

University of Louisville

ThinkIR: The University of Louisville's Institutional Repository

Electronic Theses and Dissertations

5-2014

Forecasting seasonal hydrologic response in major river basins.

A. M. Tanvir Hossain Bhuiyan
University of Louisville

Follow this and additional works at: <https://ir.library.louisville.edu/etd>

Part of the [Civil and Environmental Engineering Commons](#)

Recommended Citation

Bhuiyan, A. M. Tanvir Hossain, "Forecasting seasonal hydrologic response in major river basins." (2014). *Electronic Theses and Dissertations*. Paper 107.
<https://doi.org/10.18297/etd/107>

This Doctoral Dissertation is brought to you for free and open access by ThinkIR: The University of Louisville's Institutional Repository. It has been accepted for inclusion in Electronic Theses and Dissertations by an authorized administrator of ThinkIR: The University of Louisville's Institutional Repository. This title appears here courtesy of the author, who has retained all other copyrights. For more information, please contact thinkir@louisville.edu.

FORECASTING SEASONAL HYDROLOGIC RESPONSE IN MAJOR RIVER
BASINS

By

A. M. Tanvir Hossain Bhuiyan

B.Sc. Eng. Bangladesh University of Engineering & Technology (BUET), 2005

M. Eng. Bangladesh University of Engineering & Technology (BUET), 2009

A Dissertation

Submitted to the Faculty of the

J.B. Speed School of Engineering of the University of Louisville

in Partial Fulfillment of the Requirements

for the Degree of

Doctor of Philosophy

Department of Civil & Environmental Engineering

University of Louisville

Louisville, Kentucky 40292

May 2014

Copyright 2014 by A. M. Tanvir Hossain Bhuiyan

All rights reserved

FORECASTING SEASONAL HYDROLOGIC RESPONSE IN MAJOR RIVER
BASINS

By

A. M. Tanvir Hossain Bhuiyan
B.Sc. Eng. Bangladesh University of Engineering & Technology (BUET), 2005
M. Eng. Bangladesh University of Engineering & Technology (BUET), 2009

A Dissertation Approved on

March 6, 2014

by the following Dissertation Committee:

Dr. Mark N French (Dissertation Director)

Dr. Nageshwar R Bhaskar

Dr. Arthur C Parola

Dr. Mehmed M Kantardzic

DEDICATION

This dissertation is dedicated to my parents

Mr. A. M. Motaher Hossain Bhuiyan

and

Mrs. Khodeza Begum

ACKNOWLEDGEMENTS

This research would not have been possible without the support of many people. At first, I would like to express my profound gratitude and appreciation to my research advisor Dr. Mark N French for his indispensable support, consistent encouragement, invaluable suggestions, and constant guidance which enhanced my research interest in the field of hydro-climatology. He is the one who introduced me with this field and taught me the way to conduct a research and think critically. Discussions with him always introduced me with new issues and ideas emerging in the field, and encouraged me to think independently. His immense patience, easy accessibility, and keen interest throughout the work gave me enough freedom, confidence and motivation to pursue the research project from initiation towards completion. His constructive comments and expertise also helped me to improve my writing and presentation skills necessary for conducting a research. I consider myself very fortunate to have him as my mentor.

I am also highly indebted to my dissertation committee member Dr. Mehmed M. Kantardzic for introducing me into the wonderful world of Data Mining. By taking his course, I have learnt different techniques and methodologies frequently used for forecasting computer science related problems. This course broadened my knowledge and encourages me to bring those ideas and techniques into the field of hydrology. I am also thankful to him for his useful comments about my research. I would also like to thank the two other committee members Dr. Nageshwar R. Bhaskar and Dr. Arthur C. Parola for their valuable time, comments, instructions and suggestions. Taking their

courses helped me to learn many issues related to hydrology and water resources engineering. Thank also goes to Dr. Young Hoon Kim, Dr. Zhuhui Sun and Dr. William M. McGinley for their suggestions and helping attitude at different stages of my study.

Throughout the entire period, I was funded by the Department of Civil and Environmental Engineering (CEE) of the University of Louisville (UofL). So, I am also thankful to Dr. J.P. Mohsen, the department chair for providing me the scholarship, logistic and technical support through the CEE department. Besides this, financial support from the UofL School of Interdisciplinary and Graduate Studies (SIGS) and International Center are also highly acknowledged. A part of the research was conducted with the help of Dahlem Supercomputer Laboratory. Their help in in this regard is also gratefully acknowledged. All the departmental staffs particularly Ms. Gail Graves, Ms. Leanne Whitney, Mr. Bernie D. Miles and Mr. Brandon Shelley, Ms. Ifunanya Hilda Whitfill (Ify), were very helpful in providing me the administrative and technical support. I would also like to take this opportunity to thank all of them for being so nice and supportive throughout my stay.

I am also highly indebted to my friend Dr. Altaf Rahman, for his constant encouragement and constructive suggestions throughout my university life and career in Bangladesh and USA. Although, he is a computer scientist, he is the person who motivated me to go for higher studies in the USA. I would also like to thank my academic friends and colleague specially Abu M. Sufiyan, Abolfazl Shafaie, Venkata Gullapally, Dempsey Ballou, Liu Fengjuan, Jin-Young Hyun, Park, Dr. Raja Mohan Nagisetty, Dr. Fahim Mohammad for their help, support and friendly attitude throughout my stay in Louisville. Their company gave me the opportunities to learn about many cultures and

customs which made my stay easier and enjoyable. The author also wishes to give thanks to his friends and colleagues for their encouragement.

Finally, I am profoundly obliged to my father A. M. Motaher Hossain Bhuiyan, mother Mrs. Khodeza Begum, my sisters Dr. Noor-E-Zannat and Noor-E-Afsana, brother in law Dr. Abu Hasnath Rony, and my loving wife Dr. Sharifa Khatun for giving me the strength, and encouragement during tough times. Without their love and constant support, this study would not have been possible. The author carries his immense thanks to them. Above all, I am thankful to the Almighty for giving me the opportunity and showing me the right path.

ABSTRACT

FORECASTING SEASONAL HYDROLOGIC RESPONSE IN MAJOR RIVER BASINS

A. M. Tanvir Hossain Bhuiyan

February 1, 2014

Seasonal precipitation variation due to natural climate variation influences stream flow and the apparent frequency and severity of extreme hydrological conditions such as flood and drought. To study hydrologic response and understand the occurrence of extreme hydrological events, the relevant forcing variables must be identified. This study attempts to assess and quantify the historical occurrence and context of extreme hydrologic flow events and quantify the relation between relevant climate variables. Once identified, the flow data and climate variables are evaluated to identify the primary relationship indicators of hydrologic extreme event occurrence. Existing studies focus on developing basin-scale forecasting techniques based on climate anomalies in El Nino/La Nina episodes linked to global climate. Building on earlier work, the goal of this research is to quantify variations in historical river flows at seasonal temporal-scale, and regional to continental spatial-scale. The work identifies and quantifies runoff variability of major river basins and correlates flow with environmental forcing variables such as El Nino, La Nina, sunspot cycle. These variables are expected to be the primary external natural indicators of inter-annual and inter-seasonal patterns of regional precipitation and river flow. Relations between continental-scale hydrologic flows and external climate variables

are evaluated through direct correlations in a seasonal context with environmental phenomenon such as sun spot numbers (SSN), Southern Oscillation Index (SOI), and Pacific Decadal Oscillation (PDO). Methods including stochastic time series analysis and artificial neural networks are developed to represent the seasonal variability evident in the historical records of river flows. River flows are categorized into low, average and high flow levels to evaluate and simulate flow variations under associated climate variable variations. Results demonstrated not any particular method is suited to represent scenarios leading to extreme flow conditions. For selected flow scenarios, the persistence model performance may be comparable to more complex multivariate approaches, and complex methods did not always improve flow estimation. Overall model performance indicates inclusion of river flows and forcing variables on average improve model extreme event forecasting skills. As a means to further refine the flow estimation, an ensemble forecast method is implemented to provide a likelihood-based indication of expected river flow magnitude and variability. Results indicate seasonal flow variations are well-captured in the ensemble range, therefore the ensemble approach can often prove efficient in estimating extreme river flow conditions. The discriminant prediction approach, a probabilistic measure to forecast streamflow, is also adopted to derive model performance. Results show the efficiency of the method in terms of representing uncertainties in the forecasts.

TABLE OF CONTENTS

	PAGE
DEDICATION	iii
ACKNOWLEDGEMENTS	iv
ABSTRACT	vii
TABLE OF CONTENTS	ix
LIST OF TABLES	xiii
LIST OF FIGURES	xix
CHAPTER 1: INTRODUCTION	1
1.1 Research Background.....	2
1.2 Climate System	6
1.3 Pacific Decadal Oscillation	9
1.4 North Atlantic Oscillation	10
1.5 Sunspot Cycle.....	12
1.6 Objectives.....	13
1.7 Structure of the Dissertation.....	16
CHAPTER 2: LITERATURE REVIEW	18
2.1 Climate Variability and Streamflow	18

2.2 Hydrologic Models.....	21
2.3 Time Series Models.....	22
2.4 Artificial Neural Network Model.....	24
2.5 Probabilistic Model.....	29
2.6 Ensemble Model.....	33
CHAPTER 3: METHODOLOGY	38
3.1 Continental River Flows and External Variables.....	38
3.2 Time Series Model	39
3.2.1 Preliminary Analysis and Model Identification.....	42
3.2.2 Parameter Estimation.....	46
3.2.3 Goodness of Fit Test.....	51
3.2.4 Model Evaluation	53
3.2.5 Flow Forecasting with the ARMA Model.....	54
3.3 Artificial Neural Network Model.....	55
3.4 Forecast with the Discriminant Prediction Approach (Probabilistic Model).....	58
3.5 Persistence model and forecast	60
3.6 Performance Evaluation Criteria.....	61
3.6.1 Mean of % Error.....	62
3.6.2 Root Mean Square Error.....	62
3.6.3 Ratio of Standard Deviation (RSD).....	62
3.6.4 Correlation Coefficient.....	63
3.6.5 Pearson's Method	63
3.7 Ensemble forecast	64

3.8 Skill Measurement with Forecasting Index.....	70
CHAPTER 4: MODEL ANALYSIS	72
4.1 Data	72
4.2. Cross-correlation	77
4.3 Time Series Model Analysis	92
4.3.1 Univariate Model Analysis.....	92
4.3.2 Multivariate AR (MAR) Model.....	131
4.3.3 Time Series Modeling with Long Term Data Series	144
4.4 Model Analysis with Artificial Neural Network Model (ANN).....	150
4.5 Forecast with the Discriminant Prediction Approach (Probabilistic Model).....	177
CHAPTER 5: RESULTS AND DISCUSSION.....	188
5.1 Performance Analysis: Time Series Models (Short Data Series)	188
5.1.1 Flow Categorization Results.....	192
5.2 ANN Model Performances (Parana, Nile, and Murray Rivers)	197
5.3 Performance Analysis: Long Data Series (Congo, Yangtze, Rhine, Columbia and Parana River Flow).....	209
5.3.1 Congo River.....	216
5.3.3 Rhine River.....	220
5.3.4 Columbia River.....	223
5.3.5 Parana River	225
5.4 Flow Categorization and Forecast.....	228
5.4.1 Congo River.....	228
5.4.2 Yangtze River	231

5.4.3 Rhine River.....	234
5.4.4 Columbia River.....	238
5.4.5 Parana River	241
5.5 Ensemble Forecast (Long Data Series).....	245
5.5.1 Congo River.....	247
5.5.2 Yangtze River.....	255
5.5.3 Rhine River.....	256
5.5.4 Columbia River.....	257
5.5.5 Parana River	258
5.6 Merging of Time Series and Neural Network Model Forecasts	259
5.7 Ensemble Mean and Median Analysis	261
5.8 Discriminant Prediction Approach (Probabilistic Method)	267
5.8.1 Forecast Calibration (1906–80).....	274
5.8.2 Forecast Verification (1981–1999).....	280
CHAPTER 6: CONCLUSIONS	285
REFERENCES	292
APPENDIX A: TABLES.....	304
APPENDIX B: FIGURES	322
APPENDIX C: POSTERS.....	376
CURRICULUM VITAE.....	379

LIST OF TABLES

TABLE	PAGE
Table 4.1 River Station Information (Short Data Series), Data Used from Year 1936 to 1979	73
Table 4.2 River Station Information (Long Data Series), Data Used from Year 1906 to 1999	77
Table 4.3 Statistical Characteristics of the Observed and Transformed River Flow Series	93
Table 4.4 Linear Trend Equations, Where 'x' Represents the Sequence of the Time Series (1, 2, 3...etc.).....	96
Table 4.5 Parameters of ARMA Models with Different Model Orders for the Parana River	113
Table 4.6 Parameters of ARMA Models with Different Model Orders for the Danube River	114
Table 4.7 Parameters of ARMA Models with Different Model Orders for the Rhine River	114
Table 4.8 Parameters of ARMA Models with Different Model Orders for the Missouri River	114

Table 4.9 Comparison between the Observed and Generated Flow Statistics of the Parana River	119
Table 4.10 Comparison between the Observed and Generated Flow Statistics of the Danube River	119
Table 4.11 Comparison between the Observed and Generated Flow Statistics of the Rhine River	120
Table 4.12 Comparison between the Observed and Generated Flow Statistics of the Missouri River	120
Table 4.13 Comparison between the Observed and Generated Flow Statistics with MAR(3) models for the Parana, Danube, Rhine, and Missouri Rivers	137
Table 4.14 Performance of the Univariate ANN Model for the Murray River with Different Numbers of Lags and Hidden Nodes	155
Table 4.15 Performance of the Univariate ANN Model for the Parana River with Different Numbers of Lags and Hidden Nodes	155
Table 4.16 Performance of the Univariate ANN Model for the Nile River with Different Number of Lags and Hidden Nodes	156
Table 4.17 Performance of the Multivariate ANN Model incorporating Parana and Nile Rivers	158
Table 4.18 Performance of the Multivariate ANN Model incorporating Parana and Murray Rivers	159
Table 4.19 Performance of the Multivariate ANN Model incorporating Nile and Murray Rivers	159

Table 4.20 Performance of the Multivariate ANN Model incorporating Parana, Nile and Murray Rivers	160
Table 4.21 Performance of the Multivariate ANN Model Incorporating Parana, Murray, and SSN	160
Table 4.22 Correlations between Seasonal Yangtze and Columbia Summer Flow	178
Table 4.23 Correlations between Seasonal Rhine and Columbia Summer Flow	179
Table 4.24 Correlations between Seasonal SOI and Columbia Summer Flow	179
Table 4.25 Correlations between Seasonal PDO and Columbia Summer Flow.....	179
Table 4.26 Correlations between Seasonal NAO and Columbia Summer Flow	180
Table 4.27 Boundaries of Low and High Categorical River Flows and Forcing Variables	181
Table 4.28 Forecast of the Columbia Summer Flow Conditioned on Summer NAO (Lag 1) and Spring PDO (Lag Zero) Information.	187
Table 4.29 Forecast of the Columbia Summer Flow Conditioned on Summer NAO (Lag 1) and Winter SOI (Lag Zero) Information.	187
Table 5.1 Summary of the Performance Evaluators of Time Series Models for Predicting the Parana, Danube, Rhine, and Missouri River Seasonal Flows.....	189
Table 5.2 Validation of Parana River Low and High Flow Forecasting.	194
Table 5.3 Validation of Danube River Low and High Flow Forecasting.....	194
Table 5.4 Validation of Rhine River Low and High Flow Forecasting.....	195
Table 5.5 Validation of Missouri River Low and High Flow Forecasting.	195
Table 5.6 Summary of the Performance Evaluators of Different ANN models for Predicting the Parana, Nile, and Murray River Seasonal Flows.....	198

Table 5.7 Testing of ANN Model Forecasts for the Categorized Parana River Flow (Year 1971 to 1979).....	206
Table 5.8 Testing of ANN Model Forecasts for the Categorized Nile River Flow (Year 1971 to 1979).....	206
Table 5.9 Testing of ANN Model Forecasts for the Categorized Murray River Flow (Year 1971 to 1979).....	207
Table 5.10 Summary of the Performance Evaluators of Time Series and ANN Model Forecasts for the Congo, Yangtze, Rhine, Columbia, and Parana Rivers. ..	209
Table 5.11 Time Series Model Forecast Validation for the Categorized Congo Flow (1982-1999)	229
Table 5.12 ANN Model Forecast Validation for the Categorized Congo Flow (1982-1999)	230
Table 5.13 Time Series Model Forecast Validation for the Categorized Yangtze Flow (1982-1999)	232
Table 5.14 ANN Model Forecast Validation for the Categorized Yangtze Flow (1982-1999)	233
Table 5.15 Time Series Model Forecast Validation for the Categorized Rhine Flow (1982-1999)	235
Table 5.16 ANN Model Forecast Validation for the Categorized Rhine Flow (1982-1999)	235
Table 5.17 Time Series Model Forecast Validation for the Categorized Columbia Flow (1982-1999)	238

Table 5.18 ANN Model Forecast Validation for the Categorized Columbia Flow (1982-1999)	239
Table 5.19 Time Series Model Forecast Validation for the Categorized Parana Flow (1982-1999)	242
Table 5.20 ANN Model Forecast Validation for the Categorized Parana Flow (1982-1999)	243
Table 5.21 Rank Probability Skill Scores (RPSS) of the Ensemble Forecasts for the Congo, Yangtze, Rhine, Columbia, and Parana River Seasonal Flows	247
Table 5.22 Cross-correlation Coefficients and RMSE of Ensemble Means and Medians for Time Series (TS), Neural Network (NN), and Persistent (P) Models....	265
Table 5.23 Cross-correlations between the Ensemble Variance and the Error in the Ensemble Means and Medians of the Time Series (TS), the NN, and Persistence (P) Models	267
Table 5.24 Conditional Probability of the Columbia Summer Flow, Given the Yangtze Winter Flow, Based on Observations of 1906–1980.....	268
Table 5.25 Conditional Probability of the Columbia Summer Flow, Given the Rhine Spring and Yangtze Winter Flow, Based on Observations of 1906–1980 ..	269
Table 5.26 Conditional Probability of the Columbia Summer Flow, Given the Summer NAO index, Yangtze Winter, Rhine Spring Flow Based on Observations of 1906–1980	270
Table 5.27 Conditional Forecasting of the Columbia River Summer Flow, Based on Yangtze Winter Flow and Comparison with the Observed Flow (1981–1999)	271

Table 5.28 Conditional Forecasting of the Columbia River Summer Flow, Based on Rhine Spring and Yangtze Winter Flow, and Comparison with the Observed Flow (1981–1999)	272
Table 5.29 Conditional Forecasting of the Columbia River Summer Flow, Based on Rhine Spring Flow and Spring PDO, and Comparison with the Observed Flow (1981–1999)	273
Table 5.30 Conditional Forecasting of the Columbia River Summer Flow, Based on Rhine Spring, Summer NAO, and Winter SOI Indices, and Comparison with the Observed Flow (1981–1999)	274
Table 5.31 The mean RPSS and the FI Values at the Calibration Period (1906-1980)..	275
Table 5.32 The mean RPSS and the FI Values at the Validation Period (1981-1999)...	282
Table 6.1 Overall Performance of TS, ANN, Persistence Models based on RMSE, MPE, RSD, SPPMCC	288
Table 6.2 Overall Categorical Forecast Performance of TS, ANN, Persistence Models	289

LIST OF FIGURES

FIGURE	PAGE
Figure 1.1. Flow chart of the research objectives	15
Figure 3.1. Structure of a feedforward three layer ANN, (ASCE, 2000a)	56
Figure 3.2. Development of ensemble forecast model (flow chart)	67
Figure 4.1. Location and seasonal flow series (from year 1906 to 1999) of the five continental rivers namely Congo (Africa), Yangtze (Asia), Rhine (Europe), Columbia (North America), and Parana (South America).	74
Figure 4.2. Time series plots (seasonal) of the four external environmental variables (forcing variables): (a) Southern Oscillation Index (SOI); (b) Sunspot Cycle (SSN); (c) Pacific Decadal Oscillation (PDO); and (d) North Atlantic Oscillation (NAO) from years 1906 to 1999.	76
Figure 4.3. Cross-correlation of the seasonal flow series of Parana–Danube, Parana–Rhine, Parana–Missouri, Danube–Rhine, Danube–Missouri, and Rhine–Missouri (lags indicate three months shifts).	80
Figure 4.4. Cross-correlations between the seasonal river flow series and two forcing variables (SOI and SSN) of Parana–SOI, Danube–SOI, Rhine–SOI, Missouri–SOI, Parana–SSN, Danube–SSN, Rhine–SSN, and Missouri–SSN (lags indicate three months shifts).	81

Figure 4.5. Autocorrelation (ACF) plots of the seasonal river flow series of Congo, Yangtze, Rhine, Columbia, and Parana (lags indicate three months shifts)..	84
Figure 4.6. Autocorrelation (ACF) plots of the seasonal forcing variables of SOI, SSN, PDO, and NAO (lags indicate three months shifts).....	85
Figure 4.7. Cross-correlation plots of the seasonal river flow series of Congo-Yangtze, Congo-Rhine, Congo-Columbia, Congo-Parana, Yangtze-Rhine, Yangtze-Columbia, Yangtze-Parana, Rhine-Columbia, Rhine-Parana, and Columbia-Parana (lags indicate three months shifts).	86
Figure 4.8. Cross-correlations between five continental river flow series (seasonal) and SOI (forcing variable) of Congo-SOI, Yangtze-SOI, Rhine-SOI, Columbia-SOI, and Parana-SOI (lags indicate three months shifts).	87
Figure 4.9. Cross-correlations between the five continental river flow series (seasonal) and the SSN (forcing variable) of Congo-SSN, Yangtze-SSN, Rhine-SSN, Columbia-SSN, and Parana-SSN (lags indicate three months shifts).....	88
Figure 4.10. Cross-correlations between the five continental river flow series (seasonal) and the PDO (forcing variable) of Congo-PDO, Yangtze-PDO, Rhine-PDO, Columbia-PDO, and Parana-PDO (lags indicate three months shifts).	89
Figure 4.11. Cross-correlations between the five continental river flow series (seasonal) and the NAO (forcing variable) of Congo-NAO, Yangtze-NAO, Rhine-NAO, Columbia-NAO, and Parana-NAO (lags indicate three months shifts).	90

Figure 4.12. Cross-correlations between the four forcing variable series (seasonal) of SOI-SSN, SOI-PDO, SOI-NAO, SSN-PDO, SSN-NAO, and PDO-NAO (lags indicate three months shifts).	91
Figure 4.13. Histograms of the Parana seasonal flows: (a) before transformation and (b) after log-transformation.	94
Figure 4.14. Probability plots of the Parana seasonal flows (before log-transformation)	94
Figure 4.15. Probability plots of the Parana seasonal flows (after log-transformation)...	95
Figure 4.16. Linear trends of the Parana River flow for seasons: (a) Winter; (b) Spring; (c) Summer; and (d) Fall.....	98
Figure 4.17. De-trended and standardized Parana flows for seasons: (a) Winter; (b) Spring; (c) Summer; and (d) Fall.....	100
Figure 4.18. Plots of sample mean and sample standard deviation of (a) Parana; (b) Danube; (c) Rhine; and (d) Missouri Rivers. In the x-axis, the notations 1, 2, 3, and 4 represent winter, spring, summer, and fall seasons, respectively. .	102
Figure 4.19. Seasonal variation of the correlation coefficients for the rivers: (a) Parana; (b) Danube; (c) Rhine; and (d) Missouri.	105
Figure 4.20. Standardized seasonal river flow series: (a) Parana, (b) Danube, (c) Rhine, and (d) Missouri.....	107
Figure 4.21. The ACF and PACF plots of the Parana (a, b), Danube (c, d), Rhine (e, f), and Missouri (g, h) Rivers, respectively.....	112
Figure 4.22. Comparison between the ACFs of the observed (historical) and generated Parana River flow series with model type: (a) ARMA(1,0); (b) ARMA(2,0); (C) ARMA(1,1); and (d) ARMA(1,2) model.	116

Figure 4.23. Comparison between the ACFs of the observed (historical) and generated Danube River flow series with model type: (a) ARMA(1,1); (b) ARMA(1,2); (C) ARMA(2,0); and (d) ARMA(2,1).	118
Figure 4.24. Residuals independence and normality test for the Parana River: (a) ACF; (b) PACF; (C) Histograms; and (d) Normal probability plots of the residuals.	122
Figure 4.25. Residuals independence and normality test for the Danube River: (a) ACF; (b) PACF; (C) Histograms; and (d) Normal probability plots of the residuals.	124
Figure 4.26. Residual independence and normality test for the Rhine River: (a) ACF, (b) PACF, (C) Histograms, and (d) Normal probability plots of the residuals.	126
Figure 4.27. Residual independence and normality test for the Missouri River: (a) ACF; (b) PACF; (C) Histograms; and (d) Normal probability plots of the residuals.	128
Figure 4.28. Calibrated lead-1 forecast for the Parana River seasonal flows using univariate ARMA(1,1) model.....	130
Figure 4.29. Validated lead-1 forecasts of the Parana River seasonal flows using univariate ARMA(1,1) model.....	131
Figure 4.30. Correlograms of residuals of MAR(3) models: (a) Parana, (b) Danube, (C) Rhine, and (d) Missouri Rivers, respectively.....	134
Figure 4.31. Residuals normality test for MAR(3) model incorporating 4 rivers: (a) Histograms, and (b) normal probability plots of the residuals.	136

Figure 4.32. Calibration of the lead one seasonal forecasts of the rivers: (a) Parana; (b) Danube; (c) Rhine; and (d) Missouri, using the MAR(3) model incorporating 4 rivers.	139
Figure 4.33. Validated lead-1 seasonal forecasts of the rivers: (a) Parana River, (b) Danube River, (c) Rhine River, and (d) Missouri, using univariate and multivariate time series and persistence models.	143
Figure 4.34. Forecast validation (year 1982 to year 1999) of various time series models for the rivers: (a) Congo; (b) Yangtze; (c) Rhine; (d) Columbia; and (e) Parana	150
Figure 4.35. ANN model performance (RMSE) analysis with various numbers of lags and hidden nodes (HN) for model type: (a) Univariate ANN model for the Murray River; (b) Univariate ANN model for the Parana River; (c) Univariate ANN model for the Nile River.	157
Figure 4.36. ANN model performance (RMSE) analysis with various numbers of lags and hidden nodes (HN) for the multivariate model type incorporating (a) Parana-Nile model; (b) Parana-Murray model; (c) Nile-Murray model; (d) Nile-Parana-Murray or all-river model; and (e) Parana-Murray-SSN model.	163
Figure 4.37. Performance plots when the ANN training stopped (a) Univariate Murray model; and (b) Multivariate Parana-Nile model.	164
Figure 4.39. Regression plots of the multivariate ANN models incorporating: (a) Parana and Nile Rivers; (b) Parana and Murray Rivers; (c) Nile and Murray Rivers; (d) Parana, Nile, and Murray Rivers; and (e) Parana, Murray, and SSN. Here, (i) trained data; (ii) test data.	168

Figure 4.40. Validated lead-1 univariate ANN model forecasts of the rivers: (a) Murray; (b) Parana; and (c) Nile from the year 1971 to 1979.....	170
Figure 4.41. Validated lead-1 multivariate model incorporating Parana, Nile, and Murray River seasonal flows (multivariate all-river model) for the rivers: (a) Murray; (b) Parana; and (c) Nile from year 1971 to 1979.....	172
Figure 4.42. Forecast validation (year 1982 to year 1999) of the ANN models for the five rivers: (a) Congo; (b) Yangtze; (c) Rhine; (d) Columbia; and (e) Parana. ..	176
Figure 4.43. Time series plots of the seasonal Columbia flows	178
Figure 4.44. Data counting procedure to forecast the Columbia summer flow with one variable condition (a) Yangtze winter flow, (b) Rhine spring flow, (c) winter SOI, (d) spring PDO, and (e) summer NAO, respectively.	186
Figure 5.1. Performance indices of different time series models, predicting the Parana (a), Danube (b), Rhine (c), and (d) Missouri seasonal flows.	192
Figure 5.2. Flow categorization of the Parana River for the multivariate model including 4 rivers, SOI, and SSN.....	193
Figure 5.3. Ensemble forecast for the Parana winter flow (short data series).	197
Figure 5.4. Results of the RMSE, MPE, RSD, and SPPMCC (Pearson) performance indices of the ANN models, predicting the Parana, Nile, and Murray Rivers seasonal flows.....	200
Figure 5.5. Regression plots of the univariate model (M1): (a) Parana River; (b) Nile River; and (c) Murray River.	203

Figure 5.6. Performance evaluation of time series (TS) and neural network (NN) models for the Congo River (a, b), Yangtze River (c, d), Rhine River (e, f), Columbia River (g, h), and Parana River (i, j), respectively.	215
Figure 5.7. Ensemble forecasts of the Congo River winter flow: (a) Ensemble of time series models with persistence (TS-P); (b) Ensemble of NN models with persistence (NN-P); and (c) Ensemble of time series and NN models with persistence (TS-NN-P).....	249
Figure 5.8. Ensemble forecasts of the Congo River spring flow: (a) Time series model forecasts ensembles with persistence (TS-P); (b) NN model forecasts ensembles with persistence (NN-P); and (c) Ensembles of the time series and NN model forecasts with persistence (TS-NN-P).	251
Figure 5.9. Ensemble of the Congo River summer flow: (a) Time series model forecasts ensembles with persistence (TS-P); (b) NN model forecasts ensembles with persistence (NN-P); and (c) Ensembles of the time series and NN model forecasts with persistence (TS-NN-P).	252
Figure 5.10. Ensemble of the Congo River fall flow: (a) Time series model forecasts ensembles with persistence (TS-P); (b) NN model forecasts ensembles with persistence (NN-P); and (c) Ensembles of the time series and NN model forecasts with persistence (TS-NN-P).	254
Figure 5.11. Root mean square errors (RMSE) and cross-correlation coefficients of the seasonal river flow ensemble means and medians along with individual time series, NN, and persistence model forecasts. The rivers are represented by (a) Congo; (b) Yangtze; (c) Rhine; (d) Columbia; and (e) Parana.....	264

Figure 5.12. Forecast skills of the models with lagged variables or variable combinations in the calibration period (year 1906-1980): (a) Rank probability skill score (RPSS) and (b) Forecast Index (FI).....	276
Figure 5.13. Forecast skills of the models with lagged variables or variable combinations in the validation period (year 1981-1999): (a) Rank probability skill score (RPSS) and (b) Forecast Index (FI).....	283

CHAPTER 1

INTRODUCTION

Global climate variation has an observable effect on the natural environment resulting in intense heat waves, more frequent temperature extremes, enhanced seasonal precipitation and runoff. A study described in Lubchenco and Karl (2012), shows global occurrence of extreme meteorological and hydrological events, defined in terms of economic and human impacts, more than doubled over the past 20 years. For example, in summer 2010, intense heat wave resulting severe forest fires in Western Russia killed 55,000 people and caused \$15 billion in economic losses Schultz (2012). In 2011, new records were set in the United States for heat waves, drought, wind, floods, wildfires, etc., among which 14 such events were identified as extreme events (\$1 billion or more in damages) and caused nearly \$55 billion in total damages (Lubchenco & Karl, 2012). The extent and devastating nature of natural calamities and extreme events prompt scientists to consider a link to climate variation. Several studies and assessments have linked occurrences of heavy rainfall, extreme heat waves and flooding to climate variation (Lubchenco & Karl, 2012). An upward trend of these extreme events indicates the importance of enhancing current prediction and forecast methods to indicate the onset of these unusual events, and allow after-event recovery actions to be planned. This research study attempts to assess and quantify the historical occurrences and evaluate existing forecast estimation methods for these extreme events.

1.1 Research Background

Several categories or types of hydrologic modeling and forecasting methods exist to predict extreme events and related hydrological consequences. These include physically-based models, conceptual models, empirical models and stochastic models, with some approaches incorporating external variables influencing precipitation and streamflows.

Providing an accurate forecast involves identification of uncertainties in observed historical data series, limitations in prediction methodologies, such as rainfall-runoff information, and knowledge of the physical processes involved in rainfall-runoff mechanisms at the time and space scales of interest. The more common forecasting model categories are physically-based, conceptual-based, empirical and stochastic models. Physically-based models are based on laws of physics representing hydrological processes including complex interaction between water, energy, soil moisture and surface runoff. These models include detail physics of land-surface processes and can be characterized into fully distributed, semi distributed and lumped model forms. In a fully distributed model, the river basin is discretized into number of grids or mesh where rainfall and energy are used as forcing to determine evapotranspiration, soil moisture and surface runoff. Semi distributed models differ from the fully distributed in a sense that the basin is sub-divided into number of sub-basins based on surface characteristics and drainage networks. In the lumped approach, a watershed is characterized as a single entity and elements of the hydrological cycle (i.e. evaporation, surface runoff etc.) are included to represent the process based on a watershed scale. Any method can be challenging to apply due to calibration demands and number of model parameters. Also,

the mechanisms involved in physical processes of runoff generation are nonlinear with temporal and spatial variation (Sivakumar et al., 2002). If the mechanisms and variables are identified accurately and represented well mathematically, data are available for a calibration and validation process, a physically-based model may provide acceptable accuracy in flow estimation.

In conceptual models, equations represents the hydrological processes are lumped in a sense that physical transformation processes involved in the system are accumulated in space and time. Here, model formulation and parameters are conceptualized to reproduce the input output characteristics of the system rather than to represent the details of the physical processes. Therefore, the model is not a direct representation of the detailed hydrological process, but mimics the response to forcing variables.

Stochastic models are similar to the lumped model approach in the sense that limited information of physical processes is required. The simplest form of a stochastic model only requires the information of the historical time series of interest. In this form of the model, the relationship between input and output as represented by the persistence characteristics of the historical data series is studied. There is no direct consideration of the physics behind a process i.e. understanding of the mechanisms involved in the process is not essential. In this context, events such as floods or droughts are predicted based on the historical occurrences of these events.

In this study, several forms of stochastic models, artificial neural network models (ANN) and probabilistic models were developed to forecast seasonal flows and extreme events such as floods and droughts. Flow forecasts based on persistent characteristics are included as a baseline performance criterion. In general applications, stochastic time

series models may be used to generate synthetic hydrological records for planning and management of water resources systems, to forecast hydrological events, to detect trends and shifts in hydrological records, and to fill in missing data and extend record (Burlando et al., 1993). Stochastic time and spatial methods enables hydrologist to account for dependence when studying time or space related sequences of events (Carlson et al., 1970). These mathematical models are formulated in the theory of linear dependence in time and space, implying the methods apply where linear relationships between input and output variables exist. This means there is often an approximation to natural phenomenon considering the non-linear variability and persistence characteristics of natural systems. However, the formulation of linear stochastic modeling is straightforward to develop and has been shown to be useful for forecasting many types of hydrologic processes.

The artificial neural network (ANN) approach is a technique widely used in fields of cognitive science and machine learning. Inspired from the study of McCulloch and Pitts (1943) on the human brain and biological neuron system, ANN gained popularity in the computer science and artificial intelligence fields. Cognitive research which applied artificially created neuron works equivalently to the biological neural network by abstracting all the complexity involve in the process and focusing more on the outcome of the model. Hopfield (1982) and Rumelhart et al. (1986) provided a mathematical basis that paved the way for application of ANN methods in science and engineering fields. However, only in the last decades of the 20th century, ANN applications have had an impact in the field of hydrological modeling, forecasting precipitation, streamflow and water quality parameters (ASCE, 2000b).

The ANN methods are appealing due to simplicity, flexibility and an ability to represent highly nonlinear relationships where the complex physical processes of the system are not required to be known (Toth et al., 2000; Toth & Brath, 2007). Modeling hydrological phenomena such as rainfall runoff mechanisms is complex due to variations of watershed characteristics, rainfall patterns, snow water relationships and soil moisture condition across temporal and spatial scales. These relationships are highly nonlinear in nature and often difficult to represent by mathematical equations. This nonlinearity in the system imparts complications to the process of forecasting streamflow. For this reason, the ANN has gained much attention in the field of water resources and hydrological prediction. It works by considering the hydrological system as a blackbox and provides predictions based on establishing complex nonlinear relationships between the inputs and outputs where parameters are adjusted to produce output similar to the observed data. (Solomatine & Dulal, 2003). This characteristic of the model admits the ANN model into a class of data driven approaches that learn and characterize the system response from the observation data (Toth & Brath, 2007) and has the ability to identify the critical variables of the hydrological system suitable for predicting the streamflow (Zealand et al., 1999). Based on an extensive review of the existing literature by the ASCE task force committee, specifically formed to address the importance of ANN in the field of hydrology, also revealed that ANN can apply as a robust modeling tool to predict rainfall and streamflows (ASCE, 2000b).

1.2 Climate System

Before selecting the climate variables required for streamflow forecast models, it is important to understand the relationships between land, atmospheric and oceanic phenomenon along with snow and ice that create the climate system. The physics of phenomena that exist between ocean and atmosphere, in the form of exchanging energy which involves evaporation, condensation and solar radiations are relatively complex. Sun (sunlight) is the main source of energy in the climate system and reaches earth in the form of radiation. The energy is absorbed by the land, ocean and earth's atmosphere while some is reflected back into space. Evaporation uses this latent heat energy from the atmosphere to produce water vapor whereas condensation at height releases this energy to form clouds. Therefore, there exists a balance in the earth's temperature which is dependent upon the overall energy balance between the incoming and outgoing heat waves. Moreover, this heat energy is distributed unevenly in the earth, intense at the equator but the weakest at the poles. This non-uniformly distributed energy results in a temperature difference which causes the wind flows that forms the ocean currents, evaporation and precipitation, the phenomenon known as weather. Therefore, the interactions among land, atmospheric and oceanic components determine the earth's weather as well as the long-term averages of that weather referred to as 'climate'. Any perturbation in the climate system due to changes of energy causes alterations in the processes described above, which may influence hydrological conditions in the form of floods and droughts. These changes in the natural climate system can occur both due to the alteration of the earth's internal dynamics and may be evident in observed records of climate variables. These variables can be classified as natural (such as volcanic eruptions,

solar variations, and changes in the ocean atmosphere interactions) or anthropogenic (due to human activities). A change in the climate system may result changes in the frequency or severities of hydrological events. Thus, it is important to analyze those unusual hydrological events and their relationships with the changing climate variables.

To characterize and understand climate variability, researchers have utilized the information of global sea surface temperature and atmospheric pressure differences as indicators of changes in land, atmospheric and oceanic phenomenon and hydrological response. Anomalies in temperature and pressure between certain regions of the ocean are used to define climate indices, which represent status, duration and timing of climate variation responsible for influencing hydrological conditions. Therefore, potential previsions of these events can be made through the development of relationships between climate variables, precipitation, and streamflow.

Recognized climate indicator variables include El Nino, La Nina, and Sunspot number cycle. El Nino Southern Oscillation (ENSO), a large atmospheric oceanic circulation, specifically in the central and east-central equatorial Pacific. The ENSO includes El Nino and La Nina as the warm and cold episodes of the ENSO cycle. Historical records of temperature indicate a relation of ENSO to the inter-annual and inter-seasonal pattern of local and regional precipitation, and results in floods and droughts in particular regions of the world. The relationships between activities in the equatorial Pacific and regional precipitation and streamflow are also known as teleconnections. Teleconnections occur through the association between rainfall and sea surface temperature (SST) in the equatorial Pacific. Increased SST in the eastern Pacific during El Nino causes water vapor to rise and form clouds. Wind flow due to pressure

difference between the east and west central equatorial Pacific brings these clouds and, therefore, increased precipitation to the low pressure region (west equatorial Pacific). In this way, two regions in the tropic, far away from each other, can experience wet and dry conditions at the same time. These changes in the SST alter the tropical and sometimes extra tropical rainfall by changing the prevailing wind patterns circulating around the globe.

Recent advancement in the understanding of the ENSO dynamics and the use of statistical and numerical coupled ocean-atmosphere models, make it easier to predict ENSO with a lead time of several seasons ahead (Chen et al., 1995). Moreover, ENSO related climate anomalies and effects are region specific. In a study, Amarasekera et al. (1997) assessed the predictability of large tropical river flows including the Amazon, Nile, Congo and Parana, and found a percentage of flow variability associated with ENSO. In another study, Chiew et al. (1998) found correlations between hydro-climatic variables (rainfall and streamflow), ENSO indicators (SOI and equatorial Pacific SST) and droughts in Australia. They suggested this information as well as streamflow persistence may be used to develop forecast models. Eltahir (1996) found an association between annual flow variability of the Nile River and ENSO, and used this to improve Nile flood predictability. Based on the results of previous studies linking Ganges basin precipitation to El Nino, Whitaker et al. (2001) found a relationship between variability of Ganges annual flow and the ENSO index, useful for enhancing the forecast lead time of the flow up to one year. Kahya and Dracup (1993) analyzed the relationship between ENSO and streamflow of the contiguous United States, and found river flows were influenced by the tropical ENSO phenomena particularly in the four regions, the Gulf of

Mexico, the Northeast, the North central and the Pacific Northwest. If relationships are established between ENSO and regional precipitation and streamflow, the early predicted ENSO may be useful to enhance the prediction skills of floods and droughts.

1.3 Pacific Decadal Oscillation

Another El Nino like climate variable is the Pacific Decadal Oscillation (PDO). The PDO is a climate variability pattern in the North Pacific Ocean because of its ability to produce some of the climate variability observed during the El Nino period. However, the two differ in their persistence time. El Nino is known to persist for 6 to 18 months whereas the PDO occurs in a decadal timescale reoccurring every 20 to 30 years. It is calculated as the leading principal component mode of the 20 degree poleward North Pacific SST (Mantua et al., 1997). It was discovered first by Hare (Hare, 1996) in a study of relationships between climate variability and Pacific Ocean salmon production. Similar to other climate indices, it consists of two phases, warm and cool. During the warm phase, the Central North Pacific Ocean experiences below average SST and the west coast of North America above average or warmer SST. The opposite is true when the PDO phase is identified as cool. Since 1890 to 1998, only two complete cycles of PDO were observed with alternating warm and cool phases during the years 1890-1924, 1925-1946, 1947-1976 and 1977-1998 respectively.

Although PDO dynamics are not yet understood (Mantua et al., 1997), the contribution of PDO in developing hydro-climatic forecasts has been discussed in previous studies. Nigam et al. (1999) described PDO as one of two modes of the Pacific decadal SST anomalies that influences warm season drought and streamflow conditions

in the United States. This was expressed during the severe Northeastern drought in the 1960s which was found to correlate with above average SST anomalies of the North Pacific Ocean. This study also indicated that the relationship of the North Pacific SST with low frequency droughts in the warm season can provide important information in the management of drought, agriculture and water resources in the United States. A study by Mantua and Hare (2002) found that warm and cool phases of PDO are associated with dry and wet conditions of the Western North American climate. The influence of PDO is also evident in the decadal variation of the SOI-precipitation relationships in the western United States which were responsible for relatively a weaker ENSO effect from 1920 to 1950 in comparison to the recent decades (McCabe & Dettinger, 1999). The interdecadal variability of the ENSO-streamflow relationship in south western Canada has also been found to be influenced by the PDO which is constructive when in phase with ENSO or destructive otherwise (Gobena & Gan, 2006). Moreover, the PDO has shown its impact on the variation in winter season temperature of western Canada while the ENSO influence is either positive (El Nino) or negative (La Nina) (Bonsal et al., 2001).

1.4 North Atlantic Oscillation

The North Atlantic Oscillation (NAO) is a time varying climatic phenomenon in the North Atlantic Ocean, due to fluctuation of sea level atmospheric pressure differences between the Icelandic Low (Arctic) and the Azores High (sub-tropical Atlantic) (Hurrell, 1995; Hurrell et al., 2002). Through this activity, NAO controls the intensity and direction of the westerly winds as well as the frequency of the storm tracks across the

North Atlantic onto Europe. It is also responsible for nearly one third of the sea-level pressure and surface temperature variances over the North Atlantic and the entire Northern Hemisphere (especially during the winter season), respectively (Durkee et al., 2008). This variability of the NAO is measured by the NAO index which is the pressure difference between the Azores high and the Icelandic low pressure systems (Cannaby & Hüsrevoğlu, 2009). It can also be characterized into two phases: a positive phase and a negative phase. The positive NAO phase demonstrates below-normal heights and pressure across the high latitudes of the North Atlantic, and above-normal over the central North Atlantic, the eastern United States and the Western Europe (NCDC, 2012). The opposite is true for the negative NAO phase. Both the NAO phases are responsible for changing in the intensity and directions of the North Atlantic jet stream and storm track, and modify the zonal and meridional heat and moisture transport, which consecutively results in changes in temperature and precipitation patterns often extending from eastern North America to western and central Europe (Rogers & Van Loon, 1979; van Loon & Rogers, 1978). Studies showed that the influence of NAO is very pronounced on the climate of the Atlantic basin (Hurrell et al., 2002). This variability on regional climate underscores the need for understanding the physical mechanism of NAO and its impact on hydrology.

Anomalies in the climate system due to NAO-variability result in changes in the strength and direction of the North Atlantic Ocean winds which regulate winter time climate in Europe. Positive NAO phase creates strong westerly winds, that are responsible for milder than normal winters, cooler summers and more frequent rainfall events in central Europe and the Atlantic coast (Oubeidillah, 2011). Conversely, the

negative NAO phase weakens or blocks the westerly winds, bringing very hot summer and colder than average winters into the region (Gallego et al., 2005; Hurrell, 1995).

The impacts of NAO is also significant in the United States, particularly in the East coast and Northeast part (Hurrell, 1995; Hurrell et al., 2002) where the positive NAO is associated with the higher than average rainfall and increase in snowfall, respectively (Durkee et al., 2008). Yin (1994) found that wet climate condition in the Tennessee River Valley might be associated with the positive NAO condition. The negative NAO phase, on the other hand, is responsible for cold air outbreaks and snowy weather conditions to the East Coast (Oubeidillah, 2011).

1.5 Sunspot Cycle

Another variable for climate anomalies is solar activity such as fluctuations in the cosmic ray flux or solar irradiance either of which could influence the global climate (Prokoph et al., 2012). These solar activities are directly responsible for increasing aerosols and ion-charged raindrops which successively leads to the greater cloud cover, and potentially raises precipitation (Svensmark & Friis-Christensen, 1997). Solar activities have periodic components of approximately 11 year cycles measured as sunspot numbers. Sunspots appear as visibly dark spots on the sun compared to adjacent regions due to the activities on the photosphere of the sun. Many previous studies explored the influence of solar activities on regional climate time series. Zhongrui et al. (2003) found the length of solar cycle as a good indicator of floods and droughts in China after conducting the study using 108 years of data. Perry (2007) examined the effects of solar variability on regional climate time series using the relationships between solar

irradiance, galactic cosmic rays, and ocean and atmospheric patterns influencing precipitation and streamflow. Results of this study indicate an evidence of physical linkage between galactic cosmic rays and regional climate time series in the Midwestern United States. The influence of long-term solar activity on the South American river Parana is evidenced in a study by Mauas et al. (2008). Another study of Mauas et al. (2011) demonstrated a strong positive relationship between the sunspot numbers and the Colorado, San Juan, and Atuel River flows. Prokoph et al. (2012) also found varying degrees of correlation between sunspot cycle and maximum annual streamflow in various watersheds of the Southern Canada.

Temperature directly influences precipitation frequency and the occurrences of extreme hydrological conditions such as flood and drought (Trenberth, 2011). Increasing temperature affects the intensity and duration of droughts, resulting in greater evaporation and surface drying (Trenberth, 2011). This increase of temperature also induces an increase of water vapor in the atmosphere which ultimately produces more intense precipitation events. Since, streamflow rates are largely driven by precipitation, there may be a connection between temperature and streamflow.

This work intends to identify and quantify changes in continental scale runoff as evident in correlations between flows of major rivers globally.

1.6 Objectives

It is evident from the above discussion that seasonal hydrological extremes are dependent upon the inter-annual and inter-decadal variations of the climate system. However, the established relationships between the climate variables and streamflows

indicate indirect relations between global rivers, although geographically distant from each other. Therefore, to estimate river flows, global river flows may serve as potential predictors and provide information to develop a river flow model.

Skillful seasonal predictions of flow events are very challenging and yet may provide benefits to the society in terms of managing irrigation water requirements, reservoir operations, flood and drought management, etc. (Chowdhury & Sharma, 2009). The goal of this research is to develop innovative techniques to model and forecast extreme events as well as evaluate the influence of climate variation. Interest is primarily in extreme events, such as droughts and floods on a seasonal to annual basis. To attain this goal, this project seeks the following objectives:

- Identify and quantify changes in continental scale runoff and identify correlations between major river flows globally.
- Characterize hydrologic flow variations and quantify the relation of external environmental processes influencing flow on a seasonal to annual time scale.
- Develop a technique combining major rivers flow conditions with environmental forcing variables such as El Nino, La Nina, and the sunspot cycle to improve flow forecasting skill.
- Use ensemble forecasts to define the likelihood of an extreme event.

Present research addresses the following important issues regarding the studies of hydrological extremes: (i) Quantify relationships between occurrence of seasonal streamflow extremes in major river basins and fluctuations of external environmental variables; (ii) Evaluate stochastic models of seasonal flow extremes; (iii) Evaluate prediction of seasonal streamflow extremes using stochastic and probabilistic models;

and (iv) Illustrate the ensemble forecast method for river flow forecasting. The objectives can be shown in Figure 1.1 below:

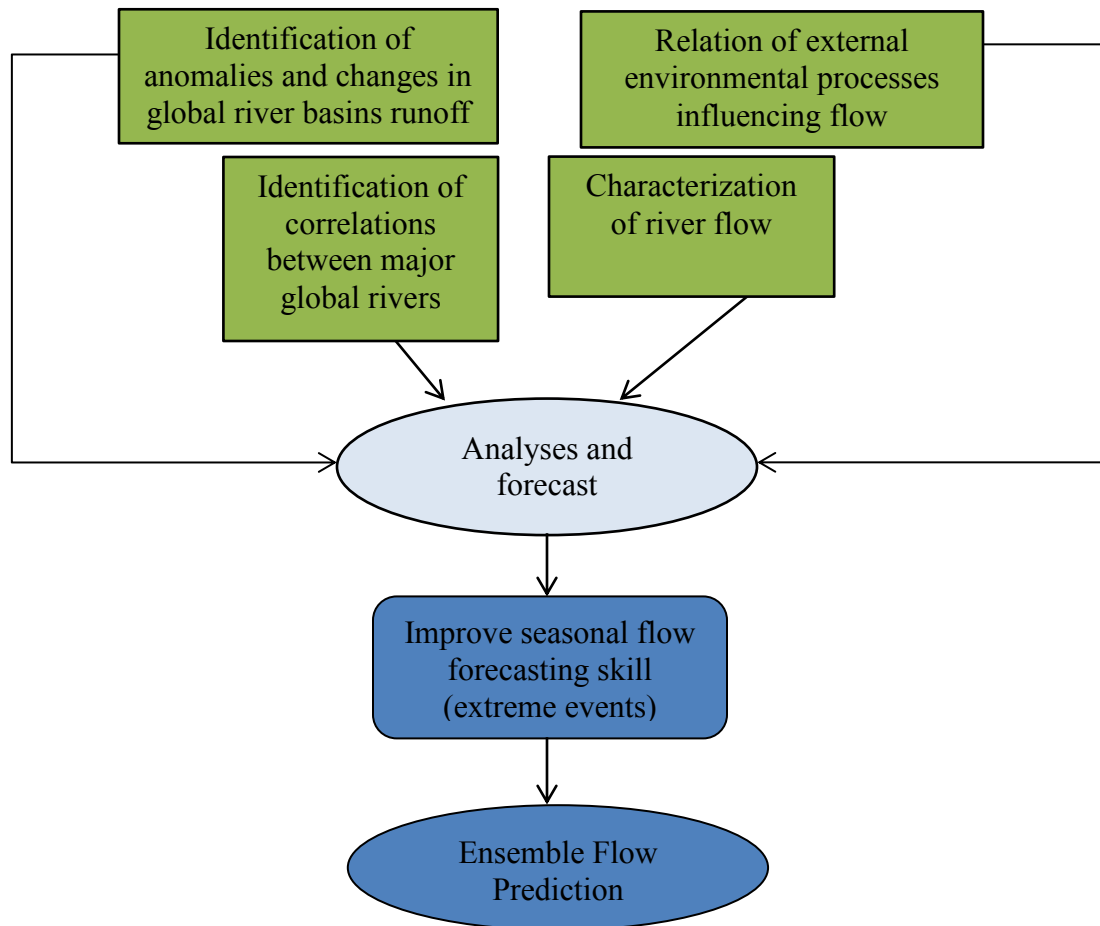


Figure 1.1. Flow chart of the research objectives

In order to attain the goals of this project, the SOI of El Nino and La Nina episodes, PDO, NAO, and sunspot number cycles (SSN) were incorporated in stochastic and probabilistic models as external environmental variables. Both univariate and multivariate time series, neural network, and probabilistic model methods were adopted.

Results provide a means to identify the role of climate variables in the performance of streamflow forecast models. Univariate time series analyses were performed using forms of the autoregressive moving average (ARMA) model to forecast the seasonal river flow. After that, multivariate ARMA analyses of seasonal flow incorporating four rivers and combinations of the SOI, PDO, NAO and SSN historical series were developed. Similarly, univariate and multivariate ANN model analyses were performed and the results were compared with the time series model predictions. An ensemble approach merging the time series and ANN model forecasts including persistence was developed and evaluated to examine its usefulness in predicting seasonal river flow. In addition, the discriminant prediction approach, a probabilistic measure to predict streamflows, was also adopted here to evaluate model's flow prediction skills.

1.7 Structure of the Dissertation

This thesis consists of six chapters. Chapter 1 provides the introduction part where background research, an overview of the factors responsible for changing the climate system, and the hydrological relations are discussed. Moreover, relationships between the climate anomalies and streamflows along with the potential for seasonal streamflow predictions are interpreted.

Chapter 2 covers a literature review of past studies relevant to this research. A brief review of different time series, neural network, and probabilistic methods is provided. The advantages of the ensemble approach for considering the uncertainties involved in the prediction methodologies have also been presented in this chapter.

Chapter 3 provides a description of the methodologies required for developing a mathematical framework and simplifications necessary for application of the time series, neural network models as well as the ensemble approach for predicting streamflows. Methods for developing probabilistic prediction approach are also discussed. Details of performance indices for assessing the skills of different models are presented.

Chapter 4 details the applications of the methodologies developed in Chapter 3 and consists of data preparation, selection of appropriate model parameters and variables, model setup, calibration and validation of the forecasts.

Chapter 5 summarizes the results obtained from the model application. Performance indices were evaluated to compare different models. Categorical forecasts are discussed to examine the efficiencies of models. Influence of river flow information and forcing variables on model performances are presented. Later, ensembles incorporating time series, ANN and the persistence models are examined for considering the uncertainties involved in the prediction methodologies. Results obtained from the discriminant prediction approach are also evaluated to derive model performance.

Finally, Chapter 6 includes the concluding remarks based on overall research outcomes.

CHAPTER 2

LITERATURE REVIEW

This chapter presents a review of literature related to continental scale runoff variation with assessment of external environmental variables for use in predicting river flow. Studies related to time series, including neural network methods and probabilistic approaches are discussed. Ensemble method applications, and comparative advantages and limitations with other methodologies, are included.

2.1 Climate Variability and Streamflow

In order to manage availability of fresh water for the world population, it is essential to understand the natural variability and long-term changes in the continental runoff and global water budget. These are of great concern to water managers for planning and policy making (Dai et al., 2009). In the previous chapter, it was discussed that fluctuations in climate variables are responsible for changes in precipitation as well as streamflow, and linked to changes in the global water balance.

Many previous studies have established relationships between the indices of climate variables such as El Nino Southern Oscillation (ENSO), Sunspot Numbers Cycle (SSN), Pacific Decadal Oscillation (PDO), North Atlantic Oscillation (NAO) and corresponding flow variations in river basins around the globe. The study of Eldaw et al. (2003) found that the Blue Nile floods are influenced by the Pacific Ocean sea surface

temperature (SST), indicating a correlation with ENSO development, information which was used to produce long range forecasts of the Blue Nile River flow. A recent study by Taye and Willems (2012) supported previous findings, indicating a significant correlation between rainfall and runoff extremes of the Blue Nile basin and climate indices of the Pacific and Atlantic Oceans, therefore, driving the occurrence of regional high and low water availability. A study by Cullen et al. (2002) showed that inter-annual and inter-decadal flow variability of Middle Eastern rivers are influenced by a dominant mode of Atlantic sector climate variability, the NAO. Precipitation and streamflow in the southwestern United States (Hidalgo & Dracup, 2003; Hurkmans et al., 2009) and southwestern Canadian streamflow anomalies (Gobena & Gan, 2006) are found to be largely influenced by the ENSO and PDO.

However, these studies have focused on individual river basin flow fluctuations and correlations with climate variables. For example, the seasonal/annual rainfall and streamflow in Australia correlated with the ENSO phenomenon and inter-decadal Pacific Oscillation (IPO) (inter-decadal ENSO-like SST variability, closely related to PDO), indicating the potential for long term hydrological prediction (Simpson et al., 1993; Chiew et al., 1998; Piechota et al., 1998; Piechota et al., 2001; Verdon et al., 2004). Chiew et al. (1998) also found ENSO influences on dry conditions in Australia. This study concluded that serial correlation in streamflow data must be used together with ENSO indicators in developing streamflow forecast models. Piechota used these findings to develop probabilistic methods for seasonal streamflow prediction (Piechota et al., 1998; Piechota et al., 2001).

Natural global hydrological variability is also evident in many of the previous studies. Studies have focused on integrating and predicting streamflow conditions on a regional scale by relating these with climate variables. Therefore, the need to understand seasonality and inter-annual variability of streamflow in a global time-space scale has become more compelling. This information can aid in discovering linkages between basins and regions, and across time (Dettinger & Diaz, 2000). In an earlier study by Probst and Tardy (1987), 50 major global rivers were selected and analyzed for annual flow fluctuations, time lags, phase oppositions, and synchronisms. This study revealed alternate relationships between North American and European runoffs, while fluctuations of South American runoffs were found to be synchronous with African runoffs.

In another study, Pekárová et al. (2003) investigated annual flow of twenty large rivers in the world based on the occurrence of wet and dry periods. This study revealed that the temporal shift in the discharge extremes occurrence (both maxima and minima) was shown to depend on longitude and latitude. This study demonstrated alternating dry and wet conditions were found in the northern and southern hemisphere. Interestingly, this study also revealed continental rivers of the Northern Hemisphere such as Magdalena (South America), Niger (Africa), and Yangtze (south-eastern Asia) create alternating dry and wet conditions as opposed to continental rivers of the Southern Hemisphere such as La Plata (South America), Zambezi (Africa), Murray (Australia) etc. Pekárová et al. (2003) demonstrated that the time shift between the Neva and Amur discharge time series is about four years, between the Amur and St. Lawrence about sixteen years, and between the St. Lawrence and Neva about nine years. The time shift between the Congo and

Amazon is about seven years (Pekárová et al., 2003). Moreover, runoff extremes in Europe and in North America do not occur in the same years.

The preceding literature described the influence of various climate variables responsible for changing regional precipitation and streamflow around the globe. Studies which demonstrate incorporation of these variables into precipitation and streamflow forecast models are described briefly in the next few sections.

2.2 Hydrologic Models

A model is the simplified conceptualization of a complex natural system which is characterized by variables highly dependent upon space and time (Viney et al., 2009). Accurate forecasts depend on the identification of relevant variables and uncertainties involved in input data, parameter estimation, and prediction methodologies or models (Beven & Freer, 2001). These uncertainties are difficult to quantify and together they inevitably result in prediction differing from that which is observed. Therefore, no model associated with this system to forecast the actual flow conditions in rivers can produce a perfect realization (similar to observation) (Viney et al., 2009). These models may also be classified as deterministic or stochastic. Physics based and empirical models are types of deterministic models, which have already discussed in Chapter 1. In this study, stochastic models, including the time series, artificial neural network (ANN), ensemble, and probabilistic models currently being used widely to forecast river flows are adopted. The literatures regarding these models are described briefly in the following sections. The reasons for not choosing the physics based and conceptual models were explained in Chapter 1.

In addition, the linear and nonlinear regression models (stochastic models) as well as the global circulation models (GCM) (physics based model) are other types of models utilize in hydrological predictions. The methods and studies regarding these models are beyond the scope of this research, therefore omitted here.

2.3 Time Series Models

The autoregressive integrated moving average (ARIMA) model (Box & Jenkins, 1970) is a popular and widely used time series (TS) model form in the field of hydrology and water resources. The approach is based on persistence and allows incorporation of other correlated variables. The ARIMA class models can be divided into AR (Autoregressive Model) and ARMA (Autoregressive Moving Average Model). The other models related to this group are the SARIMA (Seasonal Autoregressive Moving Average Model), PAR (Periodic AR), PARMA (Periodic ARMA), etc. and all belong to the extended family of ARMA models (Hipel & McLeod, 1994).

The ARMA class models can be sub-classified into two categories, univariate and multivariate. Univariate ARMA models are based on a single time series, whereas multivariate models include more than one time series. Both may have constant parameters, parameters varying with time or a combination of both (Salas et al., 1980). If data consists of an annual time series which exhibits homogeneity (constant with time) in its mean, variance, skewness and dependence structure (serial correlation), mostly non-periodic models are adopted (Salas et al., 1980). For daily, monthly or seasonal time series where seasonality (occurring repetitively in a periodic manner) in the mean and variance are evident in the time series and autocorrelation plot, periodic models are

preferred. The presence of seasonality in the data is evaluated by observing the time series and autocorrelation plots, showing periodic, repetitive, and predictable patterns.

The ARMA class models are applied to forecast natural inflows to reservoir systems and selected types of climatic variables (Salas et al., 1980). After Box and Jenkins (1968) and Box and Jenkins (1970), numerous studies have been published in literature including Carlson et al. (1970); McKerchar and Delleur (1974); Tao and Delleur (1976); McLeod et al. (1977); Hipel and McLeod (1978); Salas et al. (1980); Bras and Rodríguez-Iturbe (1994); Chatfield (2004); Mondal and Wasimi (2006) which describe improvements, advancement of the basic Box-Jenkins procedures and provide practical applications of these models in hydrology. Proper selection of a model is necessary to provide accurate forecasts which will be useful in planning, operation and management of water resources systems. According to McLeod and Hipel (1978), poor model selection or inaccurate parameter estimation are two possible sources of errors in application of time series models. Errors in model-type identification and parameter estimation are minimized by following a systematic parameter estimation approach as described in Hipel et al. (1977); McLeod et al. (1977); Salas et al. (1980); Bras and Rodríguez-Iturbe (1994). Brief descriptions of the processes are summarized later.

Carlson et al. (1970) applied Box and Jenkins' ARMA model to annual streamflow series of four rivers, then predicted a one-year forecast. And results indicated a reduction in the variance of the best selected model for each river in comparison to the original model with one or two parameters. Delleur and Kavvas (1978) used non-seasonal and seasonal ARIMA models and found that a non-seasonal model was most suitable for synthetic generation and prediction of a monthly rainfall series. Mujumdar and Kumar

(1990) used an ARMA model to forecast monthly and ten-day lead-time streamflow in three rivers in India and the goodness of fit of the models were tested for the significance of residual means, residual periodicities, and residual correlations. Test results demonstrated the models were appropriate for predicting river flows. Soltani et al. (2007) used the ARIMA model for monthly rainfall to analyze regional climate in Iran and found it useful in reproducing temporal precipitation characteristics. McKerchar and Delleur (1974) applied a seasonal ARIMA model to monthly river flows and found the AR model performed well. Thompstone et al. (1985) performed a comparative study applying a transfer function noise model, a deseasonalized ARMA model, a Periodic AR (PAR) model, and a conceptual model to predict quarter-monthly river flows. Results indicated the transfer function noise model performance was better, and, therefore, was the preferred choice. Noakes et al. (1985) assessed a one-step-ahead forecast of mean monthly flow of thirty rivers in North and South America by applying a seasonal ARIMA, deseasonalized ARMA and PAR models. The forecast performances were evaluated by using mean absolute percentage error, median absolute percentage error, mean absolute deviation, and root mean square error criteria. Results indicated the PAR model performed the best, producing the most accurate forecasts. Therefore this model was recommended for use in forecasting monthly river flow.

2.4 Artificial Neural Network Model

The artificial neural network (ANN) approach is conceptually based on mimicking the biological neural processors of the brain. The concept structure consists of massively parallel distributed processors composed of interconnected neurons. The

distributed computational function is derived from properties of the biological neural network that forms the structure of the human brain (French et al., 1992). The human brain is a highly complex, nonlinear information processing and storage unit, composed of billions of massively connected biological neurons running in parallel. The ANN model concept can be characterized as an abstract computational representation of the human brain (Kantardzic, 2011). Although a conventional computer system is able to provide a complex mathematical solution instantly, it cannot readily distinguish things such as noisy speech, facial recognition, and other fuzzy data types. Yet the human brain may be challenged by relatively simple mathematical solutions but is capable of nearly instantaneous facial recognition or voice and sound identification. Moreover, if the brain is damaged, all information is not lost, and often the brain is capable of recalling previously learned information and past events. The reason lies in the fact that the brain is composed of highly interconnected neurons and stores information in a massively distributed structure. The conceptual neural network mathematical model representing this activity can be described through the information processing of a single neuron.

Similar to biological neurons, an artificial neural network mathematical structure consists of a configuration of interconnected artificial neurons, collecting information from single or multiple sources, processing it by transformation through a nonlinear function (known as transfer function). The result of the nonlinear function or value produced represents the response activity or firing rate of the mathematical neuron. A mathematical or artificial neural network (ANN) does not fully mimic the complex biological activities among millions of biological neurons that form the human brain. It attempts to represent complex brain activities as a black box where information is

collected, processed, and stored. Therefore, the main elements that give an ANN resemblance to the form of biological neural network are its distributed representation, local operations and non-linear processing of information (French et al., 1992).

One of the main appealing features of the ANN method is the ability to learn or detect relationships between variables from representative examples, and derive a generalized function representing the underlying interconnections. The result provides a neural network function or model representing the relationship and applicable to new data from similar events. The process of learning from data is called training and is a form of model calibration. The training process, an important component of ANN application, requires no initial values or specific knowledge of the system or underlying process producing the data of interest. Another notable property of the ANN approach is the ability to solve nonlinear problems and adapt to changes in the system. The approach has the ability to tolerate faults such as noisy or missing data due to, changes in data availability that mimic situations such as disconnection of neurons. Additionally, no a priori assumptions of data structure are needed such as those required for regression-based modeling. These properties of the ANN method make it associated to artificial intelligence and cognitive science.

Numerous studies have been published discussing the usefulness of using a neural network model in predicting rainfall and precipitation. Kumar et al. (2004) demonstrated the use of two neural network models, a feed forward network (FFN) and a recurrent neural network (RNN) to predict monthly flow of a single river in India. In the FFN models, the information flows in one direction i.e. the input layer information is forwarded to the output layer through hidden layers. Cycles and loops are absent in this

network. Conversely, in the RNN, inputs and outputs are connected through a number of feedback loops, which provide the ANN facilities to consider dependence of the state of the network in the previous time step (persistence or memory). Results showed that although the performance of recurrent ANN method is better than the FFN method, both methods can be successfully applied in performing single and multi-step ahead forecasts.

The ANN applications include a wide variety of water resource areas in the field of hydrological modeling and prediction. The applications can be classified primarily as modeling either rainfall or streamflow. Toth et al. (2000) investigated the accuracy of flood forecasting by incorporating predicted rainfall information from the models including time series, ANN and k-nearest-neighbor (K-NN) methods. Their study showed a significant improvement achieved in flood prediction using the ANN approach compared with the time series and K-NN methods. Guhathakurta (2008) showed the nonlinearity and spatial variability of Indian monsoon seasonal rainfall was well captured by the ANN model and it successfully forecast the next monsoon rainfall. Nayak et al. (2007) explored the potential of integrating neural network and fuzzy logic to model the rainfall-runoff process in two basins, the USA (Kentucky basin) and India (Narmada basin), which are hydrologically different from each other. The results were encouraging and were found to explain more than 92% variability of the process.

Although, ARMA type models are often applied in predicting hydrological time series, the method is based on linear relationships between the variables in time and space. This is often a limitation, as nonlinear relations and non-stationaries cannot be explicitly incorporated. Mishra and Desai (2006) performed a comparative analysis to discover the usefulness of different types of ANN models over ARIMA models to

forecast drought over short and long lead times. The results obtained from the ANN models were better in terms of predicting droughts for one-month and four-month lead time, compared to ARMA models. The ANN method has also proved useful in predicting water quality. Maier and Dandy (1996) used ANN to forecast the salinity of the river Murray in Australia fourteen days in advance. A study by Sivakumar et al. (2002) included an ANN model and the phase space reconstruction approach (PSR) to forecast daily river flow from the Nakhon Sawan station at the Chao Phraya River basin in Thailand. In the PSR approach the non-linear function domain is sub divided into number of sub-domains in which an identified approximation is valid only for that particular sub-domain (Sivakumar et al., 2002). Therefore, the PSR differs from the ANN approach in the sense that the former is a local approximation approach; whereas the latter is a global approximation approach (past values are used as input to forecast) (Sivakumar et al., 2002). Results indicated although the PSR approach performed better than the ANN approach, both methodologies yielded reasonably good forecasts. They concluded that additional study is required to find an alternative to multilayer perceptron (MLP) [a feed-forward artificial network]. The ANN was trained with back propagation algorithm and found it may not be the appropriate model for long term streamflow prediction. Also, they pointed out the importance of selecting training data containing representative behaviors or conditions to be included in the ANN learning. This is necessary in any ANN application since the training data sets will bias ANN calibration and constrain best performance toward relations most appearing in training data.

Among the other types of ANN methods, multi-layer feed forward neural network with back propagation training algorithms have been implemented on an average of 90%

of the application cases in hydrological modeling and prediction (Coulibaly & Baldwin, 2005). Therefore, in this study, this type of ANN method is implemented to compare with time series methodologies for predicting continental river flows as a function of selected continental runoffs and external environmental variables.

2.5 Probabilistic Model

The probabilistic forecasts differed from the single valued forecast (deterministic forecast) in that a variety of flow scenarios (conditioned on the predictor variables) are presented, rather than a single estimate of flow. However, there are uncertainties in the process of selecting appropriate predictors and forecasting methods. The non-linear relationship between the streamflow and climate signals such as ENSO, PDO, NAO, and etc. (due to complex ocean-atmosphere interactions with the regional climate) makes the traditional methods (such as multiple linear regressions) difficult to use accurately (Araghinejad et al., 2006). Because of these uncertainties, deterministic forecasts are often less convincing in decision making. The probabilistic forecast is better than the deterministic one, as the uncertainties are presented in terms of likelihood. For this reason, probabilistic forecast is a requirement for operational hydrological systems and thus quantification of uncertainty needs to be considered in hydrological modeling (Krzysztofowicz, 1998, 2001a; Chen & Yu, 2007). In studies, Krzysztofowicz (Krzysztofowicz, 1998, 2001a) listed four advantages of the probabilistic forecast: (1) It admits uncertainty and expresses the degree to which a certain event can occur; (2) Flood warnings can be issued with explicitly stated probabilities so that a risk based flood warning can assist decision makers to prepare contingency plans; (3) Users are informed

about uncertainty, which allows them to consider the probable risks in decision making; and (4) The use of this forecast could be economically beneficial to the society and decision makers.

The probabilistic hydrological forecasts can be broadly classified as the Bayesian forecasting system (BFS) and the ensemble method (Chen & Yu, 2007). The detail descriptions and literatures related to ensemble forecasts are described separately in the next sections. Regarding the Bayesian probabilistic forecast, a series of studies have been performed by Krzysztofowicz et al. in order to investigate the usefulness and application of method (Krzysztofowicz, 1998, 1999, 2001a, 2001b, 2002; Krzysztofowicz & Kelly, 2000).

Among probabilistic forecast techniques, the Bayesian forecasting system demonstrated a strong fundamental basis and capability in hydrological forecasting (Chen & Yu, 2007). The efficiencies of this method have been explored in many of the previous studies. Simpson et al. (1993) provided a technique to perform probabilistic forecasts for annual river discharges in southeastern Australia, conditioned on the prior seasonal SOI and SST. The Murray and Darling river flows were categorized into low, medium, and high and SST were categorized as cool, moderate, and warm. Occurrence frequencies of the three categorical river flows as well as the mean exceedance probabilities were also determined based on prior condition of the SST. Findings of this study indicated that the method successfully incorporated the SST information to forecast annual flows of the two rivers. In another study, Moss et al. (1994) used the SOI to predict conditional probability of low streamflow in New Zealand. Eltahir (1996) used the SST of the ENSO to predict natural variability of annual Nile flow. The Nile flows and the SST values were classified

into three categories and conditional probabilities of each category were obtained using prior SST information. Results indicated that the method was useful in capturing the Nile flow variability. Wang and Eltahir (1999) successfully applied the same technique with the Bayesian theorem (also known as discriminant prediction approach) to forecast annual Nile floods by incorporating multiple predictors such as ENSO, rainfall, and prior streamflow. In a study, Sharma (2000) used a probabilistic method (using non-parametric Kernel density estimation technique) to forecast quarterly rainfall at the Warragamba dam near Sydney, Australia for lead times ranging from 3 to 24 months. Two variables, the ENSO and SST were used separately as predictors. Results indicated the method was efficient in forecasting Warragamba seasonal rainfall. However, the forecast performance with the combination of two variables was not explored.

Builds on the work of Simpson et al. (1993), Piechota et al. (1998) applied the linear discriminant approach to determine the probabilities of seasonal streamflow of southeastern Australia falling into three defined categories (below normal, normal, above normal), incorporating SOI, SST, persistence and climatological information as predictors. These four model forecasts were then combined, using optimal linear combination technique. The outcomes of this model indicated the efficiencies of the model to predict the seasonal river flows. Piechota et al. (2001) extended this work to develop an exceedance probability streamflow forecast (the streamflow amount will be equal to or exceeded a given flow value) instead of categorical forecasts. This probabilistic forecast is continuous, therefore could be useful in evaluating risks at different levels. Tamea et al. (2005) used a probabilistic approach to estimate the

distribution of the forecasted discharge values, utilizing a non-linear prediction method. Results indicated the method was useful in quantifying forecast uncertainties.

Wang et al. (2009) applied a Bayesian joint probability (BJP) approach to predict seasonal streamflow forecast at multiple sites, incorporating antecedent streamflows, ENSO indices, and other climate indicators as predictors. Results indicated impressive BJP model performance in terms of producing good quality forecast. The BJP approach was also used to forecast seasonal zero flow occurrence in many of the rivers in Australia (Wang & Robertson, 2011).

The above studies demonstrated the usefulness of probabilistic methods in hydrological predictions. In most studies, various climate signals and hydrological variables were used as predictors. However, there are opportunities for improving forecasting skills, including alternate sets of variables and variable combinations as inputs (Sharma, 2000). The discriminant prediction approach using Bayesian theorem is useful as multiple variables can be incorporated as predictors. Therefore, this method was selected in this study for seasonal river flow prediction.

The goal of the above discussion is to describe the efficiency of the stochastic models in hydrological predictions. Many of these studies incorporated SST as a predictor. The mechanism of SST influencing precipitation and streamflow is described in Chapter 1. However, the use SST as a predictor is beyond the scope of this research, therefore, omitted here.

2.6 Ensemble Model

In ensemble method, the diversity of different model predictions is utilized for skillful integration of the predictions of single or multiple models. When multiple models are available, the goal is to identify the best models or combine model results to make predictions that follow the observed flow conditions. Uncertainties in seasonal flow predictions can be considered in ensemble streamflow prediction (ESP) methods, which combine a variety of model predictions and allow the variability of estimation to be considered. This is a very useful and economically feasible technique in operational hydrology in terms of providing effective forecasts for a wide range of potential users. In a single model ensemble, realizations are produced from an individual model either by perturbing the input data series or by using different sets of variables. In a multi-model ensemble, realizations from different model results are exploited to produce skillful streamflow prediction.

The combination of model predictions is very common in economic forecasting. A significant number of studies were conducted to examine the performance of model combination. Bates and Granger (1969) was one of the first to examine the performance of model combinations. Their study revealed that the ensemble or the composite of two separate sets of forecasts for airline passenger data produced root mean square error less than either of the individual model forecasts. A study by Bates and Granger (1969) revealed that combining forecasts from two or more methodologies proved to be more accurate than using individual methods when obtained through weighted averages. A review study by Clemen (1989) combined literature from forecasting, psychology, statistics, and management science. This study showed that the accuracy of forecasts can

be significantly improved by model combination. Palm and Zellner (1992) demonstrated that the simple average of individual forecasts often showed very efficient results in comparison to weighted average forecasts. Similarly, numerous studies such as Winkler and Clemen (1992); Batchelor and Dua (1995); Fischer and Harvey (1999); Donaldson and Kamstra (1999); de Menezes et al. (2000); Hibon and Evgeniou (2005); Jose and Winkler (2008) discussed the superiority of model combination over other models.

Hydrological application of ensemble forecasts is relatively new, although its application has already been established in climate and atmospheric science. In all fields, skillful predictions can be issued for which either the best model is identified or multiple model forecasts are aggregated into a single forecast. This aggregation combines the forecast strengths of individual models and can prove to be efficient. Many studies describe the efficiency of model combination or ensembles wherein the influence of different inputs, parameters and model structure errors were considered to describe prediction uncertainties (Beven & Freer, 2001; Krzysztofowicz, 2001a; Georgakakos et al., 2004;). A study by McLeod et al. (1987) is considered to be one of the first ones to combine forecasts from different stochastic and conceptual models to predict monthly streamflows. Their study revealed that this forecast combination significantly produced better predictions than individual models. Thereafter, Shamseldin et al. (1997) combined the output from five rainfall-runoff models using simple average, weighted average, and the ANN methods, and found improved results. In another study, Shamseldin and O'Connor (1999) combined one conceptual and two empirical models to propose a real-time model, which outperformed discharge forecasts of individual models. In comparing single model and multi-model ensembles, studies indicate that forecasts with the later

outperformed the former in most cases (Ziehmman, 2000). In all cases data and model uncertainties need to be considered for the accuracy of predictions (Ajami et al., 2006). Overall, research studies demonstrate that ensemble models have the potential to provide better realizations of physical processes because of the consideration of uncertainties and may achieve improved performance relative to single forecasting models. Two types of multi-model ensemble forecasts are possible. One type of forecast identifies the best results either by using different statistical techniques such as linear regression, an ANN approach or by taking the simple mean of the available forecasts from the models (Georgakakos et al., 2004). Another one is a probabilistic approach which represents the variability of the results based on likelihoods.

From the above discussions, it is evident that models for seasonal streamflow forecasts are usually developed based on precipitation, prior streamflow and external environmental variable as predictors or forcing variables. To study the role of climate extremes on hydrologic response and understand the occurrence of extreme hydrological events, the relevant forcing variables must be identified. Existing reviews have already indicated regional hydrologic influence of climate variables and forecasting potential for precipitation and streamflow. For example, ENSO related hydro-climatic variations are evident in many regions around the globe. Regional hydrologic responses due to natural climate anomalies such as ENSO indicate the presence of indirect relationships between the continental river flows through the relation with precipitation. This offers an opportunity to assess and quantify the relationships between continental river flows and correlates with climate variables such as El Nino, SSN, PDO, and NAO. As accurate forecasts depend on proper identification of forcing variables besides model

uncertainties, the identified river flows and climate variables can serve as additional information to provide skillful streamflow prediction. This can also be useful in identifying the primary relationship indicators of hydrologic extreme event occurrence. Building on earlier work, this research quantifies the variations in historical river flows at both seasonal temporal-scale and regional to continental spatial-scale.

The reviews of existing literature indicate the prevalence and applicability of time series models in hydrological prediction. Strong theoretical basis, well understood techniques, and reduced computational burden due to availability of software are some of the main reasons for popularity of this type of model (Salas, 1993; Sharma et al., 1997). However, one of the drawbacks of the time series model is linearity assumptions among the variables to describe the behavior of the natural system, although the system is complex and highly nonlinear. Besides this, presence of non-stationarity and temporal variability in the data often make the models inadequate to provide accurate forecasts (Raman & Sunilkumar, 1995). Conversely, studies regarding the ANN model demonstrated its ability to model and capture nonlinearities and non-stationarities in the data series (Mishra & Desai, 2006). This indicates the ANN models can be very efficient in predictive hydrological modeling. In search of better models, methods including stochastic time series and neural network were adopted to simulate the seasonal variability evident in the historical river flow records.

The studies regarding ensemble forecasts demonstrates improved performance in comparison to the single model deterministic and single model ensemble forecasts (perturbing the initial conditions). Discussion of the above literatures also revealed the performance of various stochastic models currently being used in hydrological

predictions. However, studies regarding both univariate and multivariate time series and ANN models driven by continental river flow data along with external environmental variables have not yet been reported. As both time series and ANN approaches demonstrated capability in predictive hydrological modeling, combining forecasts from these stochastic models can prove to be very efficient in providing reliable seasonal streamflow forecasts. Therefore, ensemble forecasts, combining the time series and ANN model predictions were decided to evaluate.

CHAPTER 3

METHODOLOGY

This chapter presents the theoretical background of the methods applied to develop the time series, neural network, and probabilistic model in this study. The ensemble forecasts methodologies are also described.

3.1 Continental River Flows and External Variables

While previous studies have addressed regional river flow variations, this study focuses on the seasonal fluctuation of continental scale runoff. The concept is hypothesized that relationships between runoff and primary climate variables influencing flow may be identified and incorporated into methods to forecast seasonal river flows. The relationships are identified through linear and non-linear methods. Correlation analysis provides an indication of linear relationships between river flows and external environmental variables. Temporal dependence of flow records are examined using autocorrelation and partial autocorrelation analyses. The rivers were selected based on availability of long-term flow data series.

However, no flows in nature or any natural system follow a given “model”. River flow belongs to the natural system, which is highly dynamic. It is constantly changing due to natural variation or anthropogenic activities. The influence of

precipitation over river flow due to natural variations or anomalies of large scale ocean atmospheric climate circulations has already been discussed in Chapter 1. Climate anomalies such as El Niño, La Niña episodes, Pacific Decadal Oscillation (PDO), etc. are responsible for changing the frequencies and severity of extreme hydrological conditions (flood and drought). The anthropogenic activities modulating the river flow conditions are urbanization, construction of dams and reservoirs, irrigation activities, etc. Besides this, data collection procedures are also susceptible to uncertainties due to human error, instrumentation error, errors due to shifting of data stations, etc. These human activities and errors together with natural climate variations initiate uncertainties into models that usually incorporate precipitation and indices of climate variables as predictors. Moreover, improper identification of variables and linearity and stationarity assumptions in models such as the time series models also introduce uncertainties, although the natural process is inherently non-stationary and nonlinear. These uncertainties inevitably produced outcomes differing from observations and limiting the models' ability to produce accurate forecasts.

3.2 Time Series Model

The time series model identification and evaluation (both univariate and multivariate) procedure is comprised of five major steps: (1) Preliminary analysis and model identification, (2) Estimation of model parameters, (3) Tests of goodness of fit for the selected model, (4) Additional tests of the model, and (5) Model calibration and model validation. The detailed procedure and techniques of modeling are described in Matalas (1967); Tao and Delleur (1976); Salas et al. (1980); Vecchia (1985);

Thompstone et al. (1985); Hipel and McLeod (1994) with examples of application in hydrology. Preliminary analysis outlines the criteria for identifying and selecting the model order. The second step involves only parameter estimation, whereas the third step describes goodness of fit tests, which includes several tests, including the tests for residual independence and normality, evaluating correlograms (plots of the autocorrelation functions) of the observed and the model generated flow, and the model parsimony tests. The fourth step comprises the optional tests, which compares the statistical characteristics of a model-generated time series (synthetic time series) and the corresponding characteristics of the observed flow series. In the fifth step, the selected model order and parameters (calibration) are used to validate the forecast performance

The initial step in modeling is a preliminary review of short and long-term dependence of the flow series to identify the general and persistent characteristics. This dependence over time is represented with the autoregressive model as model order. The presence of any definite pattern (e.g., high flows tend to follow high flows and /or low flow tends to follow low flows) indicates the possibility of an autoregressive (AR) component. Conversely, the absence of any identifiable pattern (i.e., equal chance of having a sequence of flow values above or below the mean value) indicates absence of the AR behavior. The presence of a definite pattern indicates AR(1) model with positive parameters, dominated by low frequency fluctuations whereas alternating high and low flows exhibit negative parameter AR(1) model with dominating high frequencies (Bras & Rodríguez-Iturbe, 1994). However, the preliminary reviews are useful to indicate short term dependence of the series but the observations for higher order model are difficult at this stage. Therefore, analyzing a correlogram (plots of autocorrelation functions) and

partial correlogram is required to identify the appropriate model order to approximate the flow series characteristics. The next step is preparation of the data series, which evaluates normality, appropriate transformation towards normality (if necessary), and removal of non-stationarity and seasonality of the data series (if necessary).

Tests for normality include a skewness coefficient test and a graphical test. The skewness coefficients are compared with standard tabulated skewness values (0.508 for 2% significance level and sample size 125) given by Snedecor and Cochran (1967), described in Salas (1980). If a coefficient value falls below 0.508, the hypothesis of normality is accepted. The graphical test comprises two types: (i) histograms and, (ii) frequency distribution on normal probability paper. Depending on the test results, data are log-transformed, and thereafter evaluated for stationarity and seasonality. The procedure of transforming the data into normal (align the original distribution to normal distribution) is referred to as normalization. The presence of a linear trend, a deterministic component, indicates non-stationary flow. For the time series methods to function as theorized any series must be stationary, therefore any detectable trend must be removed. A simple linear regression test was applied to identify linear trends. Trends were removed by simply de-trending the series using a single mean. Seasonality was identified using time series plots and correlograms. Any seasonality detected was removed using a standardization procedure. Standardization was performed by subtracting a seasonal mean and dividing by the corresponding seasonal standard deviation. This process allows for series with differing means to be compared on a similar scale, and indicates relative variability. The standardized series is defined by:

$$z = \frac{y - \mu}{\sigma} \quad (3.1)$$

Here, μ and σ represent the seasonal mean and the seasonal standard deviation, respectively; y is the transformed normalized series and z is the standardized series.

3.2.1 Preliminary Analysis and Model Identification

At first, a data series is plotted to identify the general and persistent characteristics (short and long term dependence). The presence of any definite pattern (high flows tend to follow high flows and low flows tend to follow low flows) indicates the behavior resembling AR characteristics, whereas the absence of any identifiable pattern (equal chance of having the flows above or below the mean) indicates lack of autoregressive characteristics. The autocorrelation and the partial autocorrelation functions are used to identify the order of the univariate model most appropriate to approximate the statistical behavior of a data series. Usually, autocorrelation function (ACF) and partial autocorrelation function (PACF) are used to identify autoregressive (AR) and moving average (MA) model order (dependence over time). For an AR model, the ACF dies gradually after the order of the model, whereas the reverse happens for the MA model [i.e. the PACF dies abruptly] (Bras & Rodríguez-Iturbe, 1994). The significance of the decaying correlations is evaluated by approximating the 95% confidence limits as $\pm 2/\sqrt{N}$, where N represents the sample size. The ACF and the PACF values, which lie above the confidence limits indicate the corresponding order of the MA(q) and the AR(p) model, respectively. Correlations found to be significant after lag p or q without decay, indicate a seasonal series. In this case, analysis with the non-stationary seasonal models is required. If the ACF and PACF show irregularities as well as infinite extension at the first

q-p (p-q) lags, and decays abruptly afterwards, the model is identified as an ARMA(p,q) model.

The ACF indicated by $\rho_k(k = 1,2,3 \dots)$ is obtained by estimates of the ACF with equation 3.2 by Hipel et al. (1977):

$$r_k = \frac{\frac{1}{N} \sum_{t=1}^{N-k} (X_t - \bar{X})(X_{t+k} - \bar{X})}{S^2} \quad (3.2)$$

where, \bar{X} and S^2 represent the sample mean and the sample standard deviation of a series, N is the number of data in the series, and k represents time lag or distance between the correlated pairs (X_t, X_{t+k}) . Due to increasing variability of the above estimator, the ACF must be estimated to lag k on the order of $N/10$ to $N/4$ (Bras & Rodríguez-Iturbe, 1994). The calculation of population ACF requires the measure of population mean and population standard deviation. However, the mean and standard deviation used in the analysis are estimated from the sample of the river flow series. Therefore, the ACF are estimates rather than exact values of the population ACF. These are also referred as the biased estimates of the population ACF and often may misinterpret the characteristics of a time series (Salas et al., 1980).

The recursive estimation of PACF is described by Box and Jenkins (1976) and shown in equations below:

$$\hat{\phi}_{11} = r_1 \quad (3.3)$$

$$\hat{\phi}_{p+1,p+1} = \frac{r_{p+1} - \sum_{j=1}^p \hat{\phi}_{p,j} r_{p+1-j}}{1 - \sum_{j=1}^p \hat{\phi}_{p,j} r_j} \quad (3.4)$$

where,

$$\hat{\phi}_{p+1,j} = \hat{\phi}_{pj} - \hat{\phi}_{p+1,p+1}\hat{\phi}_{p,p-j+1} \quad (3.5)$$

$$j = 1, 2, \dots, p$$

Here, r_i represents the i^{th} sample autocorrelation, p is the order of the AR model, $\hat{\phi}$ is the estimate of the parameter ϕ of the AR model, and $\hat{\phi}_{pp}$ represents the estimate of the partial autocorrelation function ϕ_{pp} of the model. The symbol $\hat{}$ indicates the estimates of the corresponding parameter.

The general form of the periodic univariate ARMA (p,q) model, where p is the autoregressive (AR) order and q the moving average (MA) order with constant autocorrelation coefficient is:

$$z_t = \sum_{j=1}^p \varphi_j z_{t-1} + \varepsilon_t + \sum_{i=1}^q \theta_i \varepsilon_{t-1} \quad (3.6)$$

Here, z_t represents the standardized time series, where $t = (v - 1)\omega + \tau$ and v denotes year and τ denotes seasons with $\tau = 1, 2, \dots, \omega$. Here, ω is the number of time intervals within the year (for instance $\omega = 4$ for seasonal series). The φ_j is the autoregressive parameter of order j ($j = 1, 2, 3, \dots, p$), θ_i is the moving average parameter of order i ($i = 1, 2, 3, \dots, q$), ε_t is the independent normal variable with mean zero and variance σ_ε .

The estimates of these parameters are described in the parameter estimation section.

Evaluation of the applicability of a multivariate model can be performed by evaluating the ACF with temporal lags over the range of a few time intervals. Any short or long term dependence is indicated by a fast or slow decay towards zero with the increasing k). Short term dependence in the correlogram indicates use of multivariate

AR(p) model. Otherwise, multivariate ARMA(p,q) model is preferable for analyzing long term dependence (Salas et al., 1980).

In this study, multivariate AR(3) model is adopted with the assumption that it can be fitted well with the data to produce seasonal flow forecast. The capital letter notations used to represent multivariate equation are identical to the univariate equation, indicating matrix representations of parameters and random variables involved in the model (Salas et al., 1980). A general equation for the multivariate AR(3) model is:

$$Z_t = A_1 Z_{t-1} + A_2 Z_{t-2} + A_3 Z_{t-3} + B \varepsilon_t \quad (3.7)$$

where, Z_t is (nx1) vector elements $Z_t^{(i)}$, $Z_t^{(i)}$ represents time series of the variables i ($i = 1, 2, 3, \dots, n$) included in the model, A_1, A_2, A_3 , and B is (nxn) parameter matrix, ε_t is (nx1) vector of independent normally distributed random variables with mean zero and variance one, respectively. The expanded form of the equation is:

$$\begin{aligned} \begin{bmatrix} Z_t^{(1)} \\ Z_t^{(2)} \\ \vdots \\ Z_t^{(n)} \end{bmatrix} &= \begin{bmatrix} a_1^{11} & a_1^{12} & \dots & a_1^{1n} \\ a_1^{21} & a_1^{22} & \dots & a_1^{2n} \\ \vdots & \vdots & \ddots & \vdots \\ a_1^{n1} & a_1^{n2} & \dots & a_1^{nn} \end{bmatrix} \begin{bmatrix} Z_{t-1}^{(1)} \\ Z_{t-1}^{(2)} \\ \vdots \\ Z_{t-1}^{(n)} \end{bmatrix} + \begin{bmatrix} a_2^{11} & a_2^{12} & \dots & a_2^{1n} \\ a_2^{21} & a_2^{22} & \dots & a_2^{2n} \\ \vdots & \vdots & \ddots & \vdots \\ a_2^{n1} & a_2^{n2} & \dots & a_2^{nn} \end{bmatrix} \begin{bmatrix} Z_{t-2}^{(1)} \\ Z_{t-2}^{(2)} \\ \vdots \\ Z_{t-2}^{(n)} \end{bmatrix} \\ &+ \begin{bmatrix} a_3^{11} & a_3^{12} & \dots & a_3^{1n} \\ a_3^{21} & a_3^{22} & \dots & a_3^{2n} \\ \vdots & \vdots & \ddots & \vdots \\ a_3^{n1} & a_3^{n2} & \dots & a_3^{nn} \end{bmatrix} \begin{bmatrix} Z_{t-3}^{(1)} \\ Z_{t-3}^{(2)} \\ \vdots \\ Z_{t-3}^{(n)} \end{bmatrix} \\ &+ \begin{bmatrix} b^{11} & b^{12} & \dots & b^{1n} \\ b^{21} & b^{22} & \dots & b^{2n} \\ \vdots & \vdots & \ddots & \vdots \\ b^{n1} & b^{n2} & \dots & b^{nn} \end{bmatrix} \begin{bmatrix} \varepsilon_t^{(1)} \\ \varepsilon_t^{(2)} \\ \vdots \\ \varepsilon_t^{(n)} \end{bmatrix} \end{aligned} \quad (3.8)$$

For example,

$$\begin{aligned}
 Z_t(1) = & a_1^{11} \times z_{t-1}^{(1)} + a_1^{12} \times z_{t-1}^{(2)} + \dots + a_1^{1n} \times z_{t-1}^{(n)} + a_2^{11} \times z_{t-2}^{(1)} + \\
 & a_2^{12} \times z_{t-2}^{(2)} + \dots + a_2^{1n} \times z_{t-2}^{(n)} + a_3^{11} \times z_{t-3}^{(1)} + a_3^{12} \times z_{t-3}^{(2)} + \dots + a_3^{1n} \times \\
 & z_{t-3}^{(n)} + b^{11} \times \varepsilon_t^{(1)} + b^{12} \times \varepsilon_t^{(2)} + \dots + b^{1n} \times \varepsilon_t^{(1n)} \quad (3.9)
 \end{aligned}$$

The multivariate model is applicable with the assumption of preserving the historical statistics such as mean, standard deviation, serial-correlations and cross-correlations at different lags. It is therefore different from the univariate model in terms of preserving the space dependence of a data series (obtained by cross correlation between two time series). Usually, it is represented in a matrix form, the solution of which is complex, and typically requires a numerical method for an approximate solution. The concept of the modeling procedure involves consideration of the influence of variables across time and space along with the persistence within the data series.

3.2.2 Parameter Estimation

In this study, the parameter estimation techniques for the univariate ARMA(p,q) model was adopted from Salas et al. (1980). Initially, the parameters of the autoregressive processes are obtained, using the Yule-Walker equations. The Yule-Walker equation for calculating the φ_j parameters is:

$$r_k = \hat{\phi}_1 r_{k-1} + \hat{\phi}_2 r_{k-2} + \dots + \hat{\phi}_p r_{k-p}, \quad k > 0 \quad (3.10)$$

Here, r_k is the sample autocorrelation function and $\hat{\phi}_j, (j = 1, \dots, p)$ is the estimate of the set of parameters of the AR model. For $r_0 = 1$ and $r_{-k} = r_k$ the equation 3.10 yields

$$r_1 = \hat{\phi}_1 + \hat{\phi}_2 r_1 + \cdots + \hat{\phi}_p r_{p-1} \quad (3.11)$$

$$r_2 = \hat{\phi}_1 r_1 + \hat{\phi}_2 + \cdots + \hat{\phi}_p r_{p-1} \quad (3.12)$$

$$r_p = \hat{\phi}_1 r_{p-1} + \hat{\phi}_2 r_{p-2} + \cdots + \hat{\phi}_p \quad (3.13)$$

which may be written as

$$\begin{bmatrix} r_1 \\ r_2 \\ \vdots \\ r_p \end{bmatrix} = \begin{bmatrix} 1 & r_1 & \cdots & r_{p-1} \\ r_1 & 1 & \cdots & r_{p-2} \\ \vdots & \vdots & \ddots & \vdots \\ r_{p-1} & r_{1-2} & \cdots & 1 \end{bmatrix} \begin{bmatrix} \hat{\phi}_1 \\ \hat{\phi}_2 \\ \vdots \\ \hat{\phi}_p \end{bmatrix} \quad (3.14)$$

The solution of equation 3.14 for $\hat{\phi}$ is

$$\hat{\phi} = R^{-1}r \quad (3.15)$$

where,

$$R = \begin{bmatrix} 1 & r_1 & \cdots & r_{p-1} \\ r_1 & 1 & \cdots & r_{p-2} \\ \vdots & \vdots & \ddots & \vdots \\ r_{p-1} & r_{1-2} & \cdots & 1 \end{bmatrix}$$

For example, the $\hat{\phi}$ of an AR(1) model ($p = 1$) can be obtained from equation 3.14 as

$$\hat{\phi}_1 = r_1 \quad (3.16)$$

For an AR(2) model, equation 3.14 yields

$$\begin{bmatrix} r_1 \\ r_2 \end{bmatrix} = \begin{bmatrix} 1 & r_1 \\ r_1 & 1 \end{bmatrix} \begin{bmatrix} \hat{\phi}_1 \\ \hat{\phi}_2 \end{bmatrix} \quad (3.17)$$

Therefore, $\hat{\phi}_1$ and $\hat{\phi}_2$ can be obtained as

$$\hat{\phi}_1 = \frac{r_1(1 - r_2)}{(1 - r_1^2)} \quad (3.18)$$

$$\hat{\phi}_2 = \frac{r_2 - r_1^2}{1 - r_1^2} \quad (3.19)$$

Here, r_1 and r_2 represent the lag 1 and lag 2 autocorrelation coefficients, respectively and can be computed from equation 3.2.

This equation is the moment estimate of the parameters, and provides an approximate first estimate of the autoregressive parameters φ_j of the ARMA model. Moment estimate is a procedure, where the population moments such as mean and variance are approximated using sample moments. After obtaining the autoregressive parameters (p), the moving average parameters (q) are obtained using the formula given by Box and Jenkins (1976) described in Salas et al. (1980).

The step by step procedures to define the MA(q) parameters were adopted from Salas et al. (1980). Maximum likelihood estimate (MLE) techniques were adopted to refine parameter estimations. The SAMS (Stochastic Analysis Modeling and Simulation) 2007 (Sveinsson et al., 2007) software was used to perform all the procedures in parameter estimation. The q moving average parameters were calculated by the following equation:

$$\hat{\theta}_j = - \left(\frac{c_j}{\hat{\sigma}_\varepsilon^2} - \hat{\theta}_1 \hat{\theta}_{j+1} - \hat{\theta}_2 \hat{\theta}_{j+2} - \dots - \hat{\theta}_{q-j} \hat{\theta}_q \right) \quad (3.20)$$

where, $\hat{\sigma}_\varepsilon^2$ is the residual variance, and c_j represents the autocovariance functions $\hat{\sigma}_\varepsilon^2$ and c_j can be obtained from the equation described below:

$$\hat{\sigma}_\varepsilon^2 = \frac{c_0}{1 + \hat{\theta}_1^2 + \hat{\theta}_2^2 + \dots + \hat{\theta}_q^2} \quad (3.21)$$

$$c_j = \sum_{i=0}^p \hat{\phi}_i^2 c_j + \sum_{i=1}^p (\hat{\phi}_0 \hat{\phi}_i + \hat{\phi}_1 \hat{\phi}_{i+1} + \dots + \hat{\phi}_{p-i} \hat{\phi}_p) d_j \quad (3.22)$$

$$d_j = c_{j+1} + c_{j-1} \quad j = 0, 1, \dots, q; \quad \phi_0 = -1 \quad (3.23)$$

Here, $\hat{\theta}$ is the estimate of the MA parameter and $\hat{\sigma}_\varepsilon^2$ represents the residual variance, whereas c_0 and c_j are the estimator of the variance and autocovariance, respectively. The autocovariance was calculated from equation 3.24, which describes the relation between autocorrelation and autocovariance function:

$$r_k = \frac{c_k}{c_0} \quad (3.24)$$

The values of $\hat{\theta}$ were obtained by iteratively solving above equations, assuming that the unknown parameters were zero in the first iterations. The use of first iteration parameter values produce less accurate outcomes because the zero assumption introduces bias into the model, which progressively increased during the analysis. The biases start reducing until improved and stable parameters are obtained successively with other iterations.

The MLE of the parameters, which is similar to the least square estimates of normally distributed residuals (Salas et al., 1980), were obtained with the residuals (residual is the difference between the predicted and observed value of the dependent variable in the equation), and the sum of squares of the residuals using equations 3.25 and 3.26. The equations for estimating residuals and sum of squares of the residuals are given below:

$$\varepsilon_t = z_t - \hat{\phi}_1 z_{t-1} - \dots - \hat{\phi}_p z_{t-p} + \hat{\theta}_1 \varepsilon_{t-1} + \dots + \hat{\theta}_q \varepsilon_{t-q} \quad (3.25)$$

$$S = \sum_{t=1}^N \varepsilon_t^2 \quad (3.26)$$

Here, ε_t^2 represents the square of the residuals and S represents the sum of the square of the residuals. The neighborhood values (nearest values) of the parameters $\hat{\varphi}_j$ and $\hat{\theta}_i$ are estimated, using the Yule-Walker and Box-Jenkin's equations described in the previous section. The parameter values for which sum of squares of the residuals is the minimum, are selected as the MLE of the parameters. The procedure is performed using the SAMS 2007 software.

The basic equations and procedure followed in this study for estimating the parameters of the multivariate AR models (MAR) are based on Bras and Rodríguez-Iturbe (1994). Before analyzing the multivariate models, it is necessary to understand the characteristics of the models. The remaining part of this paragraph discusses about the multivariate model characteristics, which were directly quoted from Salas et al. (1980). "It is often the case, where the stochastic components of the data series are mutually dependent random variables (dependent along the line, over an area or across a space). When the objective is to generate a new sample of time series at a set of points, the requirement is not only to preserve the statistical characteristics at each of the n series, but also to preserve the mutual dependence among these n time series. The dependence structure among the n time series can be determined by computing the lag-k cross-correlation between the series." The cross-correlations between two periodic series $X_{v,\tau}^{(i)}$ and $X_{v,\tau}^{(j)}$ are determined by:

$$r_{k,\tau}^{ij} = \frac{\frac{1}{N} \sum_{V=1}^N (X_{V,\tau}^{(i)} - \bar{x}_{\tau}^{(i)})(X_{V,\tau-k}^{(j)} - \bar{x}_{\tau-k}^{(j)})}{s_{\tau}^{(i)} s_{\tau-k}^{(j)}} \quad (3.27)$$

In this study, SAMS2007 software was implemented to calculate the parameters of the MAR(p) model. For understanding the parameter estimation process, the calculation procedures of the parameter matrices A_1 , A_2 , and B for the multivariate AR(2) models are included, which are obtained from the theoretical expressions of M_0 , M_1 , and M_2 , where M_0 , M_1 , and M_2 represent lag-zero, lag-1 and lag-2 cross correlation matrices. The cross-correlation matrices are determined from the equations below:

$$M_0 = A_1 M_1^T + A_2 M_2^T + CC^T \quad (3.28)$$

$$M_1 = A_1 M_0 + A_2 M_1^T \quad (3.29)$$

$$M_2 = A_1 M_1 + A_2 M_0 \quad (3.30)$$

The procedures involved in solving these equations are described in Bras and Rodríguez-Iturbe (1994). Solutions yield expressions for the parameter matrices as

$$A_2 = (M_2 - M_1 M_0^{-1} M_1)(M_0 - M_1^T M_0^{-1} M_1)^{-1} \quad (3.31)$$

$$A_1 = (M_1 - A_2 M_1^T) M_0^{-1} \quad (3.32)$$

$$BB^T = M_0 - A_1 M_1^T - BM_2^T \quad (3.33)$$

Here, B matrix can be obtained from the decomposition of the equation. The superscript T and -1 represents transpose and inverse of the matrices, respectively.

3.2.3 Goodness of Fit Test

A series of tests can be performed to evaluate a model calibrated to fit a data series. A residual independence (residuals calculated from equation 3.25) of the

univariate ARMA(p,q) model is evaluated by plotting ACF and PACF of the residual flow series up to lag k from 1 to $L = N/10 + p + q$ and the 95% confidence interval. If the ACF and PACF lie within the confidence limits, the residuals are identified as independent. The Porte Manteau lack of fitness test [described in Salas et al. (1980)], a test for checking the residual independence of an ARMA(p,q) model, uses the Q-statistics (equation 3.34) for each residual series estimated from the ARMA(p,q) model (using equation 3.25). The Q-statistic is:

$$Q = N \sum_{k=1}^L r_k^2(\varepsilon) \quad (3.34)$$

Here, $r_k(\varepsilon)$ is the ACF of the residuals.

The Q statistics results are compared with the theoretical chi-square χ^2 value with $L - p - q$ degrees of freedom. If $Q < \chi^2_{(L-p-q)}$, the residuals are expected to be independent and the model is classified as adequate. Otherwise, model is identified as an inadequate, and an alternative form of model must be developed.

Later, skewness and graphical tests (histograms and probability plots of the residuals) are performed to evaluate the normality of the residual series. The SAMS 2007 software was employed to compare competing forms of the ARMA(p,q) model based on the principle of parsimony of parameters, which requires a model with the smallest number of parameters (Salas et al., 1980). The software used the corrected Akaike Information Criterion (AIC) in this respect (Hurvich & Tsai, 1993; Sveinsson et al., 2007). The model for which the AIC(p,q) is minimum, is usually selected as the best model for further analysis. The AIC equation is:

$$AIC(p, q) = n \ln(\text{MLE of Residual Variance}) + n + \frac{2(p + q + 1)n}{n - p - q - 2} \quad (3.35)$$

where, n is the sample size.

Goodness of fit tests for the multivariate AR model is almost same as the univariate model, except the residuals are evaluated for both independence in time (by correlogram plots) and space. The equation for the MAR(3) model residual is:

$$\varepsilon_t = \hat{B}^{-1}(Z_t - \hat{A}_1 Z_{t-1} + \hat{A}_2 Z_{t-1} + \hat{A}_3 Z_{t-3} + \hat{C}_1 \hat{\varepsilon}_t) \quad (3.36)$$

where, $\hat{A}_1, \hat{A}_2, \hat{A}_3$ and \hat{C}_1 represent the estimates of A_1, A_2, A_3 and C_1 respectively. The residual independence in space is evaluated by estimating cross-correlation coefficients between the two series with different lags depending on the order of the model. If the correlations are approximately equal to zero, the assumption for zero cross-correlation is accepted, and the model is selected for further analysis. This includes comparing the basic statistics (mean, standard deviation, skewness, ACF, etc.) of the observed and model generated flow series. The procedure for this analysis is described under the 'Model Evaluation' section.

3.2.4 Model Evaluation

Both univariate and multivariate ARMA models are used to generate synthetic flows and the basic statistics (mean standard deviation, skewness, autocorrelation, etc.) are calculated. The synthetic and the observed flow series statistics are evaluated using the graphical tests described before (plotting of histograms of the series as well as frequency distributions on normal probability paper). The correlograms of the historical

and model generated flow series are also plotted with the 95% confidence limits for the graphical comparison of the two series. The model generated flow correlogram, showing closeness to the historical flow correlogram indicates a better fitted model. Any significant difference (based on graphical tests and judgment) between the two flow series statistics indicates an inadequate model, which may not be a good representative of the observed flow series. For the multivariate model, cross-correlation coefficients with across time and space lags are compared with the observed series. If the coefficients of the two series are found to be approximately equal (based on judgment), the model indicates a good fit for preserving the historical statistics.

3.2.5 Flow Forecasting with the ARMA Model

For the multivariate analysis, it is assumed that the seasonal correlation coefficients are constant. Therefore, multivariate periodic hydrologic sequences with constant parameters are chosen here to use for further analysis (Salas et al., 1980). As a result, the series $z_{v,\tau}^{(i)}$ was denoted as $z_t^{(i)}$, where $t = (v - 1)\omega + \tau$ and v, τ , and ω represent years, seasons, and the number of time intervals involved in the data series, respectively.

Following the model identification process, the models are applied to achieve a lead-one time-step forecast. For the univariate model, the minimum mean square error forecasts, $z_t(L)$, were found following Salas et al. (1980) for $L = 1$, where L represents the “lead time”, as shown in Equation 3.37.

$$z_t(1) = \phi_1 z_t + \dots + \phi_p z_{t-p+1} - \theta_1 \epsilon_t - \dots - \theta_q \epsilon_{t-q+1} \quad (3.37)$$

Here, $z_t(1)$ represents the forecast of z_t with lead time of one season.

Once the lead one forecast has been performed, inverse transformation is needed to obtain the hydrologic variable. For both univariate and multivariate ARMA(p,q) models, inverse standardizations and transformations (exponentiation) are performed to get $y_{v,\tau}$ and the desired $x_{v,\tau}$ series respectively. The linear trends subtracted previously for the stationarity requirements are also added at this stage.

In the next section, the ANN methodology for seasonal streamflow forecasts will be discussed.

3.3 Artificial Neural Network Model

Multi-layer Feedforward Artificial Neural Network

An artificial neural network (ANN) is made up of a number of computational elements (represented by circles in Figure 3.1) usually known as neurons. The Figure 3.1 shows the schematic diagram of a three layer ANN, which was adopted from ASCE (2000a). The output of each neuron results from an array of inputs (or synapses), which pass through a set of interconnected links to other layer neurons as input arrays or can be the final result outputs depending on the ANN architecture and complexity of the tasks. The interconnection strength between two neurons is defined by the weights (also known as synaptic strength), which are usually adjusted based on desired outputs from known inputs. An error convergence technique is adopted so that the weights are tuned to produce results similar to the desired known outputs. This operational procedure of the input nodes to produce an analogue output is called the firing rate (French et al., 1992). A summation function merges the input firing rate and multiplies by a weight to produce respective synaptic strengths. A bias is also often incorporated to the weighted input that

affects the net input by increasing or lowering it. This bias can also be considered as a constant input weight. An activation function (also known as transfer function) is included later to limit the amplitude of the output of a neuron (Kantardzic, 2011). This transformation can be simple within a single neuron or complex when associated with several neurons.

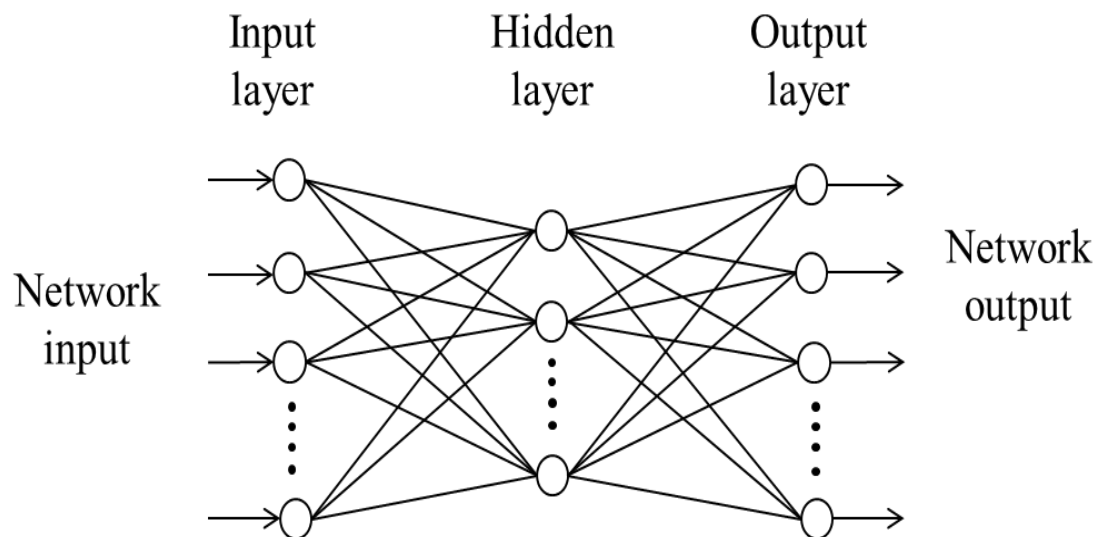


Figure 3.1. Structure of a feedforward three layer ANN, (ASCE, 2000a)

In general, the arrays represent the input variables, which are received into the input layer neurons. The next layer is the hidden layer for which neurons are connected with the input layer neurons. The hidden layer adds degrees of flexibility and complexity into the network in order to be resilient enough to deal with a more complex non-linear system. The neurons of a hidden layer are connected to the neurons of the output layer or to another hidden layer if more than one is included. The hidden layer outputs are transferred to the output layer neurons as inputs.

The use of different types of activation functions (transfer functions) depends on the nature of the network and training algorithm employed in the model (Dawson & Wilby, 2001). Some activation functions commonly used in ANN models are hard limit, symmetrical hard limit, linear, saturating linear, symmetric saturating linear, sigmoid, and hyperbolic tangent sigmoid function (Kantardzic, 2011). Among these, the logistic sigmoid function and the hyperbolic tangent functions are most popular and implemented in the majority of the research because of nonlinear behavior. The logistic sigmoid function is defined as:

$$f(x) = \frac{1}{1 + e^{-x}} \quad (3.38)$$

where, x refers to the weighted sum of inputs to the node and $f(x)$ represents the node output or firing rate.

A typical ANN consists of several interconnected nodes arranged in a particular format, known as architecture of the network (ASCE, 2000a). The characteristics of the neural architecture depend on its node-to-node connection patterns, methods required to calculate the connection weights, and selection of activation function (Dibike & Coulibaly, 2006). The ANN can be categorized either by the number of layers (i.e. single-layer, bilayer and multilayer) or by the direction of information flow processing as feed-forward and recurrent (ASCE, 2000a). In a feedforward neural network, the information is processed through nodes from the input side to the output side without any loops or feedback. In this type of ANN, nodes are arranged in layers which can be classified as input layer, one or more hidden layers, and output layer. In each step of processing, the output of a node in a layer is used as input for the next layer. However, in recurrent type neural networks, the previous network outputs can be recycled to use as present (new)

inputs, allowing the information to flow in both directions of input to output as well as output to input. In this network, information can be stored internally within the layer through lateral connections between the neurons in that layer, and can be recycled multiple time steps. This study only focused on using the multi-layer feedforward neural networks with a single hidden layer, and this network was used for calibration and verification of the model results to forecast the streamflow.

Successful training of the ANN requires a number of known inputs and outputs so that the ANN is able to learn variations of the input variables and the corresponding output. During training, the interconnection weights are initialized by assigning random numbers ranging from +1 to -1 (French et al., 1992). Here, the incremental changes of the weights are controlled by a learning rate, which performs by computing the error between the desired or targeted output and the ANN model output. Updating of the weights continues until the desired level of accuracy is reached. After completion of the training, the interconnection weights are fixed for validating the ANN model forecasts.

In the next section, the methodology involved in the discriminant prediction approach (probabilistic model) to forecast seasonal streamflow is discussed.

3.4 Forecast with the Discriminant Prediction Approach (Probabilistic Model)

The discriminant prediction approach is the conditional probabilities of the number of predictand categories given the condition of the forcing or predictor variables used in the analysis. Therefore, in this approach, forecasts are issued in a probabilistic form, which is divided into a number of categories contingent on the categories of the predictor variables (Wang & Eltahir, 1999). For this study, the predictors and the

predictands were classified into three categories: low, average, and high, such as those described in many of the previous studies (Simpson et al., 1993; Eltahir, 1996; Wang & Eltahir, 1999). To compute these conditional probabilities, the algorithm developed by Wang and Eltahir (1999), using the Bayesian theorem, was employed. The detailed descriptions of the Bayesian theory are found in many statistical books (Haan, 2002). The Bayesian Theorem for two variable conditions can be expressed by the following equation (Wang & Eltahir, 1999):

$$P(Q_i/A, B) = \frac{P(B/Q_i, A)P(Q_i/A)}{P(B/A)} \quad (3.39)$$

Here, $P(Q_i/A, B)$ represents the posterior probability of event Q_i given that both event A and B have occurred. Hence, $P(B/Q_i, A)$ is the prior probability of event B given that both event Q_i and A have occurred, $P(Q_i/A)$ represents the prior probability of event Q_i given that event A has occurred, and $P(B/A)$ demonstrates the prior probability of event B conditioned on the occurrence of event A . Therefore, the Bayesian Theorem is a way of estimating the possibility of event Q_i based on the prior probabilities of events Q_i, A , and B . If events A and B are independent, the equation can be written as

$$P(Q_i/A, B) = \frac{P(B/Q_i, A)P(Q_i/A)}{\sum_{j=1}^3 P(B/Q_j, A)P(Q_j/A)} \quad (3.40)$$

where, Q_j represents an event with all available groups. In this study $j = 1, 2, 3$ as the number of available groups are three (low, average, and high). Here, $P(B/Q_i, A)$ and $P(Q_i/A)$ are calculated based on data counting procedure. In this process, all the data points are counted in groups, which were formed according to the prior condition (low, average, and high) of a predictor variable. Thereafter, the relative frequency as well as

the probability of a flow falling into each group is calculated. In addition, the independence of the variables allows the Bayesian method to be used to calculate the conditional probability of flows, using Equation 3.40 even though any one variable data is not available on a particular period (Wang & Eltahir, 1999). Moreover, when the third variable C is included, the equation can be expressed as:

$$P(Q_i/A, B, C) = \frac{P(C/Q_i)P(Q_i/A, B)}{\sum_{j=1}^3 P(C/Q_j)P(Q_j/A, B)} \quad (3.41)$$

Therefore, for the three category forecasts, the general equation of the Bayesian Theorem for n number of variables can be expressed as:

$$P(Q_i/A_1, A_2, \dots, A_n) = \frac{P(A_n/Q_i)P(Q_i/A_1, A_2, \dots, A_n)}{\sum_{j=1}^3 P(A_n/Q_j)P(Q_j/A_1, A_2, \dots, A_n)} \quad (3.42)$$

In this Bayesian approach, the predictor variables were assumed to be independent of each other, while two or more variables were considered. However, there might be correlations which could deteriorate the forecast performance. Therefore, the variable performances need to be tested by using correlation analysis before incorporating into the equation.

3.5 Persistence model and forecast

A persistent model is developed based solely on the assumptions that the present seasonal response is the forecast for the response of the immediate next season. This is one of the simplest ways of predicting seasonal response, and the accuracy of the forecasts strongly depends on the steadiness of the data series. Persistence is sometimes defined as the forecasting method, which represents a standard of reference based on

which the skills of other forecasts are measured (Murphy, 1992). A persistence forecast can be mathematically expressed as:

$$f_{i+1} = x_i \quad (i = 1, 2, \dots, n) \quad (3.43)$$

where, x_i denotes as the flow condition at the i^{th} season and f_{i+1} represents the persistence forecast for the next season.

In the next section, the performance indices adopted in this study to measure the skills of different model forecasts are described.

3.6 Performance Evaluation Criteria

It is necessary to evaluate model forecasts so that accuracies of the models implemented in a study could be measured and the best model could be selected. Many methods are currently used to evaluate the model performance, which were published in WMO (1986), Tao and Lennox (1994), etc. The model that shows least differences of predicted discharges to the observed discharges is usually identified as a good model.

Four statistical measures were adopted to assess the performance of the forecast models incorporated in this study. These are (i) Mean of percentage error (MPE), (2) Root mean square error (RMSE), (3) Ratio of standard deviations of predicted to observed flows (RSD), and (4) Square of the Pearson product moment correlation coefficient (SPPMCC). Besides these, the correlation coefficients were also used for evaluating the model performance. The equations and performance criteria of the regarding measures are described below:

3.6.1 Mean of % Error

The model forecasts for which the MPE value approaches towards zero indicate a better model. Mean of % error for the forecasted flows were analyzed by using the following equation:

$$MPE = \frac{\sum_N \left[\frac{(y_f - y_o)}{y_o} \times 100 \right]}{N} \quad (3.44)$$

Here, subscripts ‘*f*’ and ‘*o*’ indicate forecasted and observed flows, respectively, and *N* is the total number of data points involved in the analysis.

3.6.2 Root Mean Square Error

The following equation was used to calculate the RMSE values of the models. Here, the square of the errors were calculated by subtracting the original values from the forecasted values and then taking squares:

$$RMSE = \sqrt{\frac{\sum_{i=1}^N SE}{N}} \quad (3.45)$$

Here, SE means “square error” and *N* is the total number of data points. The model for which the RMSE approaches towards zero indicates a better model.

3.6.3 Ratio of Standard Deviation (RSD)

The RSD of the forecasted to observe flows were calculated by implementing the following equation:

$$RSD = \sqrt{\frac{\sum_{i=1}^N (y_f - \bar{y}_f)}{\sum_{i=1}^N (y_o - \bar{y}_o)}} \quad (3.46)$$

Here, y_f and y_o represent forecasted and observed flows and \bar{y}_f and \bar{y}_o represent forecasted and observed flow means, respectively. For a better model, RSD values approaches to unity.

3.6.4 Correlation Coefficient

The correlation coefficient (r) is another way of comparing the forecast performance (equation 3.27). For linear regression, this coefficient is also known as Pearson product moment correlation coefficient. This is a very useful evaluation index to measure the accuracy of forecasting with respect to observed flows. It is independent of the scale of the data set, therefore an important tool to measure the performance between the observed and predicted flows. The r values vary from +1 to -1, where +1 indicates a perfect positive and -1 indicates a perfect negative forecast. The zero coefficient value indicates existence of no relationships between the observed and predicted river flows. The coefficient value of 0.9 and above indicates a very satisfactory performance.

3.6.5 Pearson's Method

The square of the Pearson product moment correlation coefficient (SPMCC) r^2 (coefficient of determination for linear regressions) is another way of measuring the performance of the model. The SPPMCC (r^2) is a statistical measure of the linear dependence between the two data sets. In other words, it shows how well a regression fits the data. The values of r^2 vary from 0 to 1, where 0 indicates nonexistence of linear

relationships and 1 represents perfectly correlated datasets (all forecasted flows equal the observed river flows). For perfect forecasts, all points lie on the 45 degree line in a scatter plot, where the x-axis and y-axis represent the observed and forecasted flows, respectively. The accuracy of forecasting is defined by the distance between the points and the 45 degree line, which also represents prediction capability of the model. The model for which the r^2 value approaches unity represents a better model. The equation used to calculate the SPPMCC is given below:

$$r^2 = \left[\frac{\sum(x - \bar{x})(y - \bar{y})}{\sqrt{\sum(x - \bar{x})^2 \sum(y - \bar{y})^2}} \right]^2 \quad (3.47)$$

Here, x and y represents the observed and forecasted flows, respectively.

In the next sections, the methodology adopted to develop an ensemble model will be described.

3.7 Ensemble forecast

Accurate forecasts depend on identification of relevant variables and uncertainties involved in prediction methodologies. Uncertainties in seasonal flow predictions can be considered in ensemble forecast methods, which combine a variety of model predictions and allow the variability of estimation to be considered. In this study, methods including time series and ANN are evaluated for seasonal flow forecasts ensembles. Forecasts based on persistent characteristics are included as a baseline performance criterion. River flows and external variables (forcing variables) are incorporated in stochastic time series and ANN methods to examine the ability to reproduce seasonal variability evident in historical flows. The forcing variables are expected to contribute to natural streamflow

conditions. Model performance is evaluated for improvement in prediction skills, while including multivariate approaches with river flow and external variables. To further assess model efficiency for predicting seasonal flow, both stochastic and ANN model forecasts are categorized into high, average and low flow levels. However, ensemble model can prove to be very efficient and more skillful than a single model forecast (Krishnamurti et al., 1999; Krishnamurti et al., 2000; Rajagopalan et al., 2002; Regonda et al., 2006). Therefore, an ensemble approach merging stochastic, ANN, and persistent forecasts are developed and evaluated for seasonal river flows.

The methodology employed in this study consists of seven major components: (i) Quantification of the relationships between different continental river flows; (ii) Identification of the influence of large-scale ocean-atmospheric variables (El Niño, La Niña episodes, SSN, etc.) on the corresponding river flows; (iii) Perform time series, ANN, and persistent model analyses to forecast seasonal streamflow; (iv) Flow categorization (low, average, and high) and forecasts (with the models employed); (v) Ensembles of the time series and ANN model forecasts, where the model predictions were obtained separately, incorporating a single or multiple variables; (vi) Combination of time series, ANN, and persistent model predictions to produce ensemble forecasts; and (vii) Ensemble mean, median, and probabilistic analysis, and evaluation of the model prediction skills. Among many of the forecasting approaches, time series and ANN models have successfully been used in a variety of hydrologic and hydro-climatic applications (described in Chapter 2). A brief illustration of methodology for these models was included in the previous sections. Therefore, the ensembles predictions from both methodologies (time series and ANN) including persistence were evaluated over

similar predictor conditions as well as their combinations. The steps followed to develop ensembles forecasts are described in the Figure 3.2.

The variables used in the time series and ANN models are required to be independent to each other in order to avoid ‘multicollinearity’ problems which causes overfitted data and erroneous forecasts (Regonda et al., 2006). For true statistical independence, the correlation matrix computed from the variables is to be a diagonal matrix with ones on the diagonal and zeros elsewhere. Multicollinearity happens statistically when two or more predictors in a multivariate regression are correlated to each other. In other words, one predictor variable is a function of the others, therefore, can be linearly predicted from the others (Haan, 2002). Therefore, the off-diagonal elements in the correlation matrix will not be zero. However, multicollinearity itself does not affect the predictability of the model but disrupt yielding better predictions by producing (i) erratic changes in the parameter estimation with small changes in the data and (ii) high standard errors in the coefficients with low significance levels even though the overall regression indicates a definite linear relationship (Haan, 2002). It may also impose wrong sign to the regression coefficients, therefore, creates problems in detecting the contribution of individual predictors in the prediction (Haan, 2002). In this study, the incorporated river flows and external variables were assumed to be independent, and the errors due to multicollinearity were also neglected.

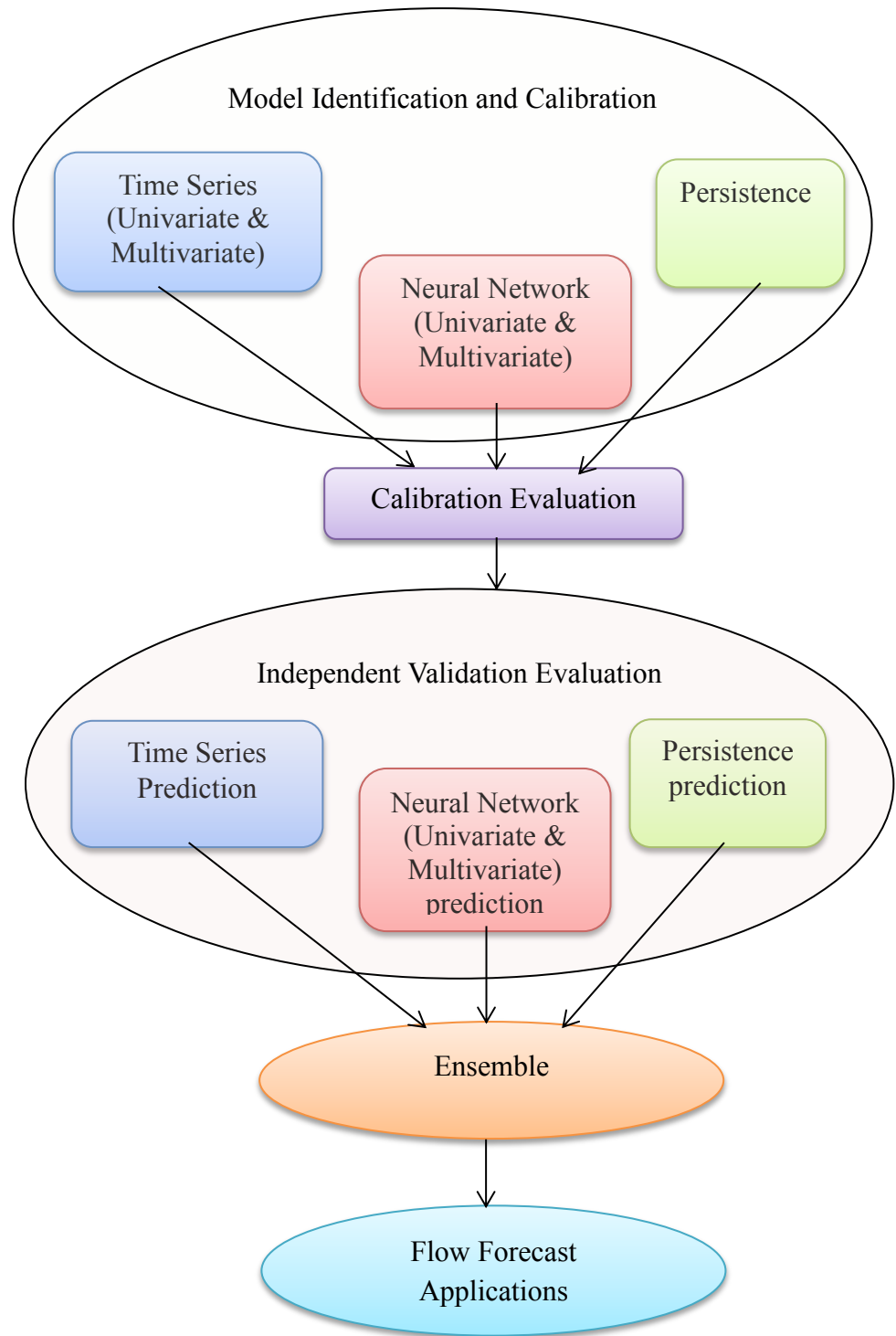


Figure 3.2. Development of ensemble forecast model (flow chart)

The uncertainties in the statistical forecasting approach due to model inadequacy can be minimized by using a combination of results from several candidate models known as ‘model averaging’ (Regonda et al., 2006). Another approach is a model average probabilistic forecast, where the predictions from several candidate models are combined to produce ensemble forecasts. This likelihood based approach has also been successfully applied in many studies and proved very efficient in outperforming the individual model forecasts (Georgakakos et al., 2004; Hagedorn et al., 2005; Krishnamurti et al., 2000; Regonda et al., 2006).

The ensemble forecast methodology employed in this study was evaluated based on the mean and median analysis as well as the probabilistic analysis. The mean and median analysis comprises estimation of mean and median of the time series and ANN model forecasts including persistence in each time step and compares results with the observed flow values. The forecasts were then evaluated, using the RMSE and correlation coefficient described in the previous sections.

The ensemble probabilistic forecasts are probability density function or PDF, as it is used to approximate the outcome of the events from a finite set of forecast realizations resulting from different models (Weigel et al., 2007). In this method, prediction uncertainties are considered by combining a variety of model predictions.

Hence, it is difficult to verify the skill of the probabilistic forecasts, using a single observation as the full information content is not considered. Therefore, skills of these forecasts are required to be evaluated in a probabilistic manner. The ranked probability skill score (RPSS), a widely used method to measure the quality of categorical probabilistic forecasts (Weigel et al., 2007), were adopted here to examine the

performances of the ensemble forecasts. Here, performance evaluations are achieved based on climatological forecasts (random guess), which acts as a base line criterion. At first, model forecasts are divided into k mutually exclusive and collectively exhaustive categories so that the portions of the of ensembles falling into each category can be calculated in a probabilistic manner represented by p_1, p_2, \dots, p_k , respectively. Thereafter, the observed flows are also categorized into the corresponding forecast categories and the observational vectors (d_1, d_2, \dots, d_k) are determined, where d_k is unity when the observation matched the k^{th} category. The equation for the RPSS is defined as follows

$$RPS = \sum_{i=1}^k \left[\left(\sum_{j=1}^i p_j - \sum_{j=1}^i d_j \right)^2 \right] \quad (3.48)$$

$$RPSS = 1 - \frac{RPS(\text{forecast})}{RPS(\text{climatology})} \quad (3.49)$$

The RPSS statistics vary from negative infinity to positive unity (Regonda et al., 2006). The RPSS value equal to unity indicates a perfect forecast i.e. the predictions completely match the observations. The zero RPSS value indicates the forecast equals the ‘climatology’ (random guess). The negative RPSS values demonstrate poor model performance as the accuracies fall below the ‘climatology’. However, the positive RPSS value indicates improved model performance in comparison to that of climatological forecast.

3.8 Skill Measurement with Forecasting Index

The forecasting index (FI) skill measure includes two types of forecast probabilities: (a) Prior probability, and (b) Posterior probability (Wang & Eltahir, 1999). Prior probability $P_r(i, j)$ demonstrates the probability of a predictand falling into each of the respective flow category (for 3 categories, $i = 1, 2, 3$) conditioned on the previous information of the predictor variables in each season ($j = 1, 2, \dots, n$). The posterior probability $P_p(i, j)$, after categorizing the observed flow into 3 categories, would be [1, 0, 0] for a low flow season, [0, 1, 0] for an average flow season, and [0, 0, 1] for a high flow. Therefore, the forecasting probability, describing the observed flow categories for a particular season, can be equated as

$$FP(j) = \sum_{i=1}^{n=3} P_r(i, j) \times P_p(i, j) \quad (3.50)$$

The overall skills of the discriminant prediction approach can be obtained by the forecasting index (FI), which is the average of these forecasting probabilities, over a certain period:

$$FI = \frac{1}{n} \sum_{j=1}^n FP(j) \quad (3.51)$$

The FI equals to unity indicates a perfect forecast, whereas the zero FI value indicates no prediction skills. However, forecasts without prior information yield the probability of 0.333 for each of the three categories (one third for three flow categories). This is also referred as climatological forecast or random guess and act as a baseline criterion for measuring the forecast performance. Therefore, any FI value below 0.333 implies less accurate forecast, whereas values larger than 0.333 indicate better forecast

performance. The advantage of the FI is its superiority over the traditional skill measurement (Wang & Eltahir, 1999), as the latter could not differentiate between the two similar categorical forecasts with different forecasting probabilities (skill difference between 90% and 50% high flow forecast for a high flow season although both predictions are accurate).

CHAPTER 4

MODEL ANALYSIS

This section describes data used in the model applications in Chapter 3. Four external environmental variables, (forcing or indicator variables) namely the Southern Oscillation Index (SOI), sun spot numbers (SSN), Pacific Decadal Oscillation (PDO), and North Atlantic Oscillation (NAO) were incorporated in combination with the river flow. Persistent forecasts were included as a baseline forecast criterion. The discriminant prediction approach, a probabilistic approach to forecast the occurrence of an event, was also examined at the end. The data and modeling procedures are described in the following sections.

4.1 Data

At first, six rivers, Parana, Danube, Rhine, Missouri, Nile, and Murray were studied to evaluate the variation in the continental scale runoff and how changes can be quantified in terms of extreme events. The river flow data were retrieved from the three sources: (i) Global River Discharge Database (RivDis v1.1) maintained by Oak Ridge National Laboratory and the University of New Hampshire (Vorosmarty, et al.,1998), (ii) study of Dai and Trenberth global river flow and continental discharge data (Dai et al., 2009) from the climate analysis section of the National Center for Atmospheric Research (NCAR), and (iii) Global Runoff Data Center (GRDC), Koblenz, Germany (GRDC,

2011). The Southern Oscillation Index (SOI) and Sunspot Number cycle (SSN) data were retrieved from the Climate Prediction Center (CPC) and the National Geophysical Data Center (NGDC) of the National Oceanic and Atmospheric Administration (NOAA), respectively. The winter, spring, summer and fall seasonal means were obtained for months December-January-February (DJF), March-April-May (MAM), June-July-August (JJA) and September–October-November (SON). The river station name, station information, upstream area and location in the map are given in Table 4.1. The PDO (Mantua et al., 1997), and NAO (Hurrell, 1995) data were collected from a data archive maintain by the Joint Institute for the Study of the Atmosphere and Ocean (JISAO) at the University of Washington.

Table 4.1

River Station Information (Short Data Series), Data Used from Year 1936 to 1979

River	Country	Continent	Station	Elevation (m)	Upstream area (km ²)	Longitude (deg.)	Latitude (deg.)
Parana	Brazil	South America	Guaira	218	802150	-54.24	-24.06
Danube	Germany	Europe	Hofkirchen		47495	13.12	48.67
Rhine	Germany	Europe	Rees	10	159680	6.40	51.76
Missouri	USA	North America	Yankton	347	273905	-97.40	42.86
Nile	Egypt	Africa	Aswan	-	-	32.90	23.96
Murray	Australia	Australia	Wakul	-	-	143.34	-34.85

Based on the length of the data series, the time series and ANN model analyses were divided into two parts: (a) short term and (b) long term. Short term study was conducted data from the year 1936 to 1979. The long-term data series were from the year 1906 to 1999. The long-term series was used to evaluate the time series and the ANN models. The rivers for which long term flow series were used are shown in Figure 4.1 and

the available information is summarized in Table 4.2. The Figure 4.2 describes the time series of the four external variables incorporated in the analysis.

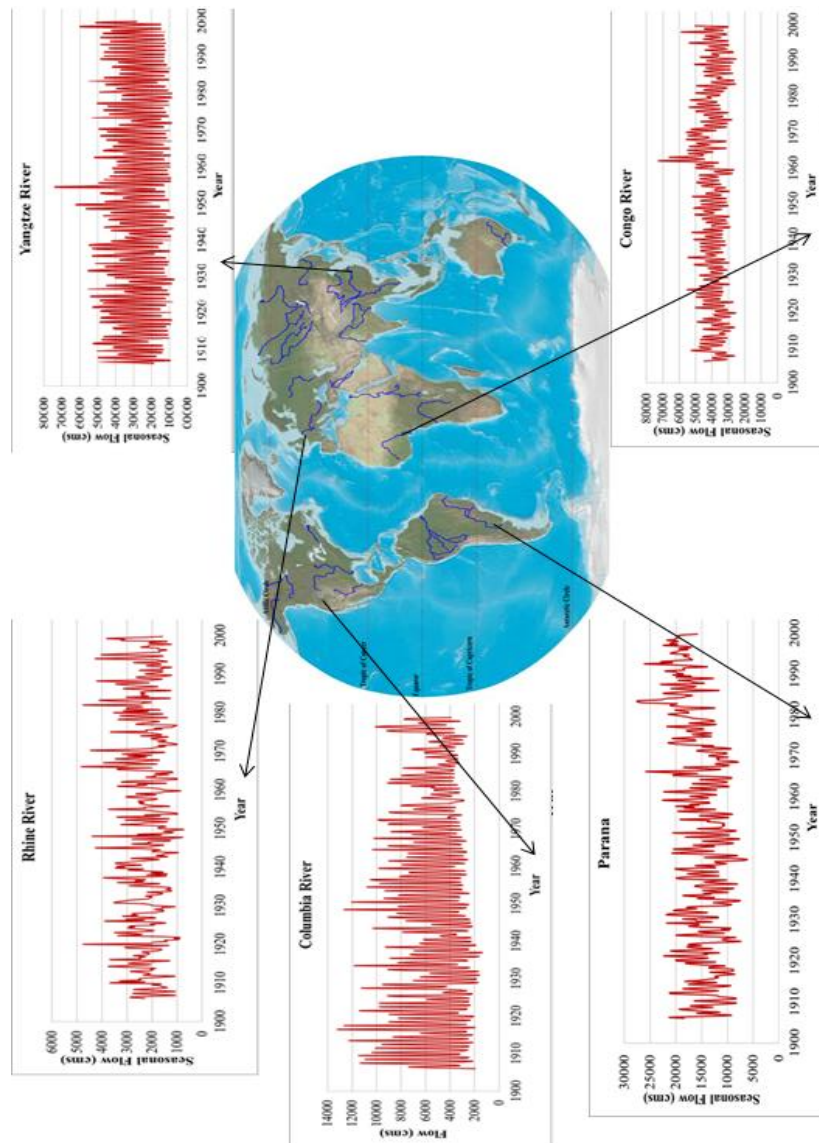
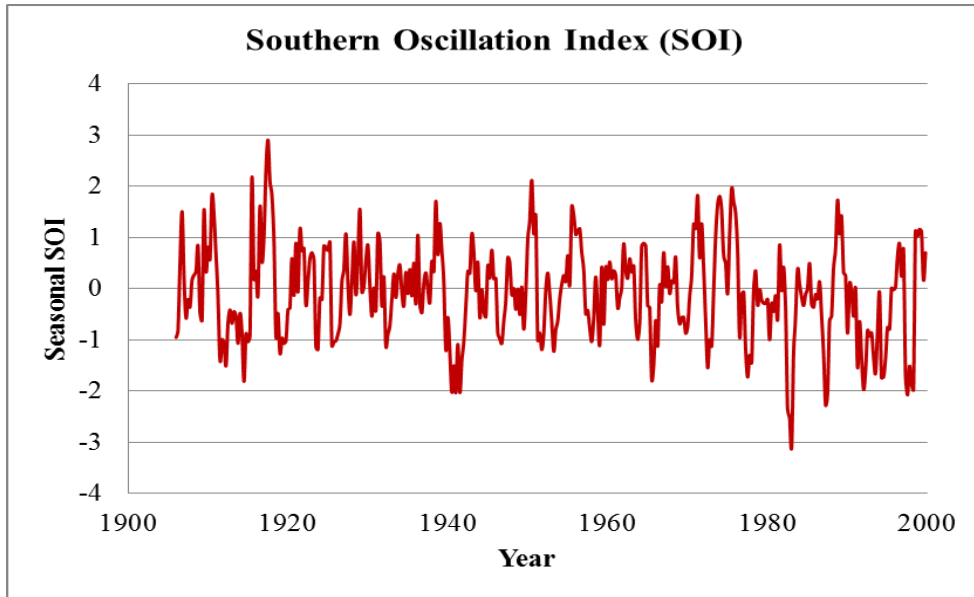
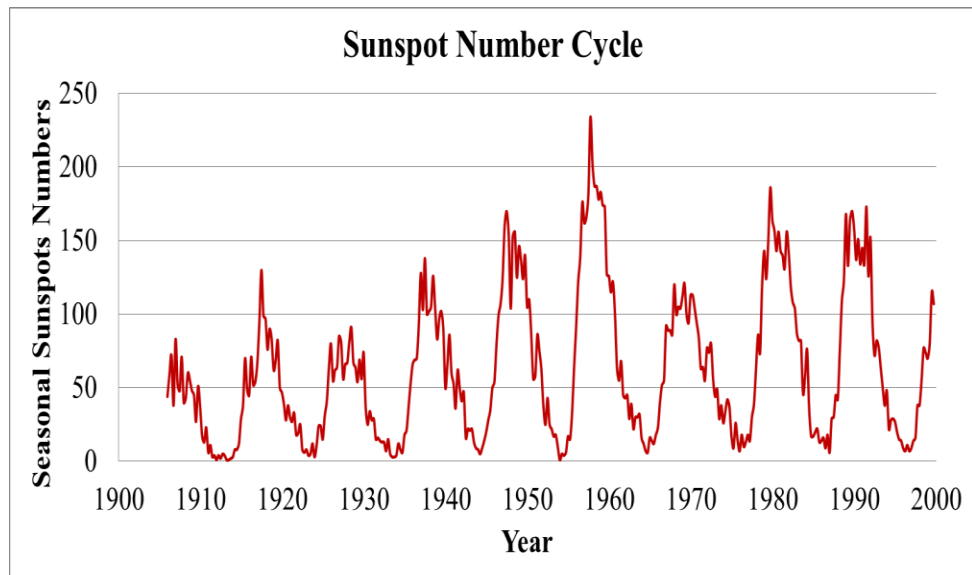


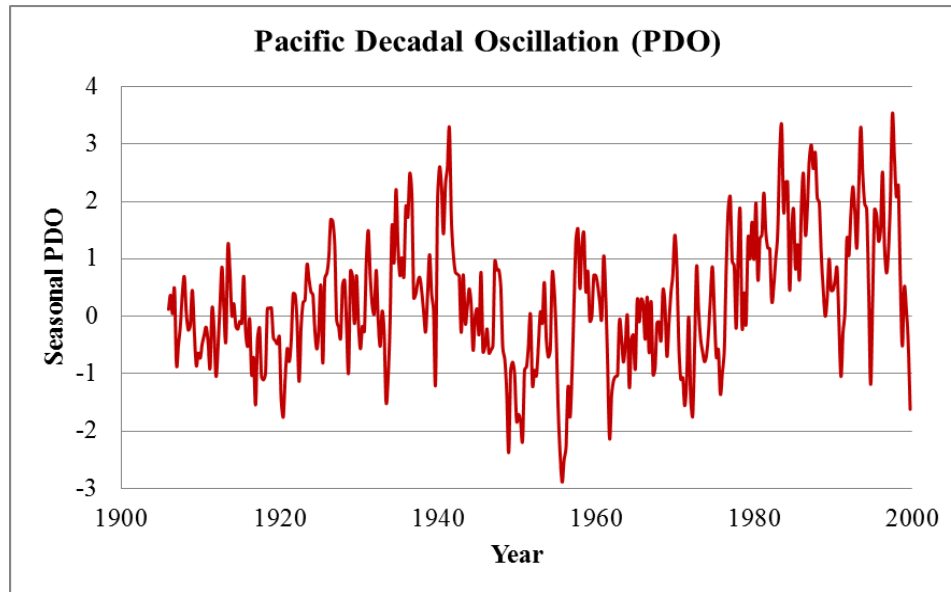
Figure 4.1. Location and seasonal flow series (from year 1906 to 1999) of the five continental rivers namely Congo (Africa), Yangtze (Asia), Rhine (Europe), Columbia (North America), and Parana (South America). (Photo Source: World's Longest Rivers Map [Photograph], 2007)



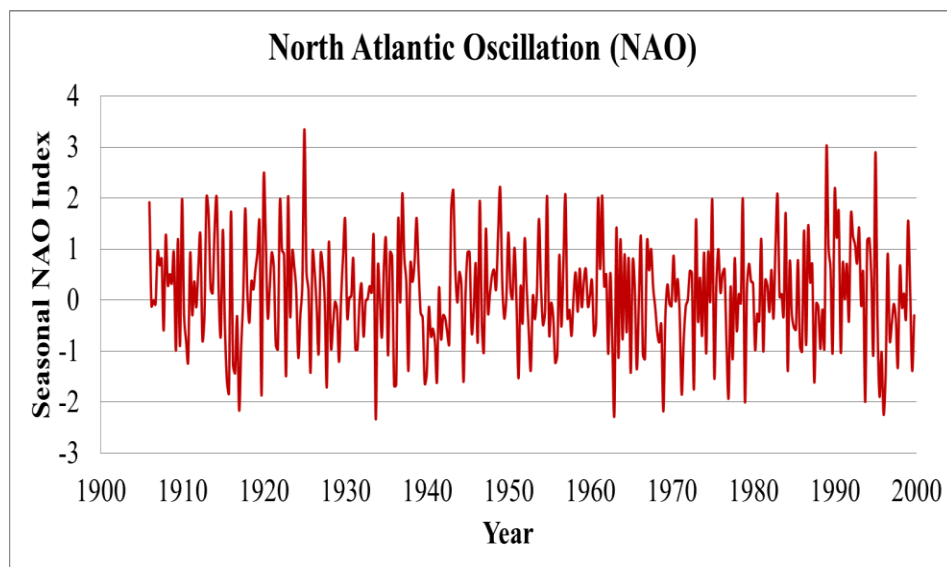
(a)



(b)



(c)



(d)

Figure 4.2. Time series plots (seasonal) of the four external environmental variables (forcing variables): (a) Southern Oscillation Index (SOI); (b) Sunspot Cycle (SSN); (c) Pacific Decadal Oscillation (PDO); and (d) North Atlantic Oscillation (NAO) from years 1906 to 1999.

Table 4.2River Station Information (Long Data Series), Data Used from Year 1906 to 1999

River	Country	Continent	Station	Elevation (m)	Upstream area (km ²)	Longitude (deg.)	Latitude (deg.)
Congo	Congo	Africa	Kinshasa	270	3475000	12.75	-5.75
Yangtze	China	Asia	Datong	19	1705383	120.75	32.25
Rhine	Netherlands	Europe	Lobith	8.53	160800	6.11	51.84
Columbia	USA	North America	Dalles	0	613827	-123.75	46.25
Parana	Argentina	South America	Timbues	4	2346000	-57.75	-34.75

The modeling procedure for both the time series and ANN methodologies are divided into two sections: (a) calibration and (b) validation. In calibration, a portion of the data series was used to estimate parameters. Thereafter, the model performances were evaluated in a validation mode. For the short data series, the seasonal (four seasons per year) flow data from 1936 to 1968 (total 33 years or 132 seasons) were used for calibration and from 1969 to 1979 (total 11 years or 44 seasons) were incorporated for validation of the model results. However, for calibrating the long data series, flow data from year 1906 to 1980 (total 75 years or 300 seasons) were used, whereas the data from 1981 to 1999 (total 19 years or 76 seasons) were used to validate or evaluate the model performance.

4.2. Cross-correlation

Cross-correlation analysis was used to examine the linear relationships between the two data series. The relationships between the data series were measured by the cross-correlation plots along with the 95% confidence limits of $\pm 2/\sqrt{N}$, where N represents the sample size. These 95% confidence limits are acting as thresholds beyond which the

values indicated significant relationships between the two data series. The cross-correlation between the river flows and different forcing variables are illustrated in Figures 4.3 to 4.12. In the plots the 95% confidence limits are represented as dashed lines. Positive correlation shows the occurrence of dry or wet condition at the same time or lagged time, whereas negatively correlated indicates occurrence of alternating dry or wet condition. The cross-correlation coefficients between the two data series were obtained for the lags or time shifts of 0, 1, 2, 3, ...seasons. The lags are both positive and negative. The positive lag refers to the relationship between the first series and the delayed second series and the alternate is true for the negative lag. However, higher order correlation values are ignored or neglected here with the assumptions that physical significance of these correlations are difficult to explain.

The cross-correlation of Parana and Danube river flow in Figure 4.3 revealed a significant negative correlations at negative lag 6 and positive correlations at lag 4 to 8. The Parana and Rhine rivers showed similar relationships, although positive correlations were not as significant as with the Danube River. The positive correlation between the Danube and Rhine rivers were expected as both are in the central European region. The correlation plots of the Parana and Missouri rivers demonstrated significant correlation at both positive and negative lag 5, whereas the Danube and Rhine rivers showed similar correlations with the Missouri River, indicating significant negative correlations at both positive and negative lag one.

A cross-correlation analysis was also performed between river flows and external variables. The negative lags indicated the relationship between delayed river flows and forcing variables, whereas the positive lags indicate river flows as variables to predict the

occurrence of the external variables. Since the goal was to forecast river flows using external variables, negative lags were discussed only.

The cross-correlation between the river flows and the external variables SOI and SSN are also included in Figure 4.4. From the figure, it is evident that the SOI is correlated with the Parana River at lag 1 and 3. The Danube and Rhine River correlations are found to be significant at lag 1 to 3. However, correlation between the Missouri and SOI indicates approximately significant at lag three, although did not exceed the 95% confidence intervals. This reveals the SOI as a potential predictor of the seasonal river flows.

In terms of the SSN, the Parana River shows significant correlations at lag 0 to 5. The Danube river cross-correlation plot indicates significant correlations at lag 4 to 10, whereas the Rhine, river was correlated at lag 4. Besides this, the Missouri River demonstrates no significant correlations with the SSN. Therefore, the SSN can serve as a potential predictor for the Parana, Danube, and Rhine rivers.

The autocorrelation (ACF) plots of the standardized seasonal five river series namely the Congo, Yangtze, Rhine, Columbia, and Parana along with the four external variables (SOI, SSN, PDO, and NAO) are included in Figures 4.5 and 4.6. These plots reveal the persistence characteristics of the data series. These characteristics are useful to predict the corresponding seasonal river flows based on the previous flow information. The detail description of the ACF and the identification of the lagged relationships were discussed in Chapter 3. The ACF plots in Figure 4.5 indicate the Congo, Yangtze, Rhine, Columbia, and Parana flows are significantly correlated up to lags 7, 4, 3, 2, and 5,

respectively. The ACFs of the four external variables are also included in Figure 4.6, which indicate the presence of significant correlations at all four variables.

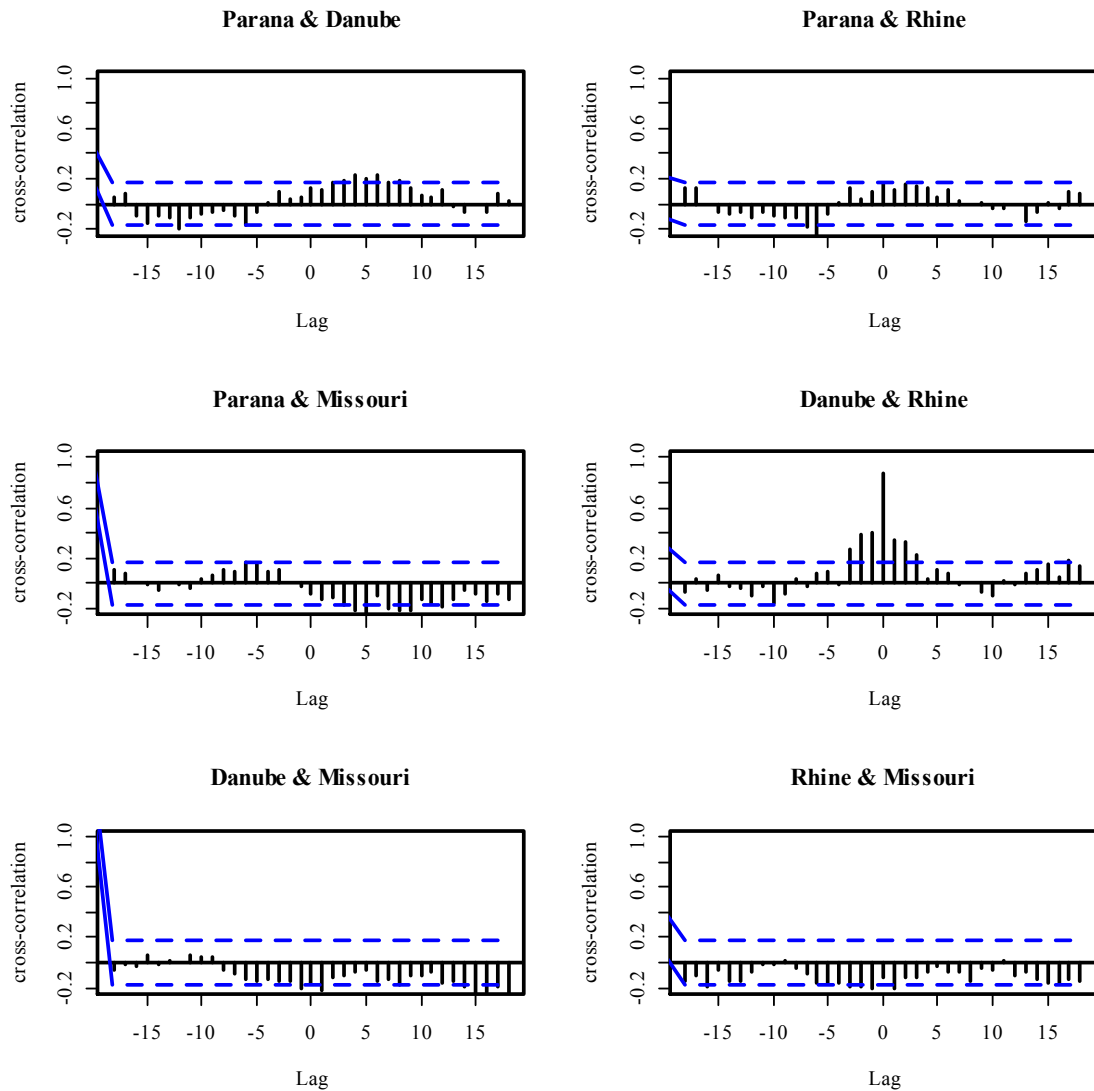


Figure 4.3. Cross-correlation of the seasonal flow series of Parana–Danube, Parana–Rhine, Parana–Missouri, Danube–Rhine, Danube–Missouri, and Rhine–Missouri (lags indicate three months shifts).

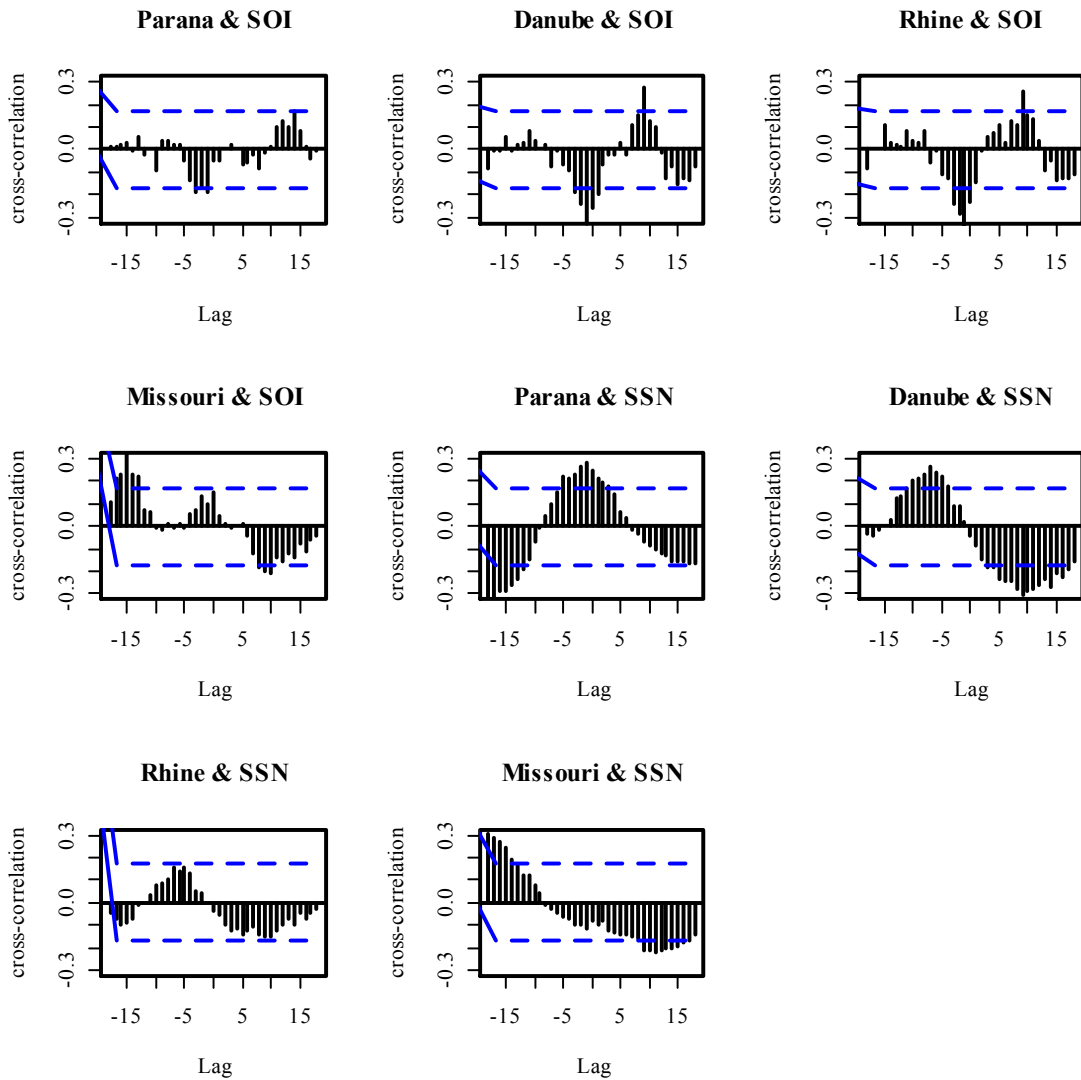


Figure 4.4. Cross-correlations between the seasonal river flow series and two forcing variables (SOI and SSN) of Parana-SOI, Danube-SOI, Rhine-SOI, Missouri-SOI, Parana-SSN, Danube-SSN, Rhine-SSN, and Missouri-SSN (lags indicate three months shifts).

The cross-correlation between the Congo and Yangtze flow shows existence of no significant correlations before lag 17 (Figure 4.7). However, higher order correlations are ignored or neglected here with the assumptions that the physical significance of those correlations are difficult to explain. For the rivers Congo and Rhine, the cross-

correlations are found to be significant at lag 3, whereas the cross correlation for the rivers Congo and Columbia shows existence of a direct correlation (lag zero). However, the correlation for rivers Congo and Parana shows significance at lag 4. This correlation also revealed lagged relationships (floods and droughts do not occur at the same time) between rivers of different longitudinal zones, in this case different continents. This lagged relationship is also evident in the Yangtze and Rhine rivers, which shows significant correlation at lag 5. The Rhine and Columbia were found to be negatively correlated at lag zero. The negative correlation demonstrates that the rivers experienced alternating flood and drought conditions at the same time. The Yangtze and Parana rivers, located in the northern and southern hemispheres, are also found to be negatively correlated at lag 4 and 5. This indicates floods and droughts do not occur at the same season in these rivers. The Columbia and Parana River cross-correlation plot shows significant correlation at lag 3. Overall, most of the correlation plots revealed existence of lagged relationships between the continental rivers.

From the cross-correlation plots in Figure 4.8, it is evident that the SOI is correlated with the Congo, Yangtze, Rhine, Columbia, and Parana Rivers at lag 7 to 14 (highest correlation at lag 8), lag 3, lag 0 to 1 including 7, lag 0, and lag 0 to 1 (highest at lag 0), respectively. This reveals that the SOI could be used as a potential predictor of the five river flows.

In terms of the SSN (Figure 4.9), the Congo and Columbia flows show no significant relationships, whereas the Yangtze, Rhine, and Parana rivers were correlated significantly at lags 1 to 4, 4 to 7, and 5 to 20, respectively. This indicates the SSN as a potential predictor for the seasonal Yangtze, Rhine, and Parana flows.

The cross-correlations between the river flows and PDO in Figure 4.10 reveal existence of lagged relationships. This figure indicates the Yangtze, Rhine, Columbia, and Parana flows are significantly correlated (coefficients exceed the 95% confidence limits shown in the correlation plots) at lag 0 to 5, lag 0 to 1, lag 0 to 3, and lag 0 to 3, respectively. Conversely, the Congo River plot demonstrates the coefficients are varying within the 95% confidence limits, consequently indicating uncorrelated with the PDO. The Yangtze and the Columbia correlations were negative, whereas the Rhine and Parana correlations were positive. Therefore, any changes in the PDO will influence changing the seasonal flow conditions of the rivers. This demonstrates the PDO as a potential predictor for the corresponding river flows.

The cross correlations between the five river flows and NAO in Figure 4.11 demonstrate insignificant correlations for most of the rivers except Rhine, which is negatively correlated at lag five. This indicates less NAO influence on the Congo, Yangtze, Columbia, and Parana seasonal flows.

Cross-correlation plots of the forcing variables the SOI, SSN, PDO, and NAO are shown in Figure 4.12. This figure indicates the SOI-SSN, SOI-NAO, SSN-NAO, and PDO-NAO cross-correlations tend to remain within the 95% confidence limits, consequently indicating a tendency of independence. However, the SOI and PDO cross-correlation plots demonstrate the variables are correlated negatively up to lag 0 to 3, then again correlated positively at lag 8. The SSN and PDO plot reveals no short term dependency between the data series, although significant correlations are evident after lag 9. As higher lag correlations are neglected in this study, the external variables were considered uncorrelated to each other.

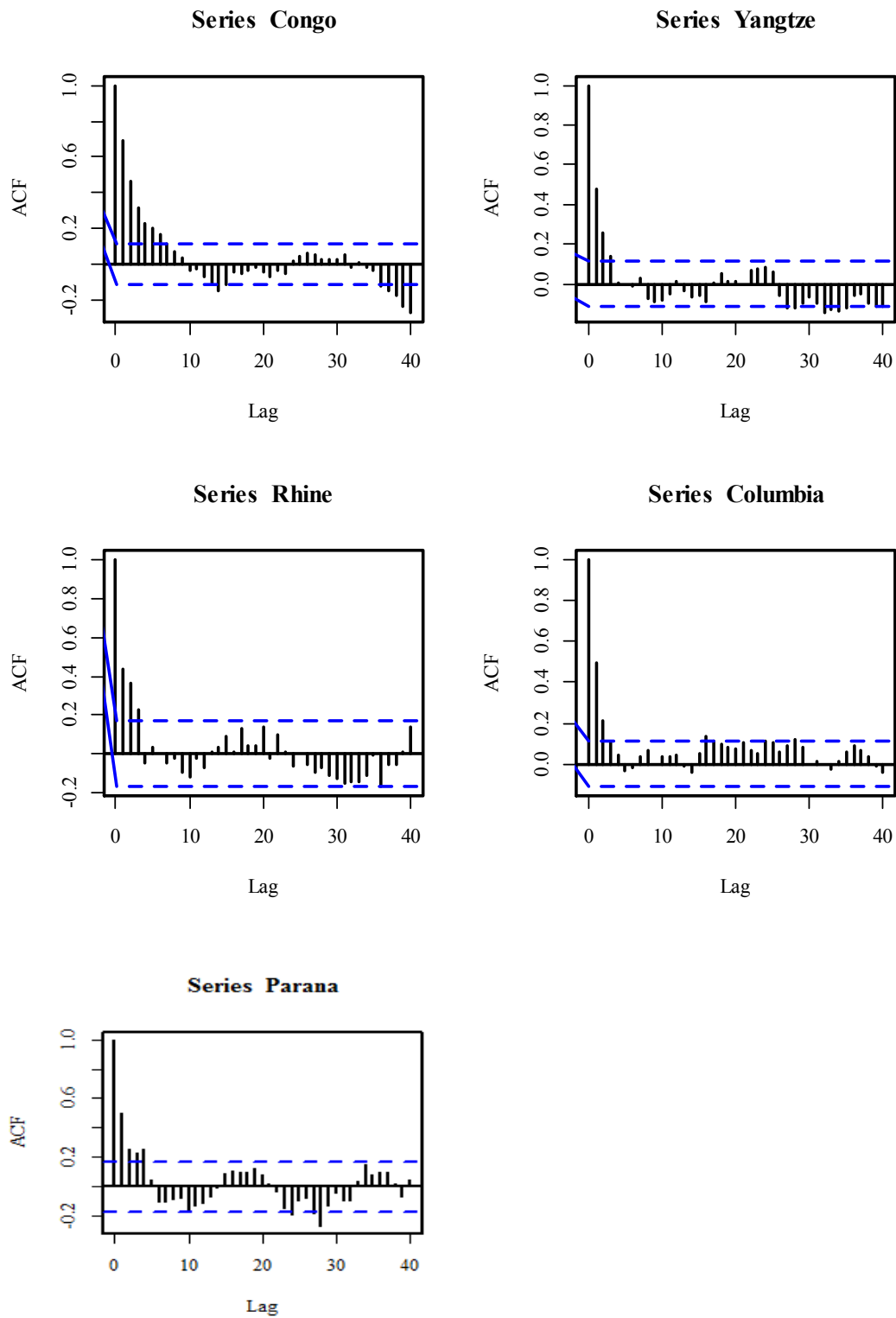


Figure 4.5. Autocorrelation (ACF) plots of the seasonal river flow series of Congo, Yangtze, Rhine, Columbia, and Parana (lags indicate three months shifts).

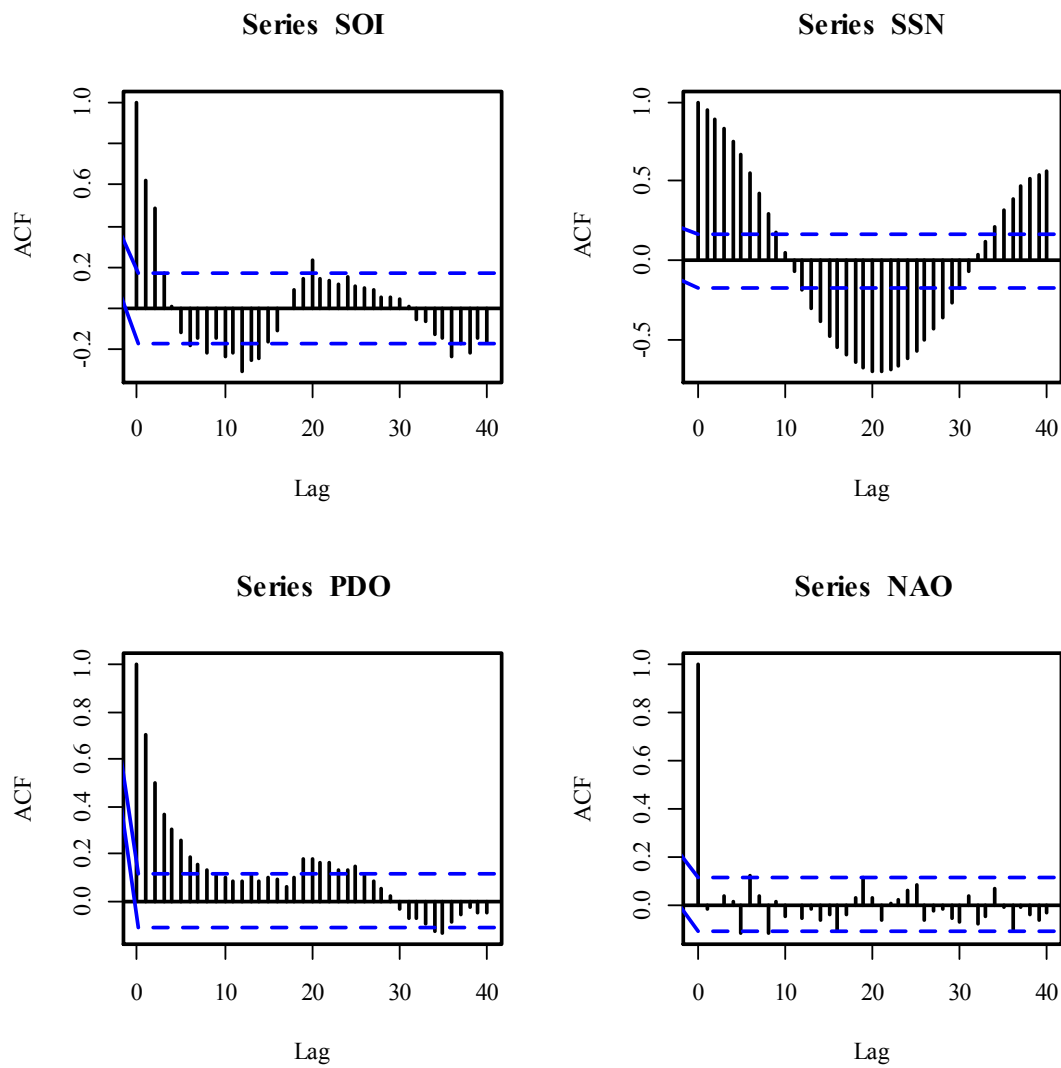


Figure 4.6. Autocorrelation (ACF) plots of the seasonal forcing variables of SOI, SSN, PDO, and NAO (lags indicate three months shifts).

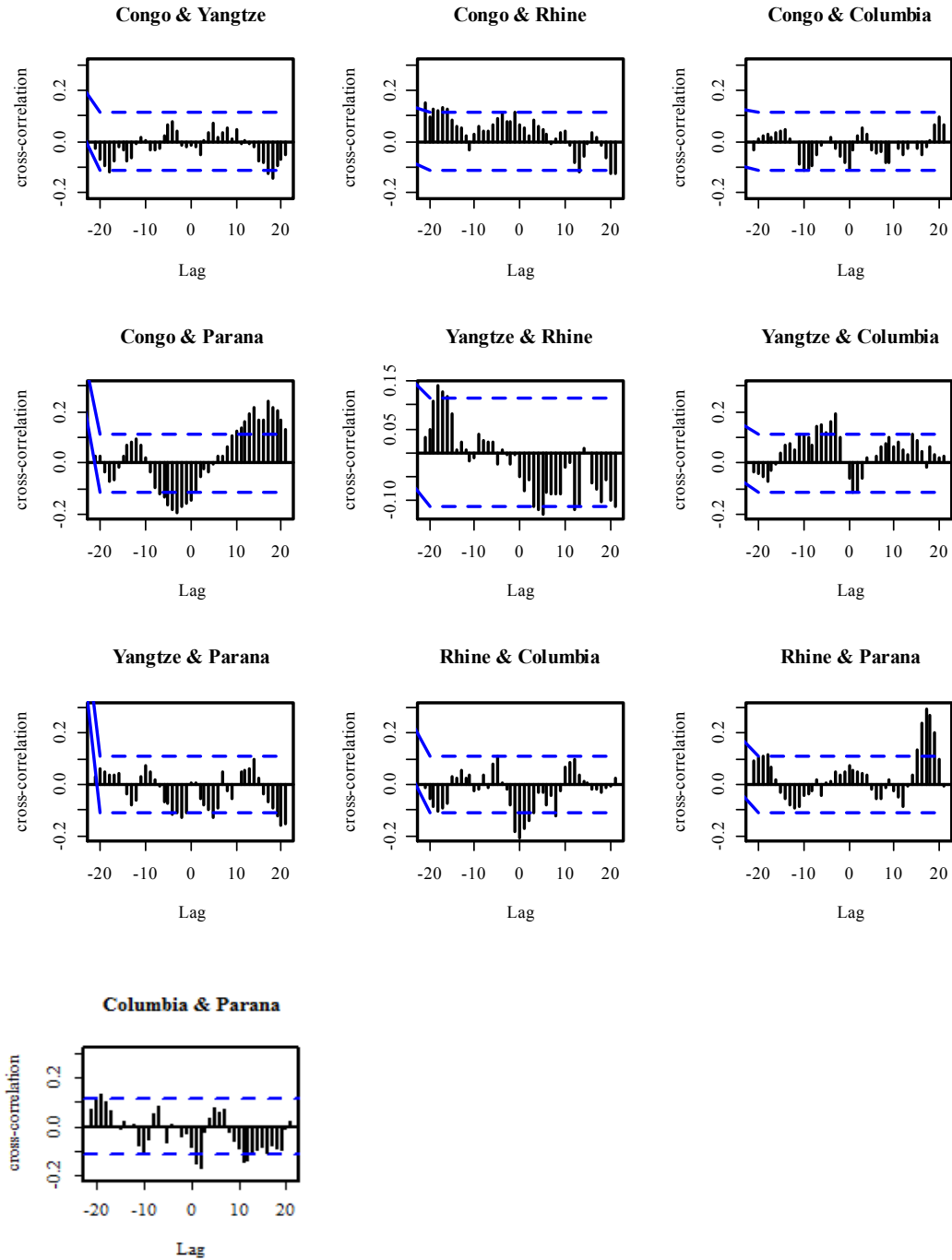


Figure 4.7. Cross-correlation plots of the seasonal river flow series of Congo-Yangtze, Congo-Rhine, Congo-Columbia, Congo-Parana, Yangtze-Rhine, Yangtze-Columbia, Yangtze-Parana, Rhine-Columbia, Rhine-Parana, and Columbia-Parana (lags indicate three months shifts).

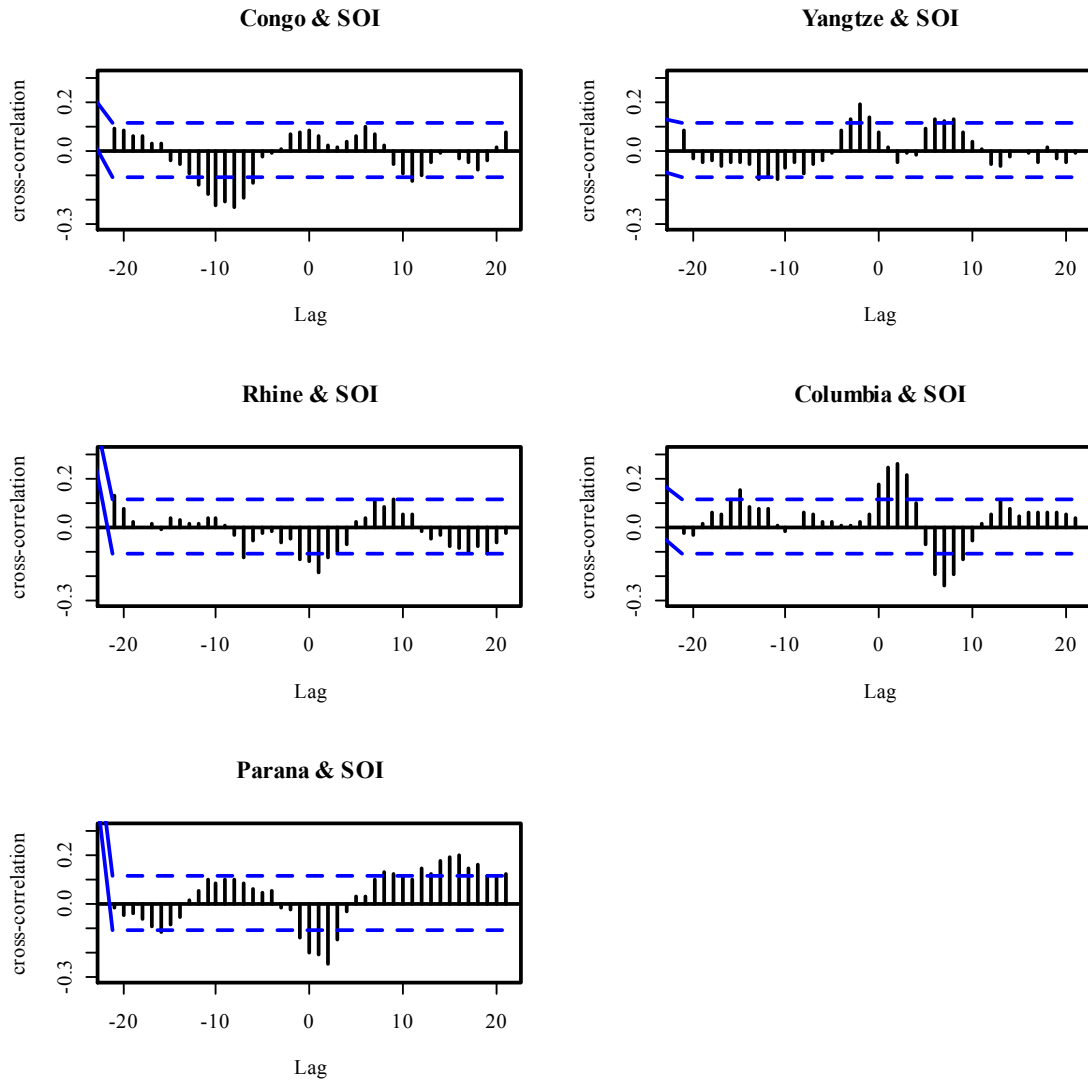


Figure 4.8. Cross-correlations between five continental river flow series (seasonal) and SOI (forcing variable) of Congo-SOI, Yangtze-SOI, Rhine-SOI, Columbia-SOI, and Parana-SOI (lags indicate three months shifts).

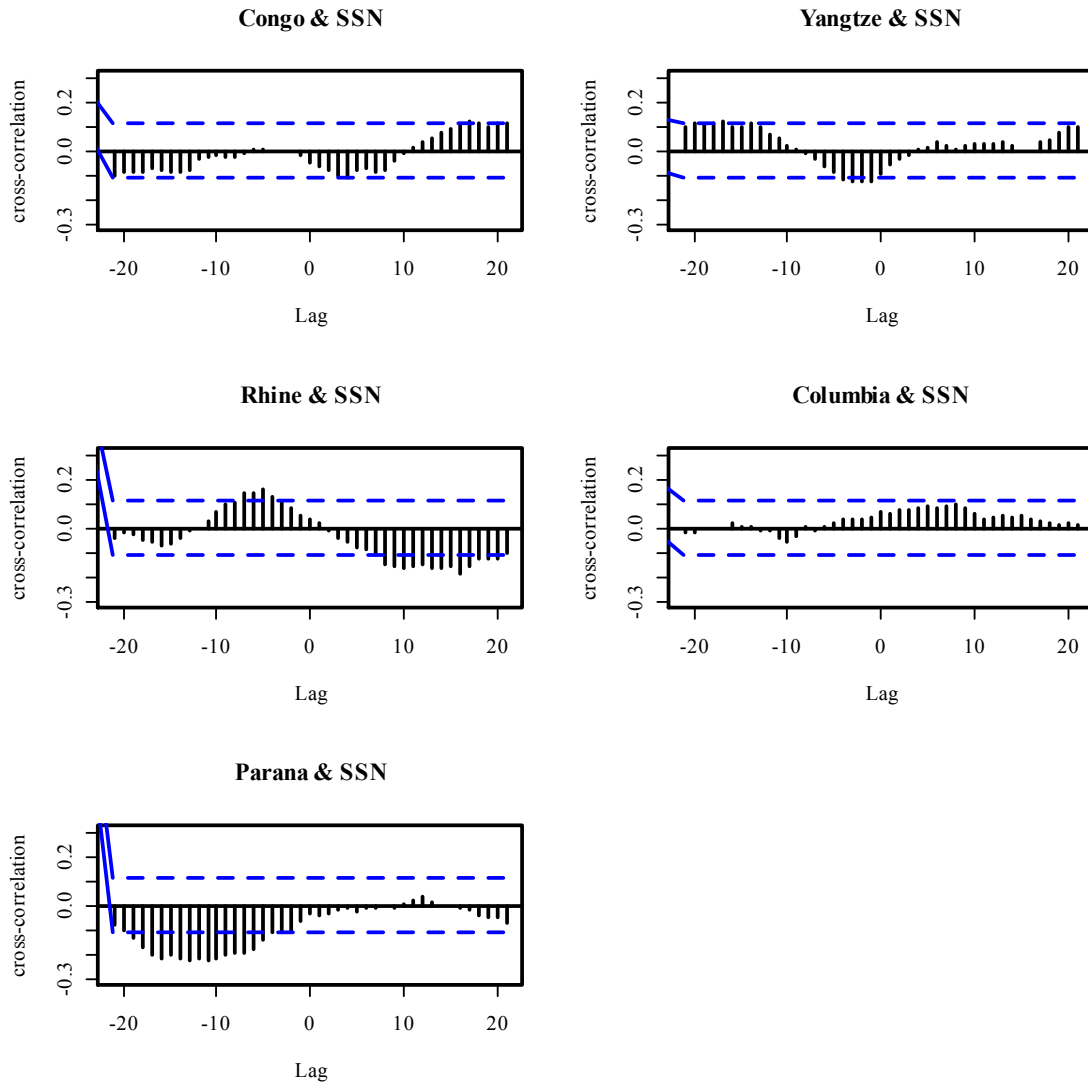


Figure 4.9. Cross-correlations between the five continental river flow series (seasonal) and the SSN (forcing variable) of Congo-SSN, Yangtze-SSN, Rhine-SSN, Columbia-SSN, and Parana-SSN (lags indicate three months shifts).

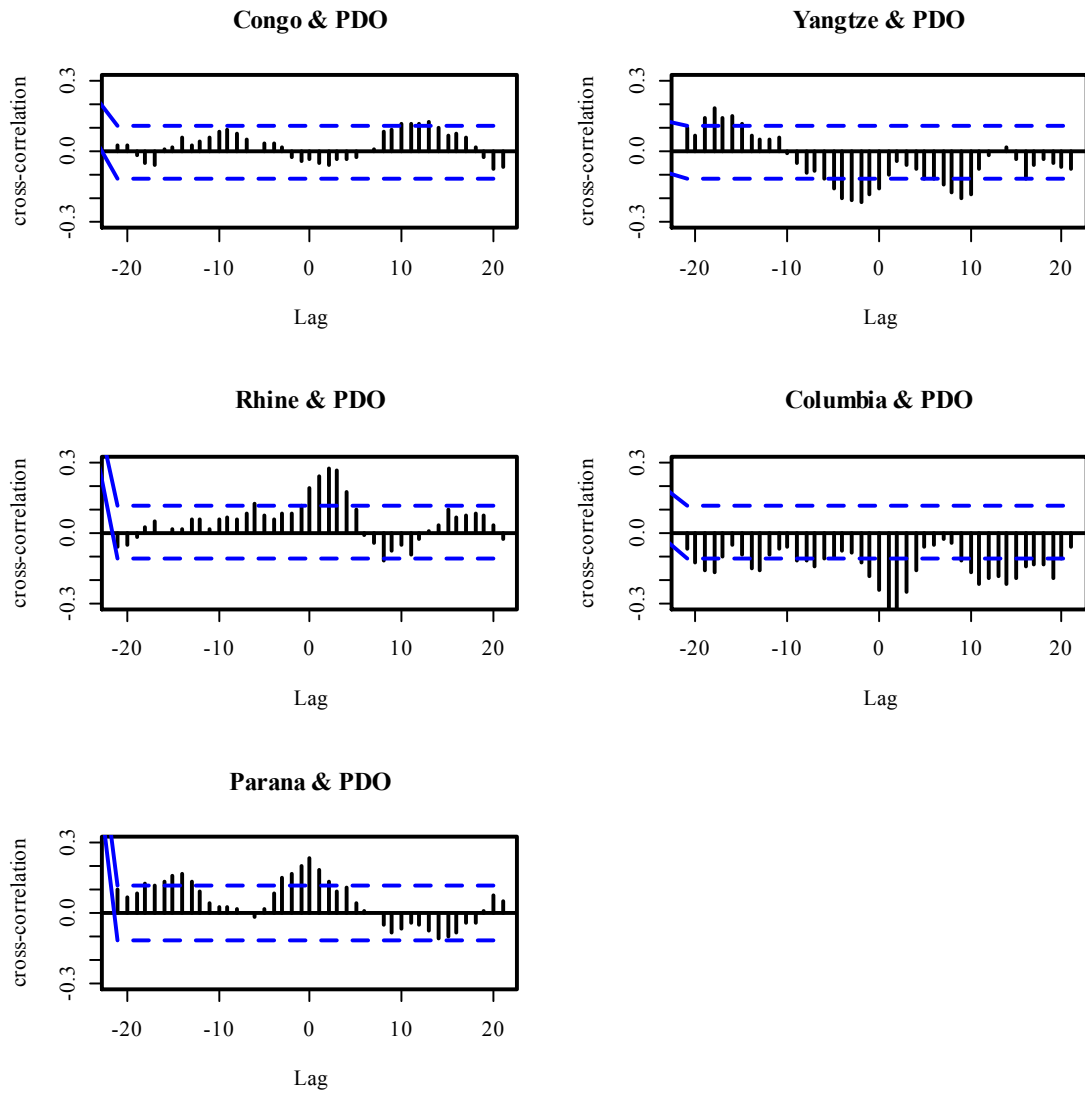


Figure 4.10. Cross-correlations between the five continental river flow series (seasonal) and the PDO (forcing variable) of Congo-PDO, Yangtze-PDO, Rhine-PDO, Columbia-PDO, and Parana-PDO (lags indicate three months shifts).

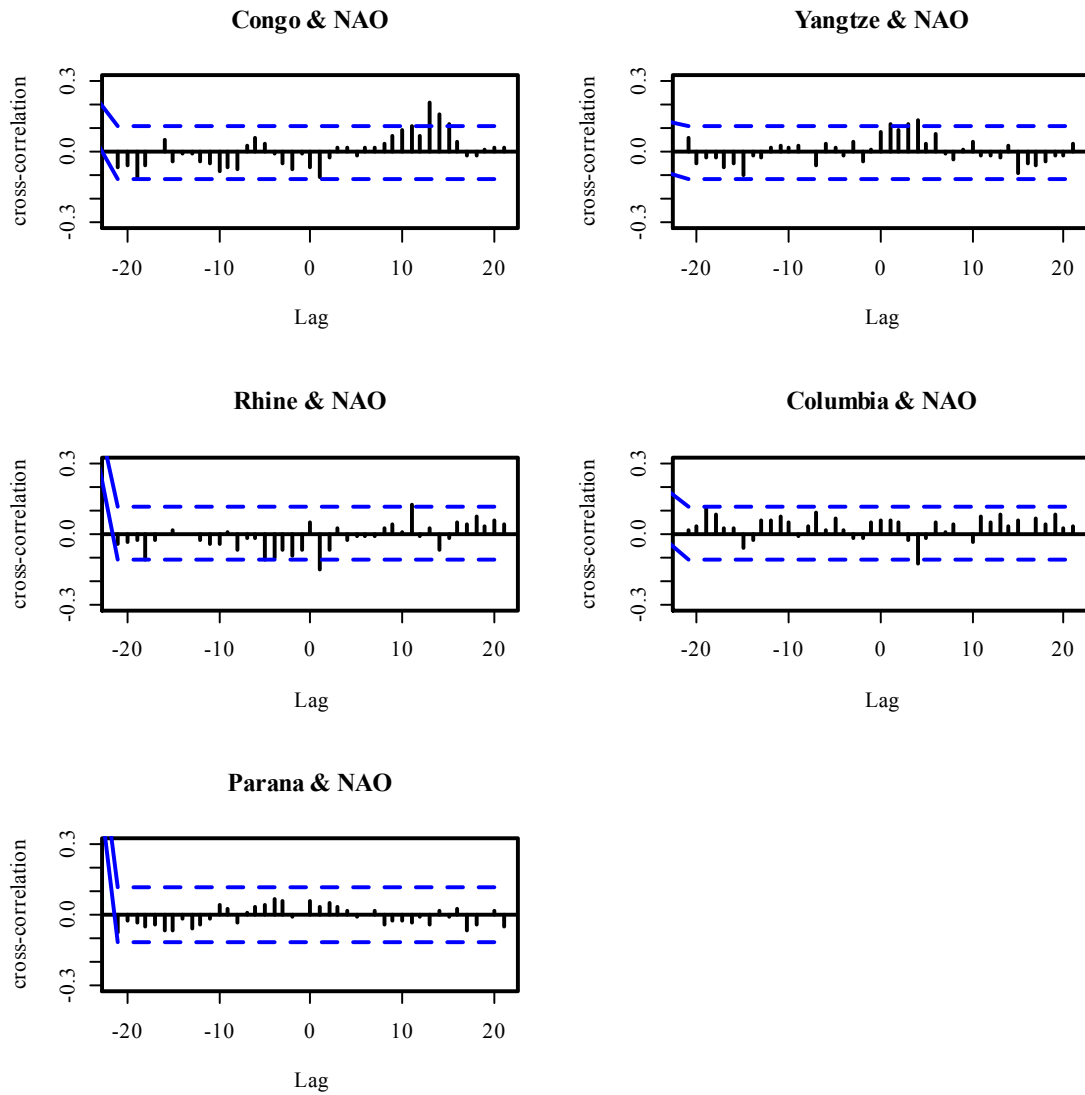


Figure 4.11. Cross-correlations between the five continental river flow series (seasonal) and the NAO (forcing variable) of Congo-NAO, Yangtze-NAO, Rhine-NAO, Columbia-NAO, and Parana-NAO (lags indicate three months shifts).

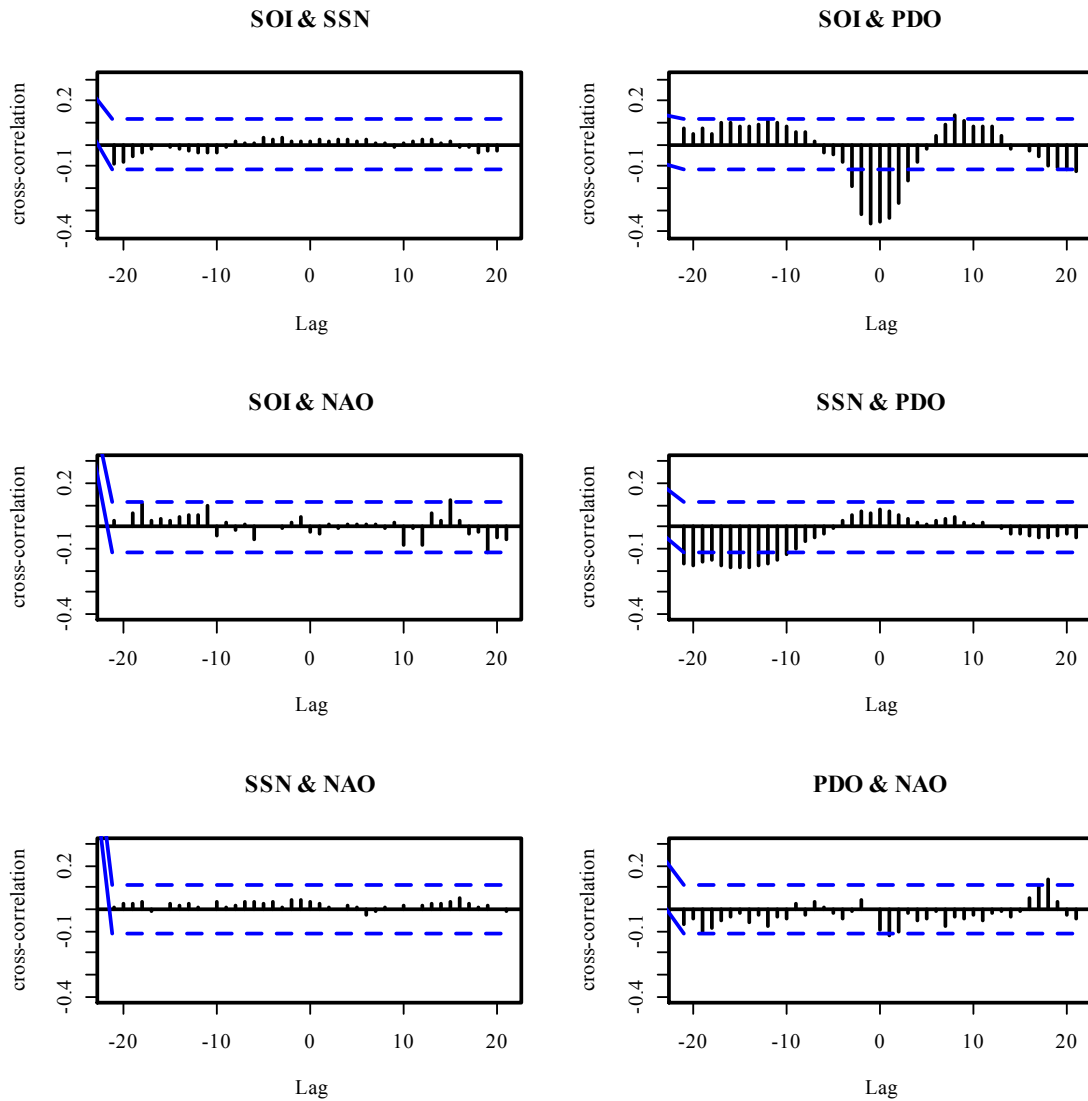


Figure 4.12. Cross-correlations between the four forcing variable series (seasonal) of SOI-SSN, SOI-PDO, SOI-NAO, SSN-PDO, SSN-NAO, and PDO-NAO (lags indicate three months shifts).

4.3 Time Series Model Analysis

For calibration, the seasonal flow data series of the four rivers Parana, Danube, Rhine, and Missouri from 1936 to 1968 (132 seasons) were used, whereas for validation, the series from 1969 to 1979 (44 seasons) were used. The modeling procedures are described in the following sections.

4.3.1 Univariate Model Analysis

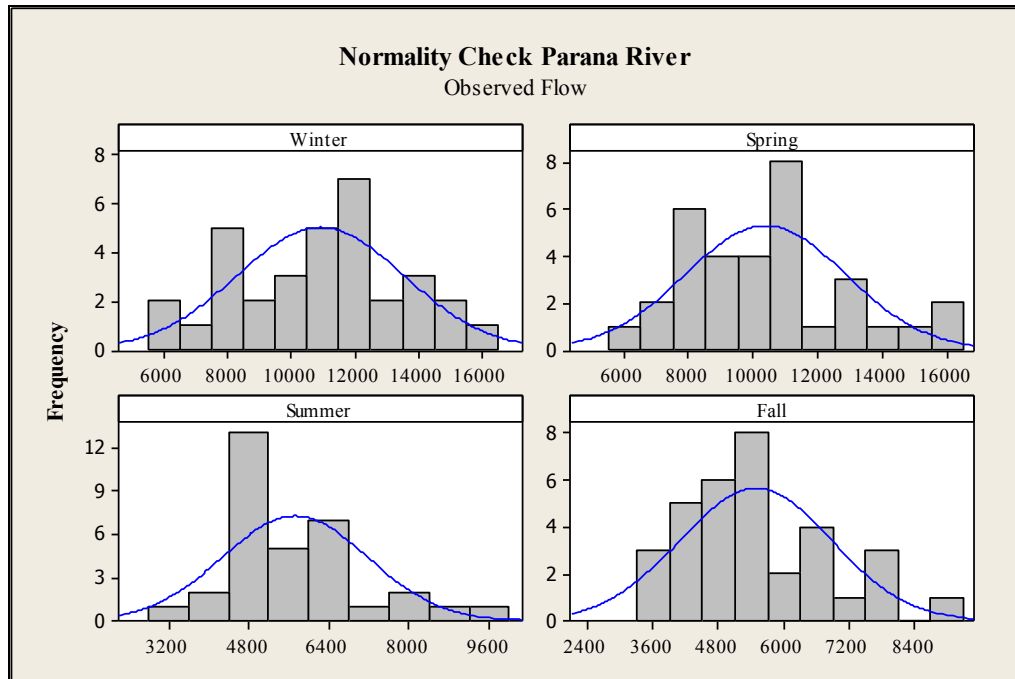
Statistical Characteristics of the Observed and Transformed Streamflow Series

The statistical characteristics of the seasonal flows, such as sample mean, sample standard deviation, and skewness coefficients are shown in Table 4.3. The skewness coefficients are useful to examine whether the river flow series are distributed normally (zero skewness). The coefficients for most of the seasonal flow series were not close to zero, indicating the distributions were not normal. Moreover, the graphical tests (plots of histograms and frequency distributions in normal probability papers) also supported the skewness results. The graphical test results of the Parana River are shown in Figures 4.13, 4.14, and 4.15.

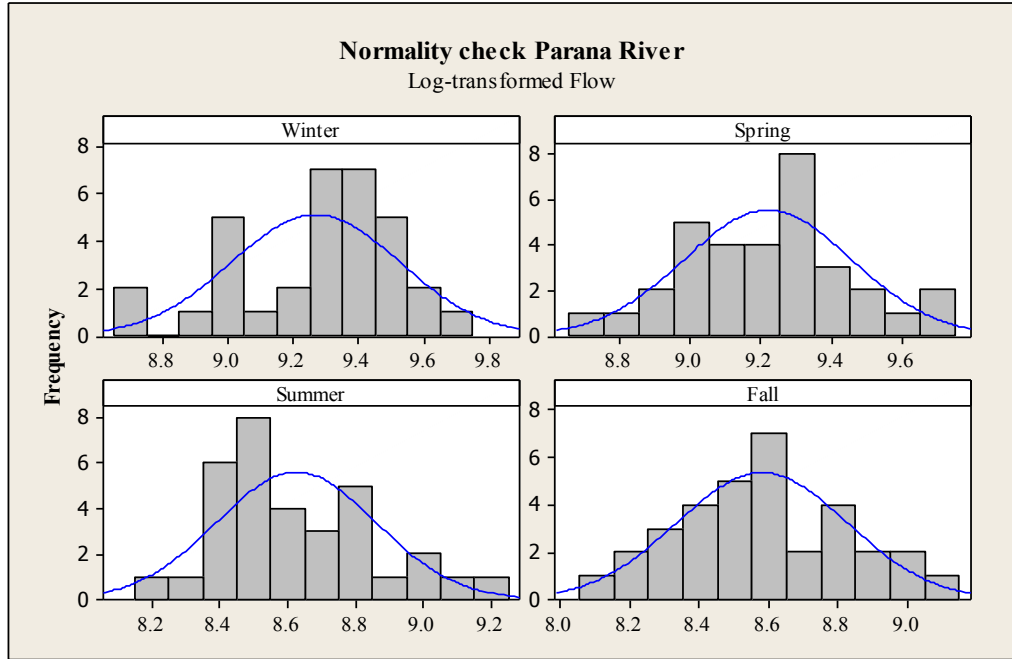
Table 4.3

Statistical Characteristics of the Observed and Transformed River Flow Series

River	Season	Mean (cms)	Standard deviation (cms)	Skewness	Average seasonal skewness	Skewness (after log-transformation)	Average seasonal skewness
Parana	Winter	10930	2627	-0.08	0.61	0.43	0.06
	Spring	10362	2486	0.56		0.59	
	Summer	5728	1449	1.15		0.59	
	Fall	5476	1396	0.82		-1.39	
Danube	Winter	622	209	0.35	0.48	-0.36	-0.14
	Spring	757	174	0.28		-0.01	
	Summer	704	197	0.35		-0.32	
	Fall	524	192	0.95		0.15	
Rhine	Winter	2708	995	0.22	0.23	-0.44	-0.38
	Spring	2446	636	0.16		-0.21	
	Summer	2131	524	0.14		-0.54	
	Fall	1817	668	0.39		-0.32	
Missouri	Winter	297	94	0.77	0.76	0.43	-0.06
	Spring	857	425	1.67		0.59	
	Summer	1009	304	1.07		0.59	
	Fall	694	199	-0.46		-1.39	



(a)



(b)

Figure 4.13. Histograms of the Parana seasonal flows: (a) before transformation and (b) after log-transformation.

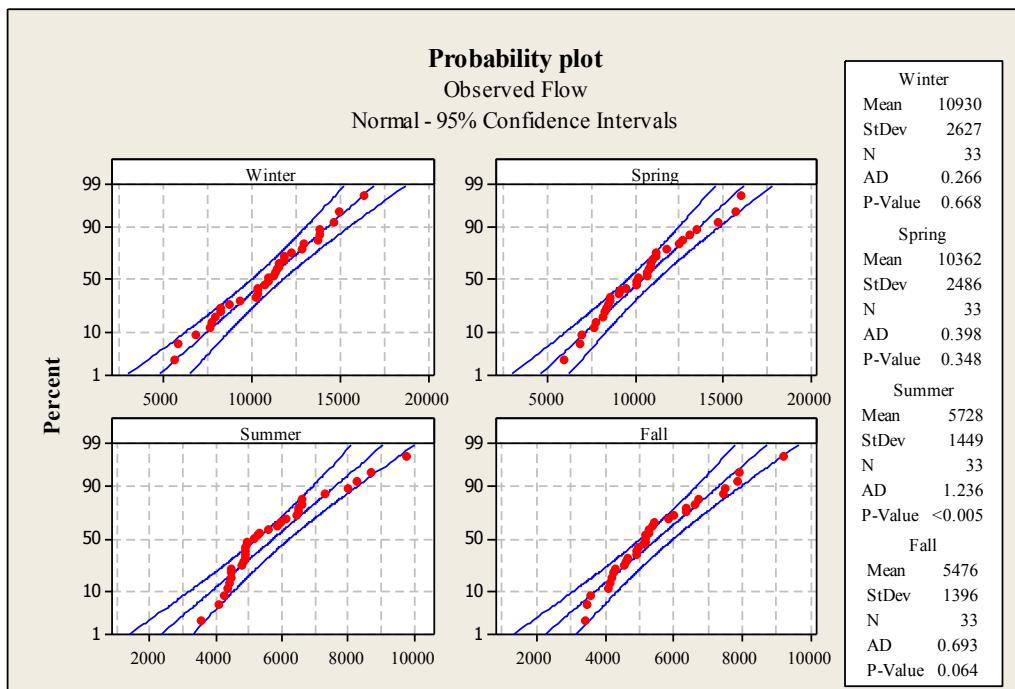


Figure 4.14. Probability plots of the Parana seasonal flows (before log-transformation)

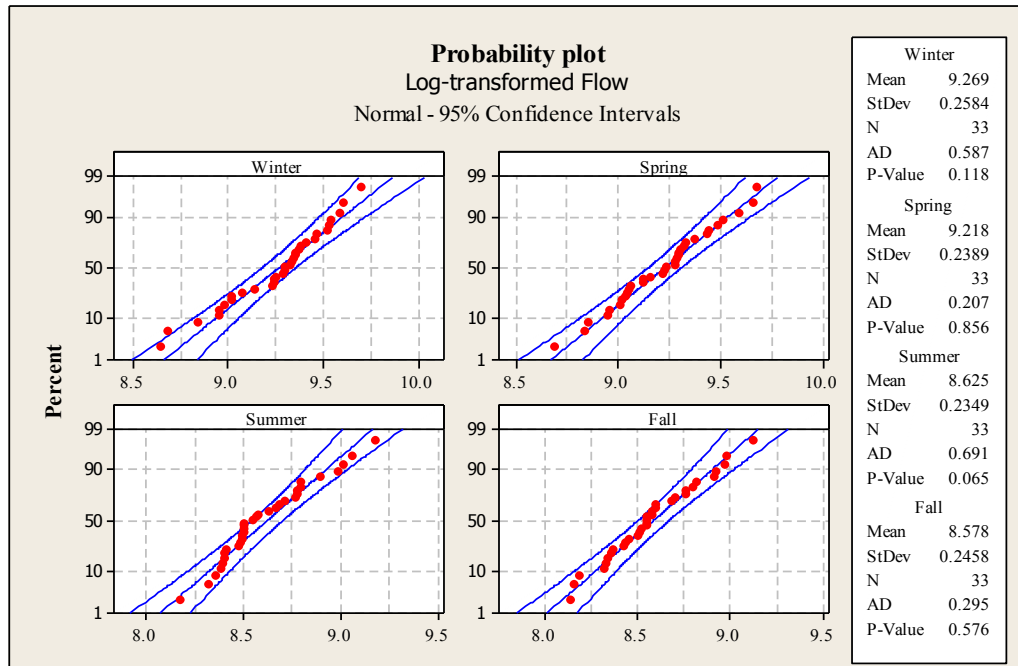


Figure 4.15. Probability plots of the Parana seasonal flows (after log-transformation)

In order to make the flow data normal, it was necessary to log-transform the data. The skewness test results of the transformed series were also included in Table 4.3, so that a comparison can be made with the observed flow (before transformation) series. These results indicated significant improvements over the observed flows (skewness closer to zero and p values well above the 5% significance level), although some of the transformed flow series showed presence of skewness in the distributions (either positive or negative). For this analysis, the log-transformed flow series were decided to use with assumptions that the distributions were approximately normal.

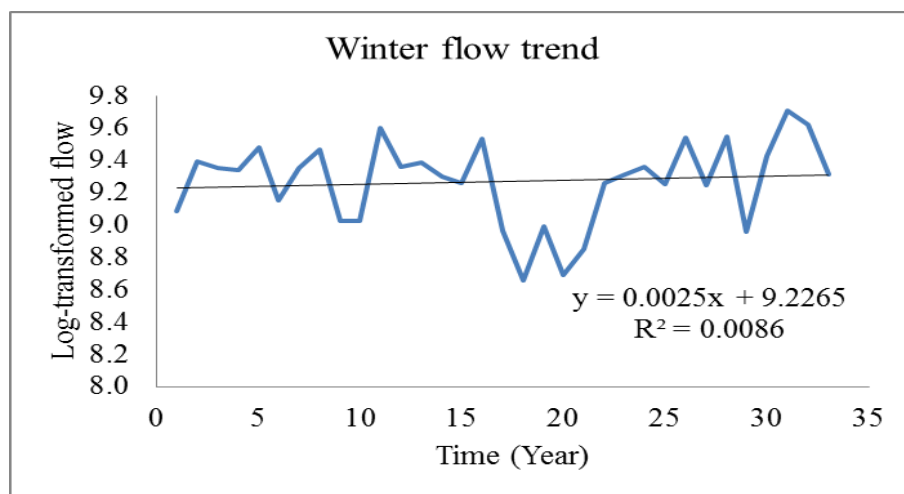
After log-transformation, the linear trend test was performed to analyze the presence of trend (non-stationary) components in the flow series (stationarity requirement, see Chapter 3). The Figures 4.16(a) to 4.16(d) showed the presence of trend components with very low correlation coefficients (R^2). This also indicated that the data

were stationary and subtractions of trend components were not necessary. Although, the identified trends were insignificant, it was decided to remove these through a de-trending procedure with the expectation of better parameter calculations and forecast performance. The identified trend components were removed through a de-trending procedure in order to make the data stationary (see Chapter 3). The corresponding linear trend equations are shown in Table 4.4. The plots, before and after the de-trended flow series for the Parana River, are shown in Figures 4.16 and 4.17, respectively. On the x-axis, the values represent the sequence of the years from 1936 to 1968.

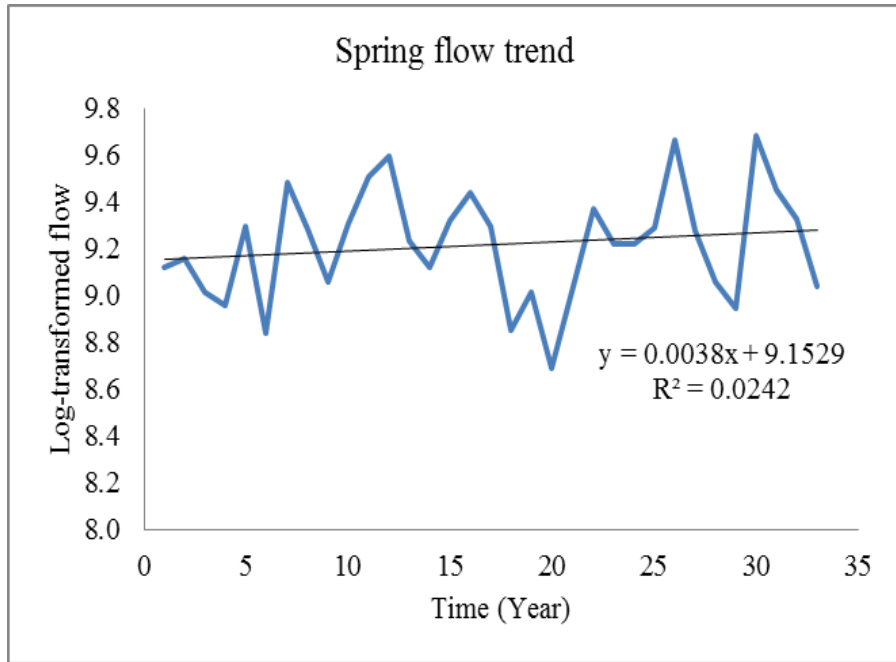
Table 4.4

Linear Trend Equations, Where ‘x’ Represents the Sequence of the Time Series (1, 2, 3...etc.)

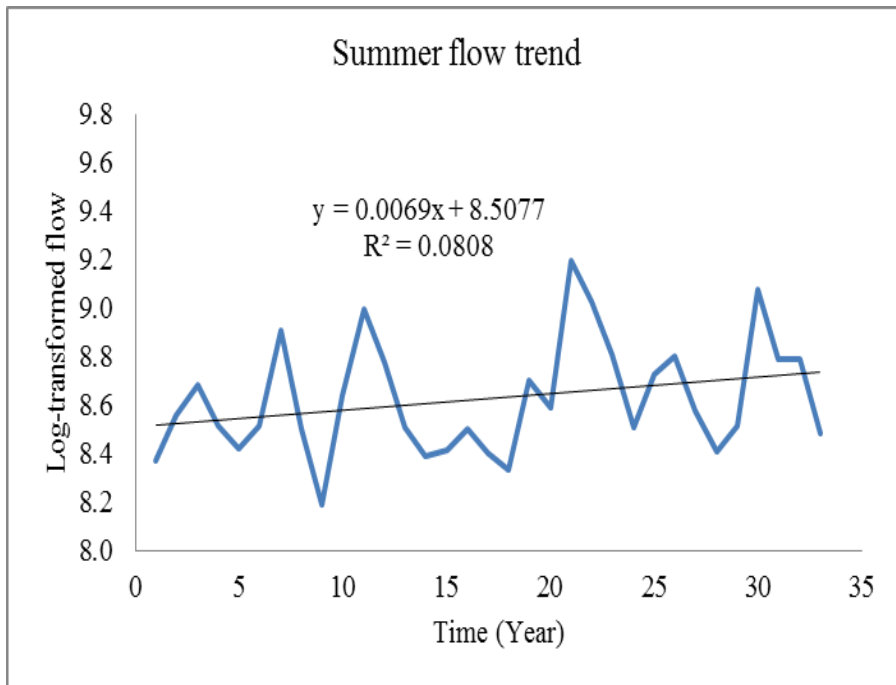
River	Winter	Spring	Summer	Fall
Parana	$0.0025x + 9.23$	$0.0038x + 9.15$	$0.0069x + 8.51$	$0.0088x + 8.43$
Danube	$-0.0046x + 6.45$	$-0.0026x + 6.65$	$-0.0018x + 6.55$	$-0.0103x + 6.37$
Rhine	$-0.0028x + 7.83$	$0.0036x + 7.74$	$0.0032x + 7.61$	$-0.0017x + 7.45$
Missouri	$0.0028x + 7.79$	$0.0036x + 7.71$	$0.0032x + 7.58$	$0.0010x + 7.42$



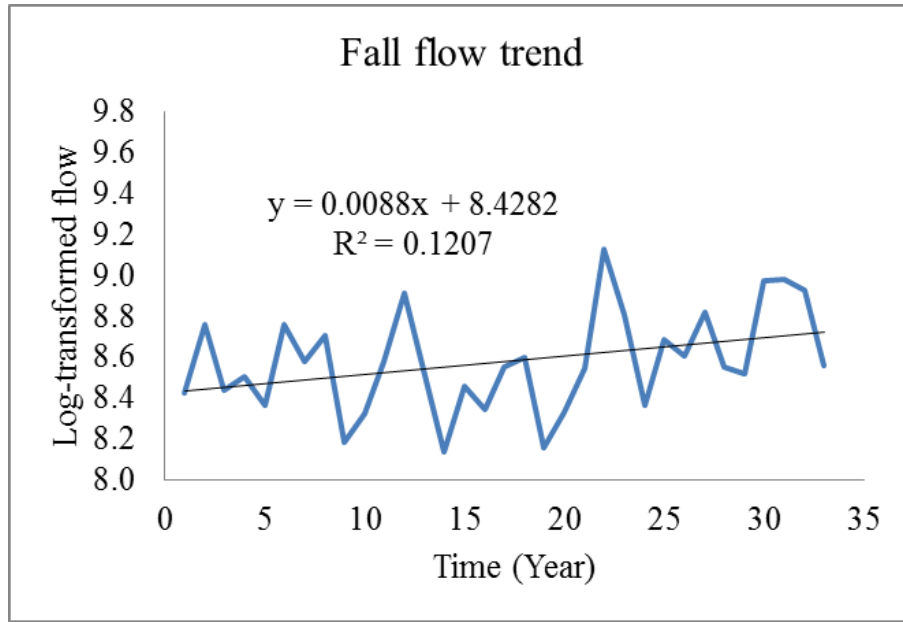
(a)



(b)

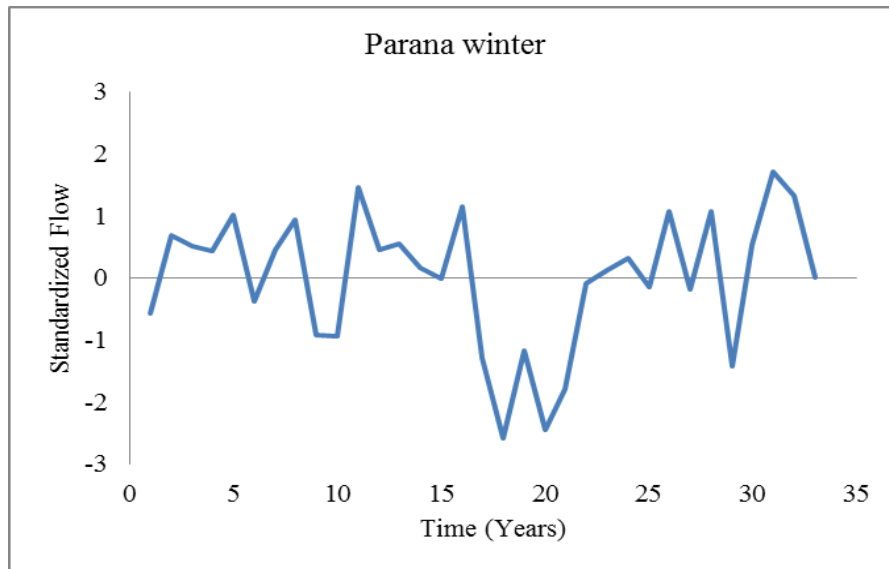


(c)

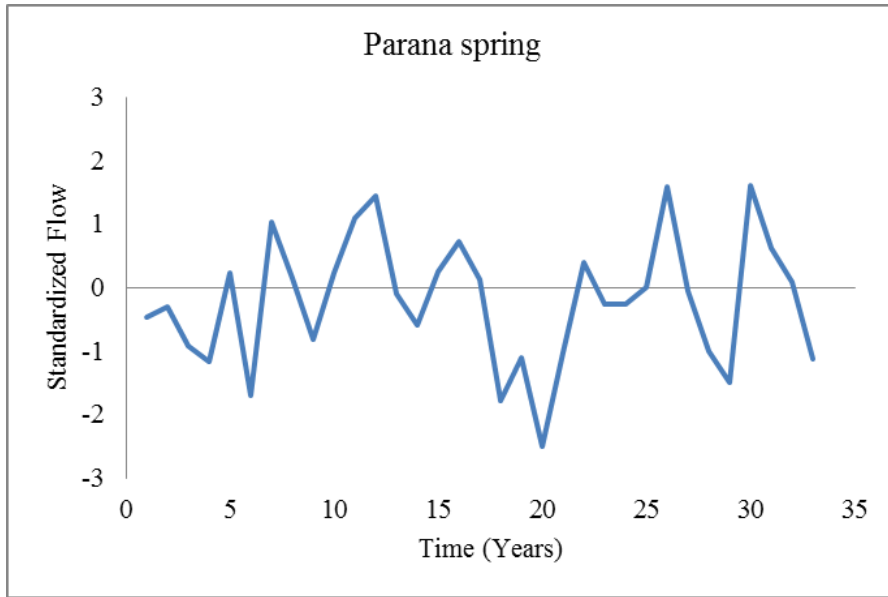


(d)

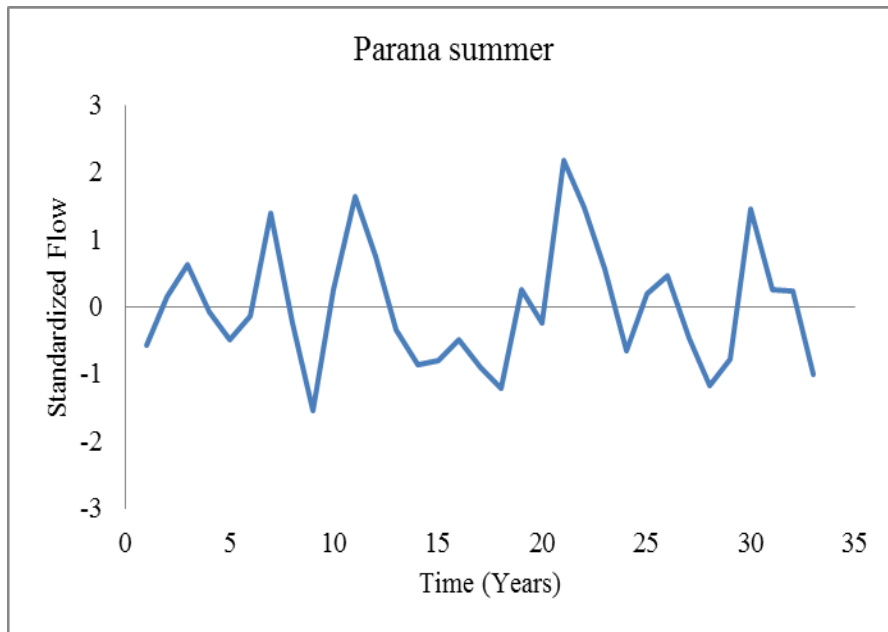
Figure 4.16. Linear trends of the Parana River flow for seasons: (a) Winter; (b) Spring; (c) Summer; and (d) Fall.



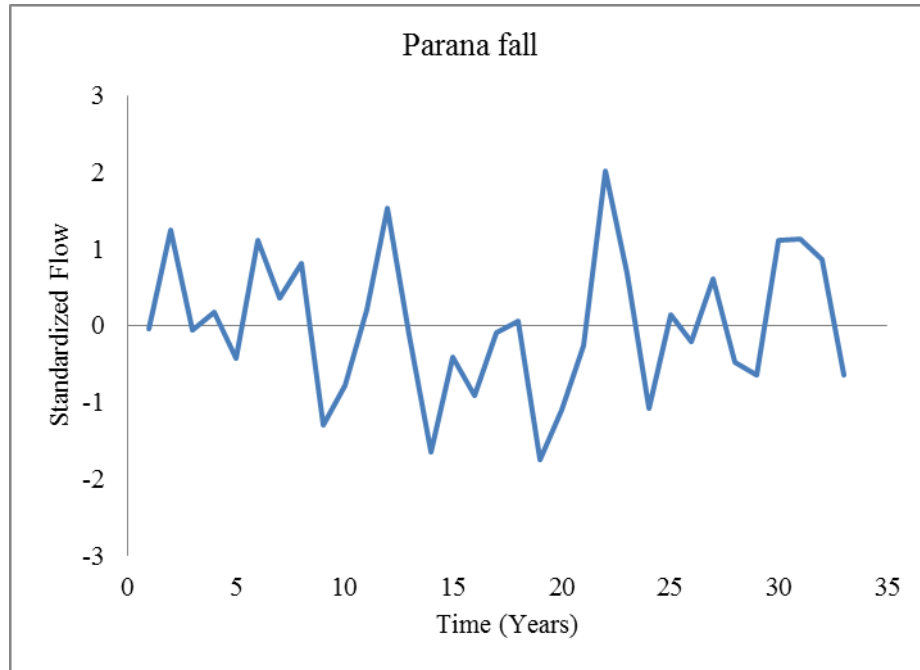
(a)



(b)



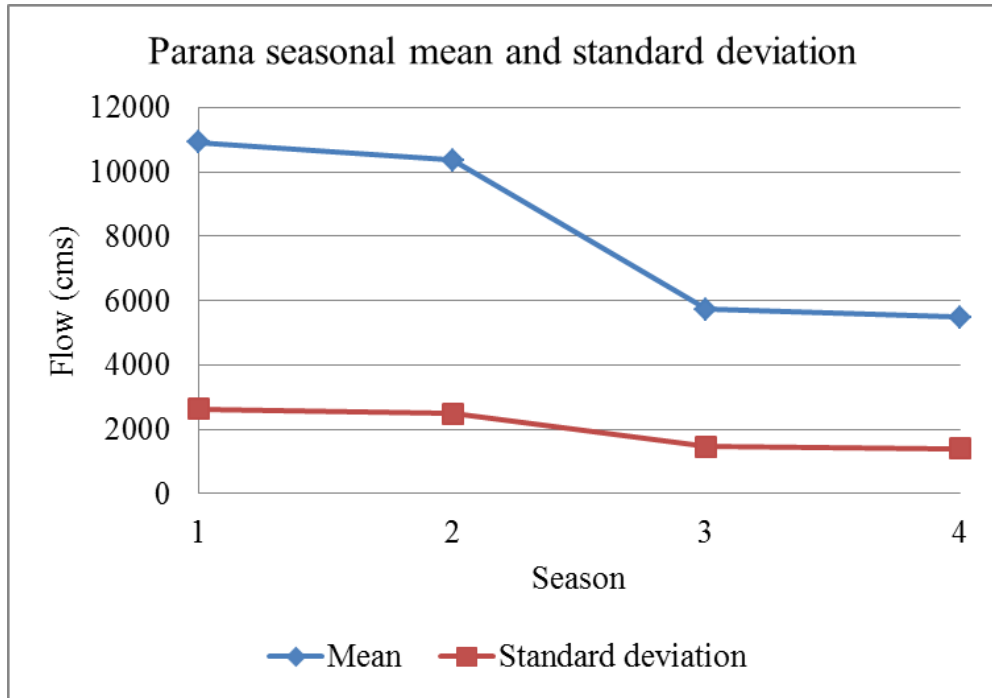
(c)



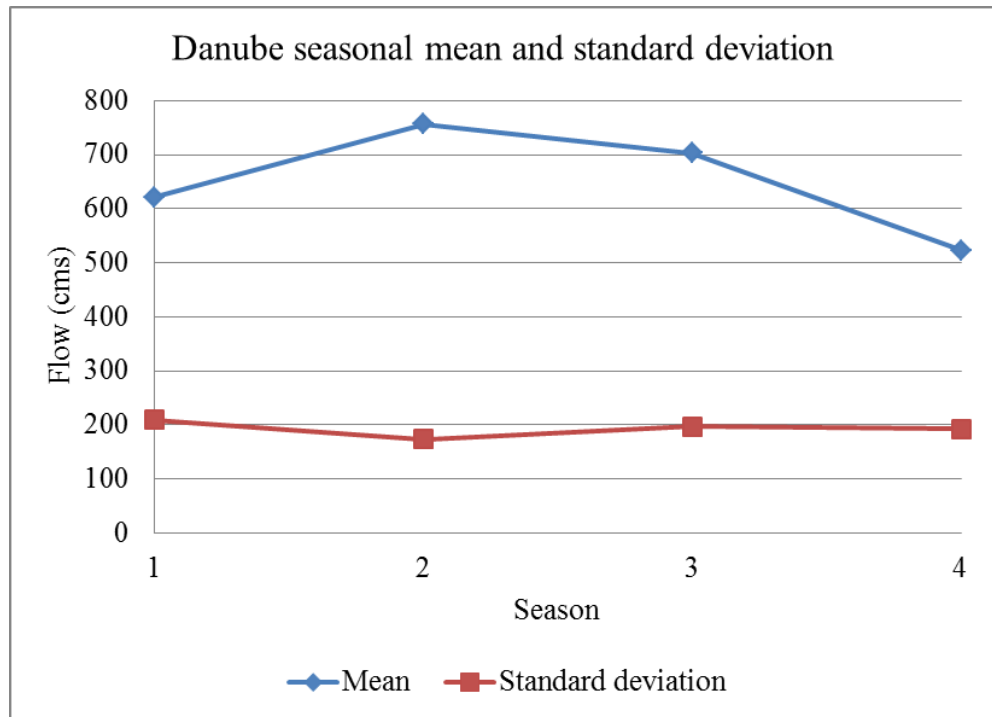
(d)

Figure 4.17. De-trended and standardized Parana flows for seasons: (a) Winter; (b) Spring; (c) Summer; and (d) Fall.

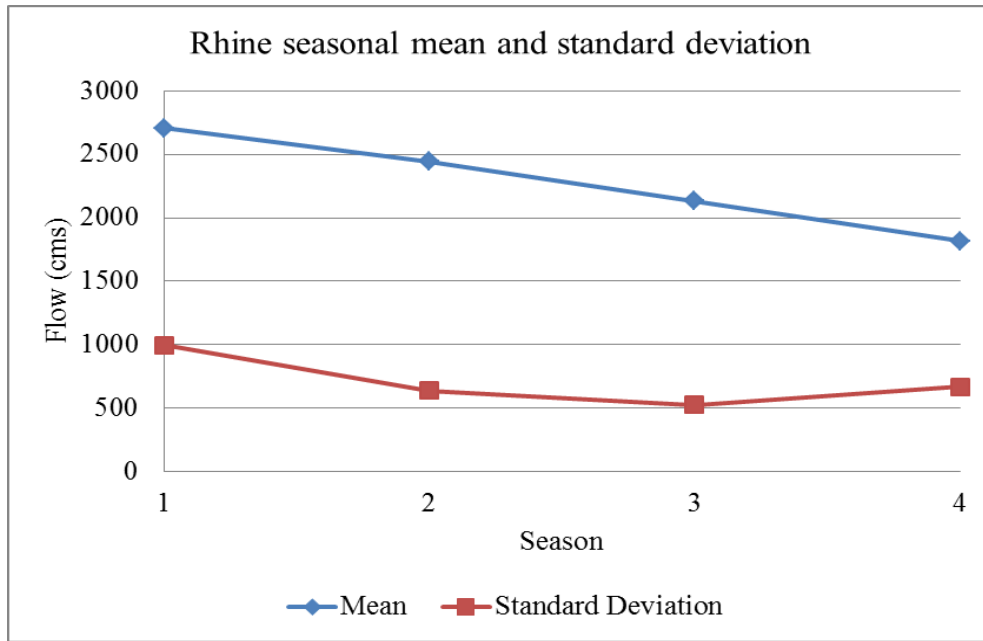
For all the seasonal river flow series, the sample mean and the sample standard deviation were plotted as shown in Figure 4.18. These plots indicated the presence of strong seasonal cycles with inter-annual variability in the flows. Moreover, the figures also indicated the occurrence of high flows in the winter seasons for the Parana and Rhine rivers, whereas the spring and summer seasons for the Danube and Missouri rivers, respectively. For all the rivers, low flows were evident in the fall seasons except the Missouri, for which low flows occurred in the winter seasons. These conditions are occurred every year in the rivers in a periodic manner.



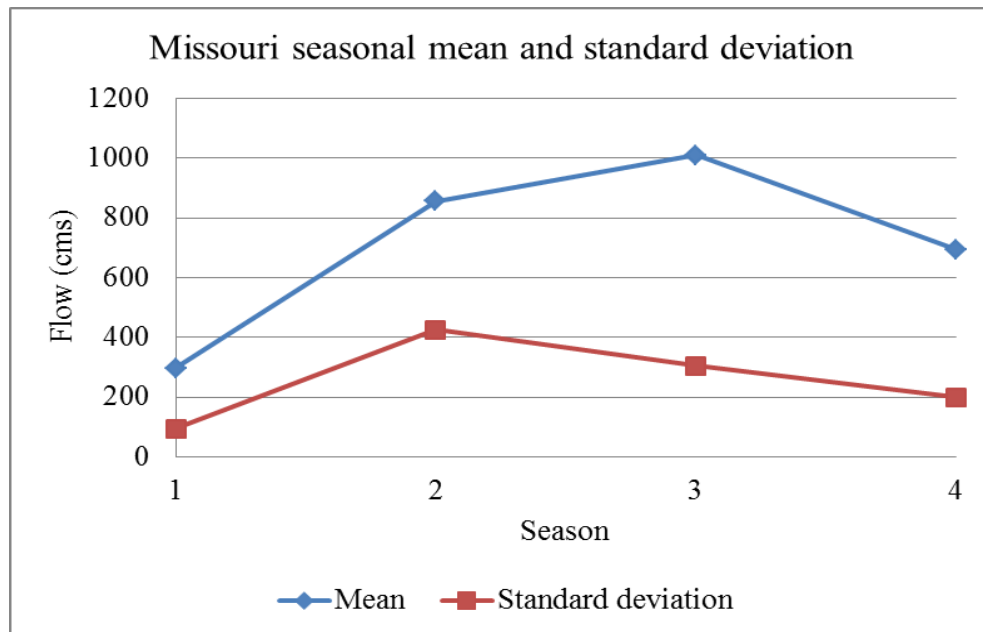
(a)



(b)



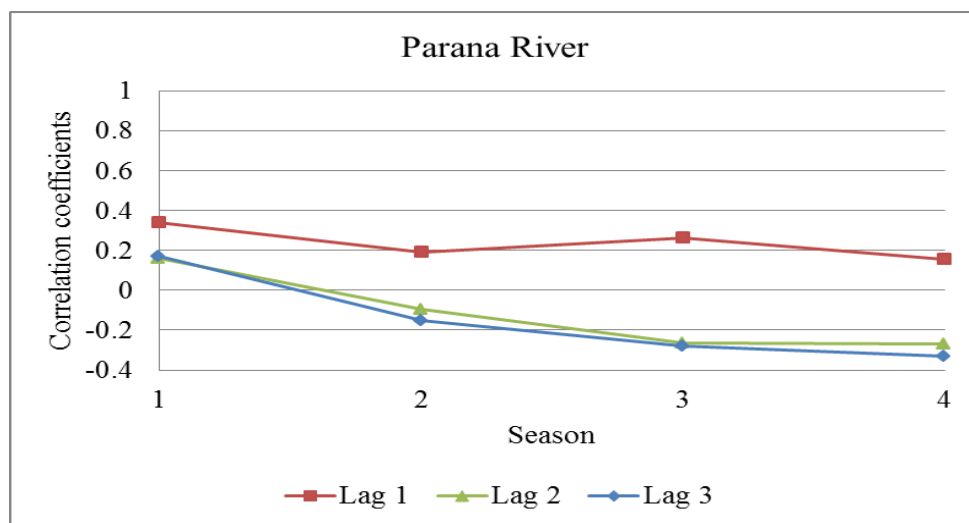
(c)



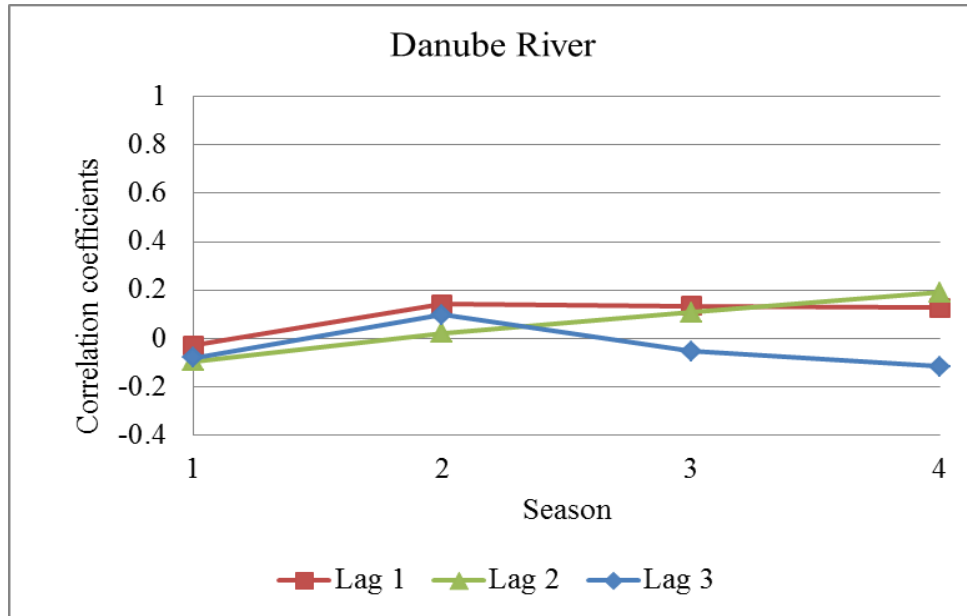
(d)

Figure 4.18. Plots of sample mean and sample standard deviation of (a) Parana; (b) Danube; (c) Rhine; and (d) Missouri Rivers. In the x-axis, the notations 1, 2, 3, and 4 represent winter, spring, summer, and fall seasons, respectively.

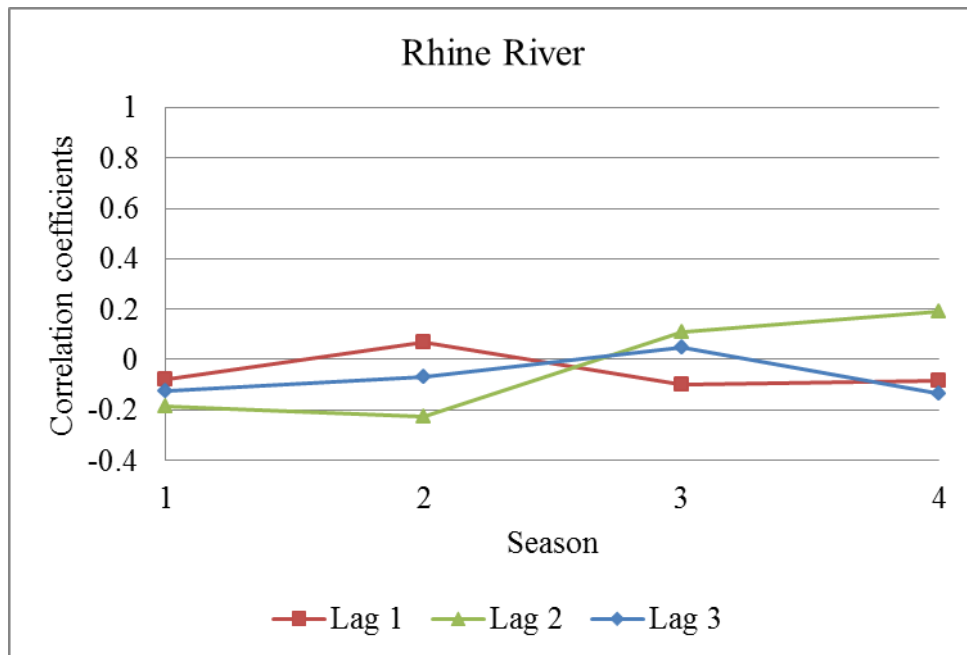
The seasonality of the river flow series ($y_{v,\tau}$) were removed by standardizing the de-trended series. The correlation coefficients ($r_{k,\tau}$) were calculated for lag $k = 1, 2, 3$ and for seasons winter, spring, summer, and fall represented by $\tau = 1, 2, 3, 4$ and plotted in Figure 4.19. Here, the notations 1, 2, 3, and 4 in the x-axis represent winter, spring, summer, and fall seasons, respectively. These plots indicate the seasonal flow variations were not large as the inter-seasonal coefficient variations were insignificant at different lags. However, the periodic parameter model (each season has different coefficient values) requires high seasonal variations of the correlation coefficients (Salas et al., 1980). The requirements for the time series model with constant and periodic parameters were described in Chapter 2 (section 2.3). The less significant coefficients in the plots indicate that the univariate and multivariate time series models with constant coefficients may fit well with the data. Considering above viewpoints, these models were selected for further analysis. The standardized Parana, Danube, Rhine and Missouri river flow series are shown in Figure 4.20.



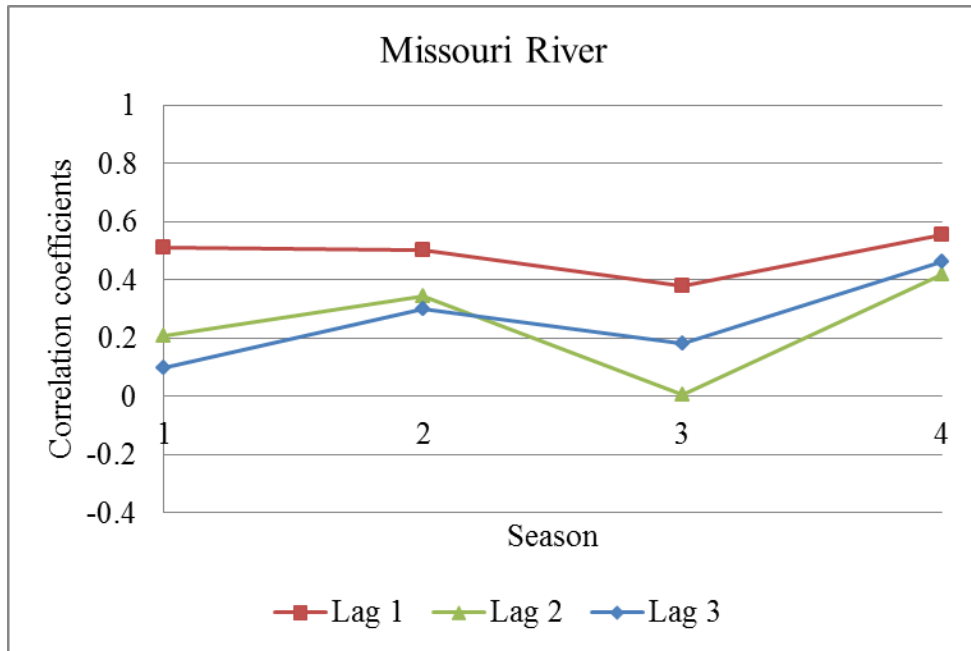
(a)



(b)

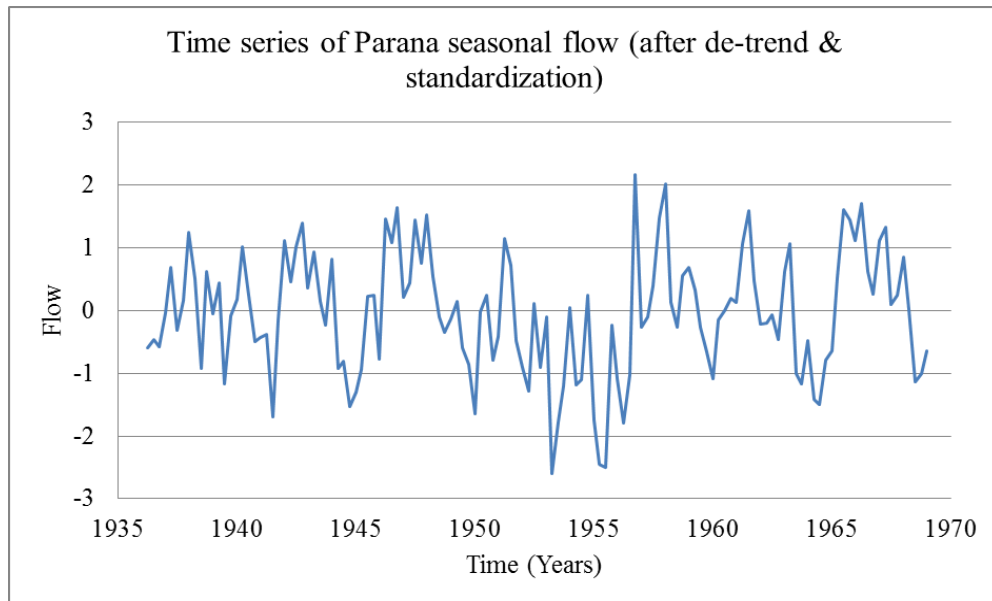


(c)

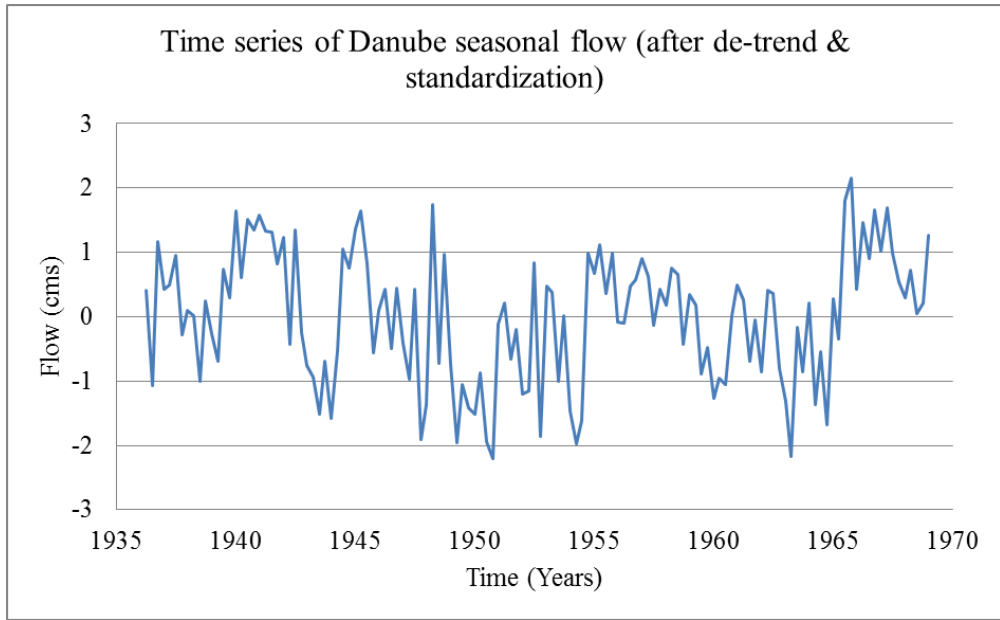


(d)

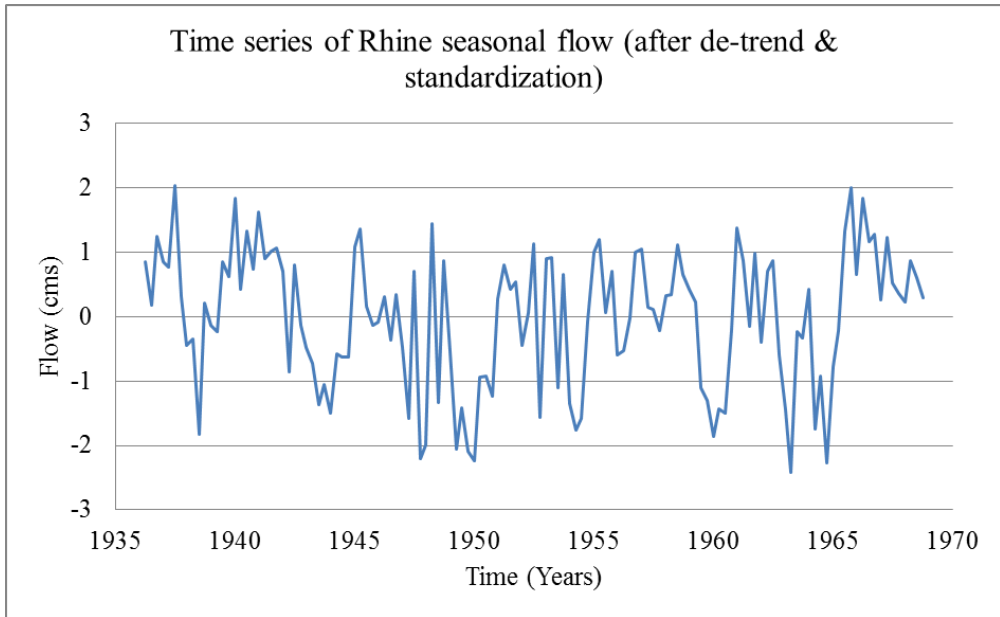
Figure 4.19. Seasonal variation of the correlation coefficients for the rivers: (a) Parana; (b) Danube; (c) Rhine; and (d) Missouri.



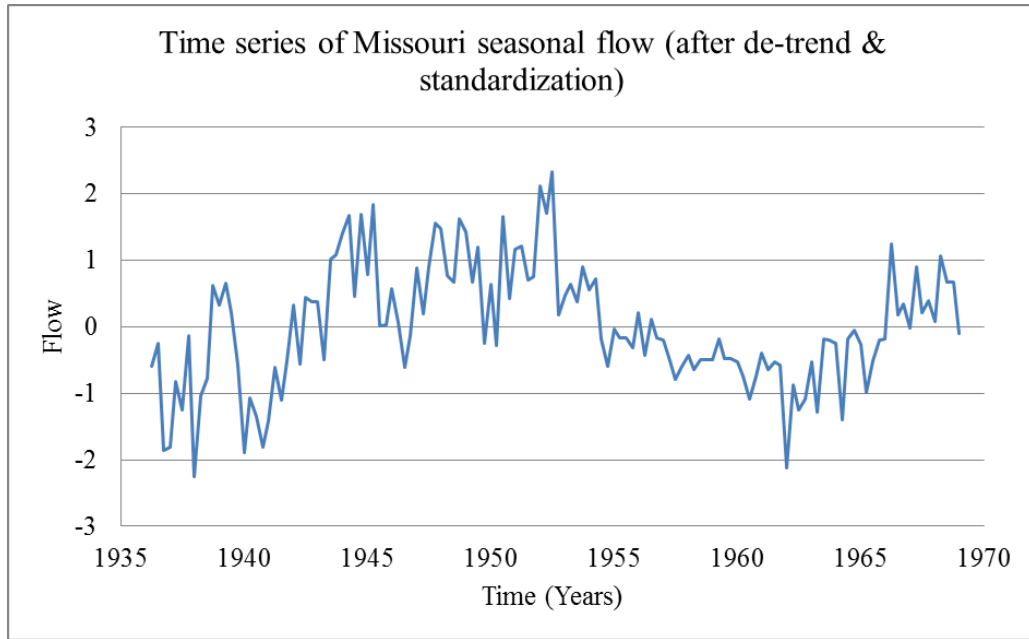
(a)



(b)



(c)



(d)

Figure 4.20. Standardized seasonal river flow series: (a) Parana, (b) Danube, (c) Rhine, and (d) Missouri.

For better understanding, each time series of the four rivers $z_{v,\tau}$ were denoted as z_t where, $t = 1, 2, \dots, 132$, since 132 seasons were involved in the calibration stage. For each river flow series, the autocorrelation (ACF) and partial autocorrelation (PACF) functions were calculated up to 25 lags and plotted within the 95% confidence interval to evaluate the persistent characteristics of the flow and also to investigate the presence of autoregressive (AR) and moving average (MA) components. It is noteworthy that the ACF and PACF are defined only for integer values of the lags. But in this study, these lag values were connected by lines in order for the better representation of the behavior of the flow series (Salas et al., 1980).

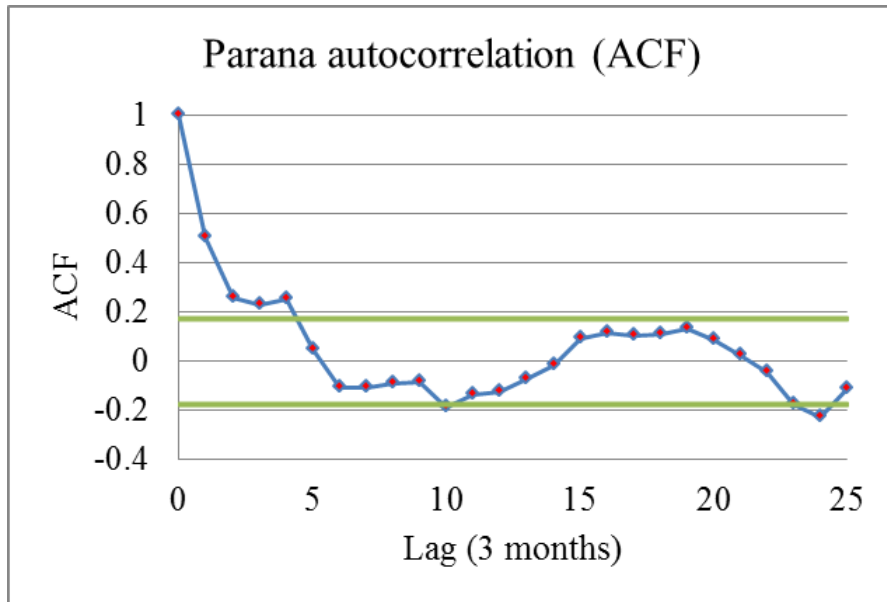
For the Parana River, the correlogram in Figure 4.21(a) seemed to be positively correlated up to lag four, then turned sharply towards zero, and oscillated within the 95% confidence limits. This indicated the presence of significant linear dependence between the seasonal observations. The PACF, shown in Figure 4.21(b), was significant at lag one, and thereafter showed wavy resemblance within the confidence intervals. The slow decay rate of the ACF indicated the possibility of the presence of a moving average component. Although the ARMA(1,4) seemed to be a reasonable model, it was decided to try AR(1) or ARMA(1,0), ARMA(2,0), ARMA(1,1), ARMA(1,2) models, and apply the one which showed the most resemblance to the observed flow characteristics.

The correlogram of the Danube River in Figure 4.21(c) showed that the ACFs were positively significant up to lag three, and thereafter died abruptly within the confidence limits. Conversely, the PACF, shown in Figure 4.21(d), was found to be significant at lag two, oscillating afterwards within the confidence limits. Although this oscillating behavior indicated an ARMA(2,3) model, it was also decided to try the ARMA (1,1), ARMA(1,2), ARMA(2,1) and AR(2) models in search for a better model.

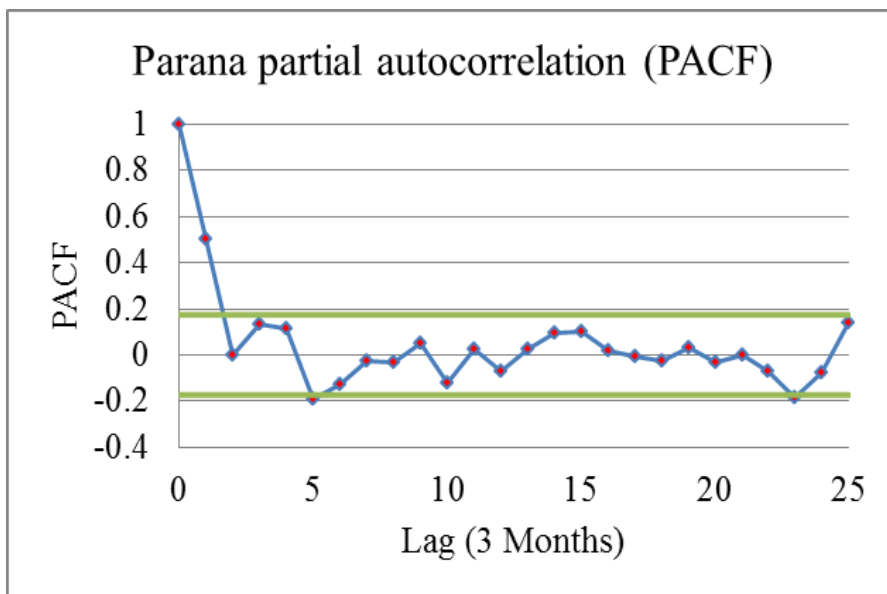
The Rhine River correlogram in Figure 4.21(e) showed significant correlations at lag three, and then started oscillating within the confidence limits. However, the PACF, shown in Figure 4.21(f), was significant at lag two, moved towards zero, and again significant at lag four. It started oscillating afterwards within the 95% confidence interval. Therefore, it was decided to try the ARMA(1,1), ARMA(1,2), ARMA(2,1) and ARMA(2,3) models.

The Missouri River ACF in Figure 4.21(g) was delaying while decaying towards zero. The delayed behavior of the autocorrelation coefficients indicated the presence of a

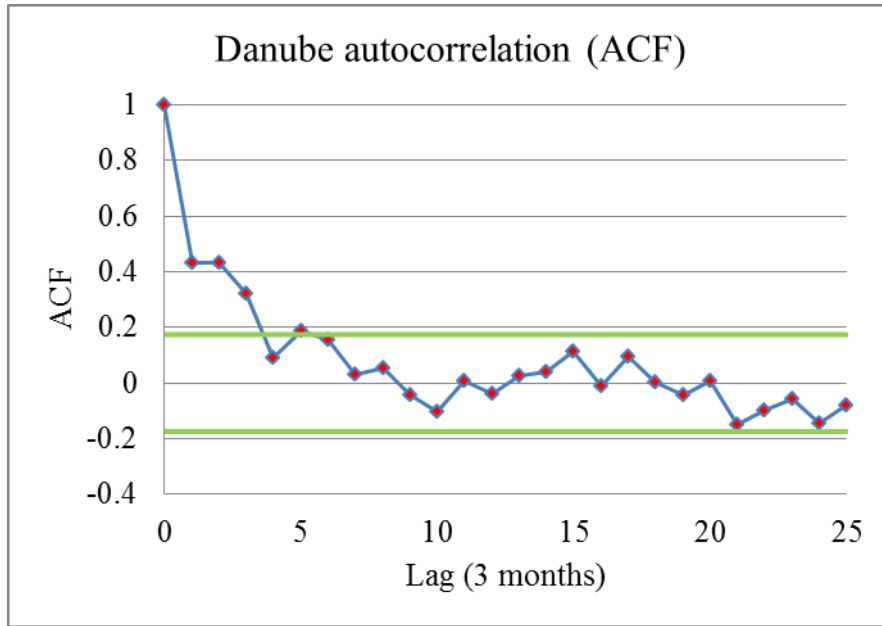
moving average component. However, the PACF in Figure 4.21(h) was correlated at lag 2. Hence, it was decided to try the ARMA(1,1) and ARMA(2,1) models.



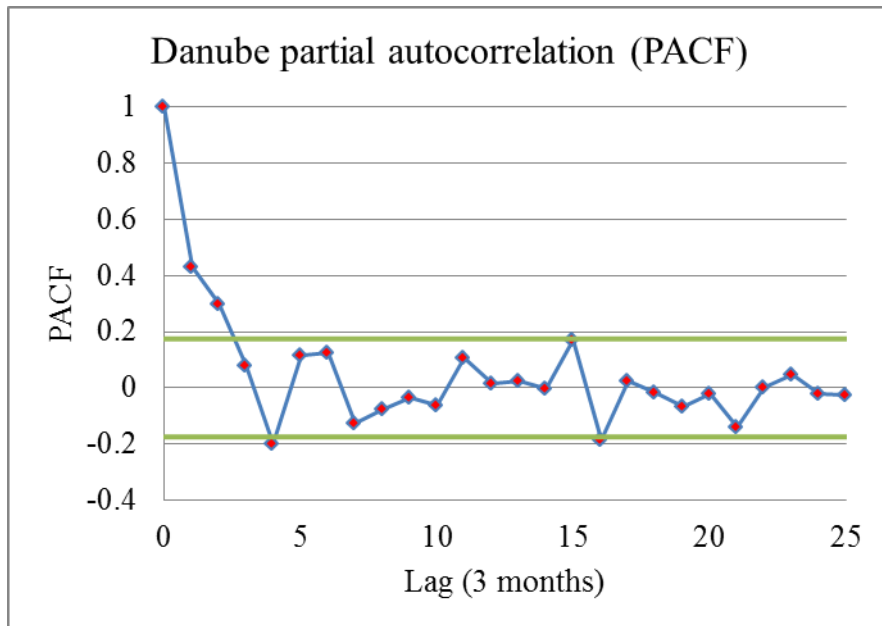
(a)



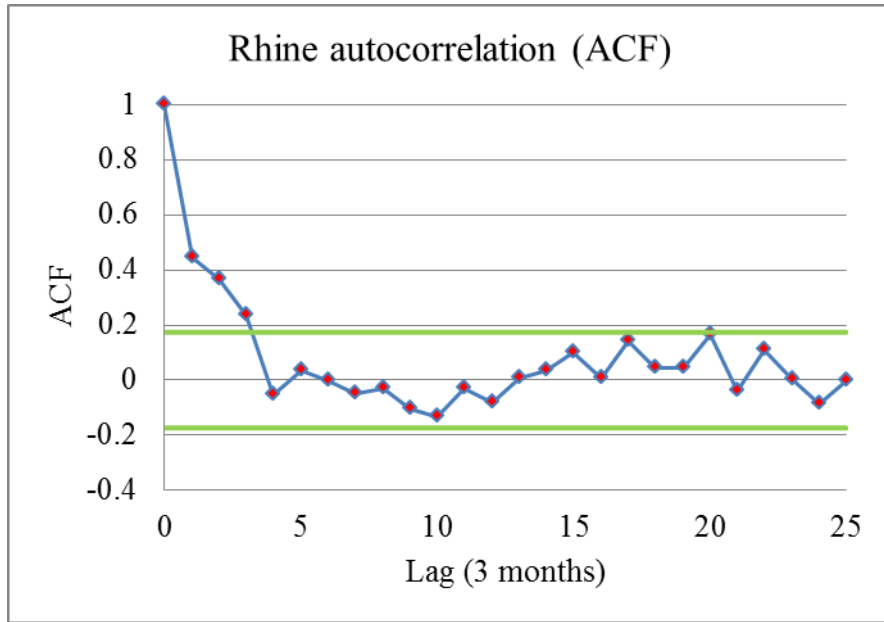
(b)



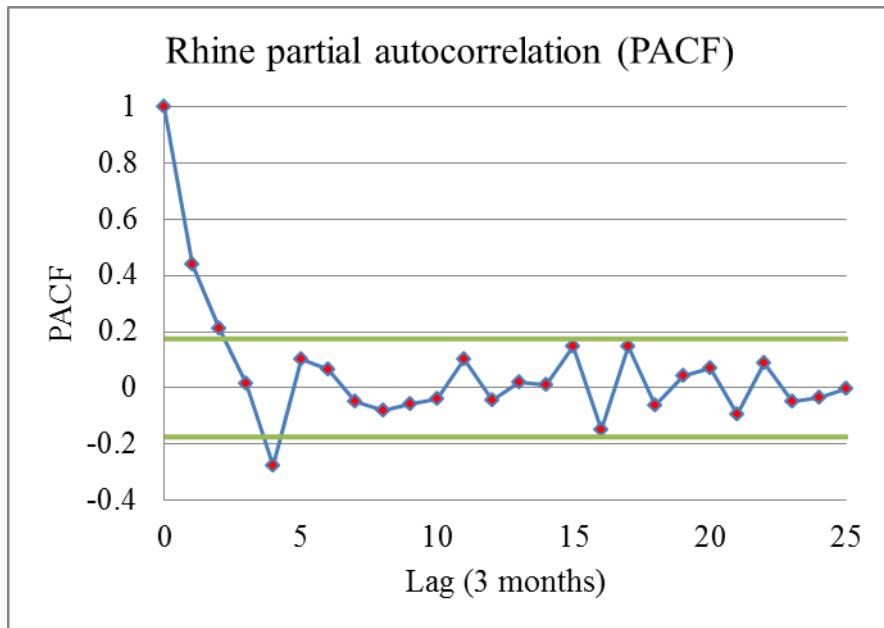
(c)



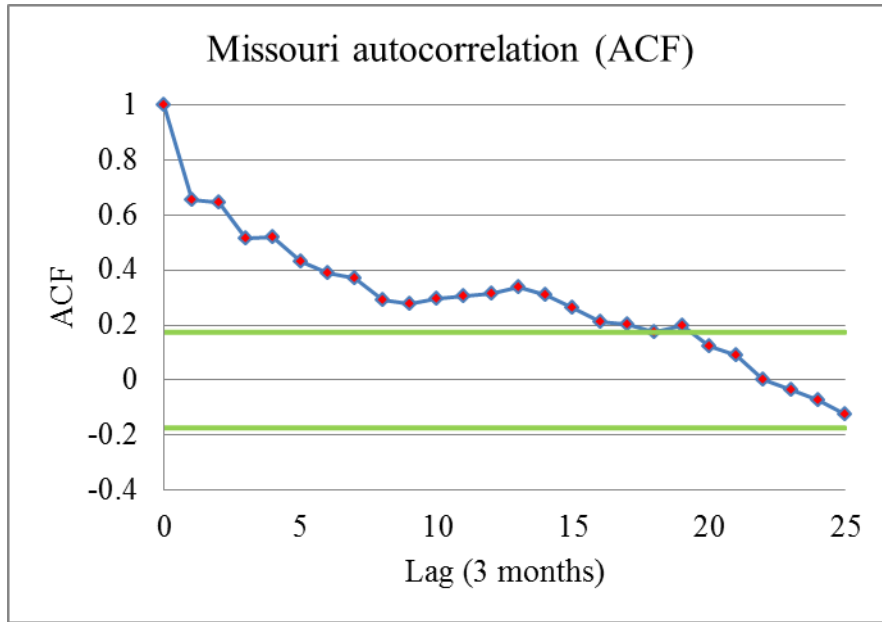
(d)



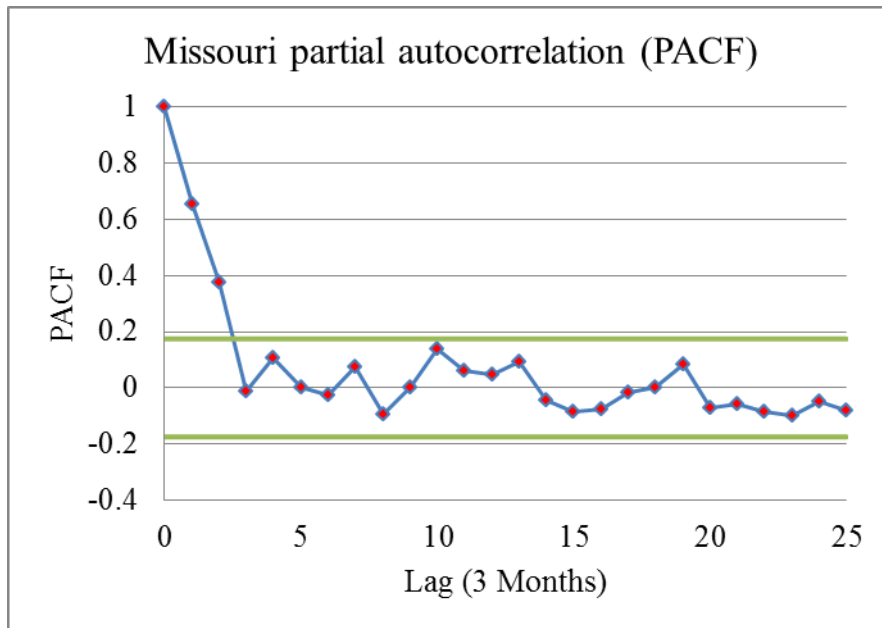
(e)



(f)



(g)



(h)

Figure 4.21. The ACF and PACF plots of the Parana (a, b), Danube (c, d), Rhine (e, f), and Missouri (g, h) Rivers, respectively.

Parameter Estimation

The estimated parameters of different ARMA(p,q) models for the Parana, Danube, Rhine and Missouri Rivers are shown in Tables 4.5 to 4.8, respectively. The SAMS 2007 software was used for estimating all the parameters and generating synthetic flows necessary to analyze the data. The software was programmed to perform all the tasks required to obtain the maximum likelihood estimate (MLE) of the parameters. The corresponding white noise variances and the Akaike Information Criterion (AIC) index values were also obtained and summarized in these tables. Later, the SAMS software was used to generate 10 samples of the 132 seasonal flows and compute the mean flow statistics. Model performances were evaluated by comparing the generated and observed flow statistics. The idea was to find out whether the fitted model can reproduce flow similar to the observed flow. The observed and generated flow correlograms were also plotted to evaluate the skills of the models in reproducing the observed flow characteristics. Any notable difference between the correlograms indicates, selecting an alternative model with new model orders and parameters. The observed and generated flow correlograms of the Parana and Danube Rivers are shown in Figures 4.22 and 4.23, respectively.

Table 4.5

Parameters of ARMA Models with Different Model Orders for the Parana River

Model	$\hat{\phi}_1$	$\hat{\phi}_2$	$\hat{\theta}_1$	$\hat{\theta}_2$	$\hat{\sigma}_\varepsilon^2$	AIC index
ARMA(1,0)	0.503	-	-	-	0.701	89.268
ARMA(2,0)	0.502	0.004	-	-	0.701	91.231
ARMA(1,1)	0.513	-	0.011	-	0.701	91.229
ARMA(1,2)	0.569	-	0.058	0.058	0.696	92.554

Table 4.6Parameters of ARMA Models with Different Model Orders for the Danube River

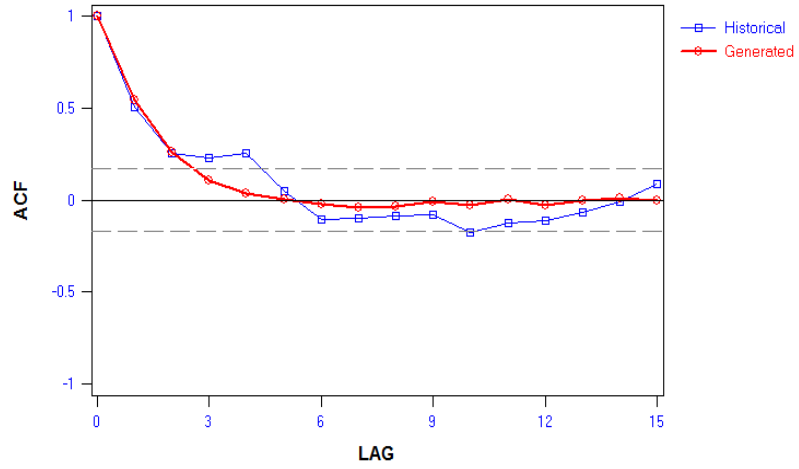
Model	$\hat{\phi}_1$	$\hat{\phi}_2$	$\hat{\theta}_1$	$\hat{\theta}_2$	$\hat{\sigma}_\varepsilon^2$	AIC index
ARMA(1,1)	0.733	-	0.407	-	0.773	104.204
ARMA(1,2)	0.613	-	0.318	-0.249	0.740	100.608
ARMA(2,0)	0.306	0.299	-	-	0.755	101.061
ARMA(2,1)	0.552	0.203	0.269	-	0.756	103.478

Table 4.7Parameters of ARMA Models with Different Model Orders for the Rhine River

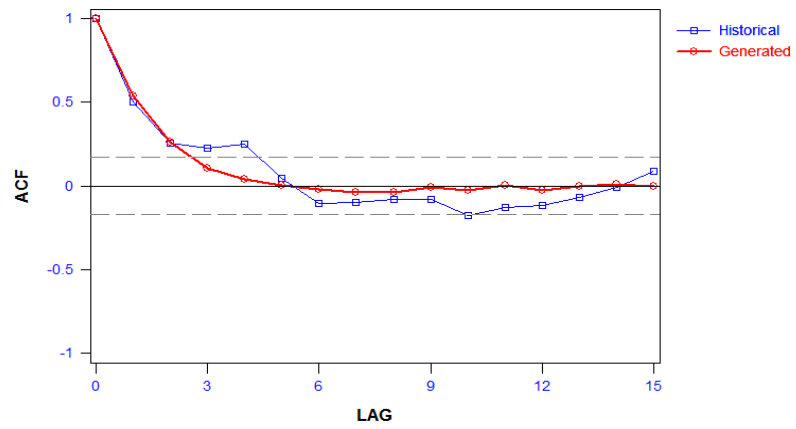
Model	$\hat{\phi}_1$	$\hat{\phi}_2$	$\hat{\theta}_1$	$\hat{\theta}_2$	$\hat{\theta}_3$	$\hat{\sigma}_\varepsilon^2$	AIC index
ARMA(1,1)	0.829	-	0.516	-	-	0.857	117.815
ARMA(1,2)	0.524	-	0.184	-0.233	-	0.842	117.588
ARMA(2,1)	0.407	0.190	0.059	-	-	0.867	121.446
ARMA(2,3)	0.349	0.205	0.000	0.000	0.000	0.867	125.800

Table 4.8Parameters of ARMA Models with Different Model Orders for the Missouri River

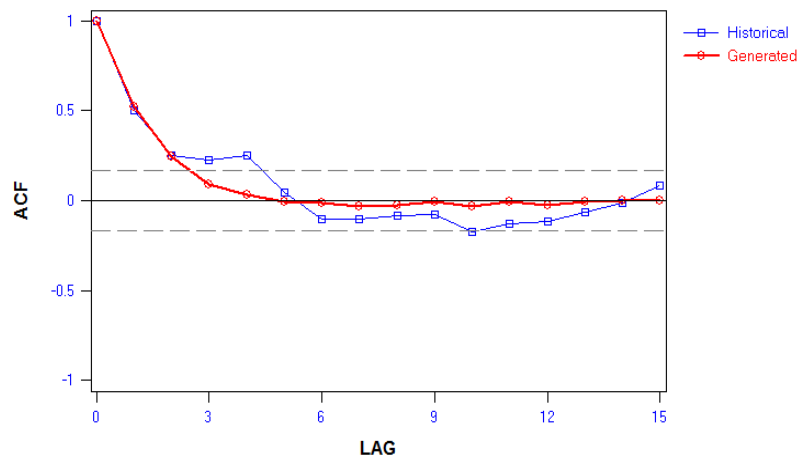
Model	$\hat{\phi}_1$	$\hat{\phi}_2$	$\hat{\theta}_1$	Variance	AIC index
ARMA(1,1)	0.919	-	0.525	0.418	23.051
ARMA(2,1)	0.374	0.399	-0.039	0.525	21.819



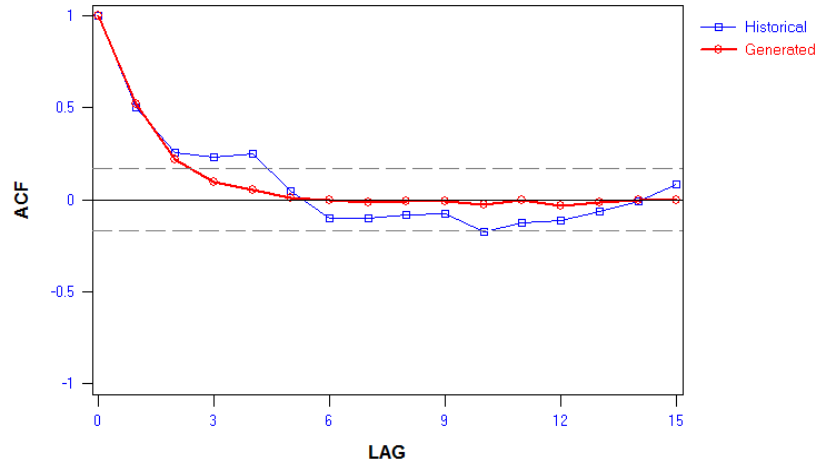
(a)



(b)

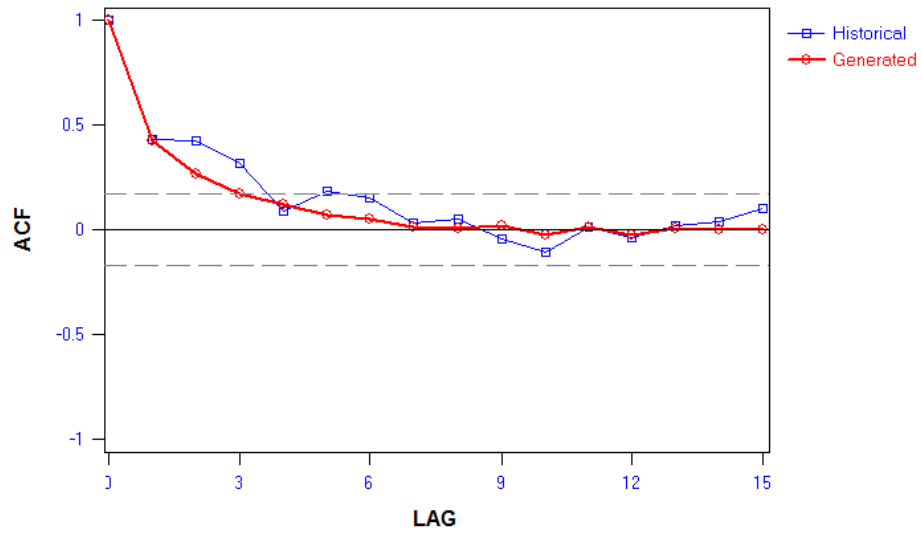


(c)

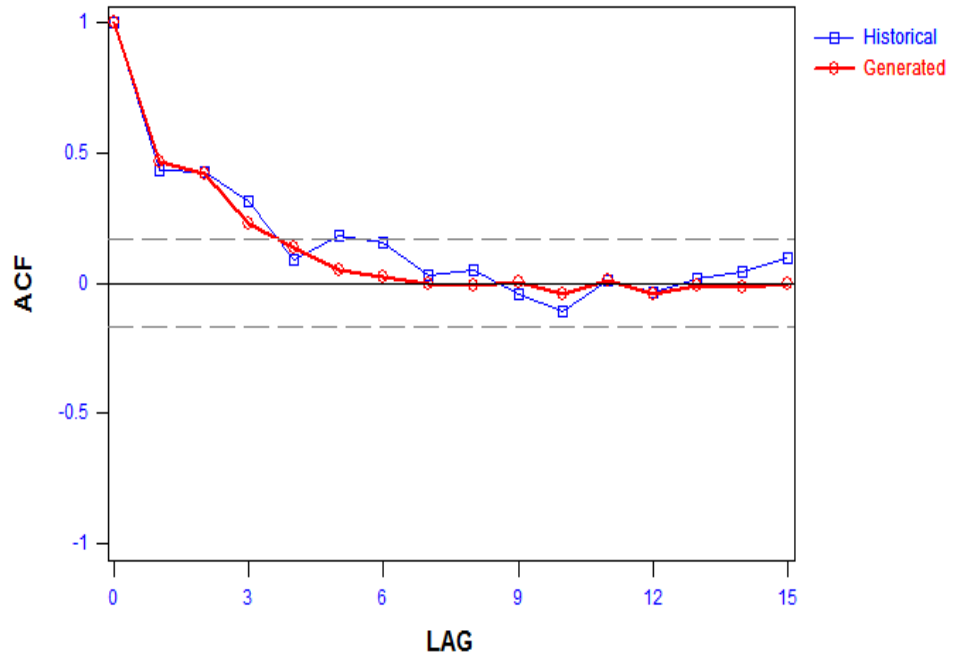


(d)

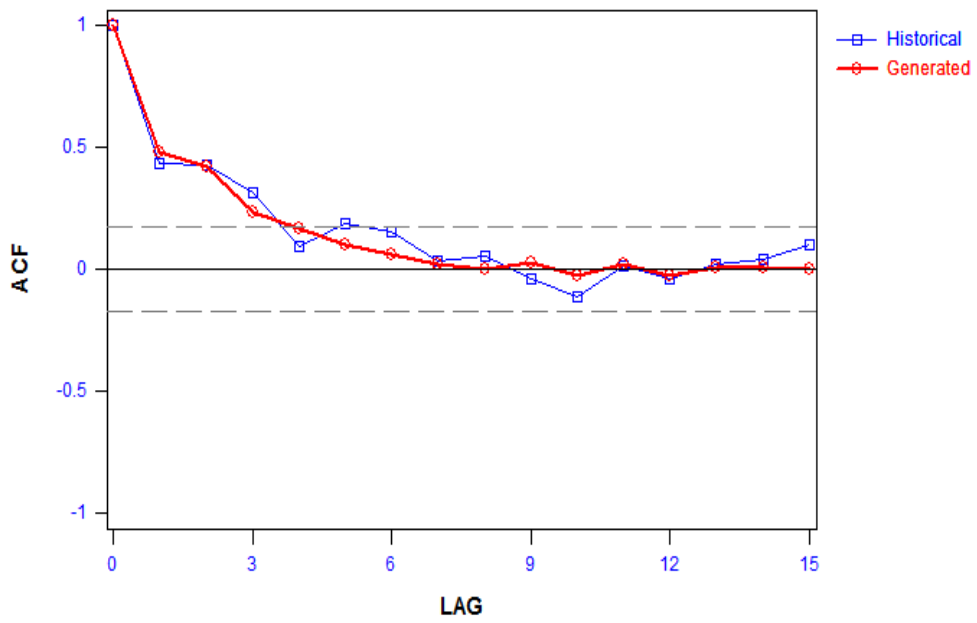
Figure 4.22. Comparison between the ACFs of the observed (historical) and generated Parana River flow series with model type: (a) ARMA(1,0); (b) ARMA(2,0); (C) ARMA(1,1); and (d) ARMA(1,2) model.



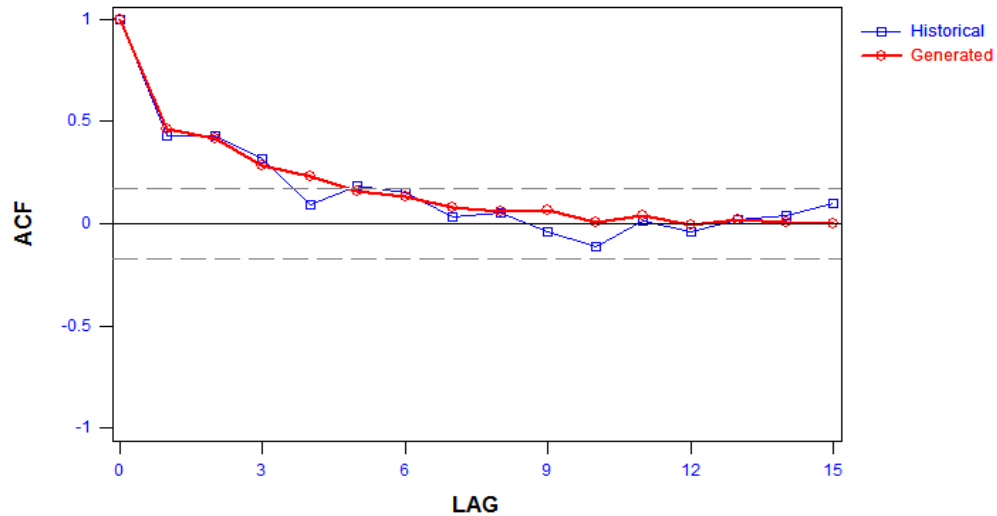
(a)



(b)



(c)



(d)

Figure 4.23. Comparison between the ACFs of the observed (historical) and generated Danube River flow series with model type: (a) ARMA(1,1); (b) ARMA(1,2); (C) ARMA(2,0); and (d) ARMA(2,1).

For the Parana, Danube, Rhine, and Missouri rivers, the ARMA(1,0), ARMA(2,0), ARMA(1,2), and ARMA(1,1) models produced the lowest AIC values for each river, respectively, and therefore were the theoretical choices. However, the variance, AIC and the basic statistics of the other competing models were almost equal, and apparently each model represented the corresponding river flows very well. Therefore, it was decided to use the ARMA(1,1) model to fit all the four rivers flow series. The corresponding equations of the ARMA(1,1) models for the Parana (equation 4.1), Danube (equation 4.2), Rhine (equation 4.3), and Missouri Rivers (equation 4.4) with the calculated parameters are given below:

$$z_t = 0.513z_{t-1} + \varepsilon_t - 0.011\varepsilon_{t-1} \dots \dots \dots (4.1)$$

$$z_t = 0.733z_{t-1} + \varepsilon_t - 0.407\varepsilon_{t-1} \dots \dots \dots (4.2)$$

$$z_t = 0.829z_{t-1} + \varepsilon_t - 0.516\varepsilon_{t-1} \dots \dots \dots (4.3)$$

$$z_t = 0.919z_{t-1} + \varepsilon_t - 0.525\varepsilon_{t-1} \dots \dots \dots (4.4)$$

All of the competing model statistics as well as their characteristics for the Parana, Danube, Rhine, and Missouri rivers are summarized in Tables 4.9 to 4.12, respectively.

Table 4.9

Comparison between the Observed and Generated Flow Statistics of the Parana River

Statistics	Observed flow	Generated flow			
		ARMA(1,0)	ARMA(2,0)	ARMA(1,1)	ARMA(1,2)
Mean	0.053	-0.079	-0.079	-0.090	-0.073
St.Deviation	0.969	0.976	0.976	0.969	0.976
Skew	-0.131	-0.044	0.043	-0.033	-0.363
Min	-2.595	-2.661	-2.659	-2.658	-2.662
Max	2.171	2.360	2.360	2.358	2.340
ACF(1)	0.503	0.540	0.540	0.525	0.521
ACF(2)	0.254	0.258	0.260	0.242	0.219

Table 4.10

Comparison between the Observed and Generated Flow Statistics of the Danube River

Statistics	Observed flow	Generated flow			
		ARMA(1,1)	ARMA(1,2)	ARMA(2,0)	ARMA(2,1)
Mean	0.001	-0.037	-0.025	-0.028	-0.044
St.Deviation	1.010	0.962	1.006	1.009	1.007
Skew	-0.200	-0.019	-0.022	-0.004	-0.003
Min	-2.210	-2.569	-2.576	-2.558	-2.596
Max	2.156	2.403	2.523	2.521	2.508
ACF(1)	0.430	0.424	0.461	0.477	0.460
ACF(2)	0.427	0.269	0.418	0.418	0.413

Table 4.11Comparison between the Observed and Generated Flow Statistics of the Rhine River

Statistics	Observed flow	Generated flow			
		ARMA(1,1)	ARMA(1,2)	ARMA(2,1)	ARMA(2,3)
Mean	-0.001	-0.046	-0.025	-0.044	-0.018
Standard Deviation	1.062	1.041	1.064	1.054	1.058
Skew	-0.389	-0.008	-0.026	-0.011	-0.039
Min	-2.417	-2.751	-2.717	-2.738	-2.734
Max	2.045	2.585	2.679	2.643	2.637
ACF(1)	0.438	0.446	0.473	0.468	0.446
ACF(2)	0.363	0.324	0.379	0.345	0.329

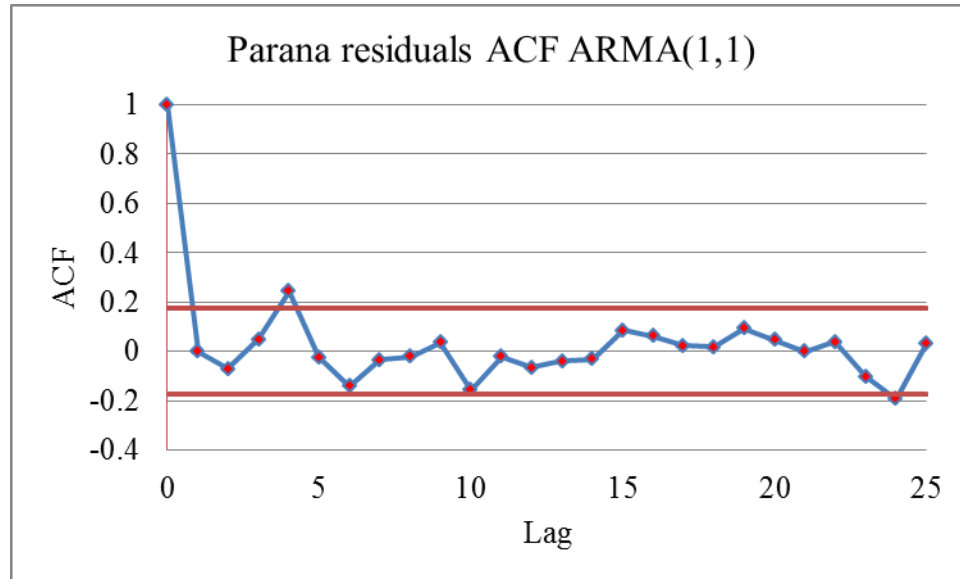
Table 4.12Comparison between the Observed and Generated Flow Statistics of the Missouri River

Statistics	Observed flow	Generated flow	
		ARMA(1,1)	ARMA(2,1)
Mean	0.001	-0.040	-0.045
Standard Deviation	1.010	0.888	0.887
Skew	-0.200	0.072	0.042
Min	-2.210	-2.165	-2.195
Max	2.156	2.140	2.123
ACF(1)	0.430	0.622	0.639
ACF(2)	0.427	0.527	0.589

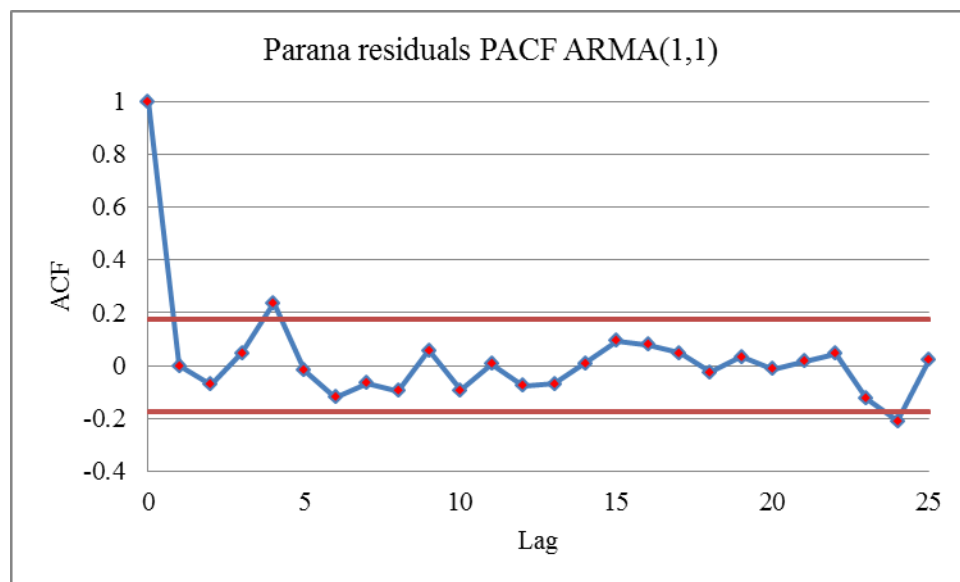
Goodness of Fit Test

The ACF and PACF were calculated for the residuals $r_k(\varepsilon_t)$ of the four rivers at least for lags up to $L = \frac{N}{10} + p + q = \frac{132}{10} + 1 + 1 = 15.2 \cong 16$ separately, and plotted within the 95% confidence limits so that the randomness of the residuals could be evaluated. Figures 4.24(a, b), 4.25(a, b), 4.26(a, b), and 4.27(a, b) showed the ACF and PACF of the residuals up to 25 lags. From these figures, it was evident that for the rivers Parana and Danube, only two points were found outside the 95% confidence limits,

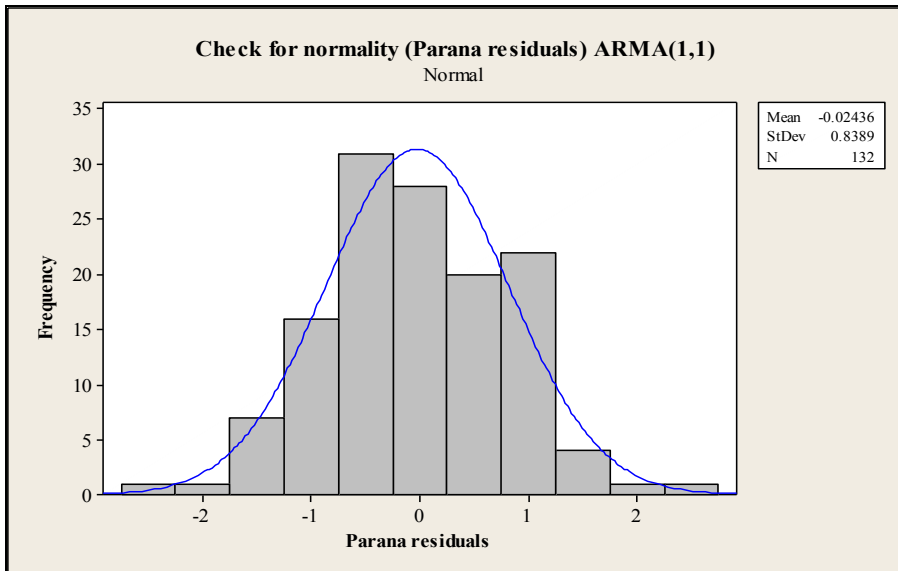
whereas for the Rhine River, only one point was out of the limits (a maximum of two of the points were allowed outside the 95% limits since $(1 - 0.95) \times 25 = 1.25 \approx 2$) (Salas et al., 1980). For the Missouri River, all of the ACF and PACF coefficients varied well within the confidence limits, indicating the randomness of the residuals.



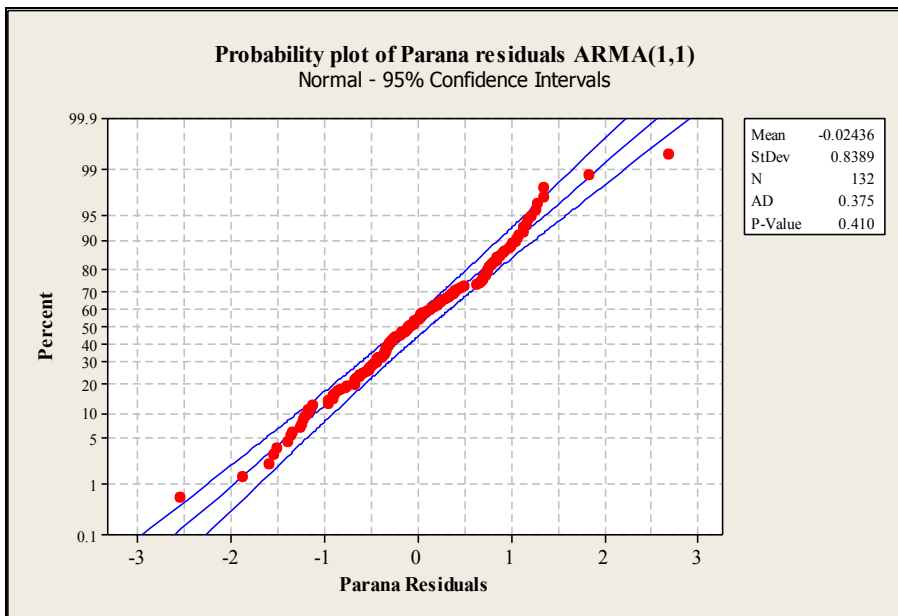
(a)



(b)

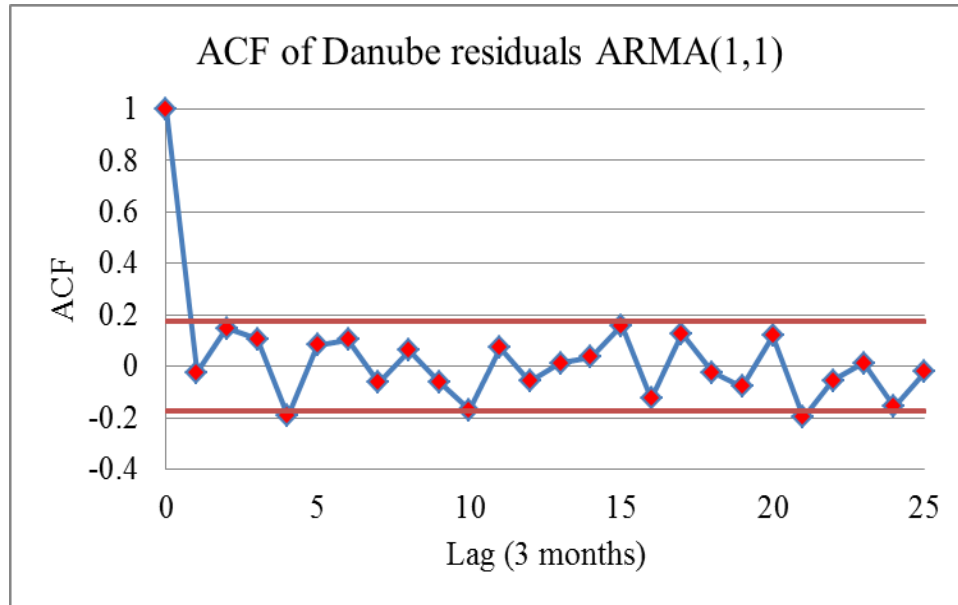


(c)

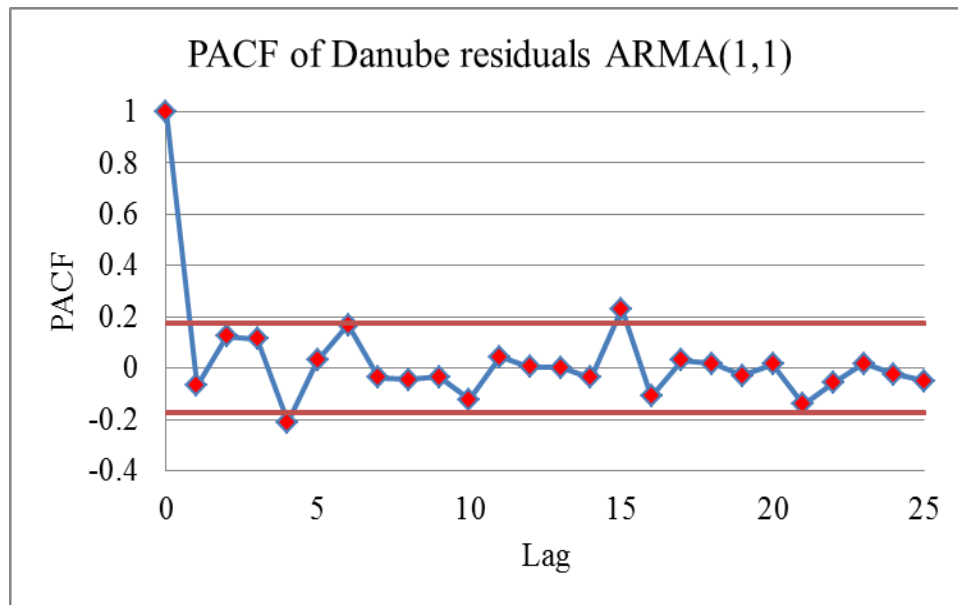


(d)

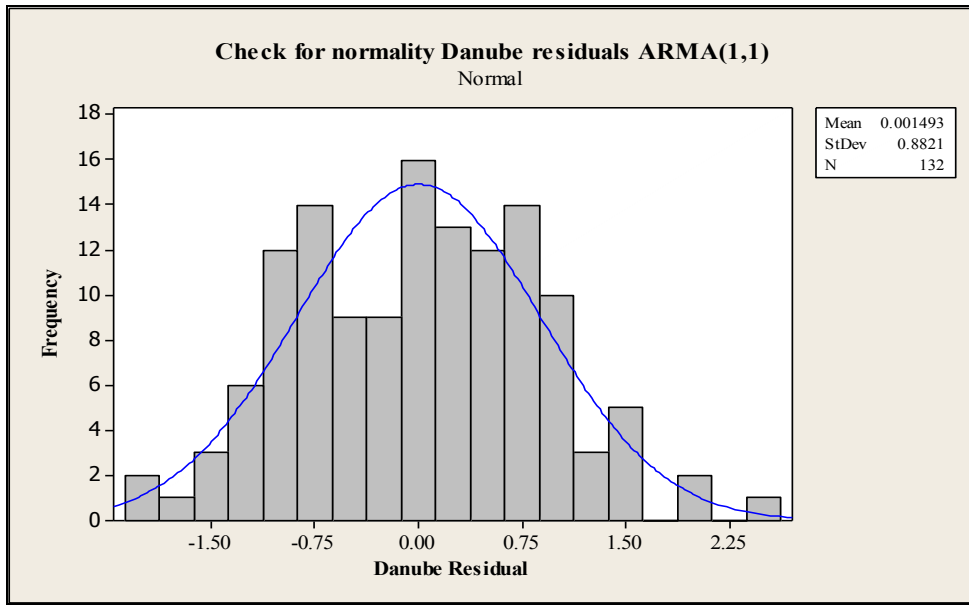
Figure 4.24. Residuals independence and normality test for the Parana River: (a) ACF; (b) PACF; (c) Histograms; and (d) Normal probability plots of the residuals.



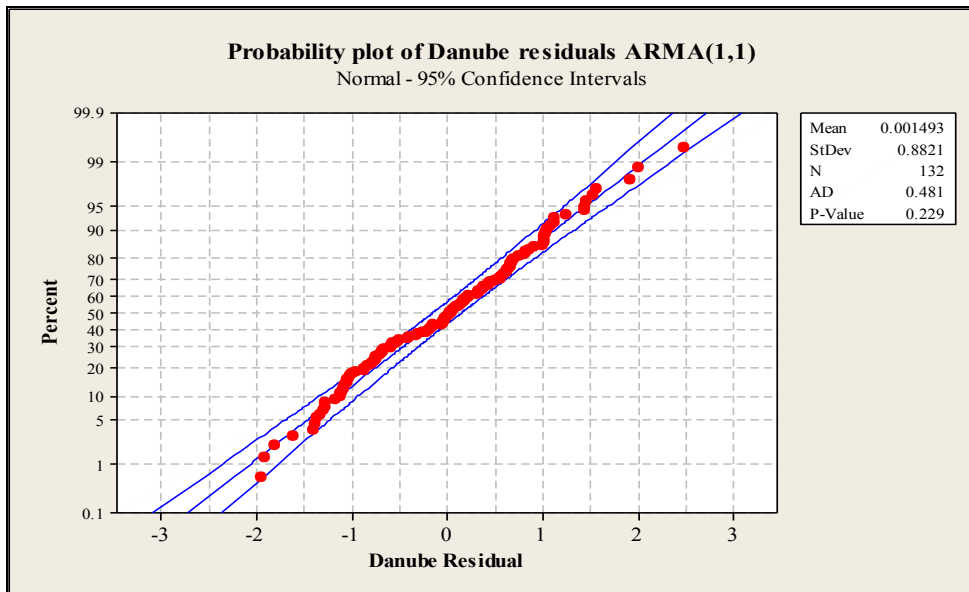
(a)



(b)

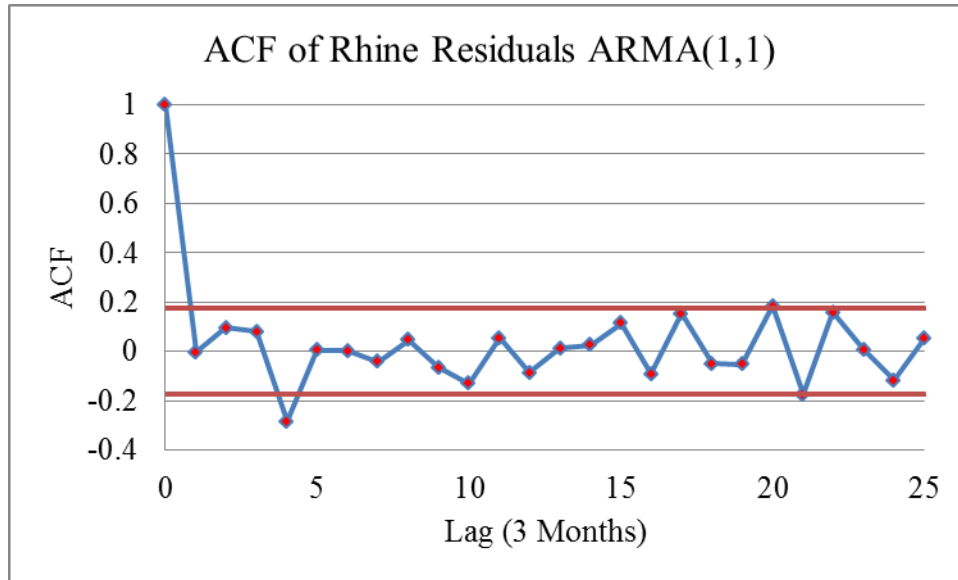


(c)

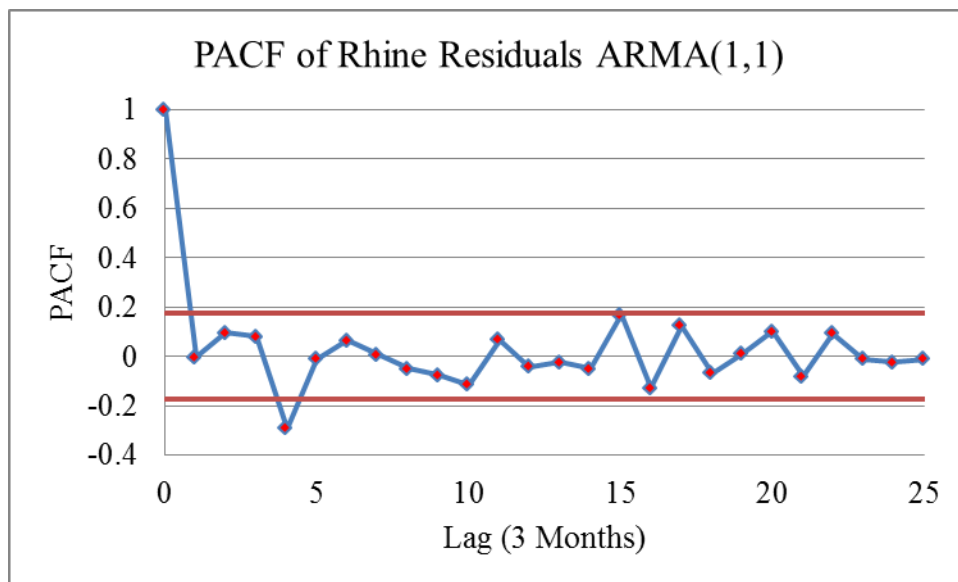


(d)

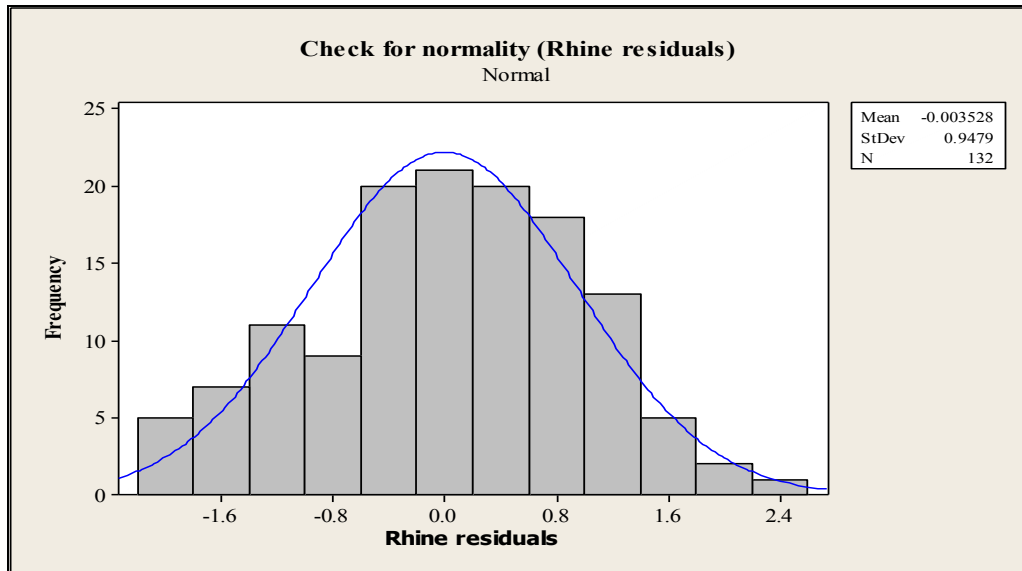
Figure 4.25. Residuals independence and normality test for the Danube River: (a) ACF; (b) PACF; (c) Histograms; and (d) Normal probability plots of the residuals.



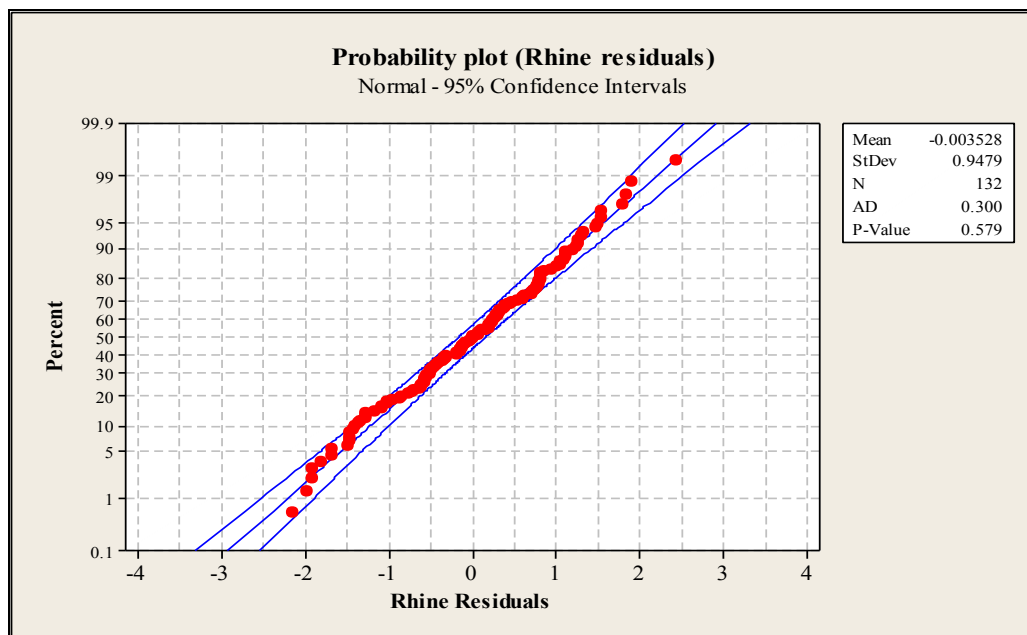
(a)



(b)

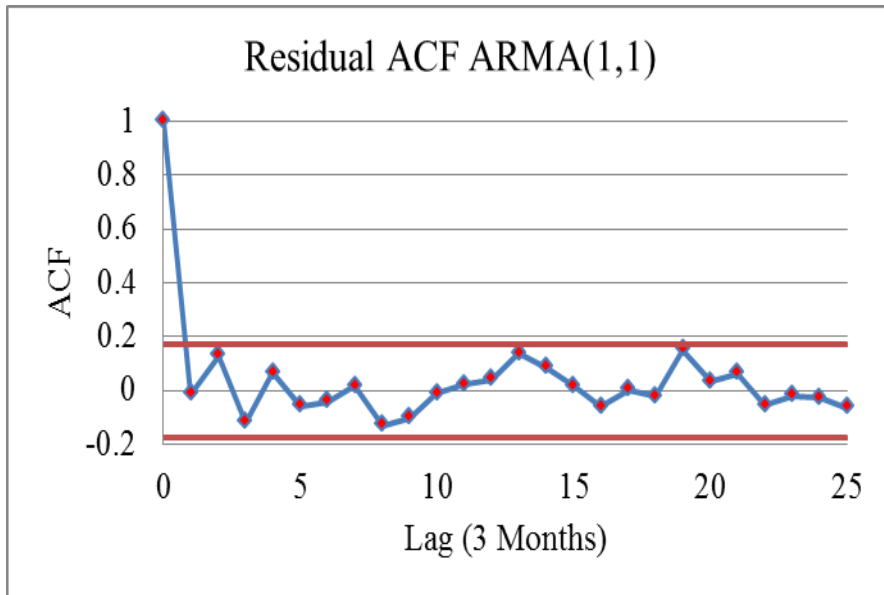


(c)

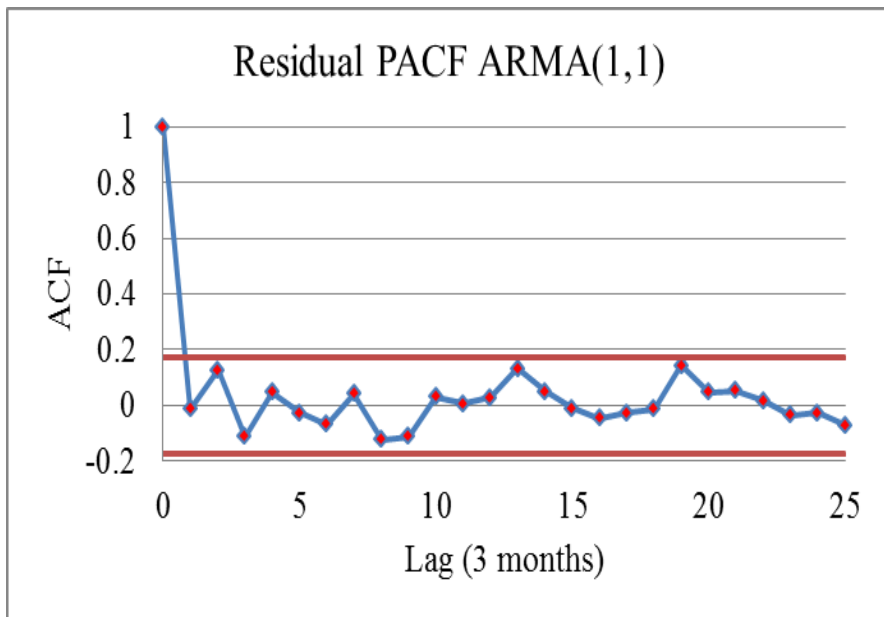


(d)

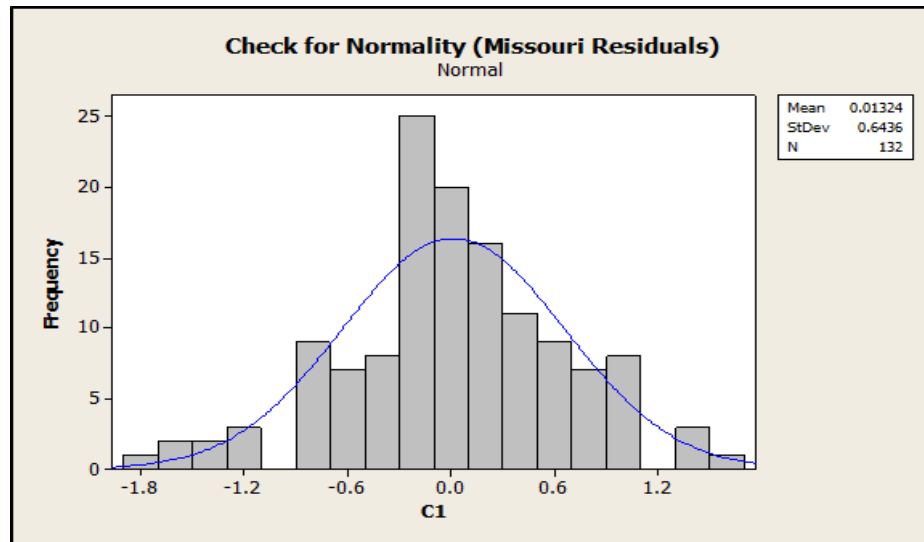
Figure 4.26. Residual independence and normality test for the Rhine River: (a) ACF, (b) PACF, (C) Histograms, and (d) Normal probability plots of the residuals.



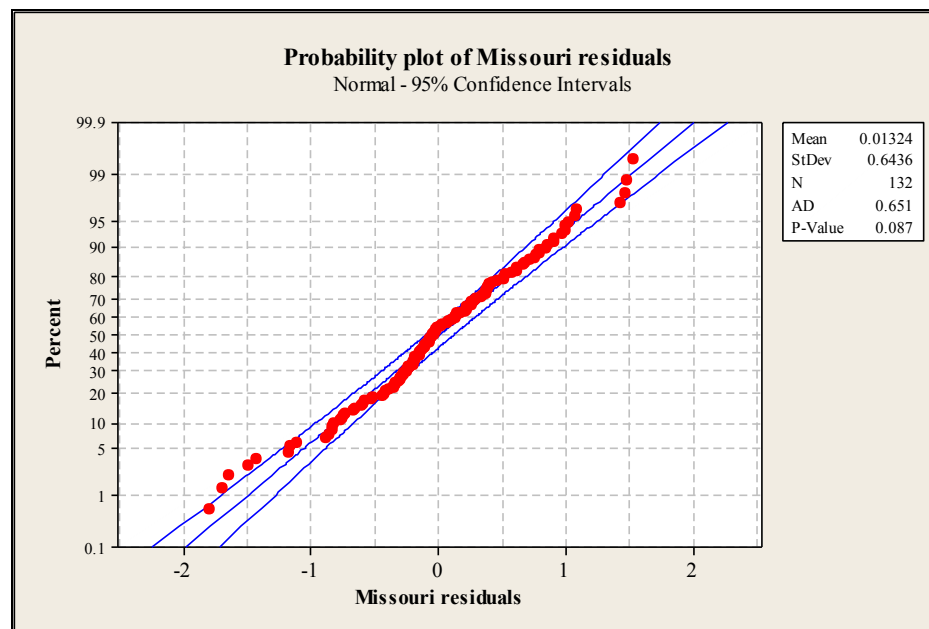
(a)



(b)



(c)



(d)

Figure 4.27. Residual independence and normality test for the Missouri River: (a) ACF; (b) PACF; (c) Histograms; and (d) Normal probability plots of the residuals.

The Port Manteau test was also applied to test the independence of the four river residuals. For this, the Q-statistics for the Parana, Danube, Rhine, and Missouri rivers

were calculated as 4.809, 7.542, 4.083 and 0.327, respectively. These values were compared with the tabulated χ^2_{L-p-q} values given in Salas et al. (1980). As the ARMA(1,1) model was applied for all the rivers, and the correlation coefficients were calculated up to 25 lags (at least 16 lags, see previous paragraph), the degrees of freedom of the residuals were obtained as 23 (25-1-1=23), and the corresponding χ^2_{25-1-1} value for the 5% significance level was 35.172. This indicated the calculated Q-statistics for all the rivers were less than the χ^2_{25-1-1} value. Therefore, the hypotheses of the residual independence were accepted.

The skewness coefficients of the four rivers residuals were obtained as 0.025, 0.078, -0.083, and -0.193. These values were nearly equal to zero and well below the tabulated coefficients for 2% significance level (in this case 0.508) given in Salas et al. (1980). Therefore, the hypotheses of normality were accepted for all the residuals. The graphical tests (histograms and probability plots of the residuals) were also performed to evaluate the normality of the residuals. The p-values of the Parana, Danube, Rhine, and Missouri rivers residual series were obtained as 0.410, 0.229, 0.579 and 0.087, respectively. These values were well above the 5% significance level, therefore, assumed to be approximately normal. The frequency distribution histograms and the normal probability plots for the Parana, Danube, Rhine, and Missouri rivers residual series are shown in Figures 4.24(c,d), 4.25(c,d), 4.26(c,d), and 4.27(c,d), respectively.

Model Calibration and Validation

In calibration, the seasonal flow series from 1936 to 1968 (132 seasons) were used to calculate the ARMA(1,1) parameters for all the rivers. These estimated

parameters were used to fit the model equations to achieve lead one forecasting $z_t(1)$. The independent normally distributed random numbers for each of the river flow series were generated for 132 seasons with mean zero and variance σ_ε^2 . The randomness and normality of the random numbers were also checked by examining the ACF and PACF along with the histogram and probability plot (graphical test), respectively. Thereafter, the forecasted $z_t(1)$ series (one season ahead) were re-transformed, and the trend components, removed initially in the data preparation processes, were added again to obtain the forecasted seasonal flows of the rivers. The calibrated and validated lead-one forecasts of the Parana River are shown in Figures 4.28 and 4.29 below. The rest of the calibrated and validated forecasts of the Danube, Rhine, and Missouri Rivers are shown in the Appendix B.

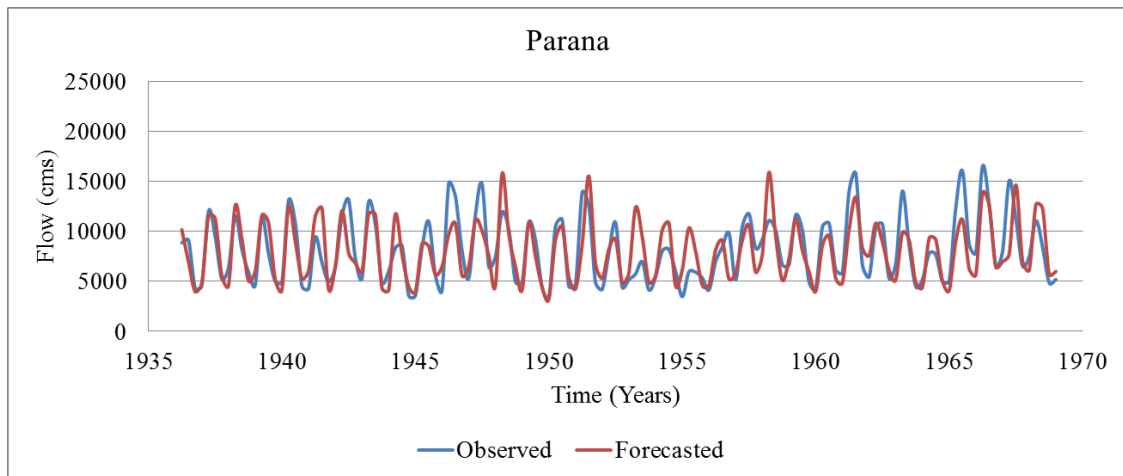


Figure 4.28. Calibrated lead-1 forecast for the Parana River seasonal flows using univariate ARMA(1,1) model.

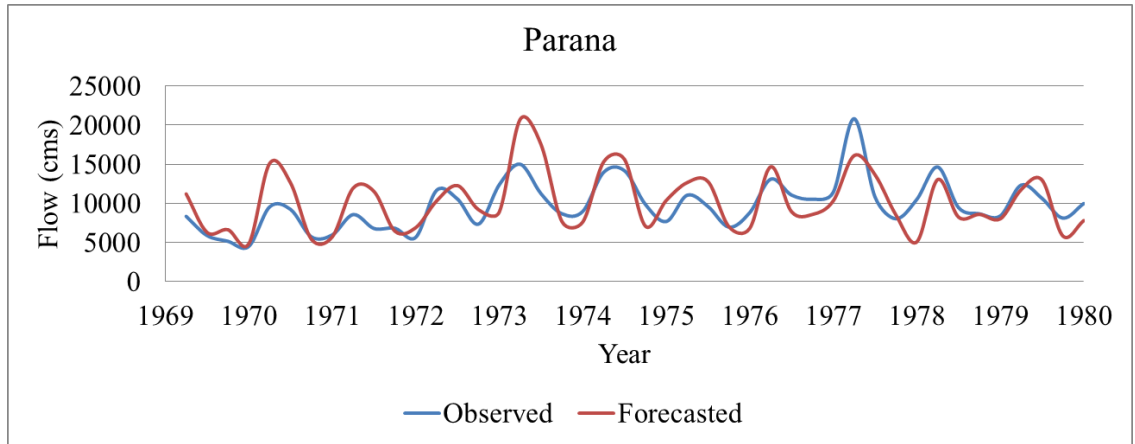


Figure 4.29. Validated lead-1 forecasts of the Parana River seasonal flows using univariate ARMA(1,1) model.

4.3.2 Multivariate AR (MAR) Model

For this study, the multivariate AR (MAR) models with the following variable combinations were used to forecast the seasonal flows of the four rivers: (i) MAR model incorporating four rivers, (ii) MAR model incorporating four rivers and SOI (iii) MAR model incorporating four rivers, SOI and SSN, and (iv) MAR model incorporating three rivers and SSN. For each model, the parameter matrices of various AR(p) models were calculated to find out the best fitted models. This was achieved by the residual analysis, where the corresponding model parameters were used to calculate the residuals of each model and examine their independence in time and space. Basic statistics (mean, variance, skewness etc.) of the historical and model generated flows were also compared to evaluate the model's capability of reproducing historical flows. If the residuals of the fitted model were found to be uncorrelated in time and space, the model was identified as adequate for those particular series. Among different types of ARMA models, the

MAR(3) indicated well fitted for all the rivers with different variable combinations. Therefore, this model was selected for further analyses.

The modeling procedure required to calculate lag zero, lag one, lag two, and lag three cross correlation matrices, represented by $\hat{M}_0, \hat{M}_1, \hat{M}_2,$ and $\hat{M}_3,$ respectively. The pre-processed standardized river flow series were used to calculate the correlation matrices. Thereafter, the correlation matrices were used to calculate the parameter matrices $A_1, A_2, A_3,$ and B of the MAR(3) model. The computed sample cross-correlation matrices for the MAR(3) model incorporating four rivers are given below:

$$\hat{M}_0 = \begin{bmatrix} 1.000 & 0.132 & 0.153 & -0.077 \\ 0.132 & 1.000 & 0.874 & -0.158 \\ 0.153 & 0.874 & 1.000 & -0.116 \\ -0.177 & -0.158 & -0.116 & 1.000 \end{bmatrix} \quad \hat{M}_1 = \begin{bmatrix} 0.475 & 0.108 & 0.112 & -0.107 \\ 0.053 & 0.439 & 0.366 & -0.209 \\ 0.101 & 0.437 & 0.494 & -0.203 \\ -0.026 & -0.186 & -0.203 & 0.543 \end{bmatrix}$$

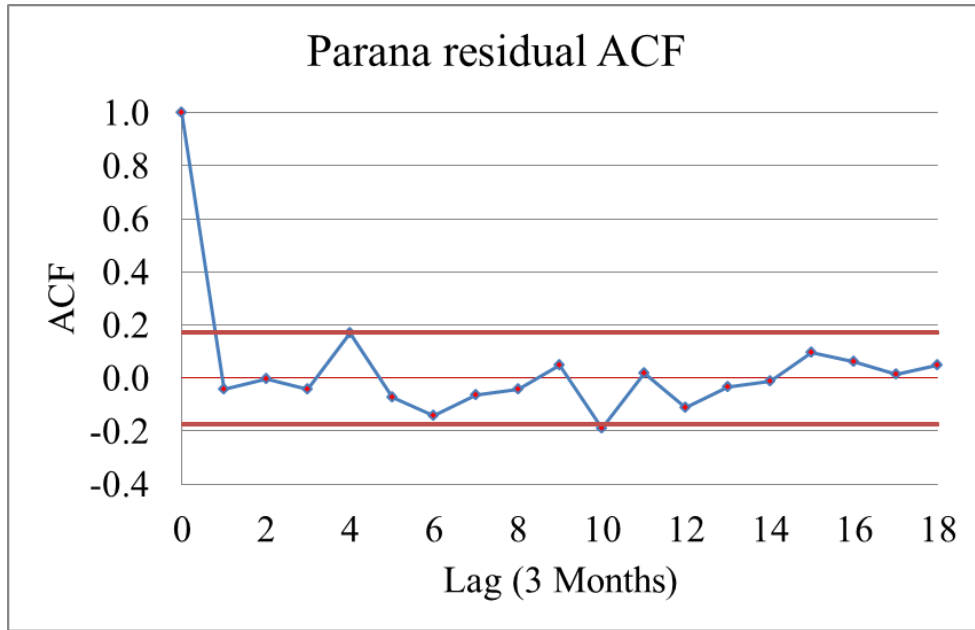
$$\hat{M}_2 = \begin{bmatrix} 0.241 & 0.162 & 0.167 & -0.099 \\ 0.043 & 0.435 & 0.358 & -0.107 \\ 0.048 & 0.411 & 0.410 & -0.118 \\ 0.005 & -0.130 & -0.189 & 0.533 \end{bmatrix} \quad \hat{M}_3 = \begin{bmatrix} 0.229 & 0.185 & 0.136 & -0.177 \\ 0.101 & 0.315 & 0.226 & -0.097 \\ 0.130 & 0.267 & 0.229 & -0.115 \\ 0.107 & -0.141 & -0.197 & 0.502 \end{bmatrix}$$

The estimated parameter matrices are given below:

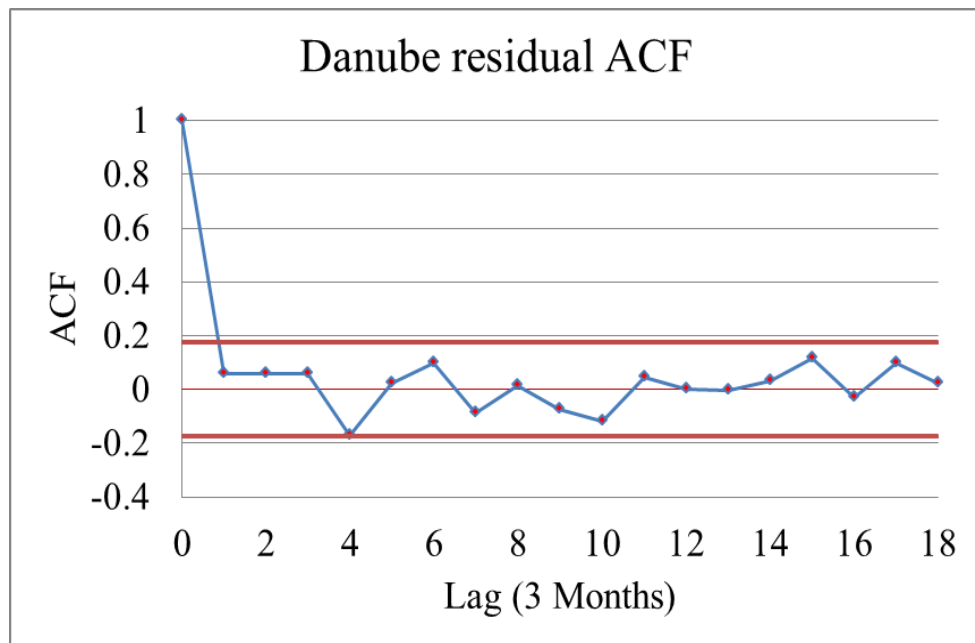
$$\hat{A}_1 = \begin{bmatrix} 0.492 & 0.000 & -0.025 & -0.054 \\ -0.025 & 0.305 & -0.044 & -0.315 \\ 0.036 & -0.085 & 0.413 & -0.299 \\ 0.037 & -0.081 & -0.001 & 0.374 \end{bmatrix} \quad \hat{A}_2 = \begin{bmatrix} -0.083 & -0.031 & 0.106 & 0.049 \\ -0.038 & 0.342 & -0.091 & 0.110 \\ -0.117 & 0.261 & -0.037 & 0.111 \\ -0.028 & 0.273 & -0.272 & 0.386 \end{bmatrix}$$

$$\hat{A}_3 = \begin{bmatrix} 0.131 & 0.230 & -0.186 & -0.098 \\ 0.118 & 0.234 & -0.159 & 0.141 \\ 0.117 & 0.150 & -0.124 & 0.102 \\ 0.132 & 0.030 & -0.025 & 0.014 \end{bmatrix} \quad \hat{B} = \begin{bmatrix} 0.903 & 0.000 & 0.000 & 0.000 \\ 0.240 & 0.883 & 0.000 & 0.000 \\ 0.208 & 0.700 & 0.405 & 0.000 \\ 0.055 & -0.077 & 0.070 & 0.644 \end{bmatrix}$$

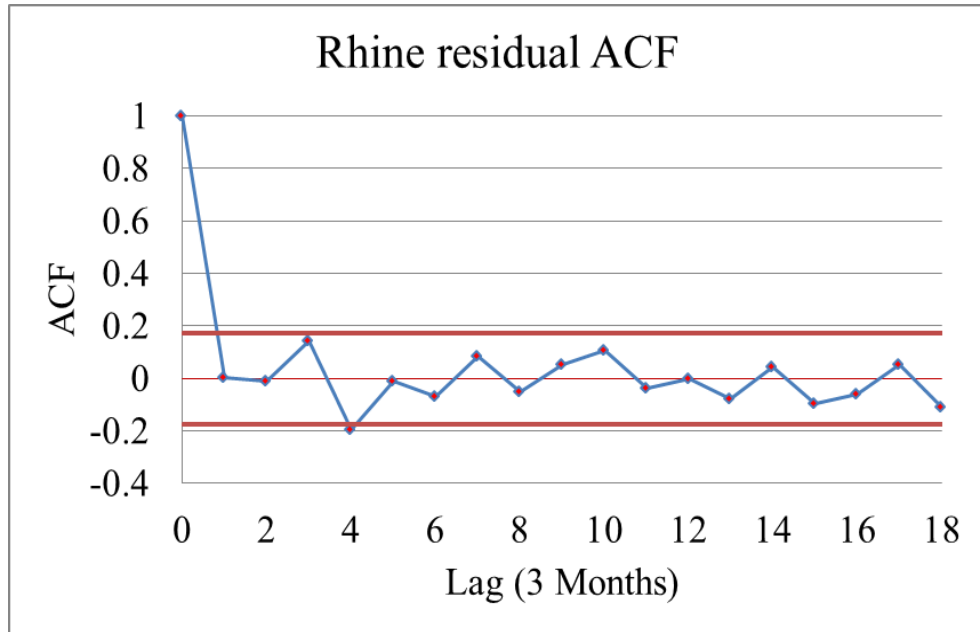
Correlograms were plotted in Figure 4.30 to investigate the time independence of the residuals. These plots showed the ACF of all the residuals were varying within the 95% confidence intervals. Therefore, the residuals of all four rivers were approximately identified as independent.



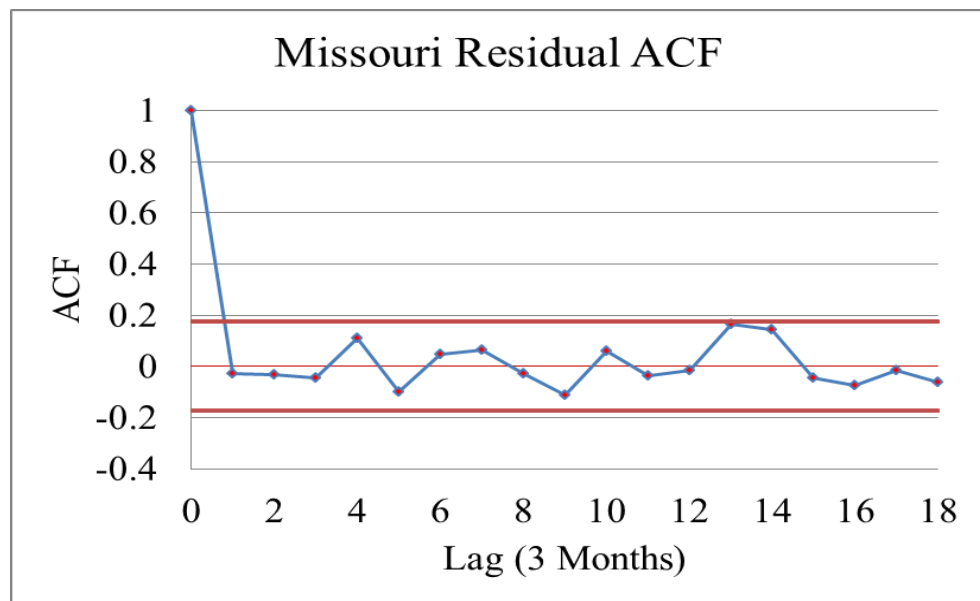
(a)



(b)



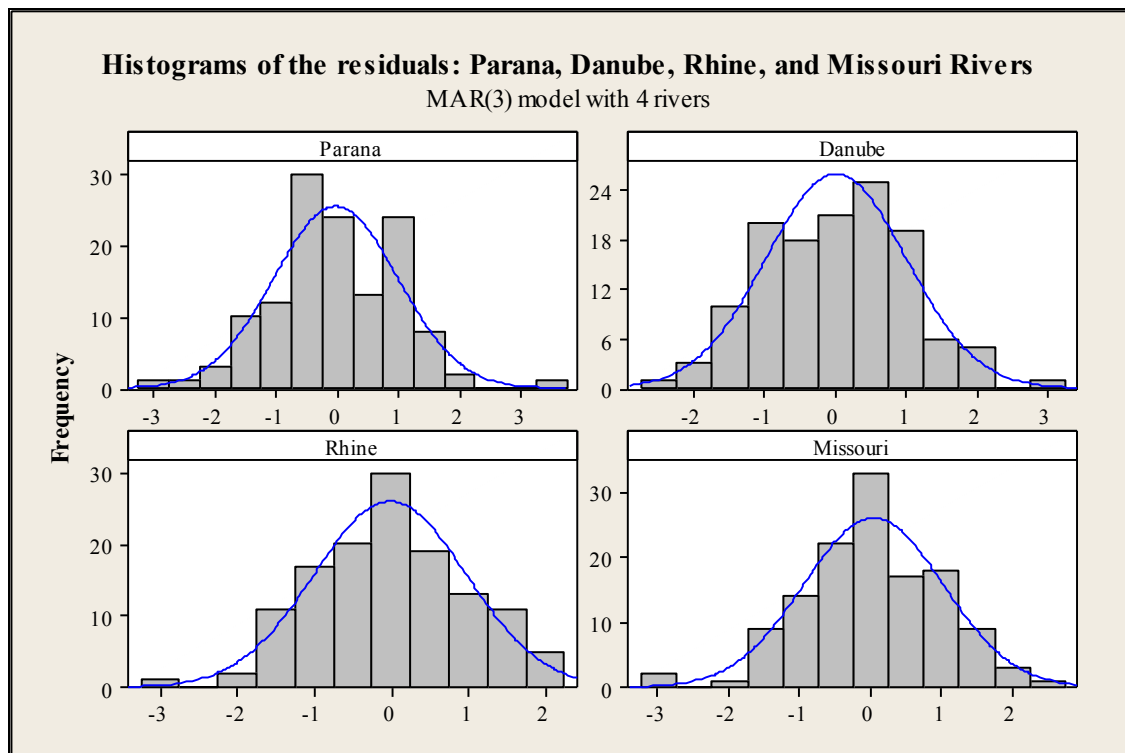
(c)



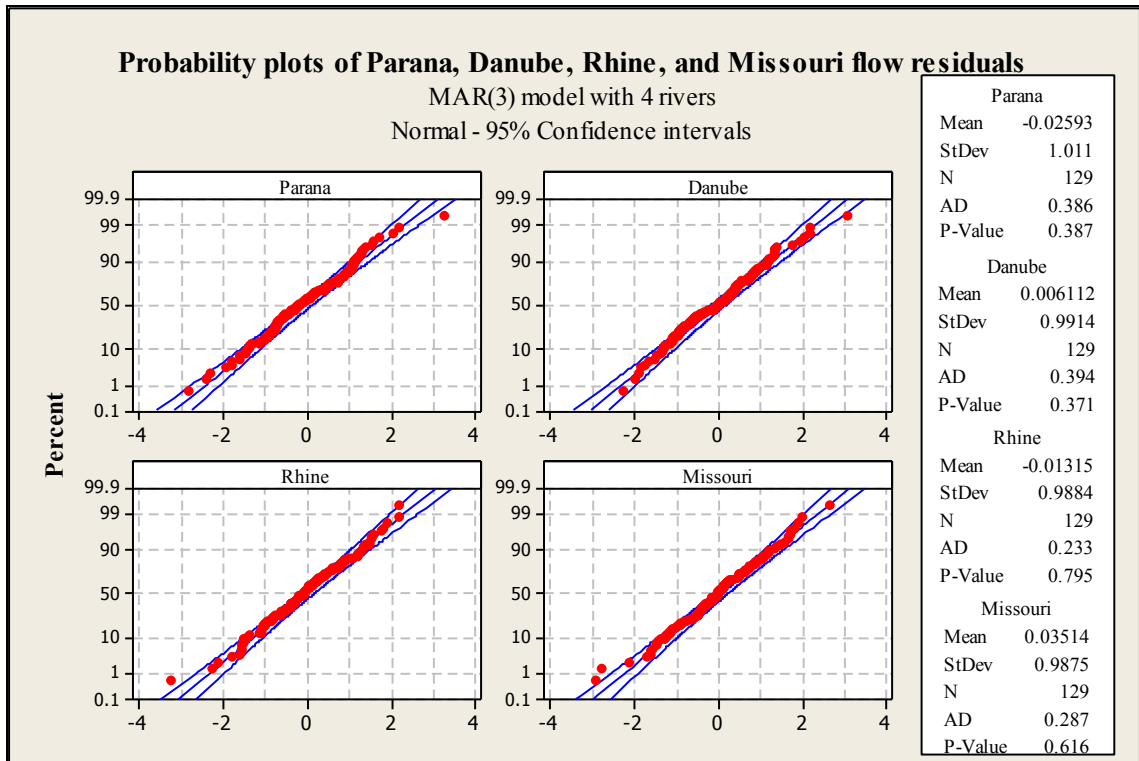
(d)

Figure 4.30. Correlograms of residuals of MAR(3) models: (a) Parana, (b) Danube, (C) Rhine, and (d) Missouri Rivers, respectively.

Besides the correlogram plots, the skewness coefficients of the Parana, Danube, Rhine, and Missouri flow residuals were computed as 0.104, 0.209, -0.089, and -0.163, respectively. These coefficients were well below the critical skewness value of 0.508 for the 2% significance level. The graphical tests were also performed by plotting the histograms and normal probability plots (shown in Figure 4.31). The corresponding p-values for the Parana, Danube, and Rhine rivers were obtained as 0.387, 0.371, 0.791, and 0.616, respectively, which are well above 0.05 (5% significance level). All the above test results indicated that the residuals series were approximately following normal distribution.



(a)



(b)

Figure 4.31. Residuals normality test for MAR(3) model incorporating 4 rivers: (a) Histograms, and (b) normal probability plots of the residuals.

The lag zero cross-correlations matrix \hat{M}_0 was also calculated to see the space independence of the residuals series. Result indicates the off diagonal matrix elements were approximately equal to zero. Therefore, in this study, the residuals were assumed to be independent in space. The estimated lag-zero cross-correlations of the residuals series were found as:

$$\hat{M}_0(\varepsilon) = \begin{bmatrix} 1.000 & 0.010 & 0.009 & -0.017 \\ 0.010 & 1.000 & 0.032 & 0.032 \\ 0.009 & 0.032 & 1.000 & 0.005 \\ -0.017 & 0.032 & 0.011 & 1.000 \end{bmatrix}$$

In addition to the normality and residual independence tests, the MAR(3) models were used to generate the synthetic flows of the four rivers series. Thereafter, the basic statistics (mean, standard deviation, ACF, etc.) of the generated and observed flow series were compared for the evaluation of the resemblance of the two data series. These calculated statistics were summarized in Table 4.13. The table results demonstrated that the statistics of the two data series for each river were nearly equal. The ACF of the two series were also shown to be approximately similar, which indicated that the MAR(3) models can be used to fit the flow data of the four rivers.

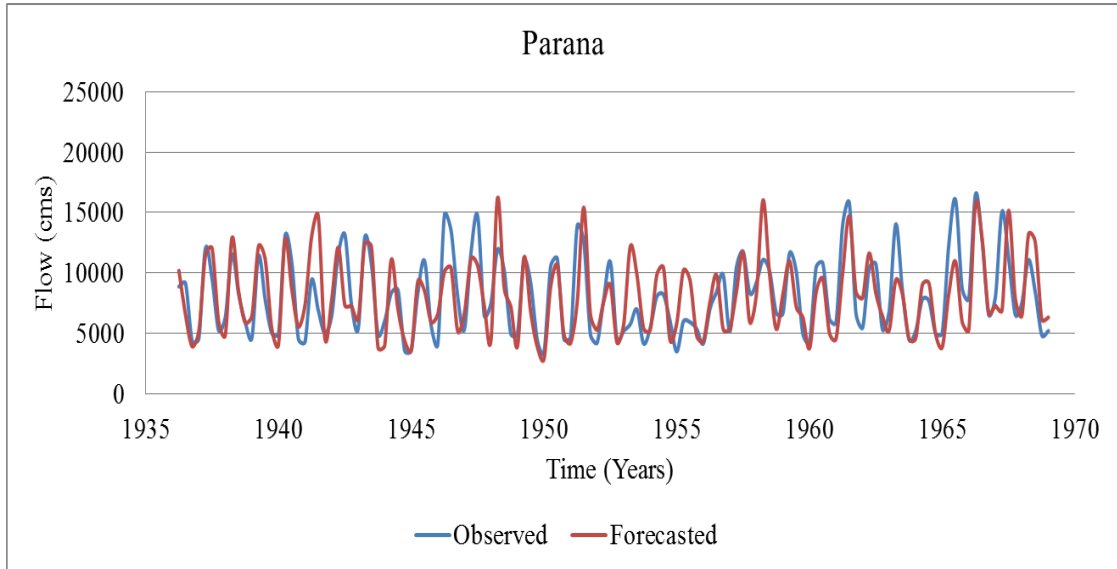
Table 4.13

Comparison between the Observed and Generated Flow Statistics with MAR(3) models for the Parana, Danube, Rhine, and Missouri Rivers

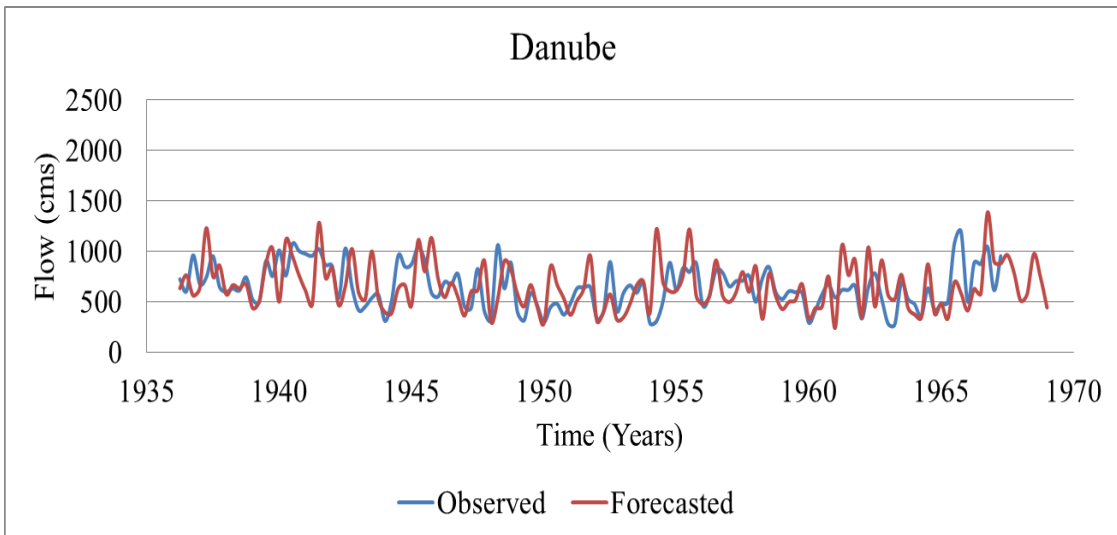
Statistics	Parana		Danube		Rhine		Missouri	
	Obs. Flow	Gen. Flow	Obs. Flow	Gen. Flow	Obs. Flow	Gen. Flow	Obs. Flow	Gen. Flow
Mean	-0.053	-0.048	0.001	-0.025	-0.002	-0.022	-0.001	-0.030
St. Dev.	0.969	0.972	1.010	0.991	1.062	1.042	0.911	0.881
Skew	-0.131	0.016	-0.199	-0.025	-0.389	-0.010	0.095	-0.019
Min	-2.595	-2.569	-2.211	-2.623	-2.417	-2.773	-2.255	-2.270
Max	2.171	2.536	2.156	2.490	2.045	2.674	2.335	2.186
ACF(1)	0.503	0.495	0.431	0.385	0.438	0.403	0.654	0.617
ACF(2)	0.254	0.239	0.427	0.394	0.363	0.336	0.642	0.588

Based on the above analyses, it was decided to apply the MAR(3) models for lead one forecasts of the Parana, Danube, Rhine, and Missouri rivers. Four random number series with mean zero and variance one were generated and used together with the estimated parameters of the calibrated models to forecast the four river flows. These forecasted series Z_t were re-transformed afterwards, and the removed trend components

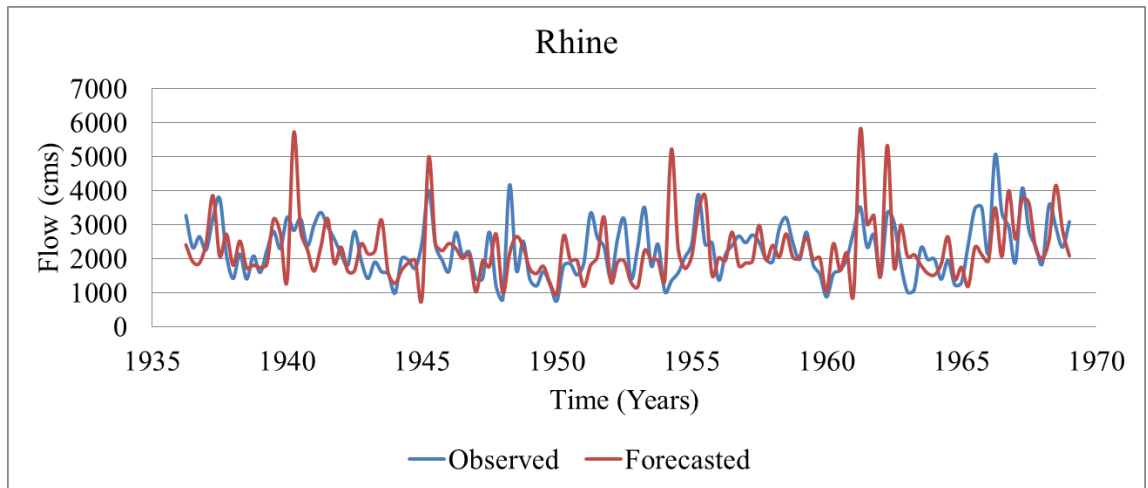
(during data preparation) were added again to get the forecasted flows of the rivers. The plots of the calibrated seasonal forecasts are shown in Figure 4.32.



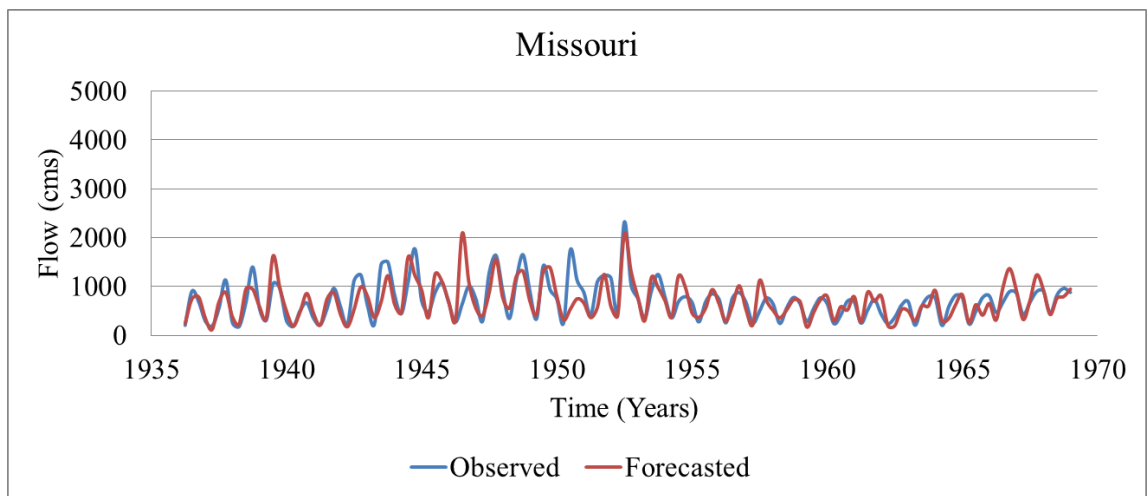
(a)



(b)



(c)



(d)

Figure 4.32. Calibration of the lead one seasonal forecasts of the rivers: (a) Parana; (b) Danube; (c) Rhine; and (d) Missouri, using the MAR(3) model incorporating 4 rivers.

Similar modeling procedure was applied to calculate the parameters of the other multivariate models and the goodness of fit were evaluated by residual analyses and comparing the synthetic and observed flow statistics. Results indicated better MAR(3) model performances for all of the river flows. Therefore, the MAR(3) model

performances were decided to evaluate for combinations of four rivers, SOI, and SSN information incorporated in terms of improving the flow prediction accuracies. The calibrated lead-one seasonal forecasts using MAR(3) model incorporating four rivers with SOI, four rivers with SOI and SSN, and three rivers (Parana, Rhine, and Missouri) with SSN are given in the Appendix B.

The parameter matrices for the MAR(3) model with four rivers and SOI information are:

$$\hat{A}_1 = \begin{bmatrix} 0.495 & 0.013 & -0.049 & -0.021 & -0.082 \\ -0.015 & 0.310 & -0.067 & -0.271 & -0.158 \\ 0.041 & -0.064 & 0.374 & -0.246 & -0.133 \\ 0.042 & -0.104 & 0.008 & 0.377 & -0.086 \\ -0.119 & -0.066 & -0.070 & -0.047 & 0.538 \end{bmatrix} \quad \hat{A}_2 = \begin{bmatrix} -0.103 & -0.010 & 0.093 & 0.026 & 0.144 \\ -0.072 & 0.363 & -0.109 & 0.074 & 0.197 \\ -0.148 & 0.296 & -0.059 & 0.076 & 0.223 \\ -0.033 & 0.265 & -0.282 & 0.393 & -0.060 \\ 0.040 & 0.095 & -0.099 & 0.058 & 0.271 \end{bmatrix}$$

$$\hat{A}_3 = \begin{bmatrix} 0.148 & 0.263 & -0.163 & -0.107 & 0.036 \\ 0.139 & 0.251 & -0.144 & 0.136 & 0.032 \\ 0.202 & 0.161 & -0.088 & 0.085 & 0.072 \\ 0.118 & 0.050 & -0.051 & 0.008 & 0.057 \\ -0.037 & 0.073 & -0.020 & -0.019 & -0.239 \end{bmatrix} \quad \hat{C}_1 = \begin{bmatrix} 0.805 & 0.000 & 0.000 & 0.000 & 0.000 \\ 0.030 & 0.826 & 0.000 & 0.000 & 0.000 \\ 0.035 & 0.763 & 0.440 & 0.000 & 0.000 \\ -0.020 & -0.033 & 0.118 & 0.592 & 0.000 \\ 0.057 & -0.097 & 0.035 & 0.101 & 0.533 \end{bmatrix}$$

The estimated parameter matrices for the MAR(3) model incorporating four rivers with SOI and SSN are:

$$\hat{A}_1 = \begin{bmatrix} 0.485 & 0.042 & -0.063 & -0.017 & -0.079 & 0.202 \\ -0.002 & 0.270 & -0.039 & -0.320 & -0.145 & -0.082 \\ 0.054 & -0.097 & 0.395 & -0.280 & -0.124 & -0.060 \\ -0.062 & -0.154 & 0.025 & 0.393 & -0.101 & -0.091 \\ -0.120 & -0.071 & -0.066 & -0.041 & 0.535 & 0.013 \\ 0.050 & 0.140 & -0.094 & -0.061 & 0.083 & 0.915 \end{bmatrix}$$

$$\hat{A}_2 = \begin{bmatrix} -0.102 & -0.006 & 0.092 & 0.047 & 0.137 & -0.089 \\ -0.064 & 0.331 & -0.105 & 0.112 & 0.167 & -0.447 \\ -0.139 & 0.277 & -0.060 & 0.099 & 0.205 & -0.301 \\ -0.035 & 0.276 & -0.284 & 0.319 & -0.025 & 0.464 \\ -0.034 & 0.092 & -0.094 & 0.045 & 0.274 & 0.112 \\ 0.002 & 0.121 & -0.050 & 0.081 & -0.033 & 0.103 \end{bmatrix}$$

$$\hat{A}_3 = \begin{bmatrix} 0.133 & 0.237 & -0.157 & 0.121 & 0.047 & 0.156 \\ 0.183 & 0.271 & -0.174 & 0.114 & 0.043 & 0.028 \\ 0.238 & 0.181 & -0.113 & 0.072 & 0.081 & 0.013 \\ 0.132 & 0.043 & -0.053 & 0.054 & 0.028 & -0.379 \\ -0.042 & 0.059 & -0.013 & -0.009 & -0.250 & -0.099 \\ -0.026 & -0.097 & 0.083 & -0.010 & 0.055 & -0.044 \end{bmatrix}$$

$$\hat{B} = \begin{bmatrix} 0.013 & 0.000 & 0.000 & 0.000 & 0.000 & 0.000 \\ 0.396 & 0.545 & 0.000 & 0.000 & 0.000 & 0.000 \\ 0.350 & 0.539 & 0.042 & 0.000 & 0.000 & 0.000 \\ 0.116 & 0.367 & 0.090 & 0.636 & 0.000 & 0.000 \\ 0.163 & 0.244 & 0.227 & 0.111 & 0.465 & 0.000 \\ -0.128 & 0.006 & 0.076 & 0.066 & -0.078 & 0.133 \end{bmatrix}$$

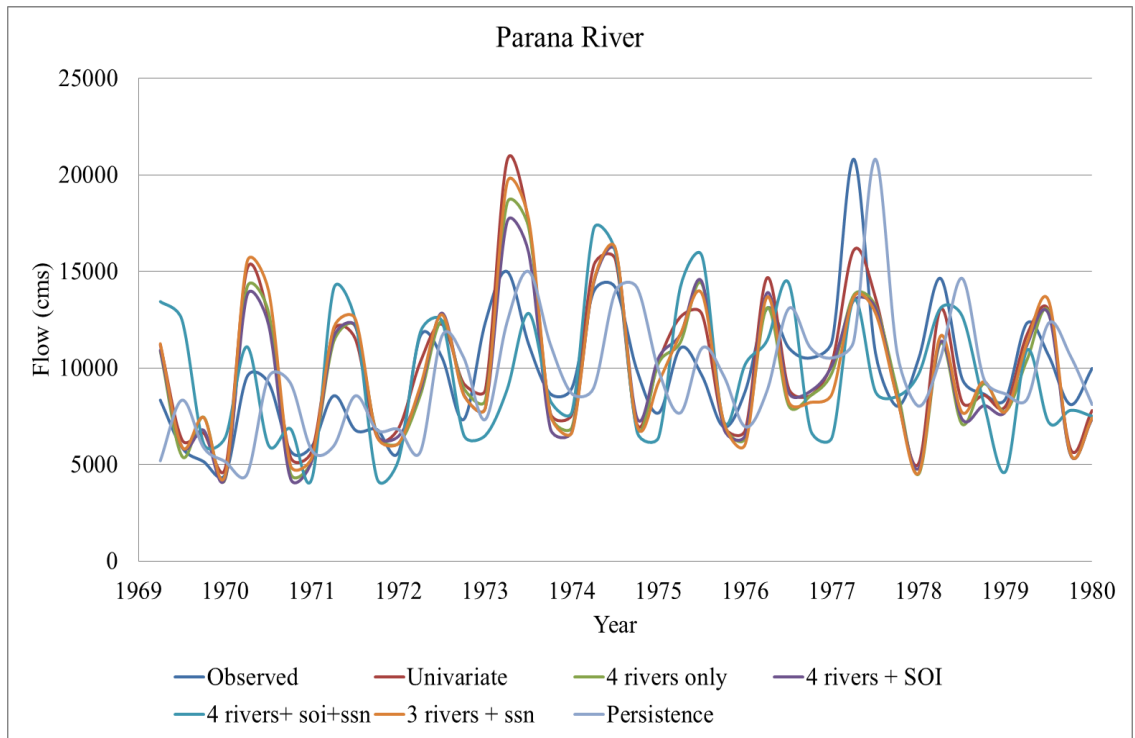
The parameter matrices for the MAR(3) model incorporating three rivers (Parana, Rhine, Missouri) and SSN data are:

$$\hat{A}_1 = \begin{bmatrix} 0.482 & -0.002 & -0.029 & 0.131 \\ 0.050 & 0.352 & -0.302 & 0.362 \\ 0.057 & -0.085 & 0.411 & -0.128 \\ 0.062 & 0.017 & -0.080 & 0.937 \end{bmatrix} \quad \hat{A}_2 = \begin{bmatrix} -0.094 & 0.078 & 0.072 & -0.114 \\ -0.118 & 0.169 & -0.125 & -0.387 \\ -0.021 & -0.028 & -0.306 & 0.431 \\ -0.027 & 0.031 & -0.054 & 0.121 \end{bmatrix}$$

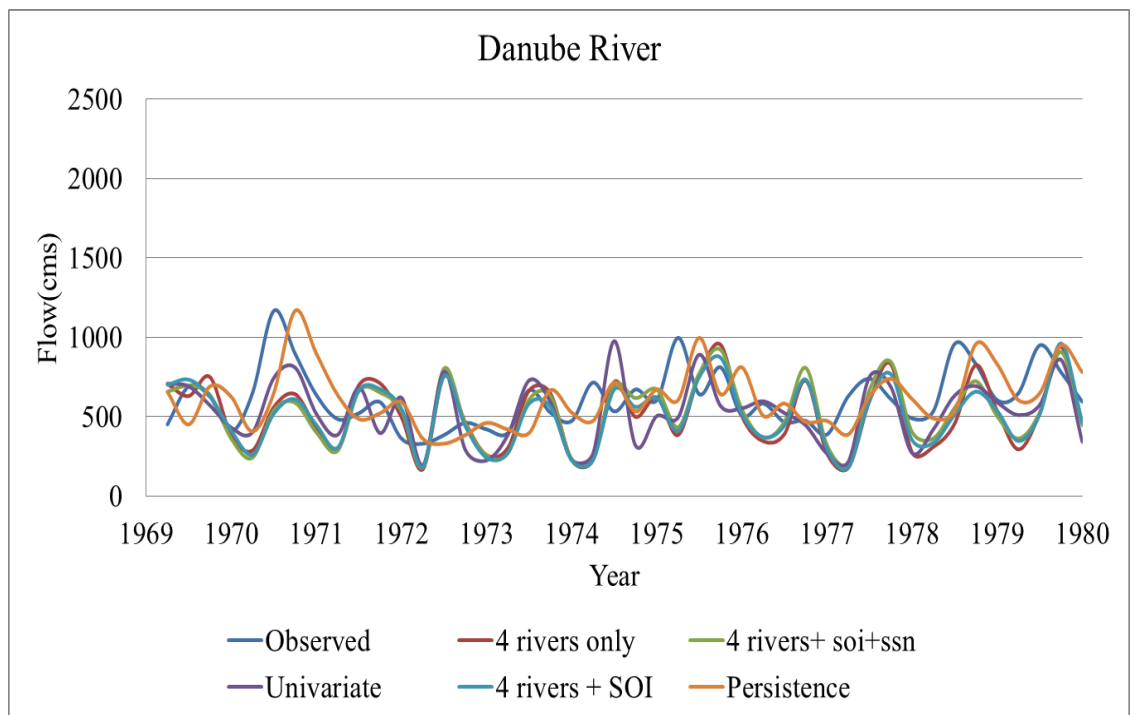
$$\hat{A}_3 = \begin{bmatrix} 0.118 & 0.003 & -0.137 & 0.063 \\ 0.205 & -0.036 & 0.055 & -0.091 \\ 0.128 & -0.030 & 0.035 & -0.394 \\ -0.020 & -0.017 & 0.025 & -0.119 \end{bmatrix} \quad \hat{B} = \begin{bmatrix} 0.813 & 0.000 & 0.000 & 0.000 \\ 0.070 & 0.890 & 0.000 & 0.000 \\ -0.007 & 0.040 & 0.605 & 0.000 \\ 0.028 & -0.010 & 0.044 & 0.304 \end{bmatrix}$$

Validation of the Multivariate AR(3) Model

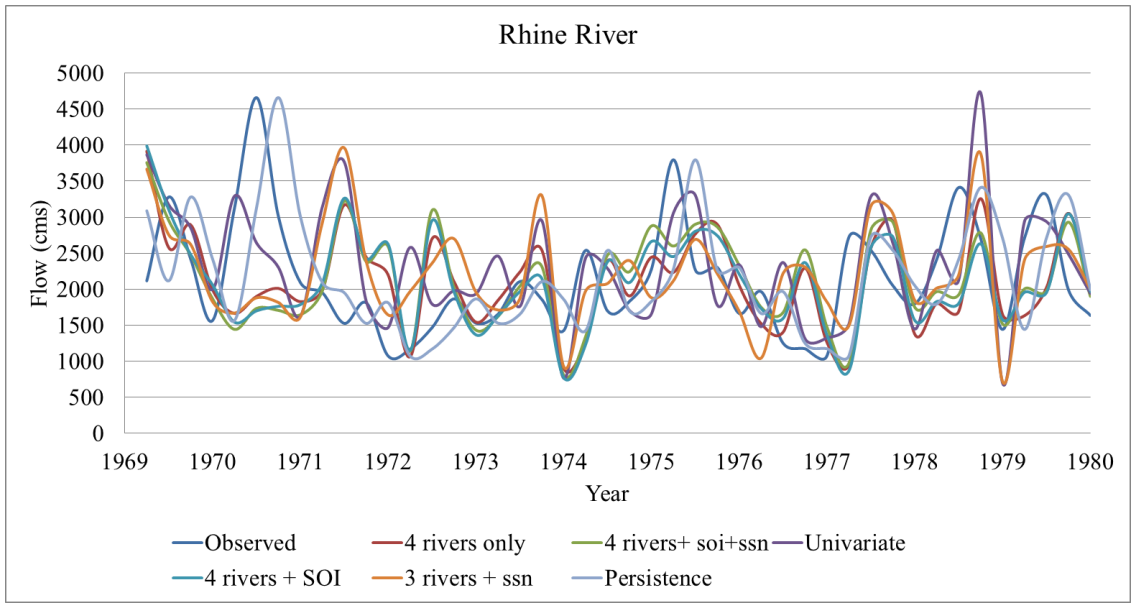
The parameters, obtained during the calibration procedure, were used to validate the model for 1969 to 1979. The persistent model forecast was also performed to compare with the other model results. The plots of the observed and the validated lead-one forecasts are shown in Figure 4.33. The individual model forecasts are shown in the Appendix B.



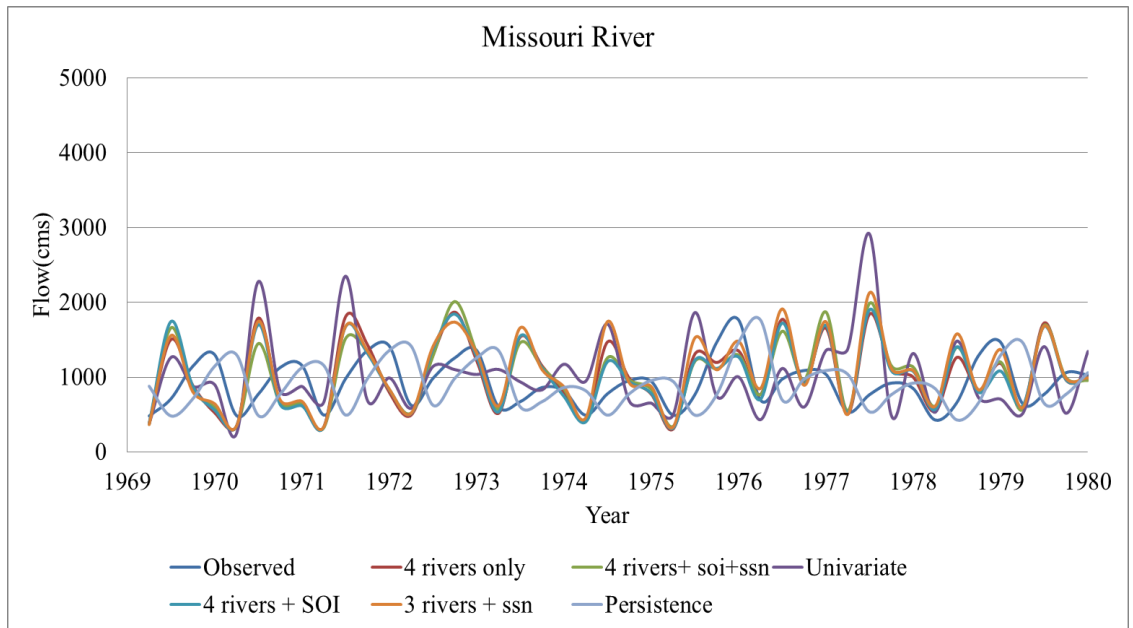
(a)



(b)



(c)



(d)

Figure 4.33. Validated lead-1 seasonal forecasts of the rivers: (a) Parana River, (b) Danube River, (c) Rhine River, and (d) Missouri, using univariate and multivariate time series and persistence models.

4.3.3 Time Series Modeling with Long Term Data Series

In the calibration with the long term flow series, the seasonal flow data of five rivers namely the Congo, Yangtze, Rhine, Columbia, and Parana, from 1906 to 1980 (300 seasons) were used to calculate the parameters of the univariate and multivariate time series models, whereas the series from 1981 to 1999 (76 seasons) were used for the validation of model forecasts. The modeling procedures followed for these analyses were similar to the procedures followed in the modeling of short term flow series, therefore, were not repeated here in order to avoid duplication of the methods.

For the multivariate model analysis, the AR models with the following variable combinations were used to forecast the seasonal flows of the five rivers: (i) MAR model incorporating five rivers, (ii) MAR model incorporating five rivers and SOI (iii) MAR model incorporating five rivers with SOI and SSN, (iv) MAR model incorporating five rivers, SOI, SSN, and PDO, and (v) MAR model incorporating five rivers, SOI, SSN, PDO, and NAO. These combinations of variables were tested with the MAR(3) model, for which the generated flow characteristics matched well with the observed flows. Therefore, this MAR(3) model was selected to forecast seasonal flows of the five rivers. The estimated parameter matrices of the MAR(3) model incorporating five rivers flow information are:

$$\hat{A}_1 = \begin{bmatrix} 0.711 & 0.008 & 0.018 & 0.021 & -0.141 \\ -0.022 & 0.439 & -0.071 & -0.107 & 0.343 \\ 0.143 & 0.032 & 0.434 & -0.051 & 0.129 \\ -0.044 & -0.007 & -0.098 & 0.472 & -0.227 \\ -0.006 & -0.027 & 0.001 & 0.012 & 0.659 \end{bmatrix} \quad \hat{A}_2 = \begin{bmatrix} -0.032 & -0.064 & -0.052 & 0.029 & 0.226 \\ -0.071 & 0.043 & 0.034 & -0.052 & -0.368 \\ -0.109 & -0.046 & 0.072 & -0.023 & -0.007 \\ -0.005 & 0.058 & 0.043 & -0.028 & -0.639 \\ -0.006 & 0.000 & -0.001 & -0.021 & -0.085 \end{bmatrix}$$

$$\hat{A}_3 = \begin{bmatrix} 0.017 & 0.073 & 0.087 & 0.031 & -0.018 \\ 0.107 & 0.008 & -0.088 & 0.020 & -0.169 \\ 0.048 & 0.032 & 0.007 & -0.016 & -0.013 \\ 0.018 & 0.081 & 0.039 & 0.045 & 0.704 \\ -0.016 & -0.003 & 0.005 & 0.014 & 0.075 \end{bmatrix} \quad \hat{C}_1 = \begin{bmatrix} 0.643 & 0.000 & 0.000 & 0.000 & 0.000 \\ 0.031 & 0.837 & 0.000 & 0.000 & 0.000 \\ -0.021 & -0.032 & 0.865 & 0.000 & 0.000 \\ -0.095 & -0.028 & -0.095 & 0.741 & 0.000 \\ 0.013 & 0.018 & 0.012 & -0.001 & 0.178 \end{bmatrix}$$

The estimated parameter matrices for the MAR(3) model incorporating five rivers and SOI data are:

$$\hat{A}_1 = \begin{bmatrix} 0.711 & 0.007 & 0.015 & 0.026 & -0.156 & 0.003 \\ -0.020 & 0.440 & -0.085 & -0.103 & 0.366 & 0.030 \\ 0.159 & 0.040 & 0.432 & -0.035 & 0.056 & -0.215 \\ -0.048 & -0.008 & -0.086 & 0.448 & -0.145 & 0.069 \\ -0.004 & -0.025 & -0.006 & 0.015 & 0.659 & -0.007 \\ -0.006 & 0.038 & -0.065 & -0.065 & -0.318 & 0.601 \end{bmatrix}$$

$$\hat{A}_2 = \begin{bmatrix} -0.029 & -0.064 & -0.052 & 0.033 & 0.218 & -0.032 \\ -0.060 & 0.046 & 0.046 & -0.046 & -0.412 & -0.145 \\ -0.117 & -0.041 & 0.057 & -0.043 & -0.012 & 0.106 \\ -0.013 & 0.054 & 0.050 & -0.034 & -0.609 & 0.074 \\ -0.002 & 0.002 & 0.002 & -0.020 & -0.103 & -0.049 \\ 0.085 & 0.078 & 0.076 & 0.045 & 0.530 & 0.169 \end{bmatrix}$$

$$\hat{A}_3 = \begin{bmatrix} 0.018 & 0.075 & 0.085 & 0.029 & -0.019 & -0.005 \\ 0.100 & 0.010 & -0.094 & 0.006 & -0.144 & 0.095 \\ 0.052 & 0.048 & 0.020 & -0.010 & 0.067 & 0.015 \\ 0.014 & 0.067 & 0.041 & 0.048 & 0.679 & 0.017 \\ -0.018 & -0.001 & 0.004 & 0.008 & 0.092 & 0.036 \\ -0.088 & -0.031 & -0.036 & 0.003 & -0.283 & -0.188 \end{bmatrix}$$

$$\hat{B} = \begin{bmatrix} 0.643 & 0.000 & 0.000 & 0.000 & 0.000 & 0.000 \\ 0.029 & 0.832 & 0.000 & 0.000 & 0.000 & 0.000 \\ -0.022 & -0.029 & 0.853 & 0.000 & 0.000 & 0.000 \\ -0.091 & -0.023 & -0.087 & 0.734 & 0.000 & 0.000 \\ -0.014 & 0.015 & 0.010 & 0.002 & 0.174 & 0.000 \\ 0.056 & 0.034 & -0.004 & 0.063 & -0.040 & 0.636 \end{bmatrix}$$

The estimated parameter matrices for MAR(3) model incorporating five rivers, SOI and SSN are:

$$\hat{A}_1 = \begin{bmatrix} 0.017 & 0.070 & 0.084 & 0.032 & -0.002 & -0.005 & -0.073 \\ 0.102 & 0.011 & -0.094 & 0.004 & -0.153 & 0.095 & 0.043 \\ 0.054 & 0.046 & 0.012 & -0.007 & 0.131 & 0.017 & -0.128 \\ 0.006 & 0.074 & 0.041 & 0.051 & 0.700 & 0.016 & -0.091 \\ -0.019 & -0.001 & 0.005 & 0.008 & 0.081 & 0.036 & 0.020 \\ -0.084 & -0.030 & -0.041 & 0.002 & -0.261 & -0.185 & -0.001 \\ -0.016 & -0.005 & 0.013 & 0.002 & -0.003 & 0.035 & -0.036 \end{bmatrix}$$

$$\hat{A}_2 = \begin{bmatrix} -0.031 & -0.062 & -0.050 & 0.035 & -0.168 & 0.004 & 0.059 \\ -0.062 & 0.045 & 0.045 & -0.045 & -0.402 & -0.146 & -0.037 \\ -0.127 & -0.033 & 0.059 & -0.039 & -0.017 & 0.104 & -0.087 \\ -0.002 & 0.059 & 0.050 & -0.042 & -0.644 & 0.078 & 0.202 \\ -0.001 & 0.001 & 0.002 & -0.021 & -0.101 & -0.049 & 0.006 \\ -0.077 & 0.080 & 0.076 & 0.049 & 0.543 & 0.166 & -0.101 \\ -0.025 & 0.011 & 0.035 & 0.000 & -0.185 & -0.032 & 0.130 \end{bmatrix}$$

$$\hat{A}_3 = \begin{bmatrix} 0.017 & 0.070 & 0.084 & 0.032 & -0.002 & -0.005 & -0.073 \\ 0.102 & 0.011 & -0.094 & 0.004 & -0.153 & 0.095 & 0.043 \\ 0.054 & 0.046 & 0.012 & -0.007 & 0.131 & 0.017 & -0.128 \\ 0.006 & 0.074 & 0.041 & 0.051 & 0.700 & 0.016 & -0.091 \\ -0.019 & -0.001 & 0.005 & 0.008 & 0.081 & 0.036 & 0.020 \\ -0.084 & -0.030 & -0.041 & 0.002 & -0.261 & -0.185 & -0.001 \\ -0.016 & -0.005 & 0.013 & 0.002 & -0.003 & 0.035 & -0.036 \end{bmatrix}$$

$$\hat{B} = \begin{bmatrix} 0.641 & 0.000 & 0.000 & 0.000 & 0.000 & 0.000 & 0.000 \\ 0.030 & 0.832 & 0.000 & 0.000 & 0.000 & 0.000 & 0.000 \\ -0.026 & -0.028 & 0.849 & 0.000 & 0.000 & 0.000 & 0.000 \\ -0.089 & -0.023 & -0.087 & 0.732 & 0.000 & 0.000 & 0.000 \\ -0.013 & 0.015 & 0.012 & 0.003 & 0.174 & 0.000 & 0.000 \\ 0.056 & 0.034 & -0.007 & 0.063 & -0.037 & 0.635 & 0.000 \\ -0.020 & -0.034 & 0.001 & 0.013 & 0.023 & -0.002 & 0.343 \end{bmatrix}$$

The estimated parameter matrices for MAR(3) model incorporating five rivers

SOI, SSN, and PDO are:

$$\hat{A}_1 = \begin{bmatrix} 0.707 & 0.008 & 0.012 & 0.024 & -0.157 & 0.001 & 0.067 & -0.013 \\ -0.017 & 0.434 & -0.075 & -0.100 & 0.383 & 0.025 & -0.008 & -0.071 \\ 0.167 & 0.064 & 0.399 & -0.001 & 0.024 & -0.182 & 0.223 & 0.091 \\ -0.047 & -0.036 & -0.070 & 0.430 & -0.025 & 0.026 & -0.052 & -0.232 \\ -0.005 & -0.027 & -0.003 & 0.015 & 0.658 & -0.007 & -0.032 & 0.001 \\ -0.003 & 0.027 & -0.057 & -0.090 & -0.278 & 0.577 & 0.145 & -0.121 \\ 0.049 & -0.039 & 0.001 & -0.025 & -0.016 & 0.011 & 0.833 & 0.027 \\ -0.019 & -0.040 & -0.044 & -0.009 & 0.123 & -0.165 & -0.143 & 0.656 \end{bmatrix}$$

$$\hat{A}_2 = \begin{bmatrix} -0.029 & -0.063 & -0.052 & 0.044 & 0.224 & -0.030 & -0.031 & -0.035 \\ -0.070 & 0.045 & 0.044 & -0.065 & -0.430 & -0.159 & -0.046 & 0.087 \\ -0.120 & -0.017 & 0.061 & -0.014 & -0.057 & 0.127 & -0.081 & 0.059 \\ -0.013 & 0.049 & 0.039 & -0.053 & -0.639 & 0.049 & 0.158 & 0.026 \\ -0.002 & 0.000 & 0.002 & -0.023 & -0.102 & -0.050 & 0.007 & 0.004 \\ 0.077 & 0.070 & 0.068 & 0.061 & 0.580 & 0.155 & -0.128 & -0.079 \\ -0.024 & 0.009 & 0.037 & -0.006 & -0.175 & -0.032 & 0.139 & -0.020 \\ 0.005 & -0.046 & -0.010 & -0.013 & -0.066 & -0.064 & 0.299 & -0.020 \end{bmatrix}$$

$$\hat{A}_3 = \begin{bmatrix} 0.017 & 0.072 & 0.082 & 0.033 & -0.021 & -0.005 & -0.076 & 0.053 \\ 0.106 & 0.002 & -0.092 & 0.000 & -0.112 & 0.092 & 0.065 & -0.084 \\ 0.049 & 0.062 & 0.014 & 0.014 & 0.057 & 0.049 & -0.159 & 0.089 \\ 0.017 & 0.058 & 0.037 & 0.037 & 0.737 & -0.002 & -0.048 & 0.006 \\ -0.018 & -0.002 & 0.006 & 0.007 & 0.088 & 0.035 & 0.022 & -0.014 \\ -0.079 & -0.034 & -0.047 & -0.007 & -0.273 & -0.198 & 0.012 & 0.097 \\ -0.017 & -0.006 & 0.014 & -0.001 & 0.012 & 0.029 & -0.036 & -0.032 \\ 0.047 & -0.003 & 0.034 & -0.013 & 0.201 & 0.142 & -0.142 & 0.014 \end{bmatrix}$$

$$\hat{B} = \begin{bmatrix} 0.640 & 0.000 & 0.000 & 0.000 & 0.000 & 0.000 & 0.000 & 0.000 \\ 0.032 & 0.829 & 0.000 & 0.000 & 0.000 & 0.000 & 0.000 & 0.000 \\ -0.026 & -0.020 & 0.834 & 0.000 & 0.000 & 0.000 & 0.000 & 0.000 \\ -0.093 & -0.032 & -0.063 & 0.711 & 0.000 & 0.000 & 0.000 & 0.000 \\ -0.013 & 0.014 & 0.013 & 0.002 & 0.174 & 0.000 & 0.000 & 0.000 \\ 0.050 & 0.033 & 0.006 & 0.038 & -0.036 & 0.625 & 0.000 & 0.000 \\ -0.019 & -0.035 & 0.004 & 0.015 & 0.021 & 0.000 & 0.341 & 0.000 \\ 0.001 & -0.075 & 0.020 & 0.028 & 0.078 & -0.020 & 0.019 & 0.649 \end{bmatrix}$$

The estimated parameter matrices for MAR(3) model incorporating five rivers, SOI, SSN, PDO, and NAO data are:

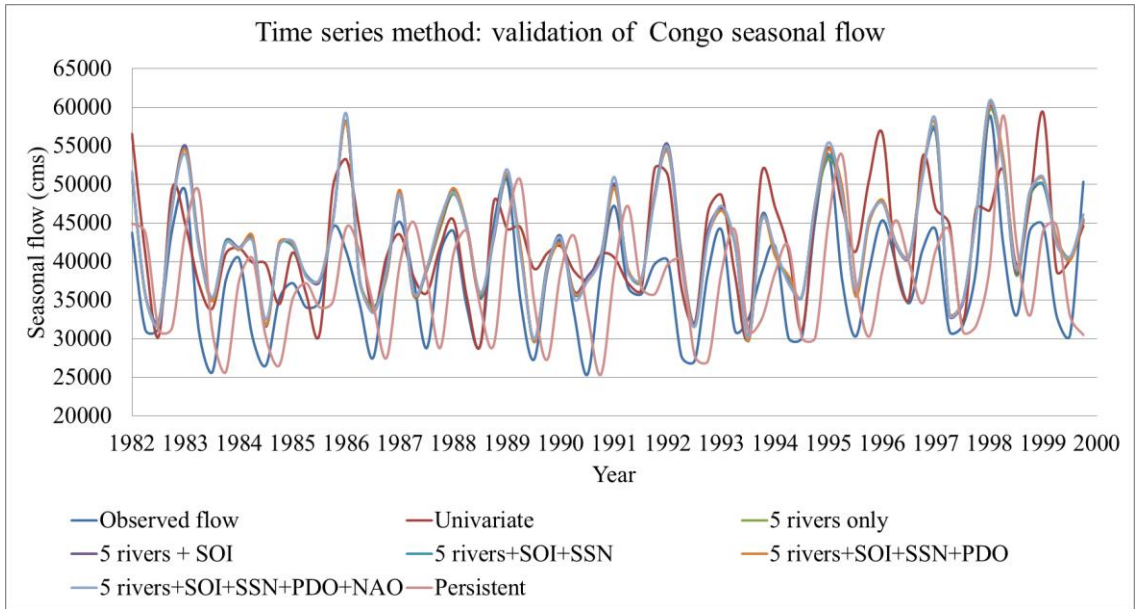
$$\hat{A}_1 = \begin{bmatrix} 0.708 & 0.006 & 0.030 & 0.026 & -0.150 & -0.001 & 0.063 & -0.016 & -0.051 \\ -0.013 & 0.421 & -0.082 & -0.106 & 0.319 & 0.037 & -0.001 & -0.043 & 0.101 \\ 0.138 & 0.078 & 0.418 & 0.010 & 0.063 & -0.195 & 0.229 & 0.063 & -0.182 \\ -0.035 & -0.035 & -0.072 & 0.428 & -0.007 & 0.026 & -0.059 & -0.235 & 0.023 \\ -0.003 & -0.028 & -0.002 & 0.015 & 0.656 & -0.007 & -0.033 & 0.003 & 0.004 \\ -0.005 & 0.032 & -0.055 & -0.088 & -0.258 & 0.573 & 0.143 & -0.130 & -0.035 \\ 0.048 & -0.038 & -0.003 & -0.025 & -0.019 & 0.012 & 0.834 & 0.028 & 0.010 \\ -0.038 & -0.031 & -0.048 & -0.005 & 0.133 & -0.171 & -0.135 & 0.644 & -0.061 \\ 0.116 & 0.033 & -0.009 & 0.111 & 0.041 & 0.028 & 0.103 & -0.063 & -0.025 \end{bmatrix}$$

$$\hat{A}_2 = \begin{bmatrix} -0.018 & -0.069 & -0.064 & 0.044 & 0.198 & -0.016 & -0.025 & -0.025 & 0.059 \\ -0.071 & 0.037 & 0.063 & -0.073 & -0.401 & -0.161 & -0.060 & 0.089 & 0.027 \\ -0.067 & -0.028 & 0.069 & 0.000 & -0.089 & 0.147 & -0.079 & 0.074 & 0.006 \\ -0.036 & 0.057 & 0.022 & -0.055 & -0.644 & 0.042 & 0.165 & 0.019 & -0.009 \\ -0.003 & 0.000 & 0.000 & -0.024 & -0.104 & -0.049 & 0.008 & 0.005 & 0.009 \\ 0.078 & 0.072 & 0.062 & 0.064 & 0.570 & 0.156 & -0.124 & -0.079 & -0.009 \\ -0.025 & 0.010 & 0.041 & -0.006 & -0.169 & -0.035 & 0.137 & -0.022 & -0.013 \\ 0.030 & -0.049 & 0.009 & -0.006 & -0.061 & -0.063 & 0.294 & -0.018 & -0.042 \\ -0.171 & -0.081 & -0.082 & -0.103 & -0.351 & 0.010 & 0.174 & 0.178 & 0.015 \end{bmatrix}$$

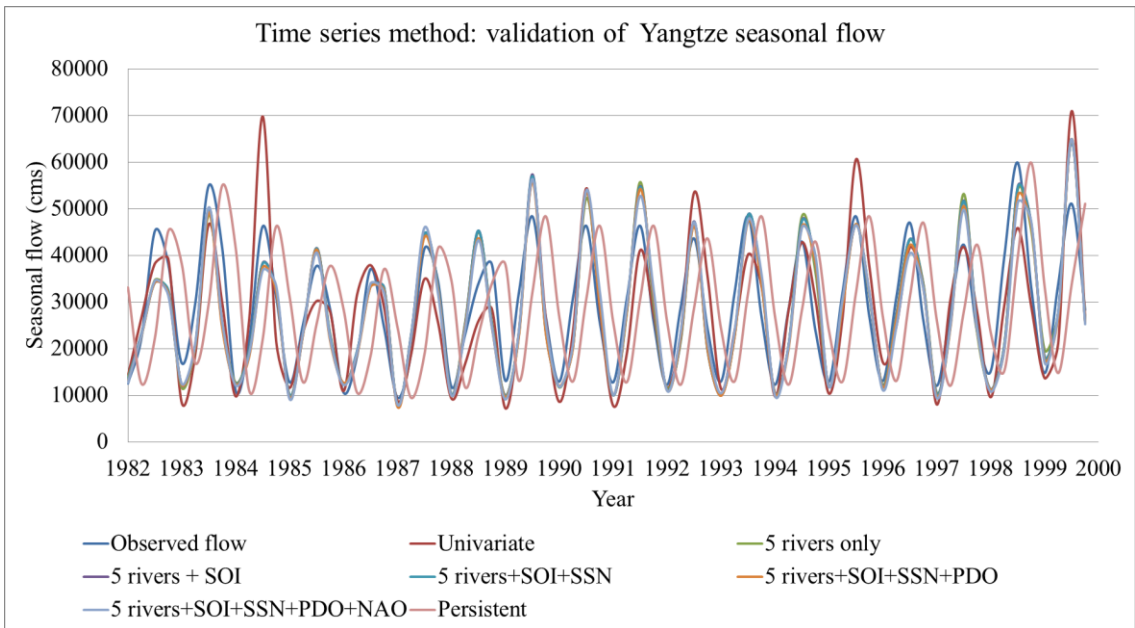
$$\hat{A}_3 = \begin{bmatrix} 0.005 & 0.070 & 0.080 & 0.026 & -0.017 & -0.012 & -0.079 & 0.051 & 0.016 \\ 0.112 & 0.007 & -0.094 & 0.002 & -0.138 & 0.093 & 0.062 & -0.097 & 0.085 \\ 0.016 & 0.046 & -0.020 & -0.006 & 0.045 & 0.054 & -0.165 & 0.113 & 0.092 \\ 0.028 & 0.063 & 0.054 & 0.044 & 0.757 & -0.006 & -0.044 & 0.002 & -0.089 \\ -0.018 & -0.001 & 0.007 & 0.007 & 0.088 & 0.033 & 0.021 & -0.016 & 0.000 \\ -0.081 & -0.036 & -0.047 & -0.008 & -0.266 & -0.198 & 0.013 & 0.101 & -0.024 \\ -0.015 & -0.006 & 0.013 & 0.000 & 0.010 & 0.031 & -0.036 & -0.031 & 0.003 \\ 0.037 & -0.012 & 0.013 & -0.021 & 0.187 & 0.151 & -0.144 & 0.030 & 0.059 \\ 0.022 & 0.063 & -0.048 & -0.016 & 0.461 & -0.021 & -0.237 & -0.080 & 0.016 \end{bmatrix}$$

$$\hat{B} = \begin{bmatrix} 0.635 & 0.000 & 0.000 & 0.000 & 0.000 & 0.000 & 0.000 & 0.000 & 0.000 \\ 0.036 & 0.820 & 0.000 & 0.000 & 0.000 & 0.000 & 0.000 & 0.000 & 0.000 \\ -0.041 & -0.009 & 0.812 & 0.000 & 0.000 & 0.000 & 0.000 & 0.000 & 0.000 \\ -0.089 & -0.026 & -0.053 & 0.707 & 0.000 & 0.000 & 0.000 & 0.000 & 0.000 \\ -0.013 & 0.014 & 0.013 & 0.002 & 0.173 & 0.000 & 0.000 & 0.000 & 0.000 \\ 0.049 & 0.039 & 0.003 & 0.036 & -0.035 & 0.623 & 0.000 & 0.000 & 0.000 \\ -0.017 & -0.036 & 0.006 & 0.016 & 0.021 & 0.001 & 0.341 & 0.000 & 0.000 \\ -0.001 & -0.074 & 0.005 & 0.035 & 0.082 & -0.021 & 0.018 & 0.643 & 0.000 \\ -0.089 & 0.091 & 0.073 & 0.016 & 0.055 & -0.045 & -0.009 & -0.133 & 0.911 \end{bmatrix}$$

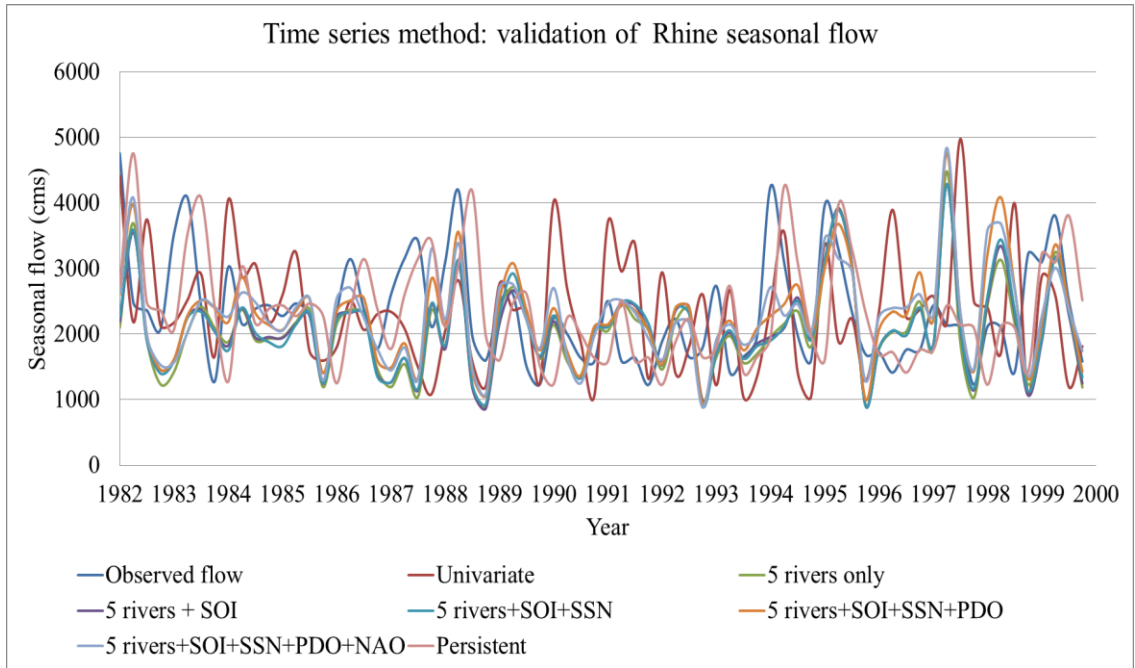
The corresponding plots of the validated seasonal forecasts of the univariate and multivariate time series models for the rivers Congo, Yangtze, Rhine, Columbia, and Parana are shown in Figures 4.34(a) to 4.34(b).



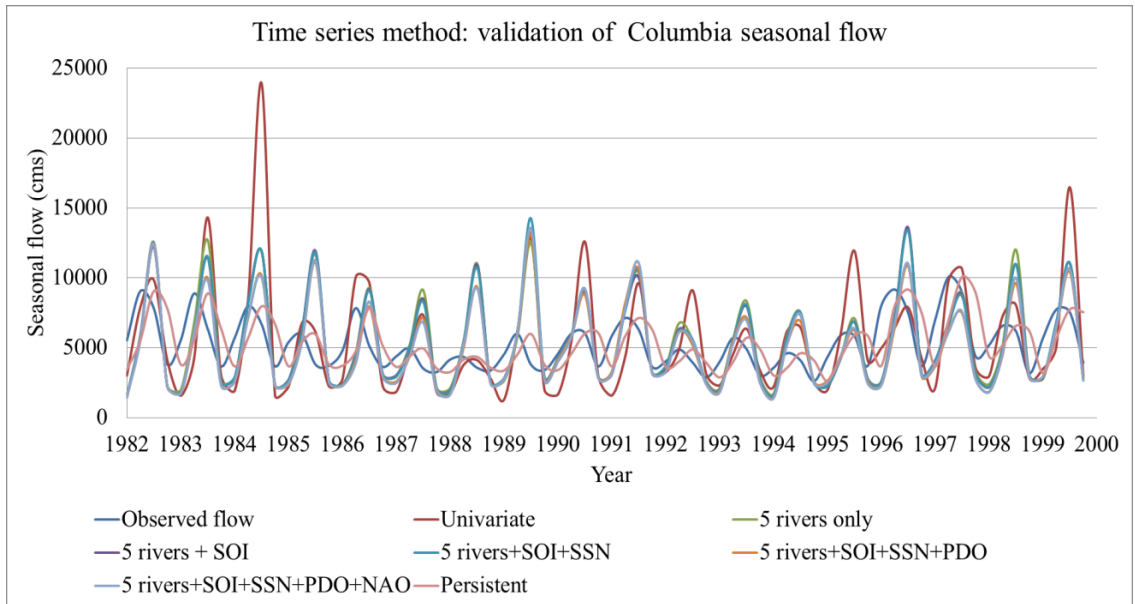
(a)



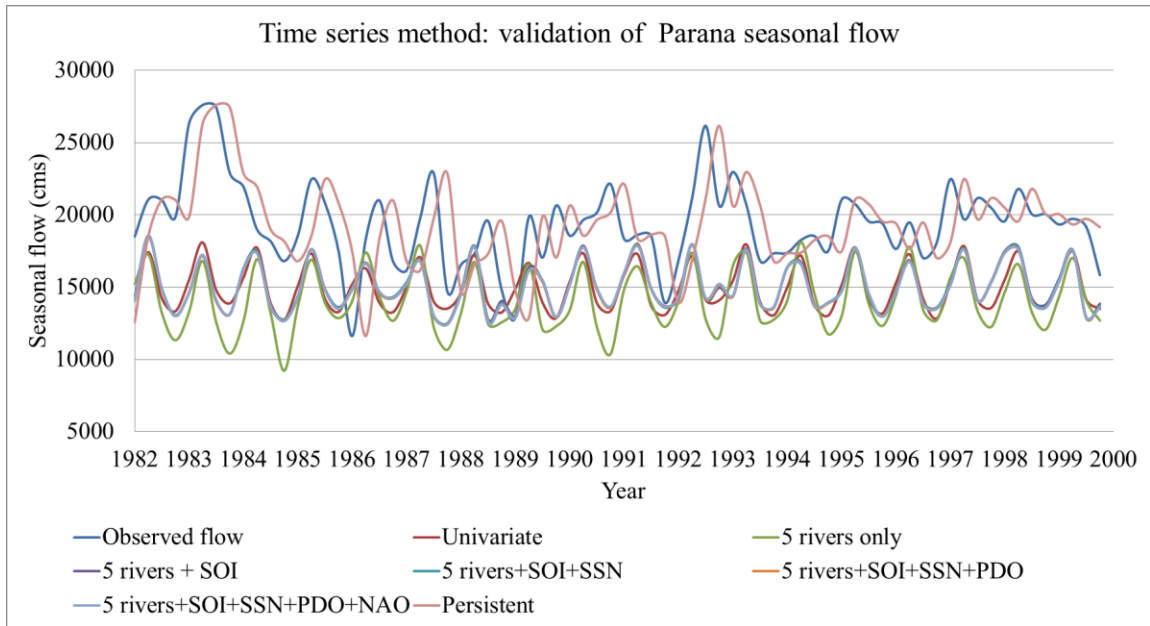
(b)



(c)



(d)



(e)

Figure 4.34. Forecast validation (year 1982 to year 1999) of various time series models for the rivers: (a) Congo; (b) Yangtze; (c) Rhine; (d) Columbia; and (e) Parana

4.4 Model Analysis with Artificial Neural Network Model (ANN)

ANN Modeling for Predicting the Parana, Nile and Murray River

In this analysis, the Parana, Nile, and Murray seasonal flows from 1936 to 1979 (178 seasons) were used as input data. The nonlinear autoregressive ANN (a type of feed forward model) was used to predict seasonal river flows. Future values of a river flow series $y(t)$ are predicted from the past values of the data series incorporating the Parana, Nile, Murray River flows and SSN. The model equation can be expressed as follows:

$$y(t) = f\{x(t-1), x(t-2), \dots, (t-d), y(t-1), y(t-2), \dots, y(t-d)\} \quad (4.5)$$

where, d is the number of delays.

Initial Condition

In this analysis, a total of 44 years (176 seasons) of flow data were used. Among those, 33 years (1936-1968 or 132 seasons) of data were used to train the ANN model. The rest of the flow data from seasons 133-152 and 153 to 176 were used for validating and testing of the models, respectively. Later, these trained models were used to forecast seasonal flows from years 1969 to 1979. Trial and error procedure was adopted for selecting the optimum number of lags and hidden nodes. The forecast values, which yielded the minimum mean square error (MSE) value, were selected for further analysis.

Model Design

Satisfactory generalization of the ANN model depends on proper selection of model architecture determined by appropriate number of inputs, outputs and hidden neurons or nodes (Coulibaly et al., 2001b). In this study, the forecasts were performed using Matlab 2011 Neural Network Toolbox (Beale et al., 2011; Demuth and Beale, 1993). For this, a memory structure is needed so that existing observations can be generalized for future predictions (Coulibaly et al., 2001). Selection of predictors, model lags, and hidden nodes is also vital in this respect. A brief discussion about the procedure of selecting predictor variables, lags, and hidden nodes is included in the following sections.

Selection of Predictors

In the analysis, a total of four variables, including three river flows and SSN, were incorporated to evaluate the importance of the variables in predicting corresponding river

flows. Similar to the time series methodology, the ANN modeling procedure was divided into two categories: (a) Univariate ANN model and (b) multivariate ANN model. The univariate model is based solely on persistent characteristics of the flow, whereas the multivariate ANN model considers persistence as well as external variables. The idea was to calculate forecast performances based solely on historical characteristics of the flow. Thereafter, other river flow variables, including the SSN, were incorporated as multivariate forms to find out better models. The performance indices described in Chapter 3 were adopted to evaluate the prediction skills of different models used in the analysis.

Selection of Lags

In order to determine the lagged relationships between the variables, the autocorrelation, partial autocorrelation, and cross-correlation plots were adopted in this analysis. The autocorrelation and partial autocorrelation plots provide initial ideas about significant lags based on persistence characteristics (time dependence) of the flow. Conversely, cross-correlation plots show the spatial dependence of the river flow series. The correlation plots indicate lags from two to eight could be useful to describe significant relationships. Therefore, trial and error procedure was adopted to determine the significant correlations from lags two to eight. The lag, for which the root mean square error (RMSE) of the forecasts was minimum, was selected for further analysis.

The ANN architecture was formed using river flows and external variables as inputs and corresponding observed river flows as outputs with a certain number of hidden

nodes in between. The procedure followed to determine the optimum numbers of hidden nodes is described in the following section.

Selection of Hidden Nodes

Selection of an appropriate number of hidden nodes or neurons is necessary for proper training and generalization of an ANN model. However, using too many neurons often over-trains the model. Overtraining refers to a situation when network performances are better for the training data sets, but poor for the independent test data sets (Bowden et al., 2012). In addition, too many neurons make the model computationally very complex and time consuming, whereas too few neurons or nodes can lead to a poorly trained model (Coulibaly et al., 2001b). Therefore, the number of hidden nodes needs to be carefully selected so that the data will neither be over fitted nor under fitted.

No standard methods have been developed so far to determine the optimum number of hidden nodes (Coulibaly et al., 2001b). Therefore, trial and error procedure, which requires inclusion of input variables and evaluation of performance with varying numbers of hidden nodes, was adopted. At the beginning, five hidden nodes were chosen to perform the analysis. Afterwards, the nodes were increased from 5 to 10, 20, 50 and 100, and the corresponding RMSE statistics were also calculated for evaluating the model performances. These numbers were chosen in such a way that the training could be done within a short period of time and allow adequate learning by providing enough working space within the ANN structure (French et al., 1992). The goal was to prevent over fitting or overtraining of the ANN models due to a higher number of hidden nodes. This

procedure was carried out for all models incorporating various input variables. The nodes for which the estimated RMSE value was the lowest were chosen for further analysis.

However, using a higher number of iterations also over-trains the ANN models. Therefore, selection of an optimum number of iterations is also necessary for a successful ANN training. A technique called “Early Stopping” was adopted here to avoid the over fitting problem due to higher numbers of iterations. It works by training the model initially and cross-checking the forecast accuracy of the validation data set using mean square error (MSE) statistics. The smaller the MSE value, the better the training. In this analysis, the trainings were designed to stop once the MSE statistics were not decreasing up to six iterations.

Training of the ANN models

The RMSE results of the univariate ANN models for selecting optimum number lags and hidden nodes are summarized in Table 4.14 to 4.16 for the rivers Murray, Parana, and Nile, respectively. The Figure 4.35 was also plotted for better visualization of the RMSE results. For the river Murray, the table results and plots demonstrated that the ANN models incorporating lag 4 with 5 hidden nodes and lag 7 with 100 hidden nodes yielded lower RMSE values of 197cms and 195 cms, respectively. The two RMSE values were almost equal; therefore, the higher number of lags and hidden nodes was neglected and lag 4 with 5 hidden nodes was selected. Similarly, for the Parana and Nile Rivers, the ANN models incorporating lag 7 with 5 hidden nodes and lag 8 with 5 hidden nodes showed better performance, yielding lower RMSE values, respectively. These lags and hidden node combinations were selected for further analyses.

Table 4.14

Performance of the Univariate ANN Model for the Murray River with Different Numbers of Lags and Hidden Nodes

No. of Lags	RMSE (cms)				
	Hidden nodes 5	Hidden nodes 10	Hidden nodes 20	Hidden nodes 50	Hidden nodes 100
Lag 2	478	536	459	599	506
Lag 3	277	635	566	248	295
Lag 4	197	234	296	286	294
Lag 5	294	366	224	432	266
Lag 6	330	236	375	337	375
Lag 7	201	234	261	337	195
Lag 8	227	226	192	281	209

Table 4.15

Performance of the Univariate ANN Model for the Parana River with Different Numbers of Lags and Hidden Nodes

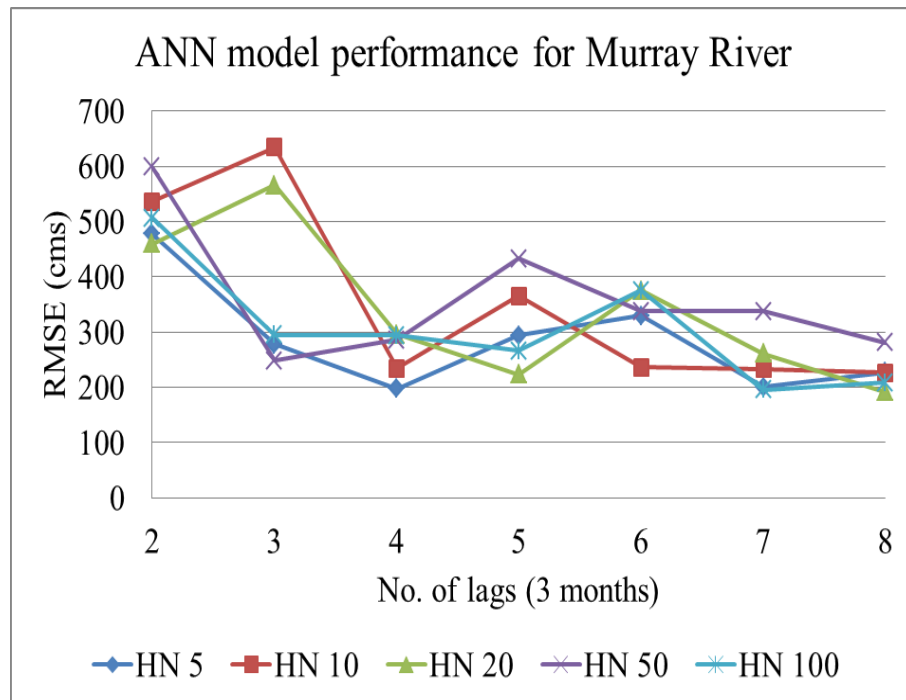
No. of Lags	RMSE (cms)				
	Hidden nodes 5	Hidden nodes 10	Hidden nodes 50	Hidden nodes 100	Hidden nodes 500
Lag 2	3237	2407	4487	4456	4102
Lag 3	2812	2980	4100	3858	3833
Lag 4	2847	2689	5356	3160	5066
Lag 5	3027	2866	3851	5410	5975
Lag 6	2574	2419	3556	3657	2712
Lag 7	2313	3132	2779	2918	6294
Lag 8	2927	3236	3657	2575	4100

Table 4.16

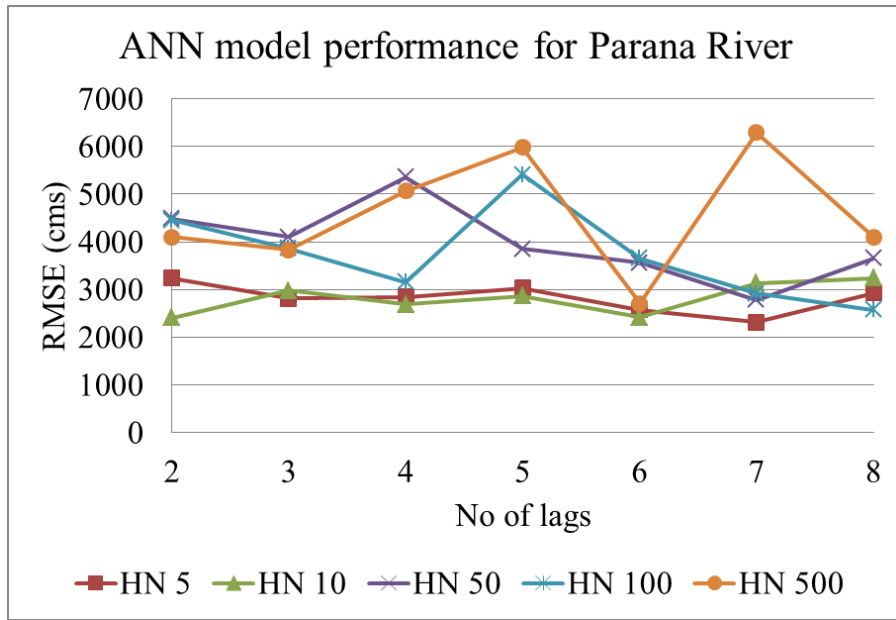
Performance of the Univariate ANN Model for the Nile River with Different Number of

Lags and Hidden Nodes

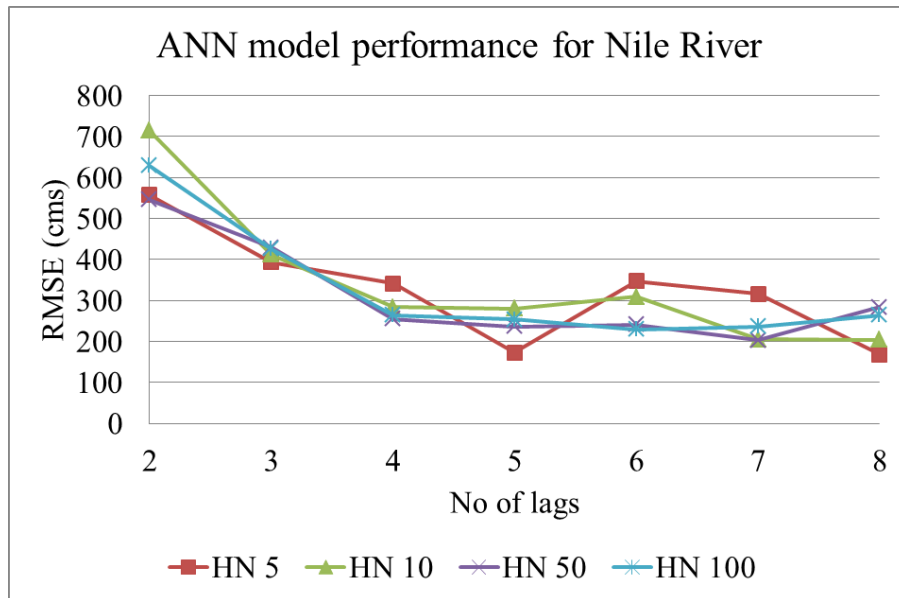
No. of Lags	RMSE (cms)			
	Hidden nodes 5	Hidden nodes 10	Hidden nodes 50	Hidden nodes 100
Lag 2	557	714	546	629
Lag 3	393	412	429	426
Lag 4	341	283	255	264
Lag 5	173	280	236	254
Lag 6	347	309	241	229
Lag 7	315	205	203	237
Lag 8	168	204	284	264



(a)



(b)



(c)

Figure 4.35. ANN model performance (RMSE) analysis with various numbers of lags and hidden nodes (HN) for model type: (a) Univariate ANN model for the Murray River; (b) Univariate ANN model for the Parana River; (c) Univariate ANN model for the Nile River.

The multivariate ANN model analyses were performed using all possible combinations of the predictor variables such as Parana-Nile, Parana-Murray, Nile-Murray, and Nile-Parana-Murray river flows. Thereafter, the SSN was incorporated with the Parana and Murray flows to see forecast improvements. Similar to the univariate models, the trial and error analyses were carried out for the multivariate models to determine the optimum number of lags and hidden nodes. Results are summarized in Tables 4.17 to 4.21 and shown in Figures 4.36(a) to 4.36(h). From the figures, it is evident that lag and hidden node combinations of (6, 20), (7, 20), (5, 10), (3, 5), and (4, 10) produced lower RMSE values. These combinations were subsequently selected to include in the ANN model trainings.

Table 4.17

Performance of the Multivariate ANN Model incorporating Parana and Nile Rivers

No of Lags	RMSE (cms)				
	Hidden nodes 5	Hidden nodes 10	Hidden nodes 20	Hidden nodes 50	Hidden nodes 100
Lag 2	2513	2557	2360	2500	2691
Lag 3	2023	1997	2487	1940	2060
Lag 4	2015	1799	1827	1806	2448
Lag 5	1861	2077	1751	2009	1637
Lag 6	2212	1949	1651	2092	2558
Lag 7	2251	1794	1875	2007	2192
Lag 8	1988	1941	2188	1712	2214

Table 4.18Performance of the Multivariate ANN Model incorporating Parana and Murray Rivers

No of Lags	RMSE (cms)				
	Hidden nodes 5	Hidden nodes 10	Hidden nodes 20	Hidden nodes 50	Hidden nodes 100
Lag 2	2585	2572	2096	2745	2664
Lag 3	1906	2294	2115	2076	2667
Lag 4	2061	2169	2157	2534	2585
Lag 5	2012	2097	2183	2156	1960
Lag 6	1823	1913	1991	2174	1845
Lag 7	1888	2072	1769	2501	2111
Lag 8	2023	2116	2082	2050	2142

Table 4.19Performance of the Multivariate ANN Model incorporating Nile and Murray Rivers

No of Lags	RMSE (cms)			
	Hidden nodes 5	Hidden nodes 10	Hidden nodes 50	Hidden nodes 100
Lag 2	698	801	783	597
Lag 3	407	402	479	528
Lag 4	368	312	358	357
Lag 5	420	269	405	339
Lag 6	383	318	414	492
Lag 7	342	367	413	363
Lag 8	382	368	405	493

Table 4.20

Performance of the Multivariate ANN Model incorporating Parana, Nile and Murray

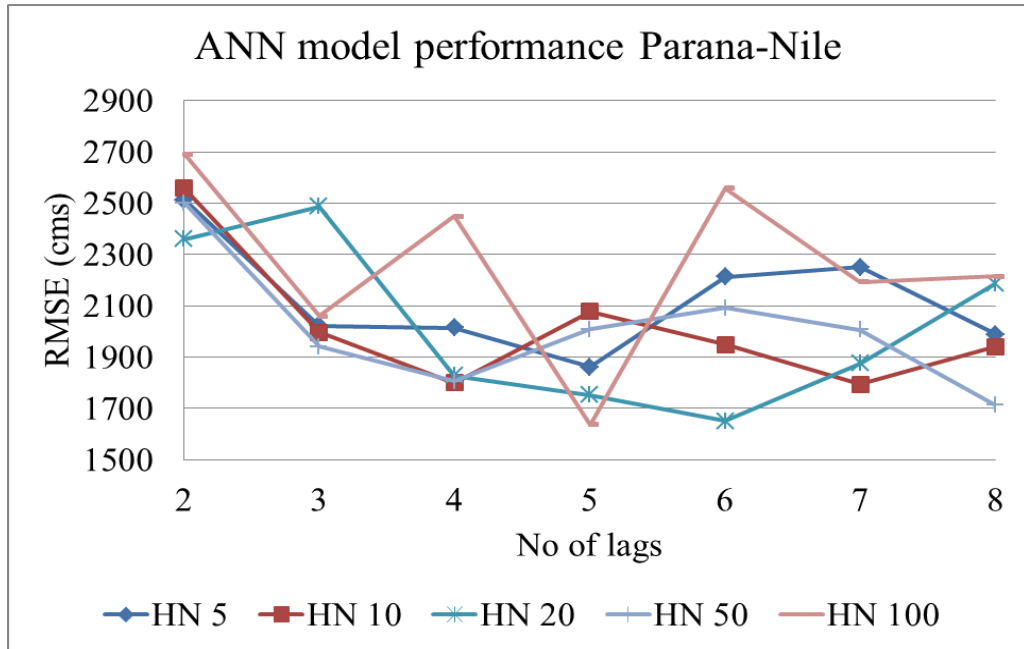
Rivers

No of Lags	RMSE (cms)				
	Hidden nodes 5	Hidden nodes 10	Hidden nodes 20	Hidden nodes 50	Hidden nodes 100
Lag 2	1945	2064	2177	1898	2185
Lag 3	1335	1623	1741	1808	2041
Lag 4	1568	1694	1709	1819	1916
Lag 5	1696	1687	1850	1549	2219
Lag 6	1708	1780	1612	1858	1880
Lag 7	1524	1712	1705	2089	2089
Lag 8	1675	1838	2079	2181	2030

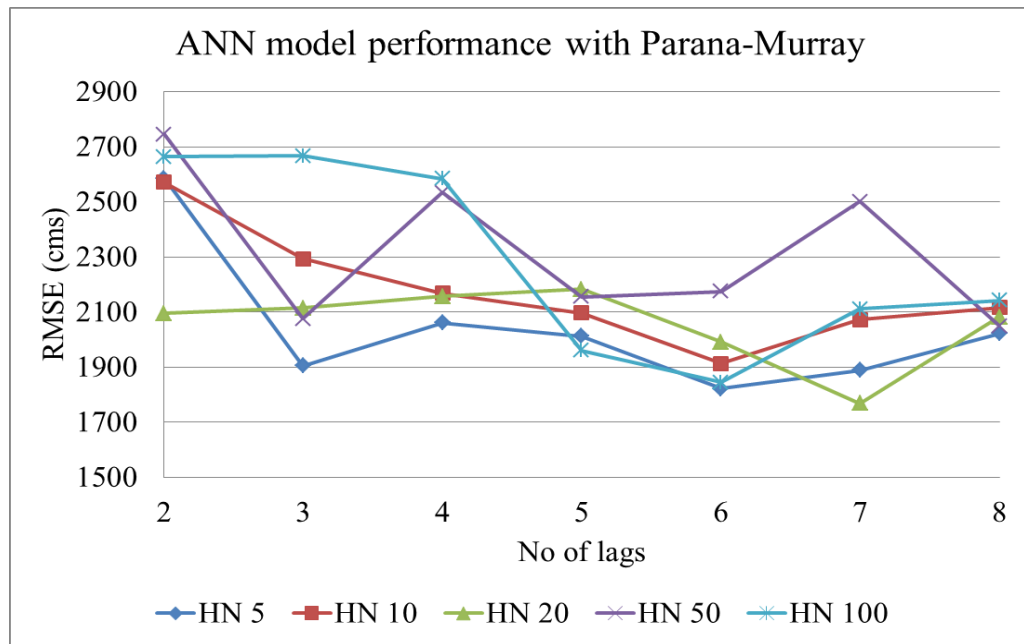
Table 4.21

Performance of the Multivariate ANN Model Incorporating Parana, Murray, and SSN

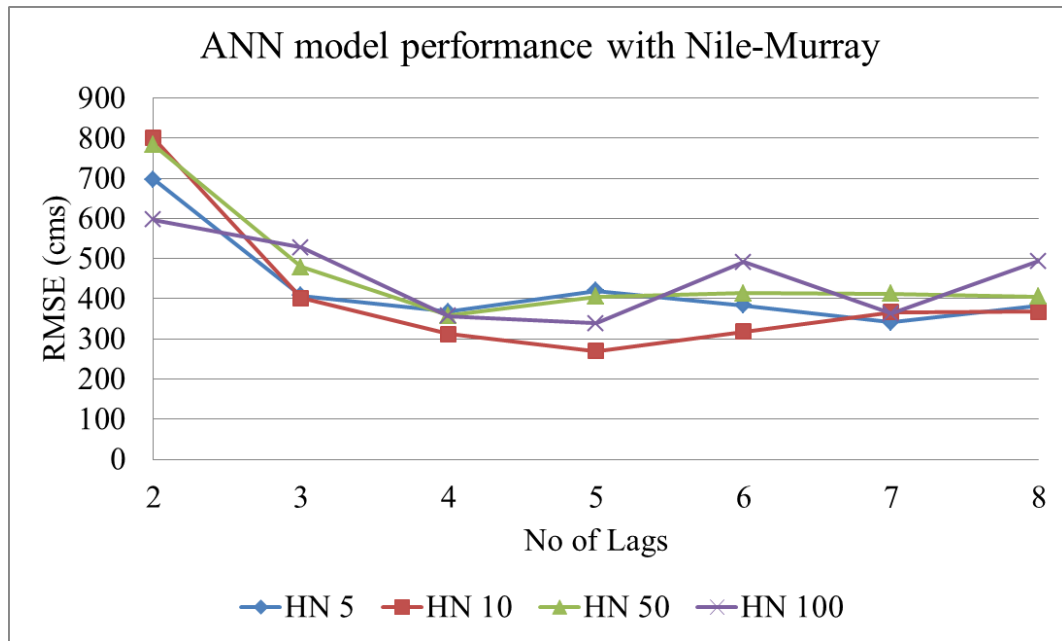
No of Lags	RMSE (cms)				
	Hidden nodes 5	Hidden nodes 10	Hidden nodes 20	Hidden nodes 50	Hidden nodes 100
Lag 2	2074	2104	2128	2157	2150
Lag 3	1622	1718	1875	1837	1685
Lag 4	1487	1434	1605	1617	1595
Lag 5	1768	1782	1463	1528	1960
Lag 6	1545	1724	1766	1487	2524
Lag 7	1570	1690	1797	1676	1622
Lag 8	1489	1746	1654	1760	1768



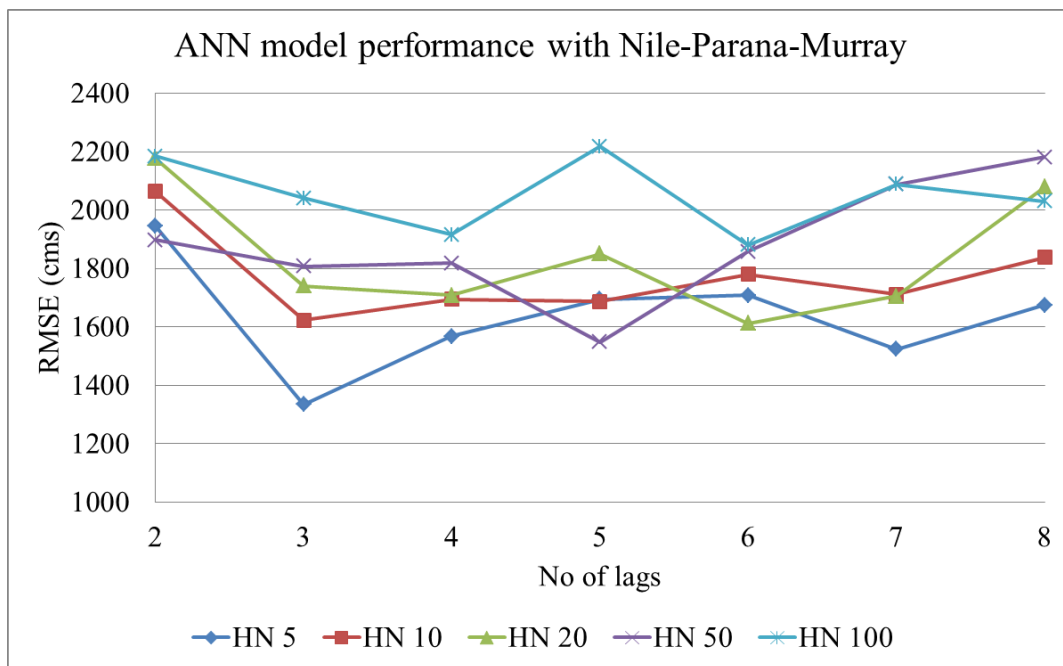
(a)



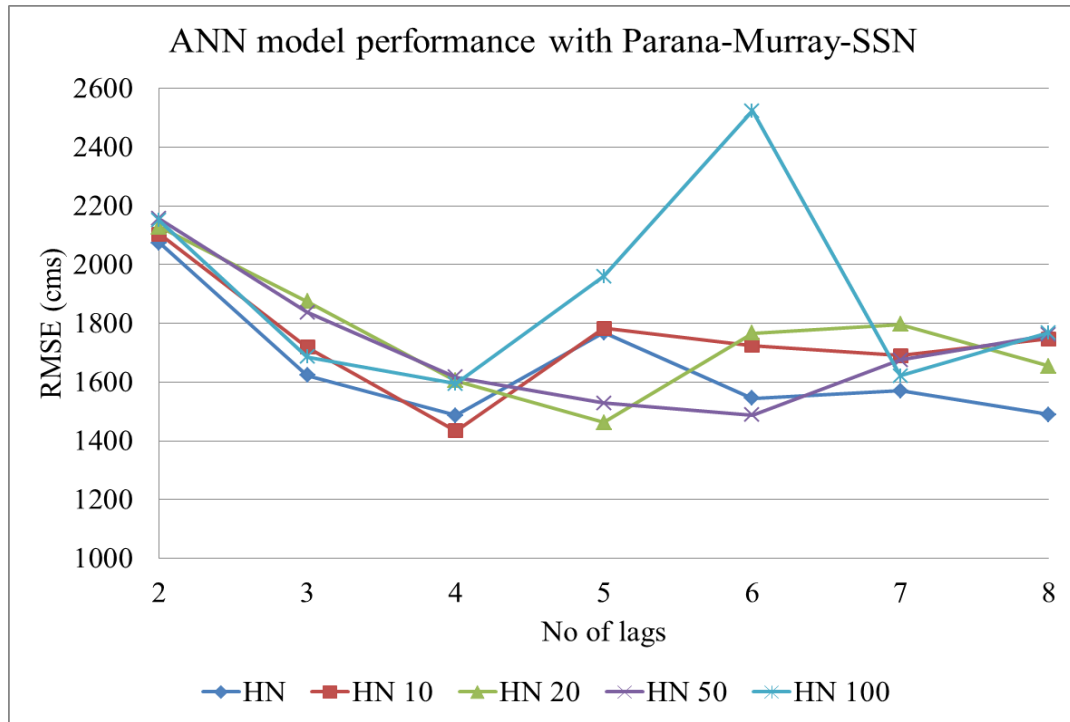
(b)



(c)



(d)

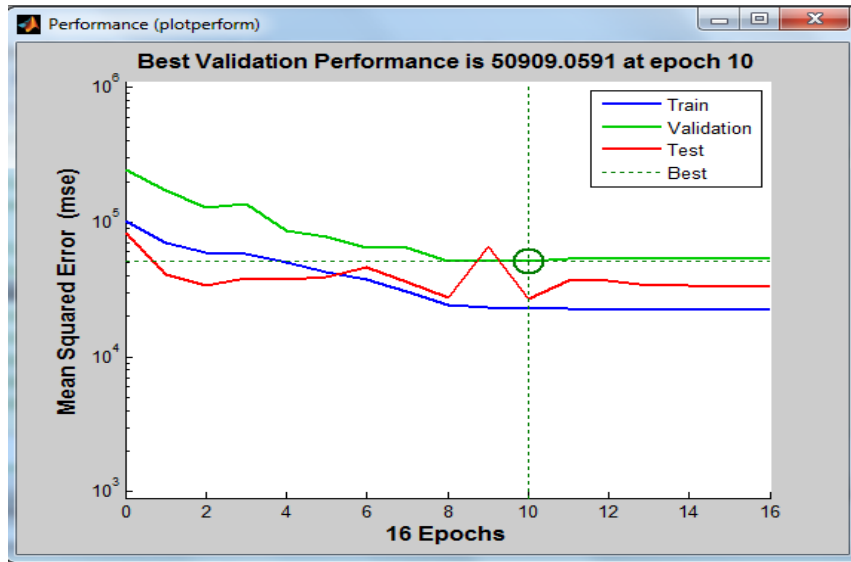


(e)

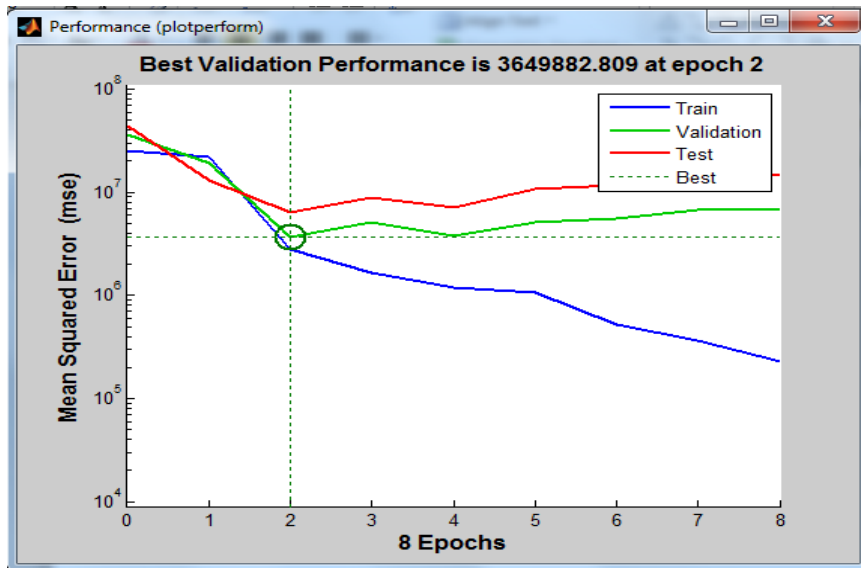
Figure 4.36. ANN model performance (RMSE) analysis with various numbers of lags and hidden nodes (HN) for the multivariate model type incorporating (a) Parana-Nile model; (b) Parana-Murray model; (c) Nile-Murray model; (d) Nile-Parana-Murray or all-river model; and (e) Parana-Murray-SSN model.

The performance plots of the univariate Murray, Parana, and Nile River models indicate the trainings stopped at the 10th, 1st, and 5th epochs, respectively. For the multivariate ANN models incorporating Parana-Nile, Parana-Murray, Nile-Murray, Nile-Parana-Murray, and Parana-Murray-SSN, the trainings stopped at the 2nd, 6th, 6th, 5th, and 2nd epochs, respectively. This indicates the calculated MSE errors were not decreasing after those points. Therefore, the model weights obtained at these epochs were used to test the three river flow predictions. The performance plots (indicating best epochs) of the

univariate Murray and multivariate Parana-Nile models are shown in Figure 4.37. The rest of the plots are included in Appendix B.



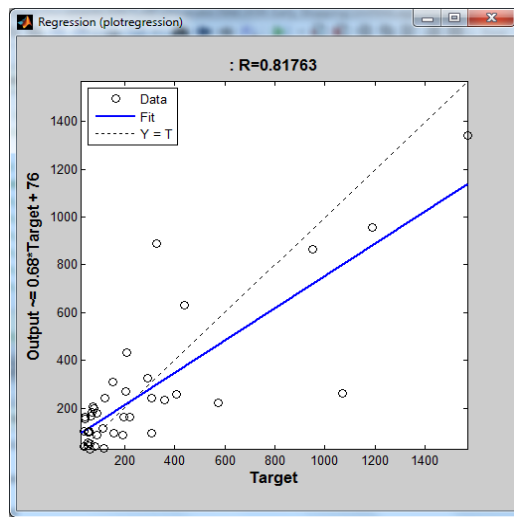
(a)



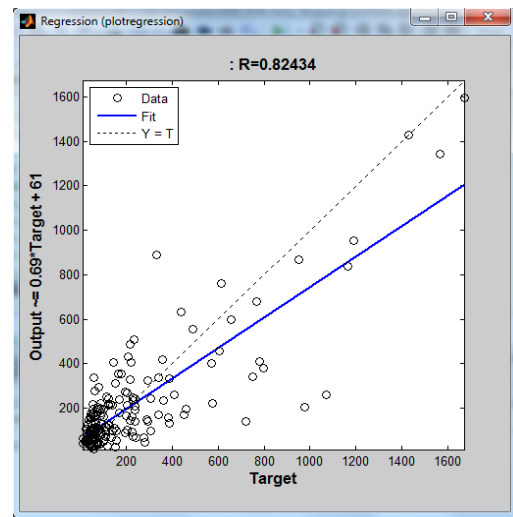
(b)

Figure 4.37. Performance plots when the ANN training stopped (a) Univariate Murray model; and (b) Multivariate Parana-Nile model.

The regression plots of the trained and tested univariate Murray, Parana, and Nile models are shown in Figures 4.38(a) to 4.38(c). The plots for the multivariate models are shown in Figures 4.39(a) to 4.39(e).

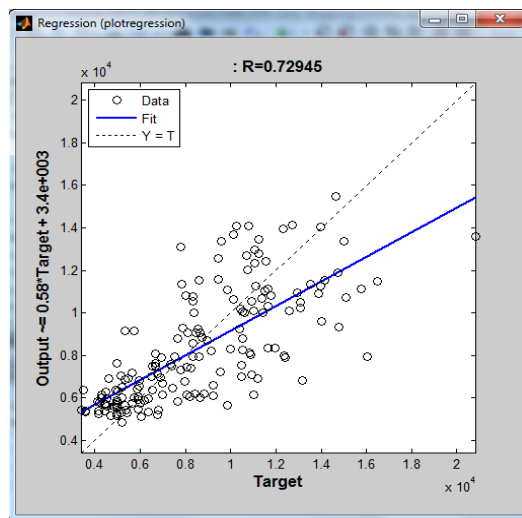


(i)

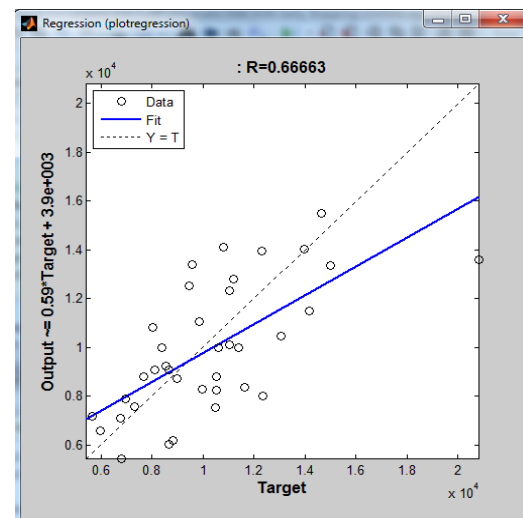


(ii)

(a)

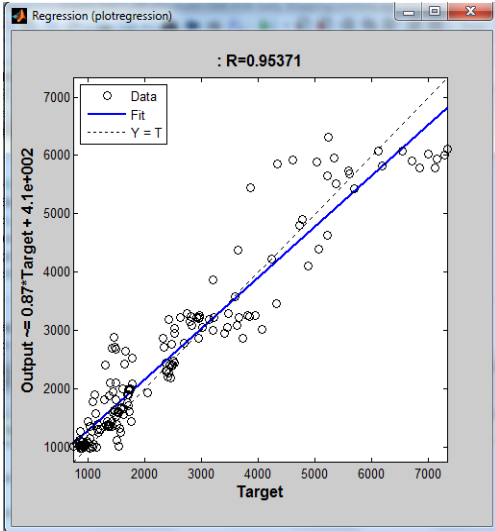


(i)

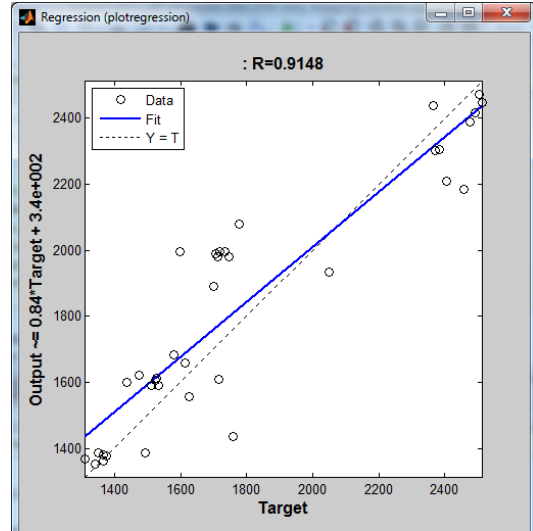


(ii)

(b)



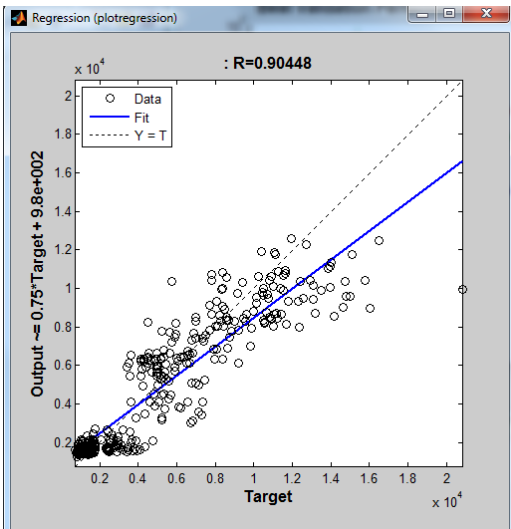
(i)



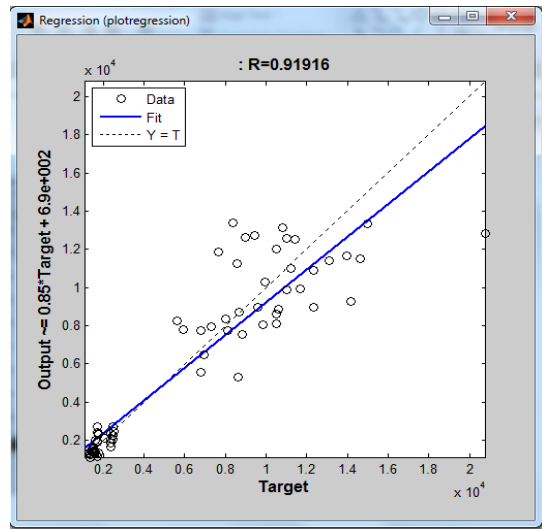
(ii)

(c)

Figure 4.38. Regression plots of univariate ANN models for the rivers: (a) Murray; (b) Parana; and (c) Nile seasonal flows. Here, (i) trained data sets and (ii) test data sets.

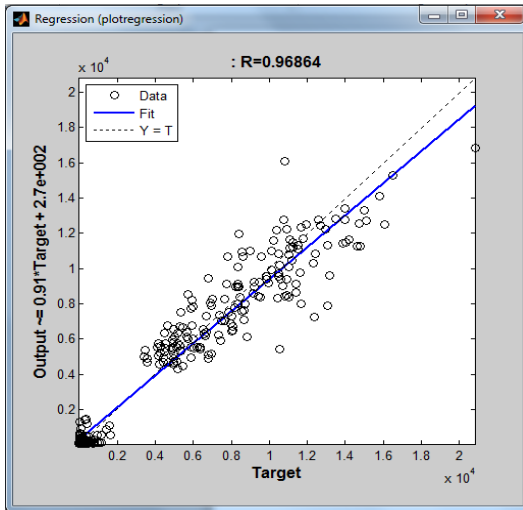


(i)

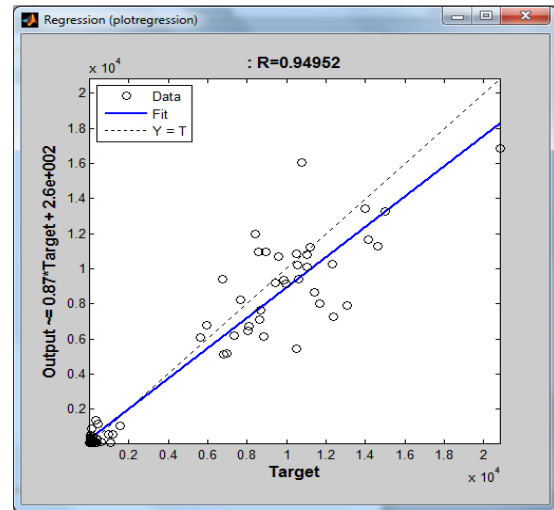


(ii)

(a)

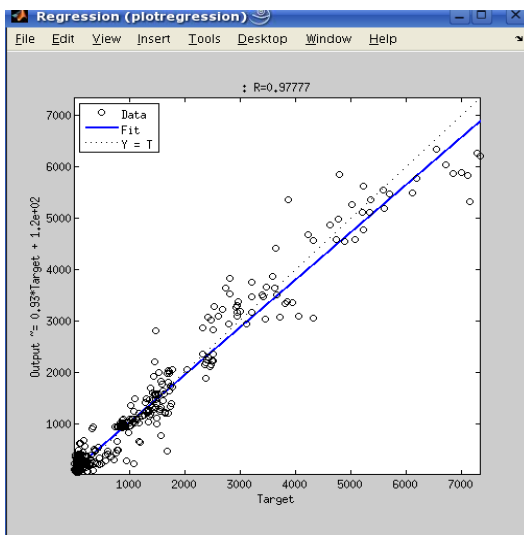


(i)

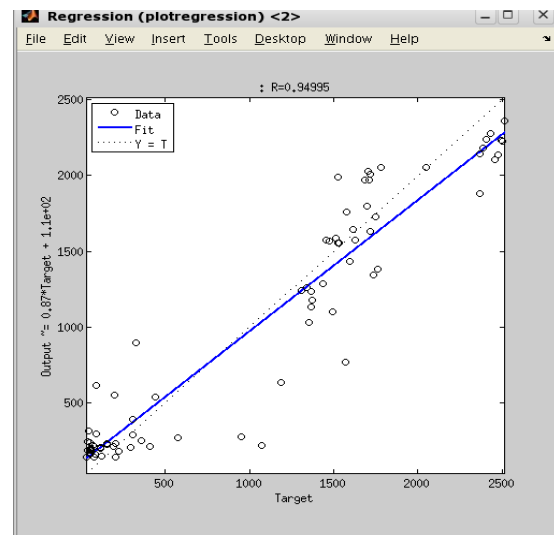


(ii)

(b)

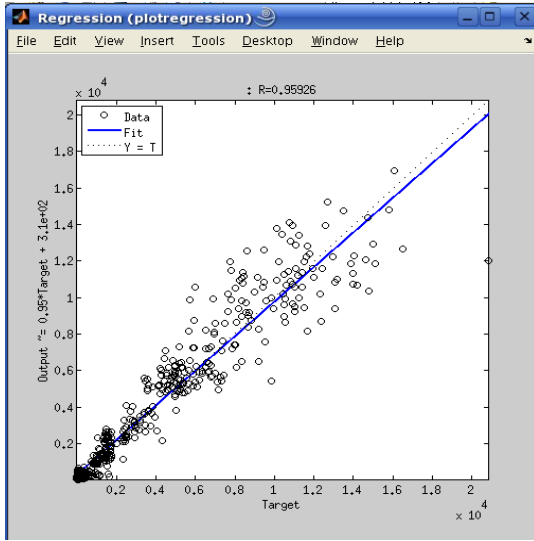


(i)

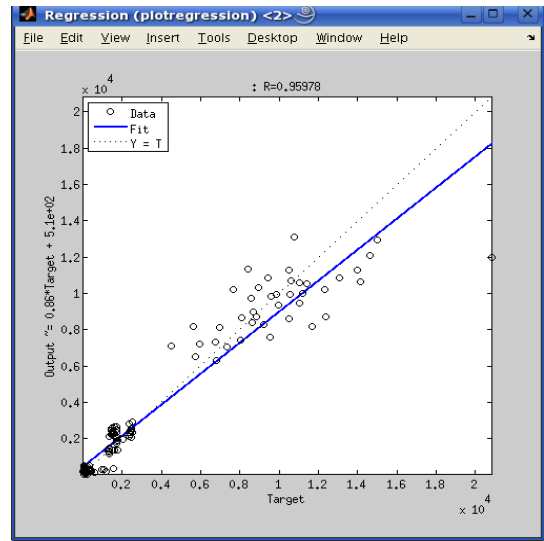


(ii)

(c)

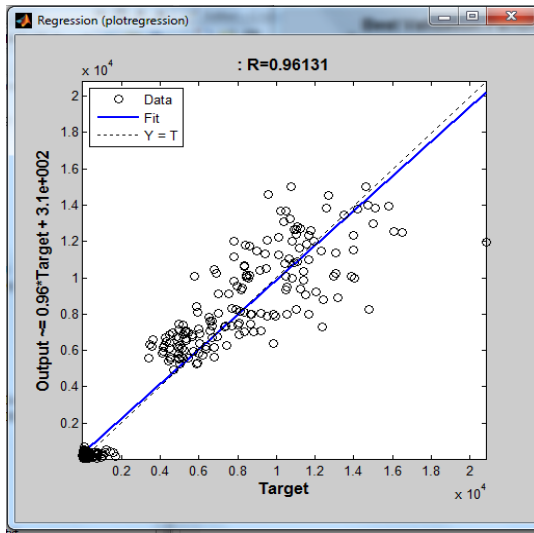


(i)

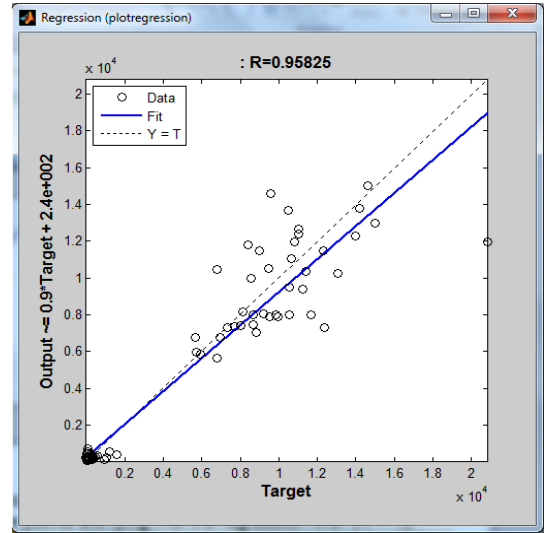


(ii)

(d)



(i)



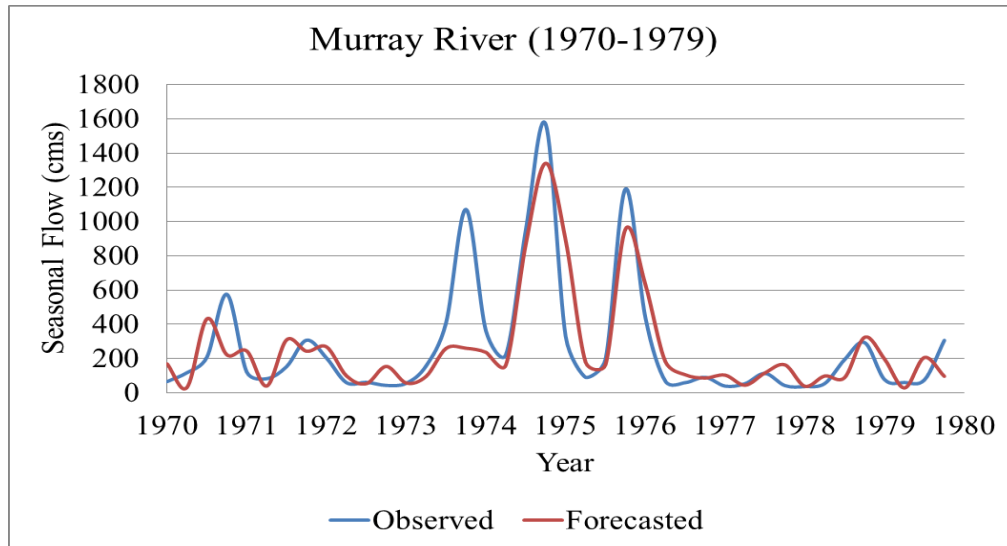
(ii)

(e)

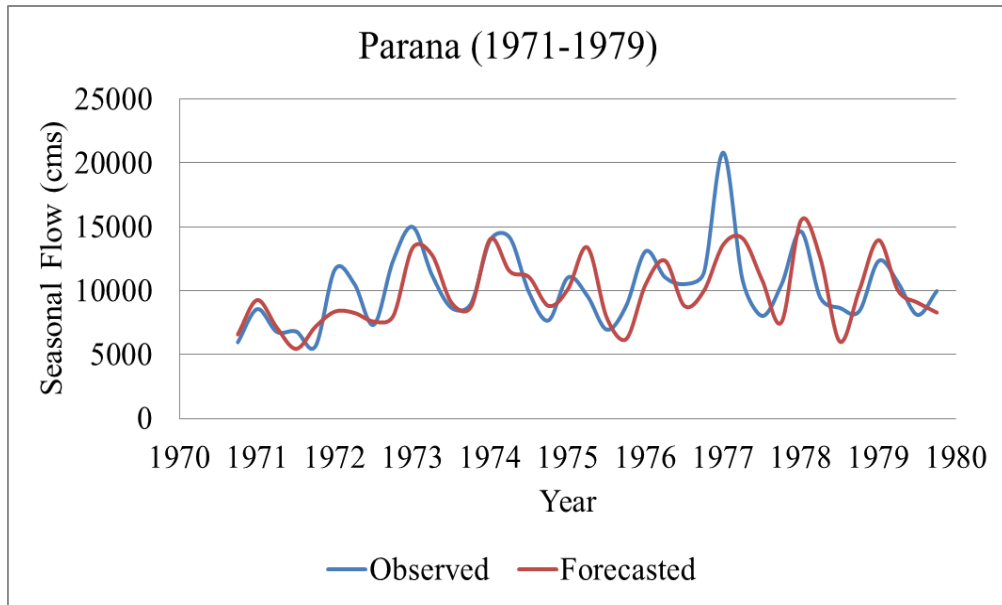
Figure 4.39. Regression plots of the multivariate ANN models incorporating: (a) Parana and Nile Rivers; (b) Parana and Murray Rivers; (c) Nile and Murray Rivers; (d) Parana, Nile, and Murray Rivers; and (e) Parana, Murray, and SSN. Here, (i) trained data; (ii) test data.

Testing of the ANN models

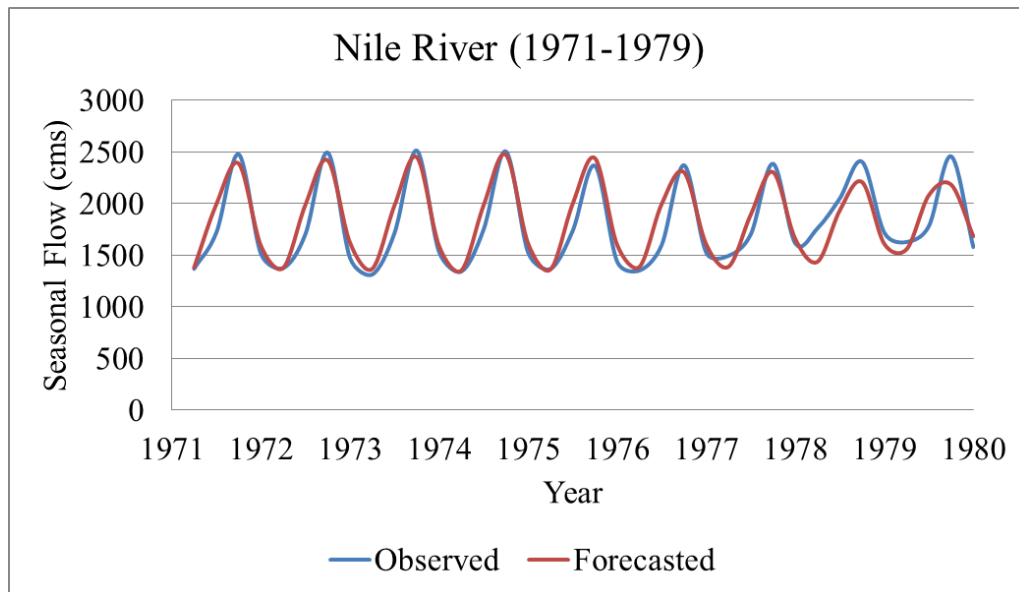
For all univariate and multivariate ANN models, the forecasted data were extracted and plotted, so that the performances of different models can be analyzed. In Figures 4.40 to 4.41, the univariate and multivariate all-river model forecasts are illustrated. The rest of the figures for the multivariate model forecasts are included in the Appendix B. These plots indicate that the forecasted flows captured the seasonal flow variability well, although often under or overestimated the observed flows. Therefore, four performance indices described in Chapter 3 were also adopted here to compare different model skills in predicting the three river flows. The results of these performance indices are summarized and discussed in Chapter 5.



(a)

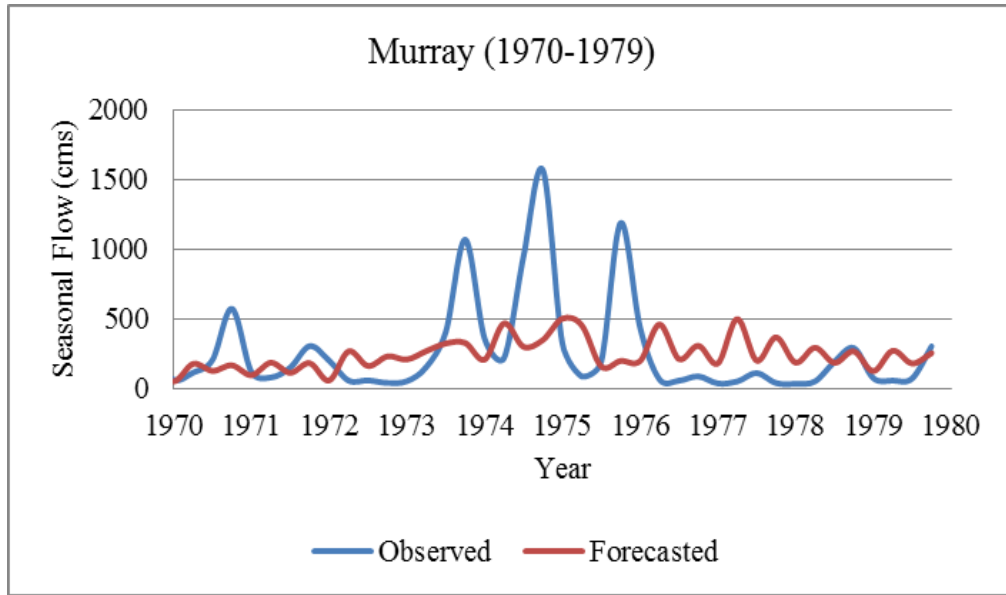


(b)

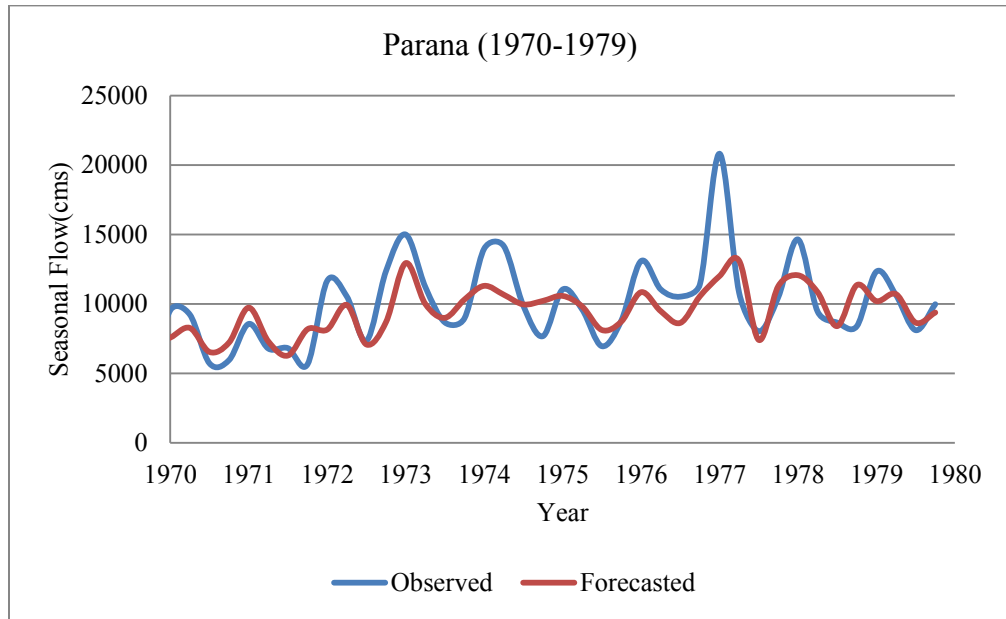


(d)

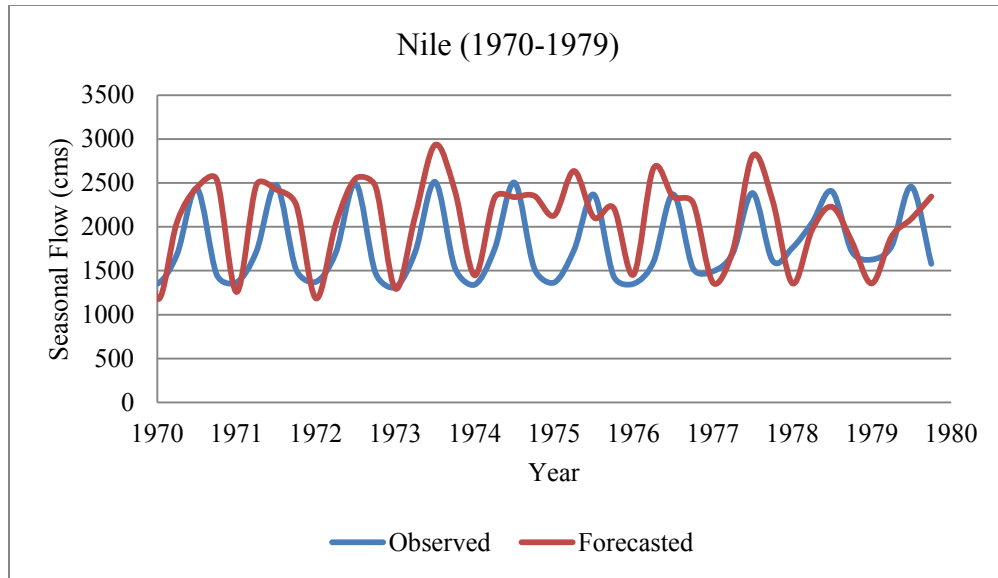
Figure 4.40. Validated lead-1 univariate ANN model forecasts of the rivers: (a) Murray; (b) Parana; and (c) Nile from the year 1971 to 1979.



(a)



(b)



(c)

Figure 4.41. Validated lead-1 multivariate model incorporating Parana, Nile, and Murray River seasonal flows (multivariate all-river model) for the rivers: (a) Murray; (b) Parana; and (c) Nile from year 1971 to 1979.

ANN Modeling with Long Term Flow Data Series

The variables used in the ANN model analyses were similar to the time series models developed previously. Seasonal flow series of five continental rivers namely, the Congo (Africa), Yangtze (Asia), Rhine (Europe), Columbia (North America), and Parana (South America) from 1906 to 1999 (376 seasons) were used as inputs. The first 75 years (1906-1980 or 300 seasons) data were used to train the model. The rest 301 to 332 (year 1981 to 1988) and 333 to 376 (year 1989 to 1999) seasonal flow data were used for validating and testing of the model, respectively. The trained models were then used to forecast all of the 72 seasonal flows (year 1982-1999). Similar to the previous study, the nonlinear autoregressive ANN model was adopted. In addition, the SOI, SSN, PDO, and

NAO indices were incorporated in the model as external environmental variables (forcing variables). The univariate and multivariate model analyses were performed to evaluate the forecast performances in order to consider time and space dependencies of the predictands and predictor variables.

In order to evaluate the ANN and time series model forecasts, the univariate and multivariate models incorporating lag three data sets were decided to use. The previous ANN analyses for the Parana, Nile, and Murray Rivers were conducted using one hidden layer and trial and error approach was implemented for selecting the optimum number of hidden nodes. The results indicated better performance with five numbers of hidden nodes for most of the models. Since the purpose of current study was to evaluate the prediction skills of the models, the same network geometry was decided to use. The early stopping technique was also adopted in order to avoid the over-fitting of the ANN models.

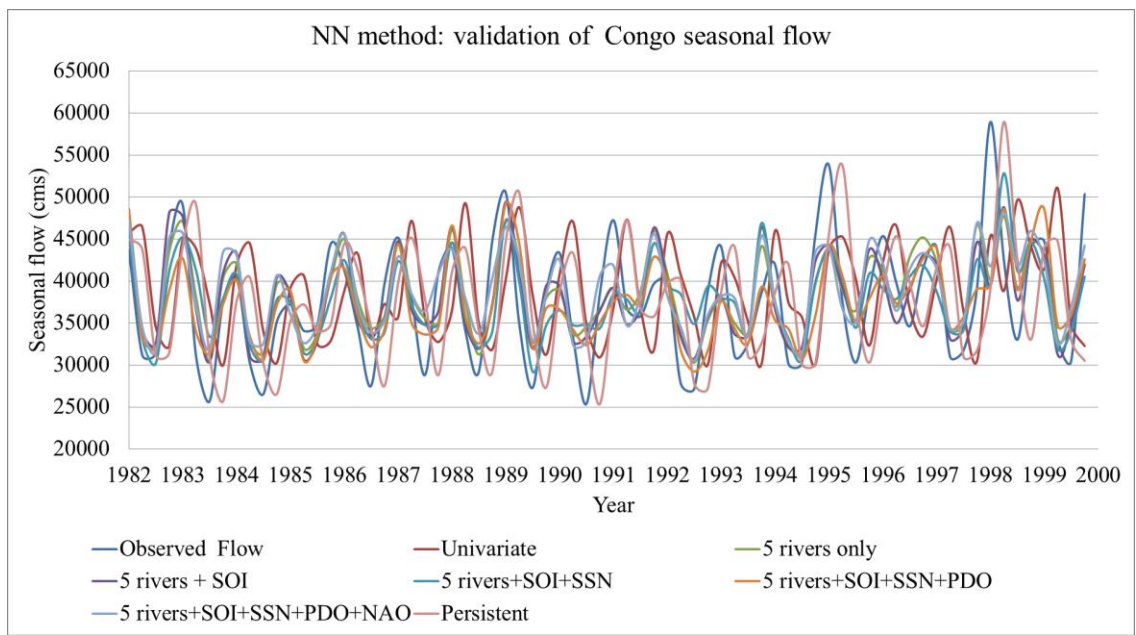
Training of the Models

After selecting appropriate numbers of lags and hidden nodes, the ANN models were trained to predict the five seasonal river flows. Although, the maximum number of epochs was set as 200 (the model was run up to 200 epochs then stopped), the training stopped well before that limit because of non-decreasing MSE statistics up to six epochs. Therefore, the weights, which were six epochs below the stopping point, were selected to use in the networks for testing the model forecasts.

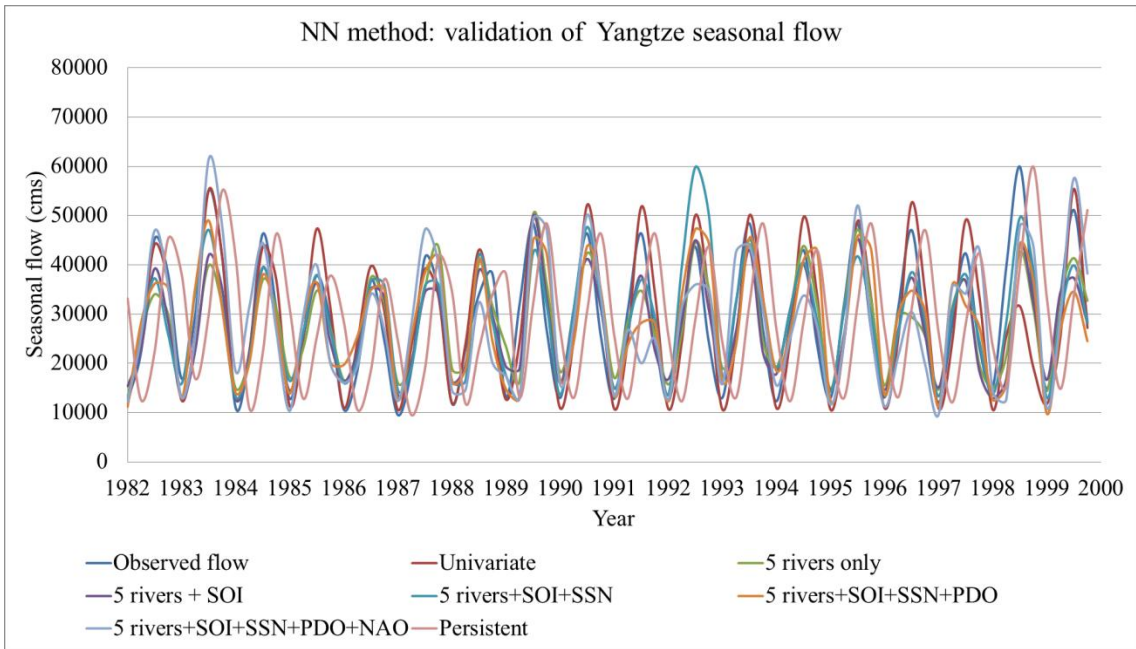
Testing of the Models

The trained ANN models were used to test the seasonal forecast of the rivers. However, 32 of the 76 seasonal flow data were used for cross-validating the model forecasts. Later, all of the 76 seasonal data were used for testing the trained ANN model performance. As lag three variable data were selected to incorporate, the first three seasonal flow data (winter, spring, and summer) were used to forecast the 4th seasonal flow (fall season).

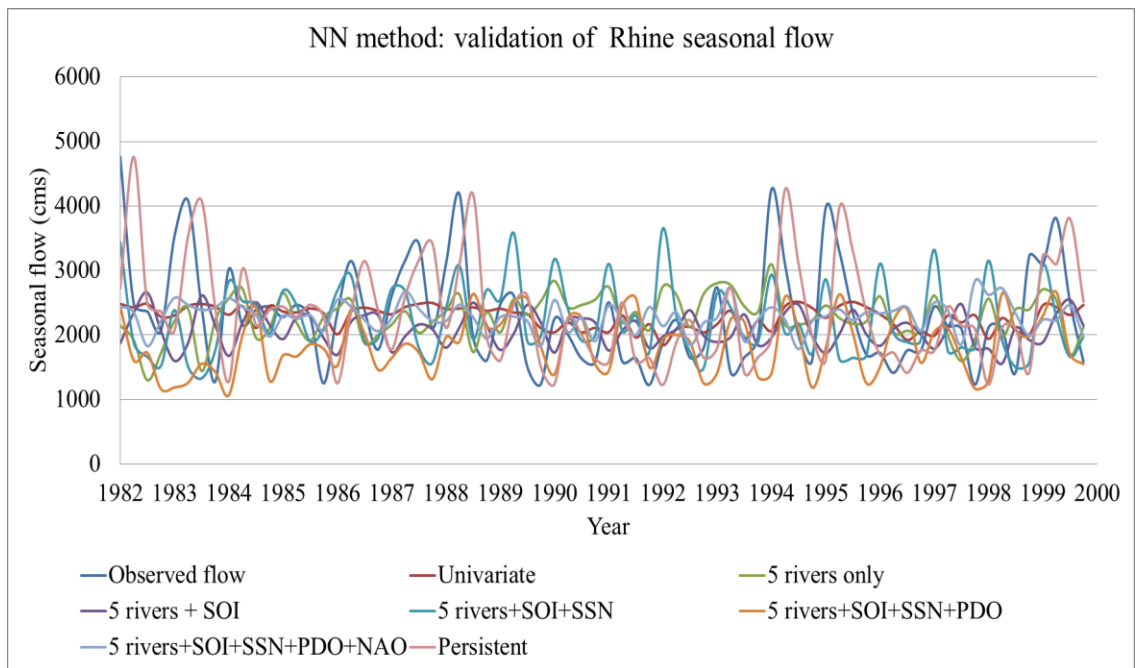
The observed and forecasted flows are plotted in Figures 4.42(a) to 4.42(e). The model performances in comparison to observed flows are difficult to explain from these figures. Therefore, four performance indices, the RMSE, MPE, RSD, and Pearson coefficients (described in Chapter 3), were adopted to compare the univariate and multivariate ANN model forecasts. The results for these performance indices are summarized and discussed in Chapter 5.



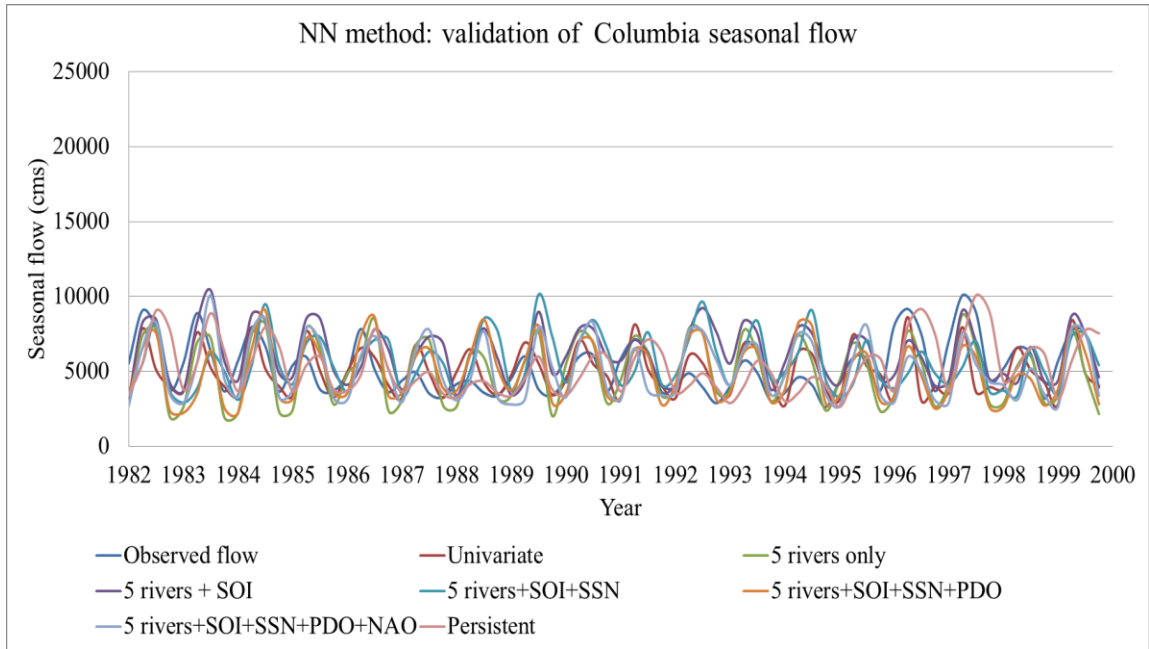
(a)



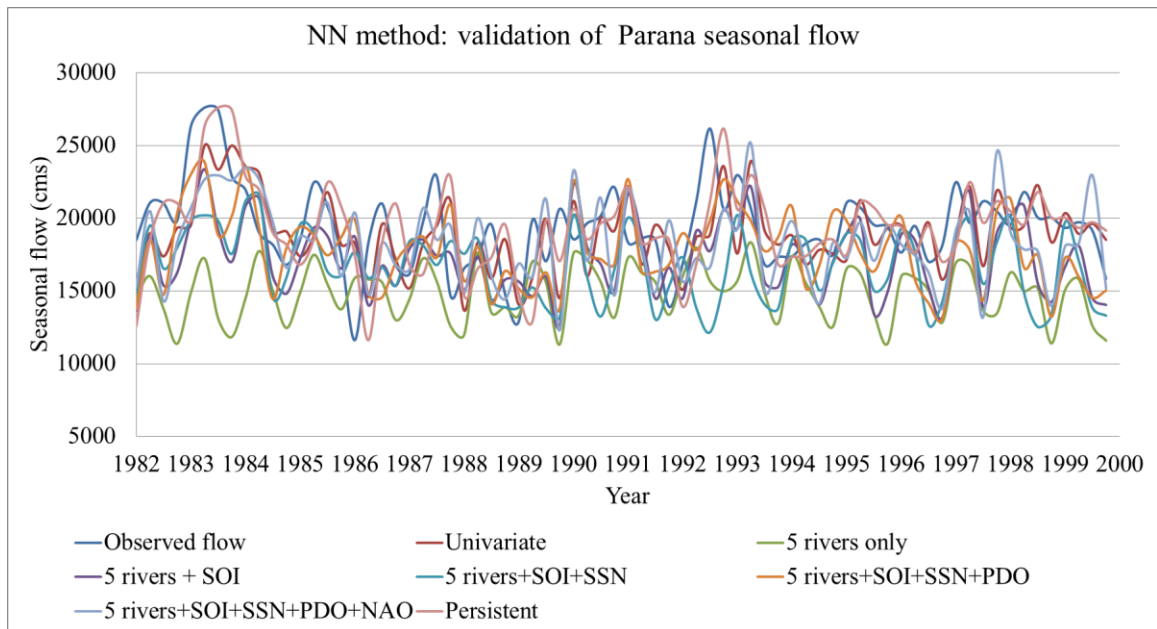
(b)



(c)



(d)



(e)

Figure 4.42. Forecast validation (year 1982 to year 1999) of the ANN models for the five rivers: (a) Congo; (b) Yangtze; (c) Rhine; (d) Columbia; and (e) Parana.

4.5 Forecast with the Discriminant Prediction Approach (Probabilistic Model)

For any river, higher seasonal flow predictions are useful if issued before the occurrence of the events. The time series of four seasonal Columbia flows are plotted in Figure 4.43. This figure indicates higher flows peaks occurred usually in the summer seasons. Therefore, the probabilistic forecasts were decided to evaluate only for the summer seasonal Columbia flow.

The correlation analyses were performed to identify the relationships between the Columbia summer flow and the predictor variables. It requires identifying the 95% confidence limits were obtained as ± 0.12 beyond which the values indicated significant correlations. Based on this, Yangtze winter flow (0.332) and summer NAO (-0.376) index were identified correlated with the Columbia summer flow at lag one (previous year), whereas Rhine spring flow (-0.364), spring PDO (-0.550), and winter SOI (0.344) indicated significant correlations at lag zero (current year). These variables with the above mentioned lags were selected to include in the analysis. However, the Congo and Parana flows demonstrated no sign of any significant correlation, therefore were neglected from the analysis. The corresponding correlation results are summarized in Tables 4.22 to 4.26.

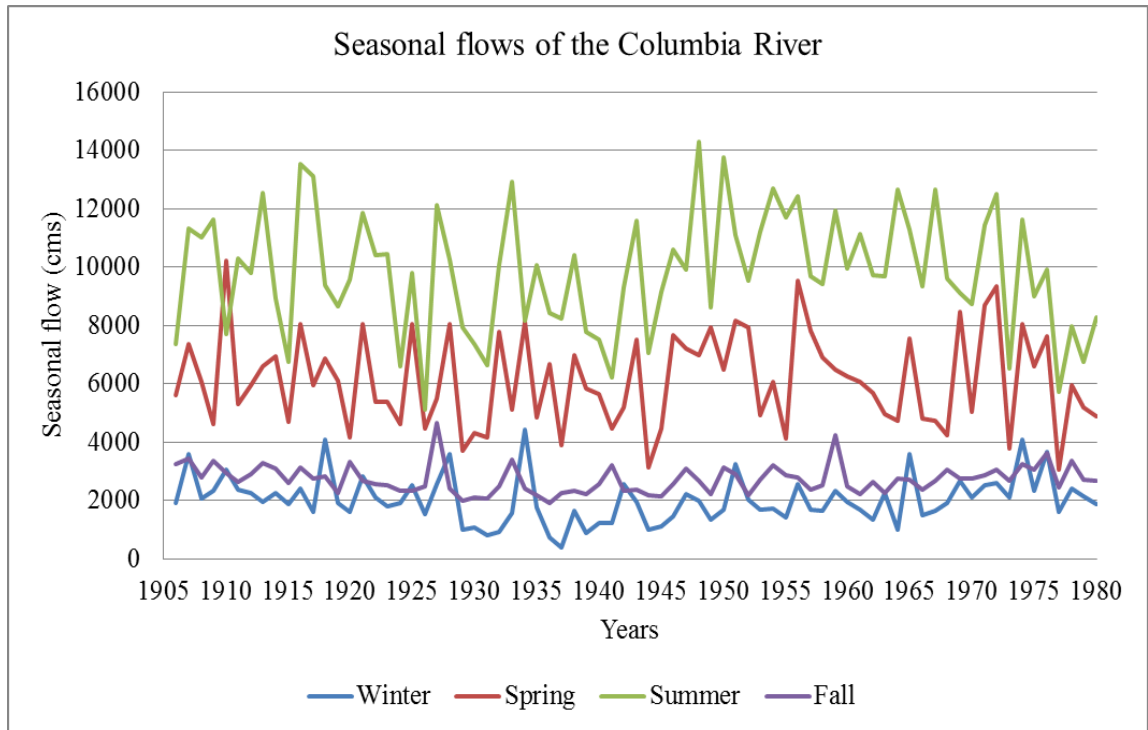


Figure 4.43. Time series plots of the seasonal Columbia flows

Table 4.22

Correlations between Seasonal Yangtze and Columbia Summer Flow

No. of lag	Winter Yangtze & summer Columbia flow	Spring Yangtze & summer Columbia flow	Summer Yangtze & summer Columbia flow	Fall Yangtze & summer Columbia flow
0	0.046	-0.015	0.098	0.006
1	0.332	0.16	0.214	0.183
2	-0.064	0.068	0.033	0.239
3	-0.046	0.134	-0.086	0.037

Table 4.23Correlations between Seasonal Rhine and Columbia Summer Flow

No. of lag	Winter Rhine & summer Columbia flow	Spring Rhine & summer Columbia flow	Summer Rhine & summer Columbia flow	Fall Rhine & summer Columbia flow
0	-0.138	-0.364	-0.203	-0.191
1	0.041	0.054	-0.007	-0.210
2	0.122	0.081	0.087	-0.160
3	0.016	0.084	0.040	0.002

Table 4.24Correlations between Seasonal SOI and Columbia Summer Flow

No. of lag	Winter SOI & summer Columbia flow	Spring SOI & summer Columbia flow	Summer SOI & summer Columbia flow	Fall SOI & summer Columbia flow
0	0.344	0.321	0.211	0.161
1	-0.296	-0.169	0.343	0.313
2	-0.231	-0.256	-0.272	-0.311
3	-0.040	-0.112	0.028	0.025

Table 4.25Correlations between Seasonal PDO and Columbia Summer Flow

No. of lag	Winter PDO & Summer Columbia	Spring PDO & Summer Columbia	Summer PDO & Summer Columbia	Fall PDO & Summer Columbia
0	-0.387	-0.550	-0.459	-0.337
1	-0.183	-0.213	-0.147	-0.265
2	-0.204	-0.097	-0.027	-0.015
3	-0.188	-0.200	-0.129	-0.222

Table 4.26Correlations between Seasonal NAO and Columbia Summer Flow

No. of Lag	Winter NAO & Summer Columbia flow	Spring NAO & Summer Columbia flow	Summer NAO & Summer Columbia flow	Fall NAO & Summer Columbia flow
0	0.046	0.152	0.243	0.131
1	0.006	0.057	-0.376	0.023
2	0.022	0.103	0.103	-0.155
3	-0.037	0.136	-0.097	0.097

In this study, the Columbia summer seasonal flows were predicted using one, two, and three predictor combinations. The data from year 1906 to 1980 (75 years) were used to calculate the probability of having Columbia summer flow, falling into a certain category of low, average, and high flow situations. These estimated probabilities were used to validate the flow forecasts of the years 1981 to 1999 (19 years). At the beginning, flow data was pre-processed by removing the trend components. Thereafter, river flows and forcing variables were divided into low, average, and high categories. The ranges of these categories are included in Table 4.27. The low and high flow thresholds were chosen in such a way that the data points fall equally into the three categories. Therefore, flow magnitudes above and below the 66th and 33rd percentile were identified as high and low, respectively. Flow magnitudes in between the two limits were categorized as average flows. However, these two boundary values do not indicate the flow magnitudes significantly different from the average flow condition. Therefore, selection of these boundaries is subjective and depends on the type of flows targeted to forecast (Eltahir, 1996). If the objective is to identify the flow events rarely occurred, a much wider ranges of average flow categories are required to be used (Wang and Eltahir, 1999).

Table 4.27Boundaries of Low and High Categorical River Flows and Forcing Variables

Category	Yangtze winter (cms)	Rhine spring (cms)	Columbia summer (cms)	SOI winter (cms)	PDO spring (cms)	NAO summer (cms)
Low(= \leq)	11674	2048	9053	-0.414	0.039	-0.310
High(= \geq)	14233	2760	10567	0.367	0.671	0.291

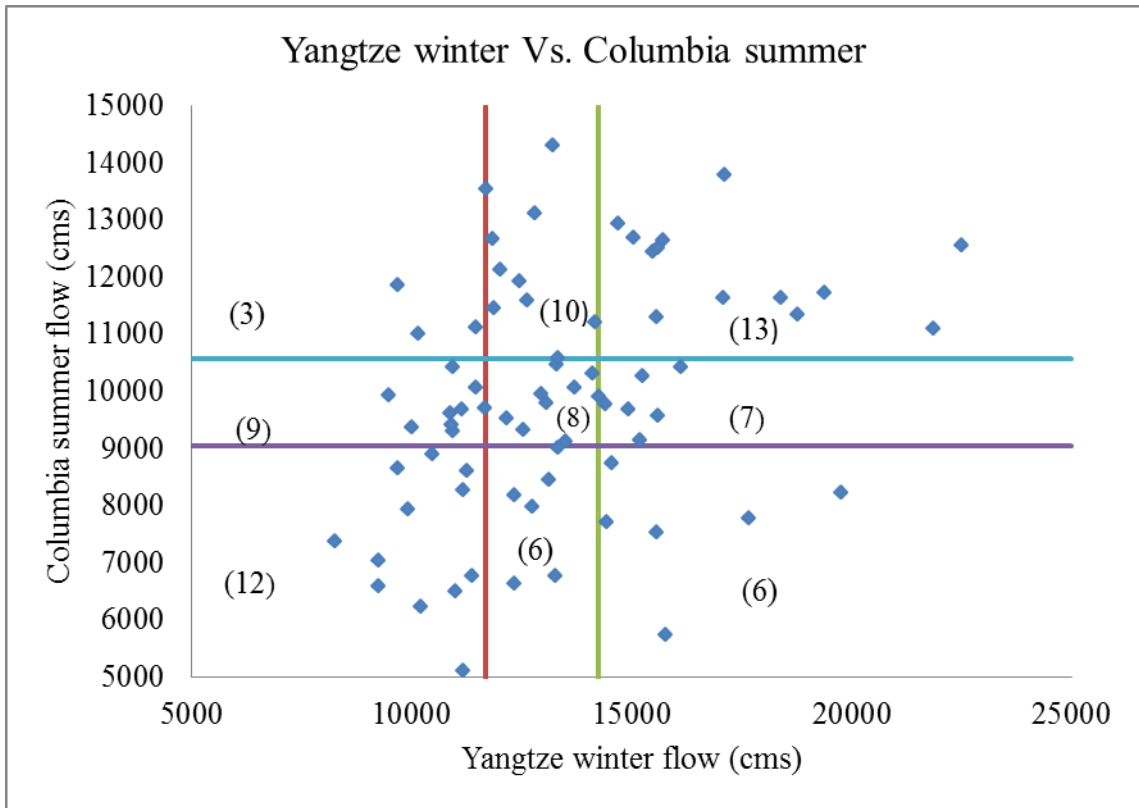
The goal of this study is to predict the probabilities of having a Columbia summer flow falling into a certain category (low, average, and high), conditioned on the observed categories of the predictor variables (low, average, and high). For instance, if the PDO, SOI, and NAO indices were used together as predictors, their observed conditions could be used to forecast the chances of having a Columbia flow falling into certain category. These conditional probabilities were obtained using the algorithm developed by Wang and Eltahir (1999). In this method, forecasts of a particular season would be issued as a likelihood of the Columbia flow, falling into each of the three categories. It was expected that incorporation of the variable information would improve the low and high flow prediction skills and provide more definite forecasts. Besides this, in order to identify the variables influencing the Columbia summer flow, various combinations of the Rhine and Yangtze flows as well as the SOI, PDO, and NAO conditions were examined and the results were compared for the calibration data sets (year 1906 to year 1980). These results were evaluated afterwards with the validation data (year 1980 to 1999). The predictors or the predictor combinations, for which the forecast more specifically indicating a particular category, were taken as the future flow condition of the river. However, this approach was unable to differentiate between a more specific and a less specific forecast (both 90% and the 60% probability indicate high flow, although 90% is more specific).

Therefore, the rank probability skill score (RPSS) and the forecast index developed by (G. Wang & Eltahir, 1999) were adopted to evaluate the performance of different variables, predicting the Columbia summer flow.

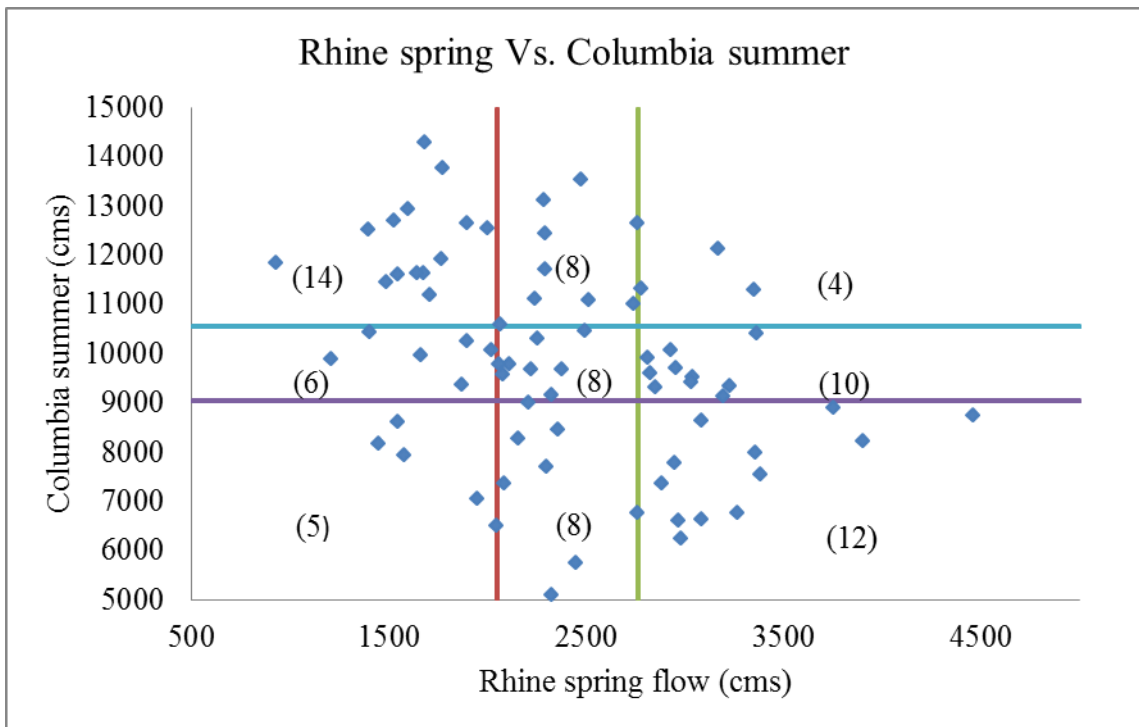
However, the predictor and predictand variable conditions together divide the corresponding data points into several groups. The numbers of groups depend on the number of variables used in the computation, and it increases exponentially with the increasing number of variables. For example, when the river flows are predicted, using one variable condition, the total number of groups is found to be nine, whereas the two and three variable conditions yielded 27 and 81 groups, respectively. The Figures 4.44(a) to 4.44(e) represents the nine groups as evident from one variable condition forecast, where Yangtze and Rhine flow as well as the SOI, PDO, and NAO were used as predictors. In the figures, the numbers within the parentheses represented the data points, belonging to each of the respective groups.

In this study, data counting procedure (counting of the data belong to a certain group) was adopted to compute the conditional probability of the river flow falling into a particular category. For this, all the data points relevant to a particular flow category (low, average, and high) as well as the data points belongs to that particular flow category based on the conditions of a predictor variable (low, average, and high) are counted to compute the relative frequency distribution. The data counting procedure is suitable up to two variable combinations (Wang & Eltahir, 1999) as each of the groups (total 27 groups) have enough data points to accurately compute the conditional probabilities of the Columbia summer flow. Because the procedure becomes time consuming and cumbersome for the number of variables greater than two and each group requires

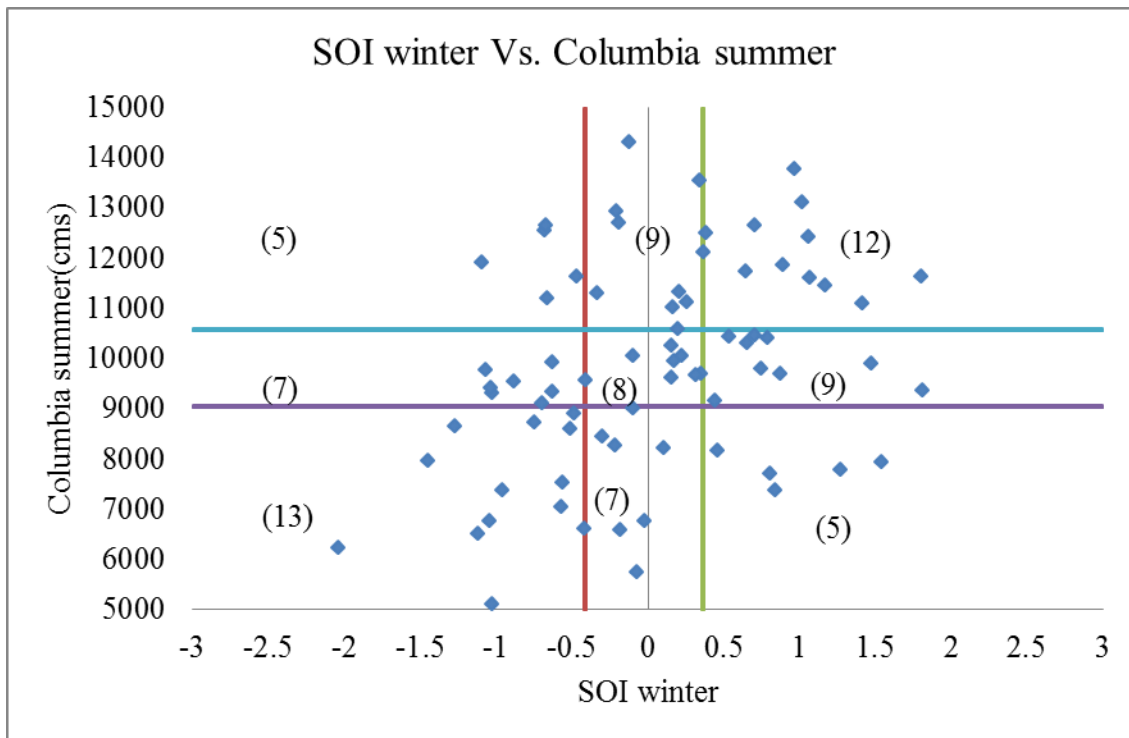
enough data points to represent a particular condition. Therefore, this procedure is not suitable for the case, where data are limited. The Bayesian method (described in Chapter 3) is advantageous in this case for which the assumption of independence is required. The results of these two methods were also compared to investigate the performance of the two methodologies. For illustration, the forecast probabilities of the Columbia summer seasonal flow obtained by using two variable combinations of NAO, PDO, and SOI are shown in Tables 4.28 and 4.29. In the tables, the values over the slash '/' represent forecast probabilities using data counting procedure and those under the slash represent probabilities, resulting from the Bayesian algorithm. Although, results of the two methodologies differed slightly, both the methodologies indicated the same categorical forecast in most of the cases. In other words, the flows indicated "high" in the data counting procedure were also indicating high flows in the Bayesian method. This indicated the performances of the two methodologies were nearly equal. In addition, it shows the advantages of the Bayesian method over the data counting procedure, where limited years of data are available and higher numbers of variables are required to be incorporated. Therefore, the errors, resulting due to the independence assumption can be neglected for calculating the two or more variable influence, improving the forecasting skills.



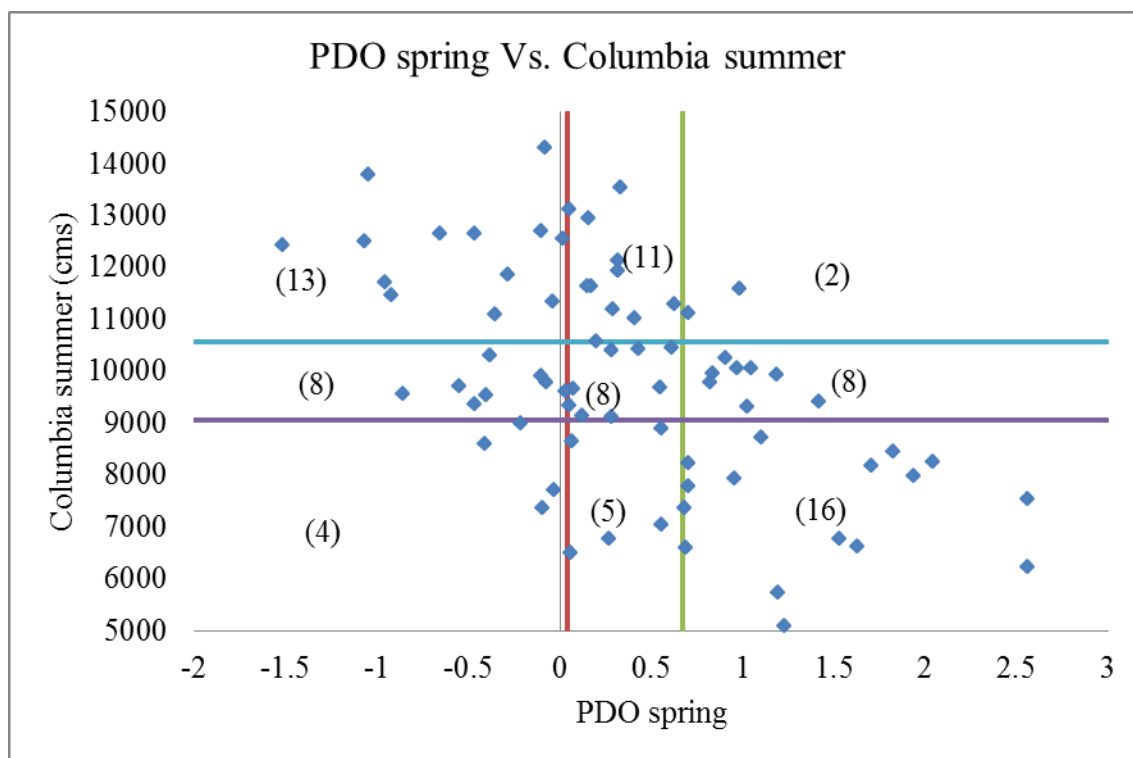
(a)



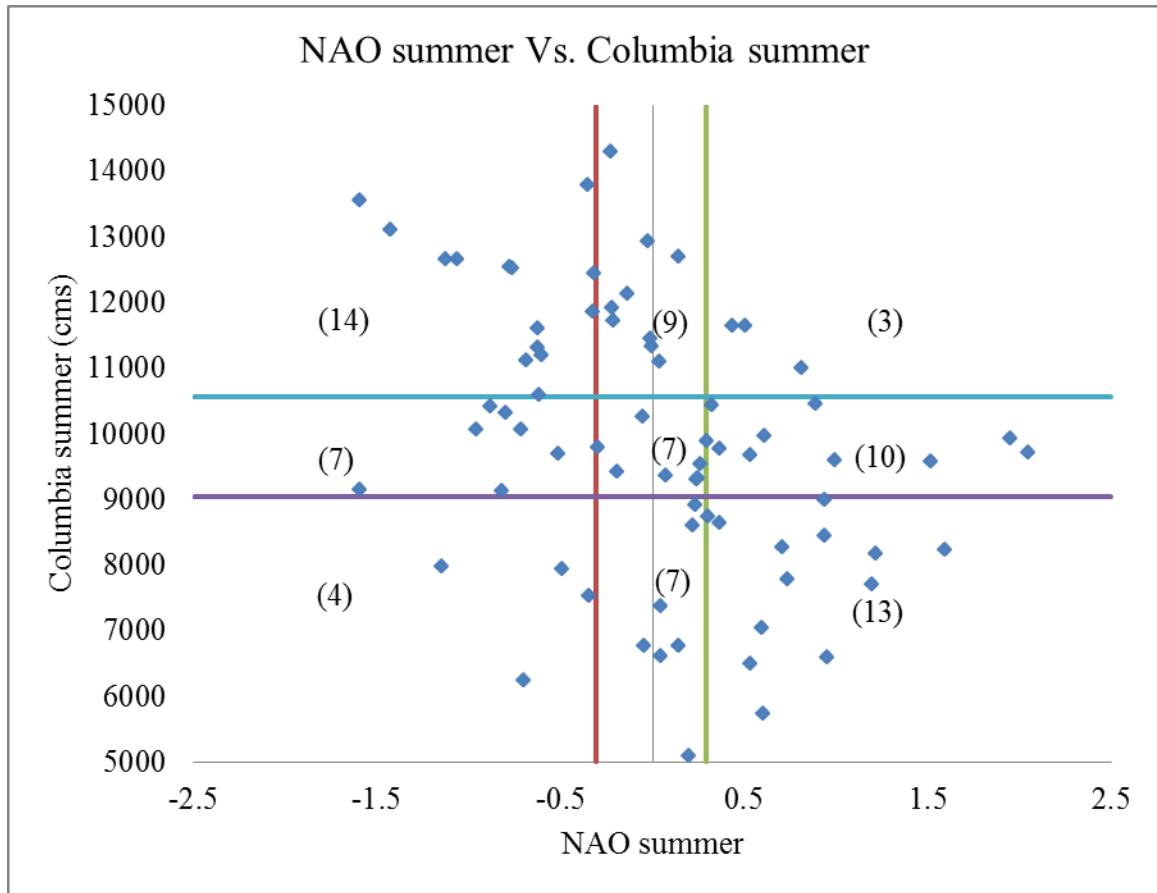
(b)



(c)



(d)



(e)

Figure 4.44. Data counting procedure to forecast the Columbia summer flow with one variable condition (a) Yangtze winter flow, (b) Rhine spring flow, (c) winter SOI, (d) spring PDO, and (e) summer NAO, respectively.

Table 4.28

Forecast of the Columbia Summer Flow Conditioned on Summer NAO (Lag 1) and Spring PDO (Lag Zero) Information.

Conditions		Columbia summer flow		
Summer NAO	Spring PDO	Low	Average	High
Low	Low	0.00/0.06	0.13/0.14	0.88/0.80
	Average	0.00/0.17	0.44/0.29	0.56/0.54
	High	0.50/0.34	0.25/0.450	0.25/0.17
Average	Low	0.20/0.13	0.20/0.16	0.60/0.72
	Average	0.33/0.29	0.17/0.29	0.50/0.42
	High	0.43/0.48	0.57/0.41	0.00/0.11
High	Low	0.29/0.37	0.71/0.30	0.00/0.32
	Average	0.33/0.54	0.33/0.35	0.33/0.12
	High	0.80/0.63	0.20/0.35	0.00/0.02

Table 4.29

Forecast of the Columbia Summer Flow Conditioned on Summer NAO (Lag 1) and Winter SOI (Lag Zero) Information.

Conditions		Columbia summer flow		
Summer NAO	Winter SOI	Low	Average	High
Low	Low	0.43/0.31	0.14/0.30	0.43/0.39
	Average	0.00/0.14	0.43/0.28	0.57/0.58
	High	0.09/0.08	0.27/0.26	0.64/0.65
Average	Low	0.50/0.48	0.40/0.26	0.10/0.26
	Average	0.17/0.25	0.17/0.29	0.67/0.46
	High	0.14/0.16	0.29/0.29	0.57/0.55
High	Low	0.57/0.70	0.29/0.24	0.14/0.06
	Average	0.55/0.50	0.36/0.37	0.09/0.14
	High	0.38/0.37	0.50/0.43	0.13/0.19

CHAPTER 5

RESULTS AND DISCUSSION

This chapter presents results for the overall prediction of flows using continental river flows and external environmental variables. The model performance in predicting seasonal river flows is discussed. First, results between selected river flows and external environmental variables are explored. Thereafter, results of the time series analyses and artificial neural network (ANN or NN) models are compared. Model forecasts are further evaluated in predicting extreme river flow conditions and also assessed in terms of variable influence on prediction skills. Methods are evaluated further for seasonal flow forecast ensembles. The results are presented and evaluated in terms of box plots to illustrate variability in prediction skills. Finally, forecasts using the probabilistic approach are presented and model performances evaluated for the Columbia River summer flow.

5.1 Performance Analysis: Time Series Models (Short Data Series)

Time series model performances are summarized in Table 5.1 as prepared. Four evaluation indices, including the mean of percentage error (MPE), root mean square error (RMSE), ratios of standard deviation (RSD) and square of the Pearson product moment correlation coefficients (SPPMCC), also known as coefficient of determination are shown. In the table, ‘M.var.’ represents multivariate model.

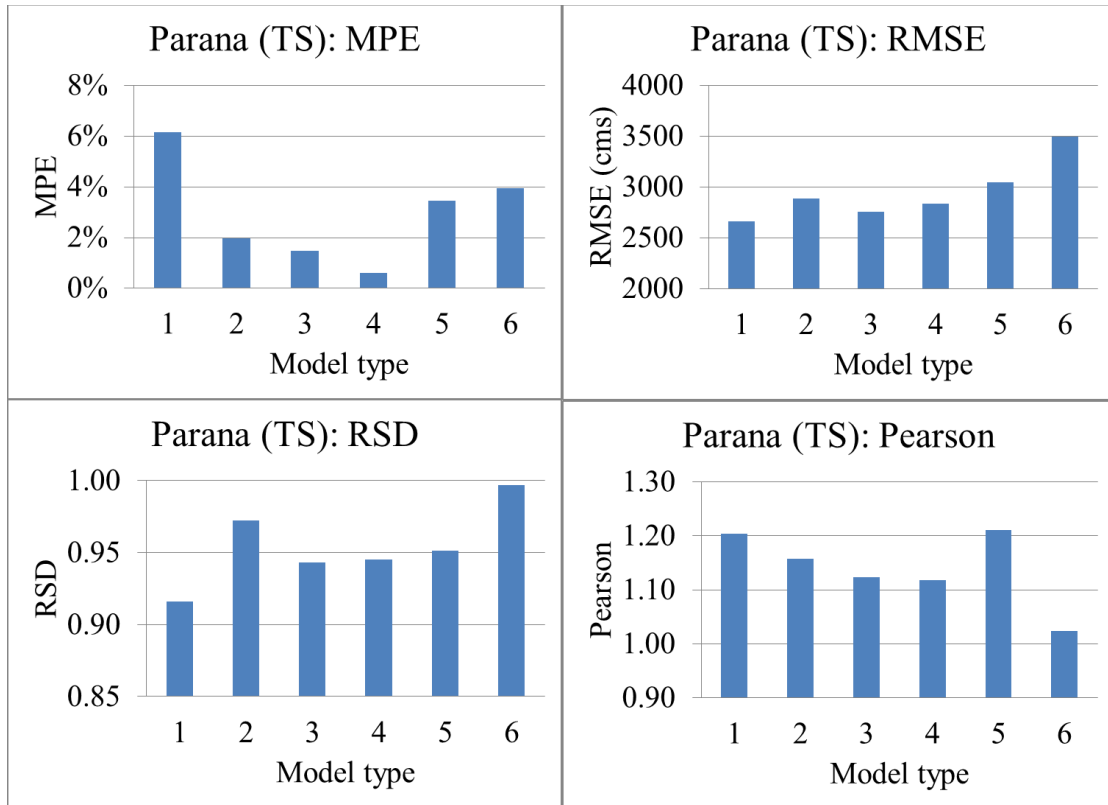
Table 5.1

Summary of the Performance Evaluators of Time Series Models for Predicting the Parana, Danube, Rhine, and Missouri River Seasonal Flows.

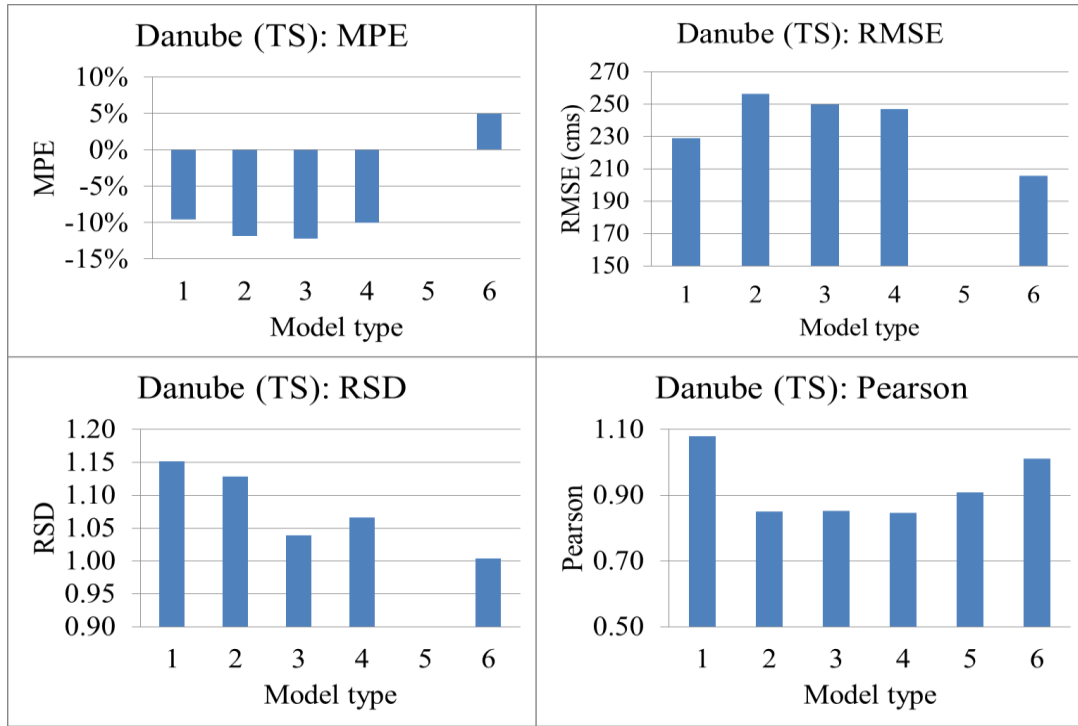
Model	MPE (%)	RMSE (cms)	RSD	SPPMCC
Parana River				
Univariate	6.17	2663	1.20	0.51
M. var. 4 rivers	1.96	2888	1.16	0.40
M. var. 4 rivers + SOI	1.48	2756	1.12	0.42
M. var. 4 rivers + SOI + SSN	0.60	2839	1.12	0.39
M. var. 3 rivers + SSN	3.46	3048	1.21	0.37
Persistence	3.96	3497	1.02	0.13
Danube River				
Univariate	-9.55	229	1.08	0.14
M. var. 4 rivers	-11.86	256	1.15	0.08
M. var. 4 rivers + SOI	-12.21	250	1.04	0.07
M. var. 4 rivers + SOI + SSN	-9.98	247	1.08	0.07
M. var. 3 rivers + SSN	-	-	-	-
Persistence	4.95	206	1.00	0.14
Rhine River				
Univariate	15.29	873	1.08	0.18
M. var. 4 rivers	8.20	958	0.85	0.01
M. var. 4 rivers + SOI	9.07	983	0.85	0.00
M. var. 4 rivers + SOI + SSN	11.26	977	0.85	0.00
M. var. 3 rivers + SSN	14.01	973	0.91	0.01
Persistence	8.15	853	1.01	0.15
Missouri River				
Univariate	25.03	627	1.70	0.01
M. var. 4 rivers	17.35	483	1.46	0.11
M. var. 4 rivers + SOI	16.47	485	1.44	0.09
M. var. 4 rivers + SOI + SSN	17.29	472	1.42	0.12
M. var. 3 rivers + SSN	23.38	523	1.53	0.09
Persistence	13.05	417	1.00	0.02

Additionally, Figure 5.1 graphically represents performance indices of the forecast models. This figure and table show that model performances are river specific as not any particular model is better for predicting the four river flows. For all of the

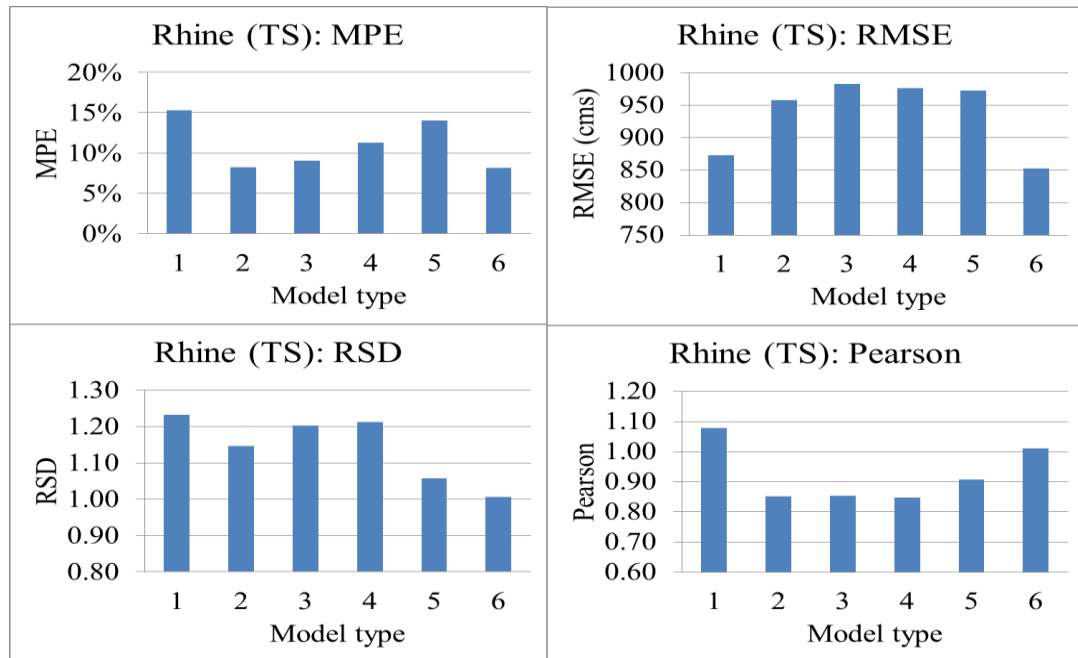
models, low R-square and high RMSE values reveal limitations for predicting seasonal flows. However, the RSD values are nearly equal to unity. This indicates model efficiency for capturing flow variability. Moreover, low MPE values for the persistence model indicate better flow prediction skills with this model.



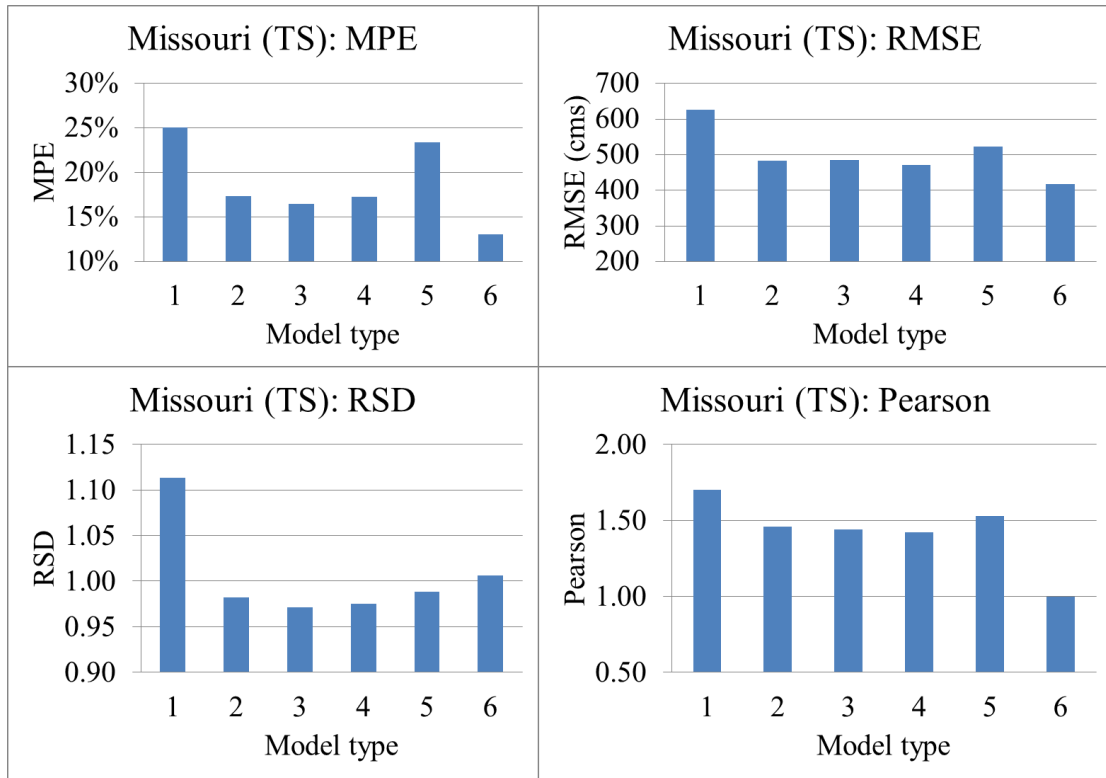
(a)



(b)



(c)



(d)

Figure 5.1 Performance indices of different time series models, predicting the Parana (a), Danube (b), Rhine (c), and (d) Missouri seasonal flows.

In the above plots, x-axis represents different models used in this analysis. These are (1) Univariate; (2) Multivariate incorporating 4 rivers; (3) Multivariate incorporating 4 rivers and SOI; (4) Multivariate incorporating 4 rivers, SOI, and SSN; (5) Multivariate incorporating 3 rivers, SSN; and (6) Persistence model.

5.1.1 Flow Categorization Results

The ability of a model to predict low and high flows are assessed by categorizing four river flows into three flow zones. River flow magnitudes below the 33rd percentile of mean are categorized as an indication of low flow and above the 66th percentile of mean

are designated high flows. Flow magnitudes between these limits are categorized as average flows. Results of the corresponding flow predictions are summarized in Tables 5.2, 5.3, 5.4 and 5.5. In the tables, ‘M. var.’ represents multivariate model. These results show that among the 44 seasonal flows of the rivers Parana, Danube, Rhine and Missouri, seasonal river flows are below the 33rd percentile limit (low flow zone) 5, 19, 20 and 6 times, respectively. For the Parana River, the persistence model shows best performance, predicting the low flows correctly three of five times. For the Danube River the multivariate model with four rivers outperforms other models as the predictions are correct 13 out of 19 low flows. However, for the Rhine River, both the univariate and persistence models are more effective than the multivariate models in terms of low flow prediction. Yet, all of the multivariate models are effective in predicting low Missouri flows as five of the six times the low flow predictions are correct.

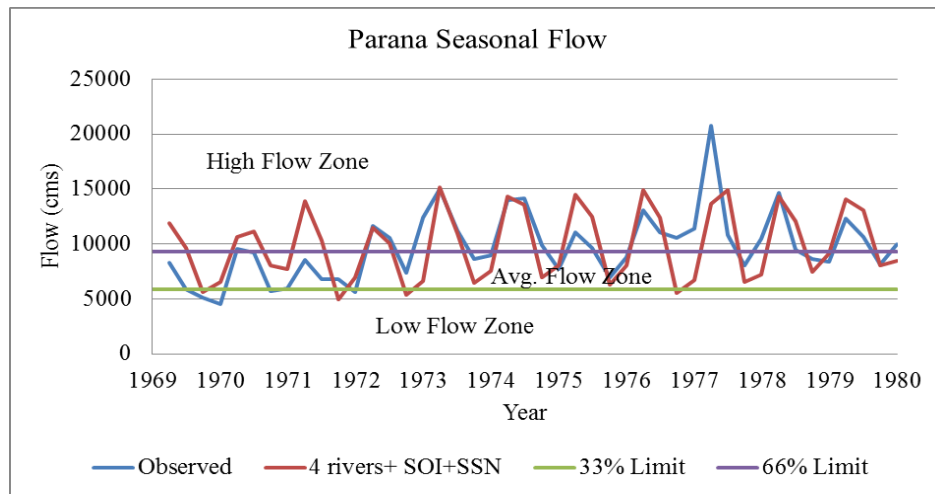


Figure 5.2. Flow categorization of the Parana River for the multivariate model including 4 rivers, SOI, and SSN.

Table 5.2Validation of Parana River Low and High Flow Forecasting.

River	Flow	Univariate	M. var. 4 rivers	M. var. 4 rivers + SOI	M. var. 4 rivers + SOI + SSN	M. var. 3 rivers + SSN	Persistence	
Low flow (total 5)								
Parana	Well predicted	2	2	2	1	2	3	
	Outside category	3	3	3	4	3	2	
	High flow (total 23)							
	Well predicted	16	16	16	15	14	14	
	Outside category	7	7	7	8	9	9	

Table 5.3Validation of Danube River Low and High Flow Forecasting.

River	Flow	Univariate	M. var. 4 rivers	M. var. 4 rivers + SOI	M. var. 4 rivers + SOI + SSN	M. var. 3 rivers + SSN	Persistence	
Low flow (total 19)								
Danube	Well predicted	12	13	12	12	10	12	
	Outside category	7	6	7	7	9	7	
	High flow (total 9)							
	Well predicted	4	3	2	4	3	4	
	Outside category	5	6	7	5	6	5	

Table 5.4Validation of Rhine River Low and High Flow Forecasting.

River	Flow	Univariate	M. var. 4 rivers	M. var. 4 rivers + SOI	M. var. 4 rivers + SOI + SSN	M. var. 3 rivers + SSN	Persistence	
Low flow (total 20)								
Rhine	Well predicted	11	8	8	9	8	11	
	Outside category	9	12	12	11	12	9	
	High flow (total 12)							
	Well predicted	7	3	3	4	4	5	
	Outside category	5	9	5	8	8	7	

Table 5.5Validation of Missouri River Low and High Flow Forecasting.

River	Flow	Univariate	M. var. 4 rivers	M. var. 4 rivers + SOI	M. var. 4 rivers + SOI + SSN	M. var. 3 rivers + SSN	Persistence	
Low flow (total 6)								
Missouri	Well predicted	3	5	5	5	5	0	
	Outside category	3	1	1	1	1	6	
	High flow (total 25)							
	Well predicted	15	20	19	22	22	14	
	Outside category	10	5	6	3	3	11	

In terms of high flow prediction, the number of times flows exceeded the 66th percentile limit for the rivers Parana, Danube, Rhine and Missouri were 23, 9, 12 and 25, respectively. For the Parana River, 16 times both the univariate and multivariate models

incorporating four rivers and four rivers and SOI correctly predicted number of flow events. For the Danube River, both the univariate and multivariate model incorporating four rivers, SOI and SSN demonstrate better performance, as the high flow category are predicted correctly four times. Conversely, the univariate model of the Rhine River outperforms other model forecasts, as five times it is effective in predicting the high flow category. For the Missouri River, the multivariate model with four rivers and the SOI and the SSN and the multivariate model with three rivers and SSN are found effective in terms of high flow prediction, as the forecasts are found correct 22 out of 25 times.

5.1.2 Ensemble Model Performance (Short Data Series)

In ensemble forecasts, the univariate and multivariate models are combined and quantified in terms of likelihood, which allows variability of models to be counted and evaluated. The boxplot in Figure 5.3 shows one example of the ensemble prediction approach, where all of the univariate and multivariate model forecasts for the winter Parana flows are plotted against the observed winter flow to consider variability of different model results. This plot indicates that the observed flows are well captured within the ensemble forecast ranges. The details of the ensemble forecast performances are evaluated using long flow data series which are discussed in the later sections.

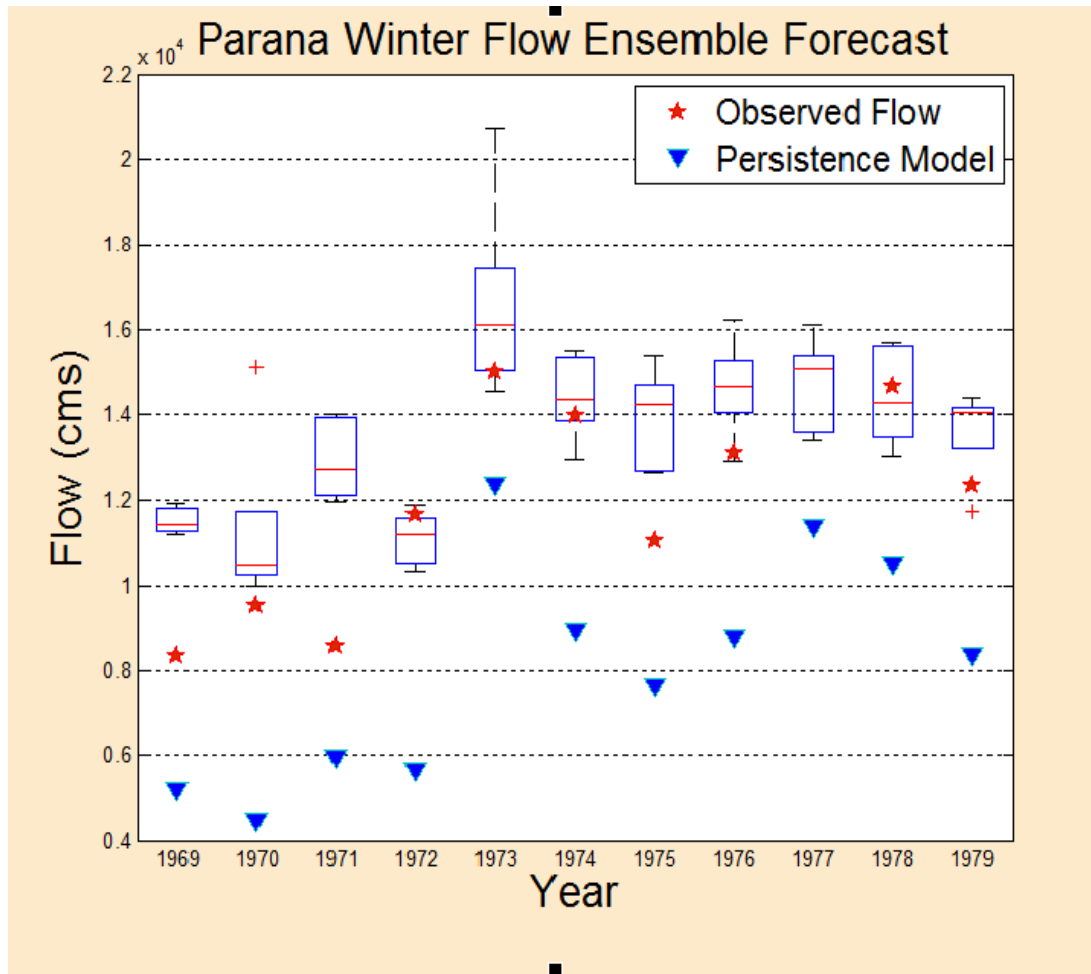


Figure 5.3. Ensemble forecast for the Parana winter flow (short data series).

5.2 ANN Model Performances (Parana, Nile, and Murray Rivers)

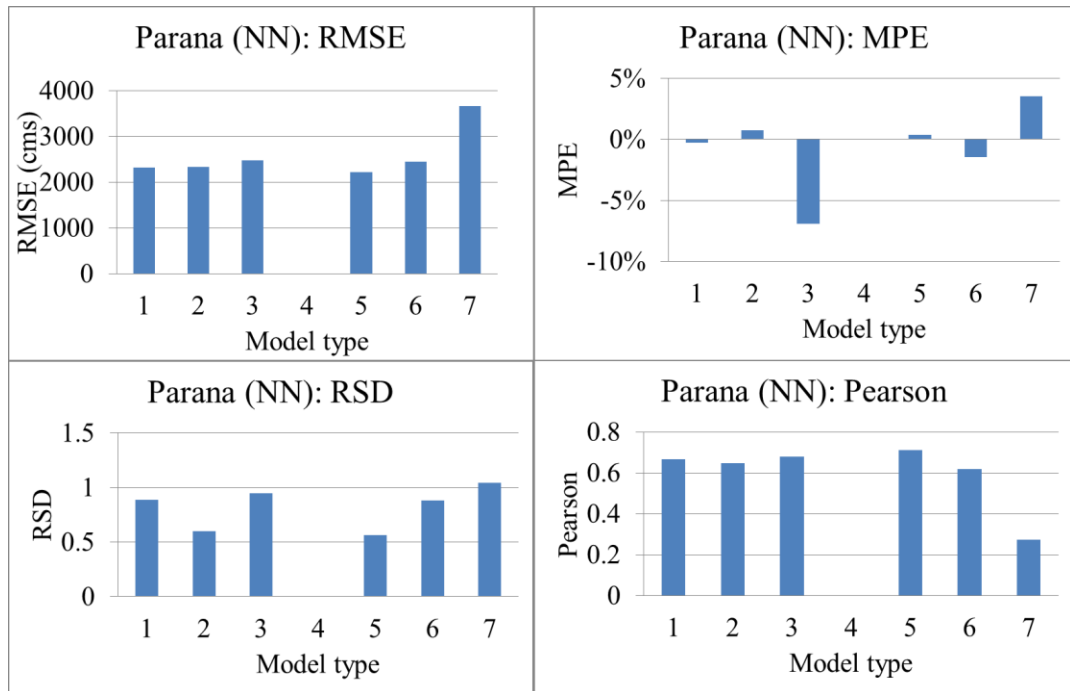
The ANN model results are evaluated using seasonal flow series of the river Parana, Nile and Missouri from 1971 to 1979. The same four performance criteria used to evaluate the time series approach, are adopted here to allow comparison with univariate and multivariate models. All performance criteria are summarized in Table 5.6. In the table, 'M. var.' represents multivariate models.

Table 5.6

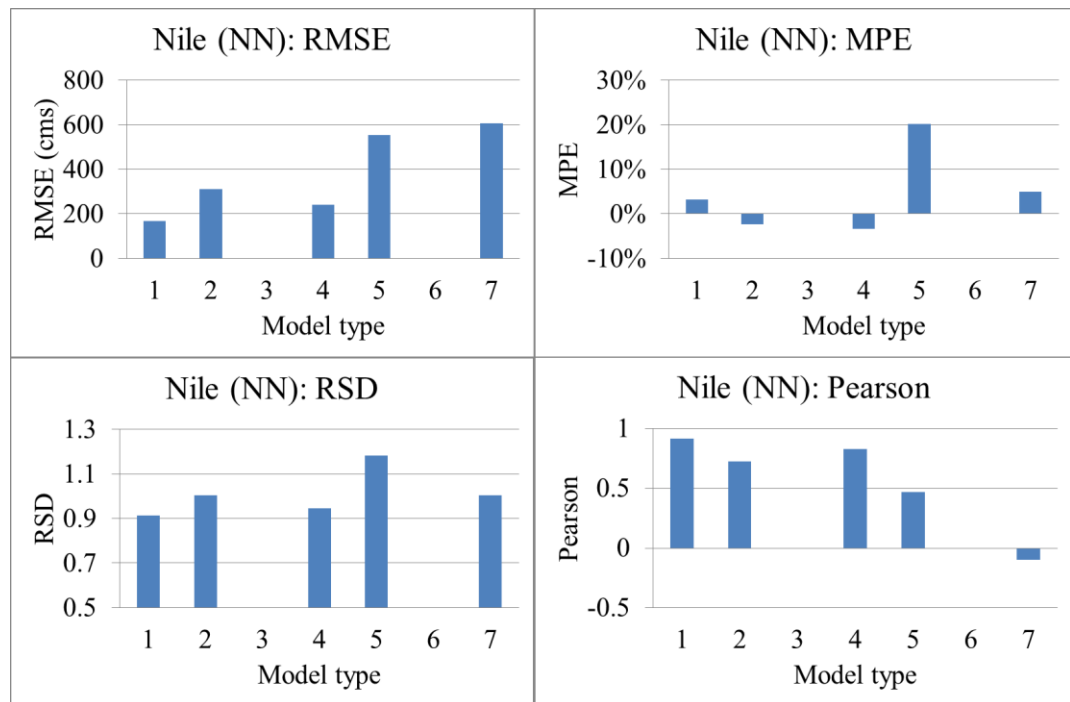
Summary of the Performance Evaluators of Different ANN models for Predicting the Parana, Nile, and Murray River Seasonal Flows.

Model	MPE (%)	RMSE (cms)	RSD	SPPMCC
Parana River				
Univariate	-0.26	2313	0.88	0.66
M. var. Parana + Nile	0.75	2341	0.59	0.64
M. var. Parana + Murray	-6.92	2473	0.94	0.68
M. var. Nile + Parana + Murray	0.35	2219	0.56	0.71
M. var. Parana + Murray + SSN	-1.46	2454	0.87	0.62
Persistence	3.5	3663	1.04	0.27
Nile River				
Univariate	3.21	168	0.91	0.92
M. var. Parana + Nile	-2.41	309	1.00	0.73
M. var. Nile + Murray	-3.31	239	0.94	0.83
M. var. Nile + Parana + Murray	20.17	553	1.18	0.47
Persistence	4.97	604	1.00	-0.10
Murray River				
Univariate	39.61	198	0.83	0.82
M. var. Parana + Murray	126.96	373	0.93	0.41
M. var. Nile + Murray	134.19	296	0.51	0.52
M. var. Nile + Parana + Murray	144.14	342	0.33	0.14
M. var. Parana + Murray + SSN	123.46	339	0.41	0.23
Persistence	55.16	386	1.00	0.38

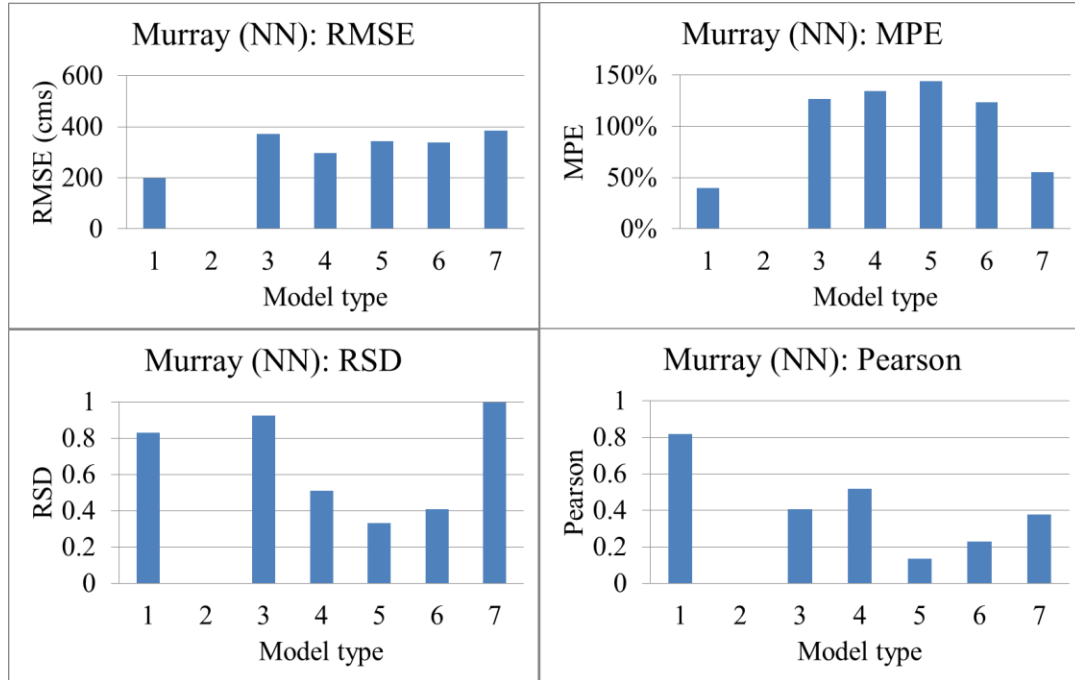
To further assess performance, criteria are plotted as shown in Figure 5.4.



(a)



(b)



(c)

Figure 5.4. Results of the RMSE, MPE, RSD, and SPPMCC (Pearson) performance indices of the ANN models, predicting the Parana, Nile, and Murray Rivers seasonal flows.

In the above figure, x-axis represents model type: (1) Univariate; (2) Multivariate model incorporating Parana and Nile Rivers; (3) Multivariate model incorporating Parana and Murray Rivers; (4) Multivariate model incorporating Nile and Murray Rivers; (5) Multivariate model incorporating Parana, Nile, and Murray Rivers; (6) Multivariate model incorporating Parana-Murray-SSN; and (7) Persistence model.

For a perfect forecast, the ANN model results have the RMSE and MPE values equal to zero and RSD and SPPMCC values equal to one. For the Parana River, Table 5.6 indicates the multivariate model incorporating three rivers has the lowest RMSE of 2219 cms. When these three rivers are used separately in a univariate model form, results are

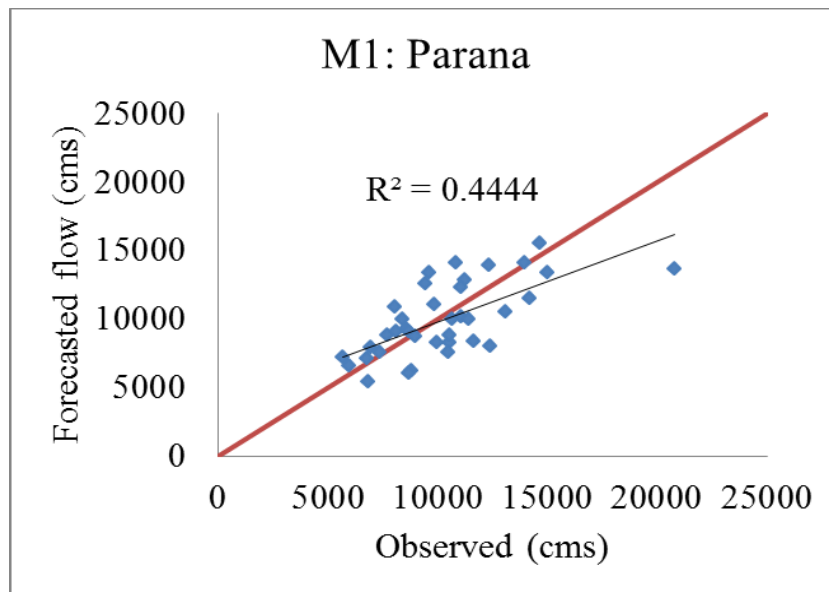
not as impressive (RMSE = 2313 cms for the Parana River). Comparing models based on the MPE, the univariate and multivariate models show an impressive performance, although the univariate model performance is the lowest and nearly equal to zero (-0.26%). However, the RSD statistics show different results for the Parana River, indicating efficiency of the multivariate model incorporating Parana and Murray Rivers. This RSD statistic also indicates that seasonal flow variability is well represented, although the RMSE, MPE and SPPMCC values indicate inferior performance compared to other models.

For the Nile River, the performance statistics for the univariate and the multivariate models based on the RMSE, MPE, RSD, and SPPMCC yield a univariate model with the lowest RMSE values (168 cms). The SPPMCC criterion also supports this as the value for the univariate model approached unity (0.91). In terms of MPE, the multivariate with Parana-Nile model indicates slightly improved performance (-2.4%) compare to the univariate model (3.2%), although the latter model performances are also close to zero percent forecast error, demonstrating impressive performance. The RSD criterion shows better performance for the univariate model with a magnitude of 0.91. However, the multivariate Parana-Nile model, and persistence model show RSD values near unity.

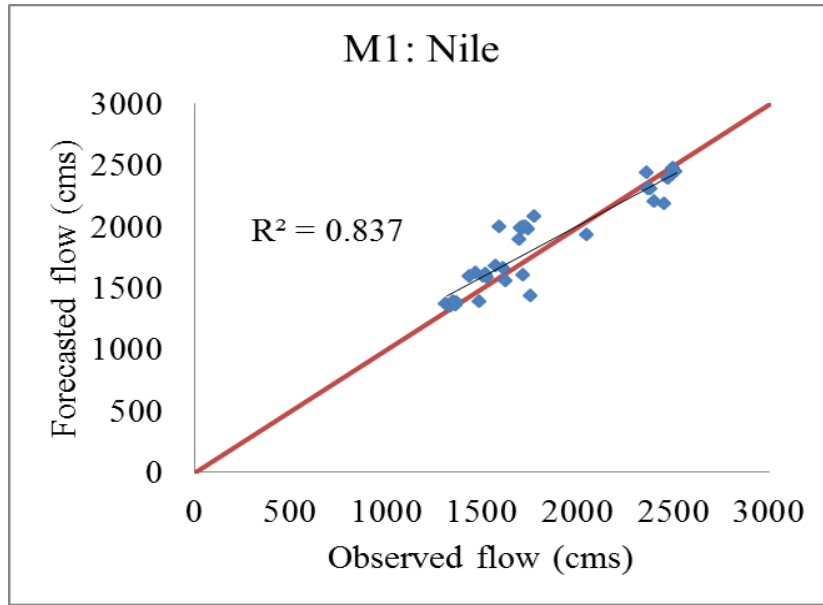
In case of the Murray River, the lowest RMSE is for the univariate model (197 cms). The MPE and the SPPMCC values for the multivariate models indicate lower performance. For the variability concern, the persistence model shows less error (RSD = 0.99) than other models although the results of the univariate (RSD = 0.83) and the multivariate Parana-Murray model (RSD = 0.93) are deemed satisfactory as near unity.

The regression plots of the corresponding river flow of testing data sets for the univariate models are included in Figure 5.5. The regression plots of the other model predictions are included in Appendix B.

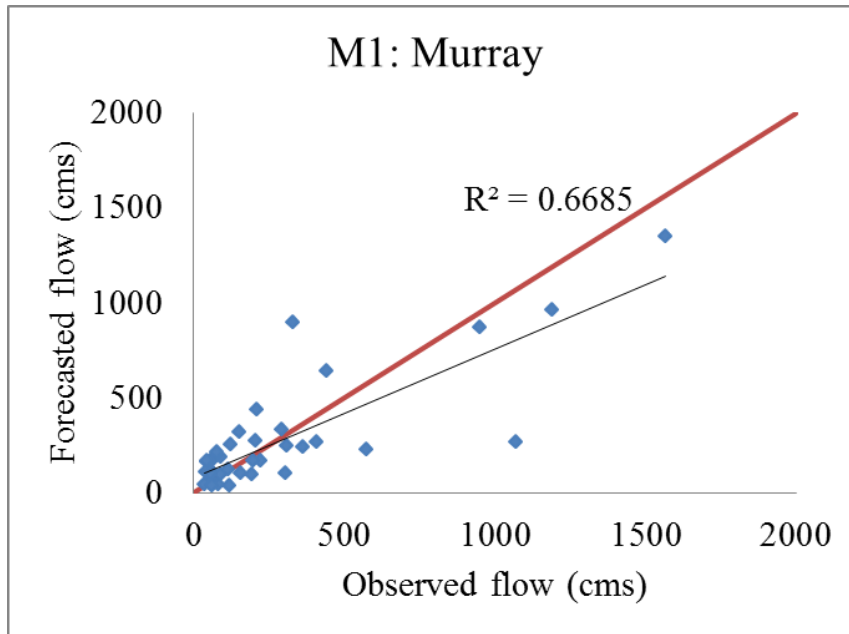
The MPE results for the Murray River demonstrate forecasting errors produced by the univariate and multivariate models are very large, ranging from 39.61% to 144.14% (far below the desired value of zero). This indicates poor model performance as the forecasted flows deviated much from the observed flows. The performance review of the multivariate models indicate inclusion of river flows and SSN are not efficient to improve Murray seasonal flows.



(a)



(b)



(c)

Figure 5.5. Regression plots of the univariate model (M1): (a) Parana River; (b) Nile River; and (c) Murray River.

Considering only a one-step-ahead forecasting in all results and model evaluations, overall, the RMSE, MPE, and SPPMCC criteria indicate the multivariate all-river model for Parana flow forecasting is best. The RSD indicates the persistence model and multivariate Parana-Murray model are better models. For the Nile and Murray River, univariate models are better in terms of RMSE, MPE, and SPPMCC criteria, whereas RSD statistics indicate persistence model is better. Results suggest that the inclusion of both river information and SSN as an external variable improve flow prediction skills under these selected criteria. It is not the case for all of the rivers, as the univariate and persistence models are often more efficient to forecast seasonal streamflow magnitude.

ANN Model Flow Categorization

The ANN model forecasted flows are categorized in high, average and low flow zones in order to assess the models' ability to predict extreme flow conditions. For the Parana and Murray Rivers, the 33rd percentile flows are 5898 cms and 60 cms, respectively. Similarly, the estimated 66th percentile flows of the Parana and Murray River are 9312 cms and 168 cms, respectively. Flow magnitudes below the 33rd percentile of the mean are designated as low flow and those above 66th percentile of the mean as high flow. For the Nile River, the flow category levels are subjectively set at 1600 cms and 2200 cms as the low and high limits. Flow magnitudes between these limits are categorized as average flow.

The ANN models are evaluated for the year 1970 to 1979 or 36 seasons. The resulting flow predictions for the Parana, Nile, and Murray Rivers are shown in Tables 5.7 to 5.9, respectively.

For seasonal Parana flow, the multivariate Parana-Nile model show better performance, predicting 27 flows correctly, whereas the univariate model performance is nearest for which the predictions are correct 26 times out of 36 flows. Performance of the multivariate Murray-SSN model is also satisfactory, as 25 times the forecasts followed the observed flow category. For the Nile and Murray Rivers, the univariate ANN models are better than the multivariate ANN models, as the predictions are correct 28 and 18 times, respectively. However, the multivariate Nile-Murray models show almost equal performance, predicting 26 out of 36 Nile seasonal flows correctly. For the Murray River, the multivariate all-river and multivariate Murray-SSN models performed well, forecasting 17 flows within the observed flow categories. Moreover, for none of the rivers, the persistence model shows better flow prediction skills, therefore, seems less attractive. However, the above analysis demonstrates overall forecasting skills of the models and do not represent the high and low flow forecast efficiency. Since the goal is to predict the seasonal flow extremes, capabilities of the models to forecast low and high flows are described in the next sections.

Model performances for the Parana, Nile, and Murray River low and high flow forecasts are also summarized in Tables 5.7, 5.8, and 5.9, respectively. For the river Parana, Nile, and Danube, total 1, 15, and 10 flows are identified as low. For the river Parana, Table 5.7 results indicate none of the models except the multivariate all-river model is efficient to predict the low flow category. However, results are different for the Parana high flow prediction, indicating the multivariate Parana-Nile model performance is better. Additionally, the multivariate all-river model is effective to forecast both the low and high flow of the Parana River. This indicates although the individual river flow

Table 5.7

Testing of ANN Model Forecasts for the Categorized Parana River Flow (Year 1971 to 1979).

River	Remarks	Univariate	M. var. Parana + Nile	M. var. Parana + Murray	M. var. Nile + Murray	M. var. Parana + Nile + Murray	M. var. Parana + Murray + SSN	Persistence
Low, average and high flow (total 36)								
	Correct forecast	26	27	22	-	21	25	20
	Outside category	10	9	14	-	15	11	16
Low flow (total 1)								
Parana	Correct forecast	0	0	0	-	1	0	0
	Outside category	1	1	1	-	0	1	1
High flow (total 22)								
	Correct Forecast	16	19	15	-	18	17	14
	Outside Category	6	3	7	-	4	5	8

Table 5.8

Testing of ANN Model Forecasts for the Categorized Nile River Flow (Year 1971 to 1979).

River	Remarks	Univariate	M. var. Parana + Nile	M. var. Parana + Murray	M. var. Nile + Murray	M. var. Parana + Nile + Murray	M. var. Parana + Murray + SSN	Persistence
Low, average and high flow (total 36)								
	Correct forecast	28	24	-	26	19	-	12
	Outside category	8	12	-	10	17	-	24
Low flow (total 15)								
Nile	Correct forecast	10	12	-	13	6	-	8
	Outside category	5	3	-	2	9	-	7
High flow (total 9)								
	Correct forecast	8	4	-	4	7	-	0
	Outside category	1	5	-	5	2	-	9

Table 5.9

Testing of ANN Model Forecasts for the Categorized Murray River Flow (Year 1971 to 1979).

River	Remarks	Univariate	M. var. Parana + Nile	M. var. Parana + Murray	M. var. Nile + Murray	M. var. Parana + Nile + Murray	M. var. Parana + Murray + SSN	Persistence
Low, average and high flow (total 36)								
	Correct forecast	18	-	15	17	17	17	16
	Outside category	18	-	21	19	19	19	20
Low flow (total 10)								
Murray	Correct forecast	4	-	0	0	0	0	4
	Outside category	6	-	10	10	10	10	6
	High flow (total 15)							
	Correct forecast	11	-	8	13	13	10	10
	Outside category	4	-	7	2	2	5	5

data is not very useful, the combination of the three river flow conditions could potentially be very useful in predicting the Parana low flows.

Model performances for the Parana, Nile, and Murray River low and high flow forecasts are also summarized in Tables 5.7, 5.8, and 5.9, respectively. For the river Parana, Nile, and Danube, total 1, 15, and 10 flows are identified as low. For the river Parana, Table 5.7 results indicate none of the models except the multivariate all-river model is efficient to predict the low flow category. However, results are different for the Parana high flow prediction, indicating the multivariate Parana-Nile model performance is better. Additionally, the multivariate all-river model is effective to forecast both the low and high flow of the Parana River. This indicates although the individual river flow

data is not very useful, the combination of the three river flow conditions could potentially be very useful in predicting the Parana low flows.

The multivariate model also shows impressive performance in forecasting low Nile River flow category. The best performance is achieved by the multivariate Nile-Murray model as the predictions are correct 13 times out of 16 low flows. However, for high Nile flows the univariate model performance is better, predicting 8 out of 9 high flows correctly. In addition, the multivariate all-river model demonstrates nearly equal performance (7 out of 9 high flows), although is inefficient in predicting low flows. Moreover, in terms of predicting both low and high flows, the univariate model is better.

The Table 5.9 reveals that for the river Murray, both univariate and persistence models are better in low flow prediction (correctly predicted 4 out of 10). Whereas, none of the multivariate model performance demonstrates low flow prediction skills. However, for high flow forecasting, the multivariate Nile-Murray model is better, predicting 14 out of 15 low flows correctly. In addition, all of the models show more or less skillful in predicting Murray high flows. These model performances are further assessed for both high and low flow prediction and the results indicate impressive performance with the univariate and persistence models.

The above analysis indicates multivariate models are better predicting low flows for the Parana (multivariate all-river model, correctly predicted the only low flows) and Nile (multivariate Nile-Murray model, 13 correct predictions) Rivers, whereas for the Murray River it is opposite (better performance with univariate and persistence models). The model performance for Parana low flow reveals an improvement in forecasting skills while the river flows are included together as predictors. The multivariate model results

differed from the Nile River as the improvements are evident with the Parana (12 correct predictions) and Murray (13 correct predictions) flows when included separately into the models as multivariate forms. The Murray low flow forecasts with the multivariate models (zero correct prediction) indicate less informative river flows and SSN to outperform the univariate and persistence model predictions (4 correct predictions).

5.3 Performance Analysis: Long Data Series (Congo, Yangtze, Rhine, Columbia and Parana River Flow)

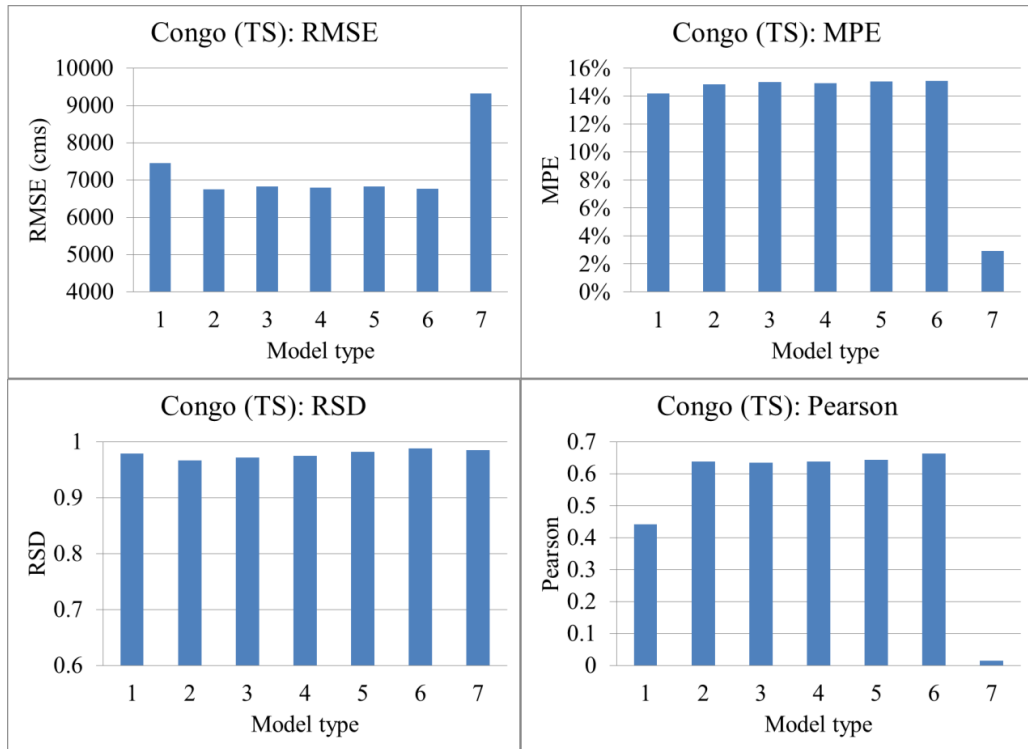
The four statistical indices, the RMSE, MPE, RSD, and SPPMCC are also adopted for evaluating time series and ANN model forecasts (from year 1982 to 1999), calibrated using seasonal flow (from year 1906 to 1980) of the Congo, Yangtze, Rhine, Columbia, and Parana Rivers. At first, the time series and ANN model performances are discussed separately. Later, both methodologies are compared and discussed briefly. Table 5.10 and Figure 5.6 represent performance statistics of time series and ANN model forecasts for the seasonal five river flow series.

Table 5.10

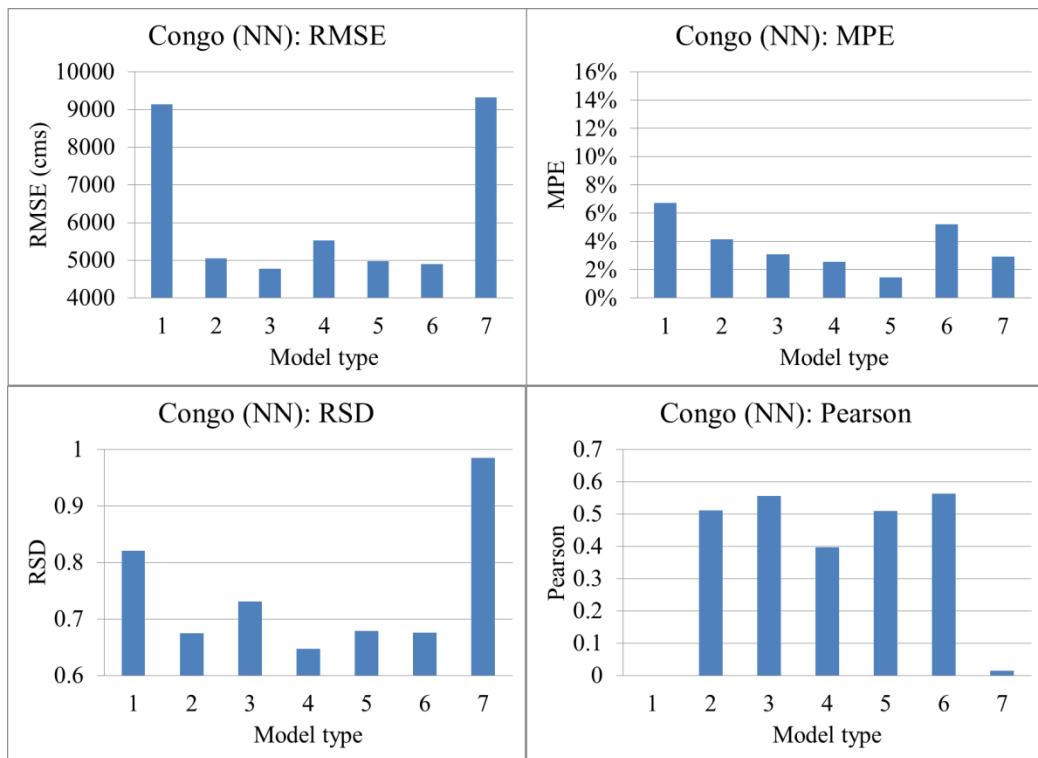
Summary of the Performance Evaluators of Time Series and ANN Model Forecasts for the Congo, Yangtze, Rhine, Columbia, and Parana Rivers.

Model	RMSE (cms)		MPE (x 100%)		RSD		SPPMCC	
	TS	ANN	TS	ANN	TS	ANN	TS	ANN
Congo River								
Univariate	7449	9144	0.142	0.067	0.979	0.821	0.443	0.001
M. var. 5 rivers	6754	5047	0.148	0.042	0.967	0.675	0.638	0.512
M. var. 5 rivers + SOI	6824	4770	0.150	0.031	0.972	0.732	0.635	0.556
M. var. 5 rivers + SOI + SSN	6796	5521	0.149	0.026	0.976	0.648	0.639	0.397

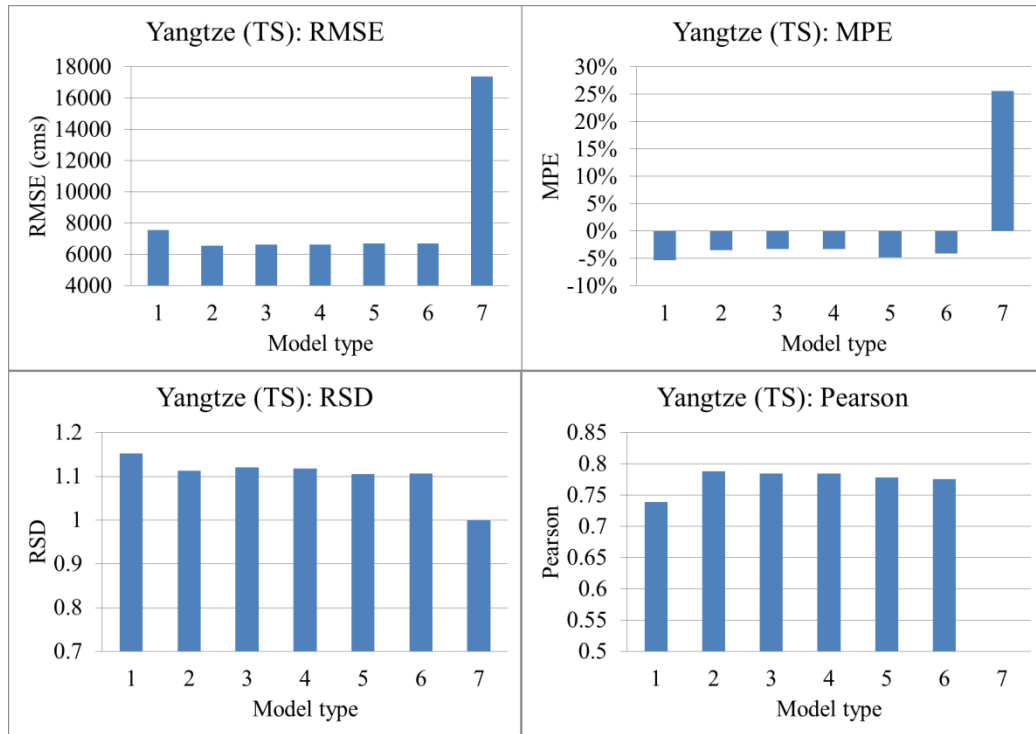
M. var. 5 rivers + SOI + SSN + PDO	6827	4980	0.151	0.014	0.983	0.679	0.643	0.511
M. var. 5 rivers + SOI + SSN + PDO + NAO	6768	4896	0.151	0.052	0.989	0.676	0.663	0.564
Persistence	9325	9325	0.029	0.029	0.985	0.985	0.016	0.016
Yangtze River								
Univariate	7545	6475	-0.053	0.001	1.152	1.080	0.739	0.777
M. var. 5 rivers	6542	6854	-0.035	0.051	1.113	0.758	0.788	0.718
M. var. 5 rivers + SOI	6629	6093	-0.033	0.005	1.120	0.765	0.784	0.803
M. var. 5 rivers + SOI + SSN	6616	6790	-0.033	0.050	1.118	0.877	0.784	0.713
M. var. 5 rivers + SOI + SSN + PDO	6707	8463	-0.048	0.035	1.105	0.881	0.778	0.571
M. var. 5 rivers + SOI + SSN + PDO + NAO	6704	8504	-0.041	0.027	1.106	1.033	0.776	0.611
Persistence	17400	17400	0.256	0.256	1.001	1.001	0.003	0.003
Rhine River								
Univariate	1035	773	0.096	0.083	1.106	0.223	0.062	0.072
M. var. 5 rivers	952	814	-0.048	0.086	0.846	0.422	0.062	0.030
M. var. 5 rivers + SOI	932	918	-0.034	0.001	0.823	0.318	0.064	0.037
M. var. 5 rivers + SOI + SSN	934	806	-0.029	0.042	0.835	0.711	0.064	0.125
M. var. 5 rivers + SOI + SSN + PDO	929	1008	0.062	-0.117	0.891	0.558	0.064	0.004
M. var. 5 rivers + SOI + SSN + PDO + NAO	914	774	0.064	0.084	0.869	0.285	0.069	0.068
Persistence	964	964	0.086	0.086	0.996	0.996	0.074	0.074
Columbia River								
Univariate	3583	1680	0.031	-0.005	2.297	0.904	0.222	0.269
M. var. 5 rivers	3033	1859	0.047	-0.026	1.882	1.191	0.179	0.312
M. var. 5 rivers + SOI	2996	2196	0.030	0.257	1.865	1.018	0.182	0.130
M. var. 5 rivers + SOI + SSN	3046	2509	0.037	0.182	1.887	1.004	0.175	0.000
M. var. 5 rivers + SOI + SSN + PDO	2775	2096	-0.036	-0.012	1.698	1.102	0.178	0.145
M. var. 5 rivers + SOI + SSN + PDO + NAO	2829	2189	-0.034	0.044	1.734	1.124	0.177	0.105
Persistence	1994	1994	0.073	0.073	1.004	1.004	0.132	0.132
Parana River								
Univariate	4786	3000	-0.213	-0.008	0.610	0.863	0.047	0.168
M. var. 5 rivers	5337	5510	-0.209	-0.218	0.574	0.637	0.032	0.032
M. var. 5 rivers + SOI	5292	3778	-0.208	-0.097	0.509	0.861	0.039	0.125
M. var. 5 rivers + SOI + SSN	5294	4273	-0.208	-0.123	0.508	0.832	0.041	0.057
M. var. 5 rivers + SOI + SSN + PDO	5323	3712	-0.211	-0.064	0.508	0.902	0.043	0.071
M. var. 5 rivers + SOI + SSN + PDO + NAO	5308	3702	-0.210	-0.038	0.508	0.995	0.047	0.066
Persistence	3073	3073	0.011	0.011	0.997	0.997	0.066	0.066



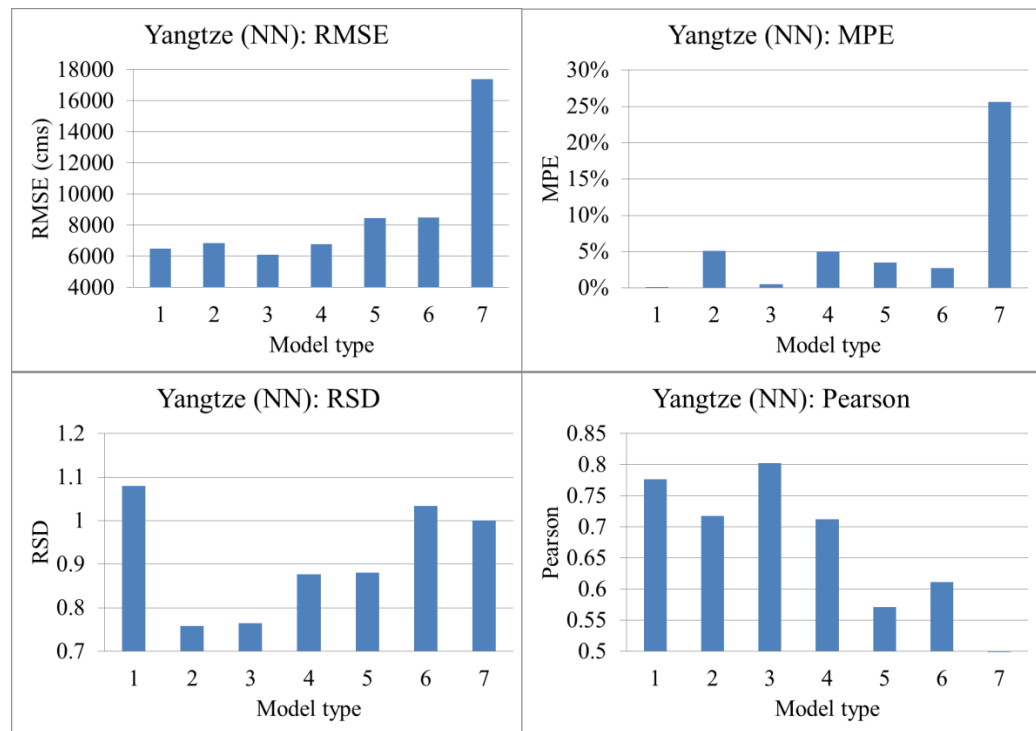
(a)



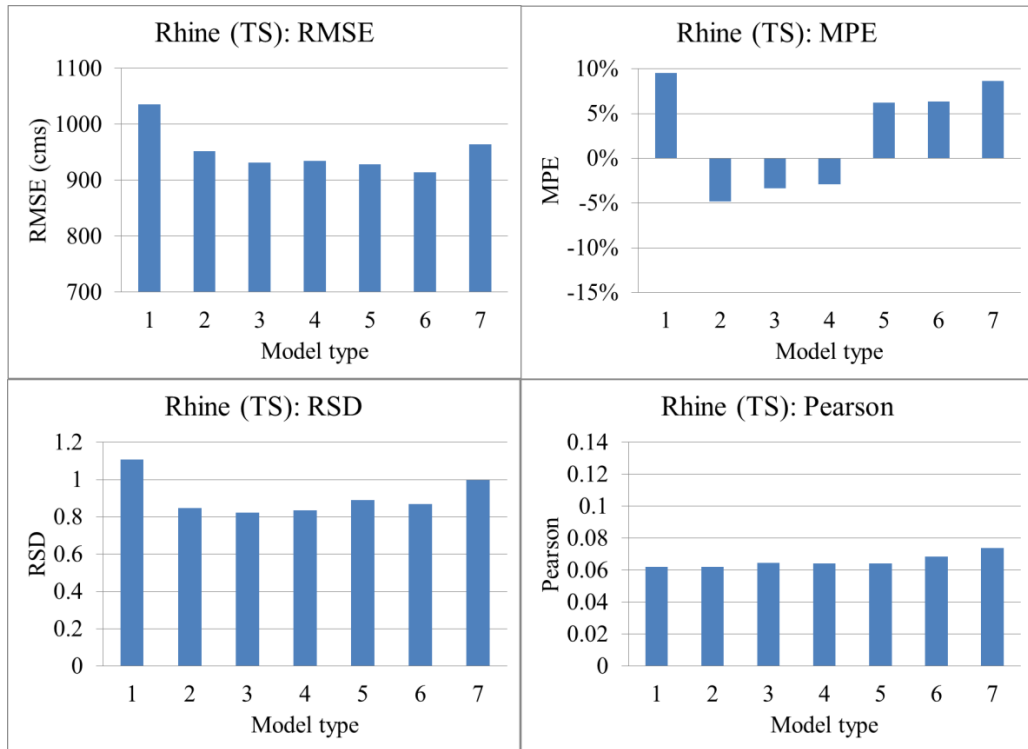
(b)



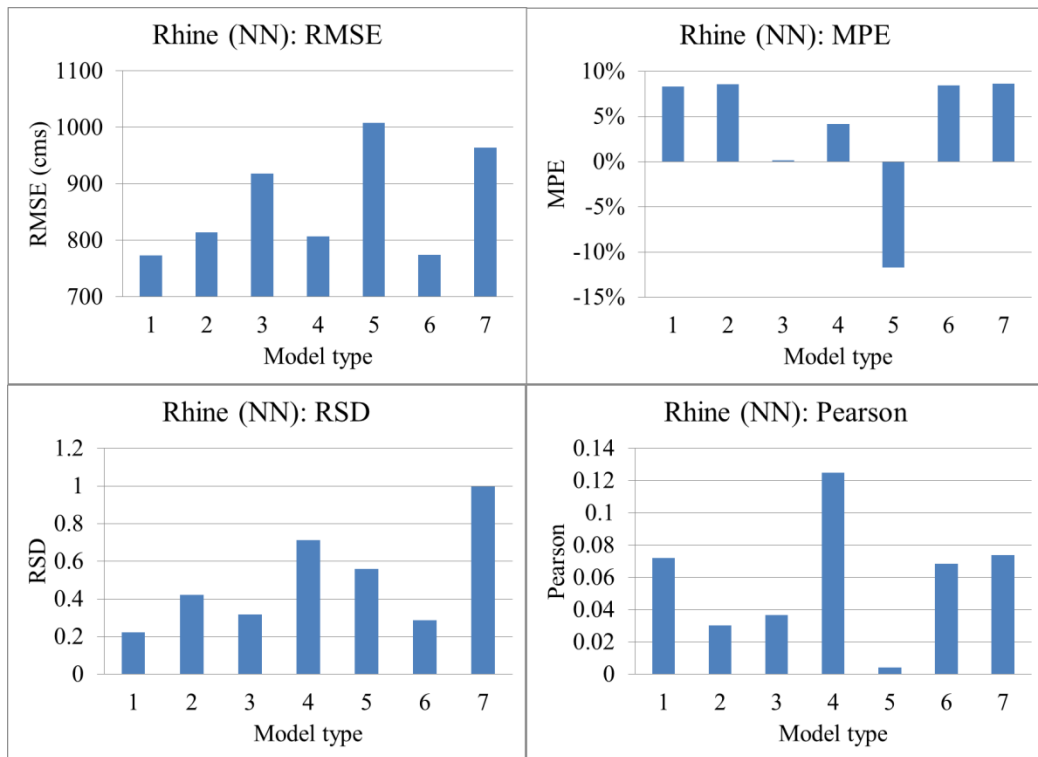
(c)



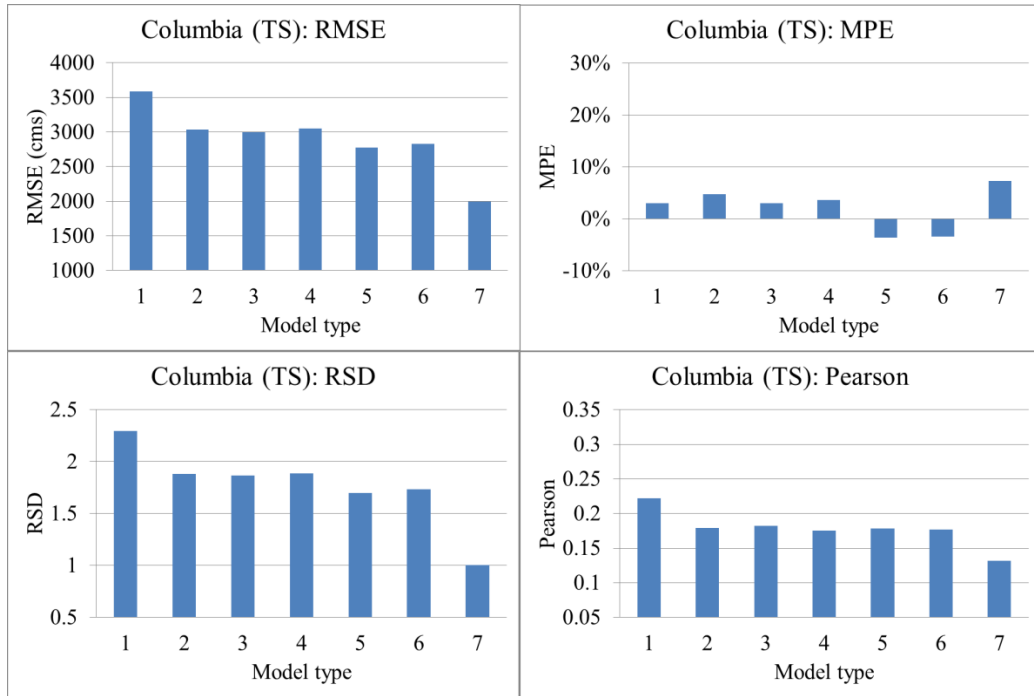
(d)



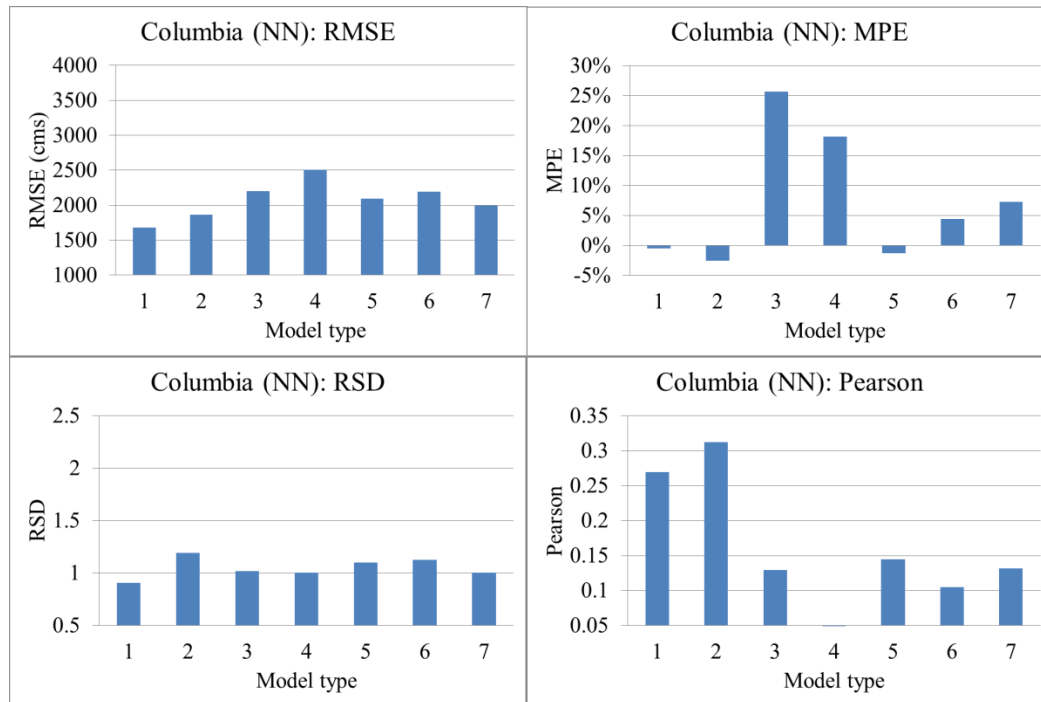
(e)



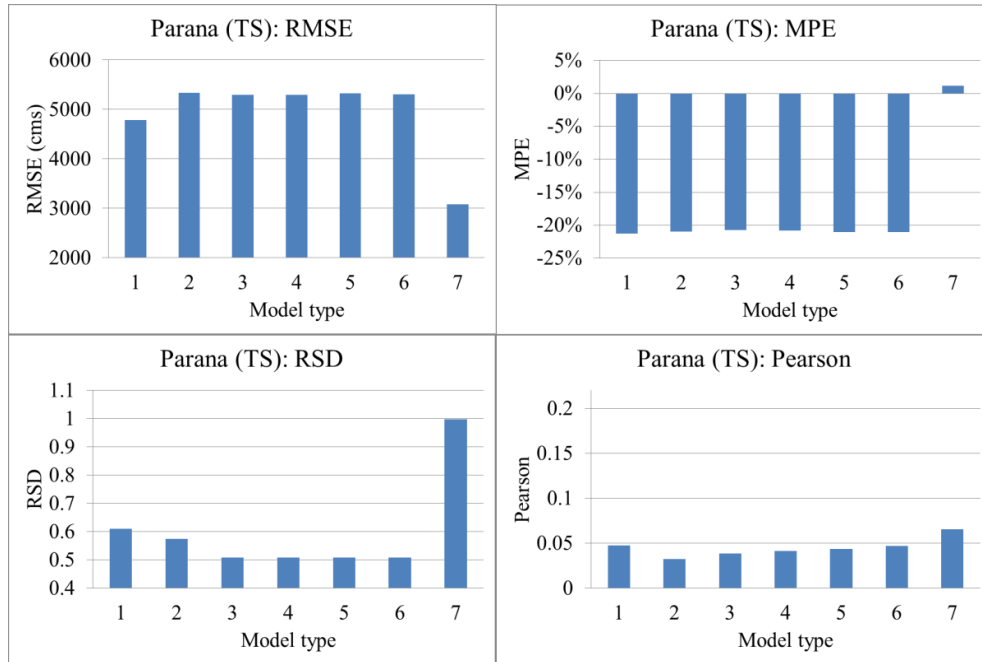
(f)



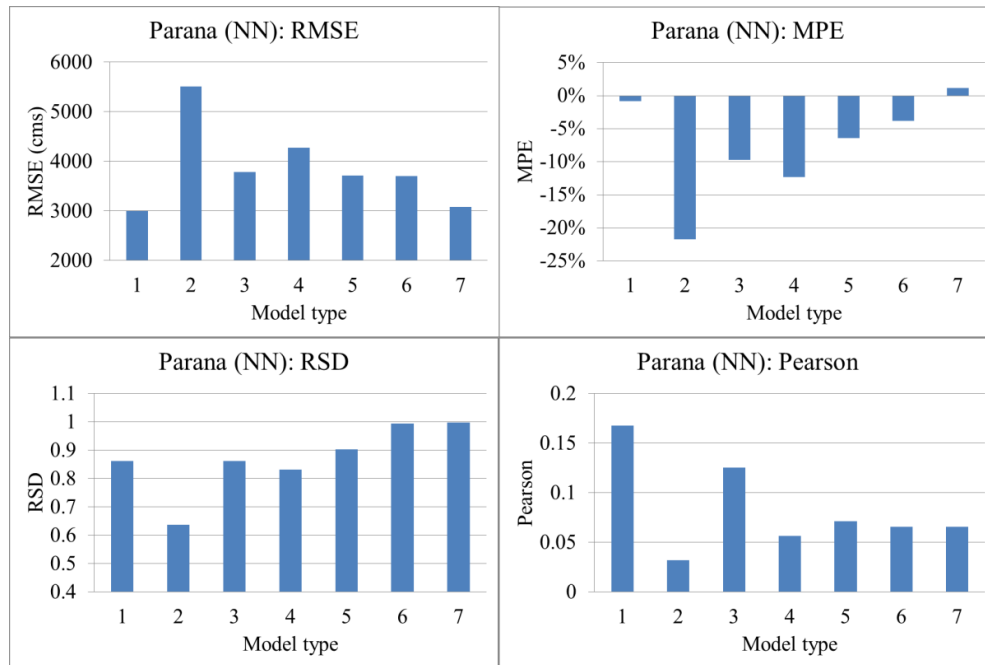
(g)



(h)



(i)



(j)

Figure 5.6. Performance evaluation of time series (TS) and neural network (NN) models for the Congo River (a, b), Yangtze River (c, d), Rhine River (e, f), Columbia River (g, h), and Parana River (i, j), respectively.

In the above figures, x-axis represents model type: (1) Univariate; (2) Multivariate incorporating 5 rivers; (3) Multivariate incorporating 5 rivers and SOI; (4) Multivariate incorporating 5 rivers, SOI, and SSN; (5) Multivariate incorporating 5 rivers, SOI, SSN, and PDO; (6) Multivariate incorporating 5 rivers, SOI, SSN, PDO, and NAO; and (7) Persistence. Left y-axis represents the root mean square error (RMSE). Right y-axis is mean % error (MPE), ratios of standard deviation (RSD), and square of the Pearson product moment correlation coefficients (SPPMCC).

5.3.1 Congo River

In terms of the RMSE, forecast based on the multivariate models are more accurate than the univariate model and persistence and the values vary from 6754 cms to 6824 cms. Among the models, the RMSE of multivariate five river model is minimum, therefore, represents a better forecast model. Based on the MPE and RSD, the univariate and multivariate models show almost equal values ranging from 14.2% to 15.1% and 0.972 to 0.989, respectively. The persistence model shows the lowest MPE value of 2.9%, whereas the highest SPPMCC value is obtained with the multivariate model incorporating five rivers and four external environmental variables (0.663). The above statistics except MPE indicate superiority of the multivariate models over the univariate and persistence models for predicting the Congo seasonal flows.

However, the performance indices used for the time series models are also adopted for the ANN models, so that the two methodologies can be compared to find out better forecast models. Similar to the time series models, the multivariate ANN model performances are better, resulting minimum RMSE values. Hence, the lowest RMSE

value of 4770 cms is obtained with the multivariate model incorporating five rivers and SOI. In terms of the MPE, the multivariate model incorporating five rivers, SOI, SSN, and PDO outperformed the other models, producing the lowest MPE value of 1.4%. However, the RSD of the ANN models differ from the time series models, indicating the persistence model as a better forecast model (RSD = 0.985). Whereas, in terms of the SPPMCC, the multivariate model incorporating five rivers, SOI, SSN, PDO, and NAO shows relatively better performance, producing the coefficient value of 0.564, although it is far below the desired value of one. This indicates the ANN models forecasts deviated much from the observed river flows. The SPPMCC statistics also show inefficient univariate (0.001) and persistence (0.016) models in predicting seasonal Parana flows.

Lower RMSE and MPE values for the ANN models over time series models indicate superiority of the ANN models over time series models, although the RSD and SPPMCC indices demonstrate time series models as better forecast models. The indices for the time series models reveal the external variables on average improved the model prediction accuracy. It is also noticeable that the inclusion of five rivers flow data decreased the RMSE value while compared with the univariate model (from 9144 cms to 5047 cms), an improvement of 44.8%. Thereafter, the added SOI information resulted in a decrease in the RMSE value from 5047 cms to 4770 cms, indicating an improvement of 5.4%. The RMSE statistics increased again from 4770 to 5521 cms (a 15.7% decrease of performance), due to the inclusion of SSN. Later, the PDO and NAO data reduced the RMSE values from 5521 to 4896 cms, an improvement of 11.3%. Therefore, the SOI, PDO, and NAO data provide better improvement on the univariate and persistence model forecasts rather than the SSN. This result deviates from the time series model for which

the model performance decreases after including the SOI and PDO, but increases after five rivers, SSN, and NAO data. This RMSE results indicate contrasting behavior of the five rivers, SOI, SSN, and PDO data when included in the time series and ANN models. The roles of these variables in the models developed to forecast Congo flow are not clear from review of RMSE values. However, in both time series and ANN models, inclusion of the NAO increase the model performance, therefore, indicating possible NAO influence on the flow.

5.3.2 Yangtze River

The time series and ANN model performances for the Yangtze River seasonal flow predictions are summarized in Table 5.10. The RMSE of time series models show the multivariate model incorporating five rivers, SOI, SSN, and PDO has the lowest RMSE value, although other multivariate model performances are nearly similar. The univariate and persistence models do not perform well, producing higher RMSE values. The MPE, RSD, and SPPMCC indicate similar performances with the multivariate models, showing almost equal values. However, the RSD of the persistence model approached to unity, indicating the seasonal flow variability is well represented in this model. Conversely, low SPPMCC (0.003) and comparatively high MPE value (0.256) stated poor performance with the persistence model.

The ANN model statistics show similar variable performances as the time series models with not much variation in the results. The RMSE values demonstrate the efficiency of multivariate models over the persistent model, although the multivariate model incorporating five rivers, SOI, SSN, PDO, and five rivers, SOI, SSN, PDO, and

NAO performances are poor. The RMSE of the multivariate ANN model incorporating five rivers and SOI is the lowest, indicating better predictions with the model. In terms of the MPE, all models are better than the persistence model, showing values almost equal to zero. The RSD of the univariate model, multivariate model incorporating five rivers and all external variables, and persistence model are approximately equal to one, indicating better performance, whereas skills of the other multivariate ANN models decrease in comparison to the multivariate time series models. The SPPMCC (varied from 0.571 to 0.803) values indicate best performance with the multivariate ANN model incorporating five rivers and SOI (SPPMCC = 0.803), although the univariate model performance was nearly equal (SPPMCC = 0.777).

From the performance review of time series and ANN models, the multivariate ANN model incorporating five rivers and the SOI shows the lowest RMSE of 6093 cms. The ANN model shows a reduced RMSE statistics when the SOI is included. The time series model performance differed from the ANN model, in terms of influence of SSN. Inclusion of the SSN decreases the time series model RMSE from 6823 cms to 6795 cms, an improvement of 0.4 % (0.004). The corresponding RMSE values for the ANN models are 4769 cms to 5521 cms, a change of 13.6%. In all other cases, incorporating multivariable data reduces time series model performances in terms of RMSE. The performance criteria of all forms of multivariate time series models evaluated are not large. This indicates either a lack of association between the external variables and the Yangtze seasonal flows or an inappropriate modeling approach.

In general, the MPE statistics indicate superiority of the ANN models over time series models, producing a forecast error of 0.1% for the univariate ANN model. The

multivariate ANN model incorporating five rivers and SOI shows similar performance, producing an MPE equal to 0.5%. The Table 5.10 summarizes model performances in terms of MPE, showing the inclusion of PDO and NAO data reduce the MPE. The MPE results also indicate contrasting behavior of the SSN data when included in the time series and ANN models. The influence of SSN improves the time series model, but decreases the ANN model performance. The role of SSN in the models developed to forecast Yangtze flow is not clear from the review of MPE values. However, the RSD values indicate improvement in the ANN model skill when multi-variable data are included, while time series model performance decreased when SOI and NAO data are included. This is indicated as a higher RSD value rather than decreasing towards one. The SPPMCC values for both time series and ANN models are similar, although the multivariate ANN five rivers and SOI model yields the best result with a value equal to 0.803.

5.3.3 Rhine River

For the Rhine River, Table 5.10 results indicate comparatively higher RMSE value for the univariate time series model (1035 cms), and lower values for the multivariate models, ranging from 914 cms to 952 cms. Interestingly, the RMSE of multivariate models are decreasing with an increasing number of variables, except the SSN for which the RMSE increases from 932 cms to 934 cms, a 0.2% decrease of performance in comparison to the model incorporating five rivers and the SOI. The inclusions of multi-variable data decrease the RMSE statistics from 1035 cms to 914 cms, a total improvement of 11.7% (0.117). Among all models, the multivariate model

incorporating five rivers and all external variables performed the best, resulting lowest RMSE value of 914 cms. The persistence model RMSE is 964 cms, 5.2% higher than the best RMSE statistics of 914 cms. In terms of MPE, the multivariate model incorporating five rivers, SOI and SSN is best, showing the lowest MPE statistics of -2.9% (-0.029). However, the RSD results differ from those of the RMSE and MPE, indicating best performance with the persistence model as the value approaches unity (0.996). The other performance criteria, the SPPMCC, for all forms of time series models evaluated, shows values nearly equal to zero. This demonstrates either an improper selection of the predictor variables or an inappropriate modeling approach.

Similar to time series model, the multivariate ANN model incorporating five rivers and all external variables indicates best performance, resulting lowest RMSE of 774 cms. The univariate ANN model also performed same, showing nearly equal RMSE value. The RMSE of all other models except the multivariate model incorporating five rivers, the SOI, and SSN increased when the variables are incorporated in the models. This indicates decrease of model performance, although the corresponding RMSE values for time series models indicate improvement in the prediction skills. These results also indicate contrasting behavior of the five river flows, the SOI, and PDO data when included in the time series and ANN models. The role of these three variables in the models developed to forecast Rhine flows are not clear just from review of the RMSE values. Both model results show improvement of model performance with the NAO information, indicating NAO influence on Rhine seasonal flows. However, the MPE statistics show superiority of multivariate model incorporating five rivers and the SOI, producing least error forecast (MPE = 0.1%). The RSD values of the ANN models

indicate similar time series model performance, as in both cases, the models are unsuccessful to outperform the persistence model forecasts. This indicates inefficiencies of the models to capture the variability of Rhine flows. However, the SPPMCC of both univariate and multivariate ANN models show values nearly equal to zero, (ranging from 0.004 to 0.125), indicating less skillful ANN models. The near zero coefficient values also demonstrate large deviations of the forecasted flows in comparison to the observed flow condition.

The table results also indicate that ANN model produces the lowest RMSE value than those of the time series models. The MPE statistics also supported the ANN models as better forecast models, resulting in relatively lower statistics. However, the RSD of the time series models are higher in comparison to the ANN models, indicating superiority of time series models. In addition, result differences between the SPPMCC of time series and ANN models are not very significant to indicate a better forecast model.

However, the RMSE of some of the ANN models behave differently than those of the time series models when the variables are incorporated such as with five river flows, the SSN and PDO data. The RMSE results indicate contrasting behavior of the five river flows, the SOI, SSN and PDO data when include in the time series and ANN models. The inclusion of five rivers, SOI, and PDO data improve the time series model but decrease the performance of ANN model. Conversely, the SSN decreases the time series model but improves the ANN model performance. Therefore, the role of five rivers, the SOI, SSN, and PDO in models developed to forecast Rhine flow are not clear from review of the RMSE results. However, association between the Columbia flows and the NAO is evident as in both time series and ANN models, the NAO data decreases the RMSE

values. Overall, these external variables thus provided the models with more or less skills.

5.3.4 Columbia River

For the Columbia River, the RMSE statistics of time series models show superiority of the persistence model over the univariate and multivariate models, yielding lowest RMSE value of 1994 cms. In terms of MPE, the multivariate model incorporating five rivers and the SOI performed better, demonstrating least forecast error of 3%. For other time series models, the errors are nearly equal, ranging from 3.1% to 4.4%. This indicates the MPE of time series models evaluated are not very large (0.1% to 1.4% higher in comparison to the lowest MPE) to differentiate model performances. However, the univariate time series model shows better performance with the RSD value of 0.863 in comparison to the multivariate models (RSD values ranging from 1.698 to 1.887). Conversely, the persistence model produces RSD value nearest to one (1.004), indicating superior forecast performance. Another performance criterion, the SPPMCC of univariate and multivariate models evaluated, show values far below the desired value of one (ranging from 0.177 to 0.222). This indicates less skillful time series models for predicting seasonal Columbia flows. The near zero values also demonstrates that the forecasted flows deviated much from the observed flows.

The ANN model performances are also summarized in Table 5.10. The RMSE of the univariate ANN model indicates minimum RMSE value of 1680 cms, therefore, outperformed the multivariate and persistence model forecasts (RMSE values ranged from 1859 cms to 2509 cms). The MPE of the ANN models also indicate superiority of

the univariate model, producing least forecast errors of -0.5%. Conversely, the multivariate model incorporating the SOI and SSN, and the persistence model show better performance in terms of RSD. However, the SPPMCC demonstrates the multivariate model incorporating five rivers is best (0.312), although coefficients of this model as well as all of the other models are nearly equal to zero. The zero proximity of the RSD statistics indicates less accurate forecasts, when comparing with the observed seasonal flows.

Results of the RMSE index for time series models indicated inclusion of five rivers flow data decreases the RMSE value from 3583 cms to 3033 cms, an improvement of 15.4%. Hence, the SOI information decreases the statistics more to 2996 cms, an improvement of 1.2%. Inclusion of the SSN information increases the RMSE value again to 3046 cms (1.7% decrease of performance). Later, the PDO decreases the statistics to 2775 cms (an improvement of 8.9%), while increases again to 2829 cms when the NAO data was added (1.9% decrease of performance). However, the ANN model performances differed from the times series models in terms of SOI. Inclusion of the SOI increased the RMSE from 1859 cms to 2196 cms, indicating a decrease of model performance of 18.1%. Therefore, the role of SOI in the models developed to forecast Columbia flow is not clear just from review of the RMSE values. Moreover, inclusion of the SSN and NAO information increase the RMSE values of both time series and ANN models, whereas the PDO data decreases the statistics. This indicates PDO influence on the Columbia flows, and lack of association with SSN and NAO.

In general, the ANN models show better forecasting skills than the time series models, while comparing the model performances based on all of the indices. Small

variation in the MPE values also made it difficult to understand the behavior of the external variables. Inclusion of five rivers as well as five rivers and the SOI decrease the RSD statistics of the univariate model from 2.30 to 1.88 and 1.88 to 1.87, an improvement of 18.3%, and 0.5%, respectively. It increases again to the value 1.89 when the SSN data is incorporated. Later, incorporation of PDO data decreases the RSD to 1.698 (an improvement of 10%), although increases again to 1.734 (1.7% decrease of performance), when NAO data is included. This indicates influence of five rivers, SOI, and PDO on the Columbia seasonal flows. However, RSD statistics of the ANN multivariate models show improvement with the SOI and SSN data. The contrasting behavior of the SSN data, when included in time series and ANN models, makes it difficult to identify the role of SSN. Furthermore, the SPPMCC of both time series and ANN models are far below the threshold value one, indicating unsatisfactory forecasting skills. Overall results of the four indices demonstrate that inclusion of river flow information and external variables thus provided skills into the models.

5.3.5 Parana River

The RMSE of the multivariate time series models vary from 5292 cms to 5337 cms, whereas the univariate model RMSE is 4786 cms. This demonstrates better univariate model forecasts, although the persistence model performance is best, producing the lowest RMSE of 3073 cms. The MPE, RSD, and SPPMCC criteria indicate superiority of the persistence model over the other models. The RSD of the univariate model is better than those of the multivariate models, although the value is well below the threshold value of unity or the persistence model statistics (0.997). In addition, the

SPPMCC of the time series models are almost equal to zero. This indicates seasonal flow variations are not represented well in the time series model forecasts.

The Table 5.10 results indicates, the univariate ANN models produce the lowest RMSE of 3000 cms, demonstrating its superiority over the multivariate ANN models (ranged from 3702 cms to 5510 cms) and persistence model (3073 cms). The RSD statistics indicates the efficiency of persistence model (RSD = 0.997), although the performance of multivariate ANN model including five rivers and all external variables is almost equal (RSD = 0.995). The MPE statistics of the univariate model ranging from -0.8% to 4.7%, demonstrate an improved univariate ANN model performance (MPE = 0.08%) in minimizing forecasting errors while compare with the persistence model statistics (MPE = 7.3%). However, the SPPMCC for all models are almost equal to zero, indicating forecasts deviated far from observed flows.

The time series and ANN model performances are further evaluated to determine the best forecast model along with the variables, influencing the Parana flows. The Table 5.10 results demonstrate the superiority of ANN models over the time series model, producing lower RMSE statistics. However, the RMSE values for the univariate time series model is 4786 cms and multivariate model incorporating five rivers is 5337 cms. This indicates addition of the five river information does not influence a decrease in the RMSE value. The model show a reduced RMSE statistics from 5337 cms to 5292 cms, when the SOI is included (an improvement of 0.8%). Inclusion of the SSN and PDO increase the RMSE again from 5292 cms to 5323 cms (a total 0.6% decrease of performance). Later, the NAO reduces the RMSE value to 5308 cms, an improvement of 0.3%. Hence, the additions of these variables are insufficient to outperform the univariate

time series and persistence model performance. For the ANN models, the RMSE statistics increases from 3000 cms (univariate model) to 5510 cms (an 83.7% decrease of performance) when the five river flows are included. Inclusion of the SOI reduces the RMSE value to 3778 cms, indicating an improvement of 31.4%. Meanwhile, the SSN information increases the RMSE value from 3778 cms to 4273 cms, whereas the PDO and NAO decreases it again to the value of 3713 cms and 3702 cms (an improvement of 13.1% and 0.3%), respectively. Improvement of both time series and ANN model performance after including the SOI, PDO, and NAO indicate associations between the Parana flows and external variables. Results also indicate that the SSN information does not improve the model performance. The reduced MPE values of the ANN multivariate models with the SOI, PDO, and NAO information indicate the variables, on average, provided skills into the models. However, the MPE, RSD, and SPPMCC criteria of all forms of multivariate models evaluated were not large to indicate the variable influence on improving the model performance; whereas the increasing tendency of the RSD values towards unity in the multivariate ANN model also demonstrate influences of the PDO, SOI, and NAO variables to modulate the Parana flows. The four performance criteria also indicate reduced model performance when the five river flows are included. Overall, results indicate although the multivariate models are not skillful enough to outperform the univariate and the persistence model performances, the external variables thus provide more or less skills into the models

5.4 Flow Categorization and Forecast

Similar to the short term data series, the ability of time series and ANN model to predict low and high flows is assessed by categorizing five river flows into three flow zones. For the rivers Congo, Yangtze, Rhine, Columbia, and Parana, the 33rd percentile flows are identified as 35823 cms, 21481 cms, 1824 cms, 3240 cms, and 12257 cms and the 66th percentile flows are found as 44031 cms, 35845 cms, 2382 cms, 6153 cms, and 15867 cms, respectively. The performance of the models to perform categorical river flow forecasts are described below:

5.4.1 Congo River

Among 72 seasonal flows of the Congo River, 32 flows are high and 14 flows are low. The remainders (26 of the 72 seasonal flows) are categorized as average flow. The time series and ANN model forecasts are also categorized accordingly to compare with the observed flows. The resulting model predictions are summarized in Table 5.11 and 5.12. The table results reveal the multivariate time series models incorporating five rivers with SOI and SSN, and five rivers with SOI, SSN and PDO, performed the best, predicting 38 of the 72 flows correctly. In addition, the multivariate models incorporating five rivers and five rivers and all external variables show nearly equal performance, as both the model predictions matched 37 times with the observed flow categories. For the performance review of time series and ANN models, the multivariate ANN models incorporating five rivers and the SOI and five rivers and the SOI, SSN, and PDO are best, predicting the flows correctly 45 of 72 times. Overall model performance revealed

superiority of multivariate models over the univariate and persistence models, when all three flow categories are considered to be forecasted.

Table 5.11

Time Series Model Forecast Validation for the Categorized Congo Flow (1982-1999)

River	Flow	Univariate	M. var. 5 rivers	M. var. 5 rivers + SOI	M. var. 5 rivers + SOI + SSN	M. var. 5 rivers + SOI + SSN + PDO	M. var. 5 rivers + SOI + SSN + PDO + NAO	Persistence
Overall Categories- low, average and high flow (total 72)								
	Correct forecast	35	37	35	38	38	37	23
	Outside category	37	35	37	34	34	35	49
Low flow (total 32)								
Congo	Correct forecast	12	13	12	13	13	12	14
	Outside category	20	19	20	19	19	20	18
High flow (total 14)								
	Correct forecast	12	13	13	13	13	13	3
	Outside category	2	1	1	1	1	1	11

Table 5.12ANN Model Forecast Validation for the Categorized Congo Flow (1982-1999)

River	Flow	Univariate	M. var. 5 rivers	M. var. 5 rivers + SOI	M. var. 5 rivers + SOI + SSN	M. var. 5 rivers + SOI + SSN + PDO	M. var. 5 rivers + SOI + SSN + PDO + NAO	Persistence
Overall forecasts- low, average and high flow (total 72)								
	Correct forecast	22	41	45	41	45	42	23
	Outside category	50	31	27	31	27	30	49
Low flow (total 32)								
Congo	Correct Forecast	12	23	26	23	25	21	14
	Outside category	20	9	6	9	7	11	18
	High flow (total 14)							
	Correct Forecast	2	3	5	2	4	5	3
	Outside category	12	11	9	12	10	9	11

The skills of model predictions can be further appreciated by considering extreme flow condition (low and high flow). An analysis is carried out to compare time series and ANN model performances for predicting low and high Congo flows. The resulting model predictions are shown in Table 5.11. The table results reveal 12 correct low flow predictions with the univariate time series model but 13 with the multivariate models, therefore, indicating relatively better multivariate model performance. Hence, the persistence model performance is best, predicting 14 of the 32 low flows correctly. The ANN model results are summarized in Table 5.12. The table results reveal almost two times more correct predictions with the multivariate models in comparison to the univariate model. However, the multivariate ANN model incorporating the SOI showed best performance, predicting 26 low flows correctly. The univariate model results are not as impressive as the multivariate models, since in only 12 of the 32 seasons the

predictions of low flow matched with the observations. It is further noticed that inclusion of the five rivers and the SOI and PDO improve the ANN model performance. This indicates that the five river flow conditions, SOI and PDO could potentially be very useful in predicting the Congo low flows. Moreover, inclusion of the SSN and NAO data slightly decrease the model skills, therefore indicating less SSN and NAO influence on the Congo River low flow condition.

The Tables 5.11 and 5.12 also summarize model performances in terms of Congo high flow predictions. Results indicated 12 correct predictions with the univariate time series model, whereas the multivariate models show 13 out of 14 correct predictions. Performances of the multivariate time series models also indicate inclusion of river flows and external variables data on average improve model prediction skills. However, among the ANN models, the multivariate models show best performance, predicting 5 of the 14 high flows correctly. Therefore, performance review of time series and ANN models indicate superiority of time series model over ANN model in terms of predicting high Congo flows, whereas low flows are predicted better with the ANN models.

5.4.2 Yangtze River

The performance of time series and ANN models for predicting Yangtze seasonal categorical flows are summarized in Tables 5.13 and 5.14, respectively. Overall results revealed the univariate time series model performance is best, predicting 61 of the 72 flows correctly. The multivariate time series models show nearly equal performances, for which 57 times the predictions matched the observed flow categories. However, similar to the time series model, univariate ANN model outperformed the multivariate ANN

models, predicting 64 of the 72 flows correctly. This indicates superiority of the univariate models over the other models. The performance of the multivariate model incorporating five rivers and the SOI is also impressive, predicting 62 flows correctly. In addition, persistence model show poor performance, as only 6 times the predictions are within the observed flow categories.

Table 5.13

Time Series Model Forecast Validation for the Categorized Yangtze Flow (1982-1999)

River	Flow	Univariate	M. var. 5 rivers	M. var. 5 rivers + SOI	M. var. 5 rivers + SOI + SSN + PDO	M. var. 5 rivers + SOI + SSN + PDO	M. var. 5 rivers + SOI + SSN + PDO + NAO	Persistence
Overall Categories- low, average and high flow (total 72)								
	Correct Forecast	61	57	57	57	57	57	6
	Outside category	11	15	15	15	15	15	66
Low flow (total 20)								
Yangtze	Correct forecast	19	19	19	19	19	19	2
	Outside category	1	1	1	1	1	1	18
	High flow (total 21)							
	Correct forecast	16	15	15	15	15	15	3
	Outside category	5	6	6	6	6	6	18

Table 5.14ANN Model Forecast Validation for the Categorized Yangtze Flow (1982-1999)

River	Flow	Univariate	M. var. 5 rivers	M. var. 5 rivers + SOI	M. var. 5 rivers + SOI + SSN	M. var. 5 rivers + SOI + SSN + PDO	M. variate 5 rivers + SOI + SSN + PDO + NAO	Persistence
Overall Categories- low, average and high flow (total 72)								
	Correct forecast	64	55	61	58	49	52	6
	Outside category	8	17	11	14	23	20	66
Low flow (total 20)								
Yangtze	Correct forecast	18	19	19	20	18	19	2
	Outside category	2	1	1	0	2	1	18
	High flow (total 21)							
	Correct forecast	18	12	15	16	12	13	6
	Outside category	3	9	6	5	9	8	15

Among 72 seasonal flows of the Yangtze validation period (1982 to 1999), a total of 20 and 21 flows were identified as low and high flows, respectively. The rest 31 flows were categorized as average flows. The time series and ANN model forecasts were categorized accordingly to compare with the observed flows. The resulting model predictions are summarized in Tables 5.13 and 5.14. Table results of both univariate and multivariate models reveal equal performances, predicting 19 of the 20 low flows correctly. The persistence model is not skillful, as only two times the predictions matched the observed low flow category. However, similar analyses with ANN models reveal the multivariate model incorporating five rivers, the SOI and SSN performance is best, predicting all the low flows correctly. This indicated improvement of model skills, when SSN data is incorporated. For the performance review of time series and ANN models,

the univariate model and the other multivariate models of both the methodologies show nearly equal performance in terms of predicting Yangtze low flows.

The Tables 5.13 and 5.14 summarize model performance in terms of Yangtze high flow predictions. Results indicate the univariate time series model performed the best, predicting 16 of the 21 high flows correctly. All of the multivariate time series models show nearly equal performances, for which the predictions match the observations 15 times. In addition, the persistence model performance is not impressive as it was able to predict only three high flows correctly. Review of the ANN model performances also indicates superiority of univariate model over multivariate models, for which predictions are correct 18 times out of 21 high flows. However, the five river information decreases the multivariate ANN model performance to 12 correct predictions (a 33.3% decrease of performance). Inclusion of the SOI and SSN information improve the multivariate model skills again, from 12 to 15 (an improvement of 25%) and 15 to 16 (a 6.7% decrease of performance) correct predictions. The model performance decreases again from 16 to 12 correct predictions, when the PDO included. Later incorporation of the NAO data improves the model performance from 12 to 13 correct high flow predictions. Therefore, influence of five river flows and the external variables are evident, although the model skills are not significant enough to outperform the univariate ANN model forecasts.

5.4.3 Rhine River

The overall performance of the time series and ANN models in predicting seasonal categorical Rhine flows are summarized in Tables 5.15 and 5.16, respectively.

Table 5.15Time Series Model Forecast Validation for the Categorized Rhine Flow (1982-1999)

River	Flow	Univariate	M. var. 5 rivers	M. var. 5 rivers + SOI	M. var. 5 rivers + SOI + SSN	M. var. 5 rivers + SOI + SSN + PDO	M. var. 5 rivers + SOI + SSN + PDO + NAO	Persistence
Overall categories- low, average and high flow (total 72)								
	Correct forecast	30	29	25	22	28	28	30
	Outside category	42	43	47	50	44	44	42
Low flow (total 24)								
Rhine	Correct forecast	11	12	11	11	10	9	10
	Outside category	13	12	13	13	14	15	14
	High flow (total 29)							
	Correct forecast	16	7	6	6	13	14	15
	Outside category	13	22	23	23	16	15	14

Table 5.16ANN Model Forecast Validation for the Categorized Rhine Flow (1982-1999)

River	Flow	Univariate	M. var. 5 rivers	M. var. 5 rivers + SOI	M. var. 5 rivers + SOI + SSN	M. var. 5 rivers + SOI + SSN + PDO	M. var. 5 rivers + SOI + SSN + PDO + NAO	Persistence
Overall categories- low, average and high flow (total 72)								
	Correct forecast	27	20	15	32	28	26	30
	Outside category	45	52	57	40	44	46	42
Low flow (total 24)								
Rhine	Correct forecast	0	0	2	8	13	0	10
	Outside category	24	24	22	16	11	24	14
High flow (total 29)								
	Correct forecast	15	13	3	18	7	14	15
	Outside category	14	16	26	11	22	15	14

In general, Table results indicate the univariate time series and persistence model performances are best, predicting 30 out of 72 flows within the selected flow categories (low, average, high). The results of the multivariate time series models incorporating five rivers, five rivers, SOI, SSN, and PDO, and five rivers incorporating SOI, PDO, and NAO also demonstrate nearly equal performances, as the predictions with the models are correct 29, 28, and 28 times, respectively. Inclusion of the SOI and SSN decrease the model performances from 29 to 25 (a 13.8% decrease of performance) and 25 to 22 correct predictions (a 12% decrease of performance), respectively. However, the PDO and NAO increase the model skills from 25 to 28 correct predictions, an improvement of 12%. This indicates PDO and NAO influence on the seasonal Rhine flows. The ANN model results differed from time series models, showing multivariate ANN model incorporating five rivers, SOI and SSN performance is best (predicting 32 of the 72 flow categories correctly). In addition, inclusion of the five rivers and SOI data decrease the ANN model performance. Addition of the SSN data comparatively improves the model performances again, but the PDO and NAO decrease the model skills. This indicates contrasting behavior of the PDO and NAO data when include in the time series and ANN models. The incorporation of the PDO, NAO improve the time series models, but decrease performance of the ANN models. Therefore, the role of PDO and NAO in the models developed to forecast Rhine categorical flows are not clear from the review of table results.

The abilities of time series and ANN models to predict low Rhine flows are summarized in Tables 5.15 and 5.16. The Table 5.15 results reveal multivariate time series model with five river information performed the best, predicting 12 of the 24 low

flows correctly. This results differ from the overall model predictions (described in the previous section) for which the univariate model shows better flow prediction skills. The univariate and other multivariate time series models indicate similar performances for which the number of accurate predictions varies from 9 to 11. However, the ANN model results in Table 5.16 differ from the time series models, demonstrating best performance with the multivariate model incorporating five rivers, SOI, SSN, and PDO. In all other cases, the ANN models are not skillful to forecast low Rhine flows.

The Tables 5.15 and 5.16 also summarize model performances in terms of Rhine high flow predictions. Table 5.15 results indicate the univariate time series model performance is best, predicting 16 high flows correctly. The improvements of model performance are also evident, when the PDO and NAO data are incorporated. However, the ANN model results differ from the time series models as the multivariate ANN model with five rivers, SOI, and SSN show best performance, predicting 18 of the 29 high flows correctly. The univariate ANN model also shows nearly equal performance, as 15 times the predictions for the high flows are accurate. The Tables 5.15 and 5.16 results also demonstrate incorporation of five rivers and the SOI decrease the high flow prediction skills of the models. The influence of NAO is also evident in both time series and ANN models which comparatively improve model performances. The SSN and PDO show contrasting behavior when included in the time series and ANN models. The SSN influence is constant in the time series model, but increases the ANN model performance. Conversely, the PDO improves the time series models, but decreases the ANN model skills. Therefore, the roles of SSN and PDO in the models developed to perform Rhine categorical forecasts are not clear from review of the table results.

5.4.4 Columbia River

The performances of time series and ANN models used to predict the categorized Columbia River flows are summarized in Tables 5.17 and 5.18, respectively. These table statistics demonstrate superiority of the persistence model over the univariate and multivariate time series and ANN models, predicting 47 of the 72 seasonal flows. The univariate time series model is able to predict only 31 flows within the respective flow categories (low, average, and high). Among the multivariate models, the model incorporating five river flows indicate relatively better performance, for which 30 times the predictions matched the observations. Moreover, the table results indicate less skillful univariate and multivariate models to outperform the persistence model forecasts.

Table 5.17

Time Series Model Forecast Validation for the Categorized Columbia Flow (1982-1999)

River	Flow	Univariate	M. var. 5 rivers	M. var. 5 rivers + SOI	M. var. 5 rivers + SOI + SSN	M. var. 5 rivers + SOI + SSN + PDO	M. var. 5 rivers + SOI + SSN + PDO + NAO	Persistence
Overall categories- low, average and high flow (total 72)								
	Correct forecast	31	30	27	28	29	28	47
	Outside category	41	42	45	44	43	44	25
Low flow (total 4)								
Columbia	Correct forecast	3	4	4	4	4	4	0
	Outside category	1	0	0	0	0	0	4
High flow (total 19)								
	Correct forecast	14	14	13	14	13	12	10
	Outside category	5	5	6	5	6	7	9

Table 5.18ANN Model Forecast Validation for the Categorized Columbia Flow (1982-1999)

River	Flow	Univariate	M. var. 5 rivers	M. var. 5 rivers + SOI	M. var. 5 rivers + SOI + SSN	M. var. 5 rivers + SOI + SSN + PDO	M. var. 5 rivers + SOI + SSN + PDO + NAO	Persistence
Overall categories- low, average and high flow (total 72)								
	Correct forecast	41	28	42	37	38	30	47
	Outside category	31	44	30	35	34	42	25
Low flow (total 4)								
Columbia	Correct forecast	0	3	0	0	4	0	0
	Outside category	4	1	4	4	0	4	4
	High flow (total 19)							
	Correct forecast	9	11	13	9	11	9	10
	Outside category	10	8	6	10	8	10	9

The performances of times series and ANN models are further analyzed to evaluate model skills in predicting Columbia low and high flows. Results indicate a total of four flows are identified as low and 19 flows are identified as high. The time series model forecasts are evaluated first to determine better models in terms of predicting low flows. The results are summarized in Table 5.17. The table results reveal equally skillful multivariate models, predicting all of the four low flows correctly. The univariate model performance is almost equal, as 3 of the 4 times the predictions matched the observations. The persistence model demonstrates poor performance, indicating inefficient to forecast Columbia low flows (zero low flow prediction), although the overall predictions with this model are the best (described in the previous section). The ANN model performances to forecast low flows are summarized in Table 5.18. The table results indicate superiority of the multivariate model incorporating five rivers, SOI, SSN, and PDO over the other

models. The multivariate model incorporating five rivers also performs well as three times the predictions matched the observations. In all other cases, the ANN model performances are poor, indicating not skillful to predict low Columbia flows.

In terms of high flow prediction skills, Table 5.17 results show the performances of univariate, multivariate time series models incorporating five rivers and five rivers, SOI and SSN are best, as 14 times the predictions are within the observed flow categories. The other multivariate models show almost equal performances, predicting 13 of the 19 high flows correctly. The time series model performance is constant with the univariate model and multivariate model incorporating five rivers as in both cases the model predictions are accurate 14 times. Inclusion of the SOI data decreases the model performance from 14 to 13 correct predictions (a 7.1% decrease of performance) while improved again with the SSN information, for which 14 times the predictions matched the observations (an improvement of 7.6%). Incorporation of the PDO data decreases the model skills a little bit, as the number of accurate predictions decreases from 14 to 13. Later, the NAO data again decreases the model efficiencies, predicting 12 of the 19 high flows within categories.

The Table 5.18 summarizes the ANN model performances in terms of Columbia high flow predictions. Table results indicate the multivariate model incorporating five rivers and SOI performed the best, predicting 11 high flows correctly. The univariate model is able to predict 9 of the 19 high flows correctly. The ANN model results differ from the times series models when five rivers and the external variables are incorporated. Inclusion of the five river flows and SOI improve the number of correct predictions from 9 to 11 (an improvement of 22.2%) and 11 to 13 (an improvement of 18.2%),

respectively. Hence, the model performance decreases to nine correct predictions when the SSN is incorporated (a 30.8% decrease of performance). Thereafter, the PDO improves the model skills again from 9 to 11 high flows, while the NAO decreases the model skills once more from 11 to 9 correct predictions. However, the role of PDO to improve high flow prediction skills of the models is evident in both time series and ANN model performances. The results also indicate contrasting behavior of five rivers and other variables when included in the time series and ANN models. Therefore, the roles of these variables in the models developed to forecast Columbia flows are not clear from review of table results. Overall model performances revealed that the variables provided more or less skills into the models.

5.4.5 Parana River

The performances of time series and ANN models for predicting the Parana River flows are summarized in Tables 5.19 and 5.20, respectively. For the validation period (1982 to 1999), 66 of the 72 seasonal flows were high, whereas one season the flow is low. The remaining 15 flows are classified as average flows. The table results indicate overall model predictions based on persistence is better in comparison to the time series model, predicting 62 of the 72 seasonal flows correctly. The univariate and multivariate time series models are not impressive because numbers of accurate predictions varies from 23 to 27. Results are assessed further to compare the prediction skills of the univariate and multivariate time series models. The Table 5.19 results indicates univariate and the multivariate model incorporating five rivers show equal performances, predicting 23 flows correctly. Incorporation of the SOI improves the forecasting skills from 23 to 27

correct predictions (an improvement of 17.4%). Later, inclusion of the SSN, PDO, and NAO data does not improve the model predictability because in all of the cases the models are able to correctly predict 27 flows.

Table 5.19

Time Series Model Forecast Validation for the Categorized Parana Flow (1982-1999)

River	Flow	Univariate	M. var. 5 rivers	M. var. 5 rivers + SOI	M. var. 5 rivers + SOI + SSN	M. var. 5 rivers + SOI + SSN + PDO	M. var. 5 rivers + SOI + SSN + PDO + NAO	Persistence
Overall categories- low, average and high flow (total 72)								
	Correct forecast	23	23	27	27	27	27	62
	Outside category	49	49	45	45	45	45	10
Low flow (total 1)								
Parana	Correct forecast	0	0	0	0	0	0	0
	Outside category	1	1	1	1	1	1	1
High flow (total 66)								
	Correct forecast	18	19	22	22	22	22	61
	Outside category	48	47	44	44	44	44	5

Table 5.20ANN Model Forecast Validation for the Categorized Parana Flow (1982-1999)

River	Flow	Univariate	M. var. 5 rivers	M. var. 5 rivers + SOI	M. var. 5 rivers + SOI + SSN	M. var. 5 rivers + SOI + SSN + PDO	M. var. 5 rivers + SOI + SSN + PDO + NAO	Persistence
Overall categories- low, average and high flow (total 72)								
	Correct forecast	59	26	46	46	52	55	62
	Outside category	12	46	26	26	20	17	10
Low flow (total 1)								
Parana	Correct forecast	0	0	0	0	0	0	0
	Outside category	1	1	1	1	1	1	1
High flow (total 66)								
	Correct forecast	58	22	43	42	50	53	61
	Outside category	8	44	23	24	16	13	5

The Table 5.20 demonstrates comparative advantages of the univariate and multivariate ANN models, performing seasonal categorical flow forecasts. Results indicated the univariate ANN model performance is best, predicting 59 of the 72 seasonal flows correctly. The multivariate model incorporating all external variables shows almost equal performance, for which 55 times the predictions matched the observations. Unlike the time series model, the multivariate ANN model incorporating five rivers is less skillful as the predictions matched only 22 times with the observations. The table results are evaluated further to substantiate the potential for external environmental variables, influencing the Parana flows. Results indicated inclusion of the SOI improves the ANN model performance, yielding 46 correct forecasts. However, inclusion of the SSN does not change the number of accurate predictions, whereas, the PDO and NAO increase the ANN model skills again from 46 to 52 and 52 to 55 correct predictions, an improvement

of 13% and 5.8%, respectively. Hence, the results also demonstrate role of the external variables either improving or decreasing the model performance. However, performance review of time series and ANN models in terms of overall predictions indicate superiority of the ANN models over the time series models (predictions with the ANN models matched the observations more than two times the time series models). Although, skills of the models improve with the ANN methodology, the persistence model substantially outperformed all of the univariate and multivariate ANN model performances by predicting 66 of the 72 flows correctly.

The model performances (time series and ANN) are further assessed specifically for predicting low flows, and the outcomes are summarized in Tables 5.19 and 5.20, which indicate none of the models are skillful to predict the only low flow observed during the validation years (year 1982 to year 1999).

In terms of high flow predictions, all of the multivariate time series models show equal performance, predicting 22 high flows correctly. The ANN model performances indicate the univariate ANN model performed the best as the prediction are correct 58 times out of 66 high flows. The multivariate ANN model incorporating five rivers and all external variables show nearest performance, predicting 53 flows correctly. However, the model accuracies are far below the accuracies of the persistence model, which are able to predict 61 of the 66 high flows. These model performances are further evaluated to identify the role of external environmental variables influencing flows. The univariate time series model is able to predict 18 high flows correctly. The model performance improves from 18 to 19 correct predictions when five river flows are included (an improvement of 5.6%). Inclusion of the SOI further improves the model skills from 19 to

22 correct predictions (an improvement of 15.8%). Later, inclusion of the SSN, PDO, and NAO do not change the model skills. However, the influence of five rivers flow data and SSN decrease the ANN model prediction skills, but improves it with SOI, PDO, and NAO information. The results indicate contrasting behavior of the other variables when included in the time series and ANN models. The role of other variables in the models developed to forecast Parana flow is not clear from review of model predictions.

The performance review of time series and ANN models indicates superiority of the ANN models to forecast Parana high flows, although it is not sufficient enough to substantially outperform the persistence model flow prediction skills.

In the following sections the performance of the ensemble forecast approach to predict seasonal flows of the five rivers are discussed.

5.5 Ensemble Forecast (Long Data Series)

The time series and artificial neural network (ANN or NN) model (univariate and multivariate) results demonstrate that model performances are space, time, and flow type (low, average, and high) specific and not any particular model is better to predict all of the five river flows. In addition, the persistence models often show better forecast skills in comparison to more complex multivariate approaches. This underscores the importance of the ensemble approach where all model forecasts are combined and variability of the forecasts can be quantified in terms of likelihood. These forecasts are usually shown as box plots, where the box indicates flow magnitudes of the 25th and 75th percentile limits of the ensembles, and the whiskers represent the 5th and 95th percentile of the ensembles. For instance, the 5% whisker indicates that there is a 5% chance that the flow would exceed that limit and a 95% chance that the flow values would fall

between the 5% and the 95% limits. The horizontal line within the box plot represents the median of the ensemble.

In this study, performances of three types of ensembles are evaluated and discussed: (a) Ensemble of the time series (TS) model forecasts with persistence (P) (TS-P); (b) Ensemble of the ANN model forecasts with persistence (NN-P); and (c) Ensemble of the time series and ANN model forecasts with persistence (TS-NN-P). Model forecasts are combined seasonally and then compared with the observed river flows. The corresponding ensemble forecasts of the Congo River are shown as box plots in Figures 5.7 to 5.10. The box plots for rest of the rivers are included in the Appendix B. The cross signs in the plots represents observed flows, which are included to determine number of times the observed flows fall within the ensemble forecast limits. This also demonstrates skills of the ensembles to forecast seasonal flows. The 33rd and 66th percentile limits of the historic (observed) flows (1906-1980) are included in the figures as dashed lines to represent high and low flows. The performance of the TS-P and NN-P forecasts for the five rivers are described in the following sections. The TS-NN-P forecast performances are discussed later. Rank probability skill scores (RPSS) are obtained for the evaluation of the forecast performance. The RPSS results are summarized in Table 5.21.

Table: 5.21

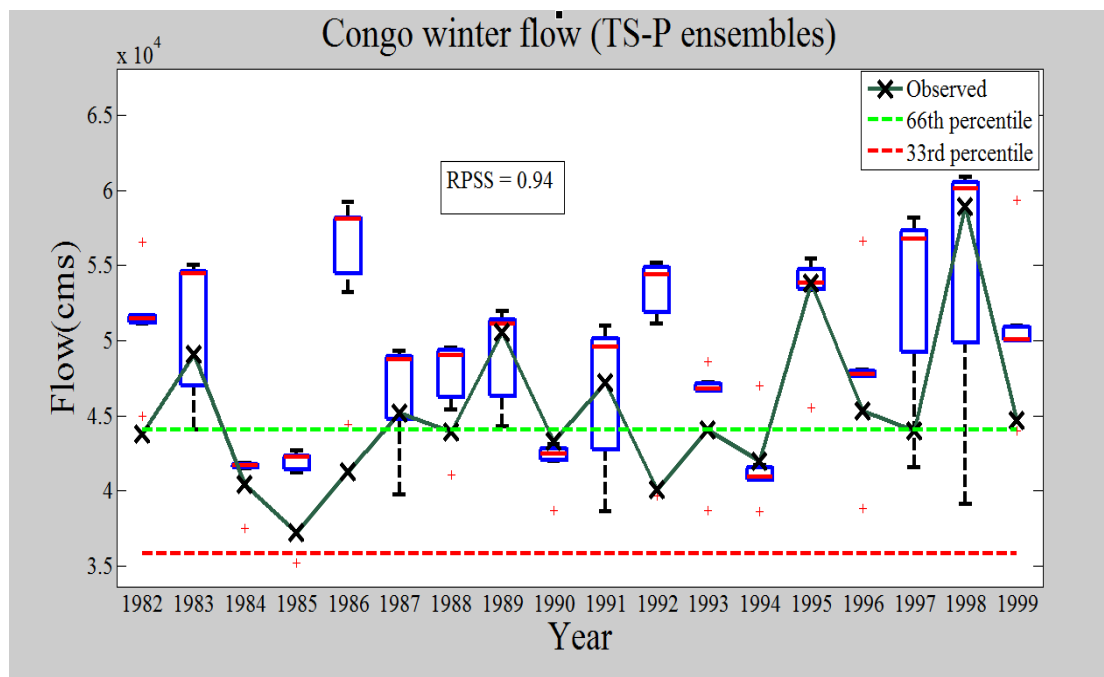
Rank Probability Skill Scores (RPSS) of the Ensemble Forecasts for the Congo, Yangtze, Rhine, Columbia, and Parana River Seasonal Flows

River	Ensemble type	Overall	Winter	Spring	Summer	Fall	Low	High
Congo	TS-P	0.57	0.94	-1.63	0.94	0.02	-0.71	0.94
	NN-P	0.45	0.33	0.57	0.97	-0.53	0.79	-1.20
	TS-NN-P	0.31	0.36	-0.13	0.96	0.06	0.10	0.36
Yangtze	TS-P	0.94	0.94	0.85	0.94	0.94	0.94	0.94
	NN-P	0.88	0.94	0.82	0.76	0.66	0.94	0.76
	TS-NN-P	0.34	0.98	0.31	0.24	0.31	0.98	0.84
Rhine	TS-P	-0.53	-0.53	-0.53	-0.59	-0.26	-0.53	-0.53
	NN-P	-0.16	-0.16	0.45	-0.41	-0.29	-0.81	0.20
	TS-ANN-P	-0.05	-0.09	-0.01	-0.36	0.17	0.13	-0.08
Columbia	TS-P	-0.71	-1.20	0.94	0.20	-1.05	0.94	0.94
	NN-P	0.45	0.76	0.45	-0.13	0.57	-0.29	0.57
	TS-ANN-P	-0.01	-0.14	0.60	-0.04	-0.01	0.70	0.84
Parana	TS-P	-0.90	-1.20	1.00	-1.20	-0.90	-1.63	-0.90
	NN-P	0.79	0.94	1.00	0.45	0.51	-2.00	0.94
	TS-NN-P	0.24	0.36	1.00	-0.44	0.06	-1.25	0.13

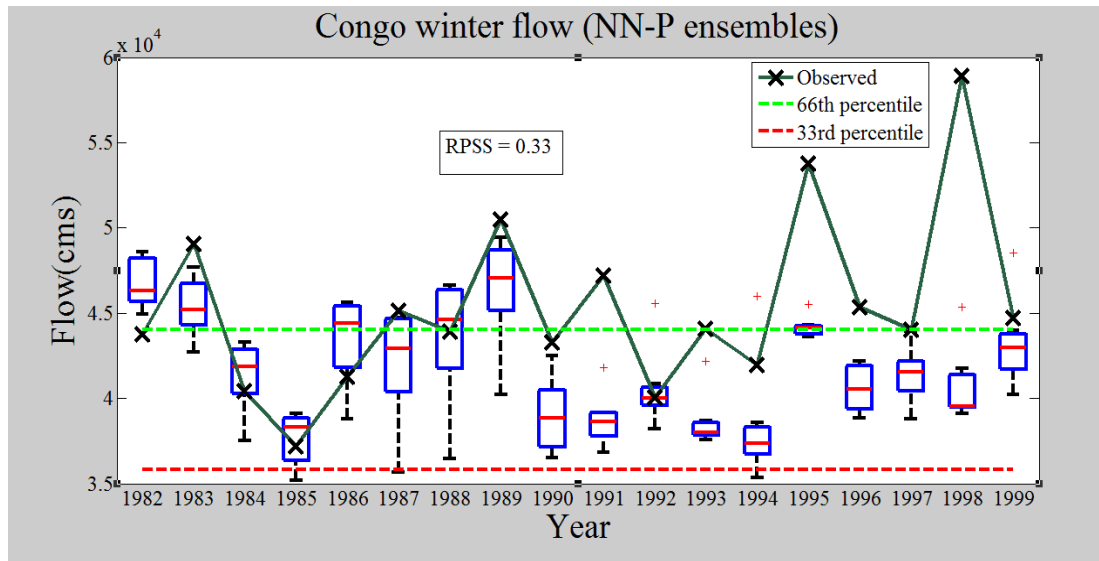
5.5.1 Congo River

The time series ensemble forecasts for winter, summer and fall season Congo flows are shown in Figures 5.7 (a), 5.9 (a), and 5.10 (a). Flow forecasts are clustered on the left side indicating the flow is overestimated during these three seasons. The spring flow ensemble forecasts [Figure 5.8(a)] show almost all forecasts shifted to the right side indicating an underestimated flow forecast. To further assess the ensemble forecast methods, the median RPSS statistics are calculated for winter, spring, summer, and fall seasonal forecasts and results are 0.94, -1.63, 0.94, and 0.02, respectively. The RPSS values indicate the mean time series ensemble forecast are skillful to estimate winter and summer Congo flow with a RPSS value near one. The RPSS for fall season is 0.02,

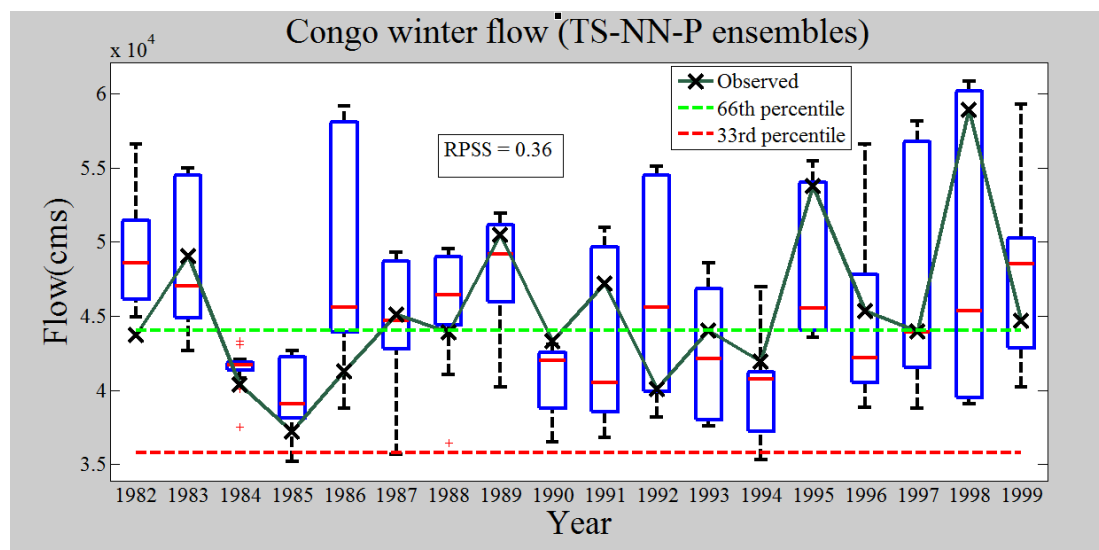
indicating slightly better performance than a random guess (RPSS = 0). Conversely, the negative RPSS statistics for the spring results indicates poor performance with forecasts deviated far from observed flows. The time series ensemble forecasts are evaluated in terms of predicting extreme river flow conditions. In this case the RPSS statistics for low and high flow forecasts are -0.53 and 0.94, respectively. The negative RPSS value of -0.53 indicates less skill and the RPSS of 0.94 is near 1, indicating better agreement between forecast and observed value.



(a)

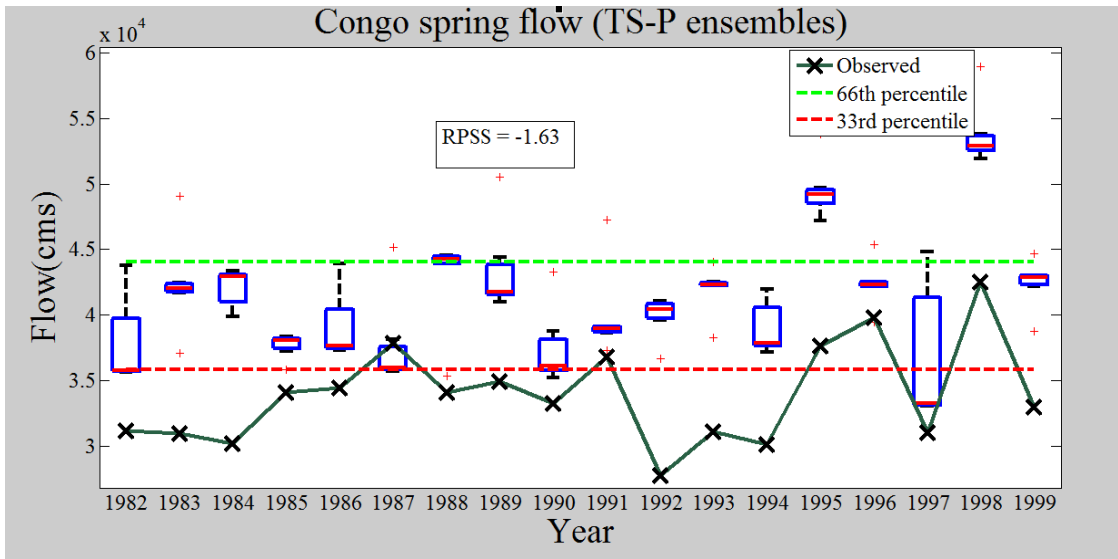


(b)

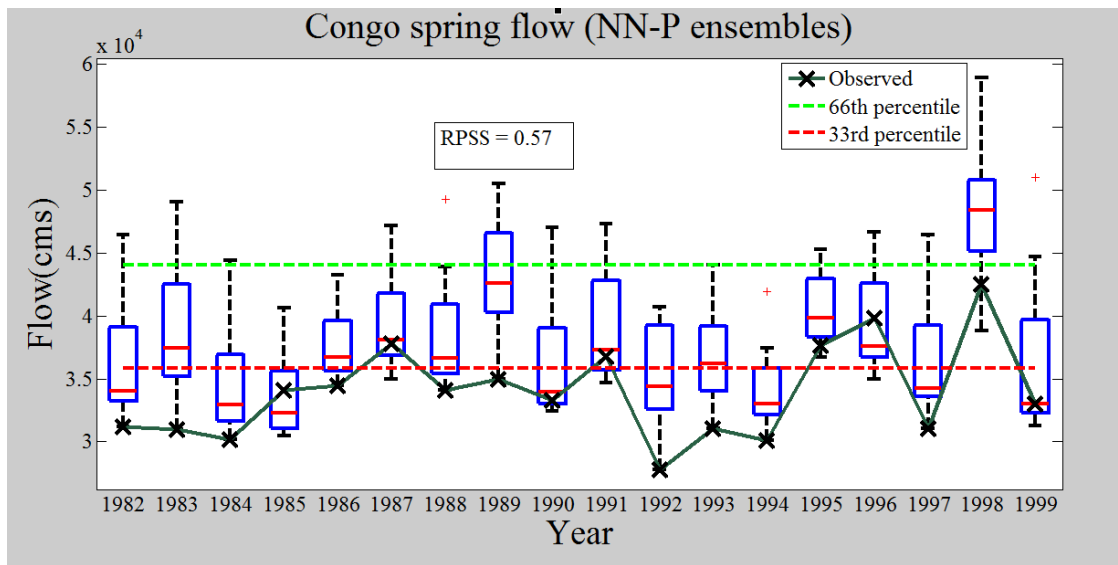


(c)

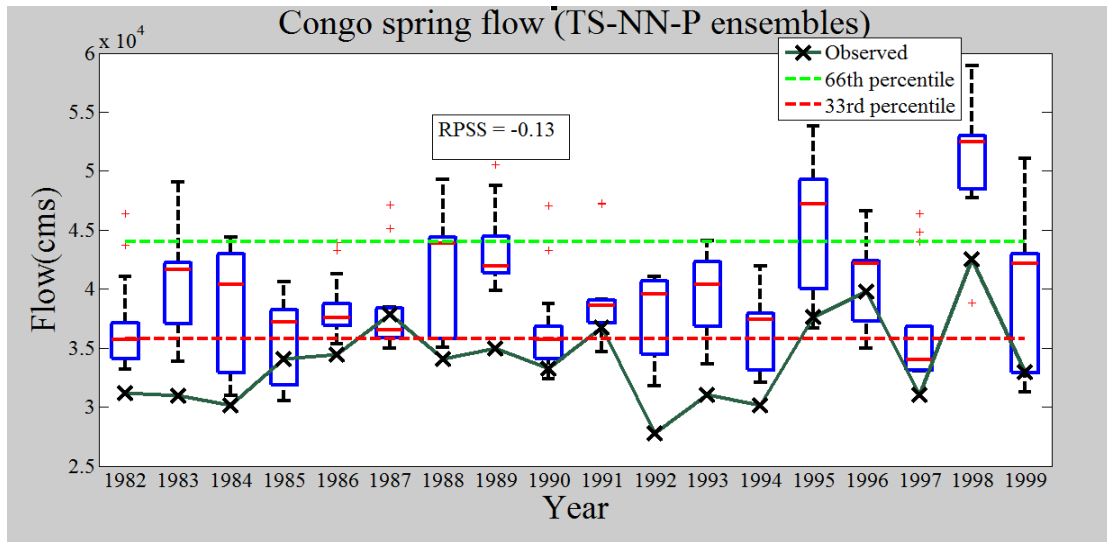
Figure 5.7. Ensemble forecasts of the Congo River winter flow: (a) Ensemble of time series models with persistence (TS-P); (b) Ensemble of NN models with persistence (NN-P); and (c) Ensemble of time series and NN models with persistence (TS-NN-P).



(a)

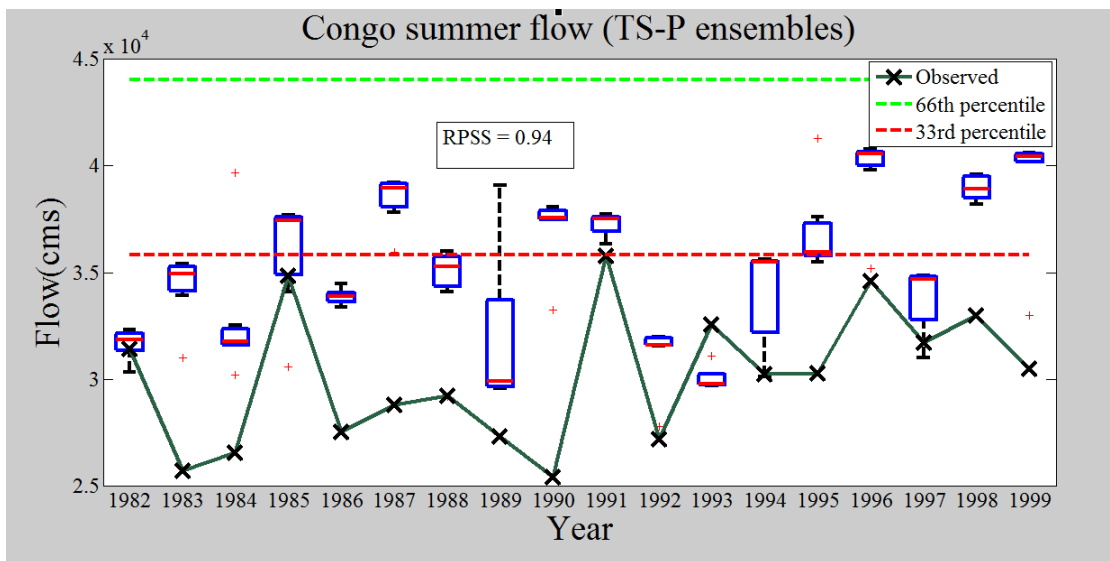


(b)

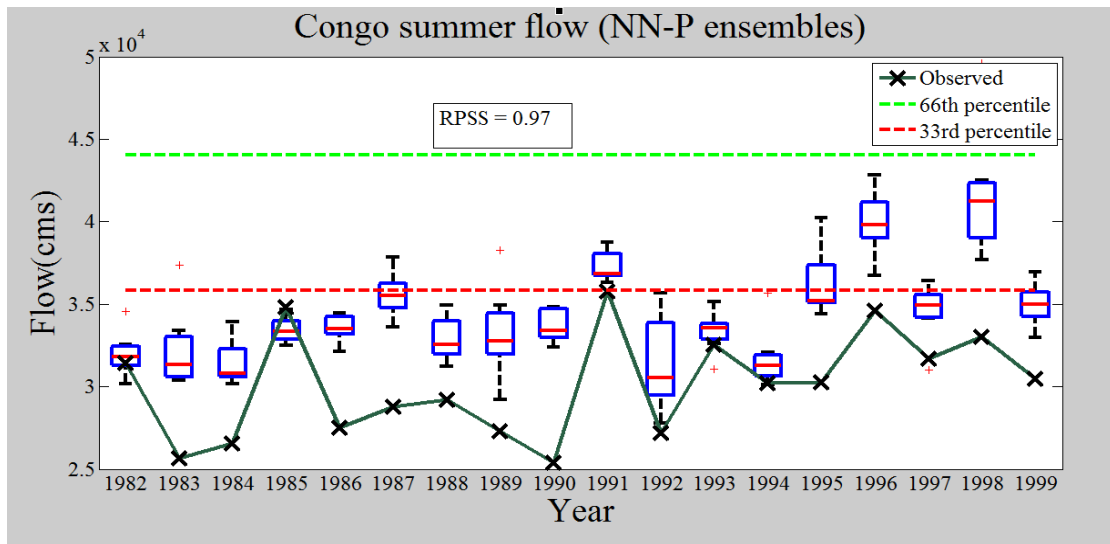


(c)

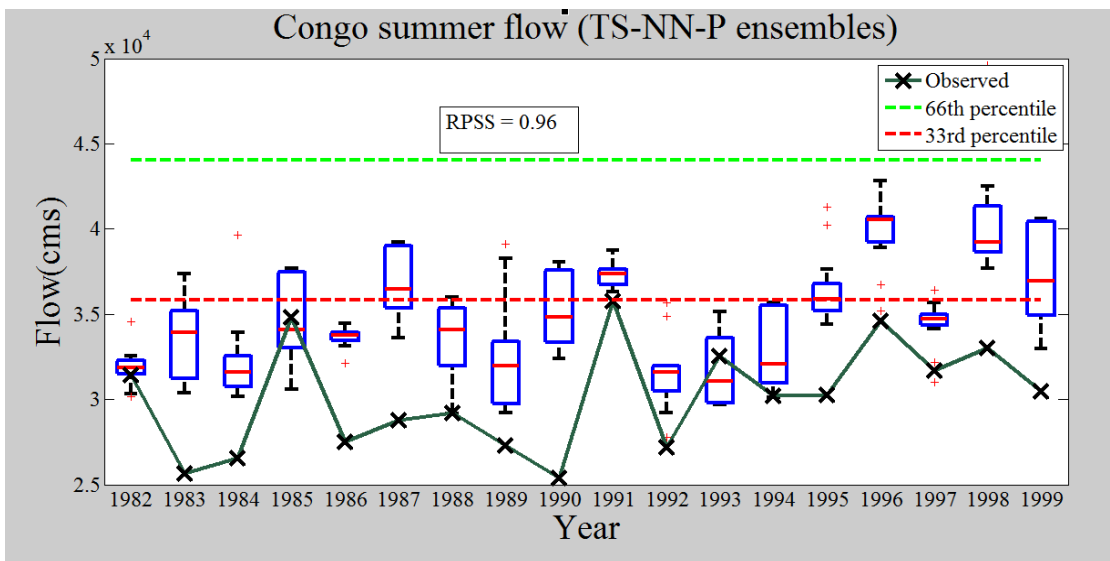
Figure 5.8. Ensemble forecasts of the Congo River spring flow: (a) Time series model forecasts ensembles with persistence (TS-P); (b) NN model forecasts ensembles with persistence (NN-P); and (c) Ensembles of the time series and NN model forecasts with persistence (TS-NN-P).



(a)

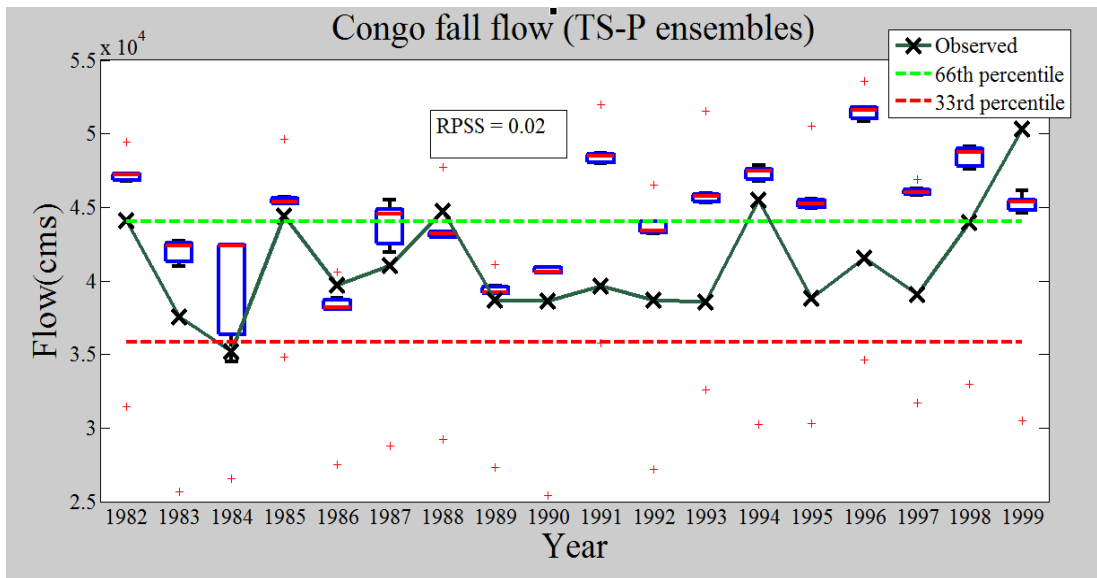


(b)

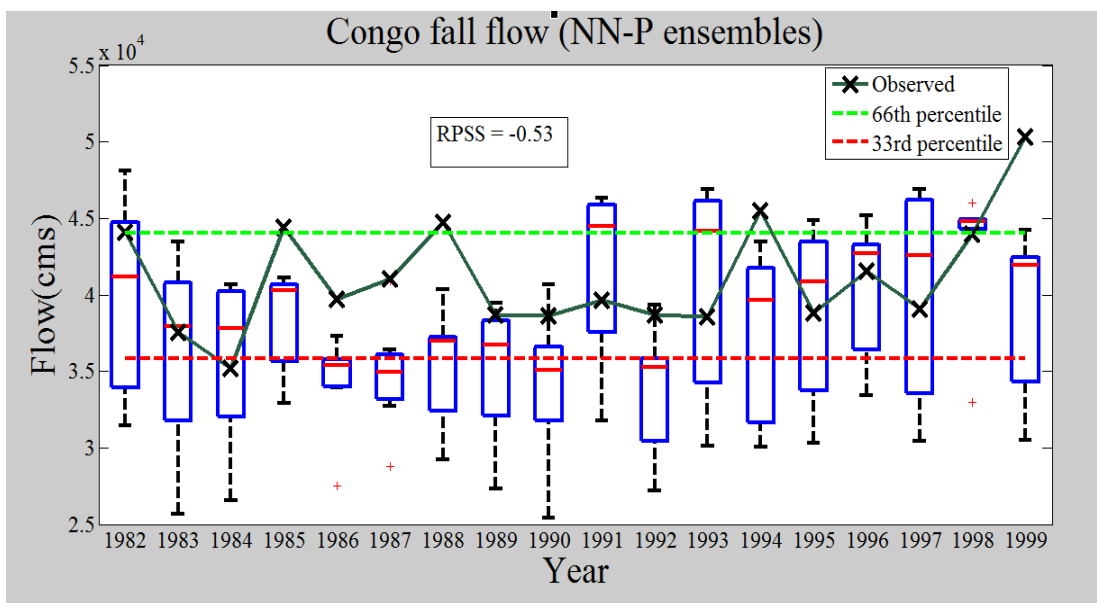


(c)

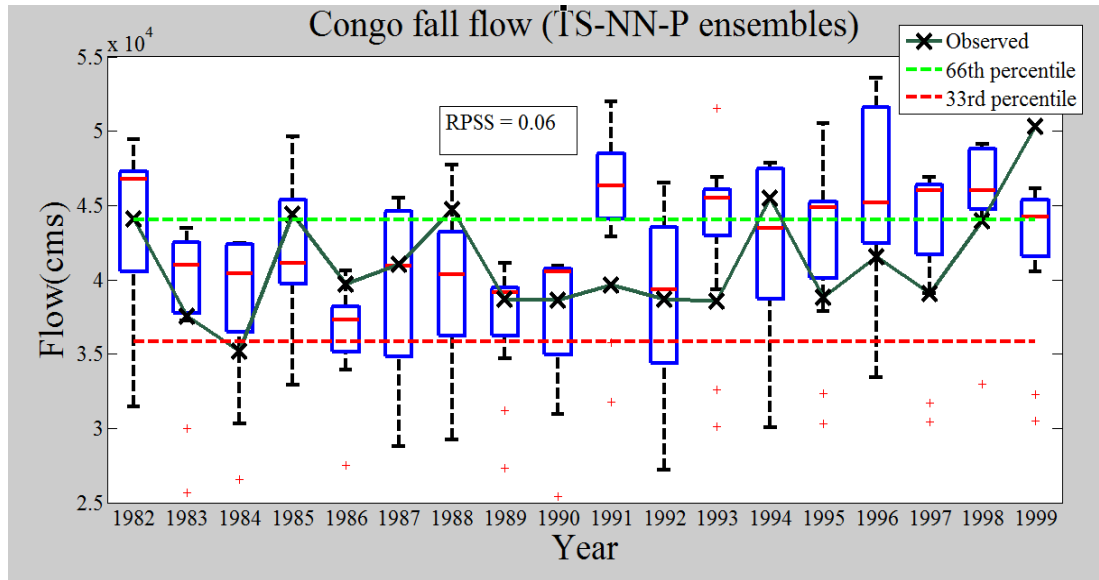
Figure 5.9. Ensemble of the Congo River summer flow: (a) Time series model forecasts ensembles with persistence (TS-P); (b) NN model forecasts ensembles with persistence (NN-P); and (c) Ensembles of the time series and NN model forecasts with persistence (TS-NN-P).



(a)



(b)



(c)

Figure 5.10. Ensemble of the Congo River fall flow: (a) Time series model forecasts ensembles with persistence (TS-P); (b) NN model forecasts ensembles with persistence (NN-P); and (c) Ensembles of the time series and NN model forecasts with persistence (TS-NN-P).

The NN-P model ensemble forecasts for the Congo seasonal flows are shown in Figures 5.7 (b), 5.8 (b), 5.9 (b), and 5.10 (b). The results are compared with the TS-P forecasts. The median RPSS statistics for winter, spring, summer, and fall forecasts are obtained as 0.34, 0.57, 0.97, and -0.53, respectively. The positive statistics indicate that ensembles are effective in predicting winter, spring, and summer flow conditions, whereas the negative fall season statistics indicates inefficient ensemble performance. The performances of the NN-P ensembles are also evaluated in terms of predicting low and high flows. The RPSS of low and high flows are 0.79 and -1.20, respectively. The positive and higher statistics of 0.79 indicates effective low flow forecasts. Conversely,

the negative RPSS value of -1.20 demonstrates that the high Congo flows were not captured well with the ensembles.

In comparing the NN-P and TS-P ensembles, it was interesting to note that the winter and fall flows are well captured in the TS-P, whereas the NN-P reveals its efficiency in capturing spring Congo flows better. Both ensembles show equally skillful performance in predicting summer flows as the RPSS statistics for the two models are almost equal (RPSS = 0.94 for TS-P and RPSS = 0.97 for NN-P). When comparisons are made based on the extreme flow RPSS, the NN-P ensembles better predicts low flows, and the TS-P approach shows more skills in predicting high flows. This indicates the challenges associated with selecting one particular method, and underscores the importance of considering alternate and multiple methods.

5.5.2 Yangtze River

For the Yangtze River, the TS-P ensemble forecasts are shown in the Appendix B. Flow forecasts are clustered on the left side during winter, spring and summer seasons, indicating the flow is overestimated. The fall seasonal ensemble forecasts show the forecasts shifted to the right side, indicating an underestimated flow. The RPSS statistics for winter, spring, summer, and fall seasonal TS-P are obtained as 0.94, 0.85, 0.94, and 0.94, respectively. The positive RPSS values indicate the TS-P is efficient to estimate seasonal Yangtze flows. The RPSS of both low and high flow ensemble forecasts are 0.94. The positive and high values (near one value) of the statistics indicate the efficiency of TS-P in capturing the high and low Yangtze flows.

The NN-P forecasts are also developed to evaluate performance in comparison to the TS-P forecasts. The box plots of the corresponding seasonal forecasts are shown in the Appendix B. Flow forecasts are clustered on the left side during winter, spring, and fall seasons, indicating an underestimated flow forecasts. Conversely, the summer flow NN-P forecasts shifted to the right side, indicating the flow is underestimated. The median RPSS statistics for winter, spring, summer, and fall seasonal flow forecasts are calculated as 0.94, 0.82, 0.76, and 0.66, respectively. The positive values of the statistics indicate effectiveness of the NN-P in capturing the seasonal Yangtze flows. The NN-P forecasts are further tested to evaluate skills, forecasting extreme river flow conditions (low and high). The corresponding RPSS statistics for low and high flows are 0.94 and 0.74, respectively. The positive and high RPSS values demonstrate effectiveness of the NN-P in estimating extreme river flow conditions.

From the RPSS statistics, it is also evident that both TS-P and the NN-P forecast performances are nearly equal. In terms of extreme flow predictions, the RPSS statistics of both TS-P and NN-P reveal equal performances for low flows, whereas the TS-P performances are slightly better than the NN-P for high flows (greater RPSS value). In general, both TS-P and NN-P ensembles are effective in predicting seasonal Yangtze flows.

5.5.3 Rhine River

The TS-P ensemble forecasts for the seasonal Rhine flows are shown in Appendix B. The RPSS statistics are calculated to evaluate the TS-P performance. The values of winter, spring, summer, and fall seasonal ensemble forecasts are obtained as -0.53, -0.53,

-0.59, and -0.26, respectively. The negative RPSS values reveal lack of forecasting skills. The TS-P performances are further evaluated in terms of predicting extreme Rhine flows (low and high), for which the RPSS statistics for both low and high flows were -0.53. The negative RPSS value of -0.53 indicates less impressive forecasts.

The NN-P ensemble forecasts for the Rhine River are shown in the Appendix B. The RPSS statistics for winter, spring, summer, and fall season NN-P forecasts are calculated as -0.16, 0.45, -0.41, and -0.29, respectively. The winter, summer, and fall seasonal RPSS indicate slightly improved performance in comparison to TS-P, although not efficient enough to outperform the random guess (zero). In addition, the RPSS of low and high flow NN-P are -0.81 and 0.20, respectively. The negative RPSS value of -0.81 demonstrates lack of low flow prediction skills, whereas the positive RPSS value of 0.20 indicates impressive high flow forecast performance.

However, the performance review of the TS-P and NN-P ensembles for predicting high flows indicate more efficient NN-P in comparison to the TS-P forecasts. The overall performance shows that the Rhine flows are not captured well with the ensembles.

5.5.4 Columbia River

The TS-P ensemble forecasts for the Columbia River are shown in Appendix B. The RPSS statistics of the ensembles forecasts for winter, spring, summer, and fall seasonal Columbia flows are -1.20, 0.94, 0.20, and -1.05, respectively. The negative RPSS values reveal inefficient winter and fall seasonal flow forecast, whereas the positive spring and summer RPSS value indicates better forecast performance. The RPSS

statistics for both low and high flows are 0.94, indicating better extreme flow prediction skills, although overall performances of the TS-P are not impressive (RPSS = -0.53).

The NN-P ensemble forecasts for the Columbia River seasonal flows are shown in Appendix B. The RPSS statistics are calculated as 0.76, 0.45, -0.13, and 0.57 for winter, spring, summer, and fall seasons, respectively. The above RPSS statistics indicate the winter, spring, and fall seasonal ensemble forecasts perform better. In terms of extreme Columbia flows, the RPSS statistics are obtained as -0.29 for low flows and 0.57 for high flows. The negative RPSS value of -0.29 indicates less skillful NN-P forecasts for Columbia low flows, whereas the positive RPSS value of 0.57 indicates better high flow prediction skills. Moreover, overall performances of the NN-P ensemble forecasts (RPSS = 0.45) demonstrates its efficiencies in capturing the Columbia seasonal flows.

However, the performance review of the Columbia extreme flow forecasts indicates more efficient TS-P in comparison to the NN-P. The overall performances of the TS-P (RPSS of -0.71) and NN-P (RPSS of 0.45) show better NN-P forecasts for the seasonal Columbia River flows.

5.5.5 Parana River

The TS-P ensemble forecasts for winter, spring, summer, and fall season Parana flows are shown in the Appendix B. Flow forecasts are clustered on the right side indicating the flow is underestimated during these four seasons. The median RPSS statistics for winter, spring, summer, and fall seasonal forecasts are calculated as -1.20, 1.00, -1.20, and -0.90, respectively. The negative RPSS statistics for the winter, summer, and fall seasonal TS-P indicates poor performance. Conversely, the RPSS value for the

spring flow is positive and one, indicating accurate spring flow predictions. The overall RPSS statistics of the TS-P is -0.90, demonstrates less efficient forecasts. The RPSS statistics for the low and high Parana flow TS-P are also calculated as -1.63 and -0.90, respectively. The negative RPSS values for both low and high flows indicate that the extreme flows are not represented well in the TS-P forecasts.

The NN-P ensembles are shown in the Appendix B. From the plots, it is evident that the model forecasts for spring, summer, and fall seasons are shifted to the right, indicating underestimated flow forecasts. Conversely, winter season flow forecasts reveals that the ensembles are often underestimated or overestimated. The RPSS statistics for winter, spring, summer, and fall seasonal NN-P are calculated as 0.94, 1.00, 0.45, and 0.51, respectively. The positive RPSS values for all seasonal NN-P demonstrate better performance in comparison to the TS-P (negative RPSS). The RPSS values for Parana low and high flow NN-P forecasts are -2.00 and 0.94, respectively. The positive and nearly one RPSS value indicates well represented high flows in the NN-P forecast ranges.

Overall, the RPSS statistics for the TS-P and NN-P ensemble forecasts are -0.9 and 0.77, respectively, indicating better NN-P forecasts. However, none of the two ensemble forecasts is better for Columbia low flows, whereas the NN-P is highly efficient for Columbia high flows.

5.6 Merging of Time Series and Neural Network Model Forecasts

However, variation of forecast magnitudes based on model-type underscores the usefulness of utilizing multi-model ensembles. Therefore, an ensemble approach merging stochastic and NN based forecasts including persistence (TS-NN-P) are developed for the

seasonal river flows. The median RPSS statistics are also calculated to compare the TS-NN-P performance with the individual TS-P and NN-P ensemble forecasts. The results are summarized in Table 5.21. The corresponding boxplots for winter, spring, summer, and fall seasonal Congo flows are shown in Figures 5.7(c), 5.8(c), 5.9(c), and 5.10(c), respectively. The boxplots of the rest of the river flows are included in the Appendix B.

The figures representing the Congo flows demonstrate seasonal flow variations are well-represented in the ensemble ranges. The box plots are extended to address the uncertainties involved in the ensemble forecasts. Table 5.21 also indicates better TS-NN-P performance for fall seasonal flows, although the other seasonal as well as low and high Congo flow RPSS statistics demonstrate better individual TS-P and NN-P forecasts.

In case of the Yangtze River, the median RPSS statistics are improved for winter and fall seasonal flows as well as low flow TS-NN-P; whereas the statistics for the spring and summer seasonal ensemble forecasts are lower than the individual TS-P and NN-P forecasts. Although, considerable variability in the skill scores is observed, the seasonal flow variations are represented well in most of the ensembles.

For the Rhine River, the median RPSS statistics improve from negative to positive for fall seasonal as well as low flow TS-NN-P forecasts, indicating better performance than climatology (random guess). The overall, winter, and summer flow statistics also show enhanced prediction skills, although the median RPSS values are negative. For high Rhine flow TS-NN-P, the RPSS statistics are lower than the NN-P ensembles, indicating less efficient forecasts.

The Table 5.21 also reveals lower median RPSS values for the Columbia and Parana seasonal TS-NN-P in comparison to the individual ensembles, indicating less efficient forecasts.

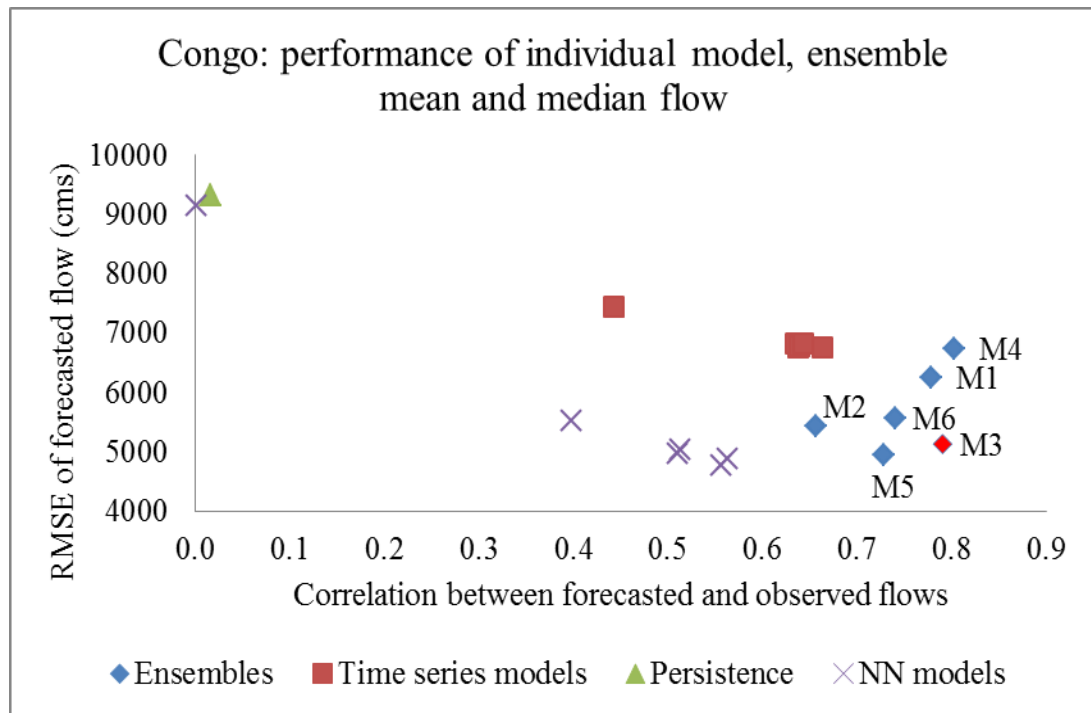
Therefore, the TS-NN-P forecast performances are season, flow-type, and river specific. The box plots also indicate that the model forecasts are well represented in the ensemble ranges.

5.7 Ensemble Mean and Median Analysis

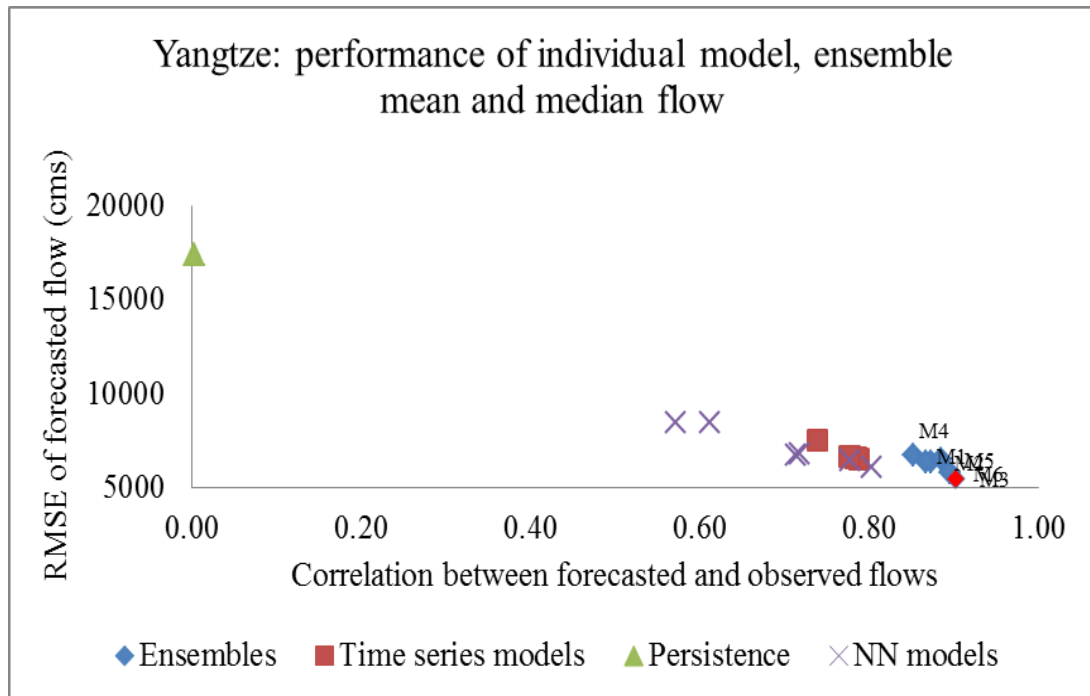
In this section, performances of the mean and median TS-P, NN-P, and TS-NN-P forecasts are discussed and evaluated on a river-by-river basis. The ensemble forecast means are calculated based on simple arithmetic averaging. The median flow values are also obtained, which separates the higher half of the flow series from the lower half. The forecast performances are examined for the years 1982 to 1999 based on the calibrated-model simulations over the periods of 1906 to 1980.

The Figure 5.11 showed the performance of ensemble mean and median flows in terms of the RMSE against cross-correlation between the forecasted and observed river flows. The corresponding performance statistics of the individual time series, NN and persistence models are also included to analyze the improvements in the prediction skills, achieved with the ensemble mean and median flows. For better representation, the six ensemble forecasts are notified with the symbols M1, M2, ..., M6. Here, M1, M2, and M3 represent ensemble mean flows of TS-P, NN-P, and TS-NN-P forecasts, respectively, whereas M4, M5, and M6 represent median flows of the above three ensembles, respectively. The corresponding RMSE statistics and correlation coefficients are

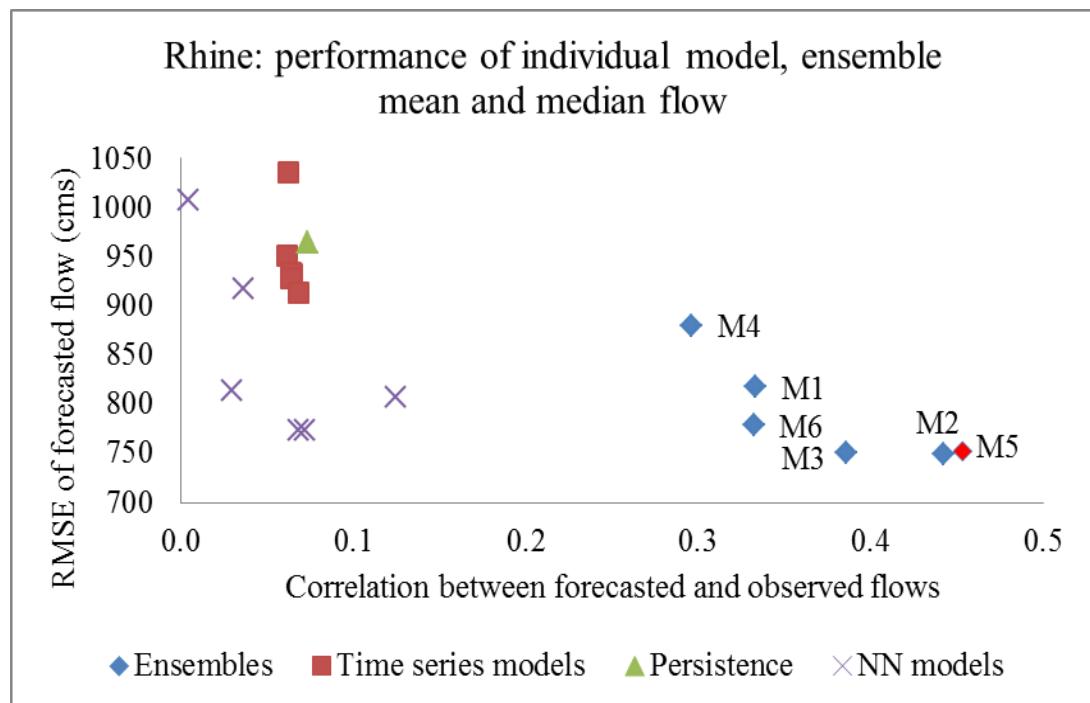
summarized in Table 5.22 for the Congo, Yangtze, Rhine, Columbia, and Parana rivers. The lower RMSE value with higher correlation coefficient represents a better forecast model. The Figures 5.11(a) to 5.11(e) also indicate significant performance discrepancies among the models for the five rivers described above. The best performed model is marked red in all these figures.



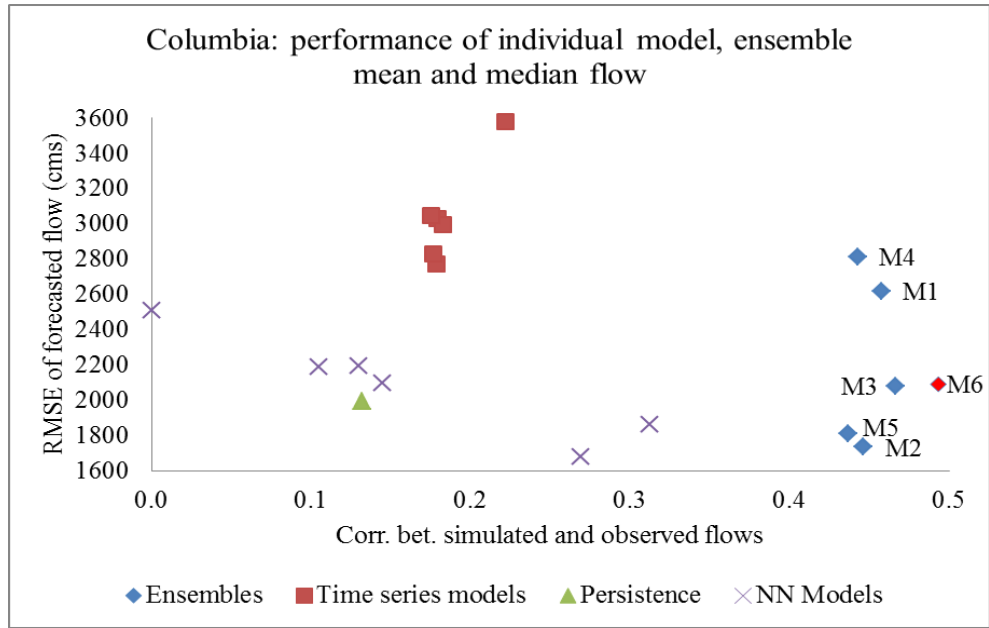
(a)



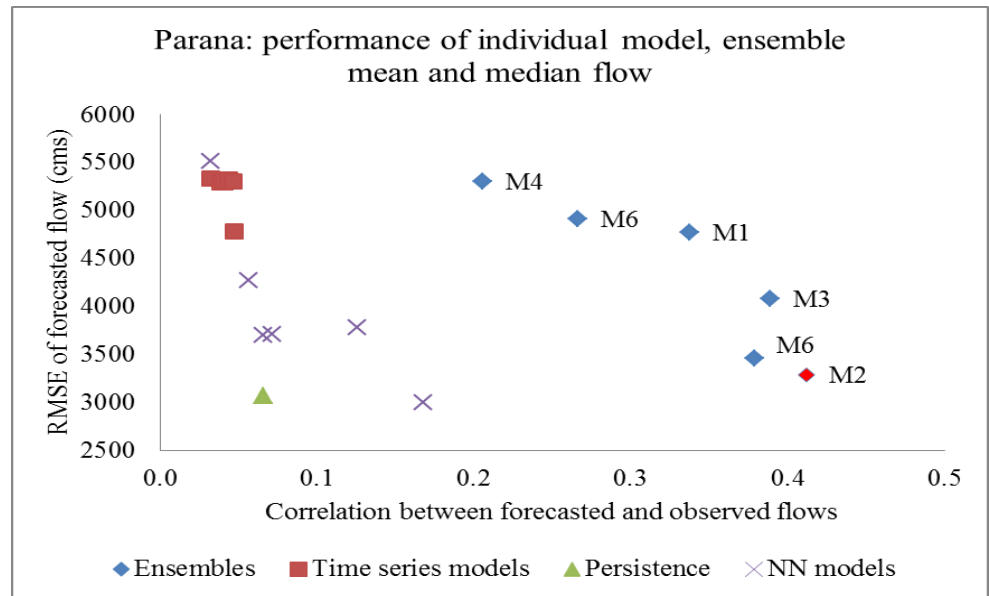
(b)



(c)



(d)



(e)

Figure 5.11. Root mean square errors (RMSE) and cross-correlation coefficients of the seasonal river flow ensemble means and medians along with individual time series, NN, and persistence model forecasts. The rivers are represented by (a) Congo; (b) Yangtze; (c) Rhine; (d) Columbia; and (e) Parana.

Table 5.22

Cross-correlation Coefficients and RMSE of Ensemble Means and Medians for Time Series (TS), Neural Network (NN), and Persistent (P) Models

Index	River	Mean (TS-P)	Mean (NN-P)	Mean (TS-NN-P)	Median (TS-P)	Median (NN-P)	Median (TS-NN-P)
Correlation coefficient	Congo	0.78	0.66	0.79	0.80	0.73	0.74
	Yangtze	0.85	0.87	0.90	0.87	0.89	0.90
	Rhine	0.33	0.44	0.39	0.30	0.45	0.33
	Columbia	0.46	0.45	0.47	0.44	0.44	0.49
	Parana	0.34	0.41	0.39	0.21	0.38	0.27
RMSE (cms)	Congo	6262	5429	5139	6740	4955	5575
	Yangtze	6736	6375	5513	6426	6562	5849
	Rhine	817	750	751	880	752	778
	Columbia	2619	1733	2081	2811	1811	2091
	Parana	4772	3287	4079	5303	3458	4915

The Figures 5.11(a) to 5.11(e) show that for the rivers Congo and Yangtze, the ensemble means of the TS-NN-P flow forecasts are best because of lower RMSE and higher correlation coefficients. Conversely, for the Rhine and the Columbia River, the ensemble medians of the NN-P and TS-NN-P flow forecasts indicate better performance, respectively. For the Parana River, the ensemble mean of the NN-P outperformed the individual model forecasts, as well as the other ensemble means and medians. This confirmed that ensemble means and medians were improvements over the individual time series, NN and persistence model predictions. It is also noteworthy that the cross-correlation coefficients of the ensemble mean and median flows of the Rhine, Columbia, and Parana Rivers are less than 0.50, indicating forecasts deviated far from observed flows. However, skills of the ensemble forecasts depend largely on the prediction skills of the participating models. High quality ensemble members resulted in enhancement of skills in the ensemble predictions. Therefore, low correlation coefficient values indicate less efficient ensemble members to forecast the Rhine, Columbia, and Parana seasonal

flows. Rigorous post processing of ensemble members including bias correction, accounting heteroscedasticity of prediction errors etc. can prove to be useful for the successful applications of multi-model ensembles (Georgakakos et al., 2004). These post processing procedures are beyond the scope of this research, therefore, not performed here.

As a part of the quality measures of the ensemble mean and median flows, cross correlation between the ensemble variance, and the error in the ensemble mean/median are obtained, which demonstrate the skills of the ensemble members to describe the level of uncertainty existing in the ensemble mean and median flow forecast. The results are summarized in Table 5.23. For the Congo River, the ensemble mean of the NN-P shows highest correlation coefficient of -0.52, indicating better efficient to represent the forecast uncertainties. For the Yangtze River, the best correlation of 0.28 is obtained with the ensemble median of the NN-P forecasts. For the Rhine River, the coefficients are less than 0.20, indicating less efficient ensemble members to describe the uncertainties involved in the ensemble mean and median flows. However, the Columbia River flow coefficients are significant for most of the ensembles for which the higher correlation coefficient of 0.70 is obtained with the ensemble mean of the TS-P forecasts. Moreover, for the Parana River, the ensemble median of the TS-P forecasts yielded most significant correlation of -0.49. Overall, these results indicate the forecast uncertainties are well represented in most of the ensembles of the five rivers.

Table 5.23

Cross-correlations between the Ensemble Variance and the Error in the Ensemble Means and Medians of the Time Series (TS), the NN, and Persistence (P) Models

River	Mean (TS-P)	Mean (NN-P)	Mean (TS-NN-P)	Median (TS-P)	Median (NN-P)	Median (TS-NN-P)
Congo	0.03	-0.52	-0.26	0.21	-0.51	-0.23
Yangtze	-0.06	0.25	0.12	-0.14	0.28	0.19
Rhine	0.20	-0.11	0.04	0.19	-0.14	-0.08
Columbia	0.70	0.22	0.55	0.66	0.25	0.48
Parana	-0.41	0.06	-0.24	-0.50	0.07	-0.45

5.8 Discriminant Prediction Approach (Probabilistic Method)

Using the Bayesian algorithm described in Chapter 3, the Columbia summer flow was predicted, using the Yangtze and Rhine River flow as predictors. The external environmental variables such as the SOI, NAO, and PDO were incorporated later to evaluate the improvements of the prediction skills. A total 95 years of data were used in this analysis. Both calibration and verification analysis were conducted for which the calibration period covers 75 years, from 1906 to 1980, and the verification period is 19 years-long, from 1981 to 1999.

In order to evaluate the forecasts improvements, the forecasts with various combinations of the predictor variables were performed and compared with the forecasts excluding those variables. The combinations were achieved using three, two, and one variables as predictors. Forecasts excluding the predictor variables are the random guess, which were obtained for the calibration period (1906 to 1980) as one third or 0.33 or 33.33% for the three categories (low, average, and high). However, forecast of a model depends on the inclusion of good quality predictor variables. In order to evaluate the

performance, the predictor variables were incorporated one after another, and the variable numbers were increased from one to three. Here, Tables 5.24, 5.25, and 5.26 were prepared to provide the forecast probabilities using one predictor (Yangtze winter flow), two predictors (Yangtze winter and Rhine spring flow), and three predictors (winter Yangtze and spring Rhine flow, and summer NAO). The rest of the tables, describing probabilities for the other variable combinations are shown in the Appendix A. Table 5.26 results indicates that in a specific year, if the Rhine spring, Yangtze winter, and summer NAO are categorized as high, average and high, then the forecasting probabilities of the low, average, and high Columbia summer flow are 0.73, 0.24, and 0.03, respectively. In addition, results (Tables 5.24 to 5.26) of some of the extreme flow conditions indicate the incorporation of river flows and external variable data tends to yield in a more definite forecast; this means the forecast probability of occurrence of a particular flow category is getting higher with the variables included into the model.

Table 5.24

Conditional Probability of the Columbia Summer Flow, Given the Yangtze Winter Flow,
Based on Observations of 1906–1980

Yangtze winter flow	Columbia summer flow		
	Low	Average	High
Low	0.50	0.25	0.25
Average	0.38	0.33	0.29
High	0.12	0.38	0.50

Table 5.25

Conditional Probability of the Columbia Summer Flow, Given the Rhine Spring and Yangtze Winter Flow, Based on Observations of 1906–1980

Predictors		Columbia summer flow		
Yangtze winter flow	Rhine spring flow	Low	Average	High
Low	Low	0.33	0.27	0.40
	Average	0.40	0.27	0.33
	High	0.70	0.20	0.10
Average	Low	0.23	0.33	0.44
	Average	0.29	0.34	0.37
	High	0.58	0.29	0.13
High	Low	0.06	0.32	0.62
	Average	0.08	0.35	0.57
	High	0.24	0.46	0.30

The Columbia summer seasonal forecasts are obtained based on the categories, demonstrating the highest probability of occurrence. Results of one variable (Yangtze winter season flow), two variables (Rhine spring with Yangtze winter season flow and Rhine spring with spring PDO), and three variables (Rhine spring season flow, winter NAO, and winter SOI) forecasts are summarized in Tables 5.27 to 5.30, respectively. The verifications using rest of the variables and variable combinations are included in the Appendix A. Results indicate 9, 7, 8, and 9 correct predictions when 1, 2, 2, and 3 variables were incorporated, respectively. Yet, beyond this categorical forecast, this type of model is unable to differentiate between skills of two similar category forecasts with different conditional probabilities. Therefore, two skill measures, the RPSS and forecast index (FI) (described in Chapter 3) for calibration and validation were adopted. The corresponding results of these two indices are described in the following sections.

Table 5.26

Conditional Probability of the Columbia Summer Flow, Given the Summer NAO index,

Yangtze Winter, Rhine Spring Flow Based on Observations of 1906–1980

Predictors			Columbia summer flow		
Rhine spring flow	Yangtze winter flow	NAO summer	Low	Average	High
Low	Low	Low	0.16	0.22	0.62
		Average	0.28	0.23	0.49
		High	0.56	0.29	0.15
	Average	Low	0.10	0.26	0.63
		Average	0.20	0.28	0.52
		High	0.43	0.40	0.17
	High	Low	0.02	0.21	0.77
		Average	0.05	0.25	0.70
		High	0.15	0.52	0.33
Average	Low	Low	0.21	0.24	0.56
		Average	0.28	0.23	0.49
		High	0.62	0.27	0.11
	Average	Low	0.14	0.28	0.58
		Average	0.25	0.29	0.46
		High	0.49	0.37	0.14
	High	Low	0.03	0.24	0.73
		Average	0.06	0.28	0.65
		High	0.19	0.53	0.29
High	Low	Low	0.51	0.25	0.24
		Average	0.67	0.19	0.14
		High	0.82	0.15	0.03
	Average	Low	0.38	0.34	0.28
		Average	0.55	0.28	0.17
		High	0.73	0.24	0.03
	High	Low	0.12	0.40	0.48
		Average	0.21	0.41	0.38
		High	0.40	0.49	0.11

Table 5.27Conditional Forecasting of the Columbia River Summer Flow, Based on Yangtze WinterFlow and Comparison with the Observed Flow (1981–1999)

Forecasting year	Observed flow category	Yangtze winter flow category	Conditional probability of flow in the Columbia (%)			Predicted flow category	Remarks
			Low	Average	High		
1981	Average	Low	50%	25%	25%	Low	Outside category
1982	High	Low	50%	25%	25%	Low	Outside category
1983	Average	Average	38%	33%	29%	Low	Outside category
1984	Average	High	12%	38%	50%	High	Outside category
1985	Low	Low	50%	25%	25%	Low	Ok
1986	Low	Average	38%	33%	29%	Low	Ok
1987	Low	Low	50%	25%	25%	Low	Ok
1988	Low	Low	50%	25%	25%	Low	Ok
1989	Low	Average	38%	33%	29%	Low	Ok
1990	Average	Average	38%	33%	29%	Low	Outside category
1991	Average	Average	38%	33%	29%	Low	Outside category
1992	Low	Average	38%	33%	29%	Low	Ok
1993	Low	Average	38%	33%	29%	Low	Ok
1994	Low	Average	38%	33%	29%	Low	Ok
1995	Average	Average	38%	33%	29%	Low	Outside category
1996	High	Average	38%	33%	29%	Low	Outside category
1997	High	Average	38%	33%	29%	Low	Outside category
1998	Average	Average	38%	33%	29%	Low	Outside category
1999	High	High	12%	38%	50%	High	Ok

Table 5.28

Conditional Forecasting of the Columbia River Summer Flow, Based on Rhine Spring and Yangtze Winter Flow, and Comparison with the Observed Flow (1981–1999)

Forecasting year	Observed flow category	Yangtze winter flow category	Rhine spring flow category	Conditional probability of flow in the Columbia (%)			Predicted flow category	Remarks
				Low	Average	High		
1981	Average	Low	High	70%	20%	10%	Low	Outside category
1982	High	Low	Average	40%	27%	33%	Low	Outside category
1983	Average	Average	High	58%	29%	13%	Low	Outside category
1984	Average	High	Average	8%	35%	57%	High	Outside category
1985	Low	Low	Average	40%	27%	33%	Low	Ok
1986	Low	Average	High	58%	29%	13%	Low	Ok
1987	Low	Low	High	70%	20%	10%	Low	Ok
1988	Low	Low	High	70%	20%	10%	Low	Ok
1989	Low	Average	Average	29%	34%	37%	High	Outside category
1990	Average	Average	Low	23%	33%	44%	High	Outside category
1991	Average	Average	Low	23%	33%	44%	High	Outside category
1992	Low	Average	Average	29%	34%	37%	High	Outside category
1993	Low	Average	Low	23%	33%	44%	High	Outside category
1994	Low	Average	High	58%	29%	13%	Low	Ok
1995	Average	Average	High	58%	29%	13%	High	Outside category
1996	High	Average	Low	23%	33%	44%	High	Ok
1997	High	Average	Average	29%	34%	37%	High	Ok
1998	Average	Average	Average	29%	34%	37%	High	Outside category
1999	High	High	High	24%	46%	30%	Average	Outside category

Table 5.29**Conditional Forecasting of the Columbia River Summer Flow, Based on Rhine Spring****Flow and Spring PDO, and Comparison with the Observed Flow (1981–1999)**

Forecasting year	Observed flow category	Spring PDO category	Rhine spring flow category	Conditional probability of flow in the Columbia (%)			Predicted flow Category	Remarks
				Low	Average	High		
1981	Average	High	Average	65%	32%	3%	Low	Outside category
1982	High	Average	High	25%	33%	42%	High	Ok
1983	Average	High	Average	65%	32%	3%	Low	Outside category
1984	Average	High	High	42%	47%	11%	Average	Ok
1985	Low	High	Average	42%	47%	11%	Average	Outside category
1986	Low	High	Average	65%	32%	3%	Low	Ok
1987	Low	High	High	65%	32%	3%	Low	Ok
1988	Low	High	High	65%	32%	3%	Low	Ok
1989	Low	Average	High	25%	33%	42%	High	Outside category
1990	Average	High	Average	37%	50%	14%	Average	Ok
1991	Average	Average	Low	20%	32%	48%	High	Outside category
1992	Low	High	Low	42%	47%	11%	Average	Outside category
1993	Low	High	Average	37%	50%	14%	Average	Outside category
1994	Low	High	Low	65%	32%	3%	Low	Ok
1995	Average	High	High	65%	32%	3%	Low	Outside category
1996	High	High	High	37%	50%	14%	Average	Outside category
1997	High	High	Low	42%	47%	11%	Average	Outside category
1998	Average	High	Average	42%	47%	11%	Average	Ok
1999	High	Average	Average	54%	31%	15%	Low	Outside category

Table 5.30

Conditional Forecasting of the Columbia River Summer Flow, Based on Rhine Spring, Summer NAO, and Winter SOI Indices, and Comparison with the Observed Flow (1981–1999)

Forecasting year	Obs. flow cat.	Winter SOI cat.	Summer NAO cat.	Rhine spring cat.	Conditional probability of flow in the Columbia (%)			Pred. flow cat.	Remarks
					Low	Avg.	High		
1981	Avg.	Avg.	Avg.	Avg.	46%	30%	24%	Low	Outside category
1982	High	High	High	High	29%	45%	25%	Avg.	Outside category
1983	Avg.	Low	Low	Avg.	53%	28%	19%	Low	Outside category
1984	Avg.	Avg.	Avg.	High	18%	27%	55%	High	Outside category
1985	Low	Avg.	High	Avg.	41%	40%	19%	Low	Ok
1986	Low	Avg.	High	Avg.	67%	28%	5%	Low	Ok
1987	Low	Low	Low	High	53%	28%	19%	Low	Ok
1988	Low	Low	Low	High	53%	28%	19%	Low	Ok
1989	Low	High	Avg.	High	11%	26%	63%	High	Outside category
1990	Avg.	Low	High	Avg.	57%	32%	11%	Low	Outside category
1991	Avg.	Avg.	High	Low	35%	41%	23%	Avg.	Ok
1992	Low	Low	High	Low	63%	29%	9%	Low	Ok
1993	Low	Low	High	Avg.	57%	32%	11%	Low	Ok
1994	Low	Avg.	High	Low	67%	28%	5%	Low	Ok
1995	Avg.	Low	High	High	82%	16%	2%	Low	Outside category
1996	High	Avg.	Low	High	7%	22%	70%	High	Ok
1997	High	High	High	Low	29%	45%	25%	Avg.	Outside category
1998	Avg.	Low	Low	Avg.	23%	29%	48%	High	Outside category
1999	High	High	Avg.	Avg.	33%	34%	33%	Avg.	Outside category

5.8.1 Forecast Calibration (1906–80)

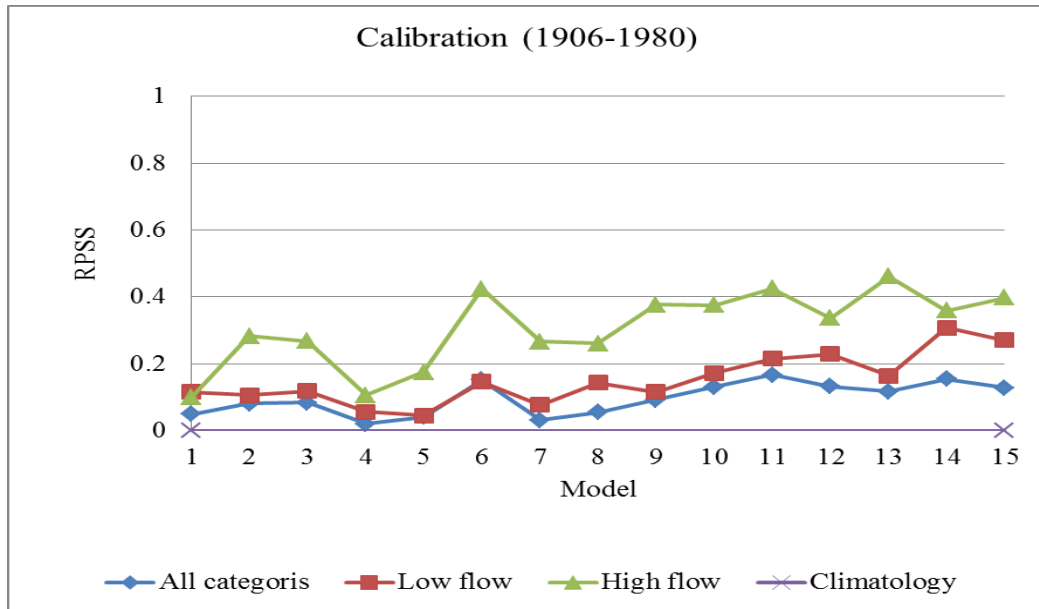
The rank probability skill score (RPSS) and forecast index (FI) values of the models are obtained for the calibration period, and the results are compared with the forecast based solely on climatology, indicated by zero RPSS and one third of the FI value (as the historical flows are divided into three categories). For a perfect forecast, the

RPSS and FI values equal to unity. Therefore, a skillful model represents a forecast with higher RPSS and FI values in comparison to the climatology. The mean RPSS and FI values for the models with various predictor combinations are summarized in Table 5.31 and shown in Figures 5.12(a) and (b).

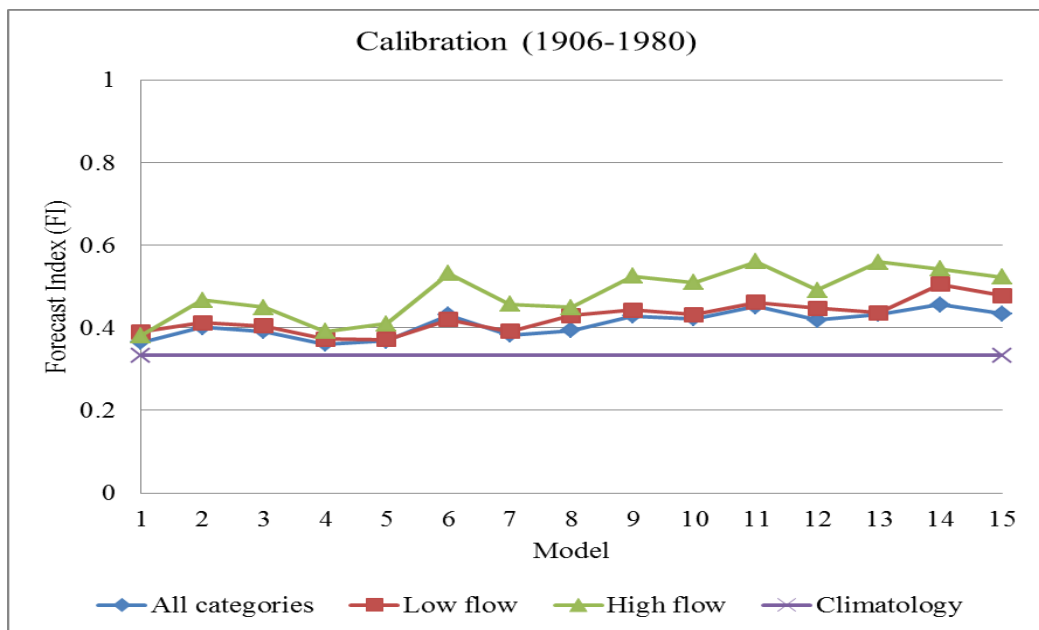
Table 5.31

The mean RPSS and the FI Values at the Calibration Period (1906-1980)

SL No	Predictors	RPSS			FI		
		Overall	Low flow	High flow	Overall	Low flow	High flow
1	Winter SOI	0.05	0.12	0.10	0.37	0.39	0.38
2	Spring PDO	0.08	0.11	0.28	0.40	0.41	0.47
3	Summer NAO	0.08	0.12	0.27	0.39	0.40	0.45
4	Yangtze winter season flow	0.02	0.06	0.11	0.36	0.37	0.39
5	Rhine spring season flow	0.04	0.04	0.18	0.37	0.37	0.41
6	Summer NAO + Yangtze winter season flow	0.15	0.15	0.42	0.43	0.42	0.53
7	Rhine spring season flow + Yangtze winter season flow	0.03	0.08	0.27	0.38	0.39	0.46
8	Winter SOI + Rhine spring season flow	0.05	0.14	0.26	0.39	0.43	0.45
9	Rhine spring season flow + spring PDO	0.09	0.11	0.38	0.43	0.44	0.53
10	Summer NAO + Rhine spring season flow	0.13	0.17	0.38	0.42	0.43	0.51
11	Summer NAO + Spring PDO	0.17	0.21	0.42	0.45	0.46	0.56
12	Summer NAO + Winter SOI	0.13	0.23	0.34	0.42	0.45	0.49
13	Rhine spring season flow + Yangtze winter season flow + summer NAO	0.12	0.16	0.46	0.43	0.44	0.56
14	Winter SOI + Summer NAO + Spring PDO	0.15	0.31	0.36	0.46	0.51	0.54
15	Winter SOI + NAO summer + Rhine spring season flow	0.13	0.27	0.40	0.43	0.48	0.52



(a)



(b)

Figure 5.12. Forecast skills of the models with lagged variables or variable combinations in the calibration period (year 1906-1980): (a) Rank probability skill score (RPSS) and (b) Forecast Index (FI).

In the above plots, the x-axis represents models used with following variable combinations: (1) winter SOI; (2) spring PDO; (3) summer NAO; (4) Yangtze winter season flow; (5) Rhine spring season flow; (6) summer NAO and Yangtze winter flow; (7) Rhine spring season flow and Yangtze winter season flow; (8) winter SOI and Rhine spring season flow; (9) Rhine spring season flow and spring PDO; (10) summer NAO and Rhine spring season flow; (11) summer NAO and spring PDO; (12) summer NAO and winter SOI; (13) Rhine spring season flow, Yangtze winter season flow and summer NAO; (14) winter SOI, summer NAO and spring PDO; and (15) winter SOI, summer NAO and Rhine spring season flow.

Among the predictor variables, the first available information was the Yangtze winter season flow and summer NAO of the previous year (lag one cross-correlation). Thereafter, the winter SOI, spring PDO and Rhine spring season flow were available and incorporated with various combinations. The Table 5.31 results reveals the RPSS/FI values for all the models are higher than zero/one third (climatological forecast), indicating improved forecast performance. The Figure 5.12 also supports this, where the line parallel to the x-axis represents the climatological forecast. In most cases, the two variable forecasts yield higher RPSS/FI value than the one variable forecasts, demonstrating improved prediction skills. For instance, the sole use of external variables such as the SOI, NAO, and PDO resulted in the RPSS statistics of 0.05, 0.08, and 0.08, respectively. The RPSS for the two-variable forecasts, including the NAO with PDO and the NAO with SOI, are found as 0.17 and 0.13, respectively, indicating superior forecasting performance. The FI values for the above two models also show similar performance, producing values of 0.45 and 0.42, respectively. The highest RPSS and FI

values for three variable combination forecasts are obtained as 0.15, and 0.46, respectively, when SOI, NAO, and PDO were incorporated. However, this value is less than the RPSS/FI values with NAO and PDO combinations. If the river flows are used in addition to the external variables, the RPSS and FI values are not improving.

The forecasts were evaluated further to identify the variables influencing the Columbia summer flow. At first, results are evaluated for the river flow variables. The sole use of the Yangtze winter and Rhine spring seasonal flows yield the RPSS and FI values of 0.02 and 0.04, respectively. The combination of these two river flow data yields the RPSS and FI values as 0.03 and 0.38, respectively, indicating approximately similar single-variable model performance. The models incorporating Rhine winter and Yangtze spring flow with NAO and the SOI, NAO, and Rhine spring flow data produced the RPSS values equal to 0.12 and 0.13, respectively, whereas the statistics for the model incorporating the NAO and PDO was 0.17. These results indicate the use of three variables do not necessarily improve the flow prediction skills while compared with the two variable combination forecast. Inclusion of the PDO with the combination of NAO and SOI increases the RPSS and FI values from 0.13 to 0.15 and 0.42 to 0.46, respectively. This demonstrates PDO influence on the Columbia summer flow.

The Figures 5.12(a) and 5.12(b) shows comparison of model skills in terms of the RPSS and FI statistics using both the river flow and the external variable information. The x-axis represents the models with different variables among which model 1 to 5, 6 to 12, and 13 to 15 represent models with a single variable, two variables, and three variables, respectively. The Yangtze winter season flow and summer NAO used here were available from the last year, therefore, their role in predicting seasonal Columbia

summer flow are evaluated first. As can be seen from the figures, the forecast skills based on the summer NAO (RPSS = 0.08), Yangtze winter season flow (RPSS = 0.02), and the combination of the summer NAO and Yangtze winter flow (RPSS = 0.15) produce skills slightly higher than the climatology (RPSS = 0). Thereafter, the winter SOI information is available and different variable combinations are examined. The results show slight improvement in the forecasting quality over the single and other dual variable forecasts with the summer NAO and winter SOI information for which the RPSS and the FI values are obtained as 0.13 and 0.42, respectively. Later, the Rhine spring season flow and the spring PDO data became available and the prediction skills gain a larger improvement particularly from the addition of the spring PDO. However, only the spring PDO data resulted in the RPSS and the FI values as 0.08 and 0.39, respectively. Therefore, it is revealed that all the three variables, the spring PDO, winter SOI and summer NAO data are useful in improving the prediction skills of the models.

In terms of low flow prediction, the model performances are similar to the overall model performance. The sole use of Rhine and Yangtze flow result the RPSS values of 0.04 and 0.06, respectively, whereas the combined use of the two river flows yields the RPSS value as 0.08 (higher than the previous two). The combination of two river flows including the NAO summer data produces the RPSS value of 0.16. This shows the river flows in combination with the external variables improve the summer flow prediction skills of the Columbia River. More interestingly, the best performance is achieved with model incorporating three-variable combination of the summer NAO, winter SOI, and spring PDO (RPSS = 0.31, FI = 0.51). However, the combined use of NAO and SOI produces the RPSS value as 0.13. This indicates the addition of PDO including SOI and

NAO improve the RPSS values from 0.13 to 0.31 (an improvement of 225%). Separately, the winter SOI, summer NAO, and combinations of summer NAO with winter SOI and summer NAO with spring PDO showed the RPSS values as 0.12, 0.12, 0.23, and 0.21, respectively. This indicates the forecasting skills were increasing with the increasing number of variables. It also shows the importance of the three external variables (NAO, SOI, and PDO) in predicting Columbia summer season low flows.

However, for forecasting the high Columbia flow, the variable results demonstrated different behavior. The results showed in the table were also plotted in the Figure 5.12 to identify the best predictor variables. This reveals the superiority of three variable combinations with Rhine spring, Yangtze winter, and the summer NAO, as the RPSS and the FI values were found as 0.45 and 0.56, respectively. However, when the Yangtze winter and Rhine spring season flows were used solely, the RPSS and the FI values were 0.11 and 0.18, respectively (corresponding FI values were 0.39 and 0.41). This shows if the external variables were used in addition to the river flow information, forecasting indices yielded higher values, indicating relatively improved model performance.

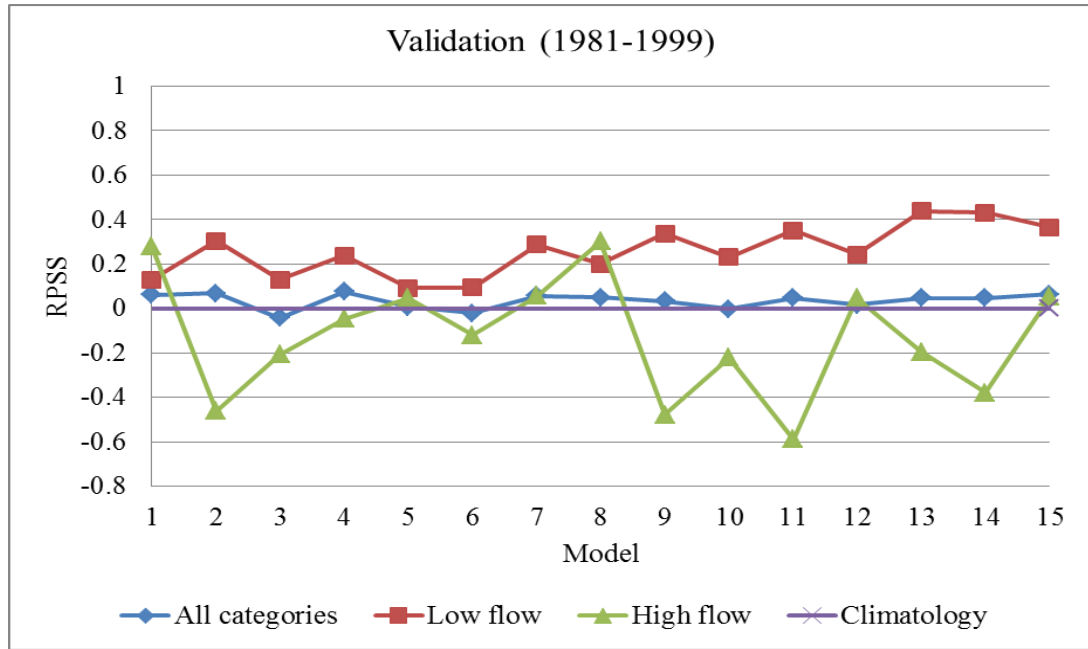
5.8.2 Forecast Verification (1981–1999)

The forecasting skills of the verification period are summarized in Table 5.32 and also shown in Figures 5.13(a) and 5.13(b). In the plots, the x-axis represents model combinations similar to Figure 5.12. The results show the performance of single variable forecasts differs from the calibrated forecasts as the summer NAO index yields the RPSS value lower than climatology, although the FI values indicate slightly higher than

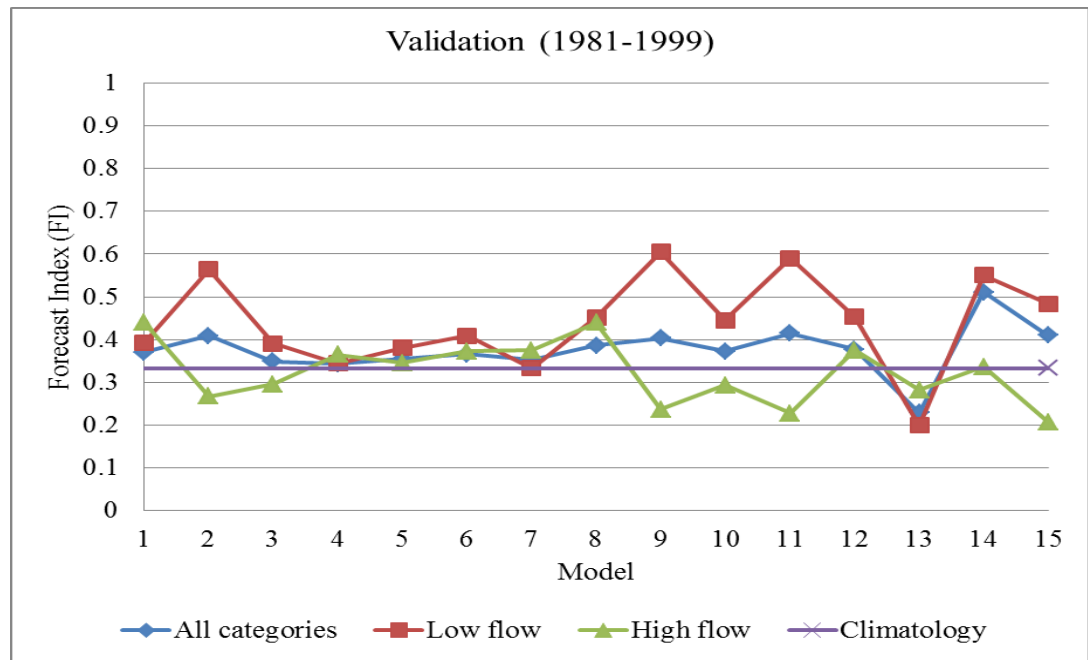
climatology. Among the single variables, higher RPSS value of 0.079 is obtained for the Yangtze winter flow. Besides this, the two variable forecasts are expected to perform similarly to the calibrated forecast. As can be seen from the Table 5.32 and Figure 5.13, the RPSS/FI values of the models incorporating the summer NAO, the Yangtze winter is -0.022/0.363, as well as summer NAO and Rhine spring flow is was -0.003/0.370. The results are contrasting as the RPSS values indicate inefficient forecast, although the FI values are above climatology. The two and three variable forecast performance indicate improvement of forecasting skills, although do not outperform the best single variable forecast (RPSS = 0.079), therefore, not very effective. Only the SOI winter and Rhine spring flow as well as the Rhine spring flow with PDO spring show slightly improved performance (evident from the RPSS and the FI values), which demonstrate better performance than those of the single variable forecasts. However, the FI values indicate different results as the three-variable combination with the SOI, PDO, and NAO performance is best (FI = 0.418). Similar to the calibration results, the FI values are increasing with the increasing number of variables.

Table 5.32The mean RPSS and the FI Values at the Validation Period (1981-1999)

SL No	Predictors	RPSS			FI		
		Overall	Low flow	High flow	Overall	Low flow	High flow
1	Winter SOI	0.061	0.130	0.277	0.370	0.393	0.440
2	Spring PDO	0.068	0.304	-0.461	0.396	0.479	0.205
3	Summer NAO	-0.043	0.131	-0.207	0.353	0.415	0.297
4	Yangtze winter season flow	0.075	0.239	-0.047	0.369	0.422	0.333
5	Rhine spring season flow	0.006	0.093	0.047	0.358	0.388	0.367
6	Summer NAO + Yangtze winter season flow	-0.022	0.095	-0.120	0.363	0.390	0.342
7	Rhine spring season flow + Yangtze winter season flow	0.058	0.288	0.058	0.387	0.470	0.360
8	Winter SOI + Rhine spring season flow	0.050	0.201	0.303	0.389	0.442	0.408
9	Rhine spring season flow + spring PDO	0.034	0.336	-0.477	0.400	0.509	0.203
10	Summer NAO + Rhine spring season flow	-0.003	0.231	-0.221	0.370	0.449	0.300
11	Summer NAO + Spring PDO	0.048	0.351	-0.588	0.405	0.517	0.180
12	Summer NAO + Winter SOI	0.018	0.244	0.047	0.380	0.460	0.379
13	Rhine spring season flow + Yangtze winter season flow + summer NAO	0.048	0.437	-0.194	0.403	0.533	0.315
14	Winter SOI + Summer NAO + Spring PDO	0.047	0.431	-0.379	0.418	0.563	0.244
15	Winter SOI + NAO summer + Rhine spring season flow	0.064	0.364	0.052	0.404	0.513	0.384



(a)



(b)

Figure 5.13. Forecast skills of the models with lagged variables or variable combinations in the validation period (year 1981-1999): (a) Rank probability skill score (RPSS) and (b) Forecast Index (FI).

In terms of low flow prediction, the variables demonstrate improved performance in comparison to the calibration period. Among the single variable predictors, the spring PDO provides the best performance, resulting in the RPSS and FI values of 0.304 and 0.479, respectively. The model with the two variables, the summer NAO and spring PDO indicates better performance, reveal from the RPSS and the FI information (the RPSS value 0.351 and the FI value 0.517). The RPSS value indicate, the best low summer Columbia flow forecast is achieved with the three-variable information, namely the Rhine spring flow, Yangtze winter flow, and summer NAO (RPSS = 0.437). However, the FI values indicate the forecasts of three external variables combination is better (FI = 0.563). In terms of the high flow prediction, the variable influences are different, as in some of the cases, single and multi-variable information demonstrate the RPSS and FI values lower than the climatology. This indicates the variables efficient to forecast low Columbia flow do not necessarily prove useful to forecast the high Columbia summer flow. In terms of the RPSS, the best high flow predictions are achieved with the combination of winter SOI and Rhine spring season flow (RPSS = 0.303), whereas the FI values indicate the winter SOI solely produced better predictions (FI = 0.440). Besides this, the PDO, which influenced by bringing skills into the models, performs not very efficiently in predicting summer season Columbia high flows.

CHAPTER 6

CONCLUSIONS

The objectives address issues regarding seasonal river flow: (i) quantify relationships between seasonal river flow and external environmental variables; (ii) evaluate stochastic, artificial neural network, and probabilistic methods to predict seasonal river flow; and (iii) evaluate ensemble forecasts for seasonal river flow. In order to address these objectives, stochastic time series, artificial neural network, and probabilistic models are adopted. A review of relevant performance criteria is conducted to objectively evaluate results. The applicable relationships between seasonal river flow and external environmental variables are summarized. The prediction skill of univariate and multivariate time series (TS) and artificial neural network (ANN) models are evaluated. The influence of external variables as predictors is evaluated. Ensemble forecasts results and performance are summarized. Finally, findings regarding the use of river flows and external variables with a probabilistic approach are stated.

Relations between continental-scale hydrologic flows and external climate variables are evaluated through direct correlations over seasonal time scale. External environmental variables include sun spot numbers (SSN), Southern Oscillation Index (SOI), Pacific Decadal Oscillation (PDO), and North Atlantic Oscillation (NAO). The cross-correlation between continental river flow records includes the following four

locations: Parana from South America, Danube and Rhine from Europe, and Missouri from North America. Later, the river flow record of the Congo (Kinshasha) from Africa, Yangtze (Datong) from Asia, Rhine (Lobith) from Europe, Columbia (Dalles) from North America, and Parana (Timbues) from South America, the Nile (Aswan) from North Africa, and Murray (Murray-Darling basin) from Australia are evaluated.

Statistical characteristics of each river flow record are identified and analyzed to illustrate the stochastic models ability to reproduce flow rates with statistical characteristics of the historical record. Results indicate univariate and multivariate time series models capture the variability of seasonal flow, although forecasted flow values deviated from the flow record. This is evident by high MPE, RMSE and low Pearson coefficients. Overall, results demonstrate time series model performance is river specific and large variations in performance for predicting seasonal river flow.

The ANN models are effective in predicting the seasonal flow for the Parana, Nile and Murray rivers. Low MPE and RMSE values, and high SPPMCC relative to persistence methods indicate ANN models produce less forecast error for these three rivers. The RSD for persistence models is nearly equal to one, indicating seasonal flow variation is well represented.

Comparison of time series and ANN models shows RMSE values of the ANN are lower indicating better performance, although other indices are nearly equal. Both methods yield low Pearson coefficients, indicating discrepancies between forecast and observed river flow.

In river flow category forecasts using low, average and high flow levels, the univariate and multivariate ANN methods, and persistence models are compared.

Performance criteria are inconclusive when comparing univariate, persistence, multivariate approaches. More complex methods do not always improve forecast estimation. Analysis performed with the Congo, Yangtze, Rhine, Missouri, and Parana Rivers indicate forecasts improved particularly with the RMSE values. The RMSE for the Congo and Yangtze rivers indicate multivariate models outperformed univariate models by 36%, 6%, and persistence models by 49% and 65%, respectively. Conversely, univariate model results for the Columbia and Parana rivers are better than the multivariate models by 10% and 19%, and persistence models by 16% and 2%, respectively. The multivariate model RMSE is 7% lower than the persistence model. For the Rhine River, both univariate and multivariate models show lower RMSE compared to persistence by 20%. The MPE values indicate univariate models are better for all the rivers except Rhine. The RSD and Pearson criteria also indicate multivariate and persistence models are relatively better. However, differences between performance criteria are not significant enough to determine the best forecast model. Table 6.1 summarizes model performance using four performance indices. The results indicate ANN performs better than times series models in most cases. Furthermore, Table 6.2 shows model rating for river flow magnitude categories. The tick marks (✓) indicate better models. Results are inconclusive and found to be river specific varying results from river to river. In general, ANN models predict low flows better, whereas time series models predict high flows better. Furthermore, results indicate multivariate models perform better than univariate and persistence models.

Evaluation of including external variables is performed in order to predict low and high seasonal flows. Results indicate equal or improved performances for most rivers,

when five rivers flow records are incorporated. Inconclusive results indicate improvement associated with inclusion of external variables depend upon specific river and method.

Table 6.1

Overall Performance of TS, ANN, Persistence Models based on RMSE, MPE, RSD, SPPMCC

River	Performance Indices	TS models		ANN models		Persistence
		Univariate	Multi-variate	Univariate	Multi-variate	
Congo	RMSE				✓	
	MPE				✓	
	RSD		✓			✓
	SPPMCC		✓			
Yangtze	RMSE				✓	
	MPE			✓		
	RSD			✓		✓
	SPPMCC				✓	
Rhine	RMSE			✓	✓	
	MPE				✓	
	RSD					✓
	SPPMCC				✓	
Columbia	RMSE			✓		
	MPE			✓		
	RSD				✓	✓
	SPPMCC				✓	
Parana	RMSE			✓		
	MPE			✓		
	RSD				✓	✓
	SPPMCC			✓		

The ensemble approach with multi-model forecasts improved seasonal flow estimates. Variation of flow magnitudes based on seasonal flow fluctuations are within the ensemble forecast range. The ensemble approach appears promising for seasonal flow predictions of flow categories. The ensemble forecasts are evaluated based on rank

probability skill score (RPSS) with median RPSS obtained separately for the time series (TS-P), ANN (ANN-P) models, and merging of the time series and ANN ensembles including persistence (TS-ANN-P).

Table 6.2

Overall Categorical Forecast Performance of TS, ANN, Persistence Models

River	Performance Indices	TS models		ANN models		Persistence
		Univariate	Multi-variate	Univariate	Multi-variate	
Congo	Overall				✓	
	Low				✓	
	High		✓			
Yangtze	Overall			✓		
	Low				✓	
	High			✓		
Rhine	Overall				✓	
	Low				✓	
	High				✓	
Columbia	Overall					✓
	Low		✓		✓	
	High	✓	✓			
Parana	Overall					✓
	Low	None	None	None	None	None
	High					✓

The ensembles are compared in terms of predicting overall, seasonal, and extreme flow categories. Results indicate performance is inconclusive and depends on the specific river and flow category. Overall flow forecasts are better for time series model ensemble forecasts for the Congo (RPSS = 0.57, 12% and 26% higher RPSS than ANN-P and TS-ANN-P, respectively) and Yangtze (RPSS = 0.94, 6% and 64% higher RPSS than ANN-P and TS-ANN-P). The ANN ensembles is better for the Columbia (RPSS = 0.45, TS-P and TS-ANN-P have negative RPSS values) and Parana Rivers (RPSS = 0.79, negative

RPSS for TS-P and 55% higher than TS-ANN-P). And the Rhine River ensemble forecasts indicate better results with the TS-ANN-P (RPSS = -0.05, tending towards zero) in comparison to the TS-P (RPSS = -0.53) and ANN-P (RPSS = -0.16), although all the three RPSS are negative. The above analysis indicate the ensemble forecasts may improve flow prediction in comparison to climatology (random guess, RPSS = 0)

The value of the mean and median ensemble flow forecast reveals improved performance relative to individual model results in all cases. For the Congo River, median ensemble correlation coefficient is 42% higher than any individual model coefficient with a corresponding low RMSE value (5% lower than the median ensemble RMSE). Similarly, ensemble mean for the Yangtze and Parana and median for the Rhine and Columbia have higher correlation coefficients of 12%, 146%, 529%, and 83%, respectively. Higher correlation coefficients for ensemble mean and median forecasts tend to yield predictions related closely with the observed flow values, although having higher RMSE values than individual models.

The probabilistic forecast using discriminant prediction approach incorporated one, two and three predictor combinations for the Columbia River summer seasonal flow. Lagged relationships of both river flows and external variables are included as predictor variables. The skills are evaluated in terms of predicting low and high flows. Results indicate improvement in the forecast performance with increasing number of variables in most of the cases. For low flow forecast, better RPSS values for one, two, and three predictor combinations indicated 30%, 35%, and 44% improvement over climatology, whereas for high flows the improvements are 46%, 59%, and 38%, respectively. Results are inconclusive since performance is flow specific and variables for a particular flow-

type do not indicate improved performance for other flows. In combination with external variables, such as Rhine spring with Yangtze winter flow, including NAO, improves low flow predictions by 44%. And Rhine spring including spring PDO improves prediction of high flows by 48%.

Overall, the continental runoff response and influence of the external environmental variables are examined through a multivariate approach. Results are promising but inconclusive. The multi-variable methods brought additional information into the models and results indicate the necessity of determining suitable variables and approaches to improve extreme event forecasting skill in specific river basins.

Components of this research were presented at three conferences: (1) 4th World Climate Research Program (WCRP) (Bhuiyan & French, May 2012), (2) American Geophysical Union (AGU) Fall Meeting 2012 (Bhuiyan & French, December 2012), and (3) AGU Chapman Conference 2013 on Seasonal to Interannual Hydroclimate Forecasts and Water Management (Bhuiyan & French, July 2013). The posters presented in these conferences are included as Appendix C.

REFERENCES

- Ajami, N. K., Duan, Q., Gao, X., & Sorooshian, S. (2006). Multimodel Combination Techniques for Analysis of Hydrological Simulations: Application to Distributed Model Intercomparison Project Results. *Journal of Hydrometeorology*, 7(4), 755-768.
- Amarasekera, K. N., Lee, R. F., Williams, E. R., & Eltahir, E. A. B. (1997). ENSO and the natural variability in the flow of tropical rivers. *Journal of Hydrology*, 200(1-4), 24-39.
- Araghinejad, S., Burn, D. H., & Karamouz, M. (2006). Long-lead probabilistic forecasting of streamflow using ocean-atmospheric and hydrological predictors. *Water Resources Research*, 42(3), W03431.
- ASCE. (2000a). Artificial Neural Networks in Hydrology. I: Preliminary Concepts. *Journal of Hydrologic Engineering*, 5(2), 115-123.
- ASCE. (2000b). Artificial Neural Networks in Hydrology. II: Hydrologic Applications. *Journal of Hydrologic Engineering*, 5(2), 124-137.
- Batchelor, R., & Dua, P. (1995). Forecaster diversity and the benefits of combining forecasts. *Management Science*, 41(1), 68-75.
- Bates, J. M., & Granger, C. W. J. (1969). The Combination of Forecasts. *OR*, 20(4), 451-468.
- Beale, M., Hagan, M., & Demuth, H. (2011). Neural network toolbox getting started guide R2011b.
- Beven, K., & Freer, J. (2001). Equifinality, data assimilation, and uncertainty estimation in mechanistic modelling of complex environmental systems using the GLUE methodology. *Journal of Hydrology*, 249(1-4), 11-29.
- Bhuiyan, T. H. & French, M. N. (2012, May). *Forecasting Seasonal Hydrologic Response in Major River Basins under Climate Variations*, Poster presented at the 4th WCRP International Conference on Reanalyses, Silver Spring, Maryland.

- Bhuiyan, T. H. & French, M. N. (2012, December). *Seasonal Streamflow Variability at Global Time-Space Scales Under Natural Climate Extremes*, Poster presented at the fall meeting of the American Geophysical Union (AGU), San Francisco, California.
- Bhuiyan, T. H. & French, M. N. (2013, July). *Ensemble Methods for Seasonal Streamflow Prediction*, Poster presented at the AGU Chapman Conference on Seasonal to Interannual Hydroclimate Forecasts and Water Management, Portland, Oregon.
- Bonsal, B. R., Shabbar, A., & Higuchi, K. (2001). Impacts of low frequency variability modes on Canadian winter temperature. *International Journal of Climatology*, 21(1), 95-108.
- Bowden, G. J., Maier, H. R., & Dandy, G. C. (2012). Real-time deployment of artificial neural network forecasting models: Understanding the range of applicability. *Water Resources Research*, 48(10), W10549.
- Box, G., & Jenkins, G. (1968). Some recent advances in forecasting and control. *Journal of the Royal Statistical Society. Series C (Applied Statistics)*, 17(2), 91-109.
- Box, G., & Jenkins, G. (1970). *Time Series Analysis Forecasting and Control*.
- Box, G., & Jenkins, G. (1976). *Times series analysis: forecasting and control*: Holden-Day.
- Bras, R. L., & Rodríguez-Iturbe, I. (1994). *Random functions and hydrology*: Dover Pubns.
- Burlando, P., Rosso, R., Cadavid, L. G., & Salas, J. D. (1993). Forecasting of short-term rainfall using ARMA models. *Journal of Hydrology*, 144(1-4), 193-211.
- Cannaby, H., & Hüsrevoğlu, Y. S. (2009). The influence of low-frequency variability and long-term trends in North Atlantic sea surface temperature on Irish waters. *ICES Journal of Marine Science: Journal du Conseil*, 66(7), 1480-1489.
- Carlson, R. F., MacCormick, A. J. A., & Watts, D. G. (1970). Application of Linear Random Models to Four Annual Streamflow Series. *Water Resources Research*, 6(4), 1070-1078.
- Chatfield, C. (2004). *The analysis of time series: an introduction* (Vol. 59): CRC press.
- Chen, D., Zebiak, S. E., Busalacchi, A. J., & Cane, M. A. (1995). An improved procedure for El Niño forecasting: Implications for predictability. *Science*, 269, 1699-1702.
- Chen, S.-T., & Yu, P.-S. (2007). Real-time probabilistic forecasting of flood stages. *Journal of Hydrology*, 340(1-2), 63-77.

- Chiew, F. H. S., Piechota, T. C., Dracup, J. A., & McMahon, T. A. (1998). El Nino/Southern Oscillation and Australian rainfall, streamflow and drought: Links and potential for forecasting. *Journal of Hydrology*, 204(1-4), 138-149.
- Chowdhury, S., & Sharma, A. (2009). Multisite seasonal forecast of arid river flows using a dynamic model combination approach. *Water Resources Research*, 45(10), W10428.
- Clemen, R. T. (1989). Combining forecasts: A review and annotated bibliography. *International Journal of Forecasting*, 5(4), 559-583.
- Coulibaly, P., Anctil, F., Aravena, R., & Bobée, B. (2001). Artificial neural network modeling of water table depth fluctuations. *Water Resources Research*, 37(4), 885-896.
- Coulibaly, P., & Baldwin, C. K. (2005). Nonstationary hydrological time series forecasting using nonlinear dynamic methods. *Journal of Hydrology*, 307(1-4), 164-174.
- Coulibaly, P., Bobée, B., & Anctil, F. (2001b). Improving extreme hydrologic events forecasting using a new criterion for artificial neural network selection. *Hydrological Processes*, 15(8), 1533-1536.
- Cullen, H., Kaplan, A., Arkin, P., & deMenocal, P. (2002). Impact of the North Atlantic Oscillation on Middle Eastern Climate and Streamflow. *Climatic Change*, 55(3), 315-338.
- Dai, A., Qian, T., Trenberth, K. E., & Milliman, J. D. (2009). Changes in Continental Freshwater Discharge from 1948 to 2004. *Journal of Climate*, 22(10), 2773-2792.
- Dawson, C. W., & Wilby, R. L. (2001). Hydrological modelling using artificial neural networks. *Progress in Physical Geography*, 25(1), 80-108.
- de Menezes, L. M., W. Bunn, D., & Taylor, J. W. (2000). Review of guidelines for the use of combined forecasts. *European Journal of Operational Research*, 120(1), 190-204.
- Delleur, J. W., & Kavvas, M. L. (1978). Stochastic Models for Monthly Rainfall Forecasting and Synthetic Generation. *Journal of Applied Meteorology*, 17(10), 1528-1536.
- Demuth, H., & Beale, M. (1993). Neural network toolbox for use with MATLAB.
- Dettinger, M. D., & Diaz, H. F. (2000). Global Characteristics of Stream Flow Seasonality and Variability. *Journal of Hydrometeorology*, 1(4), 289-310.
- Dibike, Y. B., & Coulibaly, P. (2006). Temporal neural networks for downscaling climate variability and extremes. *Neural Networks*, 19(2), 135-144.

- Durkee, J. D., Frye, J. D., Fuhrmann, C. M., Lacke, M. C., Jeong, H. G., & Mote, T. L. (2008). Effects of the North Atlantic Oscillation on precipitation-type frequency and distribution in the eastern United States. *Theoretical and Applied Climatology*, 94(1-2), 51-65.
- Eldaw, A. K., Salas, J. D., & Garcia, L. A. (2003). Long-Range Forecasting of the Nile River Flows Using Climatic Forcing. *Journal of Applied Meteorology*, 42(7), 890-904.
- Eltahir, E. A. B. (1996). El Niño and the Natural Variability in the Flow of the Nile River. *Water Resources Research*, 32(1), 131-137.
- Fischer, I., & Harvey, N. (1999). Combining forecasts: What information do judges need to outperform the simple average? *International Journal of Forecasting*, 15(3), 227-246.
- French, M. N., Krajewski, W. F., & Cuykendall, R. R. (1992). Rainfall forecasting in space and time using a neural network. *Journal of Hydrology*, 137(1-4), 1-31.
- Gallego, M., García, J., & Vaquero, J. (2005). The NAO signal in daily rainfall series over the Iberian Peninsula. *Climate Research*, 29(2), 103.
- Georgakakos, K. P., Seo, D.-J., Gupta, H., Schaake, J., & Butts, M. B. (2004). Towards the characterization of streamflow simulation uncertainty through multimodel ensembles. *Journal of Hydrology*, 298(1-4), 222-241.
- Glen Donaldson, R., & Kamstra, M. (1999). Neural network forecast combining with interaction effects. *Journal of the Franklin Institute*, 336(2), 227-236.
- Gobena, A. K., & Gan, T. Y. (2006). Low-frequency variability in Southwestern Canadian stream flow: links with large-scale climate anomalies. *International Journal of Climatology*, 26(13), 1843-1869.
- GRDC (2011). *Long-Term Mean Monthly Discharges and Annual Characteristics of GRDC Station* [data file]. Global Runoff Data Centre (GRDC), Koblenz, Germany: Federal Institute of Hydrology (BfG). Retrieved February 21, 2012 from http://www.bafg.de/GRDC/EN/Home/homepage_node.html
- Guhathakurta, P. (2008). Long lead monsoon rainfall prediction for meteorological subdivisions of India using deterministic artificial neural network model. *Meteorology and Atmospheric Physics*, 101(1-2), 93-108.
- Haan, C. T. (2002). *Statistical methods in hydrology*. Ames, Iowa: Iowa State Press.
- Hagedorn, R., Doblas-Reyes, F. J., & Palmer, T. N. (2005). The rationale behind the success of multi-model ensembles in seasonal forecasting – I. Basic concept. *Tellus A*, 57(3), 219-233.

- Hare, S. R. (1996). *Low frequency climate variability and salmon production*. University of Washington.
- Hibon, M., & Evgeniou, T. (2005). To combine or not to combine: selecting among forecasts and their combinations. *International Journal of Forecasting*, 21(1), 15-24.
- Hidalgo, H. G., & Dracup, J. A. (2003). ENSO and PDO Effects on Hydroclimatic Variations of the Upper Colorado River Basin. *Journal of Hydrometeorology*, 4(1), 5-23.
- Hipel, K. W., & McLeod, A. I. (1978). Preservation of the rescaled adjusted range: 2. Simulation studies using Box-Jenkins Models. *Water Resources Research*, 14(3), 509-516.
- Hipel, K. W., & McLeod, A. I. (1994). *Time series modelling of water resources and environmental systems* (Vol. 45): Elsevier Science.
- Hipel, K. W., McLeod, A. I., & Lennox, W. C. (1977). Advances in Box-Jenkins modeling, 1-Model construction. *Water Resources Research*, 13(3), 567-575.
- Hopfield, J. J. (1982). Neural networks and physical systems with emergent collective computational abilities. *Proceedings of the National Academy of Sciences*, 79(8), 2554-2558.
- Hurkmans, R., Troch, P. A., Uijlenhoet, R., Torfs, P., & Durcik, M. (2009). Effects of Climate Variability on Water Storage in the Colorado River Basin. *Journal of Hydrometeorology*, 10(5), 1257-1270.
- Hurrell, J. W. (1995). Decadal Trends in the North Atlantic Oscillation: Regional Temperatures and Precipitation. *Science*, 269(5224), 676-679.
- Hurrell, J. W., Hoerling, M. P., & Folland, C. K. (2002). Climatic variability over the North Atlantic. In R. P. Pearce (Ed.), *International Geophysics*, 83, 143-151.
- Hurvich, C. M., & Tsai, C.-L. (1993). A corrected akaike information criterion for vector autoregressive model selection. *Journal of Time Series Analysis*, 14(3), 271-279.
- Jose, V. R. R., & Winkler, R. L. (2008). Simple robust averages of forecasts: Some empirical results. *International Journal of Forecasting*, 24(1), 163-169.
- Kahya, E., & Dracup, J. A. (1993). U.S. streamflow patterns in relation to the El Niño/Southern Oscillation. *Water Resources Research*, 29(8), 2491-2503.
- Kantardzic, M. (2011). *Data mining: concepts, models, methods, and algorithms*: Wiley-IEEE Press.

- Krishnamurti, T. N., Kishtawal, C. M., LaRow, T. E., Bachiochi, D. R., Zhang, Z., Williford, C. E., . . . Surendran, S. (1999). Improved Weather and Seasonal Climate Forecasts from Multimodel Superensemble. *Science*, 285(5433), 1548-1550.
- Krishnamurti, T. N., Kishtawal, C. M., Zhang, Z., LaRow, T., Bachiochi, D., Williford, E., . . . Surendran, S. (2000). Multimodel Ensemble Forecasts for Weather and Seasonal Climate. *Journal of Climate*, 13(23), 4196-4216.
- Krzysztofowicz, R. (1998). Probabilistic Hydrometeorological Forecasts: Toward a New Era in Operational Forecasting. *Bulletin of the American Meteorological Society*, 79(2), 243-251.
- Krzysztofowicz, R. (1999). Bayesian theory of probabilistic forecasting via deterministic hydrologic model. *Water Resources Research*, 35(9), 2739-2750.
- Krzysztofowicz, R. (2001a). The case for probabilistic forecasting in hydrology. *Journal of Hydrology*, 249(1-4), 2-9.
- Krzysztofowicz, R. (2001b). Integrator of uncertainties for probabilistic river stage forecasting: precipitation-dependent model. *Journal of Hydrology*, 249(1), 69-85.
- Krzysztofowicz, R. (2002). Bayesian system for probabilistic river stage forecasting. *Journal of Hydrology*, 268(1), 16-40.
- Krzysztofowicz, R., & Kelly, K. S. (2000). Hydrologic uncertainty processor for probabilistic river stage forecasting. *Water Resources Research*, 36(11), 3265-3277.
- Kumar, D. N., Raju, K. S., & Sathish, T. (2004). River Flow Forecasting using Recurrent Neural Networks. *Water Resources Management*, 18(2), 143-161.
- Lubchenco, J., & Karl, T. R. (2012). Predicting and managing extreme weather events. *Physics Today*, 65(3), 31-37.
- Maier, H. R., & Dandy, G. C. (1996). The Use of Artificial Neural Networks for the Prediction of Water Quality Parameters. *Water Resources Research*, 32(4), 1013-1022.
- Mantua, N. J., & Hare, S. (2002). The Pacific Decadal Oscillation. *Journal of Oceanography*, 58(1), 35-44.
- Mantua, N. J., Hare, S. R., Zhang, Y., Wallace, J. M., & Francis, R. C. (1997). A Pacific Interdecadal Climate Oscillation with Impacts on Salmon Production. *Bulletin of the American Meteorological Society*, 78(6), 1069-1079.
- Matalas, N. C. (1967). Mathematical assessment of synthetic hydrology. *Water Resources Research*, 3(4), 937-945.

- Mauas, P. J. D., Buccino, A. P., & Flamenco, E. (2011). Long-term solar activity influences on South American rivers. *Journal of Atmospheric and Solar-Terrestrial Physics*, 73(2-3), 377-382.
- Mauas, P. J. D., Flamenco, E., & Buccino, A. P. (2008). Solar Forcing of the Stream Flow of a Continental Scale South American River. *Physical Review Letters*, 101(16), 168501.
- McCabe, G. J., & Dettinger, M. D. (1999). Decadal variations in the strength of ENSO teleconnections with precipitation in the western United States. *International Journal of Climatology*, 19(13), 1399-1410.
- McCulloch, W., & Pitts, W. (1943). A logical calculus of the ideas immanent in nervous activity. *The bulletin of mathematical biophysics*, 5(4), 115-133.
- McKerchar, A. I., & Delleur, J. W. (1974). Application of seasonal parametric linear stochastic models to monthly flow data. *Water Resources Research*, 10(2), 246-255.
- McLeod, A., Noakes, D., Hipel, K., & Thompstone, R. (1987). Combining Hydrologic Forecasts. *Journal of Water Resources Planning and Management*, 113(1), 29-41.
- McLeod, A. I., & Hipel, K. W. (1978). Simulation procedures for Box-Jenkins Models. *Water Resour. Res.*, 14(5), 969-975.
- McLeod, A. I., Hipel, K. W., & Lennox, W. C. (1977). Advances in Box-Jenkins modeling, 2, Applications. *Water Resources Research*, 13(3), 577-586.
- Mishra, A. K., & Desai, V. R. (2006). Drought forecasting using feed-forward recursive neural network. *Ecological Modelling*, 198(1-2), 127-138.
- Mondal, M. S., & Wasimi, S. A. (2006). Generating and forecasting monthly flows of the Ganges river with PAR model. *Journal of Hydrology*, 323(1-4), 41-56.
- Moss, M. E., Pearson, C. P., & McKerchar, A. I. (1994). The Southern Oscillation index as a predictor of the probability of low streamflows in New Zealand. *Water Resources Research*, 30(10), 2717-2723.
- Mujumdar, P. P., & Kumar, D. N. (1990). Stochastic models of streamflow: some case studies / Modèles stochastiques de l'écoulement—quelques études de cas. *Hydrological Sciences Journal*, 35(4), 395-410.
- Murphy, A. H. (1992). Climatology, Persistence, and Their Linear Combination as Standards of Reference in Skill Scores. *Weather and Forecasting*, 7(4), 692-698.
- Nayak, P. C., Sudheer, K. P., & Jain, S. K. (2007). Rainfall-runoff modeling through hybrid intelligent system. *Water Resources Research*, 43(7), W07415.

- NCDC. (2012). North Atlantic Oscillation (NAO). In National Climatic Data Center (NCDC), National Oceanic and Atmospheric Administration (NOAA). Retrieved February 1, 2014, from <http://www.ncdc.noaa.gov/teleconnections/nao.php>.
- Nigam, S., Barlow, M., & Berbery, E. H. (1999). Analysis links Pacific decadal variability to drought and streamflow in United States. *Eos, Transactions American Geophysical Union*, 80(51), 621-625.
- Noakes, D. J., McLeod, A. I., & Hipel, K. W. (1985). Forecasting monthly riverflow time series. *International Journal of Forecasting*, 1(2), 179-190.
- Oubeidillah, A. A. (2011). Oceanic-Atmospheric and Hydrologic Variability in Long Lead-Time Forecasting. *PhD diss., University of Tennessee*. http://trace.tennessee.edu/utk_graddiss/1111
- Palm, F. C., & Zellner, A. (1992). To combine or not to combine? issues of combining forecasts. *Journal of Forecasting*, 11(8), 687-701.
- Pekárová, P., Miklánek, P., & Pekár, J. (2003). Spatial and temporal runoff oscillation analysis of the main rivers of the world during the 19th–20th centuries. *Journal of Hydrology*, 274(1–4), 62-79.
- Perry, C. A. (2007). Evidence for a physical linkage between galactic cosmic rays and regional climate time series. *Advances in Space Research*, 40(3), 353-364.
- Piechota, T., Chiew, F., Dracup, J., & McMahon, T. (2001). Development of Exceedance Probability Streamflow Forecast. *Journal of Hydrologic Engineering*, 6(1), 20-28.
- Piechota, T. C., Chiew, F. H. S., Dracup, J. A., & McMahon, T. A. (1998). Seasonal streamflow forecasting in eastern Australia and the El Niño–Southern Oscillation. *Water Resources Research*, 34(11), 3035-3044.
- Piechota, T. C., Chiew, F. H. S., Dracup, J. A., & McMahon, T. A. (2001). Development of Exceedance Probability Streamflow Forecast. *Journal of Hydrologic Engineering*, 6(1), 20-28.
- Probst, J. L., & Tardy, Y. (1987). Long range streamflow and world continental runoff fluctuations since the beginning of this century. *Journal of Hydrology*, 94(3–4), 289-311.
- Prokoph, A., Adamowski, J., & Adamowski, K. (2012). Influence of the 11-year solar cycle on annual streamflow maxima in Southern Canada. *Journal of Hydrology*, 442–443(0), 55-62.
- Rajagopalan, B., Lall, U., & Zebiak, S. E. (2002). Categorical Climate Forecasts through Regularization and Optimal Combination of Multiple GCM Ensembles*. *Monthly Weather Review*, 130(7), 1792-1811.

- Raman, H., & Sunilkumar, N. (1995). Multivariate modelling of water resources time series using artificial neural networks. *Hydrological Sciences Journal*, 40(2), 145-163.
- Regonda, S. K., Rajagopalan, B., Clark, M., & Zagona, E. (2006). A multimodel ensemble forecast framework: Application to spring seasonal flows in the Gunnison River Basin. *Water Resources Research*, 42(9), W09404.
- Rogers, J. C., & Van Loon, H. (1979). The Seesaw in Winter Temperatures between Greenland and Northern Europe. Part II: Some Oceanic and Atmospheric Effects in Middle and High Latitudes. *Monthly Weather Review*, 107(5), 509-519.
- Rumelhart, D. E., Hintont, G. E., & Williams, R. J. (1986). Learning representations by back-propagating errors. *Nature*, 323(6088), 533-536.
- Salas, J. D. (1980). *Applied modeling of hydrologic series*. Littleton, Colo.: Water Resources Publications.
- Salas, J. D. (1993). Analysis and modeling of hydrologic time series. *Handbook of hydrology*, 19, 1-72.
- Salas, J. D., Delleur, J. W., Yevjevich, V. M., & Lane, W. L. (1980). *Applied modeling of hydrologic time series*. Littleton, Colo.: Water Resources Publications.
- Schultz, C. (2012). Warming set stage for deadly heat wave. *Eos Trans. AGU*, 93(15).
- Shamseldin, A. Y., & O'Connor, K. M. (1999). A real-time combination method for the outputs of different rainfall-runoff models. *Hydrological Sciences Journal*, 44(6), 895-912.
- Shamseldin, A. Y., O'Connor, K. M., & Liang, G. C. (1997). Methods for combining the outputs of different rainfall-runoff models. *Journal of Hydrology*, 197(1-4), 203-229.
- Sharma, A. (2000). Seasonal to interannual rainfall probabilistic forecasts for improved water supply management: Part 3 — A nonparametric probabilistic forecast model. *Journal of Hydrology*, 239(1-4), 249-258.
- Sharma, A., Tarboton, D. G., & Lall, U. (1997). Streamflow simulation: A nonparametric approach. *Water Resources Research*, 33(2), 291-308.
- Simpson, H. J., Cane, M. A., Herczeg, A. L., Zebiak, S. E., & Simpson, J. H. (1993). Annual river discharge in southeastern Australia related to El Nino-Southern Oscillation forecasts of sea surface temperatures. *Water Resour. Res.*, 29(11), 3671-3680.

- Sivakumar, B., Jayawardena, A. W., & Fernando, T. M. K. G. (2002). River flow forecasting: use of phase-space reconstruction and artificial neural networks approaches. *Journal of Hydrology*, 265(1–4), 225-245.
- Snedecor, G. W., & Cochran, W. G. (1967). *Statistical Methods* Iowa State University Press.
- Solomatine, D. P., & Dulal, K. N. (2003). Model trees as an alternative to neural networks in rainfall—runoff modelling. *Hydrological Sciences Journal*, 48(3), 399-411.
- Soltani, S., Modarres, R., & Eslamian, S. S. (2007). The use of time series modeling for the determination of rainfall climates of Iran. *International Journal of Climatology*, 27(6), 819-829.
- Sveinsson, O. G., Salas, J. D., Lane, W. L., & Frevert, D. K. (2007). Stochastic Analysis, Modeling, and Simulation (SAMS) Version 2007, User's Manual. *Computing Hydrology Laboratory, Department of Civil and Environmental Engineering, Colorado State University, Fort Collins, Colorado*.
- Svensmark, H., & Friis-Christensen, E. (1997). Variation of cosmic ray flux and global cloud coverage—a missing link in solar-climate relationships. *Journal of Atmospheric and Solar-Terrestrial Physics*, 59(11), 1225-1232.
- Tamea, S., Laio, F., & Ridolfi, L. (2005). Probabilistic nonlinear prediction of river flows. *Water Resources Research*, 41(9), W09421.
- Tao, P., & Delleur, J. (1976). Multistation, multiyear synthesis of hydrologic time series by disaggregation. *Water Resources Research*, 12(6), 1303-1312.
- Tao, P. C., & Delleur, J. W. (1976). Seasonal and nonseasonal ARMA models in hydrology. *Journal of the Hydraulics Division*, 102(10), 1541-1559.
- Tao, T., & Lennox, W. (1994). Evaluation of Streamflow Forecasting Models. In K. Hipel, A. I. McLeod, U. S. Panu & V. Singh (Eds.), *Stochastic and Statistical Methods in Hydrology and Environmental Engineering* (Vol. 10/3, pp. 77-85): Springer Netherlands.
- Taye, M. T., & Willems, P. (2012). Temporal variability of hydroclimatic extremes in the Blue Nile basin. *Water Resources Research*, 48(3), W03513.
- Thompstone, R. M., Hipel, K. W., & McLeod, A. I. (1985). Forecasting quarter-monthly riverflow. *JAWRA Journal of the American Water Resources Association*, 21(5), 731-741.
- Toth, E., & Brath, A. (2007). Multistep ahead streamflow forecasting: Role of calibration data in conceptual and neural network modeling. *Water Resources Research*, 43(11), W11405.

- Toth, E., Brath, A., & Montanari, A. (2000). Comparison of short-term rainfall prediction models for real-time flood forecasting. *Journal of Hydrology*, 239(1–4), 132-147.
- Trenberth, K. E. (2011). Changes in precipitation with climate change. *Climate Research*, 47(1), 123.
- van Loon, H., & Rogers, J. C. (1978). The Seesaw in Winter Temperatures between Greenland and Northern Europe. Part I: General Description. *Monthly Weather Review*, 106(3), 296-310.
- Vecchia, A. V. (1985). Periodic autoregressive-moving average (parma) modeling with applications to water resources. *JAWRA Journal of the American Water Resources Association*, 21(5), 721-730.
- Verdon, D. C., Wyatt, A. M., Kiem, A. S., & Franks, S. W. (2004). Multidecadal variability of rainfall and streamflow: Eastern Australia. *Water Resources Research*, 40(10), W10201.
- Viney, N. R., Bormann, H., Breuer, L., Bronstert, A., Croke, B. F. W., Frede, H., . . . Willems, P. (2009). Assessing the impact of land use change on hydrology by ensemble modelling (LUCHEM) II: Ensemble combinations and predictions. *Advances in Water Resources*, 32(2), 147-158.
- Vorosmarty, C. J., B. M. Fekete, and B. A. Tucker. (1998). Global River Discharge, 1807-1991, V. 1.1 (RivDIS). Data set. Available on-line [<http://www.daac.ornl.gov>] from Oak Ridge National Laboratory Distributed Active Archive Center, Oak Ridge, TN, U.S.A.
- Wang, G., & Eltahir, E. A. (1999). Use of ENSO information in medium-and long-range forecasting of the Nile floods. *Journal of Climate*, 12(6), 1726-1737.
- Wang, Q. J., & Robertson, D. E. (2011). Multisite probabilistic forecasting of seasonal flows for streams with zero value occurrences. *Water Resources Research*, 47(2), W02546.
- Wang, Q. J., Robertson, D. E., & Chiew, F. H. S. (2009). A Bayesian joint probability modeling approach for seasonal forecasting of streamflows at multiple sites. *Water Resources Research*, 45(5), W05407.
- Weigel, A. P., Liniger, M. A., & Appenzeller, C. (2007). The Discrete Brier and Ranked Probability Skill Scores. *Monthly Weather Review*, 135(1), 118-124.
- Whitaker, D. W., Wasimi, S. A., & Islam, S. (2001). The El Niño southern oscillation and long-range forecasting of flows in the Ganges. *International Journal of Climatology*, 21(1), 77-87.
- Winkler, R. L., & Clemen, R. T. (1992). Sensitivity of weights in combining forecasts. *Operations research*, 40(3), 609-614.

- WMO, (1986). *Intercomparison of models of snowmelt runoff*. Geneva, Switzerland: Secretariat of the World Meteorological Organization (WMO).
- World's Longest Rivers Map [Photograph]. (2007). World's Longest Rivers Map Quiz [Photograph]. In Ilike2learn.com. Retrieved April, 2012, from <http://www.ilike2learn.com/ilike2learn/Rivers/Longest%20Rivers.html>.
- Yin, Z.-Y. (1994). Moisture condition in the South-Eastern USA and teleconnection patterns. *International Journal of Climatology*, 14(9), 947-967.
- Zealand, C. M., Burn, D. H., & Simonovic, S. P. (1999). Short term streamflow forecasting using artificial neural networks. *Journal of Hydrology*, 214(1-4), 32-48.
- Zhongrui, W., Feng, S., & Maocang, T. (2003). A relationship between solar activity and frequency of natural disasters in China. *Advances in Atmospheric Sciences*, 20(6), 934-939.
- Ziehmman, C. (2000). Comparison of a single-model EPS with a multi-model ensemble consisting of a few operational models. *Tellus A*, 52(3), 280-299.

APPENDIX A

TABLES

Table A-1

Conditional probability of the Columbia Summer Flow, given the Rhine Spring Flow,
Based on Observations of 1906–1980

Rhine spring	Columbia summer Flow		
	Low	Average	High
Low	0.20	0.32	0.48
Average	0.25	0.33	0.42
High	0.54	0.31	0.15

Table A-2

Conditional probability of the Columbia Summer Flow, given the Winter SOI, Based on
Observations of 1906–1980

Winter SOI	Columbia summer flow		
	Low	Average	High
Low	0.52	0.28	0.20
Average	0.29	0.33	0.38
High	0.19	0.35	0.46

Table A-3

Conditional Probability of the Columbia Summer Flow, Given the Spring PDO, Based on Observations of 1906–1980

Spring PDO	Columbia summer flow		
	Low	Average	High
Low	0.16	0.20	0.64
Average	0.33	0.33	0.33
High	0.50	0.52	0.08

Table A-4

Conditional Probability of the Columbia Summer Flow, given the Summer NAO index, Based on Observations of 1906–1980

Summer NAO	Columbia summer flow		
	Low	Average	High
Low	0.17	0.29	0.54
Average	0.29	0.29	0.42
High	0.54	0.35	0.12

Table A-5

Conditional Probability of the Columbia Summer Flow, Given the Rhine Spring Season Flow, Summer NAO index, Based on Observations of 1906–1980

Predictors		Columbia summer flow		
summer NAO	Rhine spring flow	Low	Average	High
Low	Low	0.09	0.24	0.67
	Average	0.11	0.27	0.62
	High	0.34	0.34	0.32
Average	Low	0.17	0.27	0.57
	Average	0.21	0.28	0.51
	High	0.51	0.29	0.21
High	Low	0.39	0.40	0.20
	Average	0.45	0.39	0.16
	High	0.70	0.26	0.04

Table A-6

Conditional Probability of the Columbia Summer Flow, Given the Rhine Spring, Winter

SOI, Based on Observations of 1906–1980

Predictors		Columbia summer flow		
Winter SOI	Rhine spring flow	Low	Average	High
Low	Low	0.36	0.31	0.33
	Average	0.42	0.30	0.27
	High	0.71	0.22	0.08
Average	Low	0.17	0.31	0.52
	Average	0.21	0.33	0.46
	High	0.49	0.32	0.18
High	Low	0.10	0.30	0.60
	Average	0.14	0.32	0.54
	High	0.37	0.38	0.25

Table A-7

Conditional Probability of the Columbia Summer Flow, Given the Rhine Spring Flow,

Spring PDO, Based on Observations of 1906–1980

Predictors		Columbia summer flow		
Rhine spring flow	Spring PDO	Low	Average	High
Low	Low	0.08	0.16	0.76
	Average	0.20	0.32	0.48
	High	0.37	0.50	0.14
Average	Low	0.11	0.18	0.71
	Average	0.25	0.33	0.42
	High	0.42	0.47	0.11
High	Low	0.35	0.25	0.40
	Average	0.54	0.31	0.15
	High	0.65	0.32	0.03

Table A-8

Conditional Probability of the Columbia Summer Flow, Given the Summer NAO, Spring PDO, Based on Observations of 1906–1980

Predictors		Columbia summer flow		
Summer NAO	Spring PDO	Low	Average	High
Low	Low	0.06	0.14	0.80
	Average	0.17	0.29	0.54
	High	0.34	0.50	0.17
Average	Low	0.13	0.16	0.72
	Average	0.29	0.29	0.42
	High	0.48	0.41	0.11
High	Low	0.38	0.30	0.32
	Average	0.54	0.35	0.12
	High	0.63	0.34	0.02

Table A-9

Conditional Probability of the Columbia Summer Flow, Given the Winter SOI and Summer NAO, Based on Observations of 1906–1980

Predictors		Columbia summer flow		
Summer NAO	Winter SOI	Low	Average	High
Low	Low	0.31	0.30	0.39
	Average	0.14	0.28	0.58
	High	0.08	0.26	0.65
Average	Low	0.48	0.26	0.26
	Average	0.25	0.29	0.46
	High	0.16	0.29	0.55
High	Low	0.70	0.24	0.06
	Average	0.50	0.37	0.14
	High	0.37	0.43	0.19

Table A-10

Conditional Probability of the Columbia Summer Flow, Given the Yangtze Winter Flow,

Summer NAO index, Based on Observations of 1906–1980

Predictors		Columbia summer flow		
Summer NAO	Yangtze winter flow	Low	Average	High
Low	Low	0.31	0.41	0.27
	Average	0.11	0.25	0.64
	High	0.09	0.19	0.71
Average	Low	0.48	0.36	0.16
	Average	0.22	0.30	0.48
	High	0.20	0.24	0.56
High	Low	0.61	0.35	0.04
	Average	0.41	0.43	0.16
	High	0.42	0.37	0.21

Table A-11

Conditional Probability of the Columbia Summer Flow, Given the Spring PDO, Summer NAO, Winter SOI, Based on Observations of 1906–1980

Predictors			Columbia summer flow		
Winter SOI	Summer NAO	Spring PDO	Low	Average	High
Low	Low	Low	0.18	0.27	0.54
		Average	0.23	0.29	0.48
		High	0.53	0.28	0.19
	Average	Low	0.31	0.27	0.41
		Average	0.38	0.27	0.35
		High	0.68	0.21	0.11
	High	Low	0.57	0.32	0.11
		Average	0.63	0.29	0.09
		High	0.82	0.16	0.02
Average	Low	Low	0.07	0.22	0.70
		Average	0.23	0.29	0.48
		High	0.30	0.34	0.36
	Average	Low	0.14	0.25	0.61
		Average	0.18	0.27	0.55
		High	0.46	0.30	0.24
	High	Low	0.35	0.41	0.23
		Average	0.41	0.40	0.19
		High	0.67	0.28	0.05
High	Low	Low	0.04	0.20	0.76
		Average	0.05	0.23	0.71
		High	0.20	0.36	0.44
	Average	Low	0.08	0.24	0.68
		Average	0.11	0.26	0.63
		High	0.33	0.34	0.33
	High	Low	0.24	0.45	0.30
		Average	0.29	0.45	0.25
		High	0.55	0.37	0.08

Table A-12Conditional Probability of the Columbia Summer Flow, Given the Rhine Spring Flow,Summer NAO, and Winter SOI, Based on Observations of 1906–1980

Predictors			Columbia summer flow		
Winter SOI	Summer NAO	Rhine spring flow	Low	Average	High
Low	Low	Low	0.18	0.27	0.54
		Average	0.23	0.29	0.48
		High	0.53	0.28	0.19
	Average	Low	0.31	0.27	0.41
		Average	0.38	0.27	0.35
		High	0.68	0.21	0.11
	High	Low	0.57	0.32	0.11
		Average	0.63	0.29	0.09
		High	0.82	0.16	0.02
Average	Low	Low	0.07	0.22	0.70
		Average	0.23	0.29	0.48
		High	0.30	0.34	0.36
	Average	Low	0.14	0.25	0.61
		Average	0.18	0.27	0.55
		High	0.46	0.30	0.24
	High	Low	0.35	0.41	0.23
		Average	0.41	0.40	0.19
		High	0.67	0.28	0.05
High	Low	Low	0.04	0.20	0.76
		Average	0.05	0.23	0.71
		High	0.20	0.36	0.44
	Average	Low	0.08	0.24	0.68
		Average	0.11	0.26	0.63
		High	0.33	0.34	0.33
	High	Low	0.24	0.45	0.30
		Average	0.29	0.45	0.25
		High	0.55	0.37	0.08

Table A-13Conditional Forecasting of the Columbia River Summer Flow Based on Rhine SpringFlow and Comparison with the Observed Flow (1981–1999)

Forecasting year	Observed flow category	Rhine spring flow category	Conditional probability of flow in the Columbia (%)			Predicted flow category	Remarks
			Low	Average	High		
1981	Average	High	54%	31%	15%	Low	Outside category
1982	High	Average	25%	33%	42%	High	Ok
1983	Average	High	54%	31%	15%	Low	Outside category
1984	Average	Average	25%	33%	42%	High	Outside category
1985	Low	Average	25%	33%	42%	High	Outside category
1986	Low	High	54%	31%	15%	Low	Ok
1987	Low	High	54%	31%	15%	Low	Ok
1988	Low	High	54%	31%	15%	Low	Ok
1989	Low	Average	25%	33%	42%	High	Outside category
1990	Average	Low	20%	32%	48%	High	Outside category
1991	Average	Low	20%	32%	48%	High	Outside category
1992	Low	Average	25%	33%	42%	High	Outside category
1993	Low	Low	20%	32%	48%	High	Outside category
1994	Low	High	54%	31%	15%	Low	Ok
1995	Average	High	54%	31%	15%	Low	Outside category
1996	High	Low	20%	32%	48%	High	Ok
1997	High	Average	25%	33%	42%	High	Ok
1998	Average	Average	25%	33%	42%	High	Outside category
1999	High	High	54%	31%	15%	Low	Outside category

Table A-14Conditional Forecasting of the Columbia River Summer Flow, Based on Winter SOI andComparison with the Observed Flow (1981–1999)

Forecasting year	Observed flow category	Winter SOI category	Conditional probability of flow in the Columbia (%)			Predicted flow category	Remarks
			Low	Average	High		
1981	Average	Average	29%	33%	38%	High	Outside category
1982	High	High	19%	35%	46%	High	Ok
1983	Average	Low	52%	28%	20%	Low	Outside category
1984	Average	Average	29%	33%	38%	High	Outside category
1985	Low	Average	29%	33%	38%	High	Outside category
1986	Low	Average	29%	33%	38%	High	Outside category
1987	Low	Low	52%	28%	20%	Low	Ok
1988	Low	Low	52%	28%	20%	Low	Ok
1989	Low	High	19%	35%	46%	High	Outside category
1990	Average	Low	52%	28%	20%	Low	Outside category
1991	Average	Average	29%	33%	38%	High	Outside category
1992	Low	Low	52%	28%	20%	Low	Ok
1993	Low	Low	52%	28%	20%	Low	Ok
1994	Low	Average	29%	33%	38%	High	Outside category
1995	Average	Low	52%	28%	20%	Low	Outside category
1996	High	Average	29%	33%	38%	High	Ok
1997	High	High	19%	35%	46%	High	Ok
1998	Average	Low	52%	28%	20%	Low	Outside category
1999	High	High	19%	35%	46%	High	Ok

Table A-15Conditional Forecasting of the Columbia River Summer Flow, Based on Spring PDO andComparison with the Observed Flow (1981–1999)

Forecasting year	Observed flow category	Spring PDO category	Conditional probability of flow in the Columbia (%)			Predicted flow category	Remarks
			Low	Average	High		
1981	Average	High	50%	42%	8%	Low	Outside category
1982	High	Average	33%	33%	33%	Low	Outside category
1983	Average	High	50%	42%	8%	Low	Outside category
1984	Average	High	50%	42%	8%	Low	Outside category
1985	Low	High	50%	42%	8%	Low	Ok
1986	Low	High	50%	42%	8%	Low	Ok
1987	Low	High	50%	42%	8%	Low	Ok
1988	Low	High	50%	42%	8%	Low	Ok
1989	Low	Average	33%	33%	33%	Low	Ok
1990	Average	High	50%	42%	8%	Low	Outside category
1991	Average	Average	33%	33%	33%	Low	Outside category
1992	Low	High	50%	42%	8%	Low	Ok
1993	Low	High	50%	42%	8%	Low	Ok
1994	Low	High	50%	42%	8%	Low	Ok
1995	Average	High	50%	42%	8%	Low	Outside category
1996	High	High	50%	42%	8%	Low	Outside category
1997	High	High	50%	42%	8%	Low	Outside category
1998	Average	High	50%	42%	8%	Low	Outside category
1999	High	Average	33%	33%	33%	Low	Outside category

Table A-16

Conditional Forecasting of the Columbia River Summer Flow, Based on Summer NAO and Comparison with the Observed Flow (1981–1999)

Forecasting year	Observed flow category	Summer NAO category	Conditional probability of flow in the Columbia (%)			Predicted flow category	Remarks
			Low	Average	High		
1981	Average	Average	29%	29%	42%	Low	Outside category
1982	High	High	54%	35%	12%	Low	Outside category
1983	Average	Low	17%	29%	54%	High	Outside category
1984	Average	Average	29%	29%	42%	Low	Outside category
1985	Low	High	54%	35%	12%	Low	Ok
1986	Low	High	54%	35%	12%	Low	Ok
1987	Low	Low	17%	29%	54%	High	Outside category
1988	Low	Low	17%	29%	54%	High	Outside category
1989	Low	Average	29%	29%	42%	Low	Ok
1990	Average	High	54%	35%	12%	Low	Outside category
1991	Average	High	54%	35%	12%	Low	Outside category
1992	Low	High	54%	35%	12%	Low	Ok
1993	Low	High	54%	35%	12%	Low	Ok
1994	Low	High	54%	35%	12%	Low	Ok
1995	Average	High	54%	35%	12%	Low	Outside category
1996	High	Low	17%	29%	54%	High	Ok
1997	High	High	54%	35%	12%	Low	Outside category
1998	Average	Low	17%	29%	54%	High	Outside category
1999	High	Average	29%	29%	42%	Low	Outside category

Table A-17**Conditional Forecasting of the Columbia River Summer Flow, Based on Rhine Spring****Flow and Winter SOI, and Comparison with the Observed Flow (1981–1999)**

Forecasting year	Observed flow category	Winter SOI category	Rhine spring category	Conditional probability of flow in the Columbia (%)			Predicted flow category	Remarks
				Low	Average	High		
1981	Average	Average	High	49%	32%	18%	Low	Outside category
1982	High	High	Average	14%	32%	54%	High	Ok
1983	Average	Low	High	71%	22%	8%	Low	Outside category
1984	Average	Average	Average	21%	33%	46%	High	Outside category
1985	Low	Average	Average	21%	33%	46%	High	Outside category
1986	Low	Average	High	49%	32%	18%	Low	Ok
1987	Low	Low	High	71%	22%	8%	Low	Ok
1988	Low	Low	High	71%	22%	8%	Low	Ok
1989	Low	High	Average	14%	32%	54%	High	Outside category
1990	Average	Low	Low	36%	31%	33%	Low	Outside category
1991	Average	Average	Low	17%	31%	52%	High	Outside category
1992	Low	Low	Average	42%	30%	27%	Low	Ok
1993	Low	Low	Low	36%	31%	33%	Low	Ok
1994	Low	Average	High	49%	32%	18%	Low	Ok
1995	Average	Low	High	71%	22%	8%	Low	Outside category
1996	High	Average	Low	17%	31%	52%	High	Ok
1997	High	High	Average	14%	32%	54%	High	Ok
1998	Average	Low	Average	42%	30%	27%	Low	Outside category
1999	High	High	High	37%	38%	25%	Average	Outside category

Table A-18

Conditional Forecasting of the Columbia River Summer Flow, Based on Rhine Spring
and Summer NAO, and Comparison with the Observed Flow (1981–1999)

Forecasting year	Observed flow category	Summer NAO category	Rhine spring flow Category	Conditional probability of flow in the Columbia (%)			Predicted flow category	Remarks
				Low	Average	High		
1981	Average	Average	High	51%	29%	21%	Low	Outside category
1982	High	High	Average	45%	39%	16%	Low	Outside category
1983	Average	Low	High	34%	34%	32%	Low	Outside category
1984	Average	Average	Average	21%	28%	51%	High	Outside category
1985	Low	High	Average	45%	39%	16%	Low	Ok
1986	Low	High	High	70%	26%	4%	Low	Ok
1987	Low	Low	High	34%	34%	32%	Low	Ok
1988	Low	Low	High	34%	34%	32%	Low	Ok
1989	Low	Average	Average	21%	28%	51%	High	Outside category
1990	Average	High	Low	39%	40%	20%	Average	Ok
1991	Average	High	Low	39%	40%	20%	Average	Ok
1992	Low	High	Average	45%	39%	16%	Low	Ok
1993	Low	High	Low	39%	40%	20%	Average	Outside category
1994	Low	High	High	70%	26%	4%	Low	Ok
1995	Average	High	High	70%	26%	4%	Low	Outside category
1996	High	Low	Low	9%	24%	67%	High	Ok
1997	High	High	Average	45%	39%	16%	Low	Outside category
1998	Average	Low	Average	11%	27%	62%	High	Outside category
1999	High	Average	High	51%	29%	21%	Low	Outside category

Table A-19**Conditional Forecasting of the Columbia River Summer Flow, Based on Spring PDO and****Summer NAO, and Comparison with the Observed Flow (1981–1999)**

Forecasting year	Observed flow category	Summer NAO category	Spring PDO category	Conditional probability of flow in the Columbia (%)			Predicted flow category	Remarks
				Low	Average	High		
1981	Average	Average	High	48%	41%	11%	Low	Outside category
1982	High	High	Average	54%	35%	12%	Low	Outside category
1983	Average	Low	High	34%	50%	17%	Average	Ok
1984	Average	Average	High	48%	41%	11%	Low	Outside category
1985	Low	High	High	63%	34%	2%	Low	Ok
1986	Low	High	High	63%	34%	2%	Low	Ok
1987	Low	Low	High	34%	50%	17%	Average	Outside category
1988	Low	Low	High	34%	50%	17%	Average	Outside category
1989	Low	Average	Average	29%	29%	42%	Low	Ok
1990	Average	High	High	63%	34%	2%	Low	Outside category
1991	Average	High	Average	54%	35%	12%	Low	Outside category
1992	Low	High	High	63%	34%	2%	Low	Ok
1993	Low	High	High	63%	34%	2%	Low	Ok
1994	Low	High	High	63%	34%	2%	Low	Ok
1995	Average	High	High	63%	34%	2%	Low	Outside category
1996	High	Low	High	34%	50%	17%	Average	Outside category
1997	High	High	High	63%	34%	2%	Low	Outside category
1998	Average	Low	High	34%	50%	17%	Average	Ok
1999	High	Average	Average	29%	29%	42%	Low	Outside category

Table A-20

Conditional forecasting of the Columbia River summer flow, based on winter SOI and summer NAO index, and comparison with the observed flow (1981–1999)

Forecasting Year	Observed flow category	Summer NAO category	Winter SOI category	Conditional probability of flow in the Columbia (%)			Predicted flow category	Remarks
				Low	Average	High		
1981	Average	Average	Average	25%	29%	46%	High	Outside category
1982	High	High	High	37%	43%	19%	Average	Outside category
1983	Average	Low	Low	31%	30%	39%	Low	Outside category
1984	Average	Average	Average	25%	29%	46%	High	Outside category
1985	Low	High	Average	50%	37%	14%	Low	Ok
1986	Low	High	Average	50%	37%	14%	Low	Ok
1987	Low	Low	Low	31%	30%	39%	Low	Ok
1988	Low	Low	Low	31%	30%	39%	Low	Ok
1989	Low	Average	High	16%	29%	55%	High	Outside category
1990	Average	High	Low	70%	24%	6%	Low	Outside category
1991	Average	High	Average	50%	37%	14%	Low	Outside category
1992	Low	High	Low	70%	24%	6%	Low	Ok
1993	Low	High	Low	70%	24%	6%	Low	Ok
1994	Low	High	Average	50%	37%	14%	Low	Ok
1995	Average	High	Low	70%	24%	6%	Low	Outside category
1996	High	Low	Average	14%	28%	58%	High	Ok
1997	High	High	High	37%	43%	19%	Average	Outside category
1998	Average	Low	Low	31%	30%	39%	Low	Outside category
1999	High	Average	High	16%	29%	55%	High	Ok

Table A-21

Conditional Forecasting of the Columbia River Summer Flow, Based on Yangtze Winter
and Summer NAO Index, and Comparison with the Observed Flow (1981–1999)

Forecasting Year	Observed flow category	Summer NAO category	Yangtze winter category	Conditional probability of flow in the Columbia (%)			Predicted flow category	Remarks
				Low	Average	High		
1981	Average	Average	Low	45%	23%	32%	Low	Outside category
1982	High	High	Low	70%	23%	8%	Low	Outside category
1983	Average	Low	Average	20%	31%	50%	High	Outside category
1984	Average	Average	High	10%	32%	59%	High	Outside category
1985	Low	High	Low	70%	23%	8%	Low	Ok
1986	Low	High	Average	58%	33%	10%	Low	Ok
1987	Low	Low	Low	29%	25%	46%	Low	Ok
1988	Low	Low	Low	29%	25%	46%	Low	Ok
1989	Low	Average	Average	33%	30%	37%	Low	Ok
1990	Average	High	Average	58%	33%	10%	Low	Outside category
1991	Average	High	Average	58%	33%	10%	Low	Outside category
1992	Low	High	Average	58%	33%	10%	Low	Ok
1993	Low	High	Average	58%	33%	10%	Low	Ok
1994	Low	High	Average	58%	33%	10%	Low	Ok
1995	Average	High	Average	58%	33%	10%	Low	Outside category
1996	High	Low	Average	20%	31%	50%	High	Ok
1997	High	High	Average	58%	33%	10%	Low	Outside category
1998	Average	Low	Average	20%	31%	50%	High	Outside category
1999	High	Average	High	10%	32%	59%	High	Ok

Table A-22

Conditional Forecasting of the Columbia River Summer Flow, Based on Summer NAO, Yangtze Winter Flow, and Rhine Spring Flow, and Comparison with the Observed Flow (1981–1999)

Forecasting Year	Obs. flow cat.	Rhine spring	Yangtze winter cat.	Summer NAO cat.	Conditional probability of flow in the Columbia (%)			Pred. flow cat.	Remarks
					Low	Avg.	High		
1981	Avg.	High	Low	Avg.	67%	19%	14%	Low	Outside category
1982	High	Avg.	Low	High	62%	27%	11%	Low	Outside category
1983	Avg.	High	Avg.	Low	38%	34%	28%	Low	Outside category
1984	Avg.	Avg.	High	Avg.	6%	28%	65%	High	Outside category
1985	Low	Avg.	Low	High	62%	27%	11%	Low	Ok
1986	Low	High	Avg.	High	73%	24%	3%	Low	Ok
1987	Low	High	Low	Low	51%	25%	24%	Low	Ok
1988	Low	High	Low	Low	51%	25%	24%	Low	Ok
1989	Low	Avg.	Avg.	Avg.	25%	29%	46%	High	Outside category
1990	Avg.	Low	Avg.	High	43%	40%	17%	Low	Outside category
1991	Avg.	Low	Avg.	High	43%	40%	17%	Low	Outside category
1992	Low	Avg.	Avg.	High	49%	37%	14%	Low	Ok
1993	Low	Low	Avg.	High	43%	40%	17%	Low	Ok
1994	Low	High	Avg.	High	73%	24%	3%	Low	Ok
1995	Avg.	High	Avg.	High	73%	24%	3%	Low	Outside category
1996	High	Low	Avg.	Low	10%	26%	63%	High	Ok
1997	High	Avg.	Avg.	High	49%	37%	14%	Low	Outside category
1998	Avg.	Avg.	Avg.	Low	14%	28%	58%	High	Outside category
1999	High	High	High	Avg.	21%	41%	38%	Avg.	Outside category

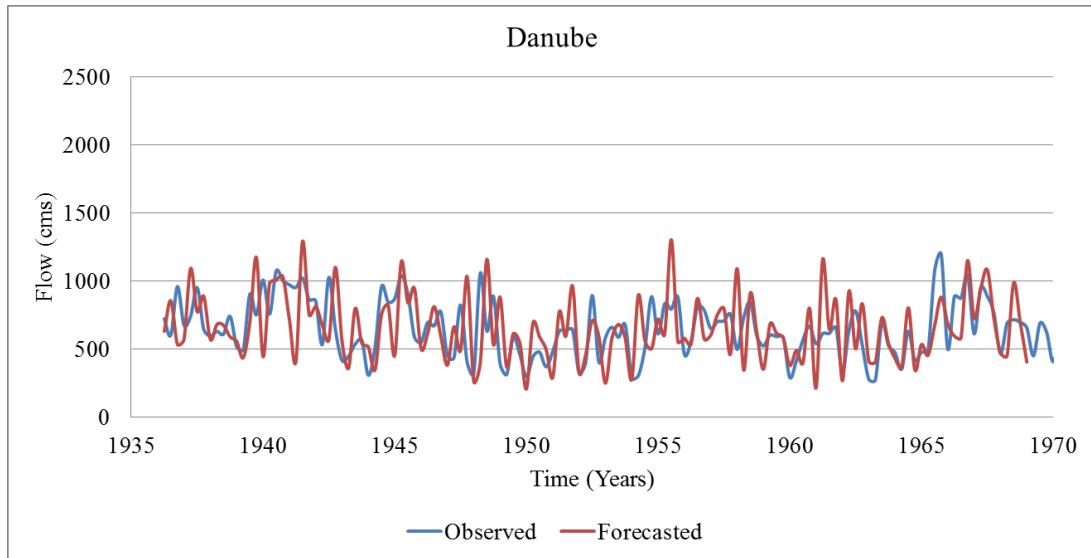
Table A-23

Conditional forecasting of the Columbia River summer flow, based on spring PDO, summer NAO, and winter SOI indices, and comparison with the observed flow (1981–1999)

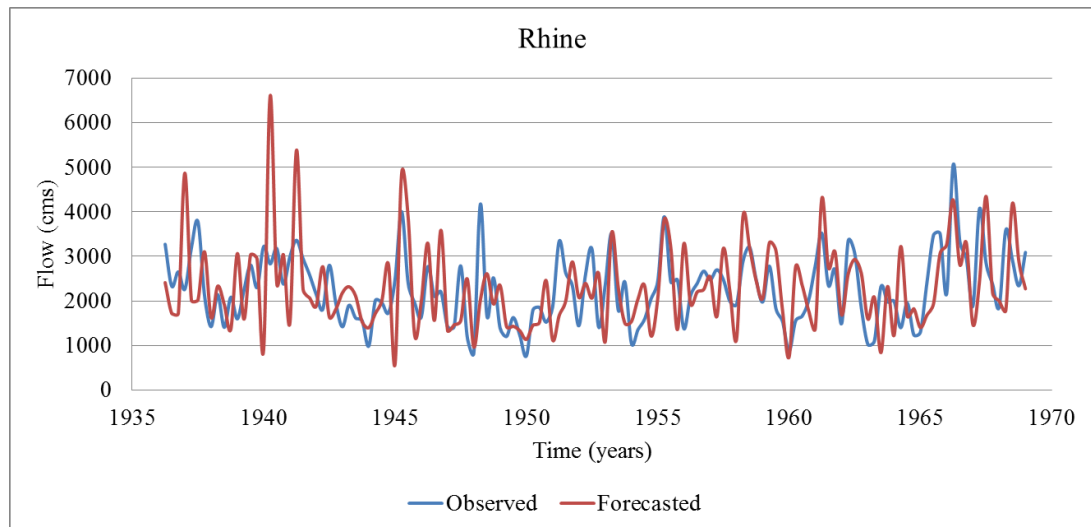
Forecasting Year	Obs. flow cat.	Winter SOI cat.	Summer NAO cat.	Spring PDO cat.	Conditional probability of flow in the Columbia (%)			Pred. flow cat.	Remarks
					Low	Avg.	High		
1981	Avg.	Avg.	Avg.	High	44%	43%	13%	Low	Outside category
1982	High	High	High	Avg.	37%	43%	19%	Avg.	Outside category
1983	Avg.	Low	Low	High	50%	40%	10%	Low	Outside category
1984	Avg.	Avg.	Avg.	High	44%	43%	13%	Low	Outside category
1985	Low	Avg.	High	High	60%	37%	3%	Low	Ok
1986	Low	Avg.	High	High	60%	37%	3%	Low	Ok
1987	Low	Low	Low	High	50%	40%	10%	Low	Ok
1988	Low	Low	Low	High	50%	40%	10%	Low	Ok
1989	Low	High	Avg.	Avg.	16%	29%	55%	High	Outside category
1990	Avg.	Low	High	High	77%	22%	1%	Low	Outside category
1991	Avg.	Avg.	High	Avg.	50%	37%	14%	Low	Outside category
1992	Low	Low	High	High	77%	22%	1%	Low	Ok
1993	Low	Low	High	High	77%	22%	1%	Low	Ok
1994	Low	Avg.	High	High	60%	37%	3%	Low	Ok
1995	Avg.	Low	High	High	77%	22%	1%	Low	Outside category
1996	High	Avg.	Low	High	30%	51%	19%	Avg.	Outside category
1997	High	High	High	High	49%	48%	4%	Low	Outside category
1998	Avg.	Low	Low	High	50%	40%	10%	Low	Outside category
1999	High	High	Avg.	Avg.	16%	29%	55%	High	Ok

APPENDIX B

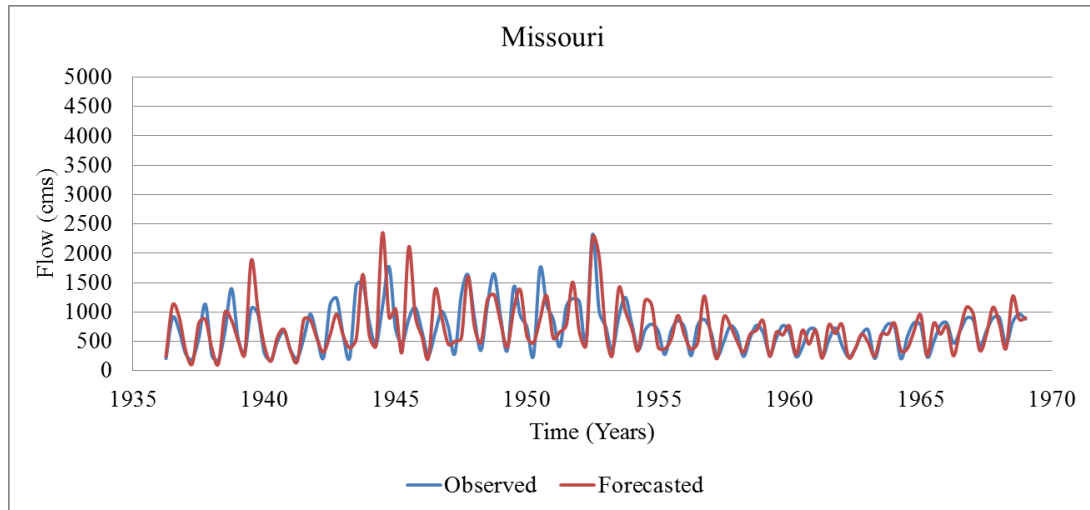
FIGURES



(a)

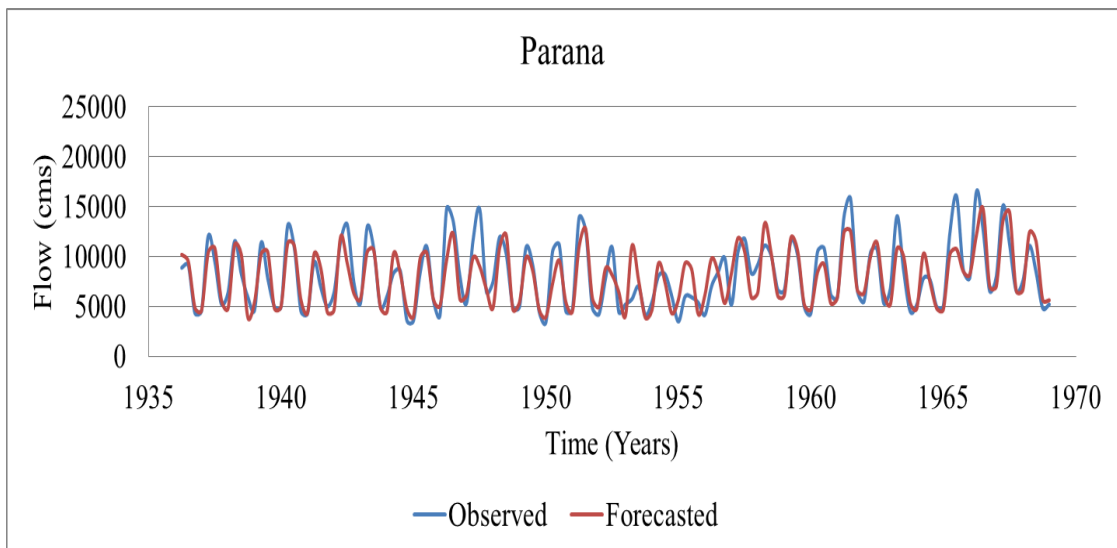


(b)

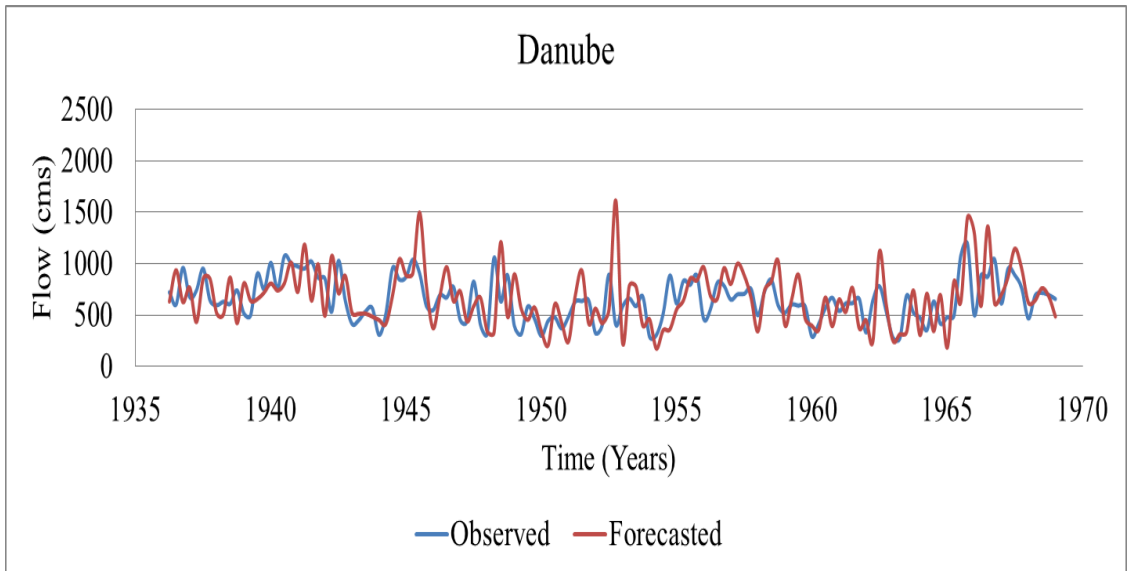


(c)

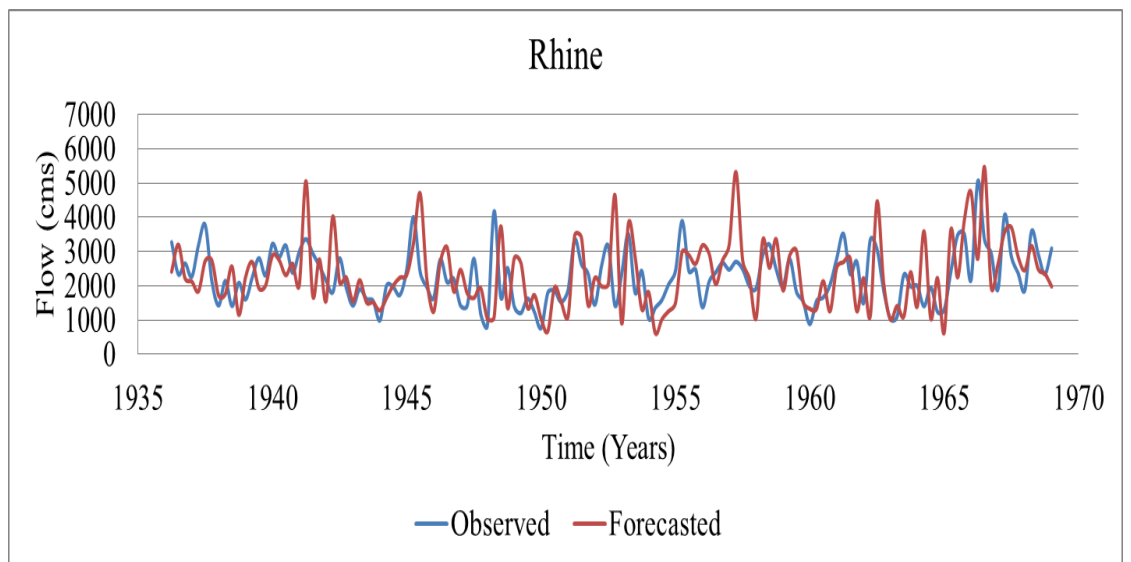
Figure B-1. Calibrated lead-1 seasonal flow forecasting of the rivers: (a) Danube; (b) Rhine; and (c) Missouri, using the univariate ARMA(1,1) model.



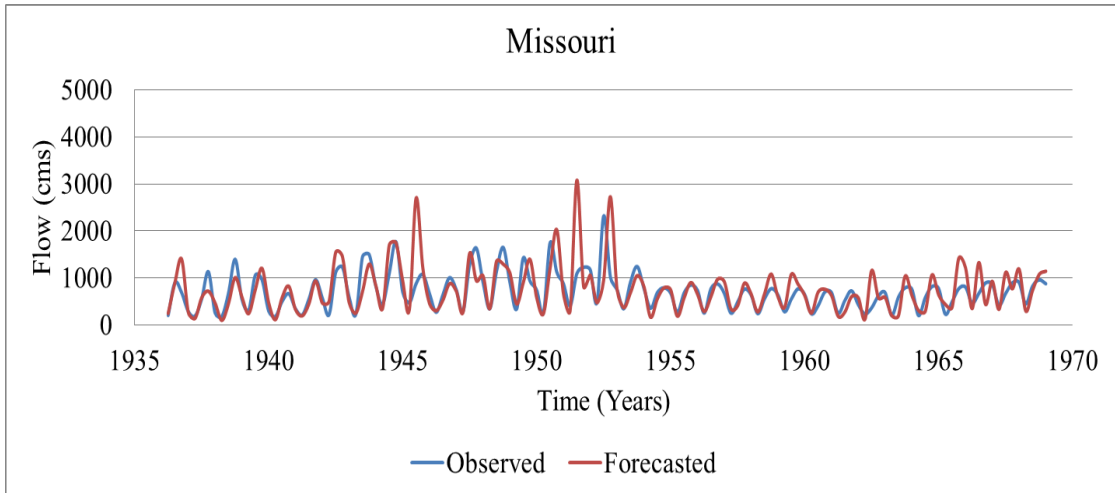
(a)



(b)

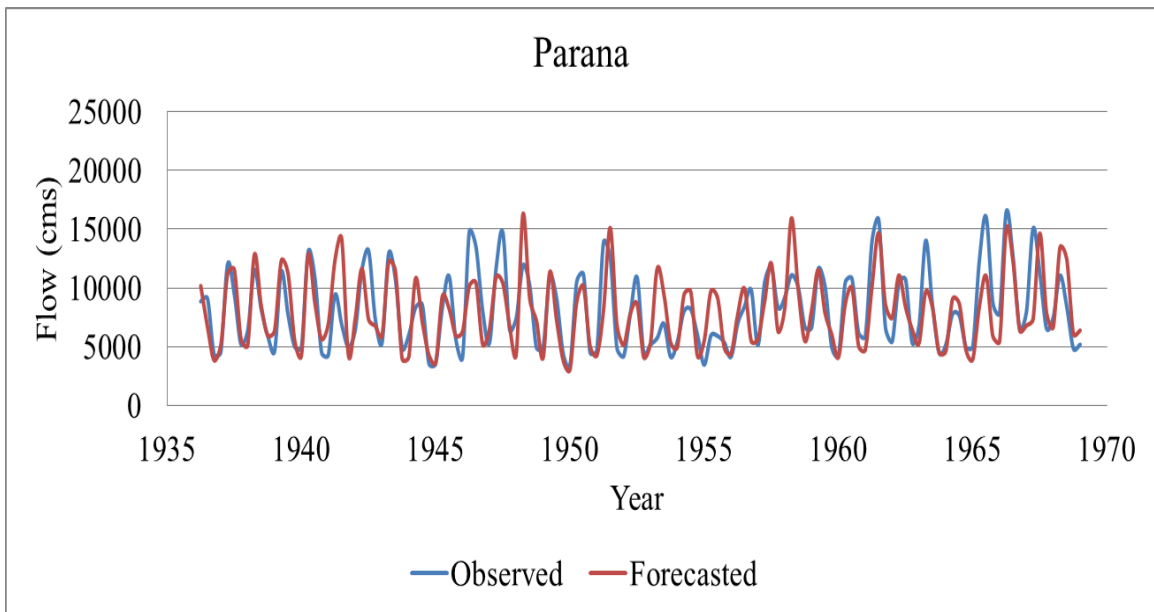


(c)

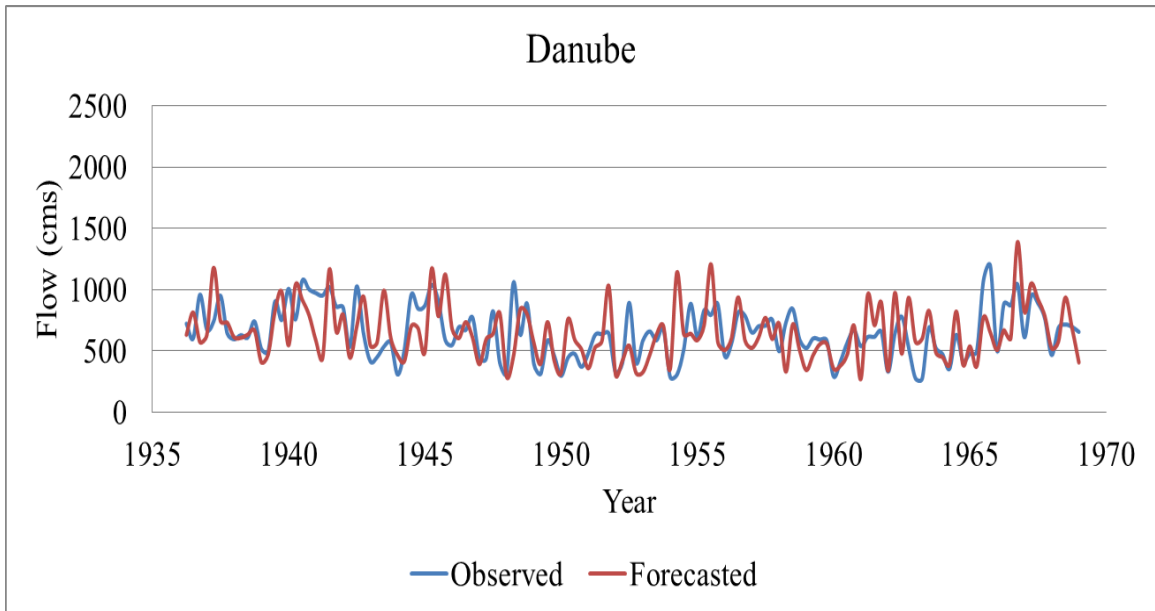


(d)

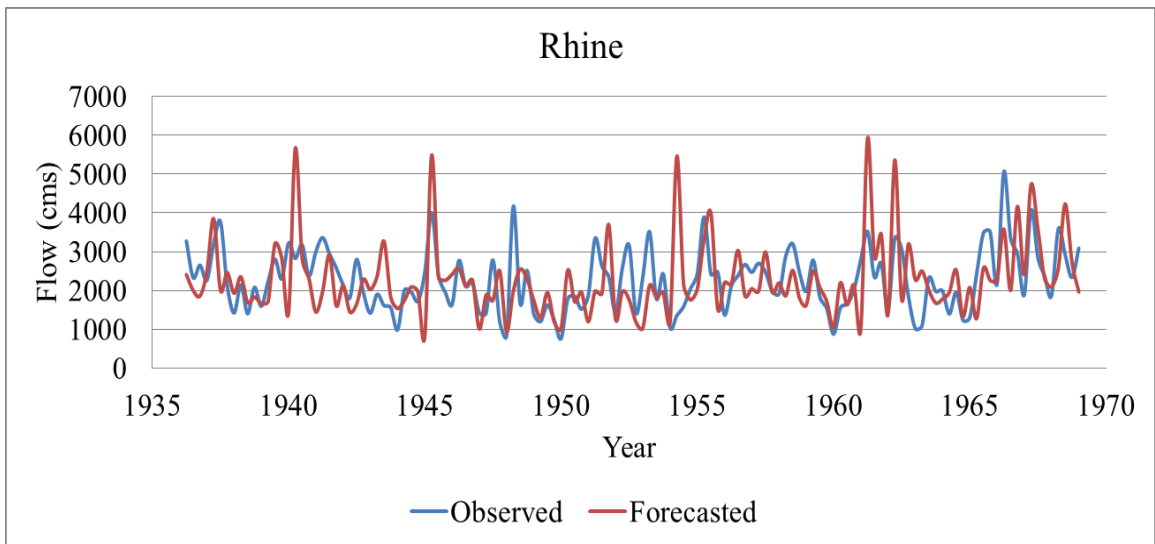
Figure B-2. Calibrated lead-1 seasonal forecasts of the rivers: (a) Parana; (b) Danube; (c) Rhine; and (d) Missouri, using the MAR(3) model incorporating 4 rivers and SOI.



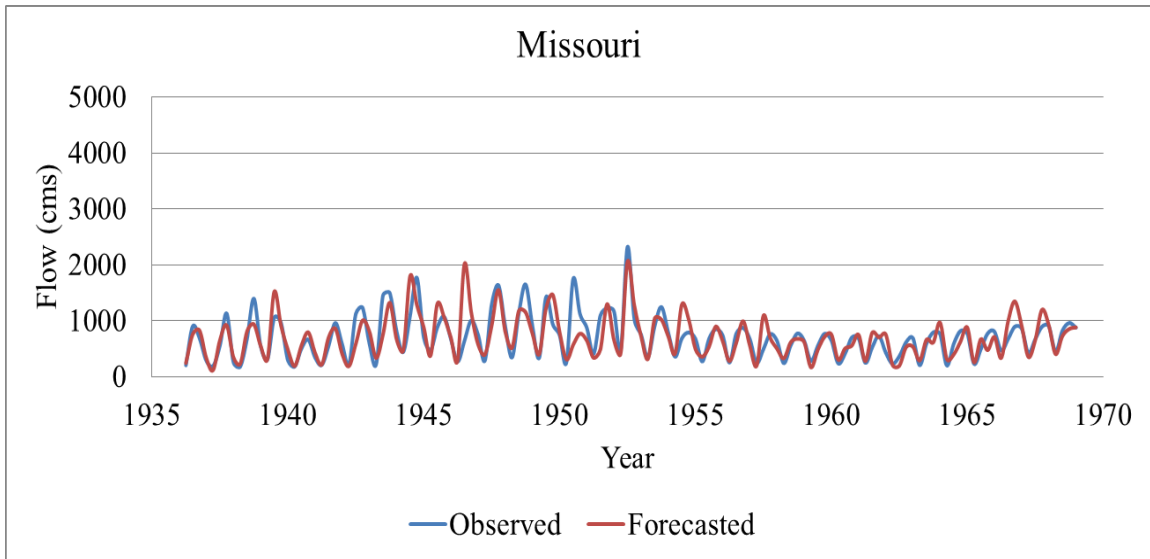
(a)



(b)

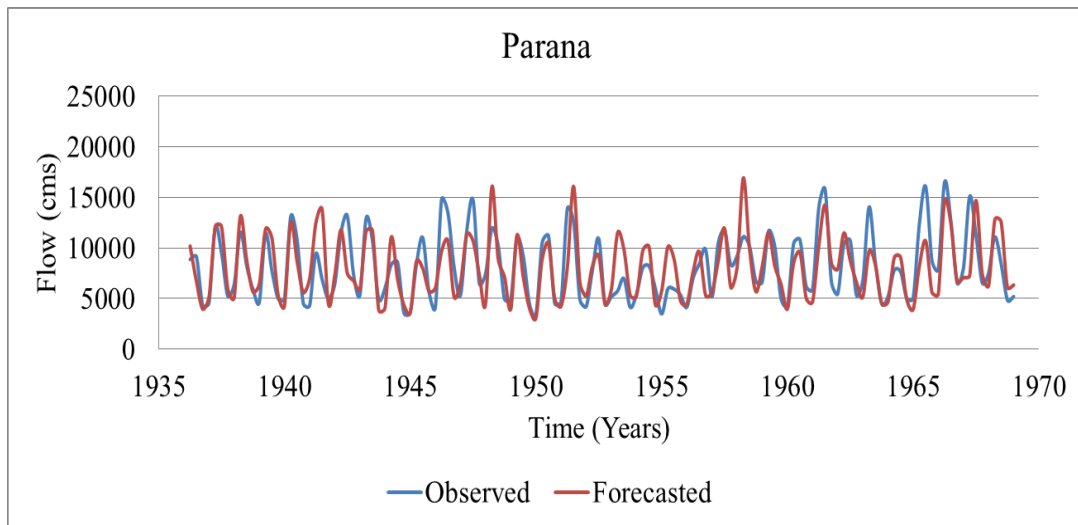


(c)

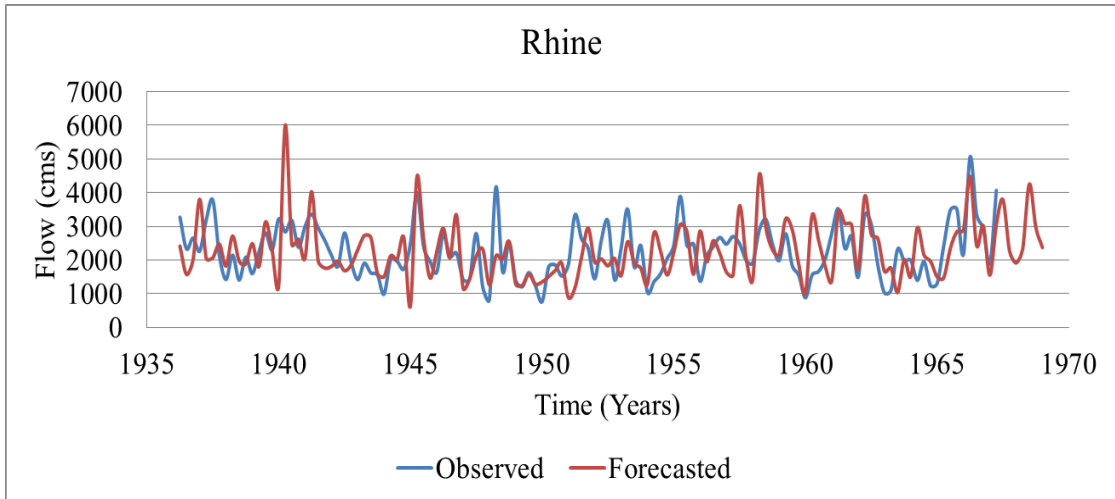


(d)

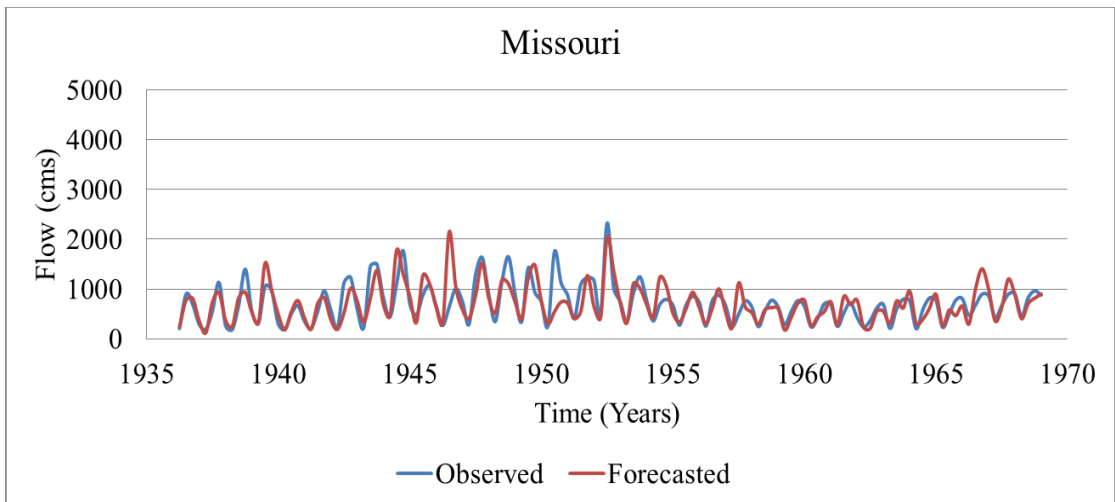
Figure B-3. Calibrated lead-1 seasonal forecasts of the rivers: (a) Parana; (b) Danube; (c) Rhine; and (d) Missouri, using the MAR(3) model incorporating 4 rivers, SOI, and SSN.



(a)

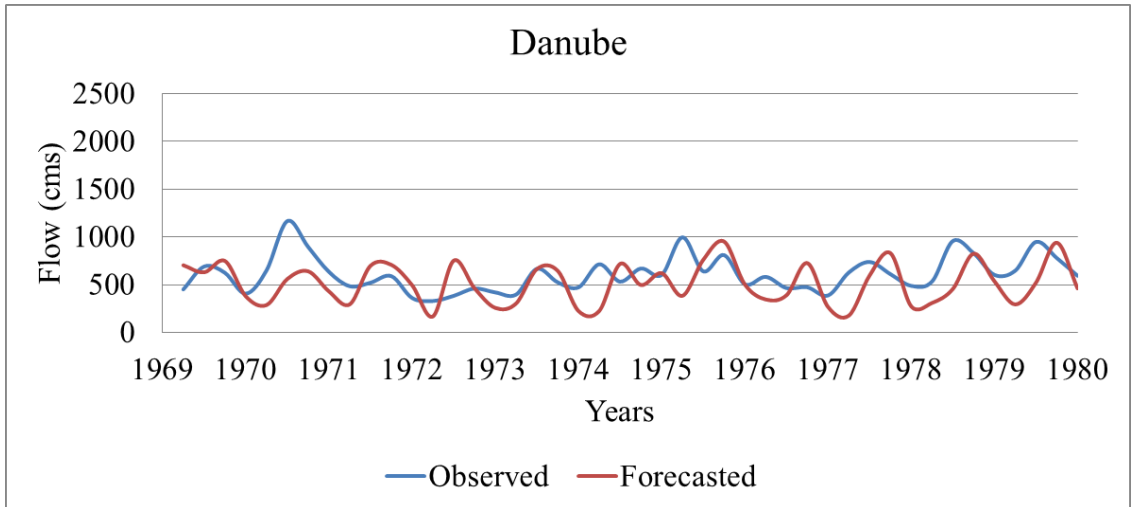


(b)

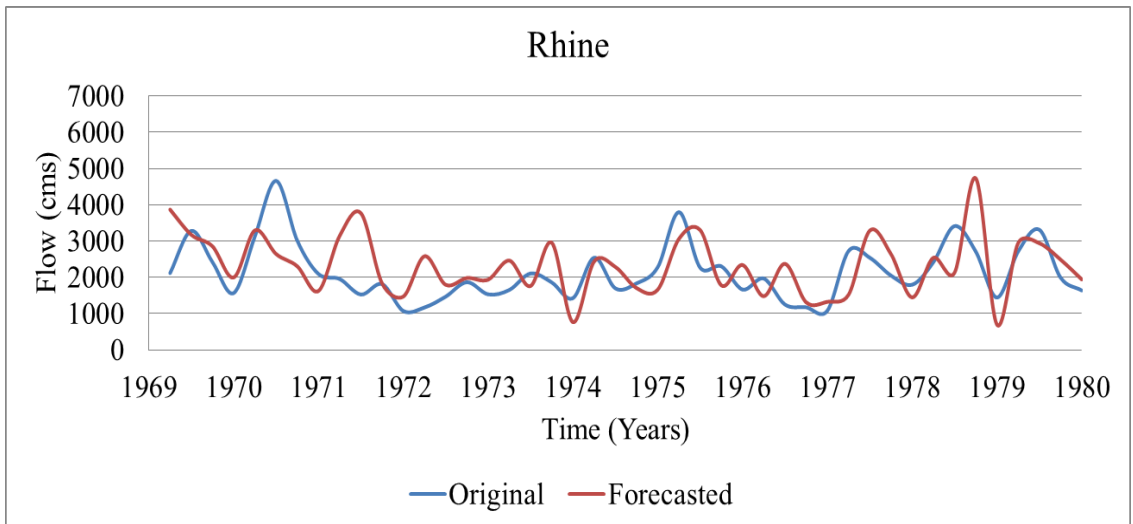


(c)

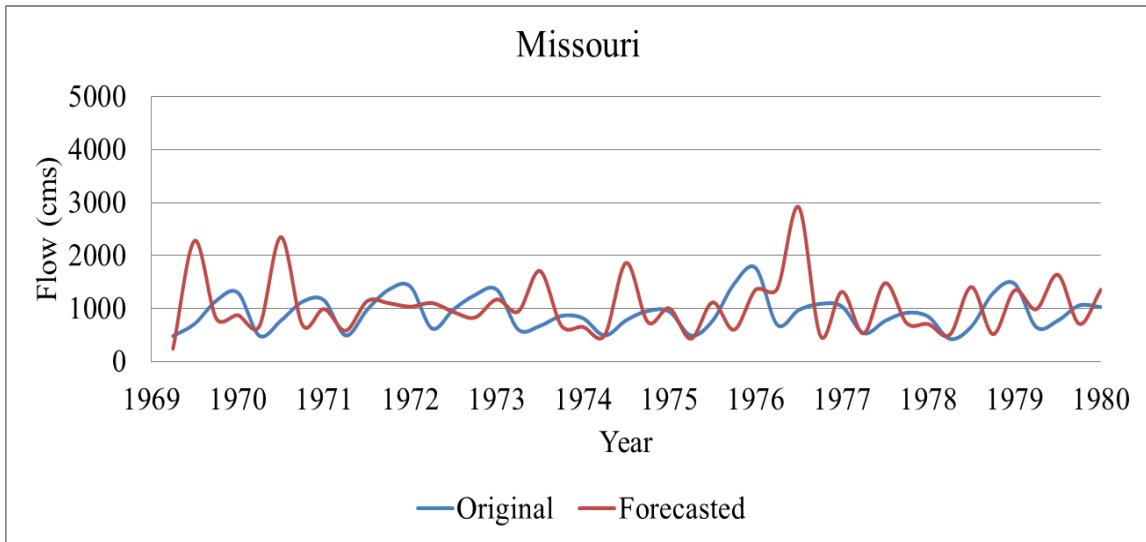
Figure B-4. Calibrated lead-1 seasonal forecasts of the rivers: (a) Parana; (b) Rhine; and (c) Missouri, using the MAR(3) model incorporating 3 rivers and SSN.



(a)

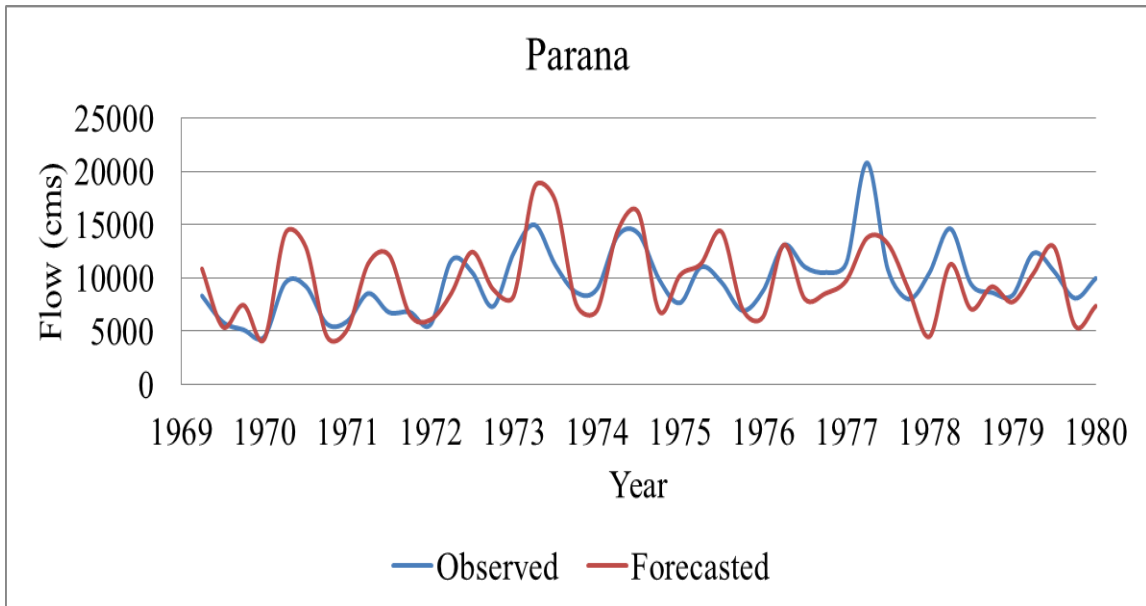


(b)

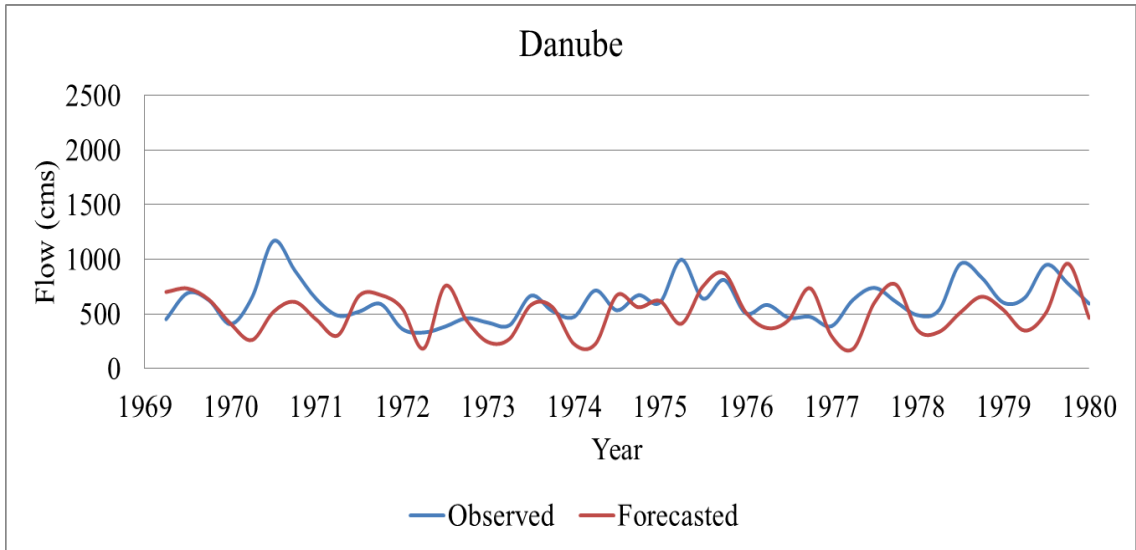


(c)

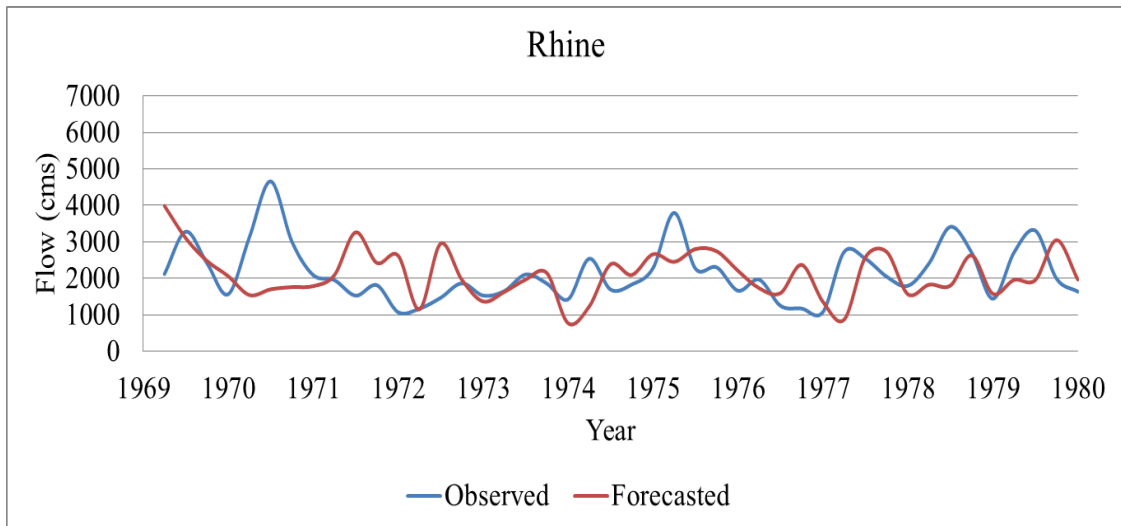
Figure B-5. Validated lead-1 seasonal forecasts of the rivers: (a) Danube; (b) Rhine; and (c) Missouri, using the univariate ARMA(1,1) model.



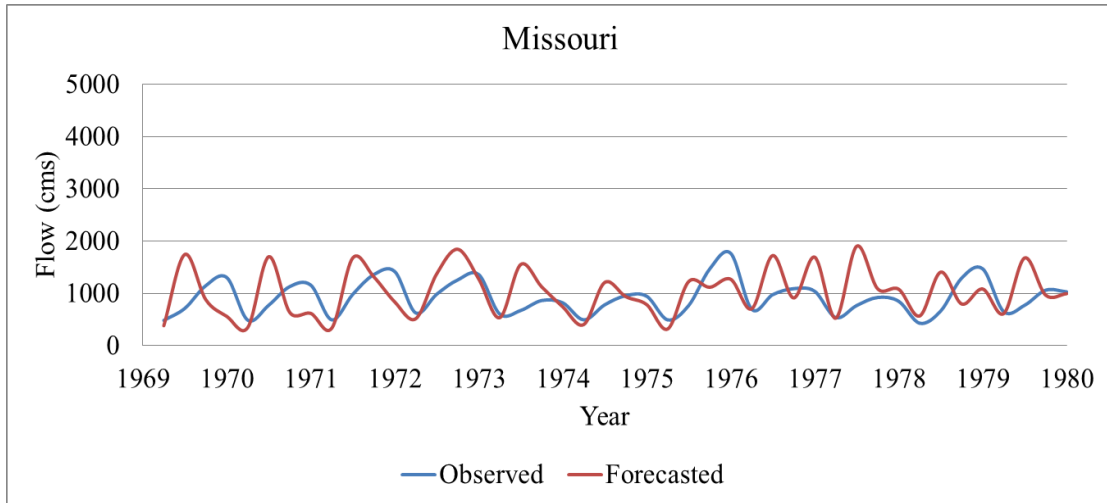
(a)



(b)

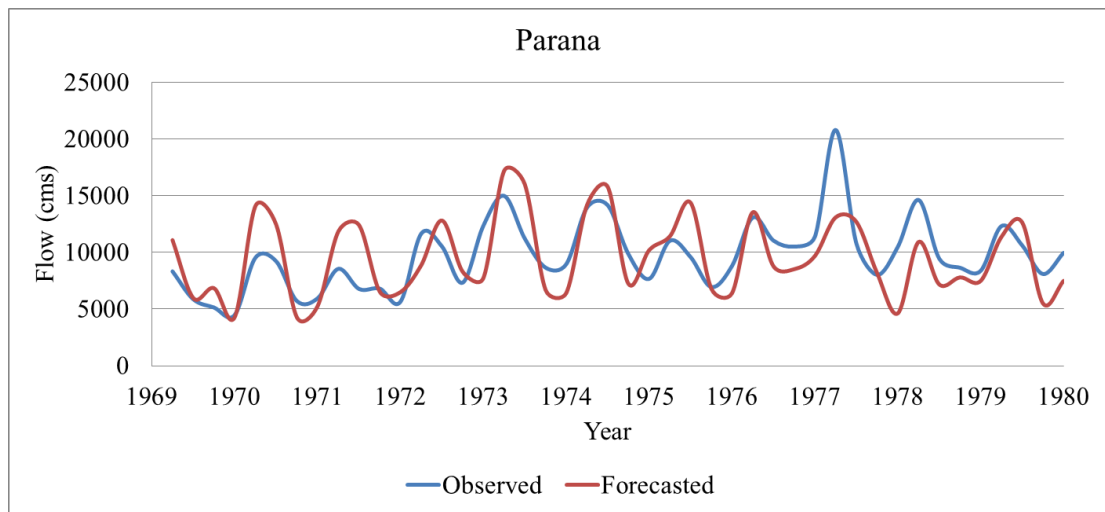


(c)

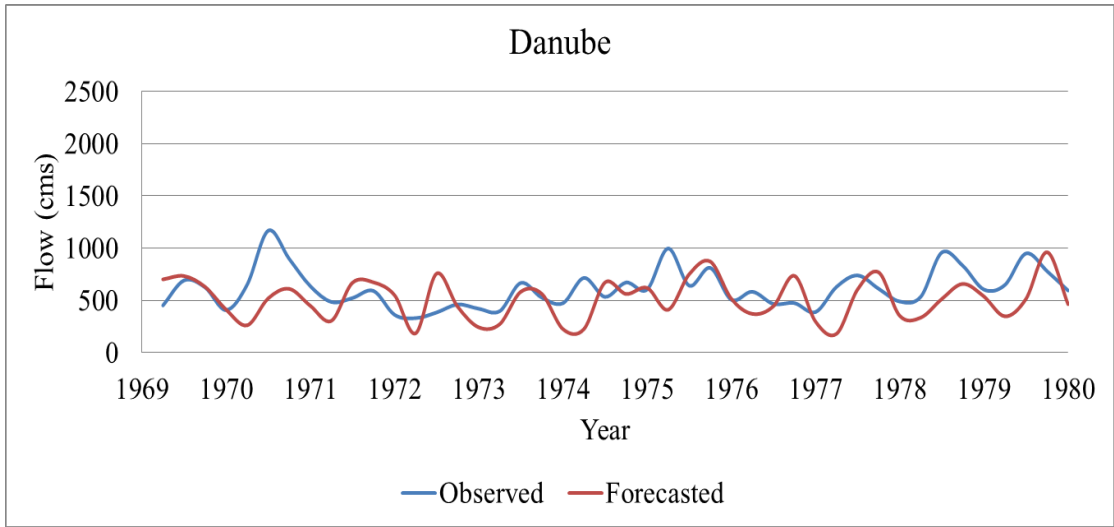


(d)

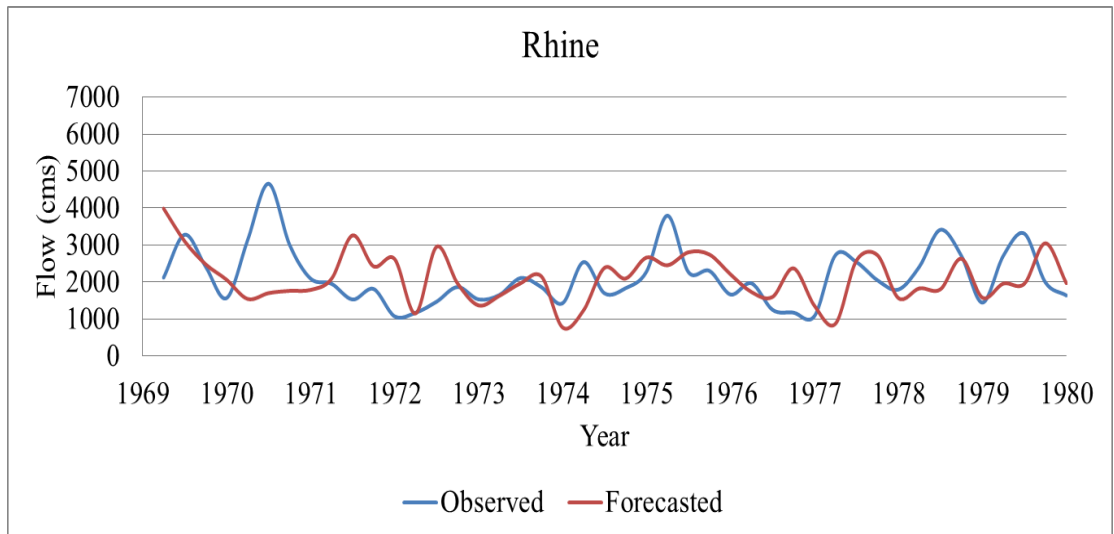
Figure B-6. Validated lead-1 seasonal forecasts of the rivers: (a) Parana; (b) Danube; (c) Rhine; and (d) Missouri, using the MAR(3) model incorporating 4 rivers flow data.



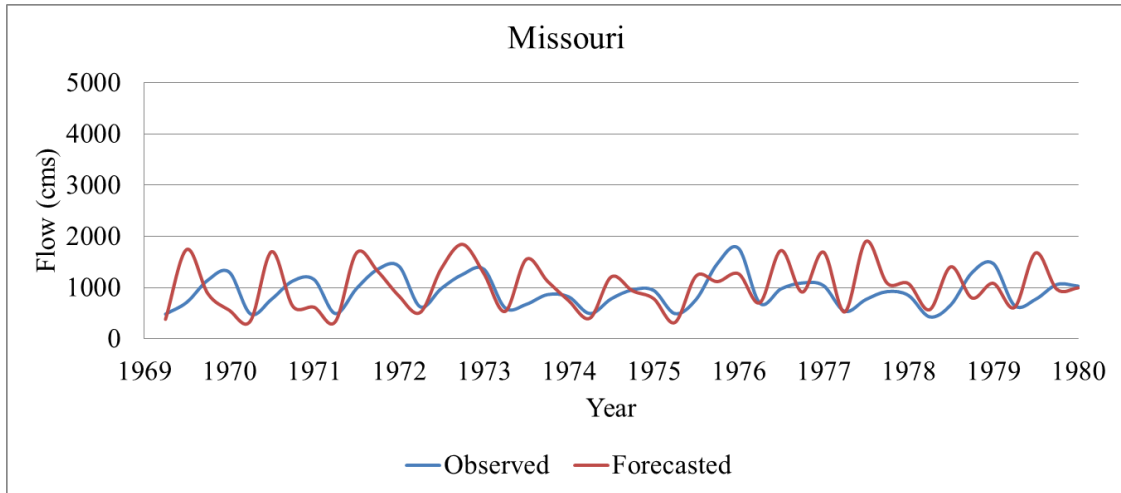
(a)



(b)

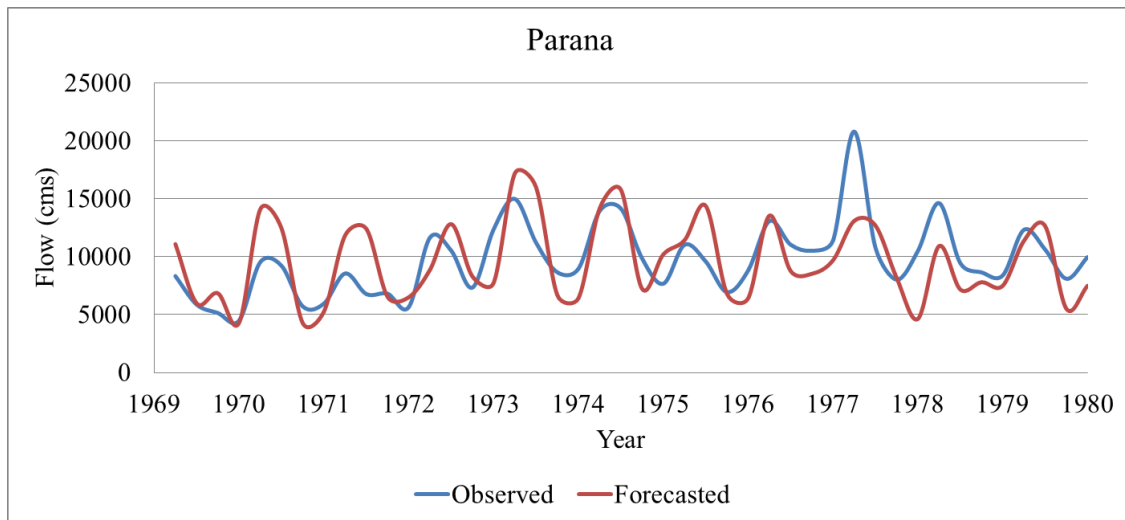


(c)

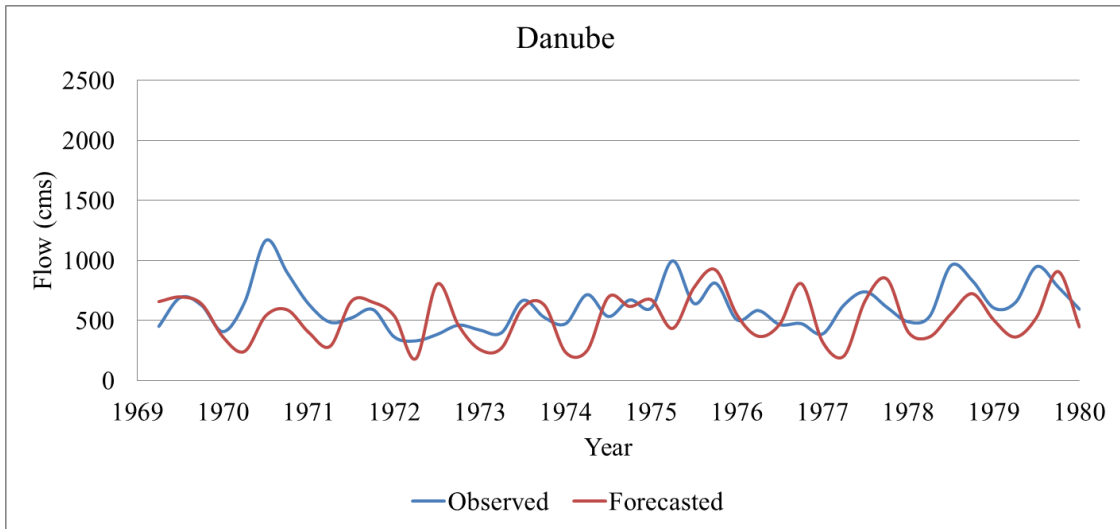


(d)

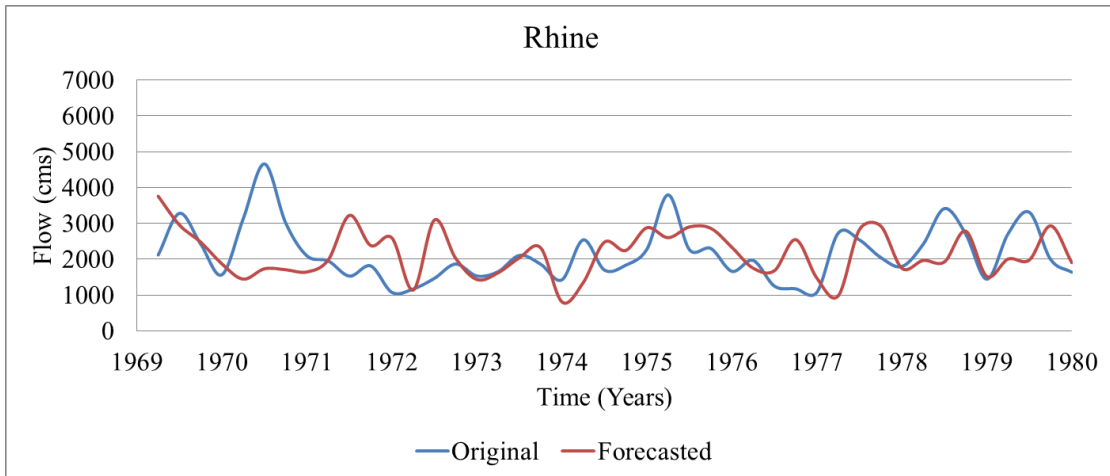
Figure B-7. Validation of lead one seasonal forecasts of the rivers: (a) Parana; (b) Danube; (c) Rhine; and (d) Missouri, using the MAR(3) model with 4 rivers and SOI information.



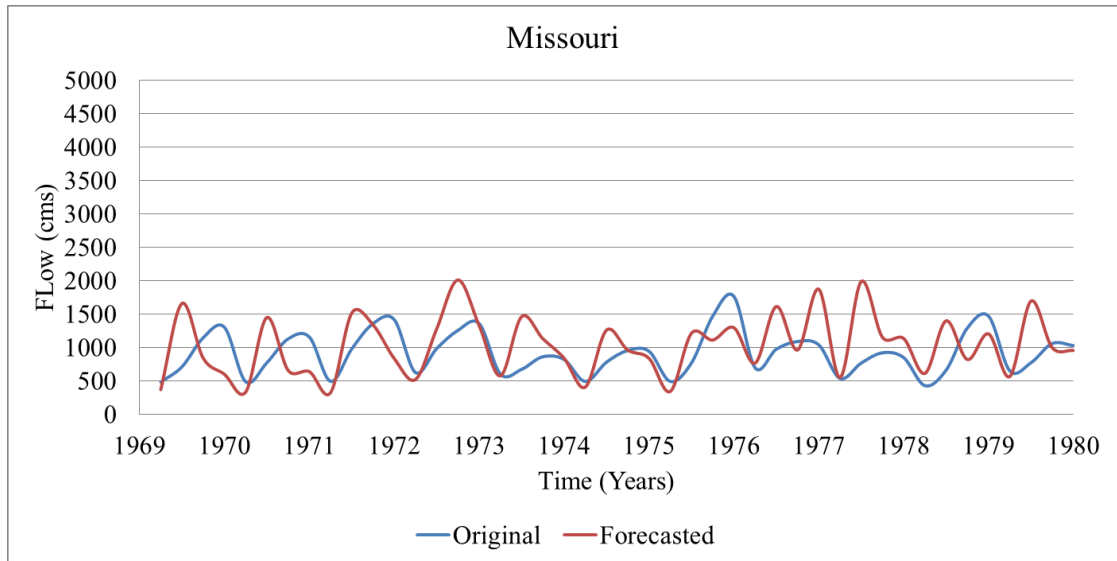
(a)



(b)

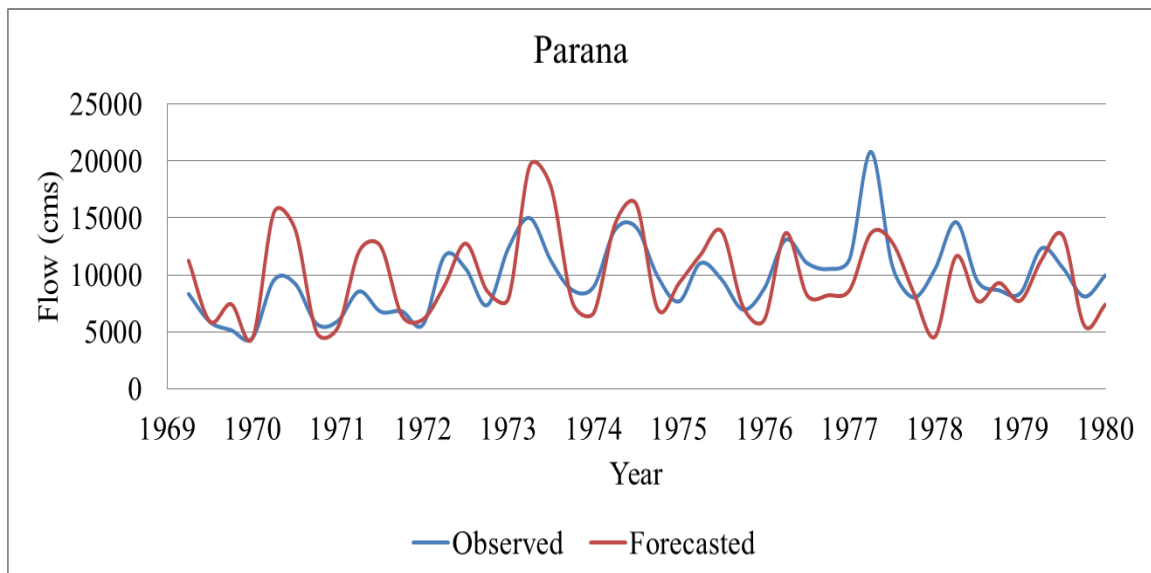


(c)

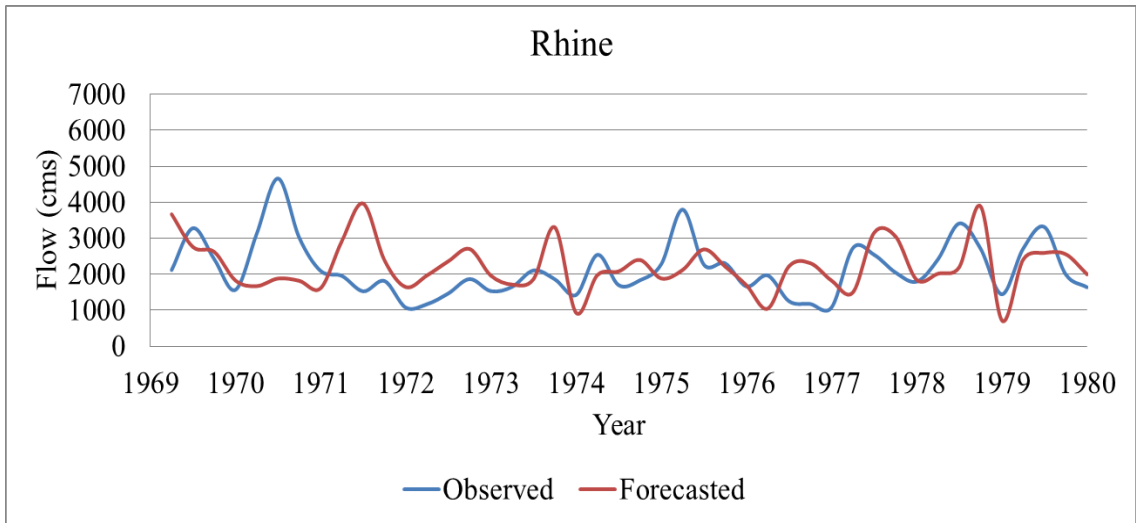


(d)

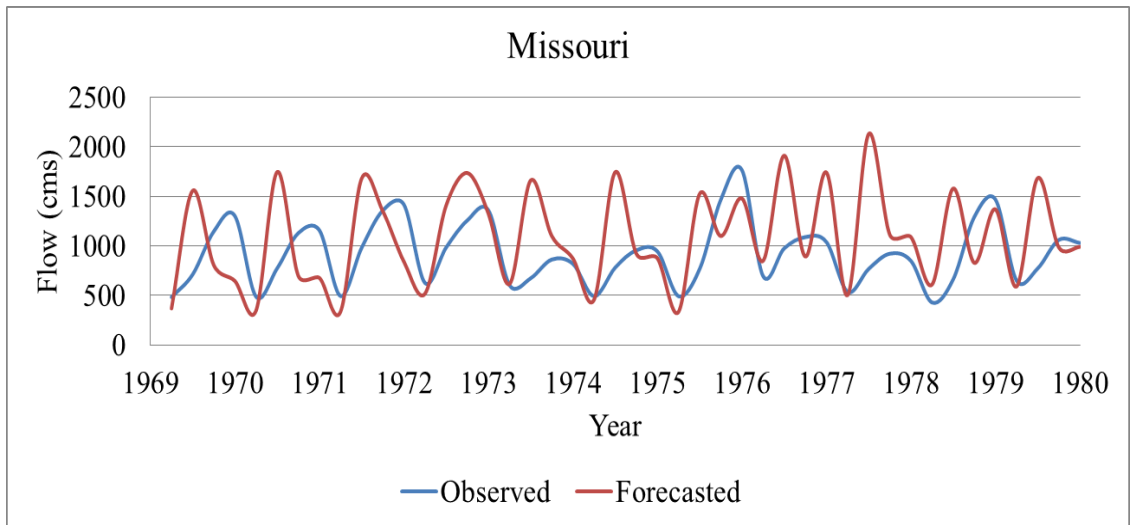
Figure B-8. Validation of lead one seasonal forecasts of the rivers: (a) Parana; (b) Danube; (c) Rhine; and (d) Missouri, using the MAR(3) model with 4 rivers, SOI, and SSN information.



(a)

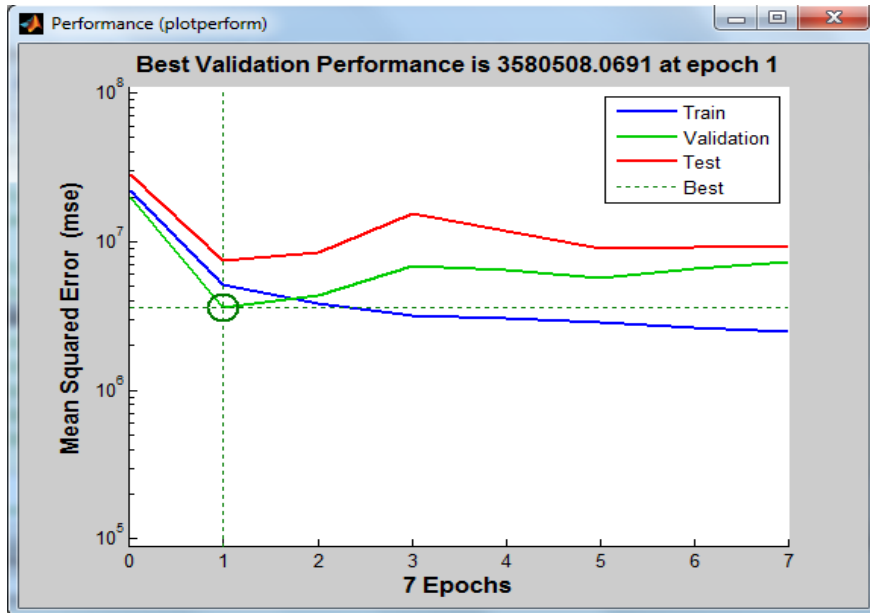


(b)

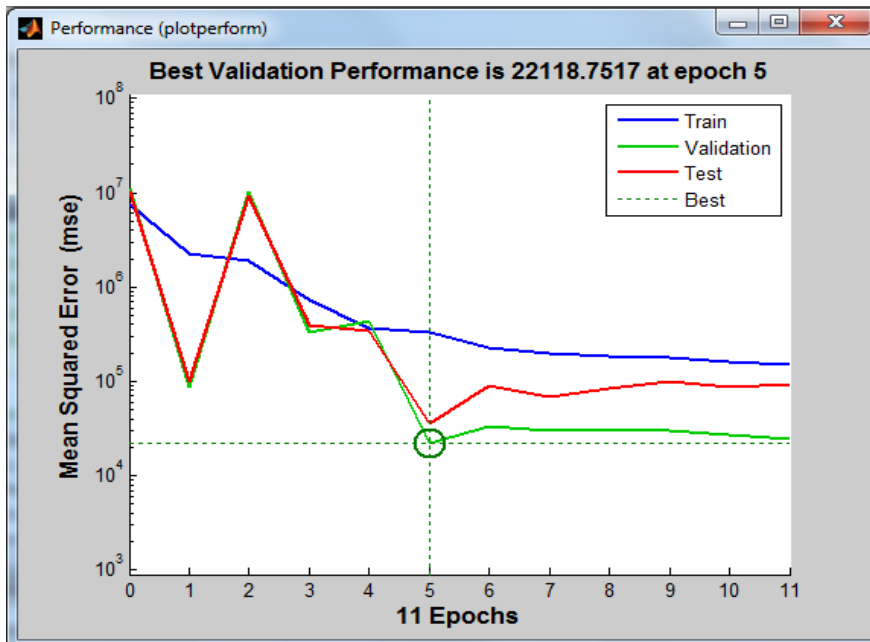


(c)

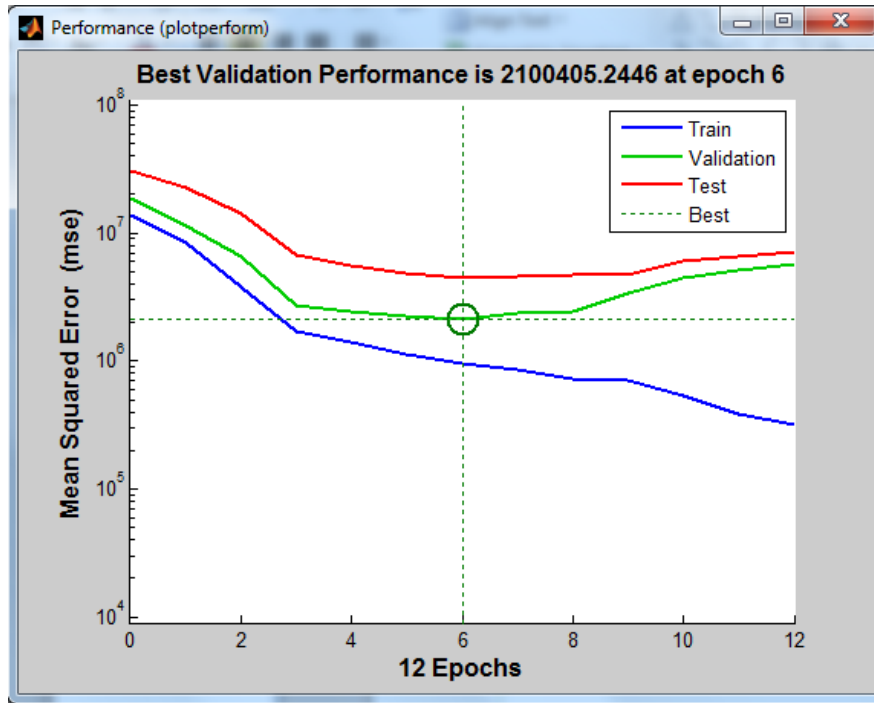
Figure B-9. Validation of lead one seasonal forecasts of the rivers: (a) Parana; (b) Danube; (c) Rhine; and (d) Missouri, using the MAR(3) model incorporating 3 rivers and SSN.



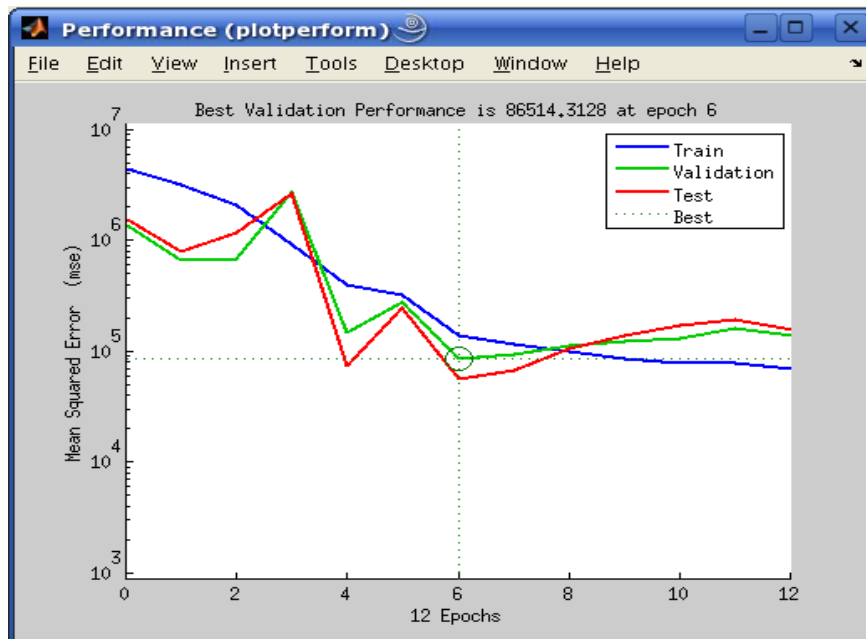
(a)



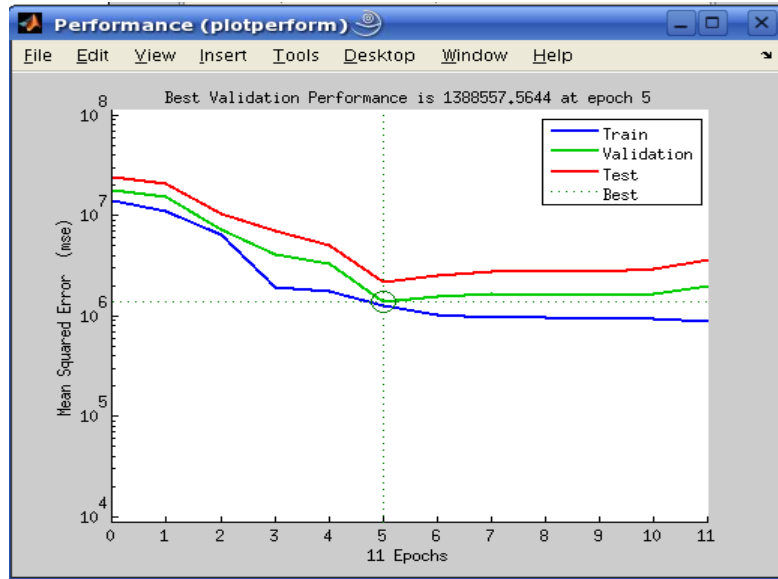
(b)



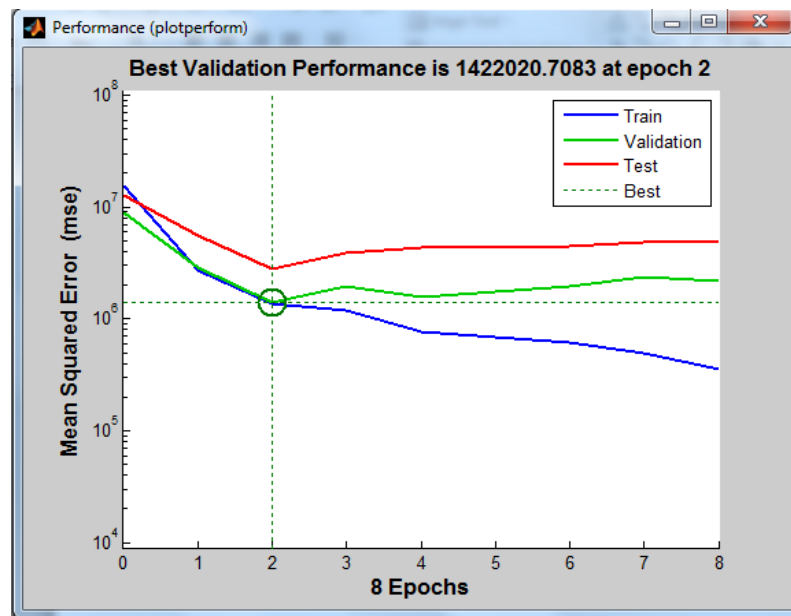
(c)



(d)

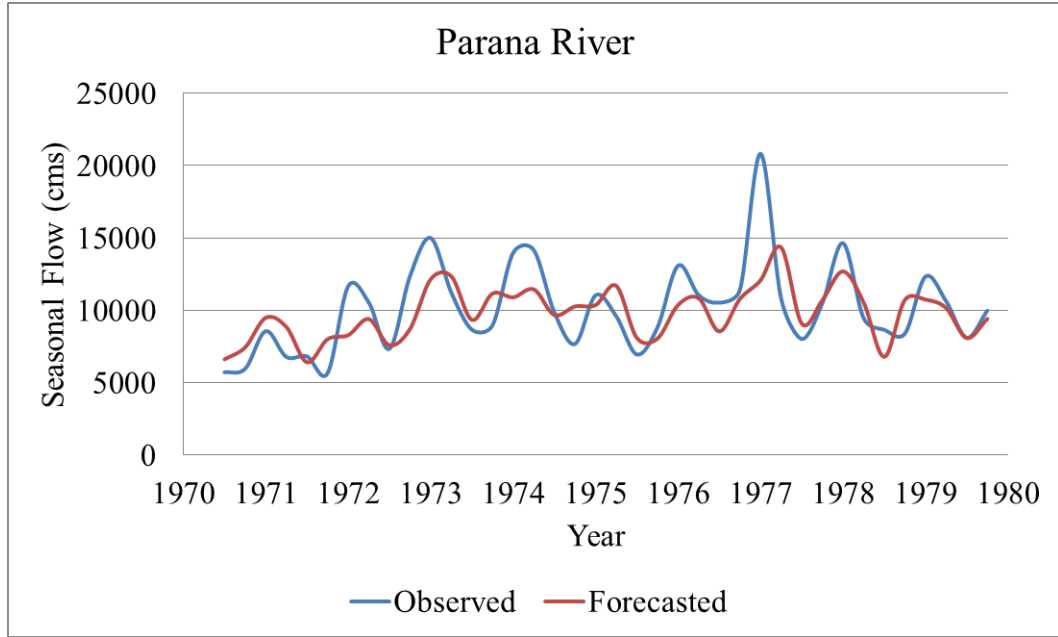


(e)

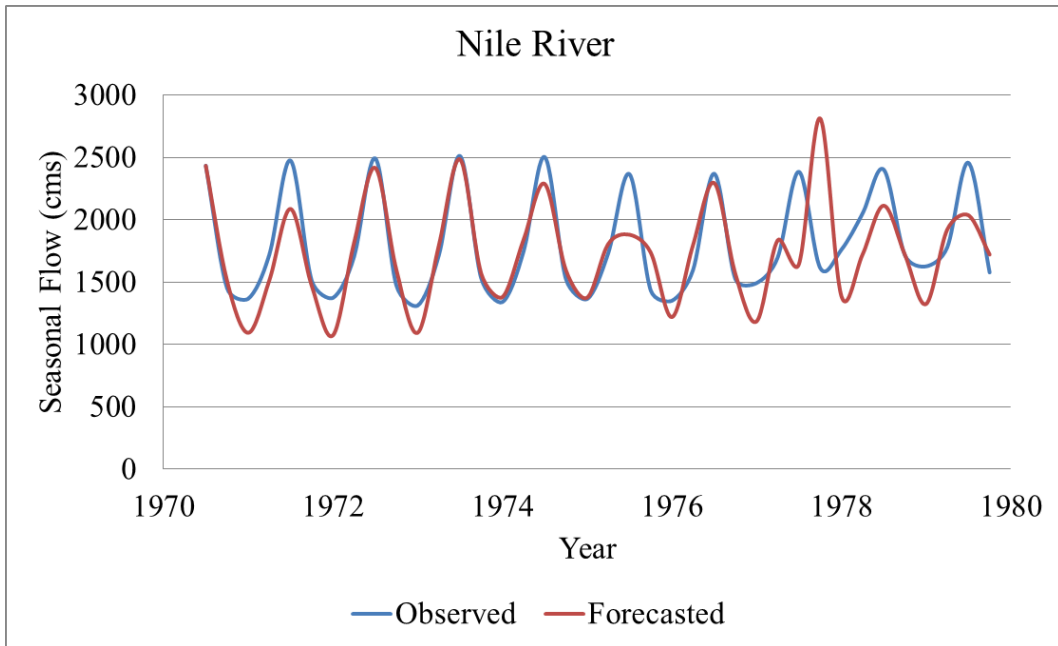


(f)

Figure B-10. Performance plots when the ANN training stopped: (a) Univariate Parana model; (b) Univariate Nile model; (c) Multivariate Parana-Murray Model; (d) Multivariate Nile-Murray model; (e) Multivariate all-river (Nile-Parana-Murray) model; and (f) Multivariate Parana-Murray-SSN model.

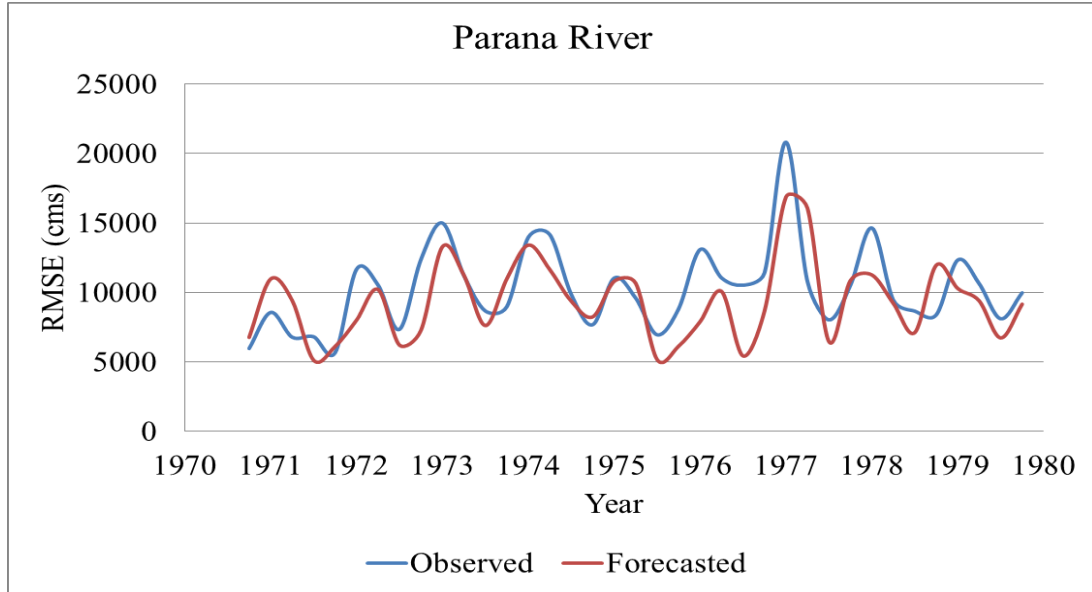


(a)

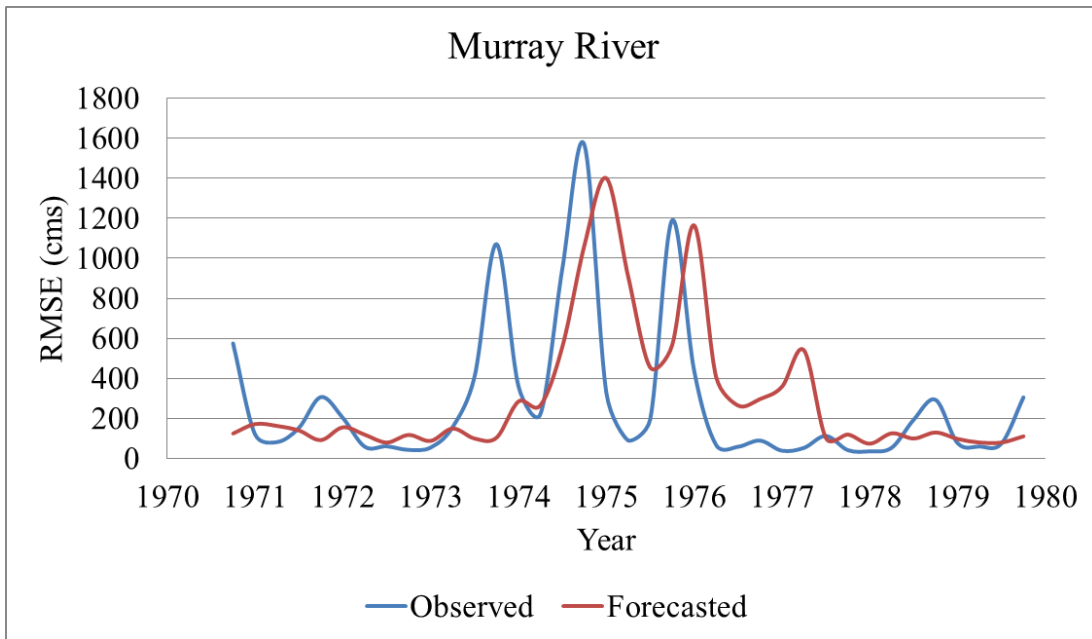


(b)

Figure B-11. Validated lead-1 multivariate ANN Parana-Nile model forecasts for the rivers: (a) Parana and (b) Nile

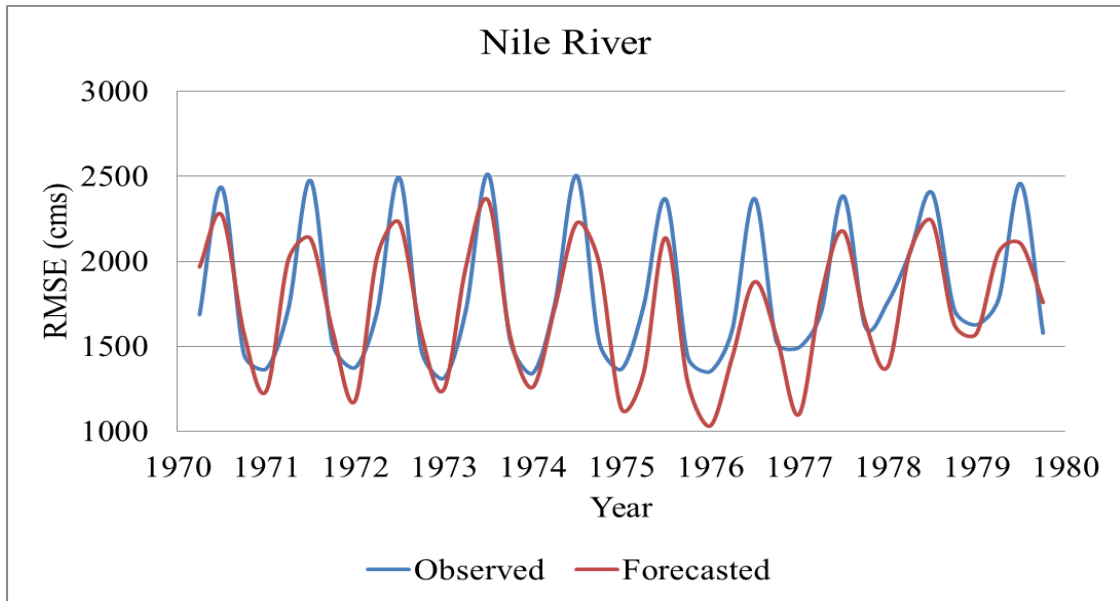


(a)

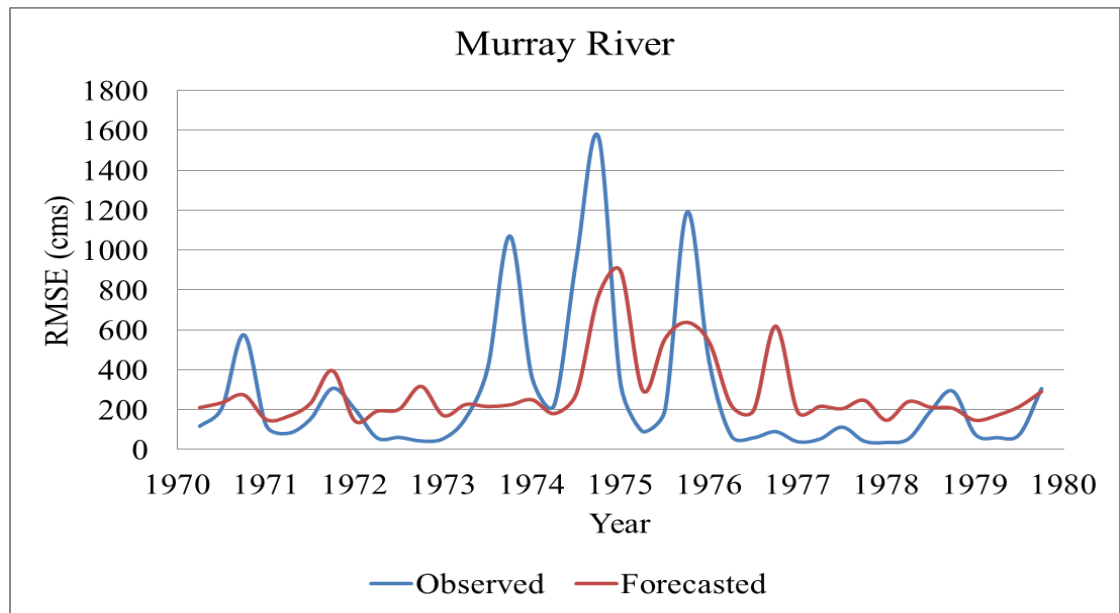


(b)

Figure B-12. Validated lead-1 multivariate ANN Parana-Murray model forecasts for the rivers: Parana and (b) Murray

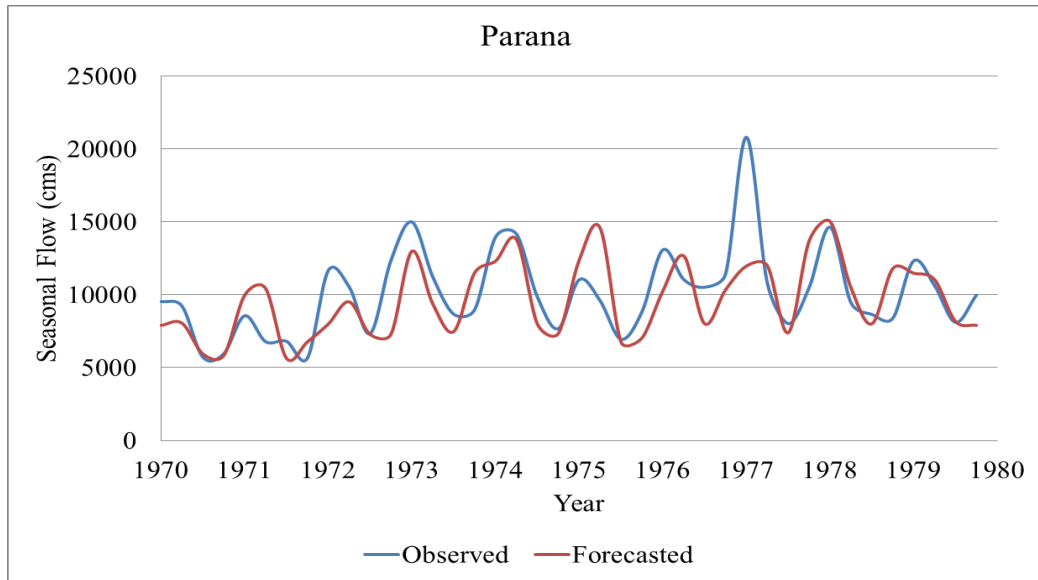


(a)

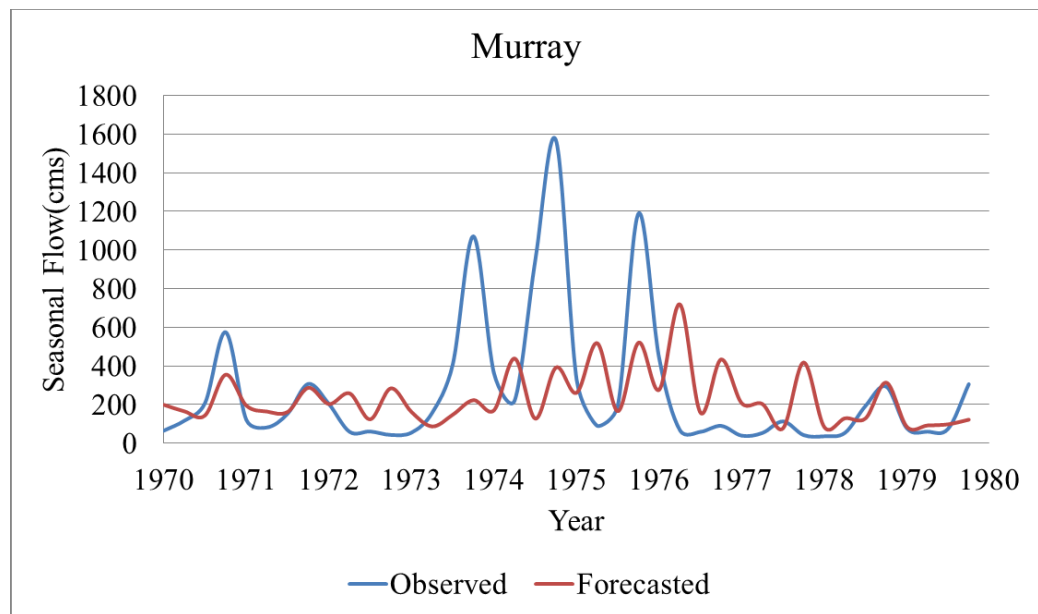


(b)

Figure B-13. Validated lead-1 multivariate ANN Nile-Murray model forecasts for the rivers: (a) Nile and (b) Murray

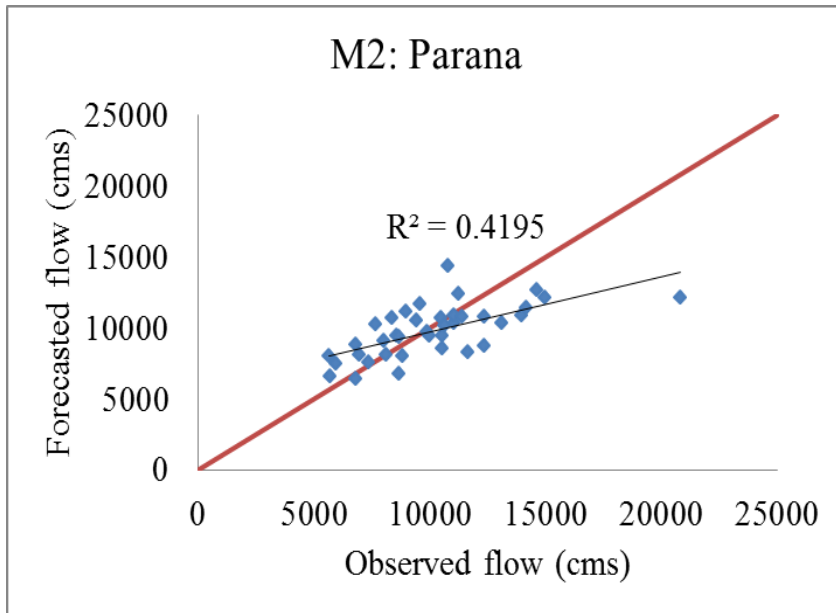


(a)

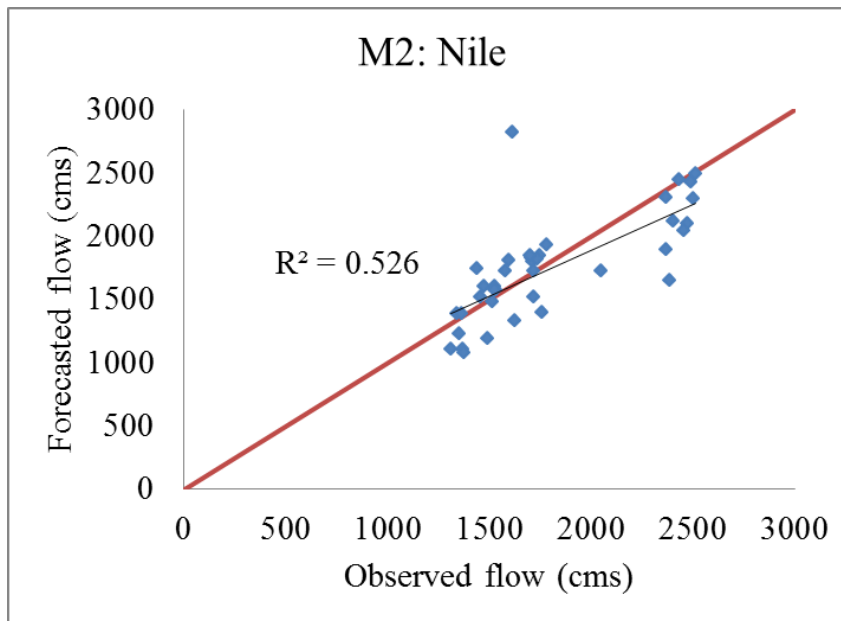


(b)

Figure B-14. Validated lead-1 multivariate ANN Parana-Murray-SSN model forecasts for the rivers: (a) Parana and (b) Murray

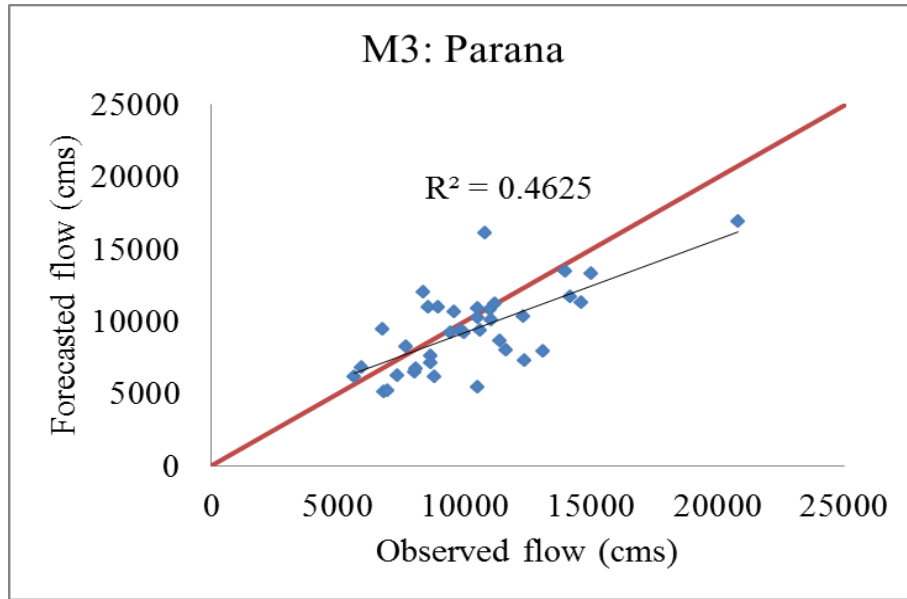


(a)

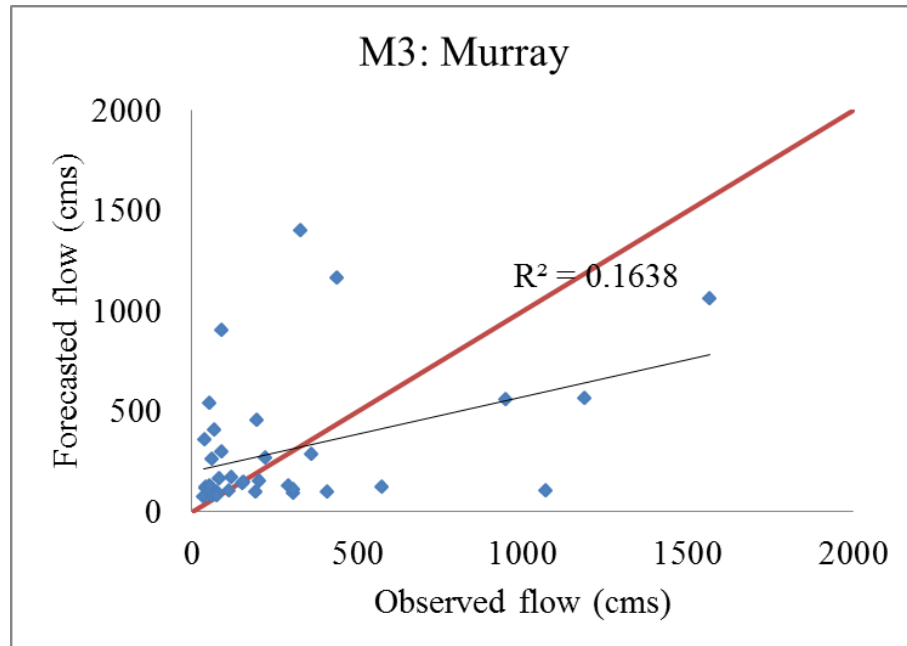


(b)

Figure B-15. Regression plots of the multivariate model with Parana and Nile River (M2): (a) Parana River and (b) Nile River.



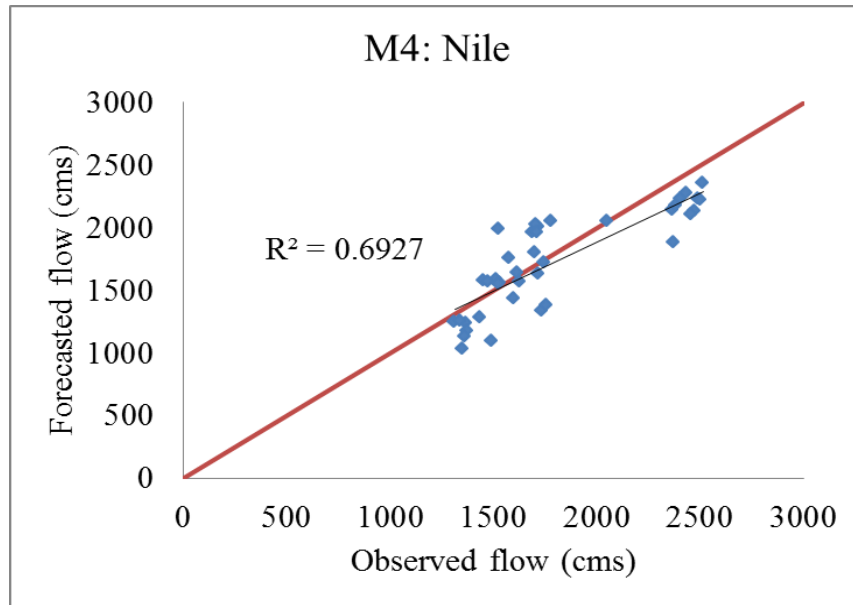
(a)



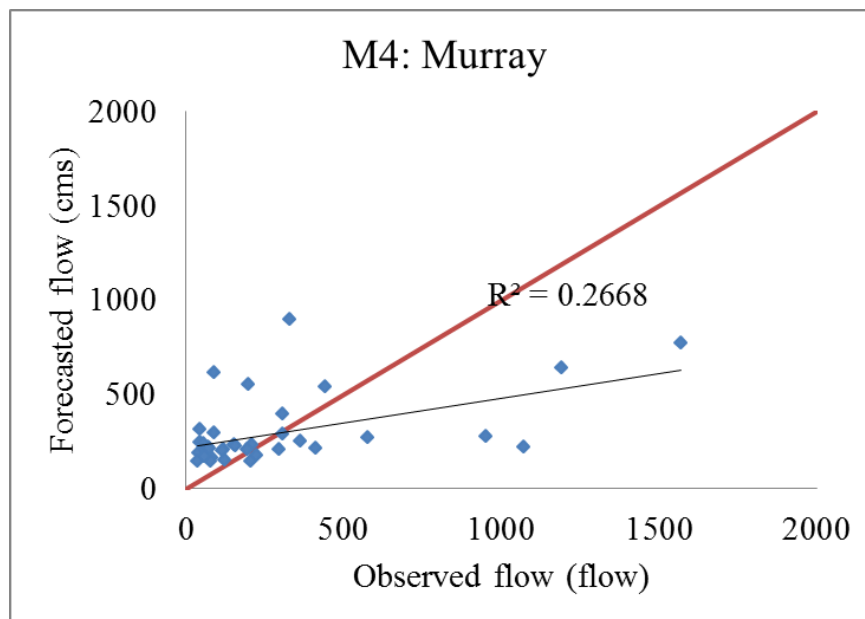
(b)

Figure B-16. Regression plots of the multivariate model with Parana and Murray River

(M3): (a) Parana River and (b) Murray River



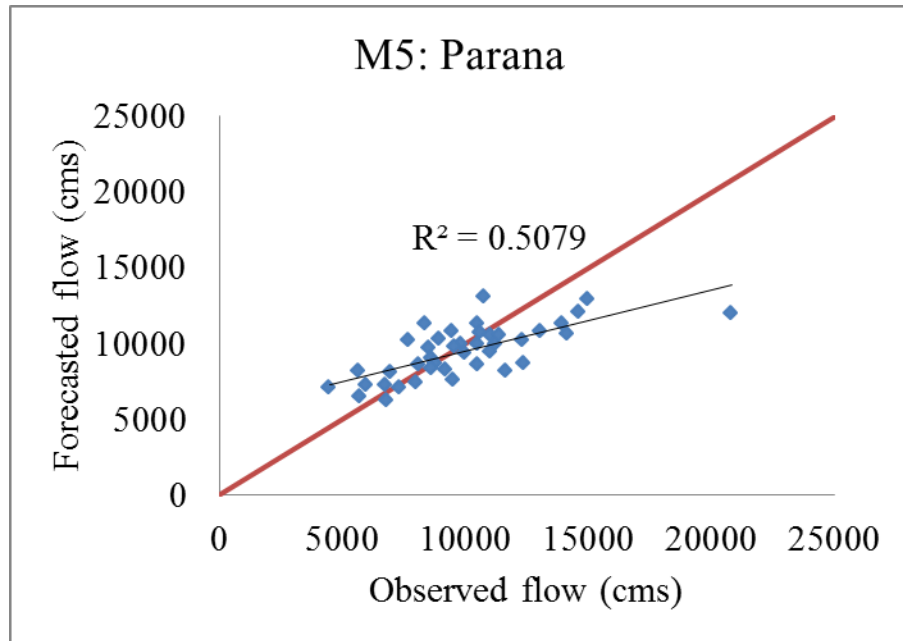
(a)



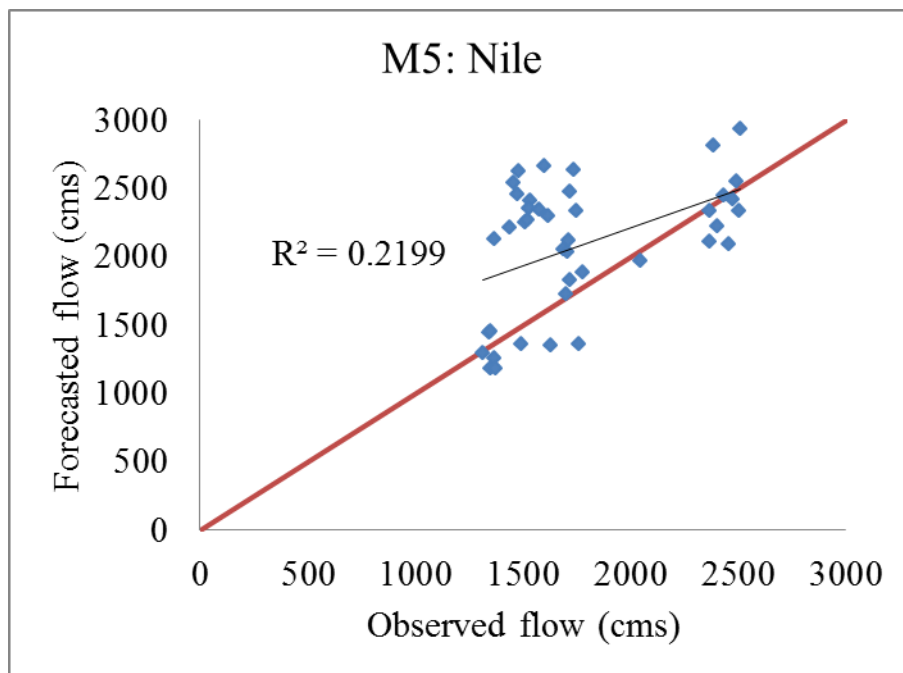
(b)

Figure B-17. Regression plots of the multivariate model with Nile and Murray River

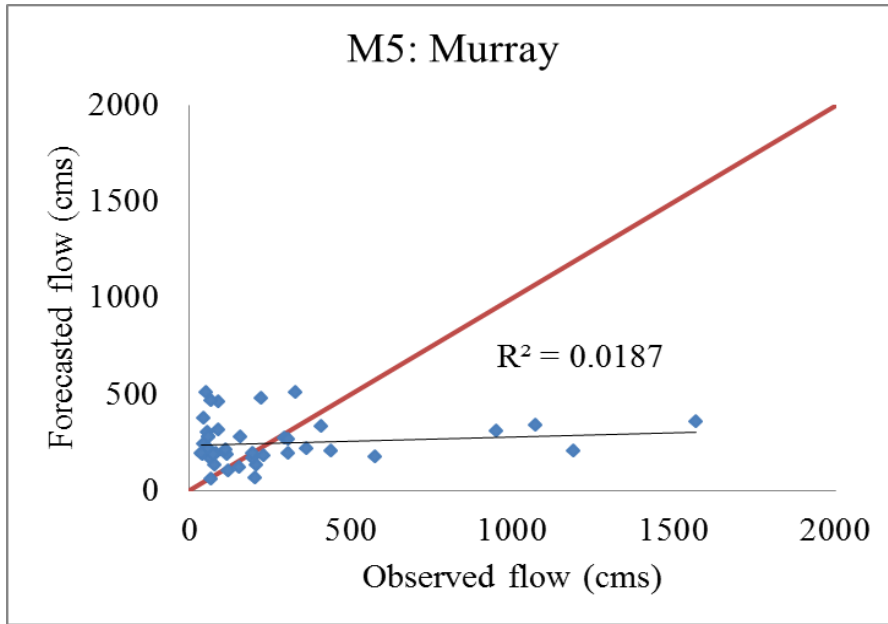
(M4): (a) Nile River and (b) Murray River



(a)

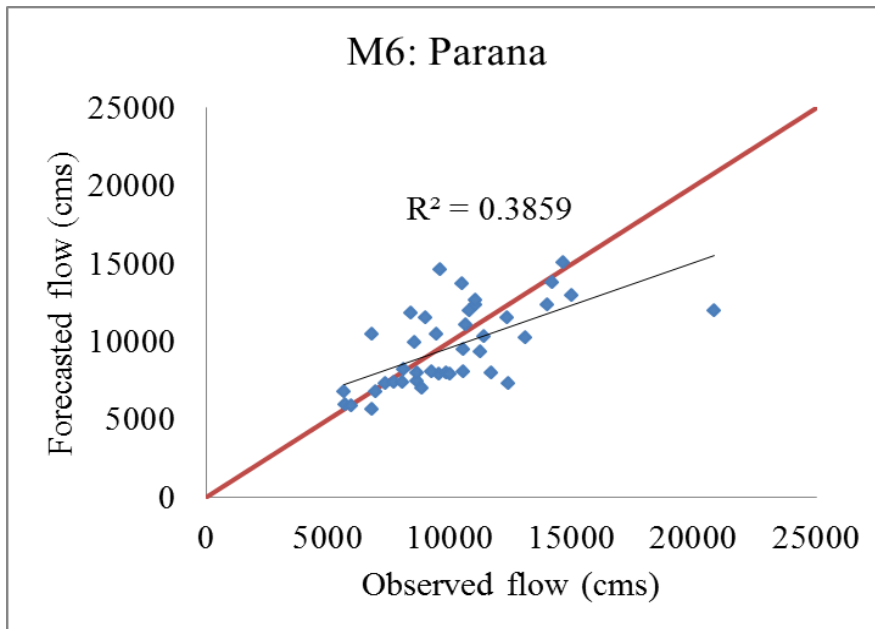


(b)

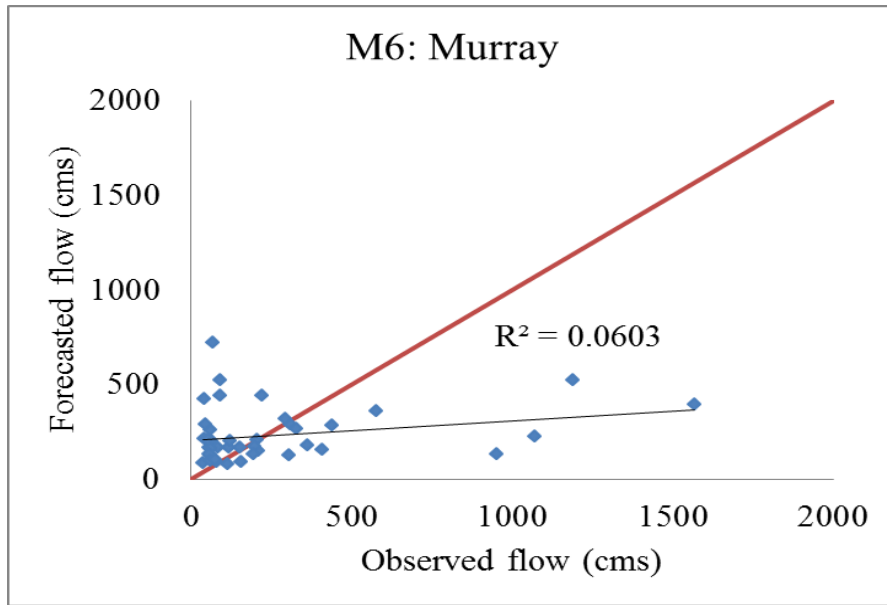


(c)

Figure B-18. Regression plots of the multivariate model with Parana, Nile, and Murray River (M5): (a) Parana River; (b) Nile River; and (c) Murray River from year 1971 to 1979



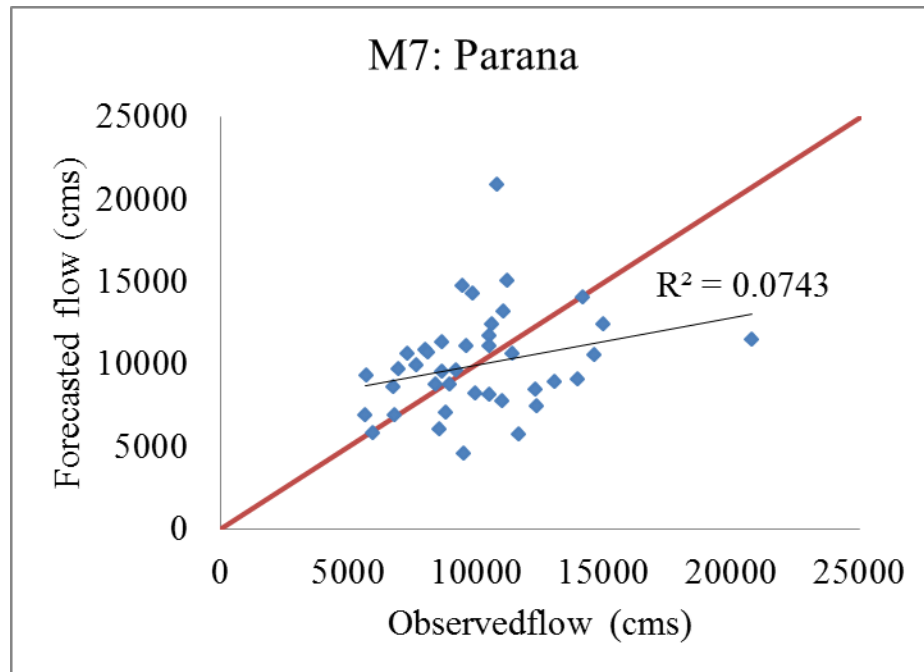
(a)



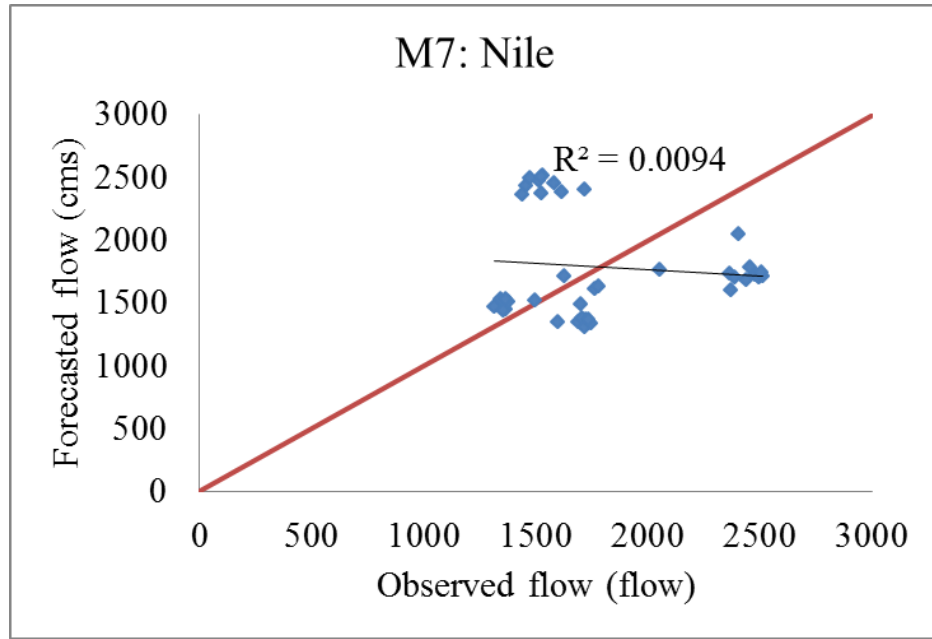
(b)

Figure B-19. Regression plots of the multivariate model with Parana, Murray, and SSN

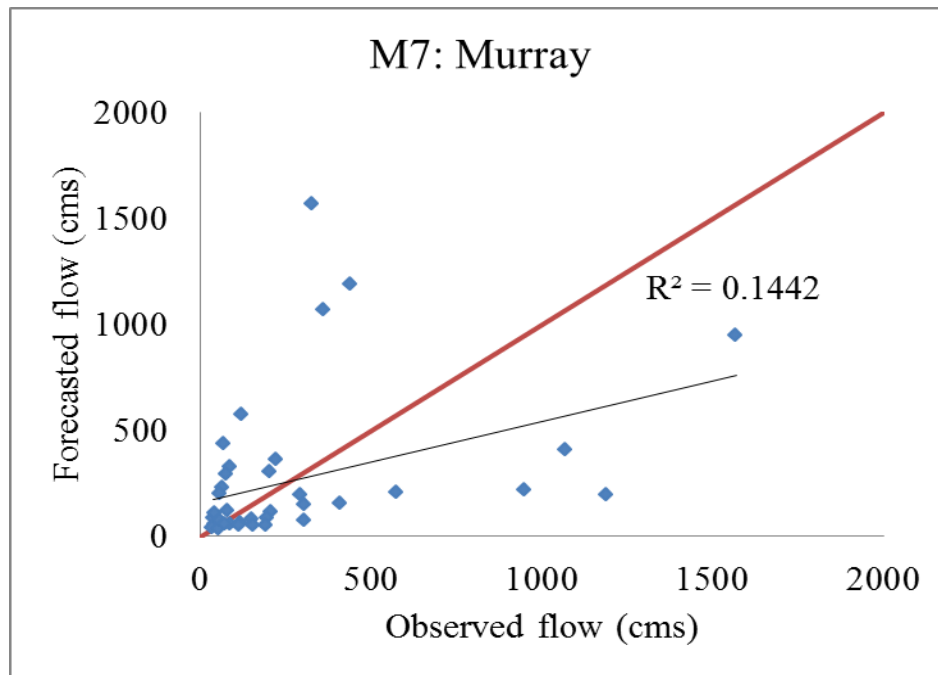
(M6): (a) Parana River and (b) Murray River from year 1971 to 1979



(a)

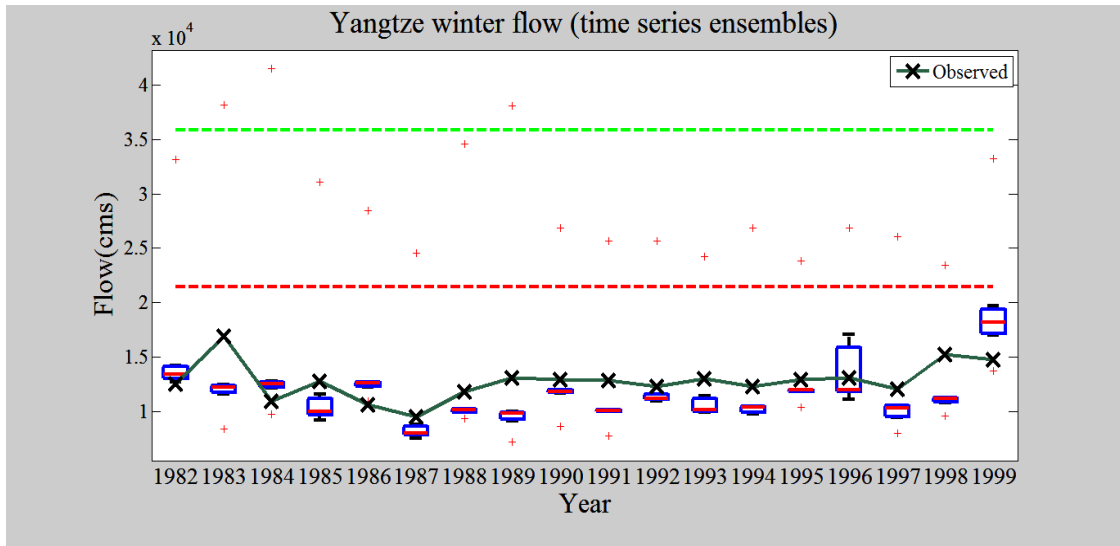


(b)

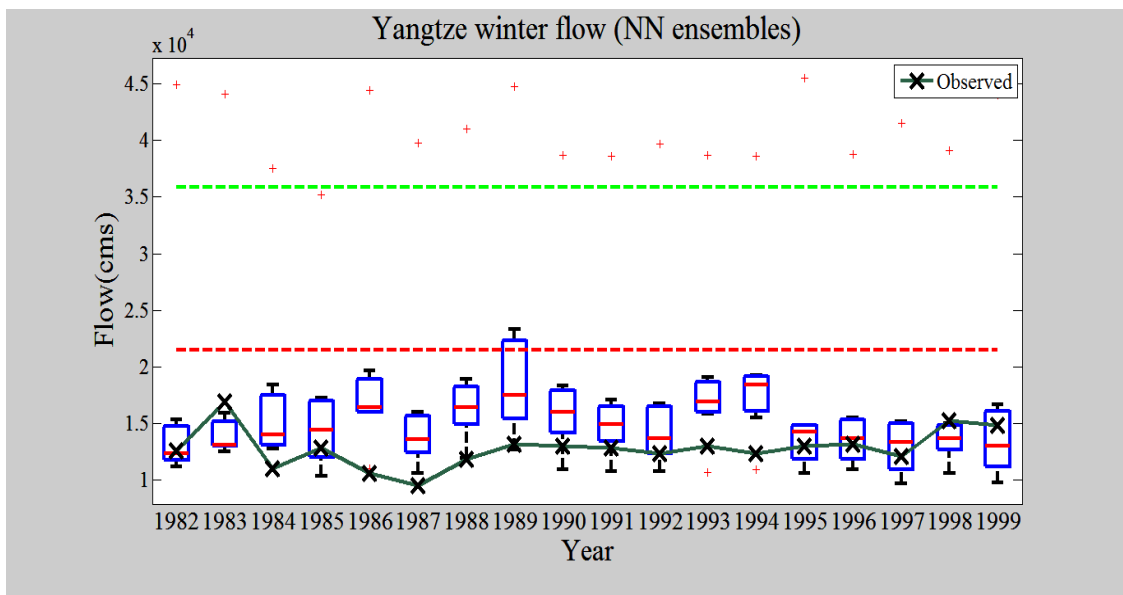


(c)

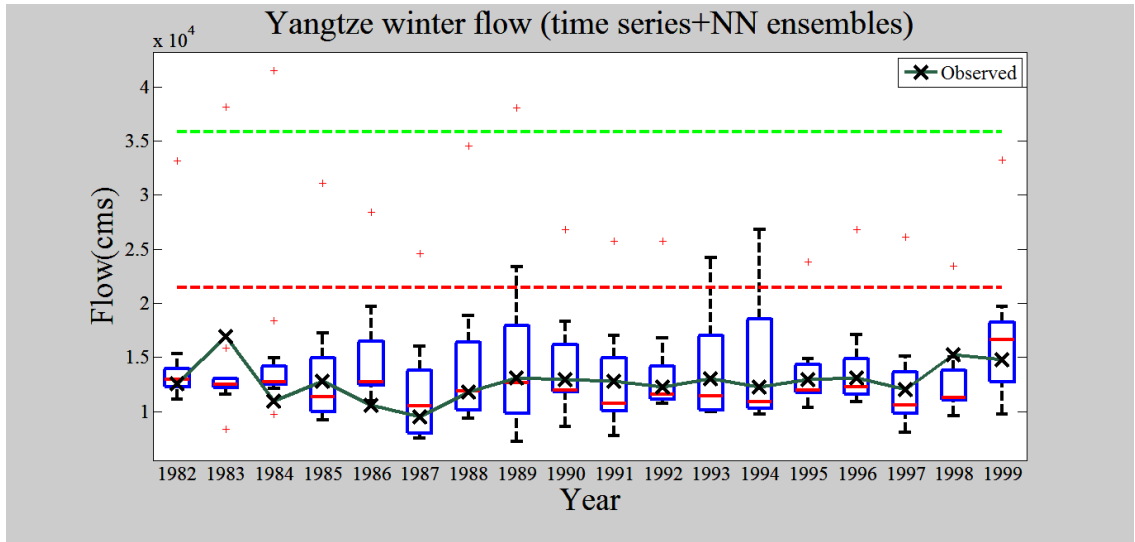
Figure B-20. Regression plots of the Persistence model (M7): (a) Parana River; (b) Nile River; and (c) Murray River from year 1971 to 1979.



(a)

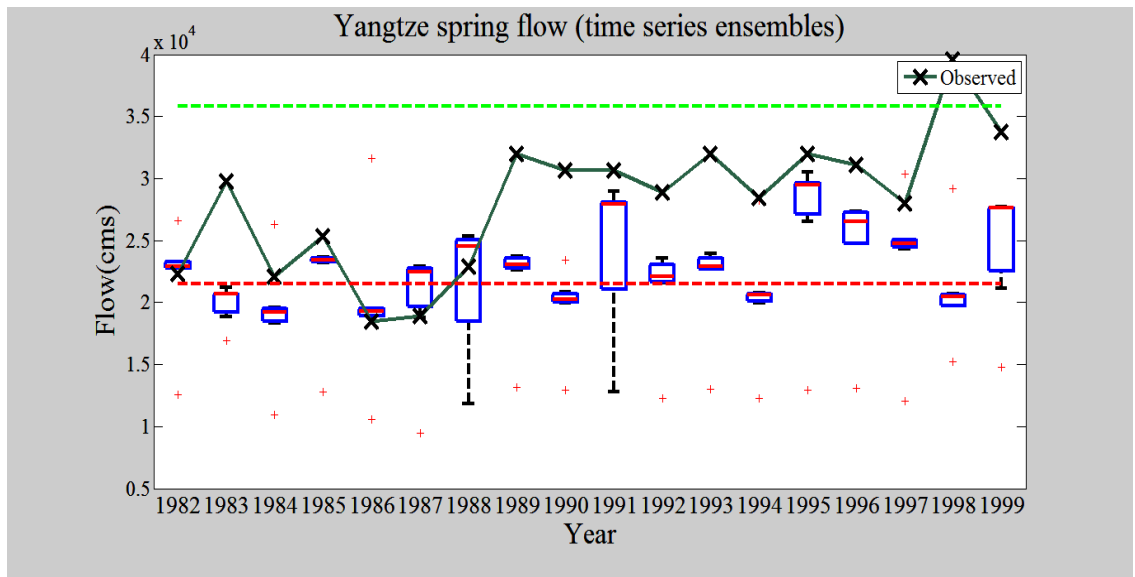


(b)

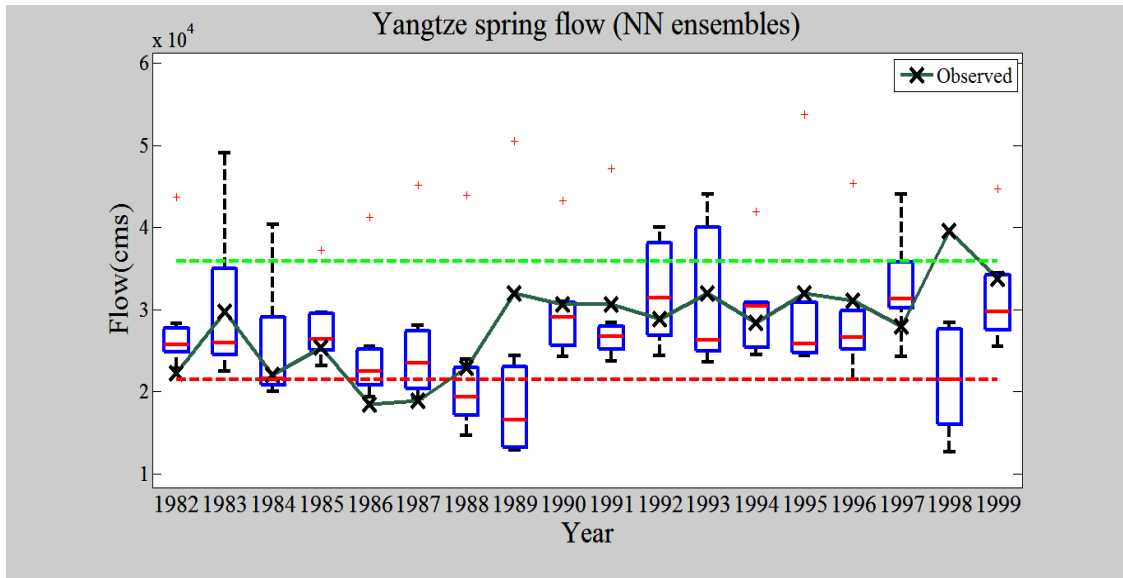


(c)

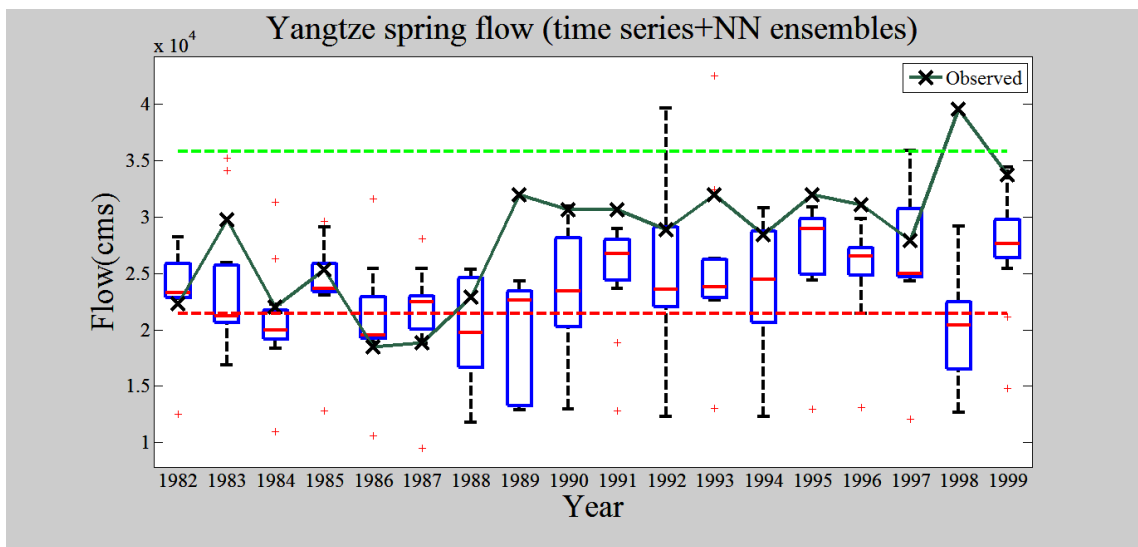
Figure B-21. Ensemble of the Yangtze River winter flow: (a) time series model forecasts ensembles; (b) NN model forecasts ensembles; and (c) ensembles of the time series and NN model forecasts.



(a)

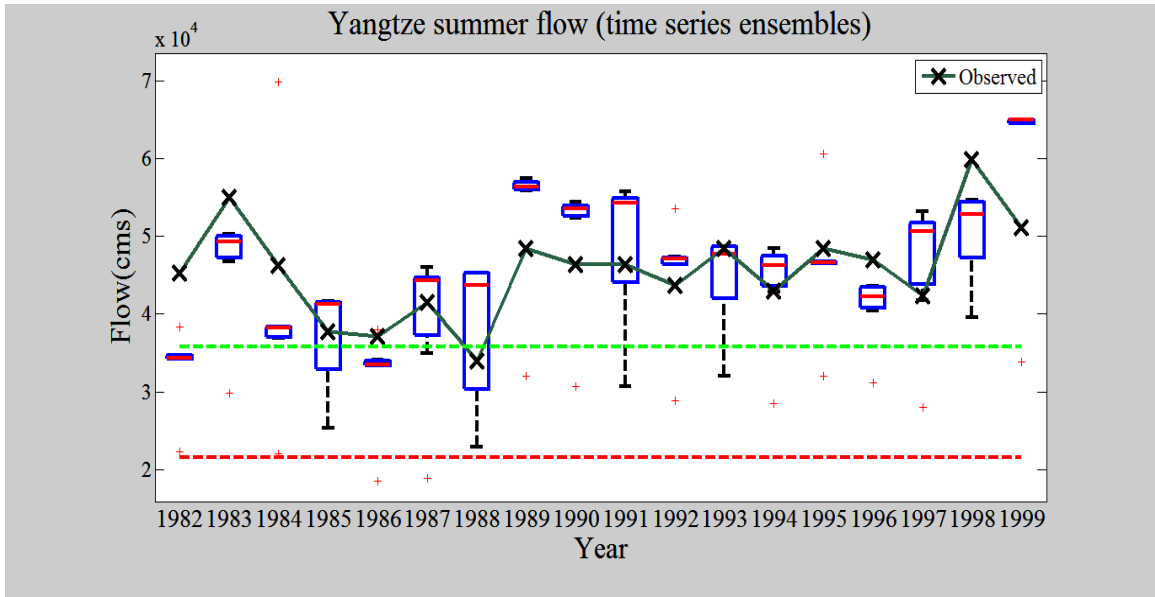


(b)

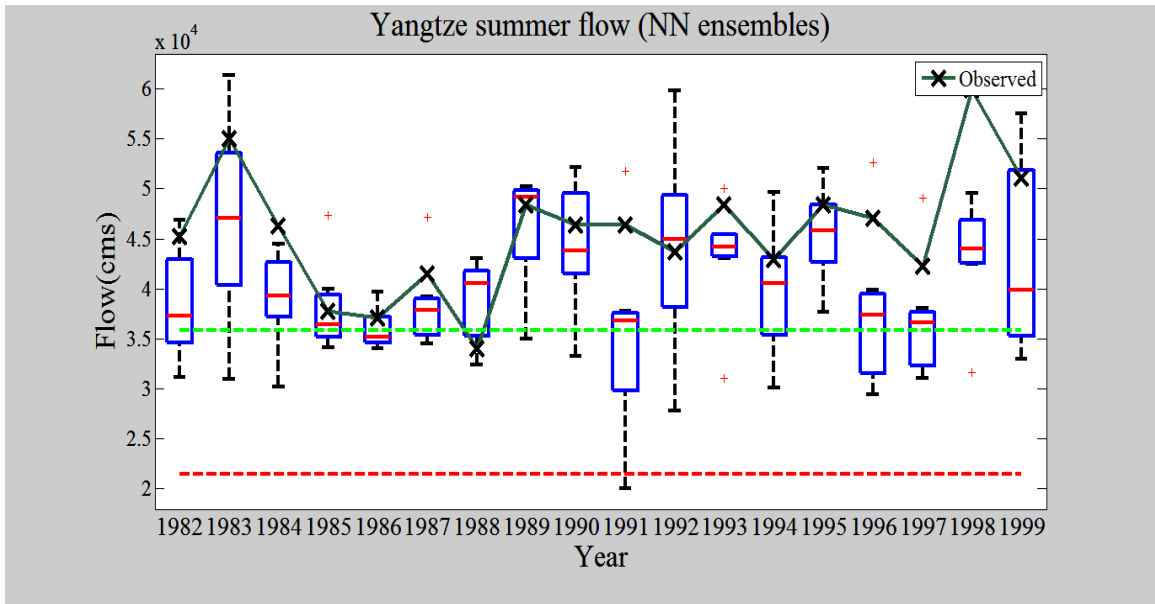


(c)

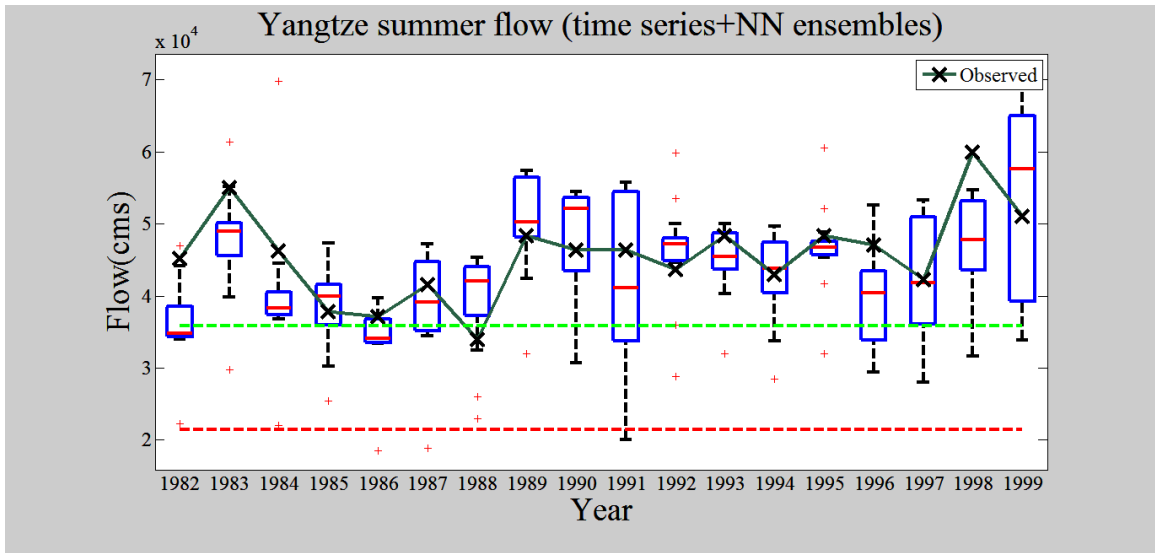
Figure B-22. Ensemble of the Yangtze River spring flow: (a) time series model forecasts ensembles; (b) NN model forecasts ensembles; and (c) ensembles of the time series and NN model forecasts.



(a)

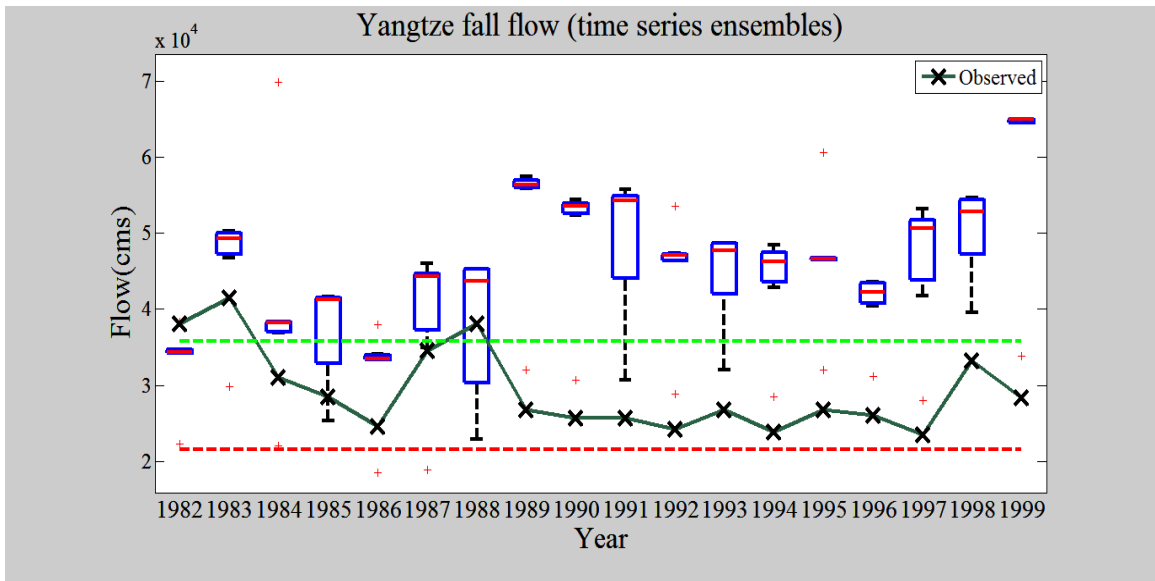


(b)

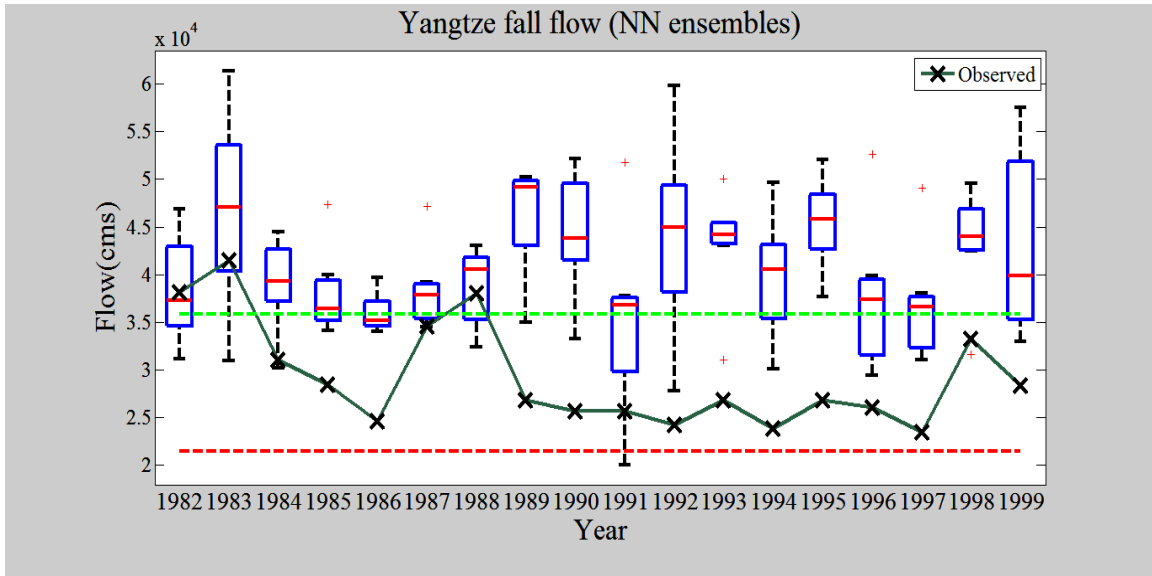


(c)

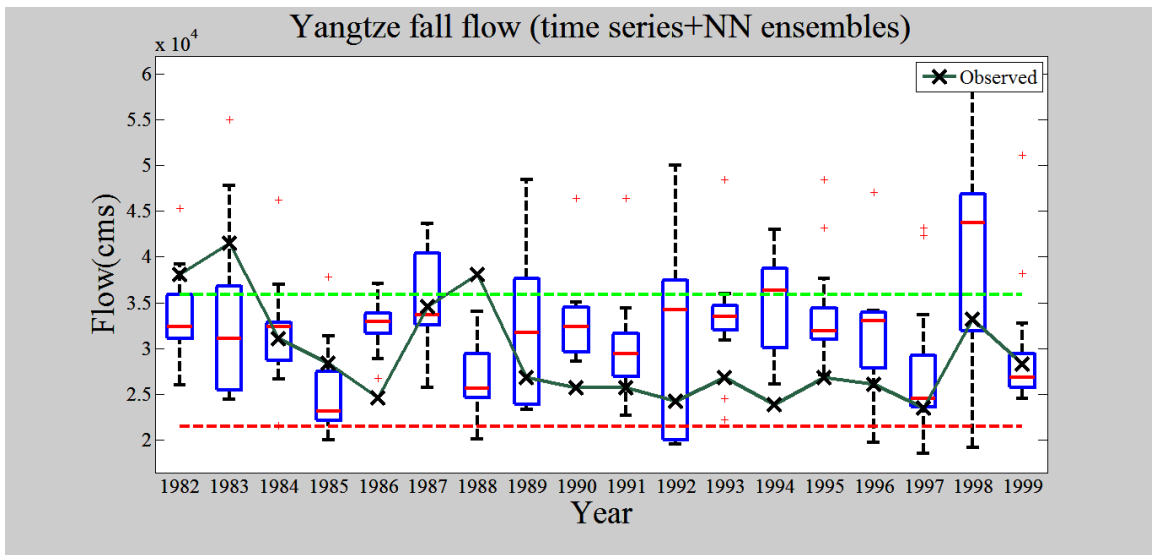
Figure B-23. Ensemble of the Yangtze River summer flow: (a) time series model forecasts ensembles; (b) NN model forecasts ensembles; and (c) ensembles of the time series and NN model forecasts.



(a)

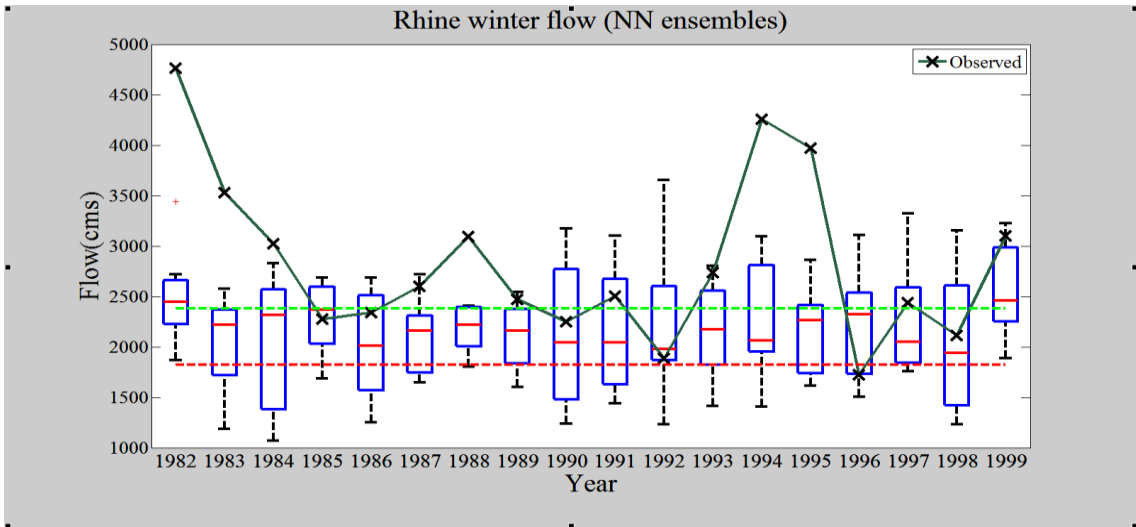


(b)

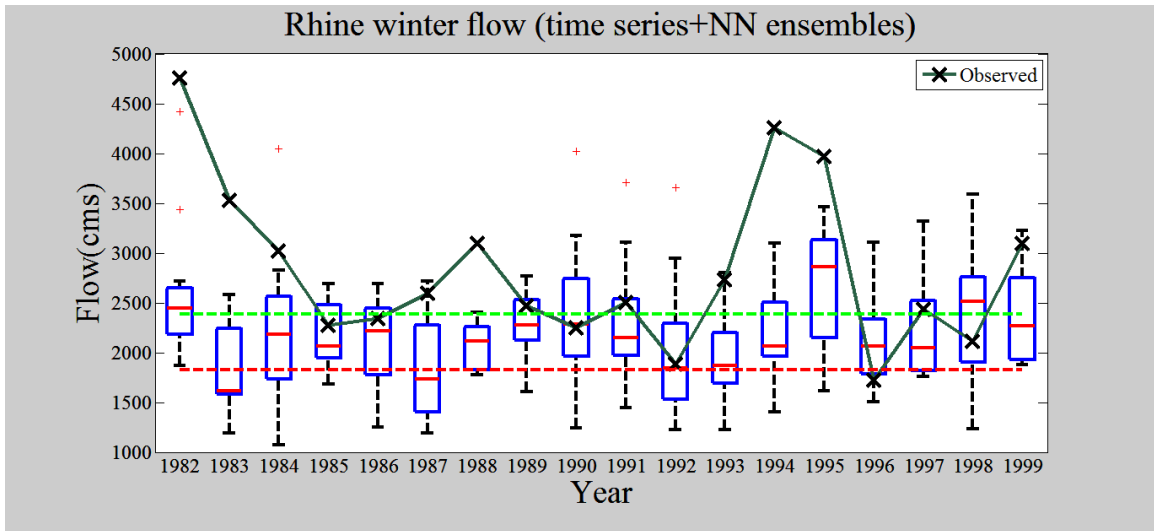


(c)

Figure B-24. Ensemble of the Yangtze River fall flow: (a) time series model forecasts ensembles; (b) NN model forecasts ensembles; and (c) ensembles of the time series and NN model forecasts.

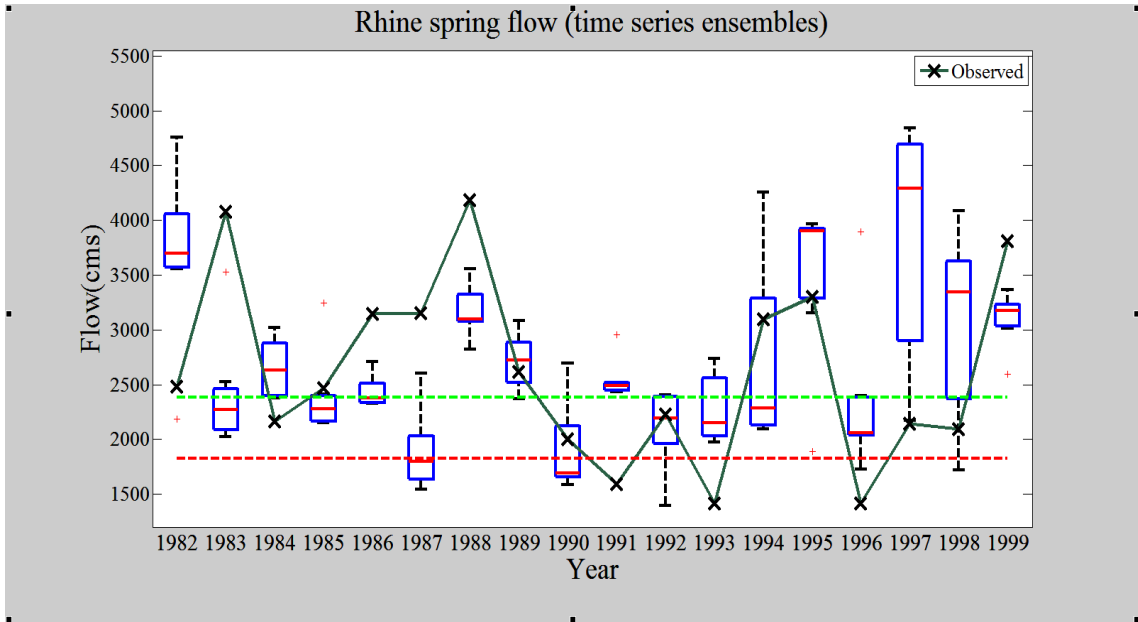


(a)

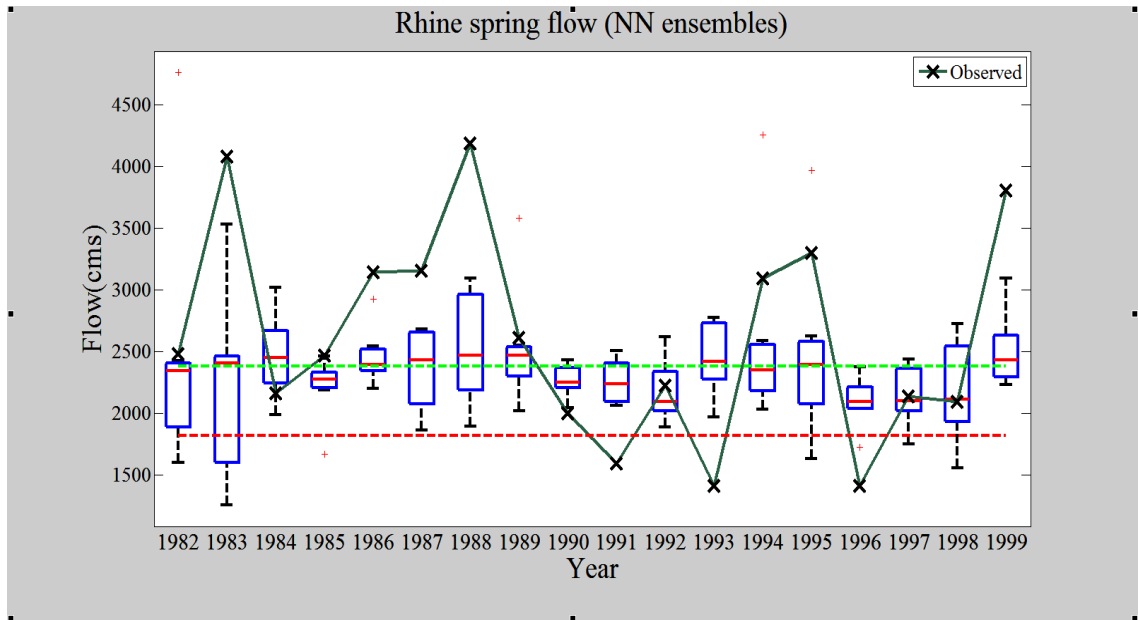


(b)

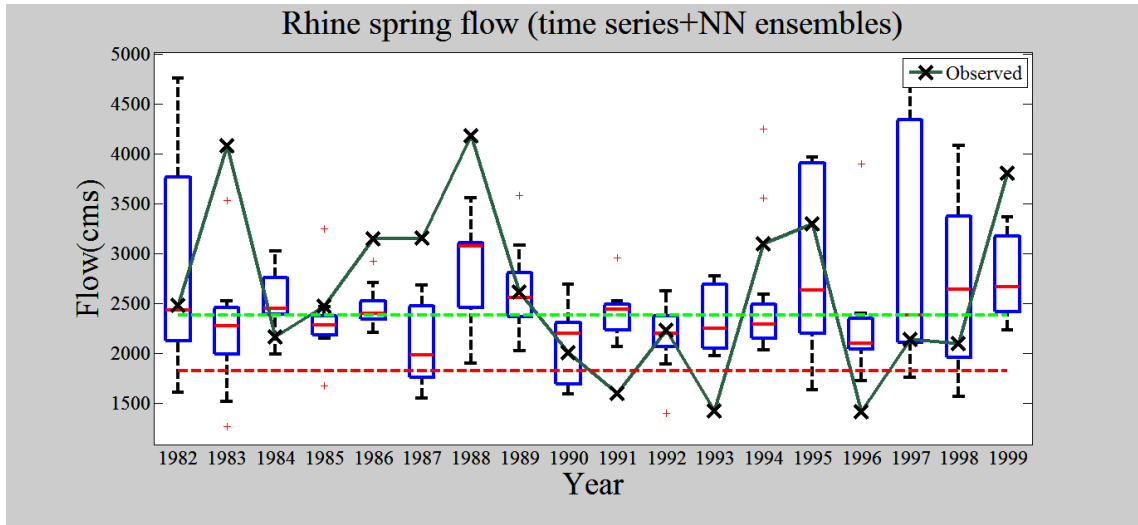
Figure B-25. Ensemble of the Rhine River Winter flow: (a) NN model forecasts ensembles and (b) ensembles of the time series and NN model forecasts.



(a)

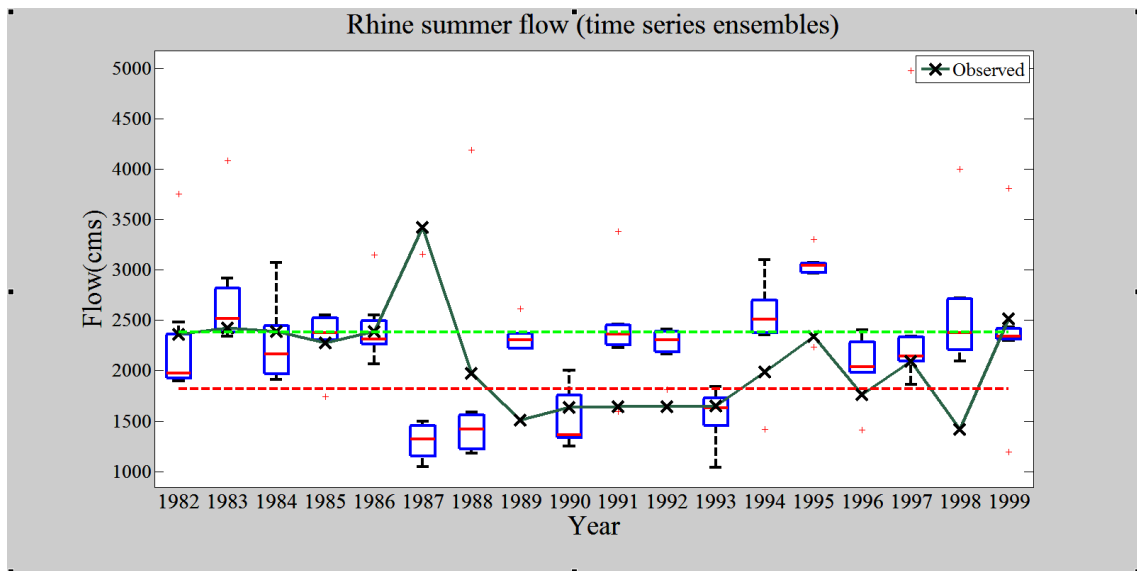


(b)

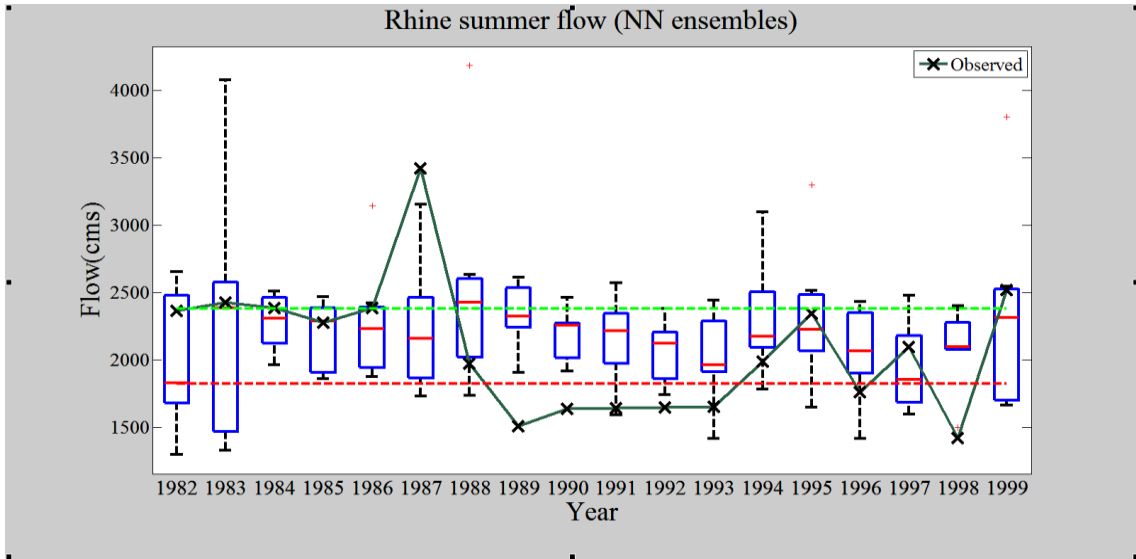


(c)

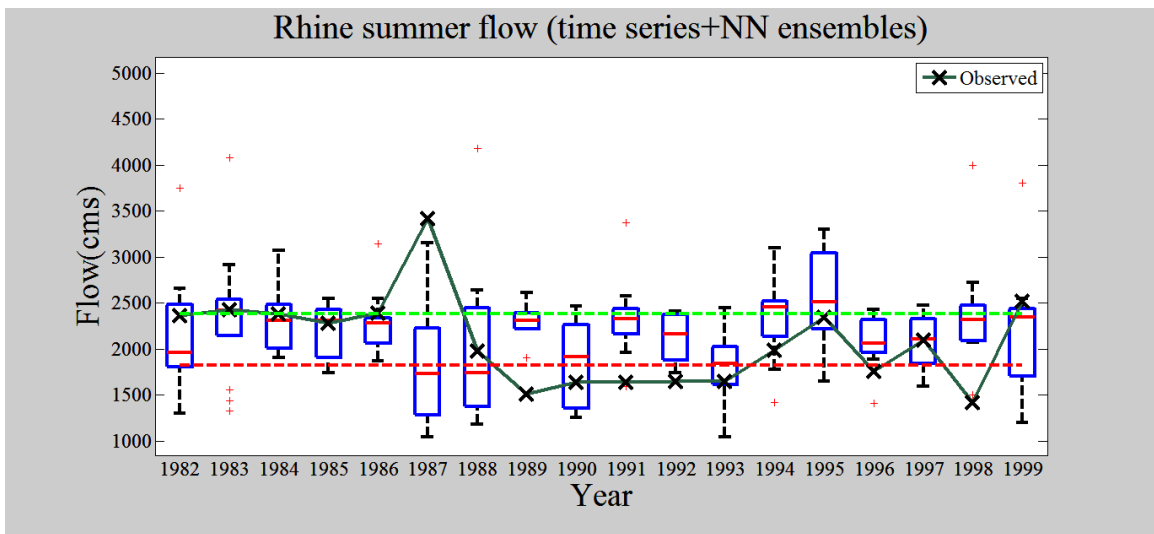
Figure B-26. Ensemble of the Rhine River spring flow: (a) time series model forecasts ensembles; (b) NN model forecasts ensembles; and (c) ensembles of the time series and NN model forecasts.



(a)

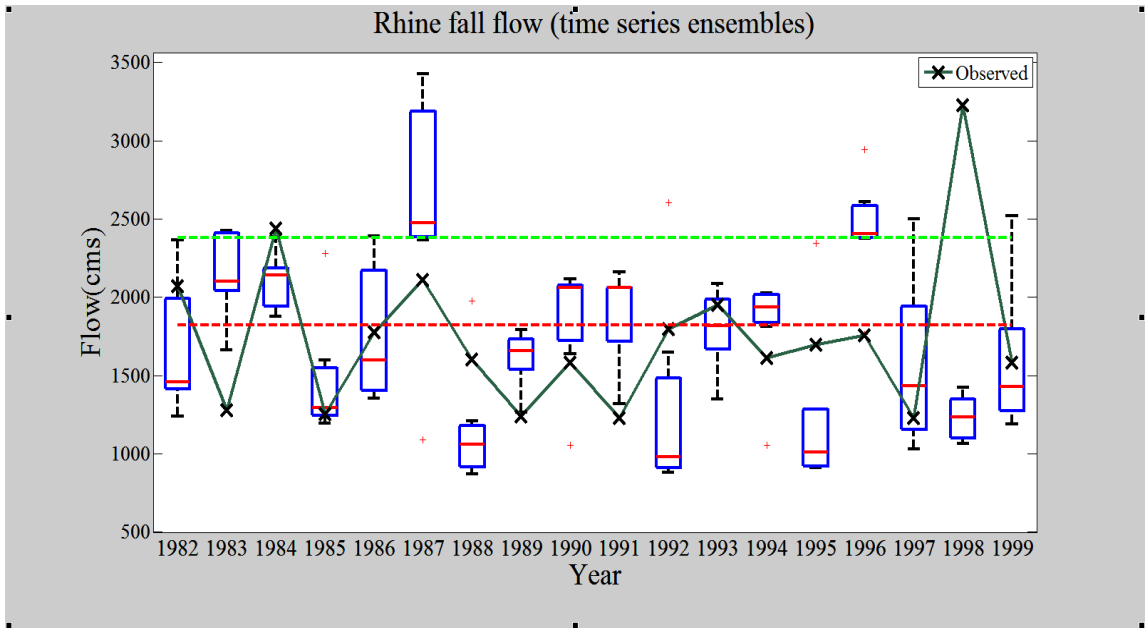


(b)

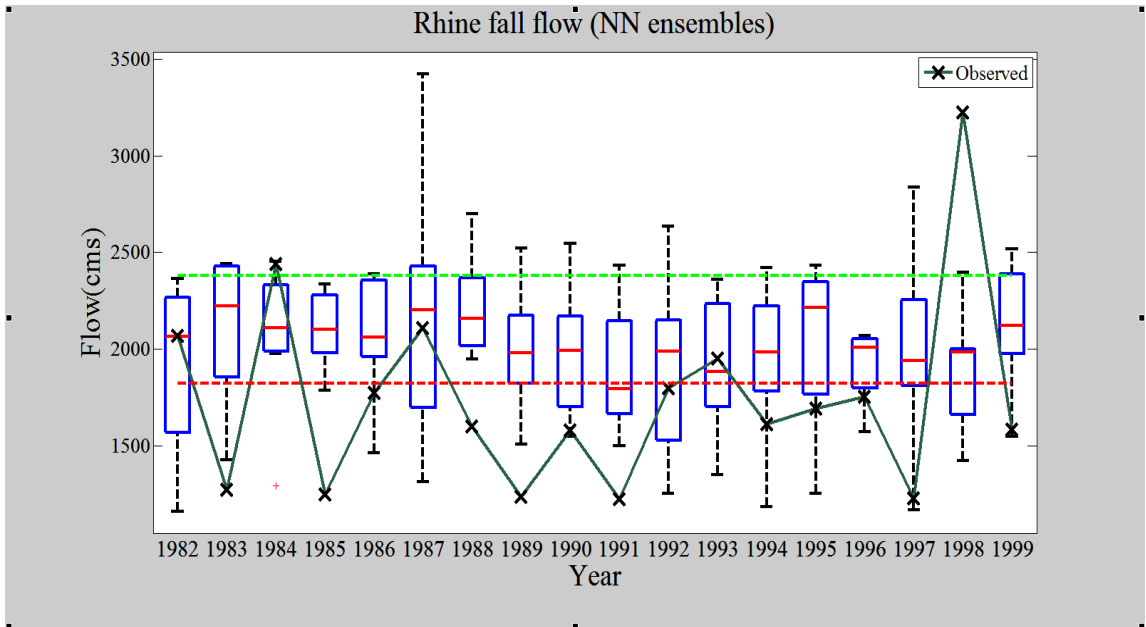


(c)

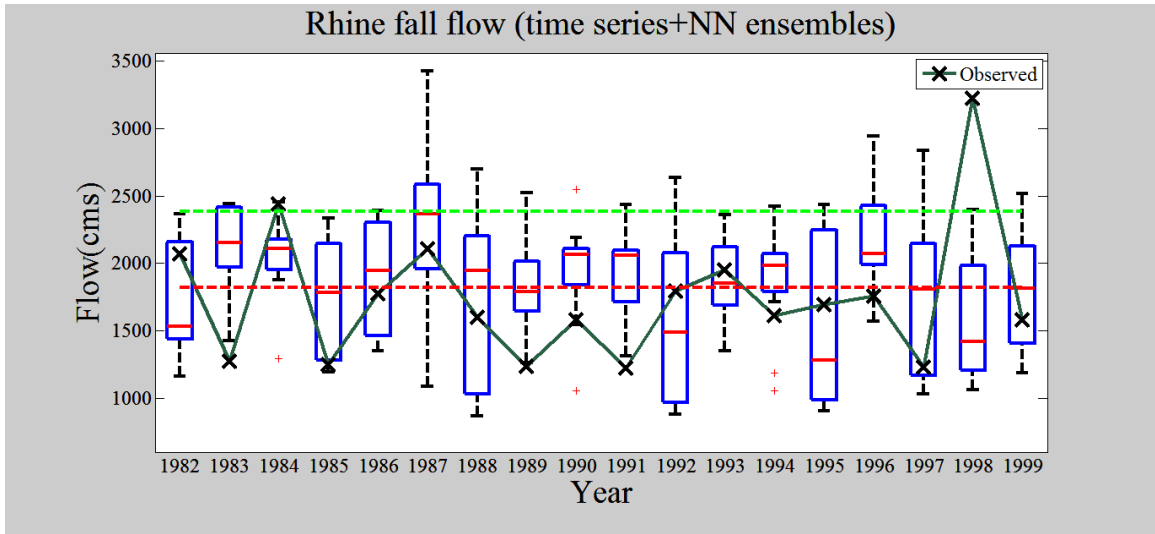
Figure B-27. Ensemble of the Rhine River summer flow: (a) time series model forecasts ensembles; (b) NN model forecasts ensembles; and (c) ensembles of the time series and NN model forecasts.



(a)

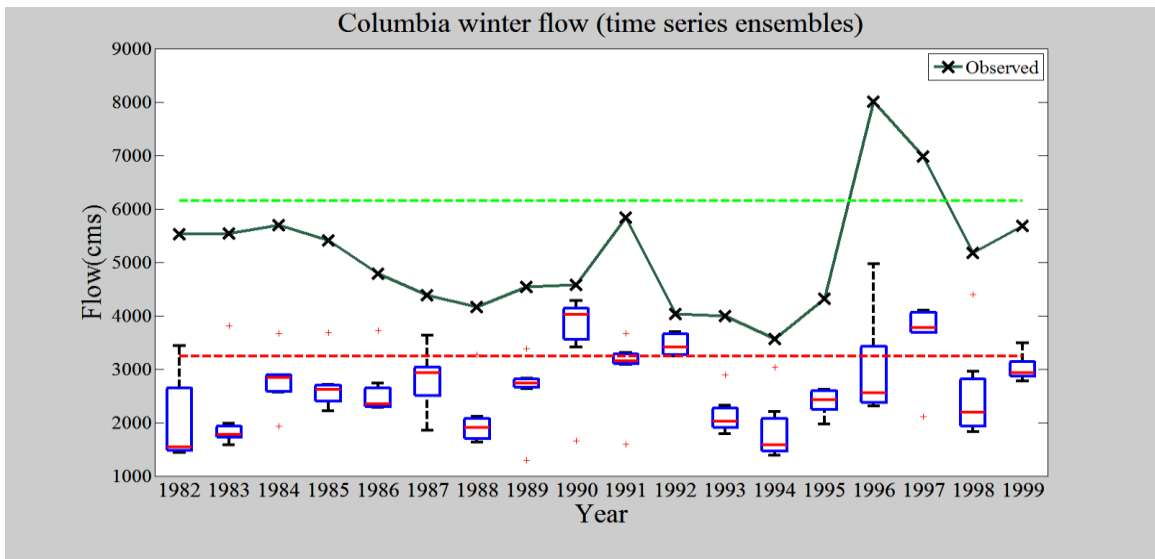


(b)

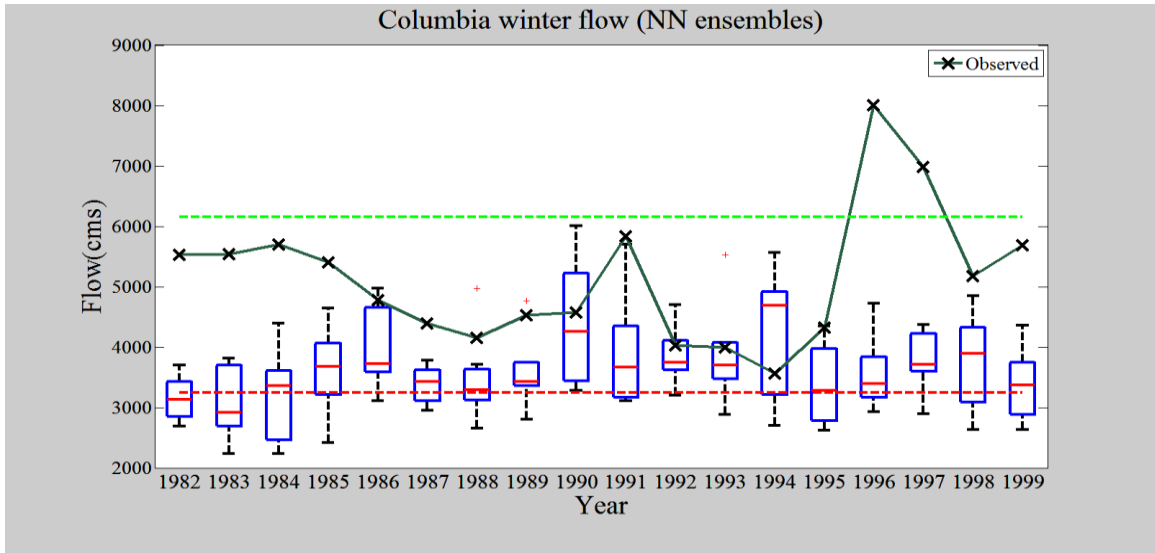


(c)

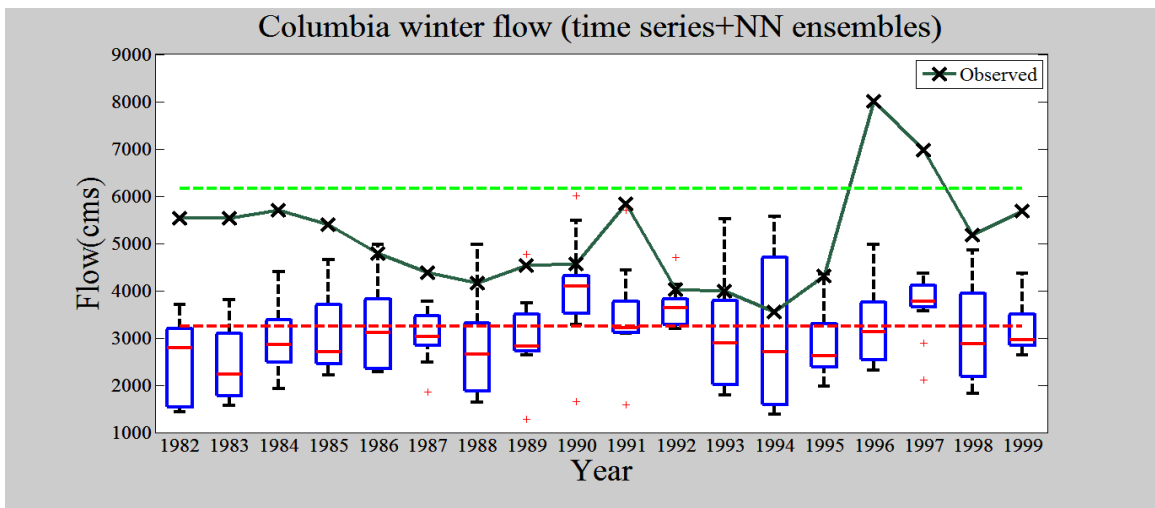
Figure B-28. Ensemble of the Rhine River fall flow: (a) time series model forecasts ensembles; (b) NN model forecasts ensembles; and (c) ensembles of the time series and NN model forecasts.



(a)

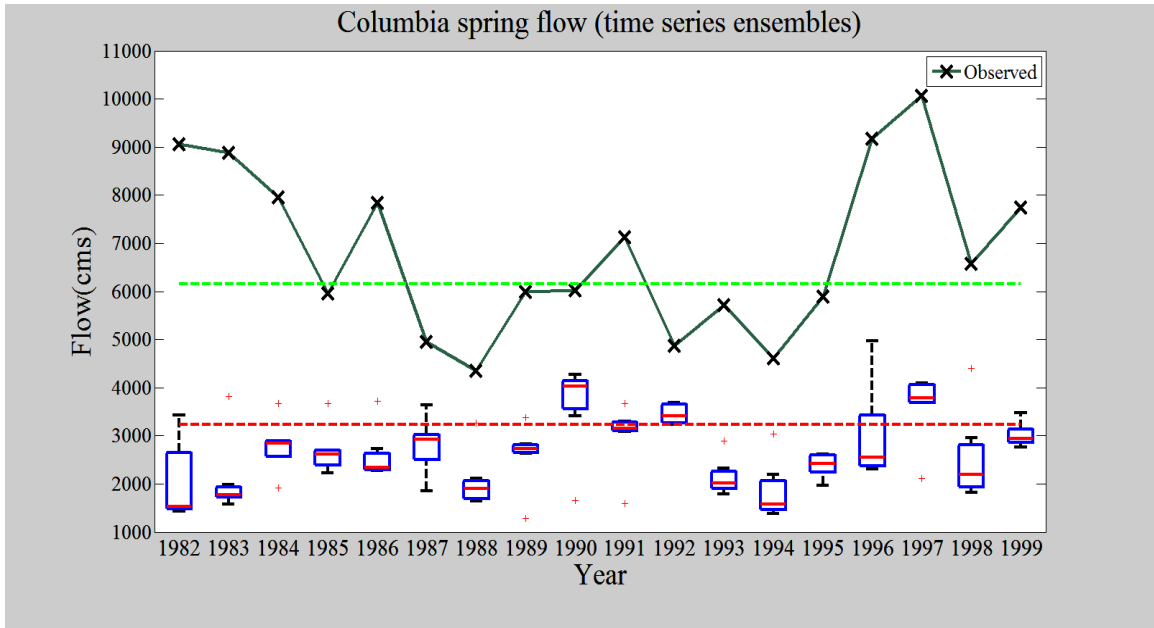


(b)

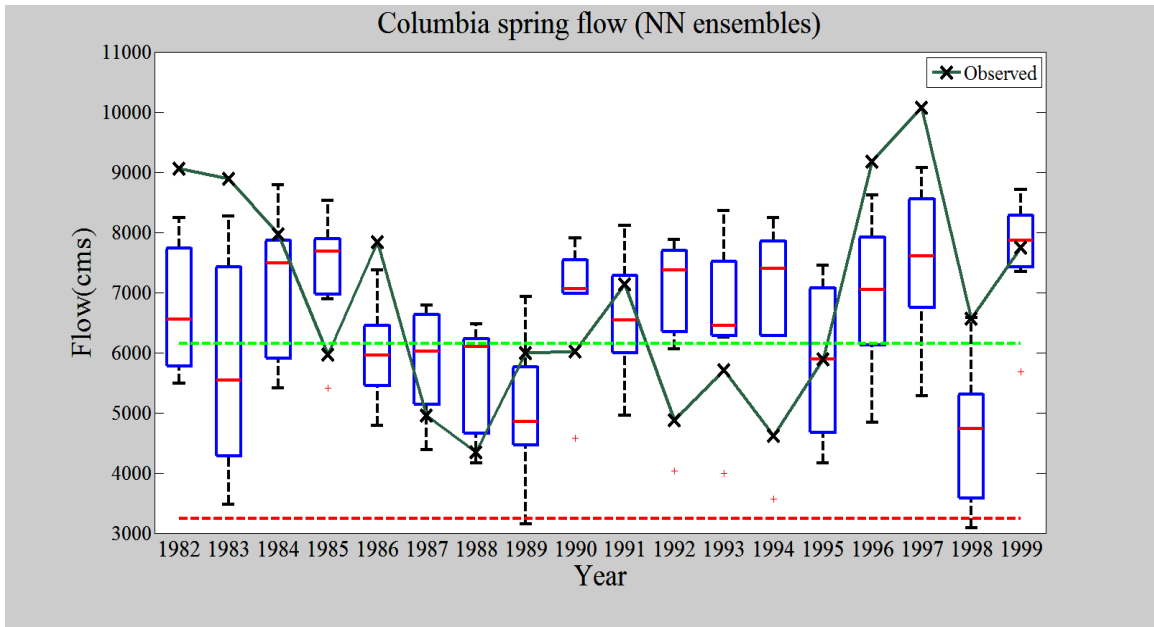


(c)

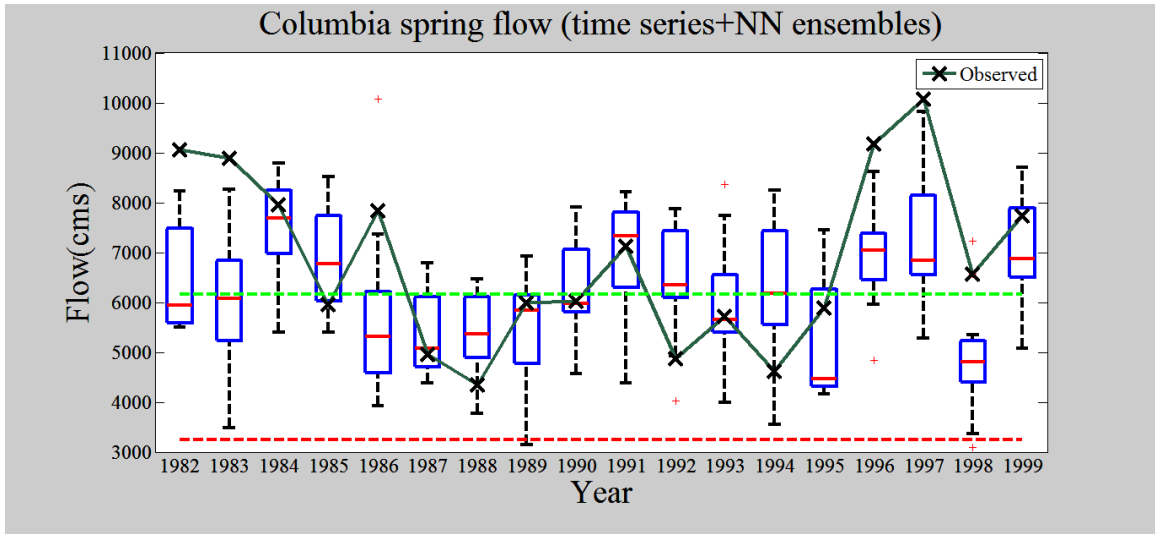
Figure B-29. Ensemble of the Columbia River winter flow: (a) time series model forecasts ensembles; (b) NN model forecasts ensembles; and (c) ensembles of the time series and NN model forecasts.



(a)

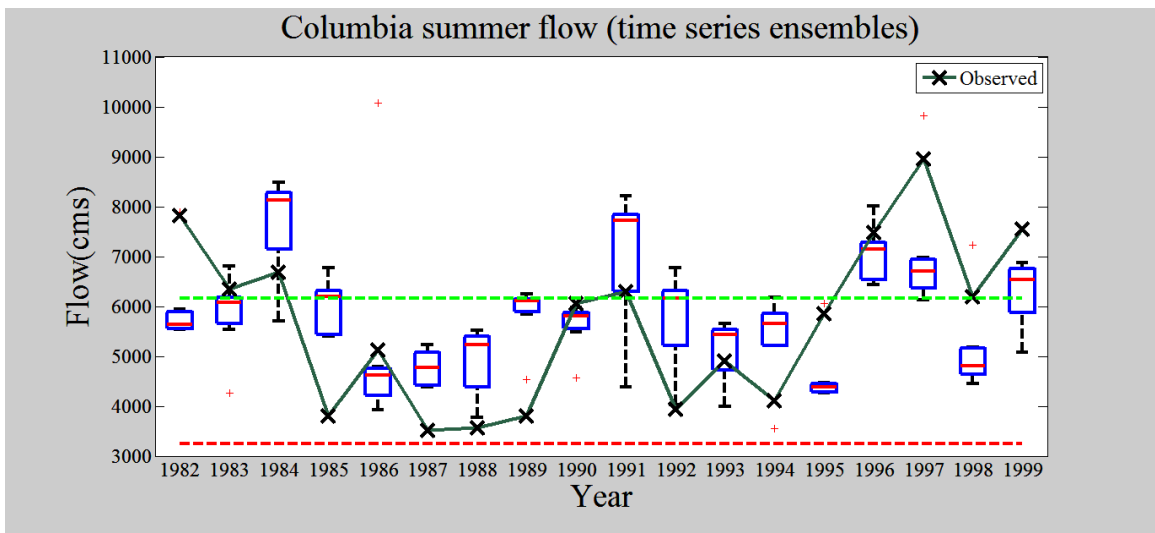


(b)

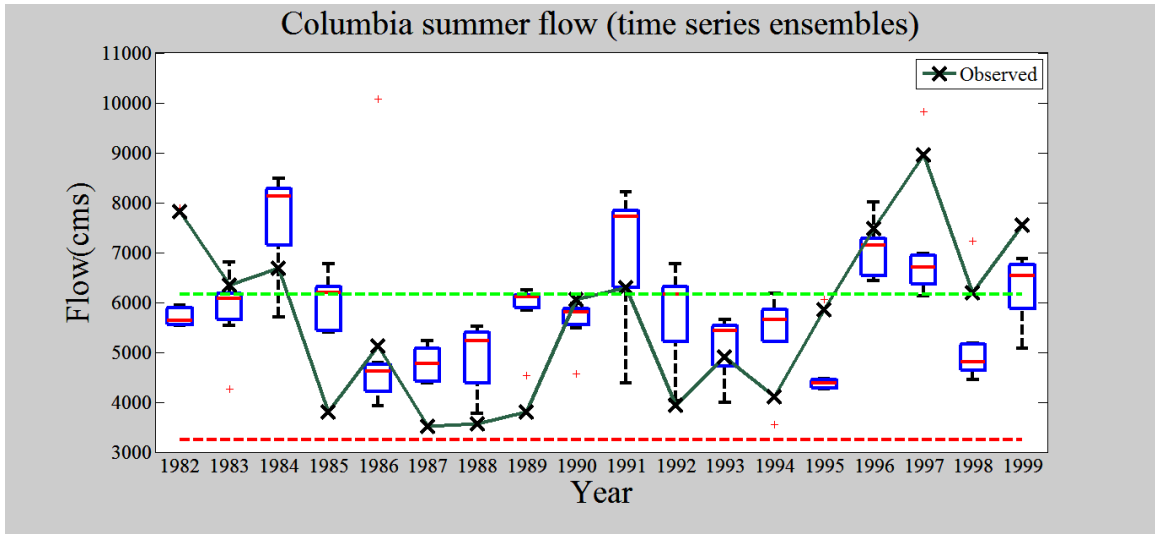


(c)

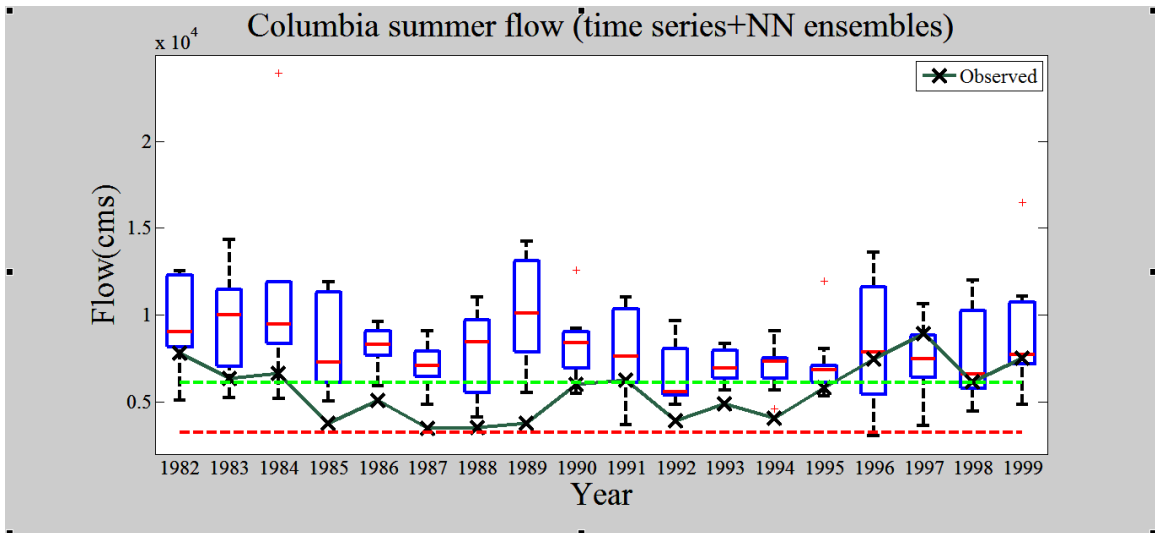
Figure B-30. Ensemble of the Columbia River spring flow: (a) time series model forecasts ensembles; (b) NN model forecasts ensembles; and (c) ensembles of the time series and NN model forecasts.



(a)

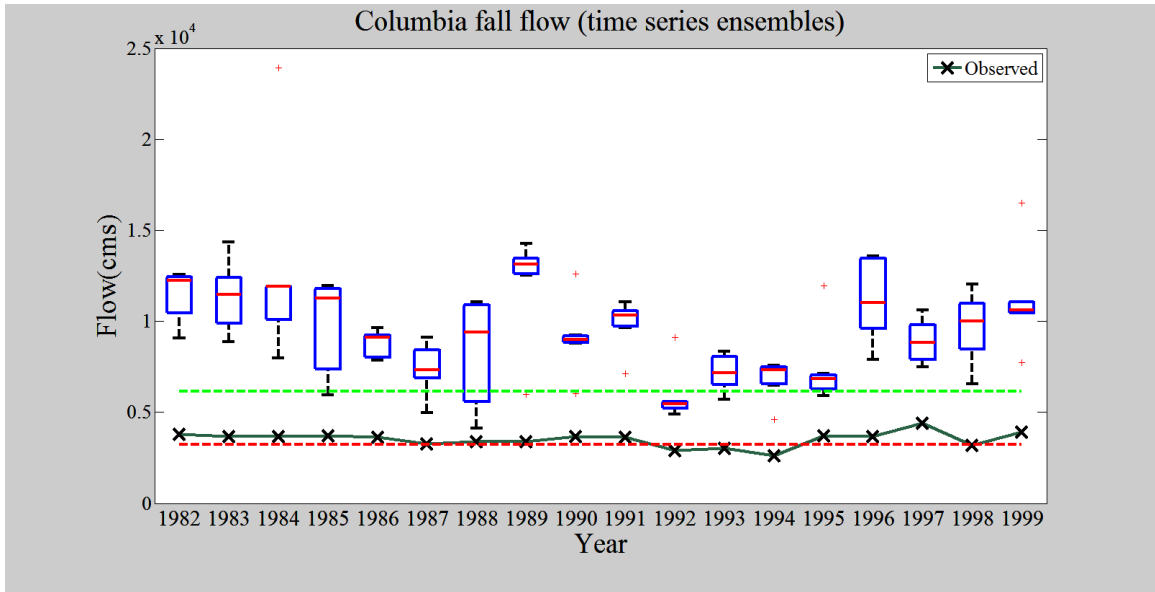


(b)

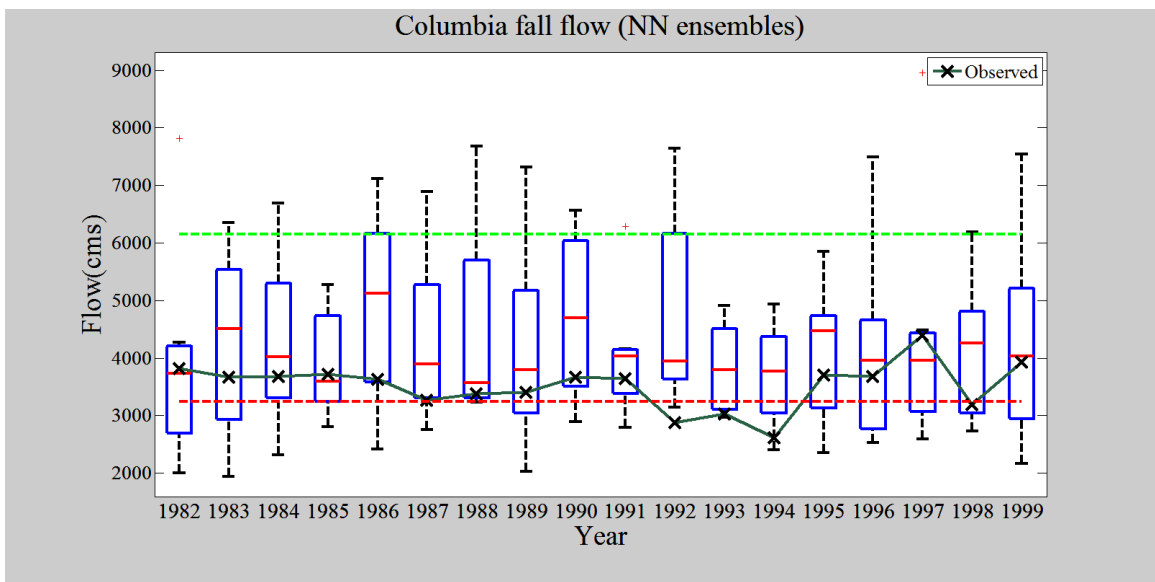


(c)

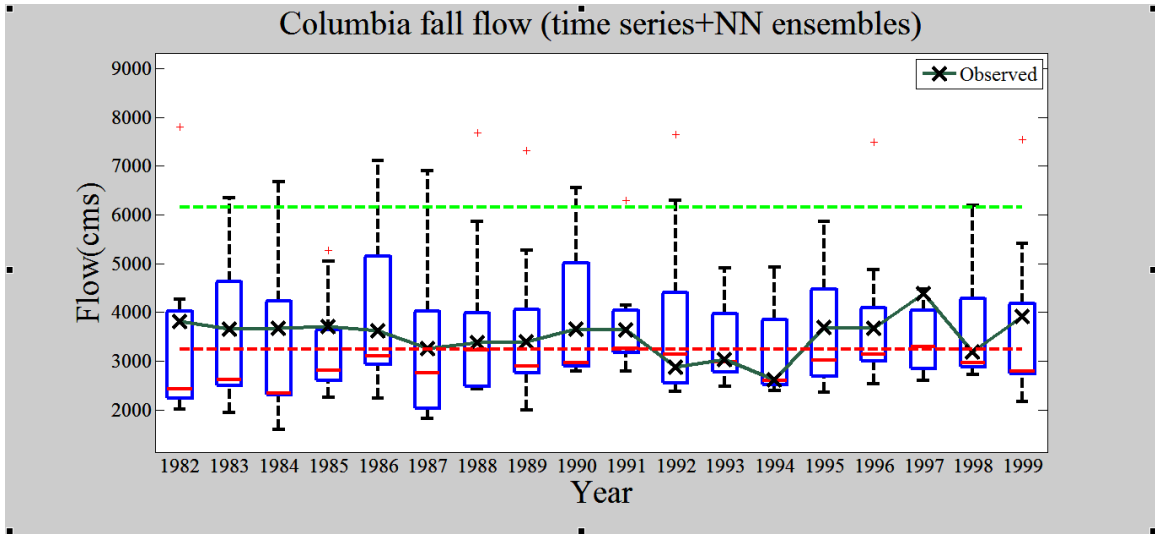
Figure B-31. Ensemble of the Columbia River summer flow: (a) time series model forecasts ensembles; (b) NN model forecasts ensembles; and (c) ensembles of the time series and NN model forecasts.



(a)

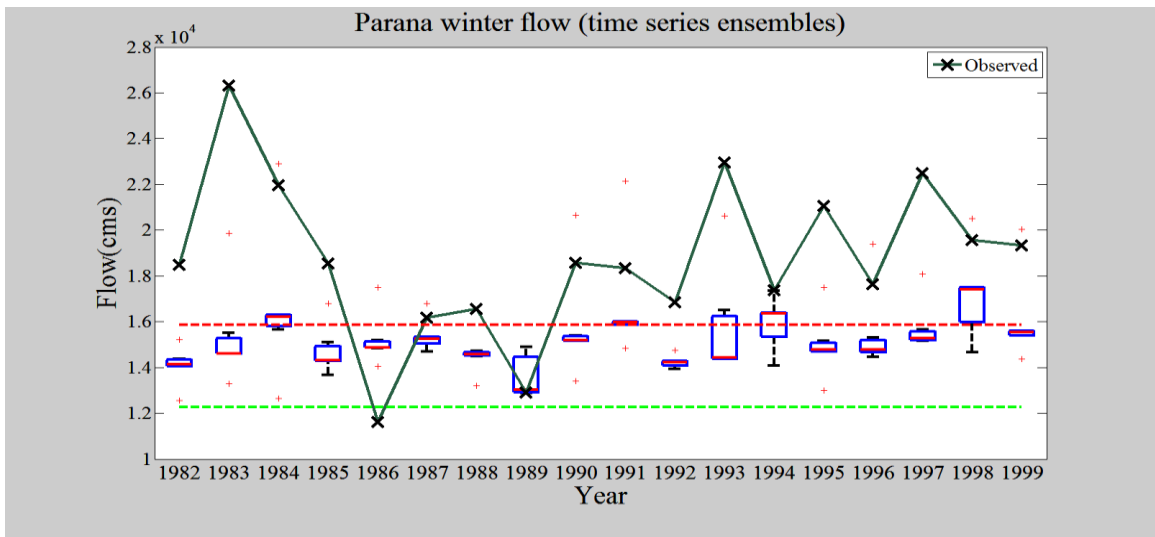


(b)

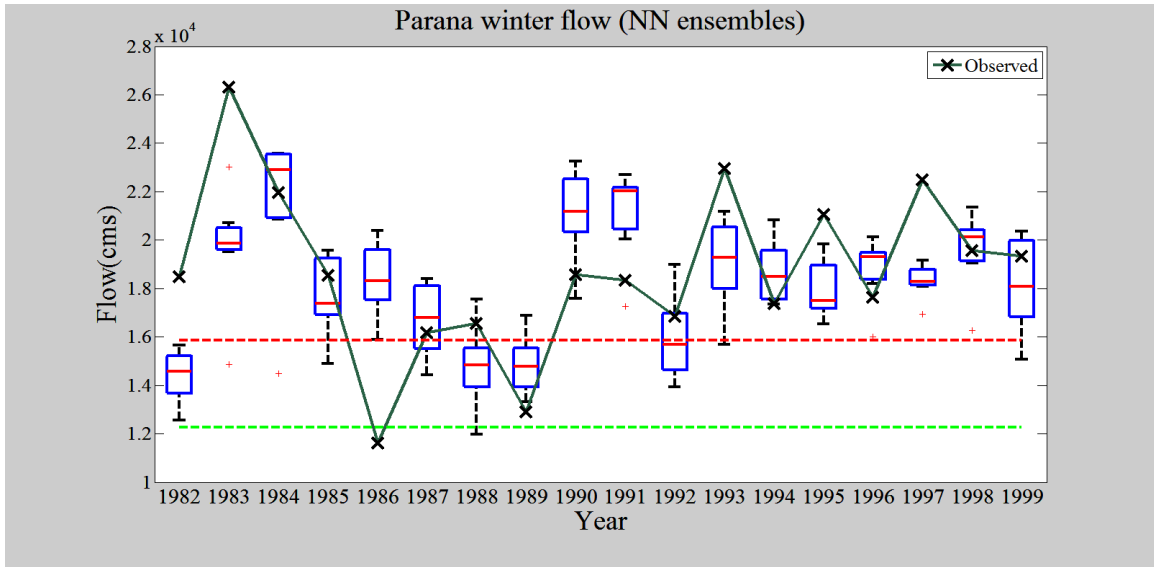


(c)

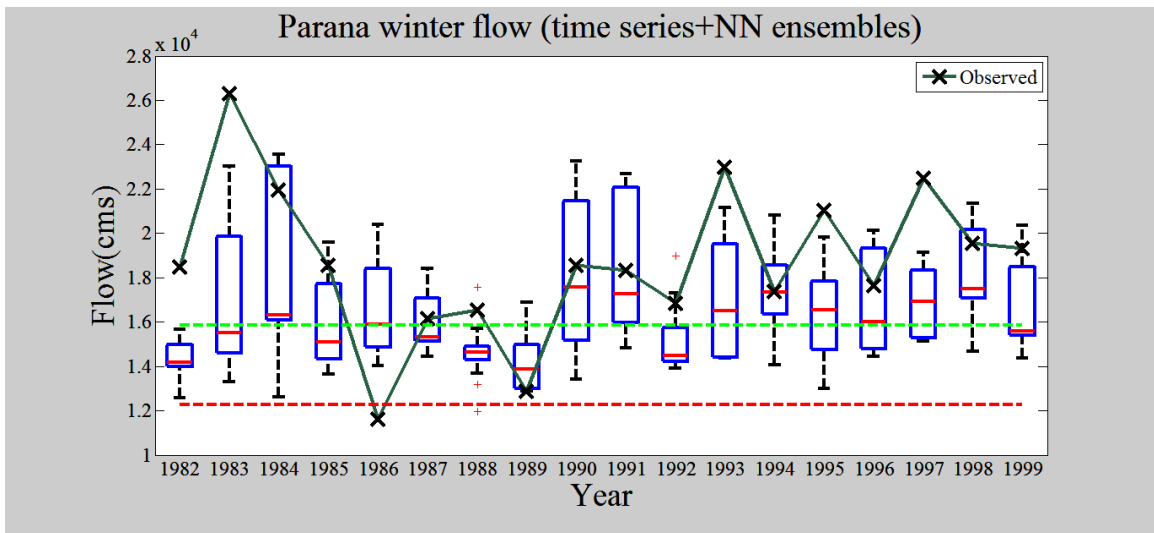
Figure B-32. Ensemble of the Columbia River fall flow: (a) time series model forecasts ensembles; (b) NN model forecasts ensembles; and (c) ensembles of the time series and NN model forecasts.



(a)

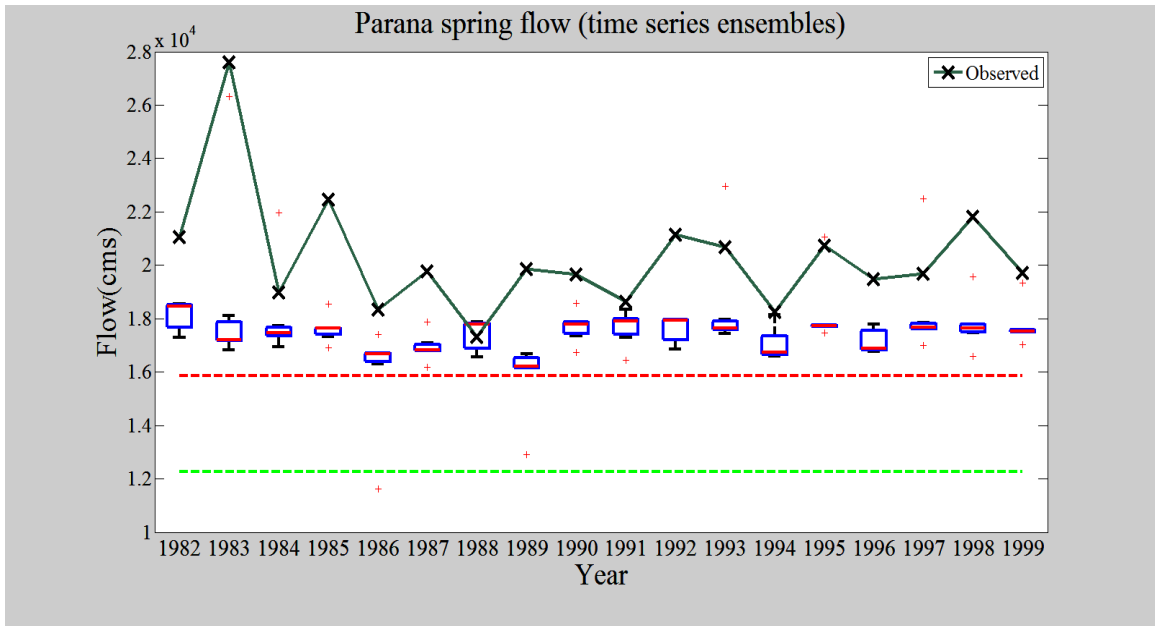


(b)

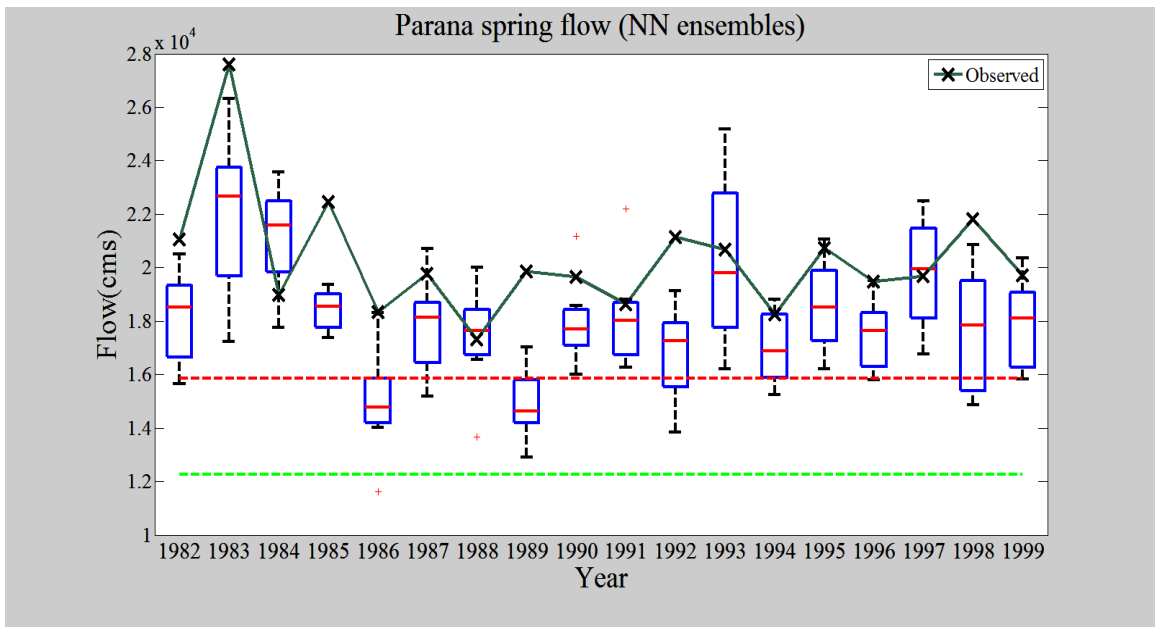


(c)

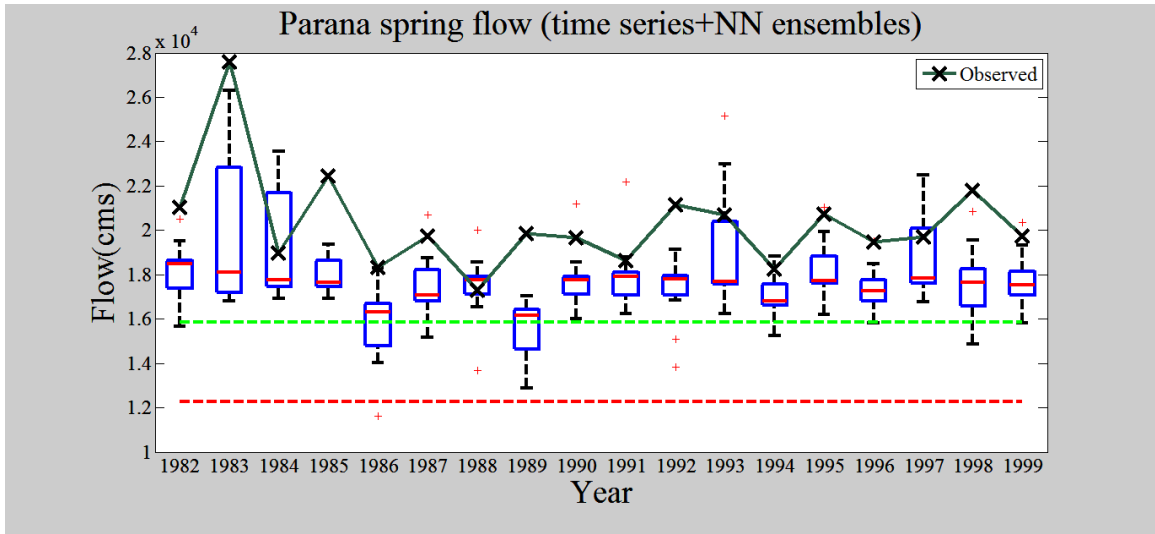
Figure B-33. Ensemble of the Parana River winter flow: (a) time series model forecasts ensembles; (b) NN model forecasts ensembles; and (c) ensembles of the time series and NN model forecasts.



(a)

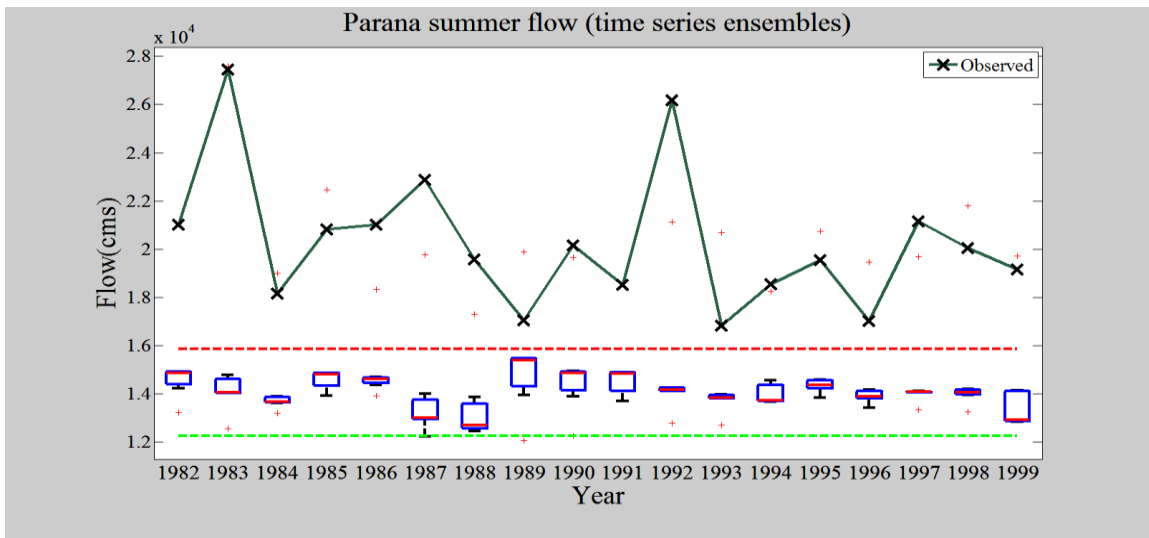


(b)

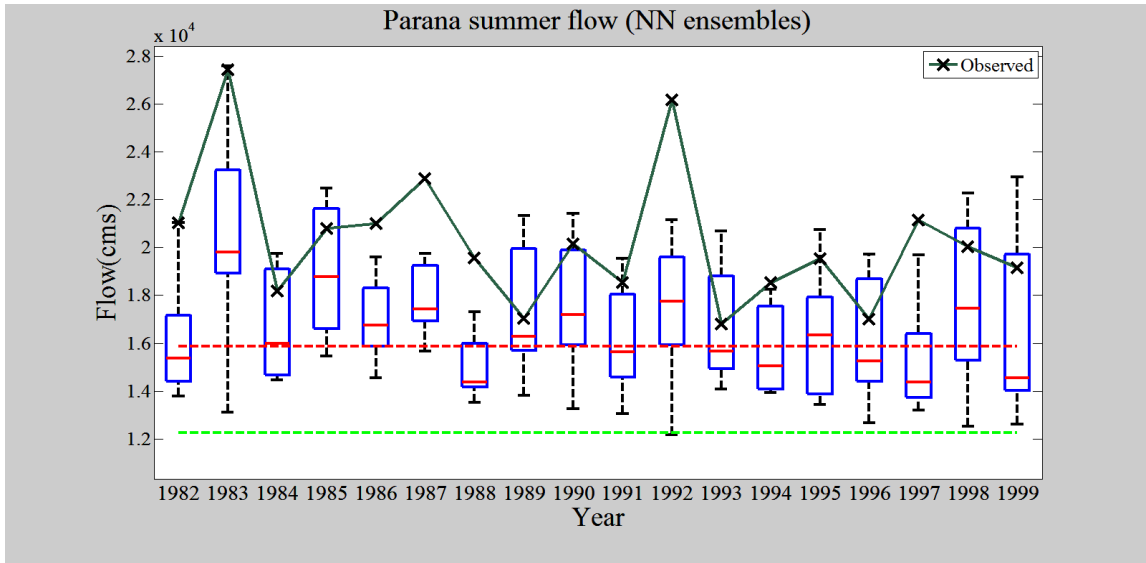


(c)

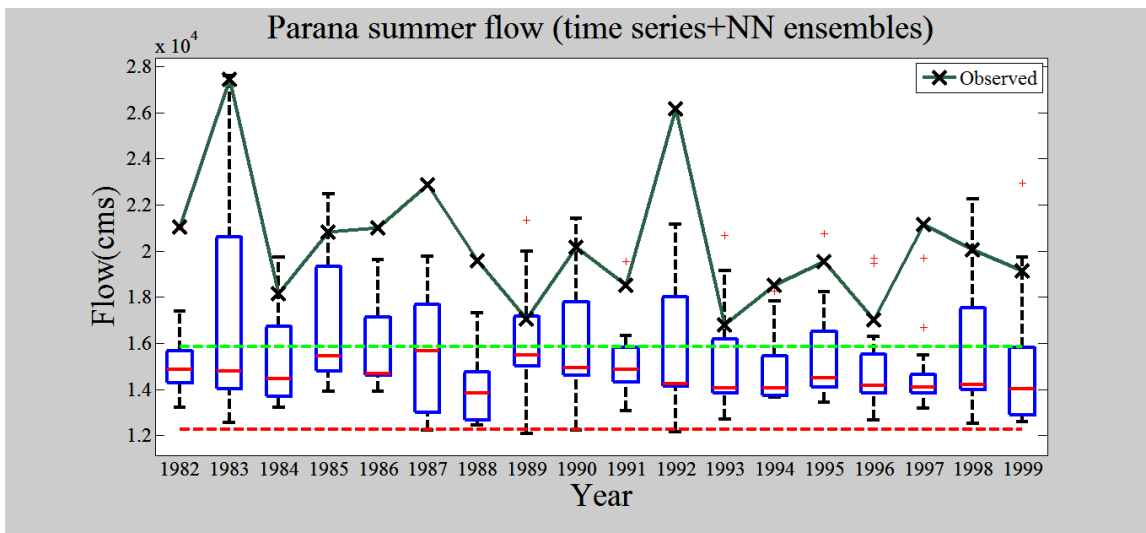
Figure B-34. Ensemble of the Parana River spring flow: (a) time series model forecasts ensembles; (b) NN model forecasts ensembles; and (c) ensembles of the time series and NN model forecasts.



(a)

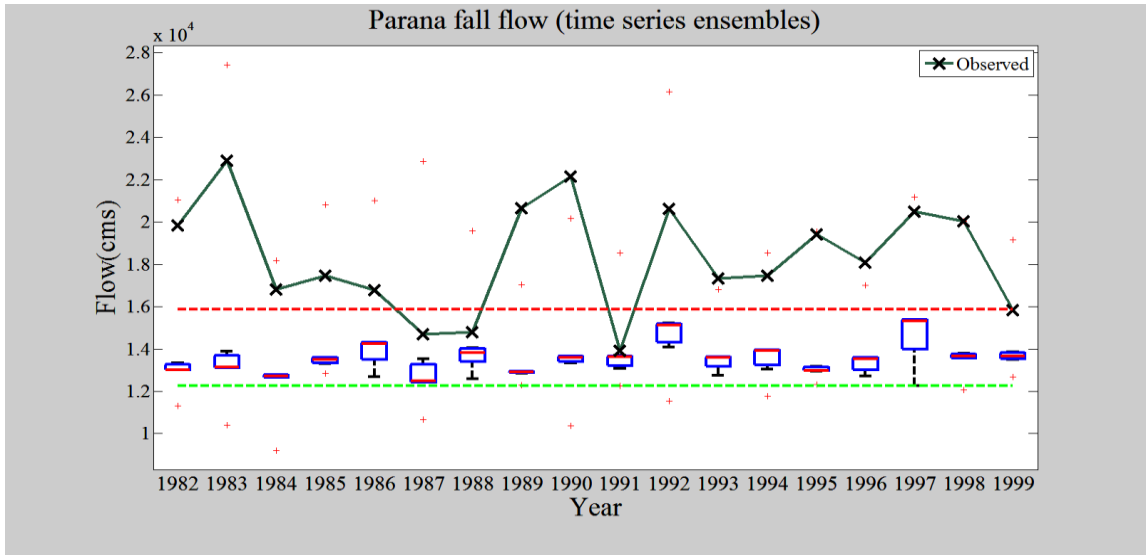


(b)

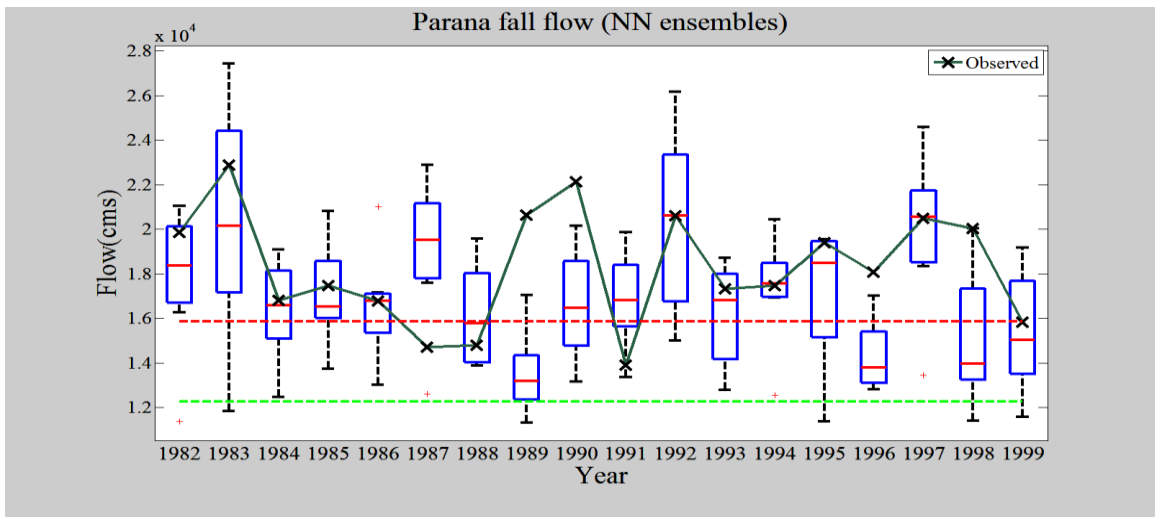


(c)

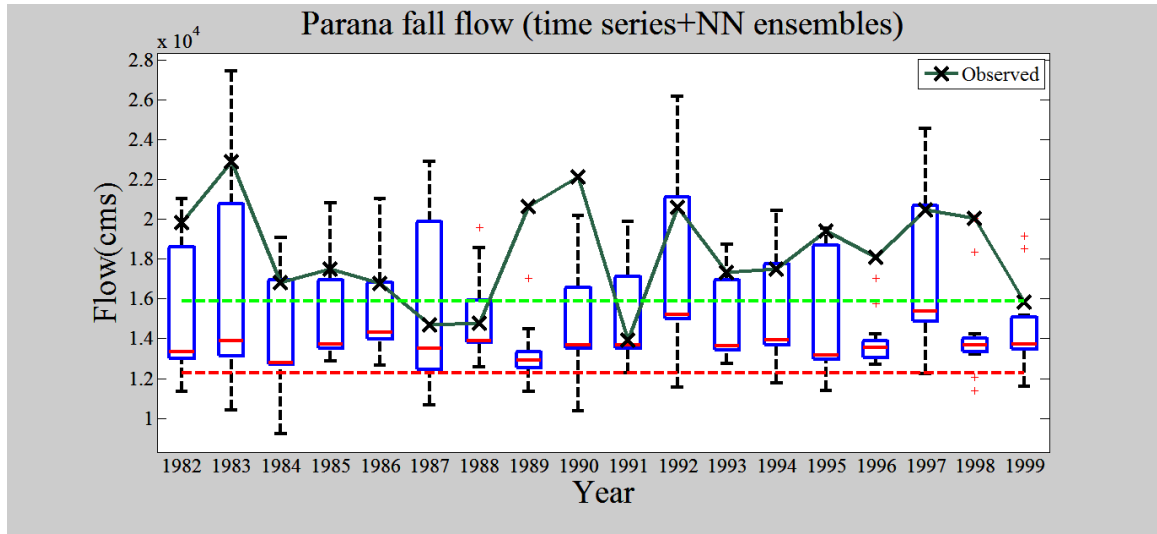
Figure B-35. Ensemble of the Parana River summer flow: (a) time series model forecasts ensembles; (b) NN model forecasts ensembles; and (c) ensembles of the time series and NN model forecasts.



(a)



(b)




(c)

Figure B-36. Ensemble of the Parana River fall flow: (a) time series model forecasts ensembles; (b) NN model forecasts ensembles; and (c) ensembles of the time series and NN model forecasts.

APPENDIX C: POSTERS

POSTER C-1




World Climate Research Programme

Forecasting Seasonal Hydrologic Response in Major River Basins Under Climate Variations

Tanvir H Bhuiyan¹, Mark N French²

Department of Civil and Environmental Engineering, University of Louisville, Louisville, Kentucky, USA
Correspondence to: Tanvir H Bhuiyan, Email: ahbhu01@exchange.louisville.edu




UNIVERSITY OF LOUISVILLE

Abstract

Global climate change has already had observable effects on the environment. Changes include sea level rise, decrease of sea ice, intense heat waves, more frequent temperature extremes, enhanced seasonal precipitation and runoff, reduced dry season precipitation etc. However, under these changing climate circumstances, science projects that these phenomenon will likely increase in frequency and extreme magnitude including events like floods, droughts, cyclones and diurnal temperature variations. Research studies are needed to assess and quantify the historical occurrence context of these extreme events and develop innovative forecasting techniques to reduce adverse impacts on society. Previous studies have focused on developing basin scale hydrologic forecasts models based on climate anomalies such as El Nino, La Nina episodes which significantly influence global climate and as well as annual and seasonal rainfall and stream flow. Specifically, the impact of climate change on streamflow could be significantly modified by anomalies in temperature and rainfall quantity and geographic distribution. This work intends to identify and quantify changes in continental scale runoff and connect with correlations between flows of major rivers globally. The goal is for this information to be used in developing a technique combining flow conditions of major rivers with environmental forcing variables like El Nino, La Nina, sunspot cycle, and others with a view to improve flow forecasting skill. The scale of interest is extreme events such as droughts and floods on a seasonal to annual basis. Additionally, this research will characterize hydrologic flow variation from large scale watersheds and quantify the relation of external environmental processes influencing flow on a seasonal to annual time scales. Preliminary work illustrates the relation among annual, monthly and seasonal flow records of 4 major rivers: Parana, Danube, Rhine and Missouri. The river flows are studied in a seasonal context with the external environmental forcings such as sun spot numbers (SSN) and Southern Oscillation Index (SOI). Initially the characteristics of each river flow records were identified and analyzed to illustrate the ability of stochastic models to reproduce simulated and forecast historical flow rates. Then relations between continental flows and external climate variables responsible for the changes in flows incorporated. The current work focuses on extreme events and evaluation of response under probabilistic variations in each component of environmental forcing to understand and quantify expected responses to stream flow under climate change scenarios.

Data & Methodology

The seasonal data (Winter, Spring, Summer and Fall) of the 4 rivers namely Parana (South America), Danube (Europe), Rhine (Europe) and Missouri (North America) from year 1936 to 1979 were used for this analysis.



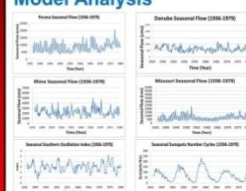
Besides that seasonal Southern Oscillation Index (SOI) and Sunspot Cycle (SSN) were also incorporated as external environmental variables. Autoregressive Moving Average (ARMA) Models of the following variable combinations were used here for forecasting seasonal flows of the rivers:

- Univariate ARMA(1,1) Models of 4 rivers
- Multivariate ARMA(3,0) Model with 4 Rivers
- Multivariate ARMA(3,0) Model with 4 Rivers and SOI
- Multivariate ARMA(3,0) Model with 4 Rivers and SOI and SSN
- Multivariate ARMA(3,0) Model with 3 Rivers and SSN - Persistence Model
- Ensemble Model

The modeling procedures were divided into 2 steps

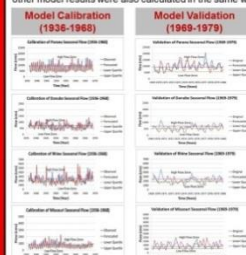
- Calibration: 33 years of data (1936-1969)
- Validation: 11 years of data (1969-1979)

Model Analysis




Seasonal Flow Forecasting

Model Calibration (1936-1969)



Model Validation (1969-1979)



Results

Pearson Correlation Coefficient

River	Univariate	4 Rivers	4 Rivers + SOI	4 Rivers + SOI + SSN	Persistence
Parana	0.568	0.514	0.550	0.550	0.536
Danube	0.178	0.165	0.166	0.201	0.128
Rhine	0.166	0.185	0.174	0.182	0.205
Missouri	0.495	0.533	0.568	0.558	0.534

Flow Categorization and Forecast

River flows below 33 percentile have been used here as an indication of low flow and above 66 percentile have been taken as high flow. Flows in between two limits are categorized as average flow.

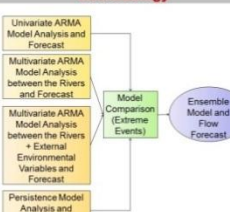
Parana River

River	Univariate	4 Rivers	4 Rivers + SOI	4 Rivers + SOI + SSN	Persistence
Correct	2	2	2	1	3
Not well Picked	3	3	3	4	2
High Flow Validation (Total: 23 Rows)	16	16	16	15	14
Not well Picked	7	7	8	9	9

Danube River

River	Univariate	4 Rivers	4 Rivers + SOI	4 Rivers + SOI + SSN	Persistence
Correct	11	9	9	8	11
Not well Picked	7	6	7	7	9
High Flow Validation (Total: 9 Rows)	4	3	2	4	3
Not well Picked	5	6	5	5	6

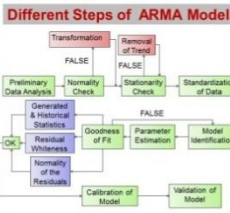
Methodology



Objectives

- Identification and quantification of changes in continental scale runoff
- Identification of correlations between major global rivers
- Characterization of hydrologic flow variation from large scale watersheds
- Relation of external environmental processes influencing flow

Different Steps of ARMA Models



Results

Ratios of Standard Deviation

River	Univariate	4 Rivers	4 Rivers + SOI	4 Rivers + SOI + SSN	Persistence
Parana	0.916	0.972	0.943	0.945	0.981
Danube	1.191	1.126	1.209	1.066	1.004
Rhine	1.222	1.147	1.201	1.212	1.057
Missouri	1.113	0.982	0.971	0.975	0.998

Ensemble Forecast

In ensemble forecasts, the results from different models were combined and quantified in terms of likelihood which allows the variability of different models to be counted and considered.

Future Work

More rivers from different continents and other variables such as precipitation, sea surface temperature etc. will be included in the analysis. Sensitivity analysis due to climate induced changes will be performed to see the accuracy of the models in predicting extreme climatic conditions in river flows such as droughts, floods etc.

POSTER C-2

AGU FALL MEETING
San Francisco | 3-7 December 2012

GC11D-1039
Seasonal Streamflow Variability at Global Time-Space Scales under Natural Climate Extremes

UNIVERSITY OF LOUISVILLE
AGU
American Geophysical Union

UL
UNIVERSITY OF LOUISVILLE
J.B. SPEED SCHOOL OF ENGINEERING

Tanvir H Bhuiyan¹, Mark N French²
Department of Civil and Environmental Engineering, University of Louisville, Louisville, Kentucky, USA
Correspondence to: Tanvir H Bhuiyan, Email: abhhu01@exchange.louisville.edu

Global Environ System

Identification of anomalies and changes in global river basins runoff

Relation of external environmental processes influencing flow

Identification of correlations between major global rivers

Characterization of river flow

Analyses and forecast

Improve seasonal flow forecasting skill (extreme events)

Ensemble Flow Prediction

Global Stream Flow System

Seasonal data (Winter, Spring, Summer and Fall) of 5 rivers from year 1906 to 1999: Congo (Africa), Yangtze (Asia), Rhine (Europe), Columbia (North America), and Parana (South America).

Seasonal Southern Oscillation (SOI), Sunspot Cycle (SSN), Pacific Decadal Oscillation (PDO), North Atlantic Oscillation (NAO) years 1906 to 1999, external environmental forcing variables

Conceptual Ensemble

Model Identification and Calibration

Time Series (Univariate & Multivariate)

Persistence

Neural Network (Univariate & Multivariate)

Calibration Evaluation

Independent Validation Evaluation

Time Series Prediction

Persistence prediction

Neural Network (Univariate & Multivariate) prediction

Ensemble

Flow Forecast Applications

Time Series Component

Univariate and multivariate Autoregressive Moving Average (ARMA) Models with spectrum of flow and environ data:

Time Series Method: Validation of Congo Seasonal Flow

Time Series Method: Validation of Yangtze Seasonal Flow

Neural Network Illustrative Concept

Neural Network Method: Validation of Congo Seasonal Flow

Results

Time Series

Congo Performance of Various Time Series Models

Neural Network

Congo Performance Analysis of various NN Models

Performance for Congo River: x axis represents model type: (1) Univariate, (2) Multivariate with 5 rivers, (3) Multivariate with 5 rivers + SOI, (4) Multivariate with 5 rivers + SOI + SSN, (5) Multivariate with 5 rivers + SOI + SSN + PDO, (6) Multivariate with 5 rivers + SOI + SSN + PDO + NAO, and (7) Persistence. Left y-axis is root mean square error (RMSE), Right y-axis is mean % error (MPE), ratio standard deviation (RSD), and Pearson correlation coefficients.

Flow Categorization and Forecast

Flow magnitude less than 33 percent of mean indicate low flow and above 66 percent indicate high flow.

Time Series

Flow	Forecast	M. Varian	M. Varian + 5 Rivers	M. Varian + 5 Rivers + SOI	M. Varian + 5 Rivers + SOI + SSN + PDO	Persistence
Congo Forecast	12	13	12	13	13	14
Congo Obs'd Category	20	19	20	19	20	18

Low Flow Validation (Total 23 Nos.)

Neural Network

Flow	Forecast	M. Varian	M. Varian + 5 Rivers	M. Varian + 5 Rivers + SOI	M. Varian + 5 Rivers + SOI + SSN + PDO	Persistence
Congo Forecast	22	20	20	20	21	18
Congo Obs'd Category	20	8	8	8	11	18

Low Flow Validation (Total 23 Nos.)

High Flow Validation (Total 14 Nos.)

Ensemble Forecast

Ensemble Time Series Approach: Congo Winter Flow

Ensemble Neural Network Approach: Congo Winter Flow

References

- Dai, A., T. Qian, K. E. Trenberth, and J. D. Milliman, 2009: Changes in continental freshwater discharge from 1948-2004. *J. Climate*, **22**, 2773-2791.
- Global Runoff Data Centre (2011): Long-Term Mean Monthly Discharges and Annual Characteristics of GRDC Stations / Global Runoff Data Centre, Koblenz, Germany: Federal Institute of Hydrology (BfG), 2011.
- Mantra, S.J. and S.K. Hare, Y. Zhang, J.M. Wallace, and R.C. Francis, 1997: A Pacific interdecadal climate oscillation with impacts on salmon production. *Bulletin of the American Meteorological Society*, **78**, pp. 1869-1878.
- Hurrell, J.W., 1995: Decadal trends in the North Atlantic Oscillation and relationships to regional temperature and precipitation. *Science* **269**, 676-679.

Photo Source: <http://www.abc20.com>, Nov 28, 2012. <<http://www.abc20.com>>

Introduction

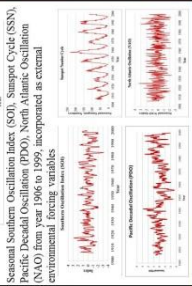
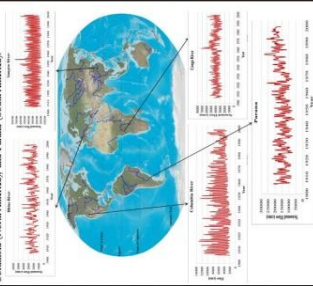
Hydrological extremes such as floods and droughts are two of the most hazardous natural disasters in context of economic loss and human impact. The frequency and the severity of these events are related to precipitation extremes, which are linked to climate variation. Predictions of precipitation extremes are essential for the development of strategies for managing irrigation water requirements, reservoir operations, and planning for recovery. Accurate forecasts depend on identification of relevant variables and uncertainties involved in prediction. The identification of relevant variables and uncertainties can be considered in ensemble forecast methods which combine a variety of model predictions and allows the variability of estimation to be considered. In this study, methods including time series and neural network (NN) are evaluated for seasonal flow forecasts ensembles.

Objectives

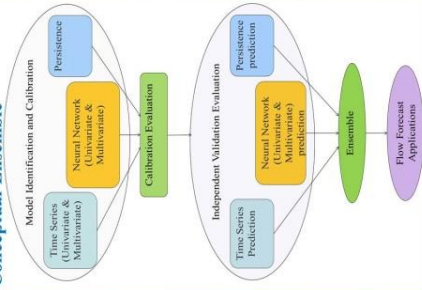
Present research seeks to address the following important issues: (a) How can we improve the accuracy of ensemble forecasts? (b) Can we improve in skill prediction for seasonal streamflow extremes include different rivers and variables in stochastic and probabilistic model predictions? (c) Can we improve the ensemble forecast can identify extreme river flow events?

Global Stream Flow System

Seasonal flow extremes are identified from year 1906 to 1999 Congo (Africa), Yangtze (Asia), Rhine (Europe), Columbia (North America), and Paraná (South America).

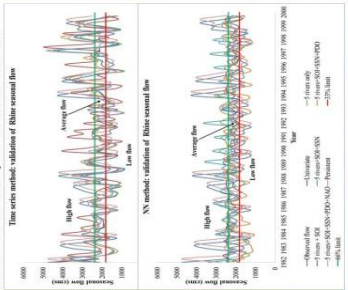


Conceptual Ensemble



Time Series and NN Components

Univariate and multivariate Autoregressive Moving Average (ARMA) Models and NN models with spectrum of flow and environ. data:



Results

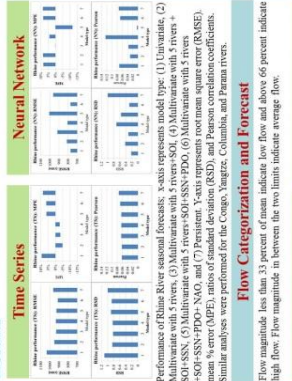
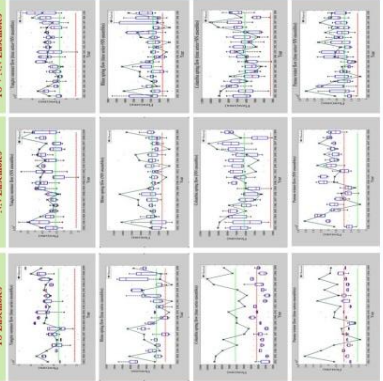
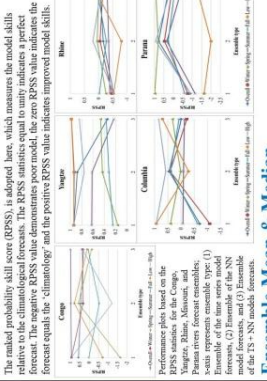


Table with 4 columns: Method, Flow Category, Mean Flow, and Performance Metrics.

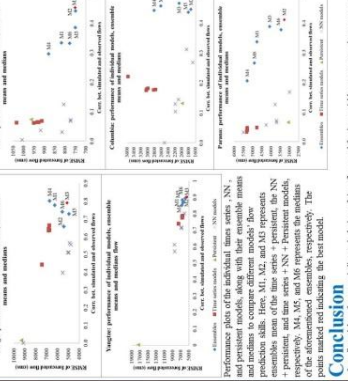
Ensemble Forecast



Ensemble Forecast Skill Evaluation



Ensemble Mean & Median



Conclusion

Overall model performance indicates inclusion of river flow and forcing variables on average improve model performance. Model results are often comparable to more complex multivariate approaches indicating the inclusion of multiple variables does not always improve model performance.

References

Blanton, James H., and Frank W. Zwiers. 2002. "Improving the Accuracy of GCMs for Regional Climate Prediction." In "Regional Climate Prediction: A Review of the State of the Science," edited by James H. Blanton and Frank W. Zwiers, 1-12. Washington, DC: American Meteorological Society.

CURRICULUM VITAE

NAME: A. M. Tanvir Hossain Bhuiyan

ADDRESS: Department of Civil & Environmental Engineering
University of Louisville
101 W.S. Speed Hall
Louisville, KY 40292

EMAIL: tanvir.h.bhuiyan@gmail.com

DOB: Dhaka, Bangladesh – January 17, 1982

EDUCATION:
and TRAINING B.Sc., Water Resources Engineering
Bangladesh University of Engineering & Technology
2001-2005

M. Eng., Water Resources Engineering
Bangladesh University of Engineering & Technology
2005-2009

Ph.D., Civil and Environmental Engineering
University of Louisville
2009-2014

RESEARCH EXPERIENCES

PHD RESEARCH: Topic: “Forecasting Seasonal Hydrologic Response in Major River Basins”
Advisor: Prof. Mark N French, PhD, PE

M.S. RESEARCH: Topic: “Performance of Geobags in River Bank and Bed Protection”
Advisor: Prof. Md. Abdul Matin, PhD

B.S. RESEARCH: Topic: “Morphological Characteristics of Gumti River”
Advisor: Prof. M. Monowar Hossain, PhD

PROFESSIONAL EXPERIENCE:

1. Graduate Research Fellow and Teaching Assistant
Department of Civil & Environmental Engineering
University of Louisville
Louisville, KY
August 2009 – Current
2. Assistant Engineer (Civil)
Bangladesh Water Development Board (BWDB) (www.bwdb.gov.bd/)
Dhaka, Bangladesh
April 2007 – July 2009
3. Deputy Program Coordinator (Infrastructure)
Intervida Bangladesh (an international NGO) (www.intervida.org)
Dhaka, Bangladesh
April 2006 - April 2007
4. Graduate Civil Engineer
Azmiri Properties and Development Ltd.
Dhaka, Bangladesh
Oct 2005 - April 2006

PUBLICATIONS

- Bhuiyan, Tanvir H. and French, Mark N., Ensemble Methods for Seasonal Streamflow Prediction, AGU Chapman Conference on Seasonal to Interannual Hydroclimate Forecasts and Water Management, Portland, Oregon, July 28-31, 2013.
<http://chapman.agu.org/watermanagement/files/2013/07/Final-Program1.pdf>
- Bhuiyan, Tanvir H. and French, Mark N., Seasonal Streamflow Variability at Global Time-Space Scales Under Natural Climate Extremes, AGU Fall Meeting, San Francisco, California, December 3-7, 2012.
<http://abstractsearch.agu.org/meetings/2012/FM/sections/GC/sessions/GC11D/abstracts/GC11D-1039.html>
- Bhuiyan, Tanvir H. and French, Mark N., Forecasting Seasonal Hydrologic Response in Major River Basins under Climate Variations, 4th WCRP International Conference on Reanalyses, Silver Spring, Maryland, May 7-11, 2012.
http://icr4.org/posters/Bhuiyan_Forecasting_Seasonal_Hydrologic.pdf
- Report of the 4th World Climate Research Programme International Conference on Reanalyses, Silver Spring, Maryland, USA, 7-11 May 2012.
http://www.wcrp-climate.org/documents/ICR4_Report.pdf

PRESENTATIONS

- Poster presented at the AGU Chapman Conference on Seasonal to Interannual Hydroclimate Forecasts and Water Management, Portland, Oregon.
- Poster presented at the fall meeting of the American Geophysical Union (AGU), San Francisco, California.
<http://fallmeeting.agu.org/2012/eposters/eposter/gc11d-1039/>
- Poster presented at the 4th WCRP International Conference on Reanalyses, Silver Spring, Maryland.
<http://icr4.org/posters.html>
- Sustainability Scholars Roundtable Panels: Water Resources, arranged by the Center for Land Use and Environmental Responsibility, University of Louisville on February 19, 2014
- Graduate Research Symposium, University of Louisville on March 23, 2012,
- PhD Seminar, spring 2012, Dept. of Civil & Environmental Engineering, University of Louisville on March 30, 2012
- PhD Seminar, Spring 2013, Dept. of Civil & Environmental Engineering, University of Louisville on March 22, 2013
- Dissertation Retreat, 2012, Writing Center, University of Louisville on May 23-25, 2012

AWARDS

1. AGU Travel Grant Award to attend Chapman Conference, July 2013
2. Matthew Aldridge Cowan PhD Fellowship-University of Louisville (2011-2013)
3. Travel Grand Award to attend 4th WCRP International Conference on Reanalyses, May 2012
4. Graduate Teaching Assistantship and Tuition Award (2009-2011)
5. Student Spotlight March 2012-University of Louisville

AFFILIATION

1. American Geophysical Union (AGU)
2. American Society of Civil Engineers (ASCE)